METHODS IN MICROBIOLOGY
VOLUME 37

Immunology of Infection
Third Edition

Edited by
Stefan H.E. Kaufmann & Dieter Kabelitz

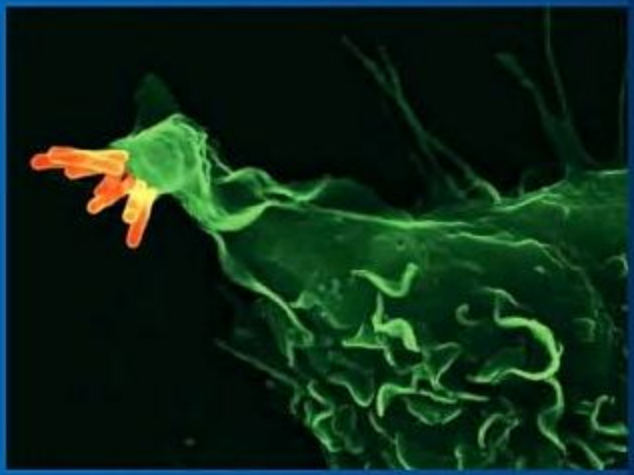

37

Recent titles in the series

Volume 24 *Techniques for the Study of Mycorrhiza*
JR Norris, DJ Reed and AK Varma

Volume 25 *Immunology of Infection*
SHE Kaufmann and D Kabelitz

Volume 26 *Yeast Gene Analysis*
AJP Brown and MF Tuite

Volume 27 *Bacterial Pathogenesis*
P Williams, J Ketley and GPC Salmond

Volume 28 *Automation*
AG Craig and JD Hoheisel

Volume 29 *Genetic Methods for Diverse Prokaryotes*
MCM Smith and RE Sockett

Volume 30 *Marine Microbiology*
JH Paul

Volume 31 *Molecular Cellular Microbiology*
P Sansonetti and A Zychlinsky

Volume 32 *Immunology of Infection, 2nd edition*
SHE Kaufmann and D Kabelitz

Volume 33 *Functional Microbial Genomics*
B Wren and N Dorrell

Volume 34 *Microbial Imaging*
T Savidge and C Pothoulakis

Volume 35 *Extremophiles*
FA Rainey and A Oren

Volume 36 *Yeast Gene Analysis, 2nd edition*
I Stansfield and MJR Stark

Methods in Microbiology

Volume 37
Immunology of Infection

Third Edition

Edited by

Dieter Kabelitz

Institute of Immunology,
University of Kiel,
Kiel, Germany

and

Stefan H E Kaufmann

Department of Immunology,
Max-Planck-Institute for Infection Biology,
Berlin, Germany

ELSEVIER

Amsterdam • Boston • Heidelberg • London • New York • Oxford
Paris • San Diego • San Francisco • Singapore • Sydney • Tokyo
Academic Press is an imprint of Elsevier

ACADEMIC
PRESS

Academic Press is an imprint of Elsevier
84 Theobald's Road, London WC1X 8RR, UK
Radarweg 29, PO Box 211, 1000 AE Amsterdam, The Netherlands
Linacre House, Jordan Hill, Oxford OX2 8DP, UK
30 Corporate Drive, Suite 400, Burlington, MA 01803, USA
525 B Street, Suite 1900, San Diego, CA 92101-4495, USA

Third edition 2010

ISBN: 978-0-12-374842-3 (Hardbound – this volume)
ISSN: 0580-9517 (Series)

Printed and bound in UK
10 11 12 10 9 8 7 6 5 4 3 2 1

***Cover image*: Macrophage (green) in the process of engulfing *Mycobacterium tuberculosis* the etiologic agent of tuberculosis. Photo kindly provided by Drs. Volker Brinkmann and Stefan H.E. Kaufmann, Max-Planck-Institute for Infection-Biology, Berlin, Germany**

Series Advisors

Contributors

Alexandre Alcaïs, Laboratory of Human Genetics of Infectious Diseases, Necker Branch, Institut National de la Santé et de la Recherche Médicale, U.550, Paris, France; University Paris Descartes, Necker Medical School, Paris, France

Sahar Aly, Microbial Inflammation Research, Research Center Borstel, Borstel, Germany

Silvia Arancia, Department of Infectious, Parasitic and Immune-mediated Diseases, Istituto Superiore di Sanità, Rome, Italy

Matthew Ardito, EpiVax, Inc., Providence, RI, USA

Jacques Banchereau, Baylor Institute for Immunology Research, Baylor Research Institute, Dallas, TX, USA; INSERM U899, Dallas, TX, USA; Department of Gene and Cell Medicine, and Department of Medicine, Immunology Institute, Mount Sinai School of Medicine, New York, NY, USA

Jay A Berzofsky, Vaccine Branch, Center for Cancer Research, National Cancer Institute, National Institutes of Health, Bethesda, MD, USA

Veit R Buchholz, Institute of Medical Microbiology, Immunology, and Hygiene, Technische Universität München, Munich, Germany

Dirk H Busch, Institute of Medical Microbiology, Immunology, and Hygiene, Technische Universität München, Munich, Germany

Ohn Chow, Department of Pediatrics, University of California, San Diego School of Medicine, La Jolla, CA, USA

Thomas E Cloke, Imperial College London, Faculty of Medicine, Department of Immunology, London, UK

Aurelie Cobat, Laboratory of Human Genetics of Infectious Diseases, Necker Branch, Institut National de la Santé et de la Recherche Médicale, U.550, Paris, France; University Paris Descartes, Necker Medical School, Paris, France

Tobias Cohen, EpiVax, Inc., Providence, RI, USA

Flavia De Bernardis, Department of Infectious, Parasitic and Immune-mediated Diseases, Istituto Superiore di Sanità, Rome, Italy

Anne S De Groot, EpiVax, Inc., Providence, RI, USA; Institute for Immunology and Informatics, University of Rhode Island, Providence, RI, USA

Gustavo A de Souza, The Gade Institute, Section for Microbiology and Immunology, University of Bergen, Bergen, Norway

René de Waal Malefyt, Schering-Plough Biopharma, Palo Alto, CA, USA

Stefan Ehlers, Molecular Inflammation Medicine, University of Kiel, Kiel, Germany

Jürgen Fritsch, Institute of Immunology, University of Kiel, Kiel, Germany

Mariam Ghochani, Department of Physics and Biology, San Diego State University, San Diego, CA, USA

Torsten Goldmann, Division of Clinical and Experimental Pathology, Department of Pneumology, Research Center Borstel, Borstel, Germany

Siamon Gordon, Sir William Dunn School of Pathology, University of Oxford, Oxford, United Kingdom

Patricia Graef, Institute of Medical Microbiology, Immunology, and Hygiene, Technische Universität München, Munich, Germany

Natascha K A Grzimek, Institute for Virology, University Medical Center of the Johannes Gutenberg-University, Mainz, Germany

Richard Haworth, Department of Pathology, Safety Assessment, Glaxosmithkline Research and Development, Park Road, Ware, Herts., UK

Christoph Hölscher, Infection Immunology, Research Center Borstel, Borstel, Germany

Rafaela Holtappels, Institute for Virology, University Medical Center of the Johannes Gutenberg-University, Mainz, Germany

Dieter Kabelitz, Institute of Immunology, University of Kiel, Kiel, Germany

Stefan H E Kaufmann, Department of Immunology, Max-Planck-Institute for Infection Biology, Berlin, Germany

Ulrich D Kadolsky, Imperial College London, Faculty of Medicine, Department of Immunology, London, UK

Hiroshi Kiyono, Division of Mucosal Immunology, Department of Microbiology and Immunology, The Institute of Medical Science, The University of Tokyo, Minato-ku, Tokyo, Japan

Eynav Klechevsky, Baylor Institute for Immunology Research, Baylor Research Institute, Dallas, TX, USA; INSERM U899, Dallas, TX, USA

Pascale Kropf, Imperial College London, Faculty of Medicine, Department of Immunology, London, UK

Kai A Kropp, Institute for Virology, University Medical Center of the Johannes Gutenberg-University, Mainz, Germany

Jun Kunisawa, Division of Mucosal Immunology, Department of Microbiology and Immunology, The Institute of Medical Science, The University of Tokyo, Minato-ku, Tokyo, Japan

Niels A W Lemmermann, Institute for Virology, University Medical Center of the Johannes Gutenberg-University, Mainz, Germany

Bill Martin, EpiVax, Inc., Providence, RI, USA

Jean-François Mathieu, BD Biosciences, Erembodegem, Belgium

Lenny Moise, EpiVax, Inc., Providence, RI, USA; Institute for Immunology and Informatics, University of Rhode Island, Providence, RI, USA

Subhankar Mukhopadhyay, Sir William Dunn School of Pathology, University of Oxford, Oxford, United Kingdom

Antje Müller, Department of Rheumatology, University of Lübeck, Lübeck, Germany

Ingrid Müller, Imperial College London, Faculty of Medicine, Department of Immunology, London, UK

Victor Nizet, Department of Pediatrics, University of California, San Diego School of Medicine, La Jolla, CA, USA; Skaggs School of Pharmacy and Pharmaceutical Science, University of California San Diego, La Jolla, CA, USA; Rady Children's Hospital, San Diego, CA, USA

Diane J Ordway, Mycobacteria Research Laboratories, Department of Microbiology, Immunology and Pathology, Colorado State University, Fort Collins, CO, USA

Marianna Orlova, McGill Centre for the Study of Host Resistance, The Research Institute of the McGill University Health Centre, Montreal, Québec, Canada; Departments of Human Genetics and Medicine, McGill University, Montreal, Québec, Canada

lan M Orme, Mycobacteria Research Laboratories, Department of Microbiology, Immunology and Pathology, Colorado State University, Fort Collins, CO, USA

A Karolina Palucka, Baylor Institute for Immunology Research, Baylor Research Institute, Dallas, TX, USA; INSERM U899, Dallas, TX, USA; Department of Gene and Cell Medicine, and Department of Medicine, Immunology Institute, Mount Sinai School of Medicine, New York, NY, USA

Leanne Peiser, Amgen Inc., Seattle, WA, USA

Jérôme Pène, Inserm U844, Montpellier, France

Jürgen Podlech, Institute for Virology, University Medical Center of the Johannes Gutenberg-University, Mainz, Germany

Matthias J Reddehase, Institute for Virology, University Medical Center of the Johannes Gutenberg-University, Mainz, Germany

Norbert Reiling, Microbial Interface Biology, Research Center Borstel, Borstel, Germany

Matthew Rogers, Imperial College London, Faculty of Medicine, Department of Immunology, London, UK

Silvia Sandini, Department of Infectious, Parasitic and Immune-mediated Diseases, Istituto Superiore di Sanità, Rome, Italy

Jens-M Schröder, Department of Dermatology, University Hospital Schleswig-Holstein, Kiel, Germany

Erwin Schurr, McGill Centre for the Study of Host Resistance, The Research Institute of the McGill University Health Centre, Montreal, Québec, Canada; Departments of Human Genetics and Medicine, McGill University, Montreal, Québec, Canada

Stefan Schütze, Institute of Immunology, University of Kiel, Kiel, Germany

Christof K Seckert, Institute for Virology, University Medical Center of the Johannes Gutenberg-University, Mainz, Germany

Ulrike Seitzer, Division of Veterinary Infection Biology and Immunology, Department of Immunology and Cell Biology, Borstel, Germany

Ulrich Steinhoff, Max-Planck Institut für Infektionsbiologie, Berlin, Germany

Vladimir Tchikov, Institute of Immunology, University of Kiel, Kiel, Germany

Hideki Ueno, Baylor Institute for Immunology Research, Baylor Research Institute, Dallas, TX, USA; INSERM U899, Dallas, TX, USA

Alexander Visekruna, Institut für Medizinische Mikrobiologie und Krankenhaushygiene, Philipps-Universität Marburg, Germany

Maren von Köckritz-Blickwede, Department of Pediatrics, University of California, San Diego School of Medicine, La Jolla, CA, USA; Department of Physiological Chemistry, University of Veterinary Medicine Hannover, Germany

John Wijdenes, Gen-Probe, Besançon, France

Harald G Wiker, The Gade Institute, Section for Microbiology and Immunology, University of Bergen, Bergen, Norway

Hans Yssel, Inserm U844, Montpellier, France

Preface

We are pleased that a third edition of this volume is now available. Immunology continues to be a rapidly moving field, and so is the progress in the development of new technologies, methods and *in vivo* models. Therefore, the third edition contains a number of new chapters on topics not present in previous editions, including the magnetic isolation of subcellular compartments, the isolation and characterization of antimicrobial peptides, proteomic approaches to the study of immune reactions, functional analysis of phagocyte extracellular traps, analysis of mucosal immunity and animal models of mucosal candida infection. In addition, this volume includes updates of several chapters in which recent progress has required the incorporation of new developments in the field.

We are very grateful to all our colleagues who have contributed new or revised chapters to this volume, and we appreciate their commitment of time and willingness to share their invaluable experience with readers.

We would like to thank the editorial staff of Elsevier Publishers, notably Lisa Tickner, Narmada Thangavelu and Sujatha Thirugnanasambandam, for their tremendous effort in the preparation of the third edition. Last but not least, we greatly appreciate the support and fantastic dedication of Birgit Schlenga and Mary Louise Grossman for their secretarial assistance.

We sincerely hope that you find this new edition helpful in your research, and we welcome your suggestions for future improvements to this volume.

1 The Immune Response to Infectious Agents

Stefan HE Kaufmann[1] **and Dieter Kabelitz**[2]
[1] *Department of Immunology, Max-Planck-Institute for Infection Biology, Berlin, Germany*
[2] *Institute of Immunology, University of Kiel, Kiel, Germany*

CONTENTS

I. INTRODUCTION

It is the task of the immune system to protect the host against invading pathogens and thereby to prevent infectious disease. A plethora of pathogens exists (i.e. viruses, bacteria, fungi, parasites and helminths) that have exploited strategies to circumvent an attack by the immune system. Conversely, the immune system has evolved to provide appropriate defence mechanisms at various levels of 'unspecific' (innate) and 'specific' (adaptive) immune responses (Hughes, 2002). In many instances, an appropriate immune response to an infectious agent requires reciprocal interactions between components of the innate and adaptive immune systems.

The various microorganisms have developed different strategies to invade their host. Viruses make use of the host cell's machinery for replication and are thus intracellular pathogens (Yewdell and Bennink, 2002; Liu *et al*., 2009). Helminths, the other extreme, are multicellular organisms that cannot live within host cells but rather behave as extracellular pathogens (Pearce and Tarleton, 2002). In between are bacteria, fungi and protozoa, which, depending on the species, live within or outside host cells (Kuhn *et al*., 2002; Pearce and Tarleton, 2002; Romani, 2002).

The successful combat of an invading infectious agent largely depends on the host's capacity to mount an appropriate protective immune response. As a consequence, the analysis of such interactions between host and invading micro-organisms requires a broad spectrum of immunological methods. This book

METHODS IN MICROBIOLOGY, VOLUME 37
0580-9517 DOI 10.1016/S0580-9517(10)37001-2

presents a collection of such methods, which are particularly useful for *in vivo*, *ex vivo* and *in vitro* analyses of murine and human immune responses towards infectious agents. In this introductory chapter, a brief overview of the immune defence mechanisms against pathogens is given to provide the reader with a guide to the subsequent chapters.

♦♦♦♦♦♦ II. THE INNATE IMMUNE SYSTEM

Several defence mechanisms exist that are ready to attack invading pathogens without prior activation or induction. They preexist in all individuals and do not involve antigen-specific immune responses. Hence they are referred to as components of the innate immune system. Among these components, granulocytes, macrophages and their relatives play an important role, especially during the early phases of the immune response. Surface epithelia constitute a natural barrier to infectious agents (Neutra and Kraehenbuhl, 2002). A one-celled layer separates our body from our intestinal microbiome, which is comprised of hundreds of trillions of bacteria. Apart from the mechanical barrier, surface epithelia are equipped with additional chemical features that help to restrain microbial invasion. Depending on the anatomical localization, such factors include fatty acids (skin), low pH (stomach), antibacterial peptides (defensins; intestine) and enzymes (e.g. lysozyme; saliva). Antimicrobial peptides (AMPs) have been recently identified as an important part of the innate immune system. In addition to constitutively expressed AMPs, β-defensins are inducibly expressed in cells of the innate immune system (Guani-Guerra *et al.*, 2010). Methods for the isolation and characterization of AMPs are described by Schröder in Section I. Once the pathogen has crossed the protective epithelial barrier, cellular effector mechanisms are activated. Granulocytes and mononuclear phagocytes represent the most important effector cells of the anti-infective immune response (Segal, 2005; Serbina *et al.*, 2008).

Invading microorganisms are sensed by surface receptors which recognize physico-chemical entities that are both unique for and shared by microbial pathogens. These entities have been termed pathogen-associated microbial patterns (PAMPs).

The receptors for PAMPs, often referred to as pattern recognition receptors (PRRs), include the Toll-like receptors (TLRs) as best known cognates. TLRs not only react with the microbial pathogens but also transduce signals into the host cell nucleus causing the prompt activation of host defence (Kumar *et al.*, 2009). Due to major research efforts, the realm of PRRs is rapidly increasing. The TLR family alone comprises around 10 different receptors. Other PRR families include the scavenger receptors (Taylor *et al.*, 2005) and the intracellular nucleotide-binding oligomerization domain (NOD)-like receptors that are coupled to molecular signalling platforms termed inflammasomes (Schroder and Tschopp, 2010).

The group of granulocytes comprises neutrophils, eosinophils and basophils, which all possess high anti-infective activity. Neutrophils phagocytose microbes and can subsequently kill them (Segal, 2005). By means of Fc receptors for immunoglobulin G (IgG) and complement receptors, phagocytosis of microbes coated by antibodies or complement breakdown products is improved. Neutrophils also kill

bacteria in the extracellular space by releasing chromatin and granular proteins, the so-called neutrophil-extracellular traps. Methods for the visualization and functional evaluation of extracellular traps are described by von Köckritz-Blickwede *et al*. in Section I. Eosinophils and basophils primarily attack extracellular pathogens, in particular helminths, by releasing toxic effector molecules (Rothenberg and Hogan, 2006). Growth and differentiation of eosinophils are controlled by interleukin-5 (IL-5) and that of basophils by IL-4. These cell types express Fc receptors for IgE, which provide a bridge between host effector cells and helminths.

The mononuclear phagocytes comprise the tissue macrophages and the blood monocytes, which circulate in the blood and migrate into tissue sites, notably, under the influence of inflammatory signals. At these sites, the monocytes differentiate into tissue macrophages or dendritic cells (DCs). This process is induced by inflammatory stimuli, and hence, these DCs are termed inflammatory DCs. The plasmacytoid DCs and the classical DCs already reside in tissue sites where they can take up antigen, process it and migrate to lymph nodes where they present antigen to T lymphocytes. Methods for the isolation and *in vitro* generation of human DC subsets are described by Ueno *et al*. in Section III. After activation by cytokines, particularly interferon-γ (IFN-γ), mononuclear phagocytes are capable of killing engulfed microorganisms. However, in their resting stage, macrophages have a low antimicrobial potential and, thus, are often misused as habitat by many bacteria and protozoa. Killing and degradation of these intracellular pathogens by activated macrophages is achieved by a combination of different mechanisms. The most important ones are as follows:

1. Activated professional phagocytes produce toxic effector molecules, in particular reactive oxygen intermediates (ROIs) and reactive nitrogen intermediates (RNIs), which often synergize in killing various intracellular bacteria and protozoa. Although RNI production is the most potent antimicrobial defence mechanism of murine macrophages, its production by human macrophages is still the subject of debate. However, an increasing amount of data supports RNI production by human macrophages during infectious diseases (Chan *et al*., 2001; Liu and Modlin, 2008).
2. Soon after engulfment of microbes, the phagosome becomes acidic and subsequently fuses with lysosomes. Lysosomal enzymes have an acidic pH optimum and, thus, express high activity within the phagolysosome. These lysosomal enzymes are primarily responsible for microbial degradation (Finlay and Cossart, 1997; Schaible *et al*., 1999; Rohde *et al*., 2007).
3. Both the intracellular pathogen and the host cell require iron. Therefore, depletion of intraphagosomal iron reduces the chance of intracellular survival for various pathogens (Lieu *et al*., 2001; Schaible and Kaufmann, 2005).
4. Tryptophan is an essential amino acid for certain intracellular pathogens, such as *Toxoplasma gondii*. Accordingly, rapid degradation of this amino acid impairs intracellular replication of susceptible pathogens (Pfefferkorn, 1984).

In this book, methods for the isolation and functional analysis of murine macrophages are described by Peiser *et al*. in Section II. Intracellular pathogens have developed various evasion mechanisms which prolong their survival inside macrophages (Schaible *et al*., 1999). Some even persist within activated macrophages, though at

a markedly reduced level. *Listeria monocytogenes* and *Trypanosoma cruzi* egress from the phagosome into the cytosol, thus escaping intraphagosomal attack. Several intracellular pathogens, such as *Mycobacterium tuberculosis*, remain in the phagosome. However, they prevent phagosome acidification and subsequent phagosome–lysosome fusion. To compete for the intracellular iron pool, some pathogens possess potent iron acquisition mechanisms, and to avoid killing by ROIs or RNIs, several microbes produce detoxifying enzymes. For example, catalase and superoxide dismutase directly inactivate ROI and indirectly impair RNI effects (Chan *et al*., 2001).

In summary, living within resting macrophages provides a niche that protects intracellular pathogens from humoral attack. Yet, once activated, macrophages are capable of eradicating many intracellular pathogens and of restricting growth of more robust ones. Such pathogens may persist for long periods of time, thus causing chronic infection and disease (Munoz-Elias and McKinney, 2002). In order to understand the intracellular processing of microbes in more detail, it is important to have methods available for the biochemical analysis of intracellular signalling pathways. In Section I, Tchikov *et al*. discuss methods based on magnetic fractionation that can be exploited for such applications.

In addition to their role in the non-specific innate anti-infective host response, macrophages contribute to the specific acquired immune response against microorganisms. Microbial degradation within macrophages delivers pathogen-derived antigenic fragments (peptides) which enter antigen processing pathways leading to the cell surface expression of 'foreign' microbial antigens in the context of appropriate major histocompatibility complex (MHC) molecules. Such antigenic peptides presented by MHC class I or class II molecules can then activate specific T lymphocytes. In addition to macrophages, DCs process and present antigens for T cells. In fact, DCs are the most efficient professional antigen-presenting cells (APCs) (Geissmann *et al*., 2010).

Among the humoral mechanisms of the innate immune system, the alternative pathway of complement activation is perhaps the most important one. While the classical pathway of complement activation requires the presence of specific antibodies (and hence is delayed upon microbial infection), the other pathways are initiated in the absence of specific immunity (Dunkelberger and Song, 2010). These pathways include the lectin pathway and the alternative pathway. All pathways join in the production of the complement component C3b, which is deposited to bacterial surfaces.

The lectin pathway is initiated by bacterial lectins. In the alternative pathway, spontaneous complement activation, which occurs under physiological conditions, is accelerated.

In contrast to host cells, bacteria lack complement controlling membrane proteins. The bound C3b initiates the lytic pathway, which leads to bacterial lysis. Moreover, C3b deposition on microbial surfaces promotes the microbial uptake *via* complement receptors. Finally, the complement breakdown products C4a and C5a are chemoattractants for phagocytes, and are, therefore, termed anaphylatoxins. They induce phagocyte extravasation into foci of microbial implantation. Another important humoral innate system is the type-I IFN system, which is mainly involved in antiviral defence. More recent findings, however, have revealed a major immunoregulatory function of these type-I IFNs (Theofilopoulos *et al*., 2005; Stetson and

Medzhitov, 2006). The plasmacytoid DCs are main potent producers of type-I IFNs in response to viral infection (Geissmann *et al*., 2010).

♦♦♦♦♦♦ III. THE ADAPTIVE IMMUNE SYSTEM

While the components of the innate immune system are appropriate as a first line of defence, the adaptive (or specific) immune system is activated if the invading microorganism cannot be eliminated, or at least be neutralized, by the above-mentioned non-specific effector mechanisms. Two major features characterize the adaptive immune system. Firstly, the immune response is antigen-specific; specificity is made possible through the usage of clonally distributed antigen receptors, i.e. surface Ig on antibody-producing B lymphocytes and T cell receptors (TCRs) on the surface of T lymphocytes. Secondly, the specific immune system develops memory (Ahmed *et al*., 2002; McHeyzer-Williams and McHeyzer-Williams, 2005). This allows the rapid response of antigen-specific effector cells upon second encounter of the relevant antigen. The underlying general principle of vaccination is the stimulation of specific immunity with long-lasting memory by harmless components of an infectious agent or by attenuated strains. This endows the host with the capacity to combat the homologous pathogen with high efficiency and thus prevents disease outbreak.

B cells recognize antigen in a fashion which is fundamentally different from that of T cells. The antibody expressed on the B cell surface (and later, secreted by the plasma cell) directly binds to native, soluble antigen. By virtue of their antibody production, B cells contribute to the humoral immune defence against extracellular pathogens and neutralize virions before they enter the host cell. By contrast, T cells recognize antigen only if it is presented in the context of appropriate MHC molecules on the surface of APCs. The surface-expressed TCR is non-covalently associated with the CD3 polypeptide complex which mediates signal transduction upon TCR triggering, leading to cytokine gene transcription and T cell activation (Smith-Garvin *et al*., 2009).

Distinct subpopulations of T cells are involved in the specific cell-mediated immune response against infectious agents (Figure 1). The expression of relevant cell surface molecules allows their identification and phenotypic characterization by specific monoclonal antibodies. Moreover, monoclonal antibodies can be used to separate subpopulations of cells on a fluorescence-activated cell sorter (FACS®) or by using magnetic beads. The dominant subsets of mature T cells are characterized by the reciprocal expression of CD4 and CD8 coreceptors. $CD4^+$ T cells recognize antigen in the context of MHC class II molecules; they produce various cytokines required for efficient activation of leukocytes – notably B cells and macrophages – and are therefore termed T helper (Th) cells. By contrast, $CD8^+$ T cells recognize antigen in the context of MHC class I molecules; one of their major tasks is to lyse virus-infected target cells. Hence, they are termed cytotoxic T lymphocytes (CTLs).

The activation of T cells requires two signals. Signal one is mediated through the CD3/TCR molecular complex following antigen recognition. Signal two is a

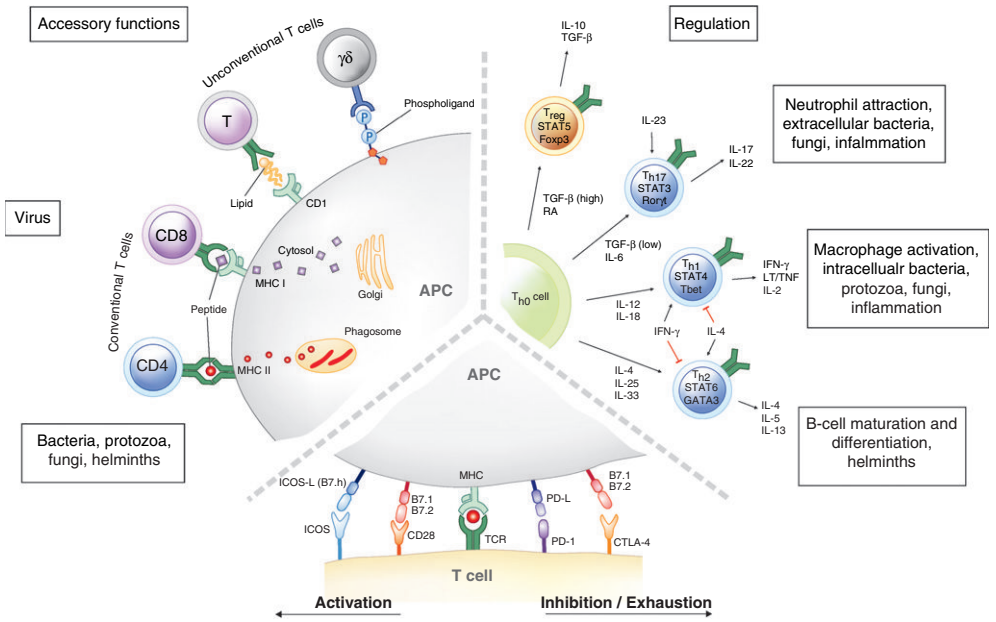

Figure 1. Role of different T cell populations in immunity to infection. Left part depicts pathways of antigen processing and presentation. Right part describes the four CD4 T cell populations, cytokines involved in their polarization, cytokines produced by the different T cell populations and the central transcription factors induced during polarization. Lower part shows costimulatory molecules involved in activation as well as inhibition/exhaustion of T cells. For further details, see text.

costimulatory signal that is delivered through receptor–ligand interactions (Figure 1). The major costimulatory molecules on APCs are CD80 (B7.1) and CD86 (B7.2). Both molecules can bind to CD28 on T cells, thereby exerting costimulation. In addition, CTLA-4 (Cytotroxic T lymphocyte antigen-4) (CD152) also binds to both ligands. The CD28/CD152 interaction with CD80/CD86 is complex. While triggering of CD28 mediates costimulation, binding to CD152 delivers an inhibitory signal (Rudd *et al.*, 2009). An overview of some important cell surface molecules with relevance to anti-infective immunity is given in Table 1.

The vast majority of the $CD4^+$ and $CD8^+$ T cells express a TCR composed of α and β chain heterodimers. These T cells are termed conventional T cells. In recent years, the existence of additional T cell subsets has been appreciated. These include $CD4^-CD8^-$ 'double-negative' (DN) T cells that express either the $\alpha\beta$ TCR or an alternative TCR composed of γ and δ chains. Furthermore, $CD8^+$ T cells expressing the $\alpha\beta$ TCR restricted by MHC I-like molecules as well as $CD4^+$ T cells coexpressing the $\alpha\beta$ TCR and natural killer (NK) receptors (NK1) have been identified. Increasing evidence suggests that there is a well-orchestrated interplay between all these subsets with a preponderance of any one of those, depending on the type of infection.

Importantly, the localization of an infection also determines the type of immune response and its regulation. In this regard, the intestinal mucosa is an important part of the immune system that is influenced by the intestinal bacteria

Table 1. Cell surface molecules with relevance to anti-infective immunity

Cell surface molecule	Function in anti-infective immunity
TCR$\alpha\beta$	MHC/peptide recognition by the major $\alpha\beta$ T cell population
TCR$\gamma\delta$	Ligand recognition by the minor $\gamma\delta$ T cell population
CD1	Presentation of lipids and glycolipids to DN $\alpha\beta$ T cells
CD3	Marker of all T cells, signal transduction in T cells
CD4	Coreceptor with specificity for MHC class II, marker molecule of Th cell
CD8	Coreceptor with specificity for MHC class I, marker molecule of CTL
CD14	Pattern recognition receptor on macrophages which, for example, binds LPS from gram-negative bacteria
CD40	Costimulatory molecule on B cells and antigen-presenting cells
CD154 (CD40L)	T cell costimulation (ligand for CD40)
CD28	Costimulatory T cell molecule (positive signal)
CD152 (CTLA-4)	Costimulatory T cell molecule (negative signal)
CD80 (B7-1)	Ligand for CD28, CD152
CD86 (B7-2)	Ligand for CD28, CD152
CD95	Fas (Apo-1), a receptor which mediates an apoptosis signal
CD279 (PD1)	Inhibition of T cell activities
CD274 (PDL1;B7-H1)	Ligand for PD1

(Hill and Artis, 2010). Steinhoff and Visekruna describe methods for the investigation of mucosal immunity in Section II.

A. Conventional T Lymphocytes

$CD4^+$ T cells expressing the $\alpha\beta$ TCR recognize foreign peptides bound in the peptide-binding groove of MHC II molecules (Figure 1). These peptides are generally derived from exogenous antigens (such as microorganisms) that are taken up by phagocytosis or endocytosis. Immunogenic peptides of 13 or more amino acids in length are generated in endosomes, bound to MHC II molecules and transported to the cell surface. Presentation of antigen to $CD4^+$ T cells is restricted to APCs that either constitutively express MHC II molecules (monocytes/macrophages, DC, B cells) or can be induced to express MHC II molecules (e.g. endothelial cells and activated human T cells). The prediction of MHC ligands and T cell epitopes based on bioinformatic analysis has developed into an important tool for vaccine development. Such methods are described by de Groot *et al*. in Section I.

There are four functionally distinct subpopulations of $CD4^+$ T cells (Figure 1). These subsets are generally distinguished based on the characteristic spectrum of cytokines which they produce upon antigenic stimulation (Zhu *et al*., 2010). Th1 cells are characterized by their secretion of IFN-γ and IL-2, whereas Th2 cells preferentially produce IL-4, IL-5 and IL-13. The Th17 cells produce the signature cytokines IL-17 and IL-22 (Korn *et al*., 2009). Finally, the regulatory T (T_{reg}) cells are characterized by production of transforming growth factor-β (TGF-β) and IL-10 (Izcue *et al*., 2009). These T cells all derive from a precursor T cell often termed naïve precursor Th0 cells. Major factors that determine polarization of different T cell

subsets from Th0 cells are the cytokines produced by the innate immune system as well as by other Th subsets. The cytokines produced by the different Th subsets play characteristic but different roles in various types of immune responses. Therefore, distinct Th cell subpopulations dominate in a given situation, thus determining the outcome of infection. Th1 cells play an important role in the initiation of the cell-mediated immune response against intracellular pathogens, due to secretion of IFN-γ (which activates macrophages) and IL-2 (which activates CTLs) (Collins and Kaufmann, 2002; Scott and Grencis, 2002; Zhu *et al*., 2010). In the mouse, IFN-γ also stimulates the production of Ig subclasses (IgG2a, IgG3) that contribute to antimicrobial immunity by virtue of their complement fixing and opsonizing activities. Th2 cells produce cytokines (IL-4, IL-5) that control activation and differentiation of B cells into antibody-secreting cells. Th2 cells are thus important for the induction of humoral immune responses. IL-4 controls the Ig class switch to IgE and hence plays a central role in the immune defence against helminths and in the regulation of the allergic response. Moreover, IL-4 stimulates the production of IgG subclasses (IgG1 in the mouse) that neutralize but do not opsonize antigens. The Th2 cytokine IL-5, together with TGF-β, induces B cells to switch to IgA, the major Ig subclass involved in local immune responses (Fagarasan *et al*., 2010). In addition, IL-5 contributes to the control of helminth infection by activating eosinophils (Scott and Grencis, 2002). The Th17 cells activate inflammatory responses and notably attract granulocytes to the site of inflammation. The T_{reg} cells are not involved in the induction of an immune response but rather in its down modulation. By producing TGF-β and IL-10, they turn off immunity after successful defence of invading pathogens to avoid collateral damage (Moore et al., 1993; Belkaid and Tarbell, 2009). The differentiation of Th1, Th2, Th17 and T_{reg} cells is initiated by cytokines produced by cells of the non-specific immune system early after infection. The polarization of Th1 and Th2 cells is closely linked as is the polarization between Th17 and T_{reg} cells. However, the different subsets also counterregulate each other. In this regard, the rapid production of IL-12 and IL-18 by monocytes/macrophages, and of IFN-γ by NK cells, drives the Th cell response into Th1 cells following bacterial infection. *Vice versa*, the early production of IL-25 and IL-33 produced by epithelial cells stimulates production of IL-4 as a major force that drives Th cells along the Th2 differentiation pathway (Eberl, 2010). The cellular source of the early IL-4 remains to be unequivocally defined. Recently, a new cell type has been described, termed nuocytes, which produce IL-13 in response to IL-25 and IL-33 and thus contribute to defence against helminth infections (Neill *et al*., 2010). Th17 cells are promoted by IL-23, which is a congener of IL-12, with support from TGF- β and IL-6. At higher concentrations of TGF-β and in the presence of IL-2, however, T_{reg} cells will develop (Li and Flavell, 2008).

Methods to measure immune responses *in vitro* and *in vivo* are a major focus of this volume. Chapters in Section II are devoted to murine cytokine analysis *in vitro* (Kunisawa and Kiyono) and *in vivo* (Ehlers *et al*.), and various methods to detect human cytokine responses are described in Section III by Müller *et al*. and Yssel *et al*.

In most instances, there is no absolute restriction in the activation of Th1, Th2 or Th17 cells during the immune response to infectious agents. Nevertheless, in many situations, there is a clear dominance of one or the other Th cell subset, and a

(genetic) failure to activate the appropriate Th cell subset may lead to a disastrous outcome after infection. A well-documented example for this is the infection of mice with the protozoan parasite *Leishmania major*. In resistant strains of mice, such as C57Bl/6, *L. major* causes a self-healing lesion, whereas in susceptible BALB/c mice, the infection is progressive and eventually fatal. The experimental model is described by Kropf *et al*. in Section II. It has been shown that during infection, resistant mice produce high levels of IFN-γ and little IL-4 (and thus display a Th1-type response), whereas the susceptible mice produce high amounts of IL-4 and little IFN-γ (and thus display a Th2-type response). In view of the known role of IL-12 in driving Th0 cells into Th1 cells, attempts were made to prevent the fatal Th2 cell differentiation in *L. major*-infected BALB/c mice. In fact, the administration of leishmanial antigens together with IL-12 induced the appearance of *L. major*-specific Th1 cells in BALB/c mice. More importantly, these mice were protected from fatal infection when challenged with *L. major*. These examples illustrate the impact of genetic background on the manifestation of disease. The chapter by Cobat *et al*. in Section I provides the methodological background for genetic analysis of susceptibility and resistance to infection.

The protective T cell response against mycobacteria is mediated by Th1 cells (Cooper, 2009). Mycobacteria induce IL-12 and IL-18 in macrophages, and IFN-γ secreted by Th1 cells is the major T cell-derived macrophage-activating mediator (Collins and Kaufmann, 2002). Tuberculosis is clearly dominated by a Th1 response, which, however, may be insufficiently protective. Ordway and Orme describe models to investigate tuberculosis in mice and guinea pigs in Section II. The spectrum of disease observed in leprosy patients can be partially explained on the basis of a Th1 or Th2 preponderance. Whereas malign lepromatous leprosy is frequently associated with the production of Th2 cytokines, the more benign tuberculoid form of leprosy is dominated by Th1 cytokine patterns. The Th17 cells dominate in infections with extracellular bacteria and fungi. *In vivo* models to study mucosal candida infections are described by De Bernardis *et al*. in Section II.

Currently, the different Th cell subsets are best distinguished by the transcription factors which they utilize (Figure 1). Thus, all three Th cells use different members of the signalling transducer and activator of transcription (STAT) molecules: the Th1 cells use STAT4, the Th2 cells use STAT6 and the Th17 use STAT3; the T_{reg} cells use STAT5. In addition, Th1 cells employ Tbet, which is critically involved in IFN-γ production. GATA3 is critical for IL-4 production by Th2 cells, and RoRγt is the central regulator for IL-17 production by Th17 cells. The T_{reg} cells can be further distinguished into different subsets, but all employ the transcription factor Foxp3. Some T_{reg} cells coexpress Tbet (similar to Th1 cells), others GATA3 (similar to Th2 cells) and still others RoRγt (similar to Th17 cells). It is possible that these different T_{reg} cells have a particular affinity for the Th cells with which they share a transcription factor.

The concept of functionally distinct $CD4^+$ T cell subsets being differentially involved in immune responses on the basis of their cytokine production has greatly helped to delineate immune defence mechanisms in infection and to devise therapeutic strategies. Even though the different CD4 T cell subsets are often viewed as stable populations, they show some plasticity. This is particularly important for long-lasting immune responses in chronic infections which can be modified by

exogenous and endogenous influences. Hence, continuous fine-tuning of an ongoing immune response is required to maintain the major Th functions required for control of chronic infections (Dorhoi and Kaufmann, 2009). Relatively little is known about disturbances of immune responses against chronic infections by coinfections. Thus, the impact of helminth infections on protective immunity, which contains *M. tuberculosis* in dormant stage, is poorly understood. Similarly little is known about the impact of coinfections on vaccine-induced protective immunity.

Termination of an immune response is important to avoid unnecessary collateral damage. T_{reg} cells play a central role in this mechanism. In addition, T cells can become exhausted after pathogen eradication. Expression of the B7 family member programmed death (PD)1 on T cells, which interacts with its ligand PDL on APCs, downregulates T cell responses (Keir *et al*., 2008) and has been shown to cause T cell exhaustion in viral infections. In a similar vein, interactions between CTLA-4 on T cells and B7-1/B7-2 inhibit ongoing immune responses (Greenwald *et al*., 2005).

The prime task of $CD8^+$ CTL is the immune defence against intracellular pathogens with an emphasis on viruses. Viruses are replicated by host cells. As a consequence, viral proteins are degraded in the cytosol of the cell. Virus-derived peptides are transported in association with the transporter associated with antigen processing (TAP) molecules into the endoplasmic reticulum, where they are introduced to MHC I molecules (Szomolanyi-Tsuda *et al*., 2002). Upon transport to the cell surface, peptides of 8–10 amino acids in length are anchored in the peptide-binding groove of MHC I molecules, ready to be recognized by $CD8^+$ CTL expressing the appropriate TCR. The important role of $CD8^+$ CTL in the elimination of cytomegalovirus in the murine model is analysed by Lemmermann *et al*. in Section II. There is clear evidence, however, that MHC I-restricted $CD8^+$ T cells also contribute to the immune defence against intracellular bacteria and protozoa (Collins and Kaufmann, 2002). Some intracellular microbes such as *L. monocytogenes* or *T. cruzi* gain access to the cytosol, which causes their antigens to enter the MHC I antigen-processing pathway. In addition, it was found that bacteria-derived antigenic peptides can be introduced into the MHC I pathway, despite the fact that the microorganisms themselves remain in the phagosome. Taken together, there is a preponderance of $CD4^+$ T cells in the immune defence against phagosomal pathogens, and of $CD8^+$ T cells in the immune defence against cytosolic pathogens independent of whether they are bacteria, fungi or protozoa (Schaible *et al*., 1999). In many instances, however, optimal protection against infectious agents requires the coordinated cooperation of $CD4^+$ and $CD8^+$ T cells.

$CD8^+$ CTL can eliminate infected cells, thereby limiting pathogen spread. Cytotoxicity is mediated through pore-forming proteins (perforins) and enzymes (granzymes) that are released by activated CTL upon cell contact-dependent recognition of relevant (e.g. virus-infected) target cells. Granulysin has been shown to directly kill a large variety of bacteria, fungi and protozoa (Clayberger and Krensky, 2003). Target cell perforation by perforin could enable granulysin to access microbes residing within target cells. This mechanism could therefore enable CD8 CTL to participate in direct attack of microbial pathogens.

CTLs can also trigger programmed cell death (apoptosis) in target cells through receptor–ligand interactions. Upon activation, CTLs are induced to express

Fas-ligand (Fas-L), a member of the TNF gene family. Fas-L interacts with the corresponding receptor Fas (CD95, APO-1) expressed on virus-infected target cells. The oligomerization of several Fas molecules triggers a rapid suicide programme which culminates in protease-dependent cell death, usually associated with fragmentation of genomic DNA into oligonucleosomal-sized fragments (Strasser *et al.*, 2009). Graef and coworkers describe various methods to measure killer cell activity in Section II. Increasing evidence indicates that the role of $CD8^+$ T cells in infection is not limited to their function as CTLs. Like $CD4^+$ T cells, $CD8^+$ T cells are equipped with the capacity to produce cytokines. More specifically, the range of cytokine(s) secreted by $CD8^+$ T cells depends on the cytokine milieu during antigenic stimulation, in a manner comparable to the situation with $CD4^+$ T cells.

B. Unconventional T Lymphocytes

Apart from the well-characterized $CD4^+$ and $CD8^+$ T cell subsets that recognize antigenic peptides in an MHC class II- or MHC class I-restricted manner *via* the conventional $\alpha\beta$ TCR, several additional T cell populations can contribute to the immune defence against infectious microorganisms. These additional T cell subsets have been collectively termed 'unconventional' T cells (Kaufmann, 1996).

In mice, $CD8^+$ T cells have been described that express the conventional $\alpha\beta$ TCR and recognize an unusual group of peptides in the context of MHC class I-like presenting molecules (Lenz and Bevan, 1996). The peptides carry the *N*-formylmethionine (*N*-f-met) sequence that represents a characteristic signal sequence required for protein export in bacteria. *N*-f-met-containing peptides are virtually absent in mammalian cells, with the exception of mitochondria. The MHC class I-like molecules that present *N*-f-met-containing peptides to $CD8^+$ T cells are far less polymorphic than classical MHC proteins, and hence are broadly distributed. $CD8^+$ T cells with specificity for *N*-f-met-containing peptides have been shown to mediate protection in experimental murine models of *L. monocytogenes* infection (Rolph and Kaufmann, 2000). The possible role of such cells during the immune response in humans is less clear, because homologues of the relevant murine MHC class I-like molecules have so far not been identified in humans.

Additional unconventional T cell subsets exist that recognize antigen in association with non-MHC molecules. Among those, T cells have been identified in humans that recognize non-peptide antigens in the context of CD1 gene products which share some similarities with MHC I molecules. These T cells express the $\alpha\beta$ TCR. Interestingly, these T cells can recognize glycolipids derived from mycobacteria, including mycolic acid and lipoarabinomannan (Schaible and Kaufmann, 2000; Brigl and Brenner, 2004). There is only limited polymorphism of the presenting CD1 molecules. The group 1 CD1 molecules (CD1a,b,c) required for presentation of glycolipids to these T cells are expressed on the surface of human macrophages or can be induced to be expressed on APCs. T cells with specificity for these glycolipids have not been described in mice possibly because the cognates of the human group 1 CD1 antigens are absent in this species. These T cells secrete IFN-γ and express cytolytic activity. Hence, they could contribute to antimicrobial defence in a way similar to that of conventional Th cells.

Another subset of unconventional T cells is characterized by coexpression of αβ TCR and NK1, a characteristic marker of NK cells. These T cells recognize glycolipids ligands in the context of group 2 CD1 molecules (CD1d) (Schaible and Kaufmann, 2000; Bendelac *et al*., 2007). Interestingly, the TCR repertoire of NK1-expressing T cells is strikingly restricted. The TCR of these T cells is composed of an invariant α chain associated with a β chain that uses a limited set of variable (Vβ) elements, suggesting that NKT cells can recognize only a restricted array of antigens. It is likely that the NKT cells perform regulatory functions. Recently, α-galactosylceramide from a marine sponge, *N*-glycosyleramides from *malaria plasmodia*, phosphatidylinositol mannoside from mycobacteria, α-galactosyl diacylglycerols from *Borrelia burgdorferi*, the causative agent of Lyme disease and glycosphingolipids from certain lipopolysaccharide (LPS)-deficient gram-negative bacteria such as *Sphingomonas sp.* and *Ehrlichia sp*. have been identified as ligands for NKT cells presented by CD1d (Schaible and Kaufmann, 2000; Bendelac *et al*., 2007). NKT cells also recognize endogenous ligands of glycosphingolipid type (Bendelac *et al*., 2007).

While the vast majority of $CD3^+$ T cells express the 'conventional' TCR composed of an αβ chain heterodimer, a minor subset (1–10%) of $CD3^+$ T cells expresses the alternative γδ TCR (Hayday, 2000). There are two major differences between αβ T cells and γδ T cells. Firstly, the majority of γδ T cells lack the expression of the coreceptor molecules CD4 or CD8, thus displaying a DN phenotype. Secondly, the number of germline gene elements that can be expressed to construct the variable regions of TCR chains is small for γ and δ when compared to α and β. Nevertheless, the available TCR repertoire of γδ T cells is as large as that of αβ T cells, because several non-germline-encoded mechanisms such as N-region diversity, usage of alternative reading frames, etc. dramatically contribute to TCR diversity. Substantial evidence suggests that γδ T cells play a role in the immune defence against various infectious microorganisms (Kaufmann, 1996; Hayday, 2000; Wang *et al*., 2001; van der Merwe and Davis, 2003; Scotet *et al*., 2008). Human γδ T cells expressing the Vγ9/Vδ2 TCR are strongly activated by live or killed mycobacteria, as well as by several other intracellular or extracellular bacteria, or protozoa such *Plasmodium falciparum* (Kabelitz *et al*., 2000). In several instances, a transient increase in circulating γδ T cells has been observed during acute infection. γδ T cells express a functional repertoire similar to that of conventional αβ T cells. Thus, activated γδ T cells exert CTL activity and produce a range of cytokines, depending on the antigenic stimulation.

The γδ T cells can be polarized into different Th effector T cells and thus follow a similar scheme as described above. For example, in experimental tuberculosis of mice, γδ T cells are the major source of IL-17. The microbial ligands recognized by human Vγ9/Vδ2 T cells have been characterized as non-proteinaceous, phosphate-containing low molecular weight compounds (Kabelitz, 2008). The most active compounds are intermediates of the non-mevalonate ('Rohmer') pathway of isoprenoid biosynthesis which is restricted to certain microorganisms (including *M. tuberculosis*) and is not available in eukaryotic cells (Altincicek *et al*., 2001). The recognition of these ligands by human γδ T cells is not restricted by classical MHC antigens or other presenting molecules (such as CD1) but requires some as yet ill-defined form of presentation. While the microbial phospholigands are potent

activators of human γδ T cells, they do not appear to be recognized by their murine counterparts.

Despite their impressive *in vitro* reactivity towards certain ligands from pathogens, the *in vivo* role of γδ T cells in infection is not precisely understood. In several experimental models of bacterial infection, a transient activation of γδ T cells during early phases of the immune response is observed. On the other hand, γδ T cells appear to contribute to protection against certain viral infections at later stages. In this context, it is interesting to note that characteristic changes in the expressed TCR repertoire of peripheral blood γδ T cells occur in HIV-infected individuals (Kabelitz and Wesch, 2001). On the basis of the rapid response of γδ T cells (frequently preceding that of αβ T cells) and their limited germline TCR repertoire, it is assumed that γδ T cells provide a link between the innate and adaptive immune systems. In addition, a more general regulatory role of γδ T cells in inflammation appears likely.

C. B Lymphocytes

B cells express surface Ig as their antigen-specific receptor molecules. Upon activation and differentiation into antibody-secreting cells, B cells produce and secrete large amounts of Ig with the same specificity as the membrane-bound Ig. T cell-dependent B cell activation requires cognate interactions between the two lymphocyte populations. In recent years, it has become obvious that the receptor–ligand interaction mediated between CD40 (expressed on B cells) and the corresponding receptor expressed on T cells (CD40-ligand; now termed CD154) is important for the initiation of humoral immune responses to T cell-dependent antigens (Elgueta *et al*., 2009). In addition, studies with gene deletion mutant mice lacking either CD40 or CD154 expression have shown that CD40/CD154 interactions are essential for secondary immune responses to T cell-dependent antigens, as well as for the formation of germinal centres (Grewal and Flavell, 1996).

Proliferation and differentiation of B cells as well as the Ig isotype class switching are driven by cytokines (Stavnezer *et al*., 2008). In the mouse, IL-4 induces IgG1 and IgE secretion, while TGF-ß and IL-5 trigger the IgA class switch. IFN-γ is known to preferentially induce IgG2a and IgG3 secretion. IgG3 (together with IgM) possesses complement-fixing activity. These Ig subclasses are thus involved in the initiation of the classical pathway of complement activation, leading to complement-mediated destruction of pathogens or infected cells. In addition, antibodies are required for antibody-dependent cellular cytotoxicity (ADCC) effector function. Lymphoid cells carrying receptors for the Fc portion of IgG (Fcγ receptor) such as large granular lymphocytes mediate ADCC of IgG-coated target cells.

The initial encounter of antigen-specific B cells with the appropriate Th cells occurs at the border of T cell and B cell areas in lymphoid tissues. Activated B cells migrate into a nearby lymphoid follicle where they form a germinal centre. In the germinal centres, somatic hypermutation occurs in rapidly proliferating B cell blasts, thus giving rise to the selection of high affinity antibodies (affinity maturation) (Rajewsky, 1996). It is possible that the CD4 T cells in germinal centres that help B cells to become antibody-producing plasma cells form a distinct Th cell

subpopulation termed T follicular helper (Tfh) cells. While it is beyond doubt that this type of T cell is essential for Ig class switching (King *et al*., 2008), it remains to be determined whether they represent a unique fifth Th subpopulation (Zhu *et al*., 2010). Long-lived memory plasma cells contribute to the maintenance of serum antibody levels (Manz *et al*., 2005).

In addition to their unique role as antibody-producing plasma cells, B cells have the capacity to present antigen to T lymphocytes. Upon binding of soluble antigen to membrane-bound Ig with homologous specificity, antigen–antibody complexes are internalized and degraded in the endolysosomal compartment. Antigen-derived peptides are then introduced into the MHC class II-dependent processing pathway and can be presented to appropriate peptide-specific $CD4^+$ T cells (Vascotto *et al*., 2007).

1. The interphase between innate and adaptive immune systems

During recent years, it has become increasingly clear that the innate immune system, in addition to providing prompt host defence mechanisms, is also instrumental for the development of the adaptive immune response. At the early stage of encounter between host and pathogen, the professional APCs, comprising DCs and macrophages, are active. Macrophages are professional phagocytes which are also capable of presenting antigens to T cells. DCs often possess lower phagocytic activity but are most efficacious in presenting soluble antigens to T cells (Geissmann *et al*., 2010). Both macrophages and DCs express non-clonally distributed PRRs which react with unique microbial PAMPs. Of critical importance are TLRs. At least 10 TLR cognates exist, each responsive to different types of PAMPs (Kumar *et al*., 2009). TLR-2 reacts with lipoproteins and lipoarabinomannans from mycobacteria. TLR-3 interacts with double-stranded RNA of various viruses, TLR-4 responds to LPS from gram-negative bacteria, TLR-5 responds to bacterial flagellin and TLR-9 responds to oligodeoxynucleotides comprising unmethylated CpG nucleotide motifs. Some TLRs form heterodimers to provide novel specificities. For example, TLR-2/TLR-6 heterodimers can react with peptidoglycans from gram-positive bacteria and zymosan from yeast. Importantly, interactions between PAMPs and TLRs initiate a signal transduction cascade which promptly mobilizes host defence mechanisms such as the production of RNIs. In addition, it also induces the surface expression of costimulatory molecules such as CD40 and CD80/CD86, as well as the secretion of immuno-stimulatory cytokines such as IL-12. In this manner, sensing PAMPs by means of TLRs promotes the development of Th1 cells. Helminths lack such PAMPs, but encompass other, so far ill-defined, molecular entities. In their presence, and in the absence of PAMPs, Th2 cell development is induced.

DCs express an enormous plasticity which allows them to develop distinct functional activities in response to different environmental stimuli (Reis e Sousa, 2001). In the presence of PAMPs, TLRs induce maturation of DCs' that preferentially stimulate Th1 cells. By contrast, helminths cause the differentiation of DCs through unknown mechanisms inducing Th2 cell development. Finally, stimulation through NOD-like receptors has been shown to stimulate DCs, which induce Th17 cell polarization.

In this way DCs are critical regulators of the adaptive immune response to various pathogens. With regard to immunity against infectious agents, the lack of highly phagocytic and degradative activities of DCs renders them dependent on cooperation with macrophages, at least in part. It is likely that intracellular microbes are engulfed and degraded by macrophages which then produce vesicles containing antigenic cargo. This cargo can be taken up by bystander DCs and presented in the most efficacious manner (Kaufmann, 2001). This cooperation is often termed cross-priming (Winau *et al*., 2006).

♦♦♦♦♦♦ IV. CYTOKINES

Collectively, cytokines are soluble mediators that exert pleiotropic effects on cells of the immune system and transduce signals *via* specific surface receptors (see Table 2).

Cytokines primarily produced by cells of the immune system with known cDNA sequence are designated interleukins. As discussed above, Th cells are functionally differentiated into subsets on the basis of their characteristic cytokine spectrum (Zhu *et al*., 2010). Upon appropriate activation, these Th subsets produce interleukins that are primarily required for immunological control of intracellular pathogens (Th1), the regulation of Ig class switching (Th2), control of extracellular pathogens (Th17) or for down-modulating immune responses (T_{reg}). In addition,

Table 2. Cytokines with relevance for the anti-infective immune response

Cytokine	Major role in antimicrobial defence
Chemokines	Leukocyte attraction to site of microbial implantation
CXC chemokine	Granulocyte recruitment to site of microbial implantation
CC chemokine	Monocyte recruitment to site of microbial implantation
C chemokine	Lymphocyte recruitment to site of microbial implantation
IL-1	Proinflammatory, endogenous pyrogen
IL-6	Proinflammatory, promotion of Th17 cells
TNF-α	Proinflammatory, macrophage costimulator, cachexia
IL-2	T cell activation
IFN-γ	Macrophage activation, promotion of Th1 cells
IL-4	B cell activation, switch to IgE, promotion of Th2 cells, activation of mast cells
IL-5	Switch to IgA, activation of eosinophils
IL-12	Promotion of Th1 cells
IL-17	Proinflammatory, attraction of granulocytes
IL-18	Promotion of Th1 cells
IL-23	Promotion of Th17 cells
IL-25	Promotion of Th2 cells
IL-33	Promotion of Th2 cells
IL-21	Proinflammatory, sustenance of Th17 cells
IL-10	Anti-inflammatory
TGF-β	Anti-inflammatory, promotion of T_{reg} cells

cytokines produced by monocytes and macrophages (frequently termed monokines) have important roles in the immune defence against infectious agents. Cytokines produced by macrophages in response to stimulation with bacterial components include IL-1 family members (Dinarello, 2009), IL-6, IL-12, IL-18, IL-23, TNF-α and TGF-β. By contrast, IL-25 and IL-33 are produced by epithelial cells in response to helminth infections.

IL-12 is a driving force for the differentiation of Th1 cells from undetermined Th0 precursor cells. Its action is supported by the more recently discovered IL-18 (Swain, 2001). IL-12 is a heterodimer of two chains. One chain is shared with IL-23, which is the driving force for Th17 cell polarization. IL-1, IL-6 and TNF-α are proinflammatory and pleiotropic cytokines that induce a variety of effects on many different target cells. The balance between IL-6 and TGF-β is instrumental in polarization of T_{reg} cells versus Th17 cells. A large group of cytokines is collectively termed chemokines. These proteins recruit phagocytic cells and lymphocytes to local sites of infection. Chemokines are characterized by four conserved cysteines forming two disulphide bridges. The position of the first two cysteines has been used to divide the chemokines into four families, the C-X-C, the C-C, the C and the CX_3C chemokines (Baggiolini *et al.*, 1997; Rot and von Andrian, 2004; Allen *et al.*, 2007). IL-8 and NAP-2 are members of the C-X-C chemokine family that promote the migration of neutrophils. Macrophage inflammatory protein-1β (MIP-1β), monocyte chemotactic protein-1 (MCP-1) and regulated upon activation normal T cell expressed and secreted (RANTES) are members of the C-C family of chemokines that promote migration primarily of monocytes and T lymphocytes (Bromley *et al.*, 2008). The C and CX_3C chemokines comprise only one or a few members. Chemokines bind to G protein-coupled receptors, some of which exert additional functions with relevance to infectious diseases (Allen *et al.*, 2007).

Chemokines can be produced by many different cell types in response to stimulation with bacterial antigens or viruses. As a consequence, local recruitment of phagocytic and effector cells due to the effect of chemokine release is a general feature of the immune response to infection. In addition, chemokines and their receptors play important roles in the control of HIV infection of target cells (Lusso, 2006).

Several cytokines possess anti-inflammatory and regulatory activities. Of note are IL-10 and TGF-β, which are both produced by a variety of cells including macrophages, but most importantly are the cytokines of T_{reg} cells.

♦♦♦♦♦♦ V. CONCLUDING REMARKS

As briefly summarized in this chapter, the immune response to infectious agents involves a broad spectrum of mechanisms of the innate and acquired immune systems. Accordingly, the analysis of these mechanisms requires a similarly broad spectrum of sophisticated immunological technologies. A better understanding of the principal mechanisms underlying the protective immune response to infectious agents will also provide guidelines for the rational design of novel vaccination strategies. Better understanding of the pathways that lead to the stimulation of a given immune response and elucidation of the decisive molecules which initiate

these pathways will provide the basis for the design of novel adjuvants. Thus, our in-depth understanding of PRRs, which recognize molecular patters of microbes and host, and signalling pathways that they stimulate, will form the blueprint for novel intervention measures.

Until recently, experimental approaches in immunology and microbiology have focused on changes in single or a few defined parameters. The elucidation of the genomes of numerous microbial pathogens and the almost completed elucidation of the human and murine genomes have led to a paradigm shift. Using DNA chips, we can now investigate the global changes in the transcriptomes of both the host and the pathogen, and new technologies allow similarly for the analysis of the differentially expressed proteome. The chapter by de Souza and Wiker in Section I provides an overview of current proteome technologies. These novel approaches broaden our interest from single molecules to the global signature responses that occur during infection.

References

Ahmed, R., Lanier, J. G. and Pamer, E. (2002). Immunological memory and infection. In: *Immunology of Infectious Diseases* (Kaufmann, S. H.E., A. Sher, and R. Ahmed, eds.), pp. 175–190. ASM Press, Washington.

Allen, S. J., Crown, S. E. and Handel, T. M. (2007). Chemokine: receptor structure, interactions, and antagonism. *Annu. Rev. Immunol.* **25**, 787–820.

Altincicek, B., Moll, J., Campos, N., Foerster, G., Beck, E., Hoeffler, J. F., Grosdemange-Billiard, C., Rodriguez-Cencepcion, M., Rohmer, M., Boronat, A. *et al*. (2001). Cutting edge: human γδ T cells are activated by intermediates of the 2-C-methyl-D-erythritol 4-phosphate pathway of isoprenoid biosynthesis. *J. Immunol.* **166**, 3655–3658.

Baggiolini, M., Dewald, B. and Moser, B. (1997). Human chemokines: an update. *Annu. Rev. Immunol.* **15**, 675–705.

Belkaid, Y. and Tarbell, K. (2009). Regulatory T cells in the control of host-microorganism interactions. *Annu. Rev. Immunol.* **27**, 551–589.

Bendelac, A., Savage, P. B. and Teyton, L. (2007). The biology of NKT cells. *Annu. Rev. Immunol.* **25**, 297–336.

Brigl, M. and Brenner, M. B. (2004). CD1: antigen presentation and T cell function. *Annu. Rev. Immunol.* **22**, 817–890.

Bromley, S. K., Mempel, T. R. and Luster, A. D. (2008). Orchestrating the orchestrators: chemokines in control of T cell traffic. *Nat. Immunol.* **9**, 970–980.

Chan, E. D., Chan, J. and Schluger, N. W. (2001). What is the Role of Nitric Oxide in Murine and Human Host Defense against Tuberculosis? Current knowledge. *Am. J. Respir. Cell Mol. Biol.* **25**, 606–612.

Clayberger, C. and Krensky, A. M. (2003). Granulysin. *Curr. Opin. Immunol.* **15**, 560–565.

Collins, H. L. and Kaufmann, S. H.E. (2002). Acquired immunity against bacteria. In: *Immunology of Infectious Diseases* (S. H.E. Kaufmann, A. Sher and R. Ahmed, eds.), pp. 207–222. ASM Press, Washington.

Cooper, A. M. (2009). Cell-mediated immune responses in tuberculosis. *Annu. Rev. Immunol.* **27**, 393–422.

Dinarello, C. A. (2009). Immunological and inflammatory functions of the interleukin-1 family. *Annu. Rev. Immunol.* **27**, 519–550.

Dorhoi, A. and Kaufmann, S. H.E. (2009). Fine-tuning of T cell responses during infection. *Curr. Opin. Immunol.* **21**, 367–377.

Dunkelberger, J. R. and Song, W. C. (2010). Complement and its role in innate and adaptive immune responses. *Cell Res.* **20**, 34–50.
Eberl, G. (2010). Immunology: close encounters of the second type. *Nature* **464**, 1285–1286.
Elgueta, R., Benson, M. J., de Vries, V. C., Wasiuk, A., Guo, Y. and Noelle, R. J. (2009). Molecular mechanism and function of CD40/CD40L engagement in the immune system. *Immunol. Rev.* **229**, 152–172.
Fagarasan, S., Kawamoto, S., Kanagawa, O. and Suzuki, K. (2010). Adaptive immune regulation in the gut: T cell–dependent and T cell–independent IgA synthesis. *Annu. Rev. Immunol.* **28**, 243–273.
Finlay, B. B. and Cossart, P. (1997). Exploitation of mammalian host cell functions by bacterial pathogens. *Science* **276**, 718–725.
Geissmann, F., Manz, M. G., Jung, S., Sieweke, M. H., Merad, M. and Ley, K. (2010). Development of monocytes, macrophages, and dendritic cells. *Science* **327**, 656–661.
Greenwald, R. J., Freeman, G. J. and Sharpe, A. H. (2005). The B7family revisited. *Annu. Rev. Immunol.* **23**, 515–548.
Grewal, I. S. and Flavell, R. A. (1996). A central role of CD40 ligand in the regulation of $CD4^+$ T-cell responses. *Immunol. Today* **17**, 410–414.
Guaní-Guerra, E., Santos-Mendoza, T., Lugo-Reyes, S. O. and Terán, L. M. (2010). Antimicrobial peptides: general overview and clinical implications in human health and disease. *Clin. Immunol.* **135**, 1–11.
Hayday, A. C. (2000). γδ Cells: a right time and a right place for a conserved third way of protection. *Annu. Rev. Immunol.* **18**, 975–1026.
Hill, D. A. and Artis, D. (2010). Intestinal bacteria and the regulation of immune cell homeostasis. *Annu. Rev. Immunol.* **28**, 623–667.
Hughes, A. (2002). Evolution of the host defense system. In: *Immunology of Infectious Diseases* (S. H.E. Kaufmann, A. Sher and R. Ahmed, eds.), pp. 67–78. ASM Press, Washington.
Izcue, A., Coombes, J. L. and Powrie, F. (2009). Regulatory lymphocytes and intestinal inflammation. *Annu. Rev. Immunol.* **27**, 313–338.
Kabelitz, D. (2008). Small molecules for the activation of human γδ T cell responses against infection. *Recent Pat. Antiinfect Drug Discov.* **3**, 1–9.
Kabelitz, D., Glatzel, A. and Wesch, D. (2000). Antigen rcognition by human γδ T lymphocytes. *Int. Arch. Allergy Immunol.* **122**, 1–7.
Kabelitz, D. and Wesch, D. (2001). Role of γδ T-lymphocytes in HIV infection. *Eur. J. Med. Res.* **6**, 169–174.
Kaufmann, S. H.E. (1996). γ/δ and other unconventional T lymphocytes: what do they see and what do they do? *Proc. Natl. Acad. Sci. U.S.A.* **93**, 2272–2279.
Kaufmann, S. H.E. (2001). How can immunology contribute to the control of tuberculosis? *Nat. Immunol. Rev.* **1**, 20–30.
Keir, M. E., Butte, M. J., Freeman, G. J. and Sharpe, A. H. (2008). PD-1 and its ligands in tolerance and immunity. *Annu. Rev. Immunol.* **26**, 677–704.
King, C., Tangye, S. G. and Mackay, C. R. (2008). T follicular helper (T_{FH}) cells in normal and dysregulated immune responses. *Annu. Rev. Immunol.* **26**, 741–766.
Korn, T., Bettelli, E., Oukka, M. and Kuchroo, V. K. (2009). IL-17 and Th17 cells. *Annu. Rev. Immunol.* **27**, 485–517.
Kuhn, M., Goebel, W., Philpott, D. J. and Sansonetti, P. J. (2002). Overview of the bacterial pathogens. In: *Immunology of Infectious Diseases* (S. H.E. Kaufmann, A. Sher and R. Ahmed, eds.), pp. 5–24. ASM Press, Washington.
Kumar, H., Kawai, T. and Akira, S. (2009). Toll-like receptors and innate immunity. *Biochem. Biophys. Res. Commun.* **388**, 621–625.
Lenz, L. L. and Bevan, M. J. (1996). H2-M3-restricted presentation of Listeria monocytogenes antigens. *Immunol. Rev.* **151**, 107–121.

Li, M. O. and Flavell, R. A. (2008). TGF-beta: a master of all T cell trades. *Cell* **134**, 392–404.
Lieu, P. T., Heiskala, M., Peterson, P. A. and Yang, Y. (2001). The roles of iron in health and disease. *Mol. Aspects Med.* **22**, 1–87.
Liu, P. T. and Modlin, R. L. (2008). Human macrophage host defense against Mycobacterium tuberculosis. *Curr. Opin. Immunol.* **20**, 371–376.
Liu, B., Woltman, A. M., Janssen, H. L. and Boonstra, A. (2009). Modulation of dendritic cell function by persistent viruses. *J. Leukoc. Biol.* **85**, 205–214.
Lusso, P. (2006). HIV and the chemokine system: 10 years later. *EMBO J.* **25**, 447–456.
Manz, R. A., Hauser, A. E., Hiepe, F. and Radbruch, A. (2005). Maintenance of serum antibody levels. *Annu. Rev. Immunol.* **23**, 367–386.
McHeyzer-Williams, L. J. and McHeyzer-Williams, M. G. (2005). Antigen-specific memory B cell development. *Annu. Rev. Immunol.* **23**, 487–513.
Moore, K. W., O'Garra, A., de Waal Malefyt, R., Vieira, P. and Mosmann, T. R. (1993). Interleukin-10. *Annu. Rev. Immunol.* **11**, 165–190.
Munoz-Elias, E. J. and McKinney, J. D. (2002). Bacterial persistence: strategies for survival. In: *Immunology of Infectious Diseases* (S. H.E. Kaufmann, A. Sher and R. Ahmed, eds.), pp. 331–356. ASM Press, Washington.
Neill, D. R., Wong, S. H., Bellosi, A., Flynn, R. J., Daly, M., Langford, T. K., Bucks, C., Fallon, P. G., Pannell, R., Jolin, H. E. *et al*. (2010). Nuocytes represent a new innate effector leukocyte that mediates type-2 immunity. *Nature* **464**, 1367–1370.
Neutra, M. R. and Kraehenbuhl, J. P. (2002). Regional immune response to microbial pathogens. In: *Immunology of Infectious Diseases* (S. H.E. Kaufmann, A. Sher and R. Ahmed, eds.), pp. 191–206. ASM Press, Washington.
Pearce, E. J. and Tarleton, R. L. (2002). Overview of the parasitic pathogens. In: *Immunology of Infectious Diseases* (S. H.E. Kaufmann, A. Sher and R. Ahmed, eds.), pp. 39–52. ASM Press, Washington.
Pfefferkorn, E. R. (1984). Interferon-γ blocks the growth of Toxoplasma gondii in human fibroblast by inducing the host cells to degrade tryptophan. *Proc. Nat. Acad. Sci. U.S.A.* **81**, 908–912.
Rajewsky, K. (1996). Clonal selection and learning in the antibody system. *Nature* **381**, 751–758.
Reis e Sousa, C. (2001). Dendritic cells as sensors of infection. *Immunity* **14**, 495–498.
Rohde, K., Yates, R. M., Purdy, G. E. and Russell, D. G. (2007). Mycobacterium tuberculosis and the environment within the phagosome. *Immunol. Rev.* **219**, 37–54.
Rolph, M. S. and Kaufmann, S. H.E. (2000). Partially TAP-independent protection against Listeria monocytogenes by H2-M3-restricted CD8+ T cells. *J. Immunol.* **165**, 4575–4580.
Romani, L. (2002). Overview of the parasitic pathogens. In: *Immunology of Infectious Diseases* (S. H.E. Kaufmann, A. Sher and R. Ahmed, eds.), pp. 25–38. ASM Press, Washington.
Rot, A. and von Andrian, U. H. (2004). Chemokines in innate and adaptive host defense: basic chemokinese grammar for immune cells. *Annu. Rev. Immunol.* **22**, 891–928.
Rothenberg, M. E. and Hogan, S. P. (2006). The eosinophil. *Annu. Rev. Immunol.* **24**, 147–174.
Rudd, C. E., Taylor, A. and Schneider, H. (2009). CD28 and CTLA-4 coreceptor expression and signal transduction. *Immunol. Rev.* **229**, 12–26.
Schaible, U. E., Collins, H. L. and Kaufmann, S. H.E. (1999). Confrontation between intracellular bacteria and the immune system. *Adv. Immunol.* **71**, 267–377.
Schaible, U. E. and Kaufmann, S. H.E. (2000). CD1 and CD1-restricted T cells in infections with intracellular bacteria. *Trends Microbiol.* **8**, 419–425.
Schaible, U. E. and Kaufmann, S. H.E. (2005). A nutritive view on the host-pathogen interplay. *Trends Microbiol.* **13**, 373–380.
Schroder, K. and Tschopp, J. (2010). The inflammasomes. *Cell* **140**, 821–832.

Scotet, E., Nedellec, S., Devilder, M. C., Allain, S. and Bonneville, M. (2008). Bridging innate and adaptive immunity through gamma-delta T-dendritic cell crosstalk. *Front. Biosci.* **13**, 6872–6885.

Scott, P. and Grencis, R. K. (2002). Adaptive immune effector mechanisms against intracellular protozoa and gut-dwelling nematodes. In: *Immunology of Infectious Diseases* (S. H.E. Kaufmann, A. Sher and R. Ahmed, eds.), pp. 235–246. ASM Press, Washington.

Segal, A. W. (2005). How neutrophils kill microbes. *Annu. Rev. Immunol.* **23**, 197–223.

Serbina, N. V., Jia, T., Hohl, T. M. and Pamer, E. G. (2008). Monocyte-mediated defense against microbial pathogens. *Annu. Rev. Immunol.* **26**, 421–452.

Smith-Garvin, J. E., Koretzky, G. A. and Jordan, M. S. (2009). T cell activation. *Annu. Rev. Immunol.* **27**, 591–619.

Stavnezer, J., Guikema, J. E. and Schrader, C. E. (2008). Mechanism and regulation of class switch recombination. *Annu. Rev. Immunol.* **26**, 261–292.

Stetson, D. B. and Medzhitov, R. (2006). Type I interferons in host defense. *Immunity* **25**, 373–381.

Strasser, A., Jost, P. J. and Nagata, S. (2009). The many roles of FAS receptor signaling in the immune system. *Immunity* **30**, 180–192.

Swain, S. L. (2001). Interleukin 18: tipping the balance towards T helper cell 1 response. *J. Exp. Med.* **194**, F11–F14.

Szomolanyi-Tsuda, E., Brehm, M. A. and Welsh, R. M. (2002). Acquired immunity against fungi. In: *Immunology of Infectious Diseases* (S. H.E. Kaufmann, A. Sher and R. Ahmed, eds.), pp. 247–265. ASM Press, Washington.

Taylor, P. R., Martinez-Pomares, L., Stacey, M., Lin, H.-H., Brown, G. D. and Gordon, S. (2005). Macrophage receptors and immune recognition. *Annu. Rev. Immunol.* **23**, 901–944.

Theofilopoulos, A. N., Baccala, R., Beutler, B. and Kono, D. H. (2005). Type 1 interferon (α/β) in immunity and autoimmunity. *Annu. Rev. Immunol.* **23**, 307–335.

van der Merwe, P. A. and Davis, S. J. (2003). Molecular interactions mediating T cell antigen recognition. *Annu. Rev. Immunol.* **21**, 659–684.

Vascotto, F., Le Roux, D., Lankar, D., Faure-André, G., Vargas, P., Guermonprez, P. and Lennon-Duménil, A. M. (2007). Antigen presentation by B lymphocytes: how receptor signaling directs membrane trafficking. *Curr. Opin. Immunol.* **19**, 93–98.

Wang, L., Kamath, A., Das, H., Li, L. and Bukowski, J. F. (2001). Antibacterial effect of human Vγ2Vδ2 T cells *in vivo*. *J. Clin. Invest.* **108**, 1349–1357.

Winau, F., Weber, S., Sad, S., de Diego, J., Hoops, S. L., Breiden, B., Sandhoff, K., Brinkmann, V., Kaufmann, S. H.E. and Schaible, U. E. (2006). Apoptotic vesicles crossprime CD8 T cells and protect against tuberculosis. *Immunity* **24**, 105–117.

Yewdell, J. W. and Bennink, J. R. (2002). Overview of the viral pathogens. In: *Immunology of Infectious Diseases* (S. H.E.Kaufmann, A. Sher, and R. Ahmed, eds.), pp. 53–64. ASM Press, Washington.

Zhu, J., Yamane, H. and Paul, W. E. (2010). Differentiation of effector CD4 T cell populations. *Annu. Rev. Immunol.* **28**, 445–489.

2 Immunomagnetic Isolation of Subcellular Compartments

Vladimir Tchikov, Jürgen Fritsch, Dieter Kabelitz and Stefan Schütze
Institute of Immunology, University of Kiel, Kiel, Germany

Immunomagnetic Isolation of Subcellular Compartments

CONTENTS

♦♦♦♦♦♦ I. INTRODUCTION

A variety of biological responses, ranging from proliferation and differentiation to cell death, are mediated by ligand-triggered receptor activation at the plasma membrane. The classical model of signal transduction involves cell surface receptors that are activated after binding to their ligands and transmit intracellular signals to generate secondary messengers. The activation of many receptors also triggers the accelerated endocytosis of ligand–receptor complexes, which suggests that endocytic vesicles are important sites for organizing the recruitment of specific components for the activated signalling cascade. Endocytosis has long been regarded solely as a mechanism to terminate signalling through receptor internalization and subsequent lysosomal degradation. However, it has become clear that certain signalling pathways require receptor internalization for full activation to occur (i.e. epidermal growth factor, Trk, nerve growth factor and insulin receptor). Thus, a more sophisticated picture emerged suggesting that endocytosis orchestrates cell signalling by coupling and integrating different cascades on the surface of endocytic vesicles (reviewed by McPherson *et al*., 2001; Sorkin and Von Zastrow, 2002; Teis and Huber, 2003; Miaczynska *et al*., 2004).

For further informations regarding the protocols described here or further applications of the free-flow high magnetic gradient chamber please contact the corresponding author.

The device described in this chapter is currently manufactured by the company HOOCK GmbH, Liebigstraße 22, D-24145 Kiel, Germany, Tel: 49-431-71577; Fax: 49-431-71578; E-mail: info@hoock-gmbh.de

METHODS IN MICROBIOLOGY, VOLUME 37
0580-9517 DOI 10.1016/S0580-9517(10)37002-4

The regulation of receptor endocytosis and signal transduction as well as the linkage of compartmentalization to select biological outcomes *in vivo* is still poorly understood. In this context, recent findings concerning death receptor signalling give novel insights into the physiological role of receptor internalization and endosomal trafficking in selectively transmitting signals that lead to either apoptosis or survival of the cell (Schütze *et al*., 1999; Schneider-Brachert *et al*., 2004, 2006; Lee *et al*., 2006; Peter *et al*., 2007; for review see Schütze *et al*., 2008; Guicciardi and Gores, 2009).

The isolation of intracellular organelles is a crucial requirement for the investigation of the functional role of subcellular compartments involved in the diversification of cell surface receptor signalling.

For this purpose, we developed a system based on target-specific immunomagnetic labelling of cell surface receptors or intracellular proteins for their selective purification. The patented free-flow magnetic chamber allows the selective purification of biological materials from cellular lysates, in particular morphological and functional intact endosomes containing activated receptors and receptor-associated proteins (Tchikov *et al*., 1999, 2001; Schütze *et al*., 2003).

As an example for the application of this approach, intact tumour necrosis factor (TNF)/TNF receptor complexes were isolated within their native membrane environment from different stages of TNF-receptosome trafficking and maturation after immunomagnetic labelling of TNF receptors with biotin–TNF coupled to streptavidin-coated magnetic nanobeads (Schneider-Brachert *et al*., 2004). Western blot analysis of the isolated magnetic fractions revealed association with marker proteins of early endosomes such as clathrin and Rab4, which dissociate after 30 min of internalization, as well as Rab5, which was retained up to 60 min on TNF receptosomes. After 30 min of internalization, fusion of TNF-receptosomes with trans-Golgi membranes was observed (indicated by markers of trans-Golgi membranes: p47A and Vti-1b, as well as GRP 78, syntaxin-6 and Rab8) resulting in the formation of multivesicular organelles. At later time points, TNF-receptosomes accumulated lysosomal proteins such as cathepsin D (CTSD) and lysosomal-associated protein 1 (LAMP-1) (see Figure 1). Analysis of TNF receptor (TNF-R1) death domain adaptor proteins in the magnetic isolates revealed the recruitment of TRADD after 3 min, as well as Fas-associated protein with death domain (FADD) and caspase-8 to establish the 'death-inducing signalling complex' (DISC). DISC formation and apoptosis are strictly dependent on TNF-R1 internalization, while the recruitment of TRAF-2 and RIP-1 to signal for NF-κB activation occurs from TNF-R1 at the cell surface. These data revealed that TNF-R1 establishes different TNF-signalling pathways by compartmentalization of plasma membrane-derived endocytic vesicles harbouring the TNF-R1-associated DISC (Schneider-Brachert *et al*., 2004). This immunomagnetic separation approach also allowed for the discovery of a novel adenoviral immune escape mechanism (Schneider-Brachert *et al*., 2006), the characterization of CARP-2, which is an endosome-associated ubiquitin E3-ligase for RIP involved in the regulation of anti-apoptotic NF-κB signalling (Liao *et al*., 2008), the complex-formation of Alix and ALG-2 with pro-caspase-8 and TNF-R1, regulating TNF-induced apoptosis (Mahul-Mellier *et al*., 2008), the identification of the enzyme riboflavin kinase as a novel TNF-R1 death domain adaptor protein, coupling the receptor to NADPH oxidase (Yazdanpanah *et al*., 2009), and the coupling of TNF-R1 via the polycomb group protein EED to neutral sphingomyelinase (Philipp *et al*., 2010).

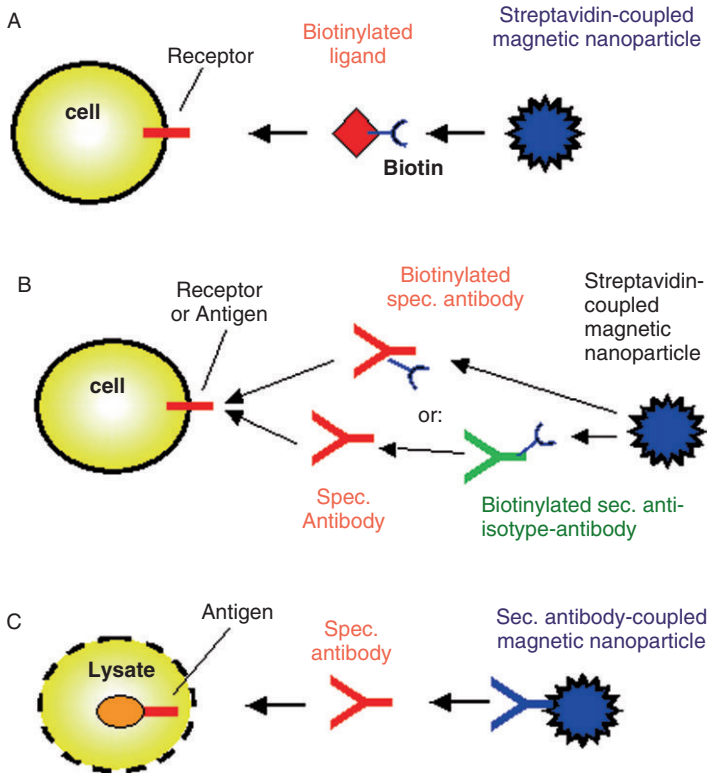

Figure 1. Approaches for immunomagnetical labelling of cellular target structures. Cell surface receptors or antigens are labelled with either the specific ligand (A) or the antibodies (B) followed by binding to magnetic nanobeads. After mechanical homogenization, magnetic membrane fractions containing the receptors or antigens can be isolated in a high-gradient magnetic field following Protocol 1. (C) For the preparation of intracellular organelles or soluble protein complexes, cells are homogenized prior to incubation with a preformed antibody–magnetic bead complex and the targets are isolated in the magnetic field according to Protocol 2.

This method was additionally applied to characterize the internalization and maturation of CD95 receptosomes. In this case, a biotinylated anti-CD95 antibody as ligand coupled to streptavidin-coated magnetic nanobeads was used for separation in the high-gradient magnetic chamber (Lee *et al.*, 2006; Feig *et al.*, 2007). Also, the DISC recruitment to internalized TRAIL receptors was analysed using this method (Lemke *et al.*, 2010). The separation approach is summarized in 'Protocol 1'.

After successful application of the magnetic separation device for the isolation and functional characterization of TNF-receptosomes, we subsequently adopted this approach for the immunomagnetic isolation of soluble proteins and other intact organelles from total cell lysates (summarized in 'Protocol 2'). By coupling antibodies specific for signature proteins of intracellular endosomal trafficking and fusion events such as Rab5 and Vti-1b to magnetic nanobeads, we isolated subcellular organelles from various stages of vesicular maturation that contain internalized TNF-R1 in early endosomes and activated TNF-R1-associated signalling

complexes such as caspase-8 and cathepsin D in late endosomes/multivesicular organelles (see Figures 3 and 4).

The free-flow high-gradient magnetic system is currently also applied to isolate intracellular phagosomes after infection of cells with pathogens such as mycobacteria, listeria and chlamydia (Steinhäuser *et al.*, manuscript in preparation).

♦♦♦♦♦♦ II. GENERAL REMARKS

Among the various approaches for organelle purification, differential centrifugation is the most frequently used protocol due to its quick and inexpensive nature. This method provides preparations in which integrity and functionality of the organelles are maintained. Another purification protocol that also results in highly enriched organelle fractions is the preparation of an isopycnic gradient followed by ultracentrifugation. However, these methods do not allow the separation of membrane compartments that share similar densities but exhibit diverse functional properties such as different stages of vesicular maturation and physiological functions. Here we describe a fast and easy method to obtain pure, functional endosomes from various stages of endosomal maturation from cultured cells. The new method is based on immunomagnetic sorting, which was originally developed for the separation of cells (Miltenyi *et al.*, 1990; Tchikov *et al.*, 1999, 2001) but has also been successfully used to purify cellular compartments such as Golgi vesicles (Mura *et al.*, 2002), endosomes (Perrin-Cocon *et al.*, 1999), lysosomes (Diettrich *et al.*, 1998), nuclei (Kausch *et al.*, 1999), mitochondria (Hornig-Do *et al.*, 2009) and plasma membranes (Lawson *et al.*, 2006). The immunomagnetic separation approach has recently been refined for the isolation of TNF-R1-, CD95- and TRAIL-receptosomes (Schneider-Brachert *et al.*, 2004, 2006; Lee *et al.*, 2006; Feig *et al.*, 2007; Liao *et al.*, 2008; Yazdanpanah *et al.*, 2009; Lemke *et al.*, 2010; Philipp *et al.*, 2010).

A. Immunomagnetic Labelling of Cellular Target Structures

Basically, cell surface proteins such as receptors can be magnetically labelled in two ways: either by a biotinylated ligand in combination with streptavidin-coated magnetic nanobeads (Figure 1A) or by using a specific antibody directed against the receptor to which a secondary anti-isotype-specific antibody, coupled to magnetic nanobeads, is linked (Figure 1B). If nanobeads carrying the respective secondary antibody are not available, the specific anti-receptor antibody can be biotinylated and then used as target for streptavidin-coated magnetic nanobeads or a biotinylated secondary antibody can be used instead (Figure 1B).

For magnetic labelling of intracellular structures in cell lysates, the cells have to be homogenized either mechanically, if organelles such as endosomes or phagosomes are to be isolated, or by using detergents, if soluble proteins will be purified. Subsequently, the specific antibody coupled to the magnetic nanobead-bound secondary antibody is added to the lysates (Figure 1C).

B. Immunoprecipitation by Using Magnetic Nanobeads

Immunoprecipitation is a widely used method to purify specific proteins from cell lysates. Conventional IP protocols use protein A or G coupled to agarose beads, to capture the antibody–antigen complex in solution. This complex is subsequently precipitated by centrifugation. Limitations of conventional IP include sample handling and processing difficulties, for example the great volume of agarose beads in the precipitate due to their great diameter, which may cause problems in case of limited volumes of material that can be loaded on a polyacrylamide gel or added to an enzymatic assay. With nanobeads there are practically no limitations in quantity, because the volume of the precipitate even from 10^{12} nanobeads does not exceed 1 μl.

As a tool for immunoprecipitation, magnetic nanobeads coated with antibodies are broadly available and offer certain advantages over conventional beads. Magnetic beads are now available at a diameter as small as 50 nm. In spite of their small volume, in a magnetic field, each bead can exhibit a magnetic moment as great as $\sim 10^6$ Bohr magnetons. This magnetic moment is sufficient to provide 'precipitation' of beads by a magnetic force additionally or instead of centrifugation. Due to the physical phenomenon of the magnetic dipole–dipole interaction between beads, the precipitation procedure can be sufficient even in a relatively low-intensity magnetic field, for example of $\sim 10^3$ Oersted.

Nanobeads of diverse specificities are commercially available from many manufacturers. Here we describe a representative protocol for immunoprecipitation with 50 nm superparamagnetic nanobeads commercially available as a solution of MACS Microbeads from Miltenyi Biotec (Bergisch Gladbach, Germany). In combination with these beads we use our self-designed magnetic field-generating system, which permits an optimal tuning of biophysical conditions regarding the parameters of the magnetic field and the liquid flow system. Our matrix-free flow column offers certain advantages over matrix-containing columns, for example MACS columns. For example, MACS columns are loaded with ferromagnetic materials such as steel balls or wires creating a porous matrix directly contacting the lysate. Our matrix-free column is empty inside. Magnets generating the magnetic field are placed outside of the column, and the biological material contacts only the plastic side wall of the column. Thus, the sample is perfectly protected from any contact to ferromagnetic materials or magnets by the wall of the column. This is an important feature to minimize contaminations. Additionally, our column can be loaded with lysates of any density or even with samples tending to spontaneous aggregation.

♦♦♦♦♦♦ III. METHODS

A. Protocol 1: Isolation of Magnetically Labelled Cell Surface Receptor Complexes

1. Cultivation and preparation of cells

1.1. U937 cells (e.g.) were obtained from the ATCC and maintained in CLICK's RPMI culture medium (Biochrom, Berlin, Germany) supplemented with 5% fetal calf serum.

1.2. Wash 10^8 cells for two times by centrifugation with 30 ml of cold phosphate-buffered saline (PBS) at $100 \times g$, 10 min. Resuspend the cell pellet in a total volume of 250 µl cold PBS; transfer the cell suspension into a fresh tube on ice.

2. Labelling of TNF receptors with biotinylated TNF and streptavidin-coated superparamagnetic nanobeads

2.1. Add 100 µl (400 ng) of biotinylated TNF (Fluorokine-Kit; R&D Systems, Wiesbaden, Germany) to the cells and incubate for 1 h on ice to label TNF receptors on the cell surface.
2.2. Add 200 µl of MACS Streptavidin Microbeads solution (Miltenyi Biotec) containing 50 nm magnetic nanobeads to the cells and incubate for another hour on ice to couple biotinylated TNF to magnetic nanobeads.
2.3. Wash the cells for two times by centrifugation with 30 ml of cold PBS at $100 \times g$, 10 min, and resuspend the cell pellet in a total volume of 250 µl cold RPMI medium without FCS, store on ice. At this step, magnetically labelled cells are cleared of contaminations from unbound labelling reactants.

3. Synchronization of receptor internalization

3.1. For synchronized activation of cells, transfer the cooled labelled cells into 20 ml of medium without FCS pre-warmed in a mixing water bath to 37°C followed by incubation for the desired duration. At this step, the TNF receptor bound to magnetic nanobeads is internalized from the cell surface into the cell by pinching off endosomes from the plasma membrane, including the nanobeads as magnetic label.
3.2. Stop the internalization by adding 20 ml of ice-cold medium without FCS into the incubation tube and transfer the tube on ice to stop the internalization immediately.

4. Gentle mechanical homogenization of cells

4.1. Centrifuge and wash cells with 30 ml of the pre-cooled homogenization buffer containing 0.25 M sucrose, 15 mM HEPES and 0.5 mM $MgCl_2$ (pH 7.4) supplemented with protease inhibitors and pepstatin (i.e. Protease Inhibitors Set from Roche Diagnostics, Mannheim, Germany). Discard the supernatant and resuspend the cells in 350 µl of homogenization buffer, supplemented with 5 µg/ml Cytochalasin D and 25 U/ml Benzonase (Merck, Darmstadt, Germany).
4.2. For the isolation of intact subcellular compartments including magnetically labelled receptosomes, the plasma membranes of cells are disrupted by a gentle mechanical procedure by vortexing cells with glass beads at 4°C. Transfer the cell suspension into the micro-homogenization device described previously (Tchikov and Schütze, 2008) and vortex the sample with glass beads for 5 min. Collect the homogenate in a separate tube and centrifuge at $100 \times g$ for 2 min. Transfer the supernatant again into a separate tube. Resuspend the pellet in 350 µl of homogenization buffer and subject repeatedly to homogenization. After three repetitions, pool the supernatants into one sample and finally clear it by centrifugation,

for example at 150 × *g* for 5 min to eliminate residual debris or intact cells. The procedure yields in approximately 700 µl of lysate (~5 mg protein) recovered from 10^8 U937 cells. Based on differences in the stability of plasma membranes between different cell lines, this protocol has to be optimized for the individual cell line used.

4.3. Alternatively, cells can also be lysed by gentle ultrasonification instead of vortexing with glass beads. For U937 cells, we used the Branson SONIFIER W-450 and the CUP-RESONATOR (from G. Heinemann, Schwäbisch Gmünd, Germany). Each sonification was for 2 min, amplitude 2 and, depending on the cell type, 80–90% duty. Electron microscopic analysis revealed intact organelles after sonification. After each sonification, samples were processed by differential centrifugation as described above. Again, this protocol has to be optimized for the individual cell line used.

4.4. Control that the lysates are devoid of unbroken cells by microscopic examination.

5. Magnetic separation of receptosomes

5.1. Load the lysate into the flow column of the magnetic device and apply the magnetic force to the sides of the column. This will result in capturing the magnetic material at the wall of the column. After approximately 3 h, the unwanted 'non-magnetic' components are removed by a flow stream of the homogenization buffer through the column. The washing is continued until a five-fold volume of washing fluid has passed through the tube to ensure adequate removal of contaminants.

After this procedure, the isolated material, the 'magnetic fraction', which is approximately 1% of the initial lysate, is retained inside the column while 'the non-magnetic fraction' which is nearly of 99% of the initial lysate is washed out.

5.2. Elute the isolated 'magnetic fraction' from the column in 1 ml of the homogenization buffer and concentrate the material by centrifugation, for example 20,000 × *g* for 1 h, store the pellet, for example resuspended in 20 µl homogenization buffer, frozen at –20°C.

6. Reconstitution for downstream applications

6.1. Reconstitute the frozen material to the desired concentration, for example by resuspension in 200 µl of ice-cold homogenization buffer and work routinely for downstream applications, for example western blotting with approximately 5 µg protein loaded per lane.

B. Protocol 2: Immunomagnetic Isolation of Subcellular Organelles from Cell Lysates

1. Preparation of immunomagnetic nanobeads coated with antibodies

1.1. If magnetic nanobeads of the desired specificity are available, wash and concentrate them by centrifugation at 20,000 × *g*, resuspend them in 1 ml PBS

and repeat the centrifugation again. Finally, resuspend the pellet in 20 µl PBS and store at 4°C up to the next step.

1.2. If magnetic nanobeads of desired specificity are not available, take 200 µl of a solution of magnetic nanobeads coated with streptavidin, protein A, protein G or for example goat-anti-mouse antibodies. Wash them as above and resuspend them in 50 µl of the primary antibody of interest, for example mouse primary antibody. Incubate the mixture overnight at 4°C by rolling. This incubation results in the formation of magnetic nanobeads coated with primary antibodies of desired specificity.

1.3. Wash and pellet the nanobeads by centrifugation and resuspend them as above. Store at 4°C for the next steps.

2. Preparation of cell lysates

2.1. Scrape 10^8 adherent cells off the flasks in PBS with a rubber policeman or wash non-adherent cells in PBS. Transfer the cell suspension into a separate tube, centrifuge at $100 \times g$ and store the cell pellet on ice.

2.2. Resuspend cells in 10 ml of growth medium without FCS and stimulate cells according to the protocols described above.

2.3. Centrifuge cells and wash with 30 ml of ice-cold PBS, drain off supernatant and resuspend cells in 30 ml of homogenization buffer. Centrifuge the cells and discard the supernatant. Store the pellet on ice.

2.4. Lyse cells depending on further applications. Subject them to mechanical homogenization to get a morphological and functional intact lysate as described above. If detergent-lysed material is desired, resuspend cells in 1 ml of ice-cold modified RIPA buffer (50 mM Tris–HCl [pH 7.4], 150 mM NaCl, 1% NP-40, 0.25% Na-deoxycholate, 1% Triton X-100, 1 mM EDTA) and protease inhibitors for 1 h on ice. Clear cell lysates by centrifugation for 10 min at $1000 \times g$ and store on ice. The lysate containing either intact intracellular organelles or solubilized target protein complexes will be fractionated by the following magnetic immunoprecipitation steps.

3. Immunomagnetic isolation of target structures

3.1. Add the immunomagnetic nanobeads prepared in steps 1.1–1.3 to the lysate and incubate by rolling overnight at 4°C. At this point, the antibodies which are coupled to the beads will bind to their targets in the lysate. This results in formation of a complex between magnetic nanobeads immunospecifically associated with the respective target structures in the lysates.

4. Isolation, washing and concentration of magnetic immunoprecipitates

4.1. Load the lysate onto the flow column of the magnetic device and apply the magnetic force to the sides of the column so that magnetically labelled

structures can precipitate on its walls. This takes approximately 1 h for lysates containing intact organelles in the absence of detergents and 10 min for detergent-solubilized lysates.

4.2. Wash the column in the magnetic field with a five-fold column volume. Alternatively, washing is accomplished by resuspending the beads (off the magnetic field) with the washing solution and then concentrating them back on the tube wall (by placing the tube back in the magnetic field). Repeat the washings several times to ensure adequate removal of contaminants.

4.3. Finally, resuspend the isolated material off the magnetic field in 1 ml of the homogenization buffer. Concentrate the material by centrifugation, for example 20,000 × *g* for 30 min and store the pellet in, for example 20 µl homogenization buffer, frozen at –20°C.

♦♦♦♦♦♦ IV. RESULTS AND CONCLUSIONS

The method of immunomagnetic isolation of cell surface receptors (Protocol 1) allows for monitoring the temporal maturation and spatial distribution of specific proteins involved in the regulation of vesicular trafficking of receptosomes and in signalling from intracellular compartments. The remarkable feature of this approach is that receptors are isolated in their native membrane environment in the absence of any detergent that might interfere with the association of adaptor proteins. Based on the gentle physical homogenization procedure, the morphology and functional integrity of the compartments is preserved. This allows for functional analysis, such as estimating the enzymatic activity of proteins contained in the vesicles. Most importantly, the method is highly specific for the receptor system of choice, based on the specificity of the ligand or antibody used for labelling the receptors.

As an example, the immunomagnetic isolation of TNF receptosomes is described using biotinylated TNF coupled to streptavidin superparamagnetic nanobeads. As shown in Figure 2, the recruitment of the TNF-R1 adaptor proteins FADD, TRADD and caspase-8 is detected in the magnetic fractions, forming the TNF-R1-associated DISC. Intracellular maturation of the receptosomes is revealed by the transient recruitment of the early endosomal marker protein Rab5, the fusion of the receptosomes with trans-Golgi vesicles which is indicated by the appearance of the v-SNARE-protein Vti-1b and the maturation to late endosomes/lysosomes concomitant with the appearance of cathepsin D.

Since these proteins are part of the TNF receptor-bearing membrane vesicle, the direct physical interaction with these proteins and the TNF receptor had to be assessed by conventional immunoprecipitation, using anti-TNF receptor or anti-TNF antibodies. By doing this, we demonstrated that FADD, TRADD and caspase-8 are directly associated with TNF-R1 (Schneider-Brachert *et al.*, 2004).

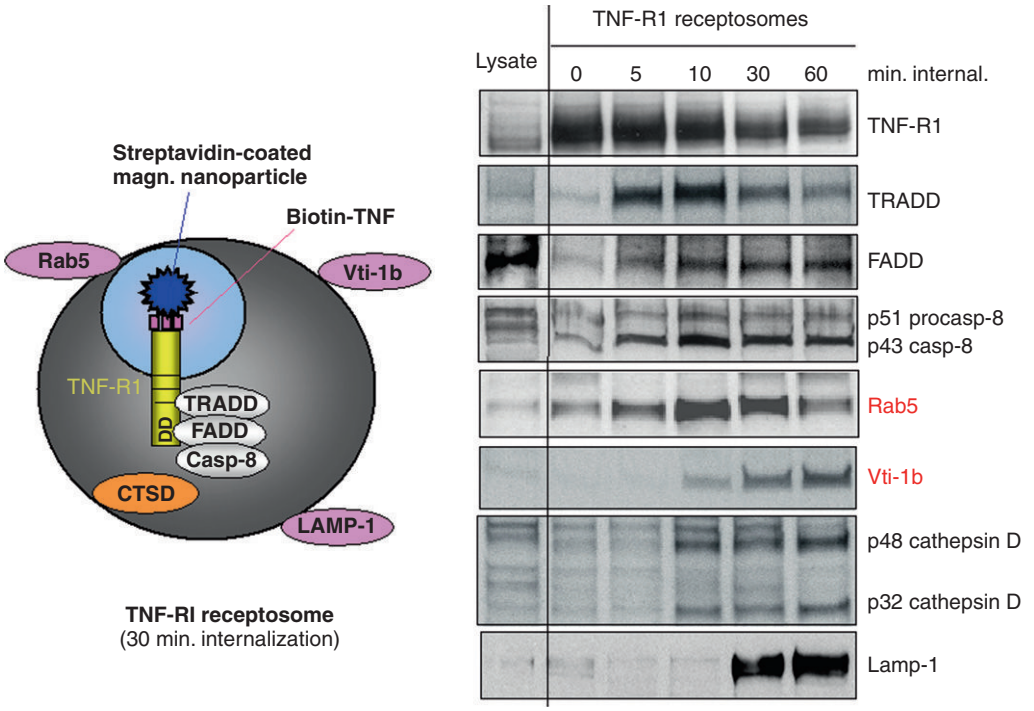

Figure 2. Immunomagnetic isolation of TNF-R1 receptosomes after labelling of TNF receptors with biotin–TNF/streptavidin magnetic beads at various stages of endosomal maturation. TNF receptors on the cell surface were labelled with a complex of biotin–TNF/streptavidin-coated magnetic beads according to Protocol 1. Cells were mechanically lysed at various time points after internalization of the activated receptor. After separation in the free-flow high magnetic gradient chamber, the magnetic fractions were analysed by western blotting for TNF-R1, TRADD, FADD, caspase-8, cathepsin D, Rab5, Vti-1b and LAMP-1.

The high-gradient magnetic chamber described here can also be used to immunomagnetically isolate phagosomes containing magnetically labelled bacteria from infected cells with high efficiency (Steinhäuser *et al.*, manuscript in preparation).

Protocol 2 was designed to immunospecifically isolate intracellular membrane compartments at various steps of vesicular trafficking and maturation, based on the employment of antibodies specific for the organelle of interest. This approach is of particular interest, if biotinylated ligands or antibodies for a specific cell surface receptor are not available, and thus receptosomes cannot be prepared according to Protocol 1.

By coupling antibodies specific for signature proteins of intracellular endosomal trafficking and fusion events such as Rab5, Vti-1b and LAMP-1, we isolated subcellular organelles at various stages of vesicular maturation containing internalized TNF-R1 in early endosomes (Figure 3) and activated TNF-R1-associated signalling complexes such as caspase-8 and cathepsin D in late endosomes/multivesicular organelles (Figure 4).

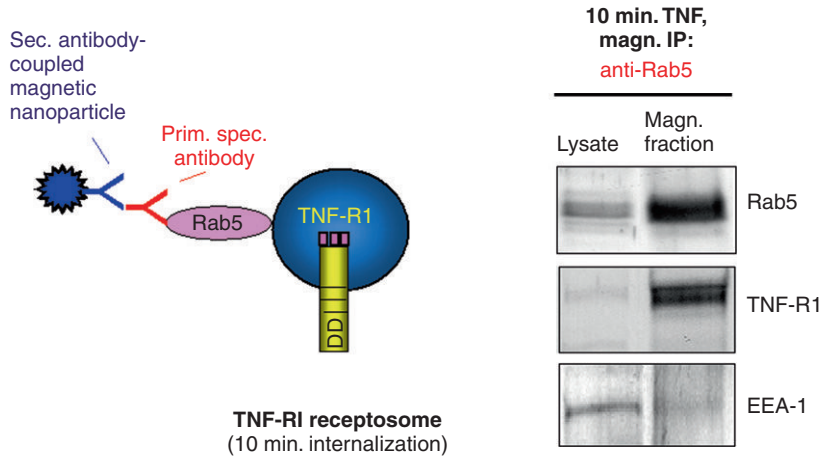

Figure 3. Early endosomes isolated by magnetically tagged anti-Rab5 antibodies contain TNF receptors. Early endosomes were isolated according to Protocol 2: After treatment with TNF for 10 min, U937 cells were mechanically homogenized. One aliquot of the lysate was incubated with anti-Rab5 antibodies coupled to magnetic nanobeads and subjected to our free-flow magnetic chamber. Both the lysates and magnetic fractions were analysed by western blotting for Rab5 and TNF-R1 and the early endosomal antigen (EEA-1). The isolated vesicles represent early endosomes, not yet fused with other membrane compartments (lack of EEA-1) and contain the TNF-R1, which is highly enriched compared with the lysates.

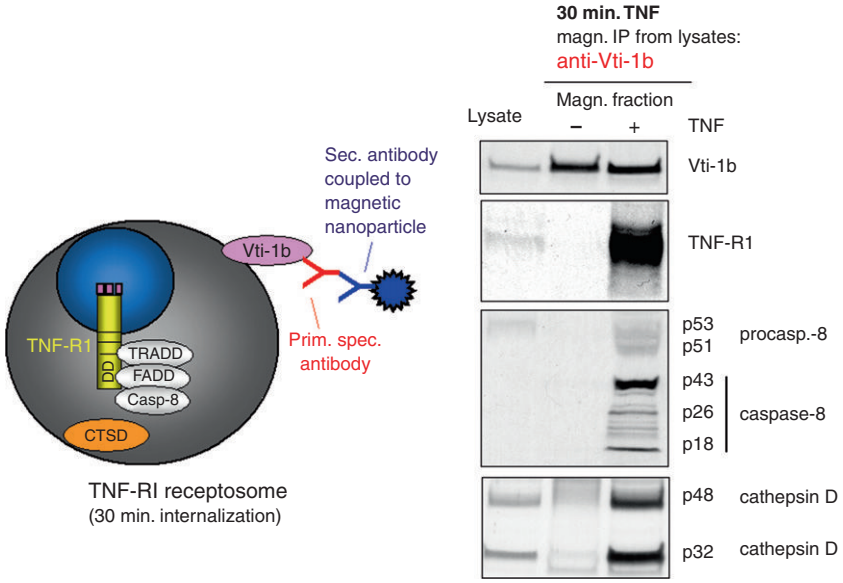

Figure 4. Late endosomes/multivesicular organelles isolated by magnetically tagged anti-Vti-1b antibodies contain TNF receptors and activated caspase-8 as well as cathepsin D. Late endosomal compartments were magnetically isolated following Protocol 2: U937 cells were either left untreated or incubated with TNF for 30 min. Cells were mechanically homogenized and one aliquot of untreated cells and one aliquot of TNF-treated cells were incubated with anti-Vti-1b antibodies coupled to magnetic nanobeads. The labelled organelles were purified in our free-flow magnetic chamber. Both the lysates and magnetic fractions were analysed by western blotting for the trans-Golgi SNARE-protein Vti-1b, TNF-R1, caspase-8 and cathepsin D. TNF-R1 and elements of the TNF-R1 signalling cascade such as activated caspase-8 and cathepsin D are detected.

References

Diettrich, O., Mills, K., Johnson, A. W., Hasilik, A. and Winchester, B. G. (1998). Application of magnetic chromatography to the isolation of lysosomes from fibroblasts of patients with lysosomal storage disorders. *FEBS Lett.* **441**, 369–372.

Feig, C., Tchikov, V., Schütze, S. and Peter, M. E. (2007). Palmitoylation of CD95 facilitates formation of SDS-stable receptor aggregates that initiate apoptosis signaling. *EMBO J.* **26**, 221–231.

Guicciardi, M. E. and Gores, G. J. (2009). Life and death be death receptors. *FASEB J.* **23**, 1625–1635.

Hornig-Do, H.-T., Günther, G., Bust, M., Lehnartz, P., Bosio, A. and Wiesner, R. J. (2009). Isolation of functional pure mitochondria by superparamagnetic microbeads. *Anal. Biochem.* **389**, 1–5.

Kausch, A. P., Owen, T. P. Jr., Narayanswami, S. and Bruce, B. D. (1999). Organelle isolation by magnetic immunoabsorption. *Biotechniques* **26**, 336–343.

Lawson, E. L., Clifton, J. G., Huang, F., Li, X., Hixson, D. C. and Josic, D. (2006). Use of magnetic beads with immobilized monoclonal antibodies for isolation of highly pure plasma membranes. *Electrophoresis* **27**, 2747–2758.

Lee, K. H., Feig, C., Tchikov, V., Schickel, R., Hallas, C., Schütze, S., Peter, M. E. and Chan, A. C. (2006). The role of receptor internalization in CD95 signaling. *EMBO J.* **25**, 1009–1023.

Lemke, J., Noack, A., Adam, D., Tchikov, V., Bertsch, U., Röder, C., Schütze, S., Wajant, H., Kalthoff, H. and Trauzold, A. (2010). TRAIL signaling is mediated by DR4 in pancreatic tumor cells despite the expression of functional DR5. *J. Mol. Med.* **88**, 729–740.

Liao, W., Xiao, Q., Liao, Z., Wincovitch, S., Garfield, S., Yang, W., Tchikov, V., El-Deiry, W., Schütze, S. and Srinivasula, S. M. (2008). CARP-2 is an endosomal ubiquitin protein ligase for RIP and regulates TNF-induced NF-κB activation. *Curr. Biol.* **18**, 641–649.

Mahul-Mellier, A. L., Strappazon, F., Petiot, A., Chatellard-Causse, C., Torch, S., Blot, B., Freeman, K., Kuhn, L., Garin, J., Verna, J. M. *et al*. (2008). Alix and ALG-2 are involved in tumor necrosis factor receptor-1 induced cell death. *J. Biol. Chem.* **283**, 34954–34965.

McPherson, P. S., Kay, B. K. and Hussain, N. K. (2001). Signaling on the endocytic pathway. *Traffic* **2**, 375–384.

Miaczynska, M., Pelkmans, L. and Zerial, M. (2004). Not just a sink: endosomes in control of signal transduction. *Curr. Opin. Cell Biol.* **16**, 400–406.

Miltenyi, S., Müller, W., Weichel, W. and Radbruch, A. (1990). High gradient magnetic cell separation with MACS. *Cytometry* **11**, 231–238.

Mura, M., Becker, I. Orellana, A. and Wolff, D. (2002). Immunopurification of Golgi vesicles by magnetic sorting. *J. Immunol. Methods* **260**, 263–271.

Perrin-Cocon, L. A., Marche, P. N. and Villiers, C. L. (1999). Purification of intracellular compartments involved in antigen processing: a new method based on magnetic sorting. *Biochem. J.* **338**, 123–130.

Peter, M. E., Budd, R. C., Desbarats, J., Hedrick, S. M., Hueber, A. O., Newell, M. K., Owen, L. B., Pope, R. M., Tschopp, J., Wajant, H. *et al*. (2007). The CD95 receptor: apoptosis revisited. *Cell* **129**, 447–450.

Philipp, S., Puchert, M., Adam-Klages, S., Tchikov, V., Winoto-Morbach, S., Mathieu, S., Jung, A., Kolker, L., Marchesini, N., Kabelitz, D., Schütze, S. *et al*. (2010). The polycomb group protein EED couples TNF-receptor 1 to neutral sphingomyelinase. *Proc. Natl. Acad. Sci. USA* **107**, 1112–1117.

Schneider-Brachert, W., Tchikov, V., Kruse, M. L., Lehn, A., Jakob, M., Hildt, E., Held-Feindt, J., Kabelitz, D., Krönke, M. and Schütze, S. (2006). Adenovirus E3-14.7K protein inhibits TNF-induced apoptosis by targeting TNF-R1 endocytosis and DISC assembly. *J. Clin. Invest.* **116**, 2901–2913.

Schneider-Brachert, W., Tchikov, V., Neumeyer, J., Jakob, M., Winoto-Morbach, S., Held-Feindt, J., Heinrich, M., Merkel, O., Ehrenschwender, M., Adam, D. *et al*. (2004). Compartmentalization of TNF receptor 1 signaling: internalized TNF receptosomes as death signaling vesicles. *Immunity* **21**, 415–428.

Schütze, S., Machleidt, T., Adam, D., Schwandner, R., Wiegmann, K., Kruse, M. L., Heinrich, M., Wickel, M. and Krönke, M. (1999). Inhibition of receptor internalization by monodansylcadaverine selectively blocks p55 tumor necrosis factor receptor death domain signaling. *J. Biol. Chem.* **274**, 10203–10212.

Schütze, S., Tchikov, V., Kabelitz, D. and Krönke, M. (2003). German patent DE 101 44 291C2.

Schütze, S., Tchikov, V. and Schneider-Brachert, W. (2008). Regulation of TNF-R1 and CD95 signalling by receptor compartmentalization. *Nat. Rev. Mol. Cell Biol.* **9**, 655–662.

Sorkin, A. and Von Zastrow, M. (2002). Signal transduction and endocytosis: close encounters of many kinds. *Nat. Rev. Mol. Cell Biol.* **3**, 600–614.

Tchikov, V. and Schütze, S. (2008). Immunomagnetic isolation of TNF-receptosomes. *Methods Enzymol.* **442**, 101–123.

Tchikov, V., Schütze, S. and Krönke, M. (1999). Comparison between imunofluorescence and immunomagnetic techniques of cytometry. *J. Magn. Magn. Mater.* **194**, 242.

Tchikov, V., Winoto-Morbach, S., Krönke, M., Kabelitz, D. and Schütze, S. (2001). Adhesion of immunomagnetic particles targeted to antigens and cytokine receptors on tumor cells determined by magnetophoresis. *J. Magn. Magn. Mater.* **225**, 285–293.

Teis, D. and Huber, L. A. (2003). The odd couple: signal transduction and endocytosis. *Cell Mol. Life Sci.* **60**, 2020–2033.

Yazdanpanah, B., Wiegmann, K., Tchikov, V., Krut, O., Pongratz, C., Schramm, M., Kleinridders, A., Wunderlich, T., Kashkar, H., Utermöhlen, O. *et al*. (2009). Riboflavin kinase couples TNF Receptor 1 to NADPH oxidase. *Nature* **460**, 1159–1163.

3 Use of Bioinformatics to Predict MHC Ligands and T-Cell Epitopes: Application to Epitope-Driven Vaccine Design

Anne S De Groot[1,2], Tobias Cohen[1], Matthew Ardito[1], Lenny Moise[1,2], Bill Martin[1] and Jay A Berzofsky[3]

[1] EpiVax, Inc., Providence, RI, USA; [2] Institute for Immunology and Informatics, University of Rhode Island, Providence, RI, USA; [3] Vaccine Branch, Center for Cancer Research, National Cancer Institute, National Institutes of Health, Bethesda, MD, USA

CONTENTS

I. INTRODUCTION

At the heart of the bioinformatics discipline is the concept that biological entities can be described as being composed of patterns. These patterns can be discovered, described and interpreted using computer-driven algorithms, enabling the discovery and comparison of biological entities as well as approximate predictions of their functions. One useful application of pattern matching algorithms is in the identification of major histocompatibility complex (MHC) ligands and T-cell epitopes. In the past two decades, new information has emerged on the peptides that bind to MHC molecules and interact with T-cell receptors to stimulate the immune system. These peptide 'epitopes' are pathogen-derived, and due to their intrinsic pattern of amino acids, they are MHC specific, i.e. restricted in presentation by a limited number of MHC molecules due to their binding specificity. The presentation of these patterned, pathogen-derived T-cell epitopes in the context of MHC is

METHODS IN MICROBIOLOGY, VOLUME 37
0580-9517 DOI 10.1016/S0580-9517(10)37003-6

pivotal to the recognition of self vs. foreign proteins and to the development of both cellular and humoral immune defence against infectious disease.

In recent years, a wide range of computer-driven algorithms have been devised to take advantage of the wealth of proteome information available in public and private databases to search for T-cell epitopes. These algorithms test each subsequence of a given protein for traits thought to be common to immunogenic peptides, thus locating regions with a greater likelihood of inducing a cellular immune response that can be assayed *in vitro*. The use of these algorithms not only significantly reduces the time and effort needed to identify putative T-cell epitopes but also decreases the number of proteins requiring *in vitro* testing for immunogenicity, as well. Thus, the bulk of *in vitro* assays can be focused on evaluating selected candidate T-cell epitopes and immunogenic proteins.

Indeed, informatics approaches to epitope mapping now make it possible to perform high-throughput screening, and comparisons, of entire proteomes for peptides that have immunogenic potential. In one of the first examples to illustrate the use of epitope-mapping tools for analyzing entire genomes, De Groot *et al*. reduced the number of potential peptide epitopes to be screened in the entire proteome of *Mycobacterium tuberculosis* (Mtb) from more than 1.3 million to less than 500, in a first-pass analysis (De Groot *et al*., 2001). Of those 500, 17 were selected for *in vitro* screening of potential immunogenicity and validated *in vitro*. In further studies, performed since 2007, an additional 49 epitopes have been tested, leading to the selection of 39 candidates for further development in a tuberculosis (TB) vaccine. Some interesting aspects of that more recent work will be described in this chapter.

The paradigm underlying vaccine development is that an effective vaccine generates epitope-specific memory immune cells, which drive the adaptive immune response upon exposure to the pathogen. Indeed, some vaccinologists would affirm that all vaccines are 'epitope-driven', since memory T cells are required for effective antibody protection, and a field of epitope-based vaccines has emerged for the production of vaccines that include the minimal essential information needed to elicit protective immune responses. The use of computational tools to screen proteomes for T-cell epitopes has accelerated efforts to develop epitope-based vaccines. As the prediction of B-cell epitopes remains beyond the reach of current immunoinformatics experts, this chapter will discuss bioinformatic tools and methods that are currently being used to mine proteomes for T-cell epitopes and associated algorithms and methods that are currently being applied to the designing and validating T-cell epitope-driven vaccines.

♦♦♦♦♦♦ II. ANTIGEN RECOGNITION BY T CELLS

T cells are activated by direct interaction with antigen-presenting cells (APCs). On the molecular level, the initial interaction occurs between the T-cell receptor and the peptides derived from endogenous and exogenous proteins that are bound in the cleft of MHC class I or class II molecules. In general, MHC class I molecules present peptides 8–10 amino acids in length and are predominately recognized by $CD8^+$

cytotoxic T lymphocytes (CTLs). Class I peptides usually contain an MHC I allele-specific motif composed of two conserved anchor residues (Elliott *et al*., 1991; Falk *et al*., 1991; Rotzschke *et al*., 1991). Peptides presented by class II molecules are longer, more variable in size and have more complex anchor motifs than those presented by class I molecules (Unanue, 1992; Brown *et al*., 1993; Chicz *et al*., 1993). MHC class II molecules bind peptides consisting of 11–25 amino acids and are recognized by $CD4^+$ T helper (Th) cells.

MHC class I molecules present peptides obtained from proteolytic digestion of endogenously synthesized proteins. Host- or pathogen-derived intracellular proteins are cleaved by a complex of proteases in the proteasome. Small peptide fragments are then typically transported by ATP-dependent transporters associated with antigen processing (TAPs) and also by TAP-independent means into the endoplasmic reticulum (ER), where they form complexes with nascent MHC class I heavy chains and beta-2-microglobulin. The peptide-MHC class I complexes are transported to the cell surface for presentation to the receptors of $CD8^+$ T cells (Germain and Margulies, 1993; Cresswell and Lanzavecchia, 2001; Trombetta and Mellman, 2005).

MHC class II molecules generally bind peptides derived from the cell membrane or from extracellular proteins that have been internalized by APCs. The proteins are initially processed in the MHC class II compartment (MIIC). Inside the MIIC, MHC is initially bound to class II-associated invariant chain peptide (CLIP) which protects the MHC from binding to endogenous peptides. Peptides generated by proteolytic processing within endosomes replace CLIP in a reaction catalysed by the protein Human Leukocyte Antigen (HLA)-DM (Appella *et al*., 1995; German *et al*., 1996). The class II molecules bound to peptide fragments are transported to the surface of APCs for presentation to $CD4^+$ helper T cells.

From these different antigen-processing and presentation pathways, two different T-cell responses are generated: a $CD8^+$ CTL immune response and $CD4^+$ Th immune response. Since these two T-cell responses are usually complementary, in terms of controlling infection by pathogens, an efficacious epitope-driven vaccine should induce both a $CD8^+$ and $CD4^+$ response.

♦♦♦♦♦♦ III. APPROACHES TO IDENTIFYING T-CELL EPITOPES FROM PROTEIN SEQUENCES

The major prerequisite for the development of an epitope-driven vaccine, or a genome-derived vaccine of any sort, is the identification of MHC class I or class II ligands that are recognized by T cells. This section will present an overview of two different approaches to identifying T-cell epitopes: the traditional overlapping peptide approach and the newer immunoinformatics approach.

A. Overlapping Method

Identification of T-cell epitopes within protein antigens has traditionally been carried out through a variety of methods, including the commonly employed

'overlapping peptide' method, as well as the method of testing whole and fragmented native or recombinant antigenic protein. The overlapping method involves synthesis of overlapping peptides which span the entire sequence of a given protein antigen, followed by testing the capacity of the peptides to stimulate T-cell responses *in vitro*. This assay was once the standard method for the identification of T-cell epitopes within protein antigens. Implementation of the overlapping peptide method is both costly and labour intensive, especially when applied to whole genomes. For example, to perform an assay using 20 amino acid long peptides overlapping by 10 amino acids spanning a given antigen of length n (a small subset of all possible 20-mers spanning the protein), one would need to construct and test (n/10)–1 peptides. For a protein 600–800 amino acids in length, more than 60 peptides would be synthesized using this approach.

This method still does not ensure the identification of all possible T-cell epitopes, considering that certain epitopes that bridge overlapping fragments could still be missed. A more 'exhaustive' overlapping approach involves manufacturing and examining every possible overlapping peptide (often including 8-mer, 9-mer and 10-mer versions of the same potential epitope), covering the entire protein sequence. While this approach is comprehensive and will identify most T-cell epitopes within the protein, it is prohibitively expensive and labour intensive for most laboratories. Moreover, it has become unnecessary with the advent of computational epitope-mapping methods that can perform exhaustive screens faster and for a lower cost in order to narrow down the epitopes most likely to elicit an immune response before testing *in vitro*.

Due to the rapid accumulation of accurate sequence information for a wide array of protein antigens, the use of algorithms for predicting antigenic sites from primary structure became more widespread. The years spanning 1991 to the present witnessed the development of a large number of computer-driven algorithms that use protein sequence information to search for T-cell epitopes.

B. Brief History of the Informatics Approach to Mapping Epitopes

1. The initial concept: periodicity and MHC-binding motifs

The idea that antigenicity could be predicted by searching for a conserved pattern of amino acids was developed in the late 1980s (DeLisi and Berzofsky, 1985; Stille *et al*., 1987; Rothbard and Taylor, 1988). It was based on empirical observations of the periodicity of amino acid residues in T-cell epitopes. Predictions based on periodicity were a clear improvement over the brute force method of epitope mapping but still did not sufficiently narrow the options, leading to the selection of a large number of false positives (Meister *et al*., 1995).

Improved computer-driven algorithms were made possible by the discovery of MHC-binding motifs (Rotzschke *et al*., 1991). Our understanding of the nature of these binding motifs has been furthered by three major technological advances: crystallographic studies of MHC molecules in complex with peptides, sequencing of naturally occurring MHC peptide ligands by Edman degradation and tandem mass spectrometry, and position-specific frequency analysis (Falk *et al*., 1991; Rotzschke *et al*., 1991; Rammensee *et al*., 1995).

The use of MHC-binding motifs to prospectively identify T-cell epitopes and the first MHC-binding motif-based algorithms were described previously (Sette *et al.*, 1989; Falk *et al.*, 1991; Rotzschke *et al.*, 1991; Lipford *et al.*, 1993; Parker *et al.*, 1994). Further variations on the MHC-binding motif-based method, known as 'extended MHC-binding motifs' or 'peptide side chain scanning' were developed (Ruppert *et al.*, 1993; Sinigaglia and Hammer, 1994). Parker described a further iteration of the MHC-binding motif approach that allowed for the construction of a matrix taking into account all possible amino acid side chain effects for a single MHC-binding motif (Davenport *et al.*, 1995; Jesdale *et al.*, 1997; Parker *et al.*, 2004). A similar approach using synthetic undecapeptides was also developed (Fleckenstein *et al.*, 1996).

2. Matrix-based epitope prediction

EpiMatrix, an algorithm developed by Jesdale and De Groot at Brown University's TB/HIV Research Lab, ranks 9 and 10 amino acid-long segments of a protein that overlap by 8 and 9 amino acids, respectively, based on the estimated probability of binding to a selected MHC molecule. This method for ranking prospective epitopes has been described in detail (De Groot *et al.*, 1997; Schafer *et al.*, 1998). The algorithm was validated through retrospective analysis of known MHC ligands. In its first trial the EpiMatrix algorithm was used to score 158 known ligands eluted from cells presenting peptide in the context of a single HLA as listed in Rammensee *et al*. (1995). The results can be seen in Table 1. In the majority of cases the EpiMatrix

Table 1. An example of the accuracy of epitope-mapping tools for the discovery of HLA ligands

HLA-B7			
Name of protein	Known ligand sequence	Protein length	EpiMatrix rank of ligand
Topoisomerase II	SPRYIFTML	1621	1
EBNA 3A	RPPIFIRRL	812	1
HLA-A2.1 signal sequence	APRTLVLLL	365	1
HLA-DP signal sequence	APRTVALTAL	258	1
Ribosomal S26 protein	APAPPPKPM	107	1
HLA-B7 signal sequence	LVMAPRTVL	255	2
HIV V3	RPNNNTRKRI	90	2
Histone H1	AASKERSGVSL	219	7
EBNA 3C	APIRPIPTRF	983	21

Well known HLA-B7-restricted ligands are shown for each of nine proteins in the table, each of which was initially discovered using the more traditional overlapping or fine mapping method. EpiMatrix (V.1, 1998) was applied to the sequences of these proteins; 10-mers overlapping by 1 were scored for each of the original protein sequences. The rank of the peptide that corresponded to the known ligand is listed in the final column in this table. For example, in the case of topoisomerase II, 1612 10-mers were evaluated and ranked by EpiMatrix score. The 10-mer that was scored the highest by EpiMatrix was identical in sequence to the published ligand for this protein. The published ligand corresponded to the highest ranked EpiMatrix prediction for the same protein in four of the remaining eight cases. A total of 4620 10-mers were scored and ranked by EpiMatrix for this analysis; in seven of nine cases the published ligand would have been correctly identified had only the top two scoring EpiMatrix peptides been synthesized and tested.

Reprinted from De Groot, A. S., Jesdale, B. M., Berzofsky, J. A. (1998). Prediction and determination of MHC ligands and T-cell epitopes. Immunology methods. In: *Methods in Microbiology,* Vol. 25, (S. H. E. Kaufmann, ed), Chapter 3, pp. 79–106, Academic Press, New York, 1998.

algorithm identified the known ligands as having a significant binding potential. In a more recent example EpiMatrix was used to score peptides eluted from the HLA of patients possessing the HLA-DRB1*0301 allele (see Table 2).

Table 2. Sequences of peptides eluted from B cells obtained by bronchiolar lavage of sarcoidosis patients (Wahlstrom *et al*., 2007) were analysed using De Groot and Martin's EpiMatrix (V.1.2, 2009) software. 62/78 (79.5%) of the peptides eluted from HLA DRB1 0301 molecules were ranked by EpiMatrix as having a *Z*-score of 1.28 or greater for the DRB1 0301 matrix (top 10% of scores, indicating high likelihood of binding)

Peptides Eluted off of DRB1*0301 in Bronchiolar Lavage Fluid of Sarcoidosis Patients			
Peptide Eluted	Gene Name	Highest EpiMatrix Assessment	9-mer Identified by EpiMatrix
SSKFQVDNNNRL	α-2-Macroglobulin	3.24	
EQAFQGDESVRIDA	Low-density lipoprotein-related protein 1	2.95	
ITSIVKDSSAARNGL	Syndecan-binding protein	2.78	
YKFQNALLVRYT	Albumin	2.78	
NKNYRIDTINLFP	Ceruloplasmin	2.74	
HAFILQDTKALHQV	Complement component 2	2.63	
KAVLTIDEKGTEAA	α-1-Antitrypsin	2.5	
FLKKYLYEIARRHPY	Albumin	2.47	YEIARRHPY
LEIFKQASAFSRAS	TGF, β-induced 68 kDa	2.43	FKQASAFSR
NTLYLQFNSLRAEDT	Ig heavy chain V region	2.4	
VKEPVAVLKANRVWGAL	Hexosaminidase B	2.32	
EAQGALANIAVDKAN	MHC class II, DR α	2.29	IAVDKANXX
ETVITVDTKAAGKGK	Filamin A, α	2.28	
KPEPELVYEDLRGSVTFH	Polymeric immunoglobulin receptor	2.23	
DPQTFYYAVAVVKKDSG	Transferrin	2.2	VKKDSGXXX
KSTITLDGGVLVH	Fatty acid-binding protein 4	2.17	
DKPVYTPDQSVKVRV	Complement component 5	2.16	YTPDQSVKV
TPTLVEVSRNLGKVG	Albumin	2.15	
NPANPAILSEASAPIPH	Syndecan-binding protein	2.12	
RVVTELGRPSAEYWNSQKDLLE	HLA-D class II antigen DR1 β chain	2.09	YWNSQKDLL
VARIVGNSGLNIYNL	Cathepsin A	2.06	
HNNYQAQSAVPLRHE	Alkaline phosphatase, liver/bone/kidney	2.01	
YLQMNSLRAEDT	Ig heavy chain V region	2.01	YLQMNSLRA
FLRFDSDVGEY	MHC class II, DR β 3	1.92	
SGTLVLLQGARGFA	CD14 molecule	1.89	LLQGARGFA
SVRFDSDVGEY	MHC class II, DR β 1	1.87	

(*Continued*)

Table 2 (*Continued*)

Peptides Eluted off of DRB1*0301 in Bronchiolar Lavage Fluid of Sarcoidosis Patients

Peptide Eluted	Gene Name	Highest EpiMatrix Assessment	9-mer Identified by EpiMatrix
VPPVQVSPLIKLGRYSAL	ATP synthase, subunit E	1.81	VQVSPLIKL
VEQGLLDKPVFSF	Napsin A aspartic peptidase	1.76	GLLDKPVFS
DTKVYTVDLGRTVTI	Polymeric immunoglobulin receptor	1.7	VDLGRTVTI
KVNVDAVGGEALGRL	Haemoglobin, δ	1.66	
TPGTEYVVSIVALNGRE	Fibronectin 1	1.61	VSIVALNGR
KVNVDEVGGEALGRL	Haemoglobin, β	1.6	
RETNLDSLPLVDTHSKRTLL	Vimentin	1.6	DTHSKRTLL
GPEGQAYDVDFTPPFR	Lysyl-tRNA synthetase	1.54	
RPVAESWNSQKDLLE	MHC class II, DR β 3	1.5	SQKDLLEXX
KDLFKAVDAALKK	Kininogen 1	1.48	
DSLPLVDTHSKRTX	Vimentin	1.42	PLVDTHSKR
EKNIMLYKGSGLWS	Mannose receptor, C type 1	1.41	YKGSGLWSX
IKEEHVIIQAEF	MHC class II, DR α	1.4	IIQAEFXXX
AIFFLPDEGKLQ	α-1-Antitrypsin	1.32	FLPDEGKLQ

This table lists the peptides that had a score higher than 1.28, duplicates not included. The highest scoring 9-mer frame in 37/62 (60%) of the original peptides was the same 9-mer as identified by Wahlstrom *et al*. The fine-mapped 9-mer identified by Wahlstrom *et al*. is underlined in the leftmost column, and, for comparison, if EpiMatrix identified a different higher scoring 9-mer, it is listed in the rightmost column.

Wahlstrom, J., Dengjel, J. *et al*. (2007). Identification of HLA-DR-bound peptides presented by human bronchoalveolar lavage cells in sarcoidosis. *J. Clin. Invest* **117**(11), 3576–3582.

3. 'Pocket profile' method

The teams of Hammer, Sturniolo *et al*. and Zhang, Anderson and DeLisi could be credited with another important advance in epitope mapping in 1999: this is the 'pocket profile' method. According to this method, similarities in MHC binding constraints are reflected in commonalties in the composition of MHC-binding pockets. This allows new motifs to be developed by mixing and matching binding pocket characteristics (Zhang *et al*., 1998; Sturniolo *et al*., 1999). The technique has also been applied to the identification of bovine T-cell epitopes (De Groot *et al*., 2003) and was also adopted for current pocket profile versions of EpiMatrix (class II epitope predictions) used by De Groot and Martin since 2002.

The concept underlying the pocket profile method is that the binding pockets of MHC are highly conserved between MHC molecules. Crystallographic studies of peptide/MHC class II complexes have identified the presence of nine 'binding pockets', which determine a given allele's peptide specificity. Each binding pocket can be described in terms of the amino acids that are likely to bind, or not bind, in that pocket. This set of amino acids is termed the 'pocket profile' (Sturniolo *et al*., 1999). Although there are many different HLA alleles, the number of different

binding pocket types (with a corresponding pocket profile) is much smaller. Different alleles appear to have evolved by a process of mixing and matching binding pockets. This observation led to the concept that the binding properties of an allele could be described by listing its constituent pocket types. Of the nine binding pockets, those located in positions 1, 2 and 3 appear to show very little difference between alleles. The greatest variation is observed in pockets 4 through 9. Due to the helical nature of MHC ligands, peptide side chains are usually directed away from the binding groove in pockets 5 and 8. Consequently, these pockets play little part in peptide binding, and the significant differences for most of the class II alleles appear to come from variation in pocket profiles for epitope positions 1, 4, 6, 7 and 9. By mixing and matching the pocket types, Sturniolo created 35 different class II binding profiles.

Careful review of the Sturniolo *et al.* (1999) data enabled EpiMatrix developers James Rayner and Bill Martin to regenerate the 35 binding profiles and to generate predictive matrices for over 90 MHC alleles [(Rayner and Martin), unpublished; De Groot *et al.*, 2003)]. These class II matrices are now included in the EpiMatrix repertoire.

4. Artificial neural networks and hidden Markov models

Other bioinformatics approaches to predicting T-cell epitopes have also emerged, including artificial neural networks (ANNs) (Brusic *et al.*, 1994) and structural (three-dimensional) modelling approaches (Altuvia *et al.*, 1995; Rosenfeld *et al.*, 1995). ANNs are computational models that are analogous to the brain in that they generate outputs based on the overall flow of numerous, small, simple pathways. ANNs actively 'learn' from their predictions and adapt their parameters on their own. ANNs require a large known database to start, and the peptides must be entered into the algorithm based on their anchor residues. This poses a problem for predicting binding in the open-ended class II MHC molecules, as the amino acid residues responsible for binding to MHC may not be as easily defined as they are for class I (Brusic *et al.*, 2004). For class I predictions, where larger well-defined training sets are available, ANNs have been shown to be more accurate than certain older matrix model systems such as SYFPETHI and BIMAS (Yu *et al.*, 2002).

Hidden Markov models (HMMs) have become popular for MHC-binding prediction because of their ability to manage the stochastic nature of biological systems. In the context of epitope prediction, a large data set of known binders is used to develop a model that can estimate the probability of a given sequence being capable of binding MHC. The model is called 'hidden' because when using the model, one does not know exactly the probabilities of each state or the path that the model takes to arrive at the conclusion. Over time though, an HMM can continue to learn as more known binders are added and thus improve its accuracy (Mamitsuka, 1998).

A list of epitope-mapping tools, ancillary algorithms and their comparative features are provided in Table 3. A number of these epitope-mapping tools are available to researchers for use via the web, including the tool available at the SYFPEITHI website (Rammensee *et al.*, 1999), and the HLA-binding prediction

Table 3. A small set of examples of the many different types of T-cell epitope prediction tools available on the internet

List of Epitope and Proteasomal Cleavage Prediction Tools

Name	*Mechanism*	*Services*	*URL*
BIMAS	Matrix	MHC Binding (Class I)	http://www-bimas.cit.nih.gov/molbio/hla_bind/
EpiDock	Homology Modelling	MHC Binding (Class I)	http://bioinfo-pharma.u-strasbg.fr/template/jd/pages/download/download.php
EpiJen	Matrix	Proteasome Cleavage, TAP transport, and MHC Binding (Class I)	http://www.jenner.ac.uk/EpiJen/
EpiMatrix	Matrix	MHC Binding (Class I and II)	http://epivax.com
EpiPredict	Matrix	MHC Binding (Class II)	http://www.epipredict.de/index.html
Epitope Predictor	Logistical Regression	MHC Binding (Class I)	http://atom.research.microsoft.com/bio/epipred.aspx
IEDB	ANN, SMM, Average Relative Binding Matrices	MHC Binding (Class I and II), TAP Transport, and Proteasome Cleavage	http://tools.immuneepitope.org/main/html/tcell_tools.html
MHCPRED	Matrix	MHC Binding (Class I and II)	http://www.jenner.ac.uk/MHCPred/
MULTIPRED	ANN, HMM	MHC Binding (Class I and II)	http://research.i2r.a-star.edu.sg/multipred/
NetChop	ANN	Proteasome Cleavage	http://www.cbs.dtu.dk/services/NetChop/
PAProC	ANN	Proteasome Cleavage	http://www.paproc.de/
ProPred	Matrix	MHC Binding (Class II)	http://www.imtech.res.in/raghava/propred/
ProPred-I	Matrix	MHC Binding (Class I)	http://www.imtech.res.in/raghava/propred1/
RANKPEP	Matrix	MHC Binding (Class I and II) and Proteasome Cleavage	http://bio.dfci.harvard.edu/Tools/rankpep.html
SMM	Matrix	MHC Binding (Class I)	http://zlab.bu.edu/SMM
SYFPEITHI	Matrix	MHC Binding (Class I and II)	http://www.syfpeithi.de/

TAP, transporters associated with antigen processing; HMM, hidden Markov model; MHC, major histocompatibility complex.

tool available on the site authored by Ken Parker at the National Institutes of Health (BIMAS) (Parker *et al.*, 1994). A recently developed set of tools has been made available through the Immunome Epitope Database; these tools have been described and validated (Wang *et al.*, 1998) and compared to EpiMatrix (De Groot and Martin, 2009) using, as a gold standard, epitopes published in the Immune Epitope Database. While none of these sites returns exactly the same predictions, all are reasonably accurate. In general, the newer and more actively maintained algorithms tend to outperform the older more static predictive methods. For an excellent review of methods used for epitope prediction, see Tong *et al.* (2007).

5. iTEM analysis

In contrast to ClustiMer, an ancillary algorithm to EpiMatrix, which identifies peptides that will be likely to bind multiple HLA molecules, individualized T-cell epitope measure (iTEM) analysis determines how likely a peptide is to be presented by an individual according to his/her HLA type. iTEM is an allele-specific scoring system developed by De Groot and Martin that can be calculated for any peptide analysed by EpiMatrix.

The overall iTEM score for a peptide to be recognized by an individual is the sum of the iTEM scores for that peptide for each of the person's HLA alleles. iTEM scores are essentially a measurement of deviation from the average and are algebraically calculated from EpiMatrix scores. When EpiMatrix analyses peptides for their HLA-binding ability, it normalizes the scores its matrix yields against its large training database and presents users with a *Z*-score for each 9-mer frame. The higher the *Z*-score, the more likely the peptide is to bind to that HLA molecule. iTEM analysis compares the scores of a peptide for a specific allele against the scores one would expect from a randomly generated peptide of the same length. The iTEM score is simply the difference between these two values. In class II binding, for example, if the sum of the scores for the DRB1* alleles is greater than 2.06, the peptide is considered likely to bind and be presented by that individual's HLA. For a more detailed description on how to calculate iTEM scores (see Figure 1).

Frame start	AA Sequence	Frame stop	Hydro-phobicity	DRB1*0101 Z-Score	DRB1*0301 Z-Score	DRB1*0401 Z-Score	DRB1*0701 Z-Score	DRB1*0801 Z-Score	DRB1*1101 Z-Score	DRB1*1301 Z-Score	DRB1*1501 Z-Score	Hits
1	VDVFKLWLM	9	1.38								1.44	0
2	DVFKLWLMW	10	.81					1.47				0
3	VFKLWLMWR	11	.70								1.29	0
4	FKLWLMWRA	12	.43			1.32			1.63			0
5	KLWLMWRAK	13	–.31									0
6	LWLMWRAKG	14	.08	1.98	1.67			2.29	2.80	1.70	1.34	5
7	WLMWRAKGT	15	–.42	1.77		2.22	2.58		1.66			4
8	LMWRAKGTT	16	–.40					1.37				0
9	MWRAKGTTG	17	–.87	1.69	1.35	1.53				1.31	1.55	1
10	WRAKGTTGF	18	–.77				1.66	2.05		1.33		2
11	RAKGTTGFE	19	–1.06									0
12	AKGTTGFEA	20	–.36									0
13	KGTTGFEAH	21	–.91									0

Summarized Results (02-DEC-2009)	DRB1*0101	DRB1*0301	DRB1*0401	DRB1*0701	DRB1*0801	DRB1*1101	DRB1*1301	DRB1*1501
Sum of Significant Z Scores	5.44	1.67	2.22	4.24	4.34	4.46	1.70	.00

0701 iTEM = 4.24–(13*.0.05*2.06) = 2.90

1101 iTEM = 4.46–(13*.0.05*2.06) = 3.12

0701/1101 iTEM = 2.90 + 3.12 = 6.02

Figure 1. Calculating an iTEM score for a single peptide–allele combination. Using the EpiMatrix report for a peptide, the iTEM score is equal to the difference between the sum of significant scores for an allele (DRB1*1101 in this example) and a peptide constant. The peptide constant is equal to the product of the number of frames (13 in this example) and 0.103. The peptide constant is the average score for a peptide of a given length. The iTEM score for this peptide on DRB1*1101 is 3.121, indicating that there is a high probability this peptide will be presented in people with DRB1*1101.

iTEM analysis is proving to be a powerful predictive tool and has the potential for a range of applications in immune profiling for vaccines and protein therapeutics. Cohen *et al*. (unpublished) have found that while overall iTEM score does not always correlate directly with the strength of the response, it can still be used as a benchmark to determine whether or not an individual is likely to respond to a given epitope. In other words, overall iTEM scores can be used as a binary test, with a threshold over which a peptide is likely to bind an individual's HLA. Overall iTEM scores often have positive predictive power in the 80% range, but their negative predictive power can be over 90%. By allowing researchers to calculate the HLA-binding potential of peptides for an individual, iTEM can be used to help analyse variability in immunogenicity evaluations of infection or vaccine responses in individuals. Moreover, it may one day play a role in mapping epitopes to design vaccines for individuals, which would be a realization of the (immuno)pharmacogenomics dream. Taken collectively these tools allow researchers to quickly and effectively identify T-cell epitopes that can be used to design epitope-based vaccines (below).

♦♦♦♦♦♦ IV. APPLIED EPITOPE MAPPING: ANALYZING THE Mtb PROTEOME

The genomes of nearly 5700 organisms can be found on the National Center for Biotechnology Information website (http://www.ncbi.nlm.nih.gov/sites/entrez?db=genome, accessed 27 July 2009). It is now possible to scan an entire genome for T-cell epitopes and subsequently develop a vaccine candidate. The laboratory standard strain *of* Mtb known as H37Rv has been sequenced by the Pasteur Institute, and it can be directly downloaded from the Sanger Centre: http://www.sanger.ac.uk/Projects/M_tuberculosis/M_tuberculosis.embl.gz (Cole *et al*., 1998). The entire sequence of a clinical isolate of Mtb (CDC strain 1551) is available at the TIGR website (http://www.tigr.org/tigr-scripts/CMR2/GenomePage3.spl?database=gmt, accessed 27 July 2009) (Delcher *et al*., 1999).

Epitope-mapping tools can be applied to the analysis of single proteins or entire proteomes. An overview of our approach to develop vaccine candidates for tularemia and TB is illustrated in the next few paragraphs and outlined in Figures 2 and 3.

A. Rationale for Mtb genome scan

Both $CD8^+$ and $CD4^+$ T cells are involved in the cell-mediated immune defence against TB. $CD4^+$ T cells orchestrate the activation of Mtb-infected macrophages through gamma-interferon release and marshal other components of cellular immune defence to the locus of Mtb infection. It is generally believed that ideal TB vaccine-component peptides or antigens would be (a) recognized by the $CD4^+$ and $CD8^+$ lymphocytes of Mtb immune individuals, (b) stimulate Th1-type

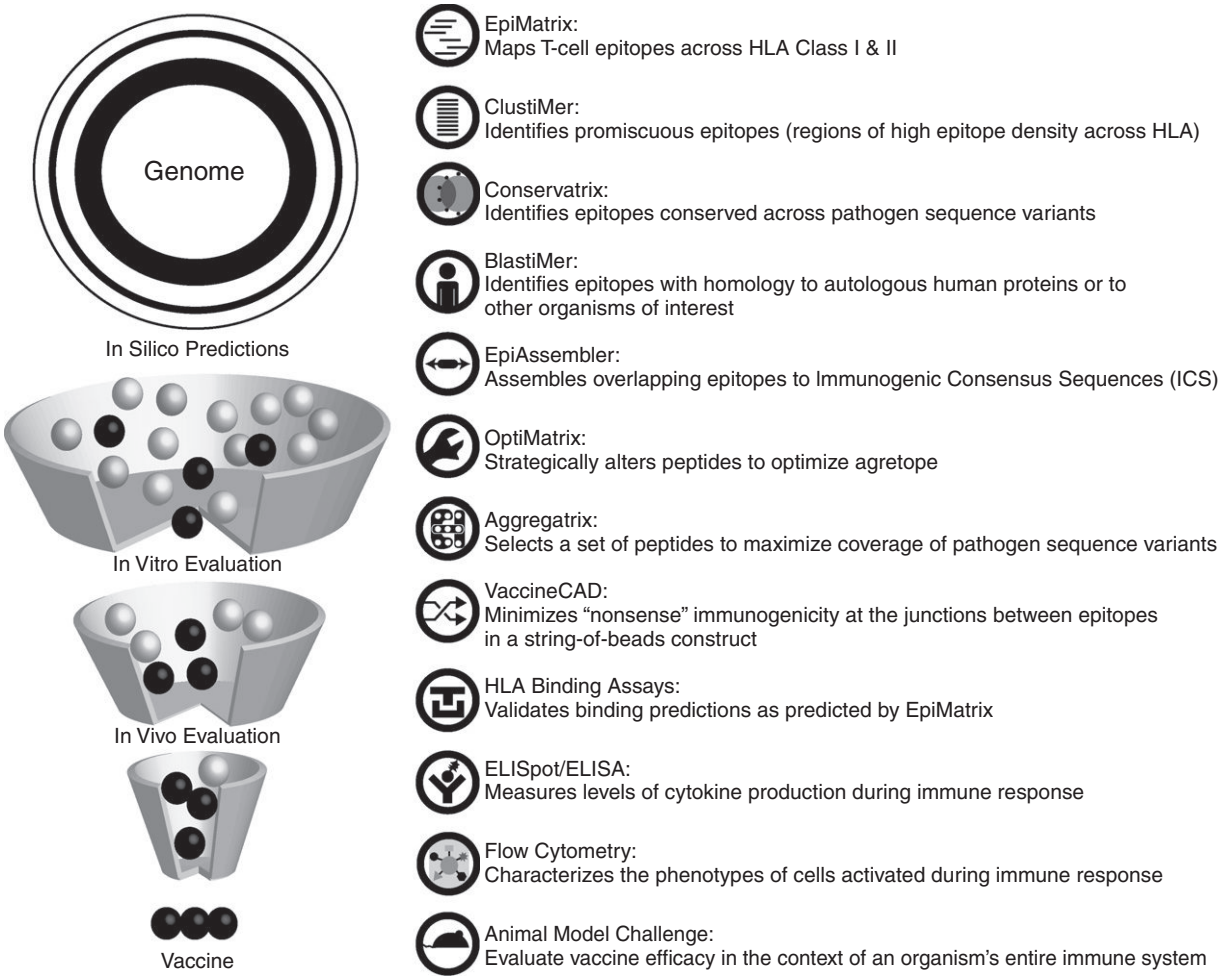

Figure 2. How the EpiMatrix tools designed by De Groot and Martin are used in the genome to vaccine pathway is shown.

responses including gamma-interferon secretion (Flynn *et al.*, 1993; Winslow *et al.*, 2008) and (c) activate macrophages, especially since non-protective and even destructive anti-TB antibodies are formed during TB infection (Glatman-Freedman and Casadevall, 1998).

I. Selection of antigen targets

The criteria for Mtb antigen selection for the development of TB vaccines have been vague at best. The failure of killed Mtb bacteria to elicit protection has led investigators to believe that secreted antigens are critical to immunity (Winslow *et al.*, 2008), and until recently, researchers have been proceeding with the evaluation of

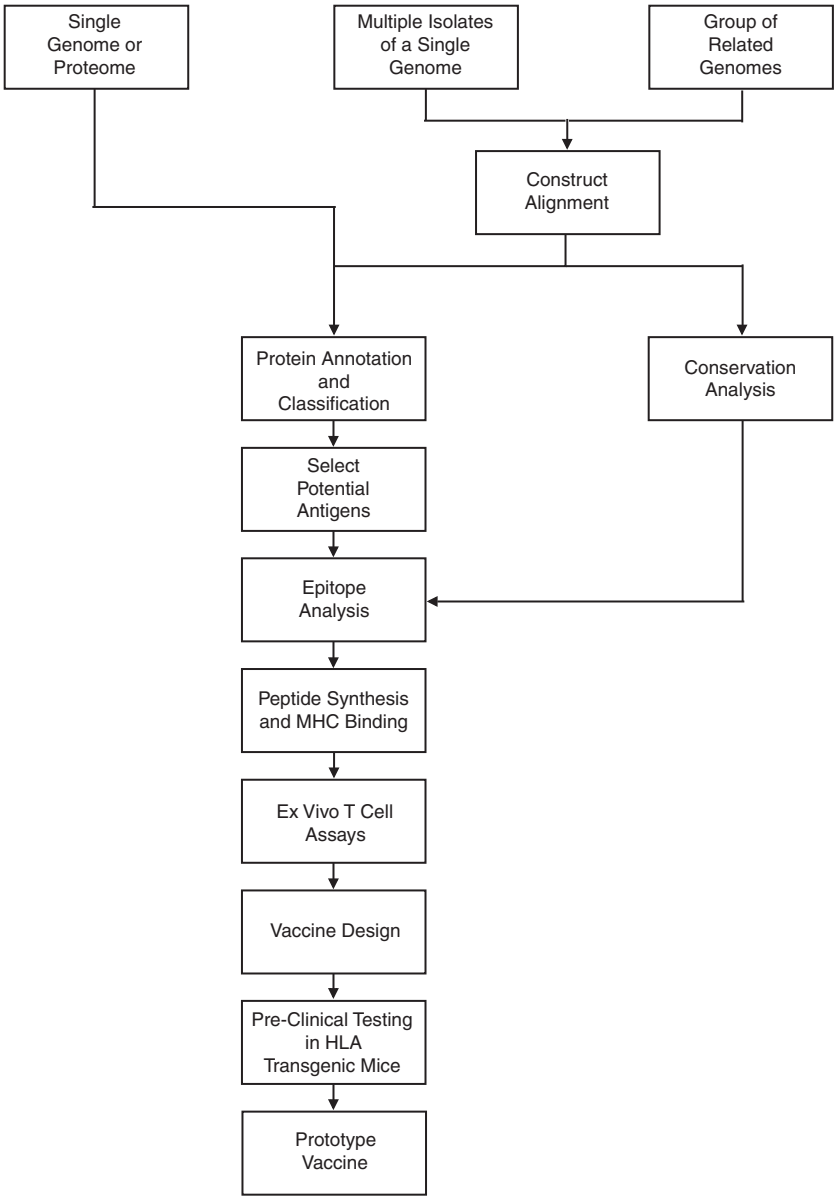

Figure 3. Illustration of several epitope-based vaccine pathways. Vaccinologists start with a pathogen's proteome, genome or multiple genomes. During *in silico* analysis, before commencing epitope analysis it is best to triage the proteins by classifying them using methods such as 2D SDS PAGE gels (2D PAGE), mass spectrometry (MS) and/or tandem MS (TMS), microarrays or bioinformatics approaches (searching for secretion tags, for example) to identify proteins of interest. If more than one genome exists either due to a variable pathogen or because a multi-pathogen vaccine is desired, then it is necessary to identify conserved regions or align the genomes to create one single genome. If the genome is small enough, it could be put directly through epitope analysis. After *in silico* analysis, the predicted epitopes are confirmed via binding and immunogenicity assays. After *in vitro* testing, a vaccine construct is usually ready for *in vivo* analysis in an effective animal model. If the animal model is successful, the vaccine prototype can often move into clinical trials.

secreted Mtb antigens one fraction at a time, using 2D gels to separate candidate antigens (Sonnenberg and Belisle, 1997). The current availability of the two whole Mtb proteomes has made it feasible to scan every one of more than 4000 putative genes for secretion signals. Algorithms such as SignalP (http://www.cbs.dtu.dk/services/SignalP/, accessed 31 August 2009) identify proteins with signal sequences that target proteins for secretion or lack of transmembrane domains using HMMs or ANNs. The other principal group of likely Mtb antigens is proteins that are upregulated during the initial growth period in the macrophage under hypoxic conditions, as described by Sherman *et al*. (2001). cDNA libraries generated by Mtb cultured in hypoxic conditions have elucidated these proteins.

In collaboration with Sherman, groups of secreted and hypoxic proteins, known as genome scans (GS)-1 and GS-2, respectively, were run through EpiMatrix, and using ClustiMer, 10- to 20-mer peptides that contained dense areas of 9-mers highly likely to bind to multiple HLA class II alleles were identified. These peptides, along with flanking residues, were analysed for homology to human sequences (as identified via a BLAST alignment using BlastiMer). If a peptide possessed 70% or greater homology to human, it was removed from the set of peptides to be tested as these peptides were believed to have the potential to elicit autoimmune responses. While epitopes from well-known TB proteins were identified in this manner, several of the proteins identified using this approach had unknown functions and were classified as 'hypothetical proteins' in the genome database. Epitopes were prepared as synthetic peptides to evaluate their immunogenicity in HLA A2/DR1 transgenic mice. Peptides were formulated in liposomes with CpG oligodeoxynucleotide (ODN) adjuvant and delivered subcutaneously. Of 67 epitopes tested, 36 elicited statistically significant responses in ELISpot measurements of gamma-interferon production by peptide-stimulated splenocytes from immunized mice in comparison to those not immunized. Importantly, based on iTEM analysis, responses to 50 of the 66 peptides (76%) correlated with EpiMatrix predictions, statistically significant proof that iTEM can be used to predict whether an immune response to a given epitope will be observed *in vivo* ($X^2 = 16.79$, df = 1, $p < .001$). In a pilot study evaluating the immunogenic epitopes for efficacy in a live aerosol challenge of peptide-immunized HLA A2/DR1 transgenic mice using the laboratory strain of Mtb, H37Rv, the peptides performed nearly as well as the current TB vaccine, BCG. This result is remarkable considering the simple vaccine design. In future studies, epitopes will be delivered in a DNA-prime/peptide-boost strategy, which promises to elicit more robust and durable responses. Importantly, this candidate Mtb vaccine was designed and tested for immunogenicity and efficacy in a mouse model in a matter of less than a year from the start of epitope prediction.

Another instance of vaccine design accelerated by computational epitope mapping comes from our recent efforts to produce a safe and effective vaccine against *Francisella tularensis*, a highly infectious intracellular bacterial pathogen thought to be a potential bioterror agent. Roughly 500,000 possible class II epitopes were computationally screened in two scans of the *F. tularensis* SCHUS4 genome (McMurry *et al*., 2007). Twenty seven epitopes were selected for experimental validation in HLA-binding assays and antigenicity studies using PBMCs obtained from tularemia survivors. Of these, 14 epitopes were shown to be immunogenic by

DNA-prime/peptide-boost vaccination in an HLA transgenic mouse model and efficacious in lethal respiratory challenge with live vaccine strain tularemia (Gregory *et al*., 2009). What could have taken 5 years or more by conventional epitope-mapping methods required about 2 years using immunoinformatics. These studies are proof-of-principle that vaccine design can be dramatically accelerated when computer-driven epitope-mapping tools are systematically applied to screen whole genomes with follow-up studies to confirm epitope predictions.

♦♦♦♦♦♦ V. EPITOPE-DRIVEN VACCINE DESIGN

The concept of epitope-based vaccines emerged soon after the tools to identify epitopes became available (Whitton *et al*., 1993; Hanke *et al*., 1998; Thomson *et al*., 1998; Wang *et al*., 1998; Velders *et al*., 2001). The epitope-based approach to vaccine design may best be described through an analogy: an *epitope* is to a *pathogen* as a *word* is to a *language*. Thus, even a single epitope may signal the presence of an infection to the immune system and stimulate a protective response, just as a single word (*bonjour*, for example) reminds the hearer of a certain language (Olsen *et al*., 2000). Due to genetic restriction, different words, or epitopes, are required to stimulate the immune system in the context of different MHC backgrounds. Also, multiple epitopes are needed to prevent immune evasion by mutation. By extending the analogy, researchers have hypothesized that a protective immune response to an entire pathogen might be generated by recognition of a repertoire of epitope 'words' derived from the proteins of the pathogen. This method of basing vaccine design on regions of pathogens that are presented by MHC molecules was termed 'reverse immunogenetics' (Davenport and Hill, 1996). An alternative term suggested here would be 'epitope-driven vaccine design' (De Groot *et al*., 2001).

The epitope-driven vaccine is an attractive concept that has been pursued in a number of laboratories since the mid-late 1990s (An and Whitton, 1997; Hanke *et al*., 1998). Multiple complex vaccines containing Th- and B-cell epitopes alongside CTL epitopes, all derived from a variety of pathogens, have already been constructed and tested (Tine *et al*., 1996; An and Whitton, 1997).

Epitope-based vaccines are frequently formulated as minigenes for genetic immunization. A basic epitope-based DNA vaccine construct contains a start codon with one epitope after another following in series, with or without intervening spacer amino acids at epitope junctions. *In vitro* studies of the earliest epitope-driven constructs have confirmed that the minigenes were expressed, that they stimulated a protective immune response and that the epitopes did not compete with one another for presentation to T cells (Whitton *et al*., 1993). Another common approach is to mix several plasmids together, each of which encodes a different multi-epitope protein. In general, this approach is expected to have no adverse effects, may elicit an enhanced response over vaccination with a more limited antigen set and may have responses shifted towards the Th1 phenotype (Morris *et al*., 2000). Together, these findings suggest that epitope-based vaccines are a reasonable and feasible approach to vaccine design.

One of the driving principles behind epitope-based vaccines is that they should deliver the smallest amount of a pathogen needed to stimulate a protective immune response. As both $CD4^+$ and $CD8^+$ T cells are critical for the generation of an effective immune response, an epitope-driven vaccine should provide T-cell epitopes presented by different MHC class I and class II alleles, as well as several epitopes for each HLA allele. Maximizing for MHC allele coverage and careful selection of promiscuous epitopes allow for the largest population to be protected by the vaccine; optimizing for strain coverage of a variable pathogen ensures that each recipient of the vaccine will be protected against the largest number of strains possible. De Groot and Martin have developed a suite of computational algorithms that address these vaccine design parameters (Figure 2). ClustiMer is used with EpiMatrix to map MHC motif matches along the length of a protein and calculate the density of motifs for eight common class II HLA alleles: DRB1*0101, DRB1*0301, DRB1*0401, DRB1*0701, DRB1*0801, DRB1*1101, DRB1*1301 and DRB1*1501. Typical T-cell epitope 'clusters', also known as promiscuous epitopes, range from 9 to roughly 25 amino acids in length and considering their affinity to multiple alleles and across multiple frames, they can contain anywhere from 4 to 40 binding motifs. These eight class II alleles were selected for use with ClustiMer because they are both common in human populations, and have relatively distinct pocket profiles. Collectively, these matrices cover the most common class II HLA-binding pockets and 95% of the human population (Southwood *et al*., 1998).

The Conservatrix algorithm is used to identify highly conserved peptide segments contained within multiple isolates of variable pathogens such as retroviruses. The amino acid sequences of protein isolates are parsed into 9-mer frames overlapping by eight amino acids. The resulting peptide set is summarized yielding a list of unique segments and appearance frequencies. Highly conserved sequences are thought to be important to the evolutionary fitness of the pathogen and are thus likely to be changed in an attempt to evade the immune system. Conserved sequences can be analysed using any epitope prediction software so that one obtains a set of sequences that are both immunogenic and conserved.

Once the most immunogenic and conserved epitopes in a pathogen have been identified, an algorithm can be used to create a vaccine that maximizes coverage across MHC alleles and pathogen strains while minimizing the amount of foreign material to be formulated in a vaccine. De Groot *et al*. coded an algorithm named Aggregatrix that maximizes strain coverage (Conservatrix output) and HLA coverage (EpiMatrix output) to select the smallest set of epitopes that would be recognized by the largest possible segment of the human population to protect against the widest variety of pathogenic strains. Aggregatrix has been applied to epitope-driven HIV vaccine design to identify epitope sets conserved over time, geography and clade (De Groot *et al*., 2008).

1. Epitope strings: spacers, alignment and flanks

Enhancing the immunogenicity of multi-epitope vaccines has been approached in several ways. One option is to present the epitopes as a 'string of beads', without any spacer sequences separating the individual epitopes. Indeed, some studies

have indicated that flanking sequences have minimal effects on epitope presentation (An and Whitton, 1997). Yet, in a 'string of beads' construct individual epitopes are very closely apposed, without their natural flanking sequences, which has raised concerns that optimal proteolytic processing of the epitopes of interest may be compromised and that other epitopes may be generated as a result (Moudgil *et al*., 1998; An and Whitton, 1999). To address this issue, spacer sequences were introduced to separate individual epitopes to help focus the immune response on the epitopes of interest (Livingston *et al*., 2001; Livingston, 2002). A study by Velders *et al*. compared the immunogenicity of two similar HPV-epitope string DNA constructs that differed only in the presence or absence of spacers between the epitopes. It was found that the addition of AAY spacers between the epitopes was crucial for epitope-induced tumour protection (Velders *et al*., 2001).

Although a potentially good solution, spacers may introduce epitopes that are homologous to naturally occurring human epitopes and lead to regulatory T-cell activation that could weaken the response to the vaccine, or even worse, generate an autoimmune response. De Groot and Martin therefore developed the VaccineCAD algorithm, which arranges putative T-cell epitopes to create optimized 'string-of-beads' vaccine immunogens without spacers. VaccineCAD (Computer-Assisted Design) arranges randomly ordered T-cell epitopes to create an optimized epitope order for vaccination, eliminating any pseudo-epitopes at the junction between two epitopes.

2. Costimulatory molecules

Costimulatory molecules play a central role during the initiation of T-cell immune responses (Kuchroo *et al*., 1995). CD28 and CTLA4 represent the costimulatory receptors on T cells, and B7 molecules represent their corresponding ligands on APCs. Several studies carried out in murine models demonstrated the signal mediated via CD28 is required for TCR-mediated T-cell activation, whereas CTLA4 has an antagonistic role in T-cell activation. The cognate ligands for CD28 and CTLA4 expressed on APCs are B7-1 (CD80) and B7-2 (CD86), the initial two members of the B7 family discovered. These two molecules show comparable affinity to CD28 molecules and differentially activate Th1 or Th2 immune responses (Kuchroo *et al*., 1995).

Lack of costimulation can lead to T-cell anergy. Peptide epitopes presented by non-professional APCs may fail to activate T cells if signal 1 (antigen presentation) is delivered in the absence of signal 2 (costimulation) and instead may lead to anergy (Mueller *et al*., 1989; Koenen and Joosten, 2000). Because of the role played by costimulatory molecules in the initiation of T-cell responses, they can be manipulated to either stimulate the immune system to prevent infection or to inhibit the immune system for immunotherapy against allergies and autoimmune diseases. Schlom and coworkers have developed poxvirus vectors expressing three synergistic costimulatory molecules, B7-1, ICAM-1 and LFA-3 (TRICOM vectors), that have been used to markedly amplify T-cell responses (Hodge *et al*., 1999; Zhu *et al*., 2001; Palena *et al*., 2003). These are now in clinical trials (Gulley, 2008; Lechleider *et al*., 2008).

3. Targeting peptides to MHC I or MHC II

One way to enhance CTL responses is to target T-cell epitopes of interest to the proteasome of the host cell (Tobery and Siliciano, 1997). It is known that the ubiquitination of proteins acts as a tag to target proteins to the proteasome and to enhance the proteolytic degradation of the introduced epitopes within the cell. This has been shown to be a promising approach for epitope-based vaccines as antigen-specific T cells were generated in vaccination of mice with a class I-restricted CTL Lewis lung cancer epitope fused to ubiquitin (Duan *et al.*, 2006). ER targeting is also promising for enhancing class I MHC presentation. The Ig-kappa signal sequence has been shown to traffic a $CD8^+$ T-cell epitope minigene vaccine to the ER, resulting in protective immunity against *Chlamydia pneumoniae* (Pinchuk *et al.*, 2005). Calreticulin is also a promising ER targeting molecule as it normally resides in the ER where it aids in antigen presentation by association with peptides that enter the ER via TAP and through association with class I MHC beta2 microglobulin molecules (Sadasivan *et al.*, 1996; Spee and Neefjes, 1997). Calreticulin fusions to human papillomavirus proteins have been shown to enhance antigen-specific $CD8^+$ responses (Peng *et al.*, 2006).

Similarly, Th responses can be enhanced by targeting the epitopes for either secretion or subcellular compartment targeting. Past studies have exploited LAMPs (lysosome-associated membrane proteins), which when fused to foreign antigens can target antigens for lysosomal entry, destruction and enhanced class II presentation (Wu *et al.*, 1995; Rodriguez and Whitton, 2000; Arruda, 2006; Chikhlikar *et al.*, 2006).

4. Promiscuous epitopes

Multi-epitope T-cell vaccines should be designed to express not only highly conserved epitopes (to circumvent strain variation for a variety of pathogens) but also epitopes recognized by a broad spectrum of different HLA alleles. An ideal vaccine would be one that can be offered regardless of an individual's HLA phenotype.

Epitope search algorithms can be configured to find promiscuous T-cell epitopes, which can be presented in the context of more than one HLA molecule. For example, EpiMatrix incorporates the 'clustering' function from a previous epitope prediction algorithm, EpiMer (Meister *et al.*, 1995). EpiMatrix measures the MHC-binding potential of each 9 amino acid long snapshot for a number of human HLA molecules and therefore can be used to identify regions of high-density clusters of potential MHC-binding sequences. Other laboratories have confirmed cross-presentation of peptides within HLA 'superfamilies' such as the A3 superfamily: A11, A3, A31, A33 and A68 (Threlkeld *et al.*, 1997; Sette and Sidney, 1998; Zhang *et al.*, 2007). Presumably, vaccines containing such 'clustered' or promiscuous epitopes will have an advantage over vaccines composed of epitopes that are not promiscuous.

5. Epitope enhancement

Because the affinity of natural viral or cancer epitopes for MHC molecules or of the peptide–MHC complexes for T-cell receptors is not necessarily optimal, it is possible to make improved vaccines by a process called epitope enhancement, in which the amino acid sequence of the epitope is modified to improve one or the other of these affinities (Berzofsky, 1993; Berzofsky *et al*., 2001). A number of cases in which viral or tumour antigen epitopes have been enhanced to improve binding to MHC molecules have been described (Pogue *et al*., 1995; Parkhurst *et al*., 1996; Ahlers *et al*., 1997; Rosenberg *et al*., 1998; Sarobe *et al*., 1998; Berzofsky *et al*., 1999; Irvine *et al*., 1999; Salazar *et al*., 2000; Slansky *et al*., 2000; Tourdot *et al*., 2000; Ahlers *et al*., 2001; Okazaki *et al*., 2003; Oh, 2004; Okazaki, 2006; Okazaki *et al*., 2006) and have even shown improved potency in human clinical trials (Rosenberg *et al*., 1998). These enhanced sequences can be determined empirically (Boehncke *et al*., 1993; Sarobe *et al*., 1998) by using known information about primary and secondary anchor residues (Ruppert *et al*., 1993). Combinatorial peptide libraries can also be used (La Rosa *et al*., 2001).

Further, it was shown that such improved affinity of a helper epitope for a class II MHC molecule, when coupled to a CTL epitope in an epitope-based peptide vaccine, resulted not only in an increased CTL response and increased protection against virus but also in a qualitatively different helper T-cell response (Ahlers *et al*., 2001). The response was skewed more towards Th1 cytokine production, due to increased induction of CD40L on the helper T cells, which was shown to result in increased IL-12 production by dendritic cells, thus polarizing Th cells towards the Th1 phenotype. Likewise, a number of examples have been published of epitope sequence modifications that result in higher affinity of the peptide–MHC complex for the T-cell receptor (Zaremba *et al*., 1997; Slansky, 2000; Fong *et al*., 2001; Tangri *et al*., 2001). In fact, a study from the group of Sette and coworkers defined specific positions in the peptide sequence at which conservative substitutions were more likely to result in higher affinity of the peptide–MHC complex for the T-cell receptor (Tangri *et al*., 2001). Both of these types of epitope enhancement should allow the development of epitope-based vaccines that are more effective than the natural pathogen or tumour antigen proteins used in conventional vaccines.

OptiMatrix (Figure 2), is a program developed by DeGroot and Martin (unpublished) that evaluates each individual amino acid's contribution to peptide immunogenicity and can recommend what amino acid substitution would most affect immunogenicity. In addition to automatically recommending what amino acid substitution would have the largest affect on HLA-binding potential, users can input their own substitutions and see the effects in real time.

6. Conserved epitopes

A number of pathogens have been shown to vary between individuals and also during the course of infection in a single individual. HIV and HCV are prime examples; both clades and subtypes (describing variation between infected individuals) and quasispecies (defining variation within a single individual) have been defined. The process of developing vaccines for variable pathogens is complicated by potential variation of key T-cell epitopes. However, the Conservatrix algorithm,

another bioinformatics tool developed by the TB/HIV Research Lab, can define regions that are both conserved (across subtypes or quasispecies) and potentially immunogenic. Conservatrix, as described above, accomplishes this by parsing every sequence in a given database into short text strings. The algorithm then identifies which text strings are most conserved and presents a summary. Highly conserved peptide text strings are then input into EpiMatrix and ranked for immunogenicity by epitope-binding probability. This tool has been applied to the analysis of HIV-1, Hepatitis C and human papillomavirus (De Groot *et al*. unpublished; De Groot *et al*., 2001).

7. Tetramers

Monitoring the specificity of the immune response following vaccination can also be accomplished using epitope-specific reagents known as MHC tetramers. These tools were first developed by Altman and colleagues (Altman *et al*., 1996). These specialized constructs bear four MHC molecules complexed with beta 2 microglobulin and a specific pathogen-derived peptide ligand. Tetramers can bind directly to T cells that recognize the MHC–peptide complex. They can be used for direct *ex vivo* analysis of the frequency and phenotypes of epitope-specific T cells by flow cytometric analysis. Tetramers permit the following types of experimental confirmations of epitope-specific T-cell responses *in vivo*: (a) Direct quantification of the number of epitope-specific T cells prior to and following vaccination; (b) phenotyping of responding T cells (examination for cell surface markers such as CD8, CD4, CD38 and additional activation markers); (c) monitoring of the immune response to specific epitopes following vaccination and (d) direct evaluation of epitope combination effects, epitope spacers or linkers and signal sequences on T-cell responses. Tetramers can be specifically designed for epitope-driven vaccines, as the same epitopes that are included in the vaccine can be used to develop tetramers to detect immune response to the vaccine. These reagents will prove to be useful as epitope-driven vaccines move into clinical trials, as they provide a means of directly measuring efficacy and phenotyping the immune response to the vaccine.

A. Proof of the Epitope-Driven Principle in Pre-clinical Models

In preparation for constructing an epitope-driven vaccine, selected peptide epitopes are synthesized, and MHC-binding studies and T-cell responses to the peptides are evaluated *in vitro*. MHC binding can be evaluated using the T2-cell-binding assay (Ljunggren *et al*., 1990) or soluble class I/class II monomers (Sylvester-Hvid *et al*., 2002; Steere *et al*., 2006). T-cell responses to the peptides can be measured in standard T-cell assays (Hiroi *et al*., 2002). Alternatively, newer techniques such as tetramers or intracellular cytokine staining can be performed.

Once T-cell epitopes are confirmed *in vitro* (using T-cell assays as described) a vaccine is constructed from these epitopes. The most rapid approach is to clone the (DNA) coding sequences of the epitopes into a vector plasmid or viral vaccine vector in a tandem string. With a prototype vaccine having been created, the research shifts towards *in vivo* models and pathogenic challenges.

1. Animal models for epitope-driven vaccines

Since the development the tools required to select epitopes and design epitope-based vaccines is a recent event, there are many epitope-driven vaccines in the pre-clinical phase of development but few in the clinical stages of development. A number of different animal models are used to evaluate the ability of vaccines derived from these epitopes to induce an immune response *in vivo*. Transgenic mice expressing human MHC class I or class II molecules represent a suitable pre-clinical model for this purpose. The advantage of using HLA transgenic animals is that they can develop physiologically relevant HLA-restricted T-cell responses. Transgenic mouse strains that express either the entire HLA-A*0201 or the DRBI*0101 molecule have been developed. HLA-A2 transgenic mice have been used to assess the immunogenicity of peptides that bind to HLA-A2. A correlation has been found between CTL responses in infected individuals and CTL responses induced in immunized HLA transgenic mice (Newberg *et al*., 1992; Sette *et al*., 1994; Man *et al*., 1995; Ressing *et al*., 1995; Shirai *et al*., 1995; Wentworth *et al*., 1996; Diamond *et al*., 1997; Sarobe *et al*., 1998; Firat *et al*., 1999).

A careful review of the literature reveals many examples of successful epitope-based vaccination and/or protection in cancer therapy and against infectious disease pathogens. For example, an adenovirus engineered to express class I Epstein–Barr epitopes has been used for both treatment and prevention of tumours associated with Hodgkin's disease in mice (Duraiswamy *et al*., 2003). Similarly in mice, p53 epitopes have been used to combat p53-associated tumours (DeLeo and Whiteside, 2008).

In pre-clinical studies, epitope-driven vaccines have also been shown to be effective against infectious diseases. What is particularly important about these vaccines is their use of T-cell help to improve immune response to many pathogens. For example, Tian *et al*. selected seven infectious bronchitis virus (IBV) T- and B-cell epitopes to be incorporated into an expression vector. They injected the vector into chickens and boosted 14 days later. The vaccine induced more antibody production and a higher proportion of activated $CD4^+$ and $CD8^+$ in circulation than any of their control groups, which included a group that received an inactivated virus vaccine for IBV. Subsequently, the DNA vaccine group had fewer infections and fewer deaths than any other group (Tian *et al*., 2008).

Epitope-based vaccines have also been proven to be effective against the other two major classes of pathogens: parasites and bacteria. Daher *et al*. created several DNA constructs that expressed different combinations of peptides associated with three regions of a malaria merozoite surface protein. The different constructs were able to elicit a Th1 response, Th2 response or both, in addition to neutralizing IgG antibodies in mice. In a western blot assay, they were able to prove that their epitope-based vaccine stimulated production of antibodies that would bind to native protein (Daher *et al*., 2010).

In a separate study, Gregory *et al*. were able to provide protection to mice against the intracellular bacteria *F. tularensis*. Starting with the entire *F. tularensis* genome, Gregory *et al*. used the EpiMatrix algorithm mentioned above to select 25 9-mer peptides, 14 of which eventually were chosen for introduction into an expression vector. The vector was administered intratracheally to mice inside a liposome vector along with CpG

ODN as an adjuvant. The mice were then boosted with a mixture of the 14 peptides a week later, and upon challenge with a live *F. tularensis* vaccine strain showed significantly better survival rates than the control group (Gregory *et al*., 2009).

B. Advantages Over Whole-Protein Vaccines

Epitope-driven vaccines offer several advantages over vaccines encoding whole-protein antigens. Not only are epitope-based vaccines capable of inducing more potent responses than whole-protein vaccines (Ishioka *et al*., 1999), they sidestep the propensity for the immune system to focus on a single immunodominant epitope by simultaneously targeting multiple dominant and subdominant epitopes (Oukka *et al*., 1996; Tourdot *et al*., 1997; Wilson, 2003). This may be particularly important to the development of vaccines against pathogens like HIV and HCV, because the breadth of an immune response appears to be a critical determinant in the progression of the infection (Couillin *et al*., 1994; Missale *et al*., 1996; McMichael and Phillips, 1997; Cooper *et al*., 1999). The use of epitopes can also overcome any potential safety concerns associated with the vaccinating antigen, such as the oncogenic proteins E6 and E7 in the case of HPV (Crook *et al*., 1989; Hawley-Nelson *et al*., 1989).

Epitope vaccines are also advantageous because they deliver a more targeted immune stimulus, and there is less chance of cross-reactive immune response to self or other pathogens. Welsh and Selin have gathered substantial evidence that unanticipated T-cell cross-reactivity between unrelated pathogens is a common occurrence and that it can contribute to altered pathogenesis, a concept that has been termed 'heterologous immunity' (Kim *et al*., 2005; Cornberg *et al*., 2006). Welsh and Selin have documented complex patterns of T-cell cross-reactivity between epitopes encoded by Epstein Barr virus (EBV) and influenza A virus in humans and between vaccinia virus and lymphocytic choriomeningitis virus (LCMV) in mice, and their data indicate that such cross-reactive responses are associated with altered disease states. In addition, their mouse studies suggest that T regulatory cells induced by influenza A virus may alter immune responses and subsequent immunopathology associated with LCMV infection (Chen *et al*., 2003). More recently, in collaboration with Hardy Kornfeld, the researchers demonstrated heterologous immunity induced between BCG and vaccinia immunization – two critically important human vaccines (Chen *et al*., 2003).

A major interest of Welsh and Selin is to define cross-reactive MHC class I and class II epitopes between unrelated pathogens and to determine whether responses to such epitopes can be correlated with altered disease courses and with adverse responses to vaccinations. For example, in humans, lesions similar to erythema nodosum, an inflammation of fatty tissue (panniculitis), can be a complication of vaccination. Welsh and Selin have been able to mimic this pathology in mouse models of heterologous immunity (Welsh and Selin). While Welsh and Kornfeld have been studying heterologous immunity in the context of murine models of viral infections, they have only recently begun to evaluate heterologous immunity using precision epitope-mapping tools. These documented interactions highlight the importance of designing vaccines with the minimum cross-reactive potential, one of the important safety attributes of epitope-driven vaccines.

Epitope-driven vaccines also have clear safety advantages over attenuated vaccines. Attenuated vaccines sometimes run a risk of mutating back into more virulent forms (the oral polio virus, for example) (Kew *et al*., 2004), and for populations where immunocompromized individuals are more prevalent, the attenuated vaccines may be contraindicated (Sester *et al*., 2008). By designing a vaccine that contains only the absolutely necessary 'words' for recognizing the pathogen, vaccine developers may be able to avoid off-target effects and unwanted auto-immunity.

♦♦♦♦♦♦ VI. ALTERNATIVE APPLICATIONS FOR EPITOPE MAPPING

1. Regulatory T-cell epitopes (Tregitopes)

In the last 5 years, the role of the regulatory T cells (Tregs) has been elucidated and attempts to harness their immunosuppressive effects are being tested in pre-clinical models (Brusko *et al*., 2008). There are two types of Tregs, adaptive and natural. Since adaptive Tregs are normal T cells that have been peripherally transformed via cytokine signalling (Curotto de Lafaille and Lafaille, 2009), their epitopes are similar to T effector epitopes and can just as easily be identified using epitope-mapping tools.

Similarly, epitope-mapping tools have been used to identify the target epitopes of natural Tregs (nTregs), although the means by which these epitopes become associated with nTregs is as yet unknown. nTregs are autoreactive T cells that are not deleted during thymic selection. They are $CD4^+$, $CD25^+$, $FoxP3^+$ cells that cause antigen-specific immunosuppression by either cytokine-mediated or contact-dependent mechanisms (Vignali *et al*., 2008). Future applications of epitope-mapping tools described in this chapter may be to seek out and identify potential regulatory T-cell epitopes that contribute to the down regulation of immune responses to pathogens and autologous proteins (De Groot *et al*., 2008).

♦♦♦♦♦♦ VII. CONCLUSION

Bioinformatics is ushering in a new era of vaccine design. The ability to induce an immune response to a broad repertoire of epitopes that are universally recognized across continents and across genetic backgrounds is considered to be a critical characteristic of an effective vaccine. Opportunities for epitope discovery are expanding as the number of entirely sequenced pathogens approaches increases access to these data improves. Cancer therapy and autoimmune disease are two additional fields that may benefit from the application of epitope-mapping tools to novel vaccine design.

Over the past decade bioinformatics tools have been systematically applied to whole genomes and are now being used in combination with immunoinformatics methods for screening and confirming epitopes. As vaccine developers begin to integrate the types of tools described in this chapter into their discovery process, the pace of vaccine development is likely to accelerate. Better designed, safer, epitope-driven vaccines for a whole host of pathogens and cancers, and autoimmune disorders, are now within reach.

Acknowledgements and Disclosures

Two of the contributing authors, Bill Martin and Anne S. De Groot, are senior officers and majority of shareholders at EpiVax, a privately owned vaccine design company located in Providence, RI, USA. The authors acknowledge that there is a potential conflict of interest related to the relationship of several of them with EpiVax and attest that the work contained in this review is free of any bias that might be associated with the commercial goals of the company.

Initial funding for the Mtb (TB) genome-to-vaccine analysis was provided by a subcontract to the TB/HIV Research Laboratory from the NIH (R01 AI 40125, Principal Investigator Robert Fleischmann). Funding for additional TB epitope analysis and T-cell assays described in this chapter was provided by the Sequella Global TB Foundation in the form of a core scientist award to Anne S. De Groot at EpiVax, Inc. Additional funding from NIH SBIR grants R21AI078800 (HIV), R43AI058376 (smallpox), R43AI075830 (TB) and R43AI058326 (Tularemia) has enabled essential proof of principle studies for the genome-to-vaccine design hypothesis. Partial support was also provided by the Center for Cancer Research, National Cancer Institute, NIH.

References

Ahlers, J. D., Belyakov, I. M., Thomas, E. K., and Berzofsky, J. A. (2001). High-affinity T helper epitope induces complementary helper and APC polarization, increased CTL, and protection against viral infection. *J. Clin. Invest.* **108**(11), 1677–1685.

Ahlers, J. D., Takeshita, T., Pendelton, D., and Berzofsky, J. A. (1997). Enhanced immunogenicity of HIV-1 vaccine construct by modification of the native peptide sequence. *Proc. Natl. Acad. Sci. U.S.A* **94**(20), 10856–10861.

Altman, J. D., Moss, P. A., Goulder, P. J., Barouch, D. H., McHeyzer-Williams, M. G., Bell, J. I., McMichael, A. J., and Davis, M. M. (1996). Phenotypic analysis of antigen-specific T lymphocytes. *Science* **274**(5284), 94–96.

Altuvia, Y., Schueler, O., and Margalit, H. (1995). Ranking potential binding peptides to MHC molecules by a computational threading approach. *J. Mol. Biol.* **249**(2), 244–250.

An, L. L. and Whitton, J. L. (1997). A multivalent minigene vaccine, containing B-cell, cytotoxic T-lymphocyte, and Th epitopes from several microbes, induces appropriate responses *in vivo* and confers protection against more than one pathogen. *J Virol.* **71**(3), 2292–2302.

An, L. L. and Whitton, J. L. (1999). Multivalent minigene vaccines against infectious disease. *Curr. Opin. Mol. Ther.* **1**(1), 16–21.

Appella, E., Padlan, E. A., and Hunt, D. F. (1995). Analysis of the structure of naturally processed peptides bound by class I and class II major histocompatibility complex molecules. *EXS* **73**, 105–119.

Arruda, L. B. (2006). Dendritic cell-lysosomal-associated membrane protein (LAMP) and LAMP-1-HIV-1 gag chimeras have distinct cellular trafficking pathways and prime T and B cell responses to a diverse repertoire of epitopes. *J. Immunol.* **177**, 2265–2275.

Berzofsky, J. A. (1993). Epitope selection and design of synthetic vaccines. Molecular approaches to enhancing immunogenicity and cross-reactivity of engineered vaccines. *Ann. N. Y. Acad. Sci.* **690**, 256–264.

Berzofsky, J. A., Ahlers, J. D., Derby, M. A., Pendleton, C. D., Arichi, T., and Belyakov, I. M. (1999). Approaches to improve engineered vaccines for human immunodeficiency virus and other viruses that cause chronic infections. *Immunol. Rev.* **170**, 151–172.

Berzofsky, J. A., Ahlers, J. D., and Belyakov, I. M. (2001). Strategies for designing and optimizing new generation vaccines. *Nat. Rev. Immunol.* **1**(3), 209–219.

Boehncke, W. H., Takeshita, T., Pendleton, C. D., Houghten, R. A., Sadegh-Nasseri, S., Racioppi, L., Berzofsky, J. A., and Germain, R. N. (1993). The importance of dominant negative effects of amino acid side chain substitution in peptide-MHC molecule interactions and T cell recognition. *J. Immunol.* **150**(2), 331–341.

Brown, J. H., Jardetzky, T. S., Gorga, J. C., Stern, L. J., Urban, R. G., Strominger, J. L., and Wiley, D. C. (1993). Three-dimensional structure of the human class II histocompatibility antigen HLA-DR1. *Nature* **364**(6432), 33–39.

Brusic, V., Bajic, V. B., and Petrovsky, N. (2004). Computational methods for prediction of T-cell epitopes–a framework for modelling, testing, and applications. *Methods* **34**(4), 436–443.

Brusic, V., Rudy, G., and Harrison, L. C. (1994). Prediction of MHC binding peptides using artificial neural networks. In: *Complex Systems, Mechanisms of Adaption* (R. J. Stonier and X. S. Yu, eds.), pp. 253–260. IOS Press, Amsterdam.

Brusko, T. M., Putnam, A., and Bluestone, J. A. (2008). Human regulatory T cells: role in autoimmune disease and therapeutic opportunities. *Immunol. Rev.* **223**, 371–390.

Chen, H. D., Fraire, A. E., Joris, I., Welsh, R. M., and Selin, L. K. (2003). Specific history of heterologous virus infections determines anti-viral immunity and immunopathology in the lung. *Am. J. Pathol.* **163**(4), 1341–1355.

Chicz, R. M., Urban, R. G. *et al*. (1993). Specificity and promiscuity among naturally processed peptides bound to HLA-DR alleles. *J. Exp. Med.* **178**, 27–47.

Chikhlikar, P., de Arruda, L. B., Gorga, J. C., Vignali, D. A., Lane, W. S., and Strominger, J. L. (2006). DNA encoding an HIV-1 Gag/human lysosome-associated membrane protein-1 chimera elicits a broad cellular and humoral immune response in Rhesus macaques. *PLoS ONE* **1**, e135.

Cohen, T., Ardito, M. *et al*. Unpublished Work.

Cole, S. T., Brosch, R. *et al*. (1998). Deciphering the biology of Mycobacterium tuberculosis from the complete genome sequence. *Nature* **393**(6685), 537–544.

Cooper, S., Erickson, A. L., Adams, E. J., Kansopon, J., Weiner, A. J., Chien, D. Y., Houghton, M., Parham, P., and Walker, C. M. (1999). Analysis of a successful immune response against hepatitis C virus. *Immunity* **10**(4), 439–449.

Cornberg, M., Chen, A. T. *et al*. (2006). Narrowed TCR repertoire and viral escape as a consequence of heterologous immunity. *J. Clin. Invest.* **116**(5), 1443–1456.

Couillin, I., Culmann-Penciolelli, B., Guegan, N., Levy, J. P, Guillet, J. G., and Gomard, E. (1994). Impaired cytotoxic T lymphocyte recognition due to genetic variations in the main immunogenic region of the human immunodeficiency virus 1 NEF protein. *J. Exp. Med.* **180**(3), 1129–1134.

Cresswell, P. and Lanzavecchia, A. (2001). Antigen processing and recognition. *Curr. Opin. Immunol.* **13**(1), 11–12.

Crook, T., Morgenstern, J. P., Crawford, L., and Banks, L. (1989). Continued expression of HPV-16 E7 protein is required for maintenance of the transformed phenotype of cells co-transformed by HPV-16 plus EJ-ras. *EMBO J.* **8**(2), 513–519.

Curotto de Lafaille, M. A. and Lafaille, J. J. (2009). Natural and adaptive foxp3+ regulatory T cells: more of the same or a division of labor? *Immunity* **30**(5), 626–635.

Daher, L. J., Demanga, C. G., Prieur, E., Catherine Blanc, C., Pérignon, J., Bouharoun-Tayoun, H., and Druilhe, P. (2010). Towards the rational design of a malaria vaccine construct: example of the MSP3 family. Part I: Immunogenicity studies in models. *Infect. Immun*. **78**(1), 477–485.

Davenport, M. P. and Hill, A. V. (1996). Reverse immunogenetics: from HLA-disease associations to vaccine candidates. *Mol. Med. Today* **2**(1), 38–45.

Davenport, M. P., Ho Shon, I. A., and Hill, A. V. S. (1995). An empirical method for the prediction of T-cell epitopes. *Immunogenetics* **42**(5), 392–397.
De Groot, A. S., Bosma, A., Chinai, N., Frost, J., Jesdale, B. M., Gonzalez, M. A., Martin, W., and Saint-Aubin, C. (2001). From genome to vaccine: in silico predictions, ex vivo verification. *Vaccine* **19**(31), 4385–4395.
De Groot, A. S., Jesdale, B. M., Szu, E., Schafer, J. R., Chicz, R. M., and Deocampo, G. (1997). An interactive Web site providing major histocompatibility ligand predictions: application to HIV research. *AIDS Res. Hum. Retroviruses* **13**(7), 529–531.
De Groot, A. S. and Martin, W. (2009). Reducing risk, improving outcomes: bioengineering less immunogenic protein therapeutics. *Clin. Immunol.* **131**(2), 189–201.
De Groot, A.S., Martin, W. *et al*. Unpublished Work.
De Groot, A.S., Martin, W. *et al*. Unpublished Results.
De Groot, A. S., Nene, V., Hegde, N. R., Srikumaran, S., Rayner, J., and Martin, W. (2003). T cell epitope identification for bovine vaccines: an epitope mapping method for BoLA A-11. *Int. J. Parasitol.* **33**(5-6), 641–653.
De Groot, A. S., Rivera, D. S., McMurry, J. A., Buus, S., and Martin, W. (2008). Identification of immunogenic HLA-B7 'Achilles' heel' epitopes within highly conserved regions of HIV. *Vaccine* **26**(24), 3059–3071.
Delcher, A. L., Kasif, S., Fleischmann, R. D., Peterson, J., White, O., and Salzberg, S. L. (1999). Alignment of whole genomes. *Nucleic Acids Res.* **27**(11), 2369–2376.
DeLeo, A. and Whiteside, T. (2008). Development of multi-epitope vaccines targeting wild-type sequence p53 peptides. *Expert Rev. Vaccines* **7**(7), 1031–1040.
DeLisi, C. and Berzofsky, J. A. (1985). T-cell antigenic sites tend to be amphipathic structures. *Proc. Natl. Acad. Sci. U.S.A* **82**(20), 7048–7052.
Diamond, D. J., York, J., Sun, J., Wright, C. L., and Forman, S. J. (1997). Development of a candidate HLA A*0201 restricted peptide-based vaccine against human cytomegalovirus infection. *Blood* **90**(5), 1751–1767.
Duan, X., Hisaeda, H. *et al*. (2006). The ubiquitin-proteasome system plays essential roles in presenting an 8-mer CTL epitope expressed in APC to corresponding CD8+ T cells. *Int. Immunol.* **18**(5), 679–687.
Duraiswamy, J., Sherritt, M., Thomson, S., Tellam, J., Cooper, L., Connolly, G., Bharadwaj, M., and Khanna, R. (2003). Therapeutic LMP1 polyepitope vaccine for EBV-associated Hodgkin disease and nasopharyngeal carcinoma. *Blood* **101**(8), 3150–3156.
Elliott, T., Cerundolo, V., Elvin, J., and Townsend, A. (1991). Peptide-induced conformational change of the class I heavy chain. *Nature* **351**(6325), 402–406.
Falk, K., Rotzschke, O., Stevanović, S., Jung, G., and Rammensee, H. G. (1991). Allele-specific motifs revealed by sequencing of self-peptides eluted from MHC molecules. *Nature* **351**(6324), 290–296.
Firat, H., Garcia-Pons, F. *et al*. (1999). H-2 class I knockout, HLA-A2.1-transgenic mice: a versatile animal model for preclinical evaluation of antitumor immunotherapeutic strategies. *Eur. J. Immunol.* **29**(10), 3112–3121.
Fleckenstein, B., Kalbacher, H., Muller, C., Stoll, D., Halder, T., Jung, G., and Weismuller, K. (1996). New ligands binding to the human leukocyte antigen class II molecule DRB1*0101 based on the activity pattern of an undecapeptide library. *Eur. J. Biochem.* **240**(1), 71–77.
Flynn, J. L., Chan, J., Triebold, K. J., Dalton, D. K., Stewart, T. A., and Bloom, B. R. (1993). An essential role for interferon gamma in resistance to Mycobacterium tuberculosis infection. *J. Exp. Med.* **178**(6), 2249–2254.
Fong, L., Hou, Y., Rivas, A., Benike, C., Yuen, A., Fisher, G. A., Davis, M. M., and Engleman, E. G. (2001). Altered peptide ligand vaccination with Flt3 ligand expanded dendritic cells for tumor immunotherapy. *Proc. Natl. Acad. Sci. U.S.A* **98**(15), 8809–8814.

Germain, R. N. and Margulies, D. H. (1993). The biochemistry and cell biology of antigen processing and presentation. *Annu. Rev. Immunol.* **11**, 403–450.

German, R. N., Castellino, F., Han, R., Reis e Sousa, C., Romagnoli, P., Sadegh-Nasseri, S., and Zhong, G. M. (1996). Processing and presentation of endocytically acquired protein antigens by MHC class II and class I molecules. *Immunol. Rev.* **151**, 5–30.

Glatman-Freedman, A. and Casadevall, A. (1998). Serum therapy for tuberculosis revisited: reappraisal of the role of antibody-mediated immunity against Mycobacterium tuberculosis. *Clin. Microbiol. Rev.* **11**(3), 514–532.

Gregory, S. H., Mott, S., Phung, J., Lee, J., Moise, L., McMurry, J. A., Martin, W., and De Groot, A. S. (2009). Epitope-based vaccination against pneumonic tularemia. *Vaccine* **27** (39), 5299–5306.

Gulley, J. L. (2008). Pilot study of vaccination with recombinant CEA-MUC-1-TRICOM poxviral-based vaccines in patients with metastatic carcinoma. *Clin. Cancer Res.* **14**, 3060–3069.

Hanke, T., Schneider, J., Gilbert, S. C., Hill, A. V., and McMichael, A. (1998). DNA multi-CTL epitope vaccines for HIV and Plasmodium falciparum: immunogenicity in mice. *Vaccine* **16**(4), 426–435.

Hawley-Nelson, P., Vousden, K. H., Hubbert, N. L., Lowy, D. R., and Schiller, J. T. (1989). HPV16 E6 and E7 proteins cooperate to immortalize human foreskin keratinocytes. *EMBO J.* **8**(12), 3905–3910.

Hodge, J. W., Sabzevari, H., Yafal, A. G., Gritz, L., Lorenz, M. G., and Schlom, J. (1999). A triad of costimulatory molecules synergize to amplify T-cell activation. *Cancer Res.* **59**(22), 5800–5807.

Hiroi, T., Kiyono, H., Fujihashi, H., and McGhee, J. R. (2002). Quantitation of T-cell cytokine responses by ELISA, ELISPOT, flow cytometry and reverse transcriptase-PCR methods. In: *Immunology of Infection* (S. H. E. Kaufmann and D. Kabelitz, eds), Academic Press, San Diego.

Irvine, K. and Parkhurt, M.R. (1999). Recombinant virus vaccination against 'self' antigens using anchor- fixed immunogens. *Cancer Res.* **59**(11), 2536–2540.

Ishioka, G. Y., Fikes, J. *et al*. (1999). Utilization of MHC class I transgenic mice for development of minigene DNA vaccines encoding multiple HLA-restricted CTL epitopes. *J. Immunol.* **162**(7), 3915–3925.

Jesdale, B., Deocampo, G., Meisell, J., Beall, J., Marinello, M. J., Chicz, R. M., and De Groot, A. S. (1997). *Matrix-Based Prediction of MHC Binding Peptides: The EpiMatrix Algorithm, Reagent for HIV Research,* Vaccines Cold Spring Harbor Press, Cold Spring Harbor, NY.

Kew, O. M., Wright, P. F., Agol, V. I., Delpeyroux, F., Shimizu, H., Nathanson, N., and Pallansch, M. A. (2004). Circulating vaccine-derived polioviruses: current state of knowledge. *Bull. World Health Organ.* **82**(1), 16–23.

Kim, S. K., Cornberg, M., Wang, X. Z., Chen, H. D. Selin, L. K., and Welsh, R. M. (2005). Private specificities of CD8 T cell responses control patterns of heterologous immunity. *J. Exp. Med.* **201**(4), 523–533.

Koenen, H. J. and Joosten, I. (2000). Blockade of CD86 and CD40 induces alloantigen-specific immunoregulatory T cells that remain anergic even after reversal of hyporesponsiveness. *Blood* **95**(10), 3153–3161.

Kuchroo, V. K., Das, M. P., Brown, J. A., Ranger, A. M., Zamvil, S. S., Sobel, R. A., Weiner, H. L., Nabavi, N., and Glimcher, L. H. (1995). B7-1 and B7-2 costimulatory molecules activate differentially the Th1/Th2 developmental pathways: application to autoimmune disease therapy. *Cell* **80**(5), 707–718.

La Rosa, C., Krishnan, R., Markel, S., Schneck, J. P., Houghten, R., Pinilla, C., and Diamond, D. J. (2001). Enhanced immune activity of cytotoxic T-lymphocyte epitope

analogs derived from positional scanning synthetic combinatorial libraries. *Blood* **97**(6), 1776–1786.
Lechleider, R. J., Arlen, P. M., Tsang, K. Y., Steinberg, S. M., Yokokawa, J., Cereda, V., Camphausen, K., Schlom, J., Dahut, W. L., and Gulley, J. L. (2008). Safety and immunologic response of a viral vaccine to prostate-specific antigen in combination with radiation therapy when metronomic-dose interleukin 2 is used as an adjuvant. *Clin. Cancer Res.* **14**(16), 5284–5291.
Leighton, J., Sette, A., Sidney, J., Appella, E., Ehrhardt, C., Fuchs, S., and Adorini, L. (1991). Comparison of structural requirements for interaction of the same peptide with I-Ek and I-Ed molecules in the activation of MHC class II-restricted T cells. *J. Immunol.* **147**(1), 198–204.
Lipford, G. B., Hoffman, M., Wagner, H., and Heeg, K. (1993). Primary *in vivo* responses to ovalbumin. Probing the predictive value of the Kb binding motif. *J. Immunol.* **150**(4), 1212–1222.
Livingston, B. (2002). A rational strategy to design multiepitope immunogens based on multiple Th lymphocyte epitopes. *J. Immunol.* **168**, 5499–5506.
Livingston, B. D., Newman, M., Crimi, C., McKinney, D., Chesnut, R., and Sette, A. (2001). Optimization of epitope processing enhances immunogenicity of multiepitope DNA vaccines. *Vaccine* **19**(32), 4652–4660.
Ljunggren, H. G., Stam, N. J. *et al*. (1990). Empty MHC class I molecules come out in the cold. *Nature* **346**(6283), 476–480.
Mamitsuka, H. (1998). Predicting peptides that bind to MHC molecules using supervised learning of hidden Markov models. *Proteins* **33**(4), 460–474.
Man, S., Newberg, M. H., Crotzer, V. L., Luckey, C. J., Williams, N. S., Chen, Y., Huczko, E. L., Ridge, J. P., and Engelhard, V. H. (1995). Definition of a human T cell epitope from influenza A non-structural protein 1 using HLA-A2.1 transgenic mice. *Int. Immunol.* **7**(4), 597–605.
McMichael, A. J. and Phillips, R. E. (1997). Escape of human immunodeficiency virus from immune control. *Annu. Rev. Immunol.* **15**, 271–296.
McMurry, J. A., Gregory, S. H., Moise, L., Rivera, D., Buus, S., and De Groot, A. S. (2007). Diversity of Francisella tularensis Schu4 antigens recognized by T lymphocytes after natural infections in humans: identification of candidate epitopes for inclusion in a rationally designed tularemia vaccine. *Vaccine* **25**(16), 3179–3191.
Meister, G. E., Roberts, C. G., Berzofsky, J. A., and De Groot, A. S. (1995). Two novel T cell epitope prediction algorithms based on MHC-binding motifs; comparison of predicted and published epitopes from Mycobacterium tuberculosis and HIV protein sequences. *Vaccine* **13**(6), 581–591.
Missale, G., Bertoni, R. *et al*. (1996). Different clinical behaviors of acute hepatitis C virus infection are associated with different vigor of the anti-viral cell-mediated immune response. *J. Clin. Invest.* **98**(3), 706–714.
Morris, S., Kelley, C., Howard, A., Li, Z., and Collins, F. (2000). The immunogenicity of single and combination DNA vaccines against tuberculosis. *Vaccine* **18**(20), 2155–2163.
Moudgil, K. D., Sercarz, E. E., and Grewal, I. S. (1998). Modulation of the immunogenicity of antigenic determinants by their flanking residues. *Immunol. Today* **19**(5), 217–220.
Mueller, D. L., Jenkins, M. K., and Schwartz, R. H. (1989). Clonal expansion versus functional clonal inactivation: a costimulatory signalling pathway determines the outcome of T cell antigen receptor occupancy. *Annu. Rev. Immunol.* **7**, 445–480.
Newberg, M., Ridge, J. P., Vining, D. R., Salter, R. D., and Engelhard, V. H. (1992). Species specificity in the interaction of CD8 with the a3 domain of MHC class I molecules. *J. Immunol.* **149**, 136–142.

Oh, S. and Terabe, M., *et al*., (2004). Human CTL to wild type and enhanced epitopes of a novel prostate and breast tumor-associated protein, TARP, lyse human breast cancer cells. *Cancer Res.* **64**, 2610–2618.

Okazaki, T., Terabe, M., Catanzaro, A. T., Pendleton, C. D., Yarchoan, R., and Berzofsky, J. A. (2006). Possible therapeutic vaccine strategy against HIV escape from RT inhibitors studied in HLA-A2 transgenic mice. *J Virol.* **80**, 10645–10651.

Okazaki, T., Pendleton, C. D., Lemonnier, F., and Berzofsky, J. A. (2003). Epitope-enhanced conserved HIV-1 peptide protects HLA-A2-transgenic mice against virus expressing HIV-1 antigen. *J. Immunol.* **171**(5), 2548–2555.

Okazaki, T., Pendleton, C. D., Sarobe, P., Thomas, E. K., Iyengar, S., Harro, C., Schwartz, D., and Berzofsky, J. A. (2006). Epitope enhancement of a CD4 HIV epitope toward the development of the next generation HIV vaccine. *J. Immunol.* **176**(6), 3753–3759.

Olsen, A. W., Hansen, P. R., Holm, A., and Andersen, P. (2000). Efficient protection against Mycobacterium tuberculosis by vaccination with a single subdominant epitope from the ESAT-6 antigen. *Eur. J. Immunol.* **30**(6), 1724–1732.

Oukka, M., Manuguerra, J. C., Livaditis, N., Tourdot, S., Riche, N., Vergnon, I., Cordopatis, P., and Kosmatopoulos, K. (1996). Protection against lethal viral infection by vaccination with nonimmunodominant peptides. *J. Immunol.* **157**(7), 3039–3045.

Palena, C., Zhu, M., Schlom, J., and Tsang, K.-Y. (2003). A triad of costimulatory molecules synergize to amplify T-cell activation in both vector-based and vector-infected dendritic cell vaccines. *Artif. Cells Blood Substit. Immobil. Biotechnol.* **31**(2), 193–228.

Parker, K. C., Bednarek, M. A., and Coligan, J. E. (1994). Scheme for ranking potential HLA-A2 binding peptides based on independent binding of individual peptide side-chains. *J. Immunol.* **152**(1), 163–175.

Parkhurst, M. R., Salgaller, M. L., Southwood, S., Robbins, P. F., Sette, A., Rosenberg, S. A., and Kawakami, Y. (1996). Improved induction of melanoma-reactive CTL with peptides from the melanoma antigen gp100 modified at HLA-A*0201-binding residues. *J.Immunol.* **157**(6), 2539–2548.

Peng, S., Trimble, C., He, L., Tsai, Y. C., Lin, C. T., Boyd, D. A., Pardoll, D., Hung, C. F., and Wu, T. C. (2006). Characterization of HLA-A2-restricted HPV-16 E7-specific CD8(+) T-cell immune responses induced by DNA vaccines in HLA-A2 transgenic mice. *Gene Ther.* **13** (1), 67–77.

Pinchuk, I., Starcher, B. C., Livingston, B., Tvninnereim, A., Wu, S., Appella, E., Sidney, J., Sette, A., and Wizel, B. (2005). A CD8+ T cell heptaepitope minigene vaccine induces protective immunity against Chlamydia pneumoniae. *J. Immunol.* **174**(9), 5729–5739.

Pogue, R. R., Eron, J., Frelinger, J. A., and Matsui, M. (1995). Amino-terminal alteration of the HLA-A*0201-restricted human immunodeficiency virus pol peptide increases complex stability and *in vitro* immunogenicity. *Proc. Natl. Acad. Sci. U.S.A* **92**(18), 8166–8170.

Rammensee, H., Bachmann, J., Philipp, N., Emmerich, N., Bachor, O. A., and Stevanovic, S. (1999). SYFPEITHI: database for MHC ligands and peptide motifs. *Immunogenetics* **50** (3-4), 213–219.

Rammensee, H. G., Friede, T., and Stevanovic, S. (1995). MHC ligands and peptide motifs: first listing. *Immunogenetics* **41**(4), 178–228.

Rayner, J. and Martin, W. Unpublished Work.

Ressing, M. E., Sette, A. *et al*. (1995). Human CTL epitopes encoded by human papillomavirus type 16E6 and E7 identified through *in vivo* and vitro immunogenicity studies of HLA-A* 0201-binding peptides. *J. Immunol.* **154**(11), 5934–5943.

Rodriguez, F. and Whitton, J. L. (2000). Enhancing DNA immunization. *Virology* **268**(2), 233–238.

Rosenberg, S. A., Yang, J. C. *et al.* (1998). Immunologic and therapeutic evaluation of a synthetic peptide vaccine for the treatment of patients with metastatic melanoma. *Nat. Med.* **4**(3), 321–327.
Rosenfeld, R., Zheng, Q., Vajda, S., and DeLisi, C. (1995). Flexible docking of peptides to class I major-histocompatibility-complex receptors. *Genet. Anal.* **12**(1), 1–21.
Rothbard, J. B. and Taylor, W. R. (1988). A sequence pattern common to T cell epitopes. *EMBO J.* **7**(1), 93–100.
Rotzschke, O., Falk, K., Stevanović, S., Jung, G., Walden, P., and Rammensee, H. G. (1991). Exact prediction of a natural T cell epitope. *Eur. J. Immunol.* **21**(11), 2891–2894.
Ruppert, J., Sidney, J., Celis, E., Kubo, R. T., Grey, H. M., and Sette, A. (1993). Prominent role of secondary anchor residues in peptide binding to HLA-A2.1 molecules. *Cell* **74**(5), 929–937.
Sadasivan, B., Lehner, P. J., Ortmann, B., Spies, T., and Cresswell, P. (1996). Roles for calreticulin and a novel glycoprotein, tapasin, in the interaction of MHC class I molecules with TAP. *Immunity* **5**(2), 103–114.
Salazar, E., Zaremba, S., Arlen, P. M., Tsang, K. Y., and Schlom, J. (2000). Agonist peptide from a cytotoxic t-lymphocyte epitope of human carcinoembryonic antigen stimulates production of tc1-type cytokines and increases tyrosine phosphorylation more efficiently than cognate peptide. *Int. J. Cancer* **85**(6), 829–838.
Sarobe, P., Pendleton, C. D., Akatsuka, T., Lau, D., Engelhard, V. H., Feinstone, S. M., and Berzofsky, J. A. (1998). Enhanced *in vitro* potency and *in vivo* immunogenicity of a CTL epitope from hepatitis C virus core protein following amino acid replacement at secondary HLA-A2.1 binding positions. *J. Clin. Invest.* **102**(6), 1239–1248.
Schafer, J., Jesdale, B. M., George, J., Kouttab, N., and De Groot, A. S. (1998). Prediction of well-conserved HIV-1 ligands using a Matrix-based Algorithm, EpiMatrix. Vaccine. *Vaccine* **16**(19), 1880–1884.
Sester, M., Gartner, B. C., and Girndt, M., Sester, U. (2008). Vaccination of the solid organ transplant recipient. *Transplant. Rev. (Orlando)* **22**(4), 274–284.
Sette, A., Buus, S., Appella, E., Smith, J. A., Chesnut, R., Miles, C., Colon, S. M., and Grey, H. M. (1989). Prediction of major histocompatibility complex binding regions of protein antigens by sequence pattern analysis. *Proc. Natl. Acad. Sci. U.S.A* **86**(9), 3296–3300.
Sette, A. and Sidney, J. (1998). HLA supertypes and supermotifs: a functional perspective on HLA polymorphism. *Curr. Opin. Immunol.* **10**(4), 478–482.
Sette, A., Vitiello, A. *et al.* (1994). The relationship between class I binding affinity and immunogenicity of potential cytotoxic T cell epitope. *J. Immunol.* **153**, 5586–5592.
Sherman, D. R., Voskuil, M., Schnappinger, D., Liao, R., Harrell, M. I., and Schoolnik, G. K. (2001). Regulation of the Mycobacterium tuberculosis hypoxic response gene encoding alpha-crystalline. *Proc. Natl. Acad. Sci. U.S.A* **98**(13), 7534–7539.
Shirai, M., Arichi, T., Nishioka, M., Nomura, T., Ikeda, K., Kawanishi, K., Engelhard, V. H., Feinstone, S. M., and Berzofsky, J. A. (1995). CTL responses of HLA-A2.1-transgenic mice specific for hepatitis C viral peptides predict epitopes for CTL of humans carrying HLA-A2.1. *J. Immunol.* **154**(6), 2733–2742.
Sinigaglia, F. and Hammer, J. (1994). Defining rules for the peptide-MHC class II interaction. *Curr. Opin. Immunol.* **6**(1), 52–56.
Slansky, J. E., Rattis, F. M., Boyd, L. F., Fahmy, T., Jaffee, E. M., Schneck, J. P, Margulies, D. H., and Pardoll, D. M. (2000). Enhanced antigen-specific antitumor immunity with altered peptide ligands that stabilize the MHC-peptide-TCR complex. *Immunity* **13**(4), 529–538.
Sonnenberg, M. G. and Belisle, J. T. (1997). Definition of Mycobacterium tuberculosis culture filtrate proteins by two-dimensional polyacrylamide gel electrophoresis,

N-terminal amino acid sequencing, and electrospray mass spectrometry. *Infect. Immun.* **65**(11), 4515–4524.

Southwood, S., Sidney, J., Kondo, A., del Guercio, M. F., Appella, E., Hoffman, S., Kubo, R. T., Chesnut, R.W., Grey H.M., and Sette, A. (1998). Several common HLA-DR types share largely overlapping peptide binding repertoires. *J. Immunol.* **160**(7), 3363–3373.

Spee, P. and Neefjes, J. (1997). TAP-translocated peptides specifically bind proteins in the endoplasmic reticulum, including gp96, protein disulfide isomerase and calreticulin. *Eur. J. Immunol.* **27**(9), 2441–2449.

Steere, A. C., Klitz, W., Drouin, E. E., Falk, B. A., Kwok, W. W., Nepom, G. T., and Baxter-Lowe, L.A. (2006). Antibiotic-refractory Lyme arthritis is associated with HLA-DR molecules that bind a Borrelia burgdorferi peptide. *J. Exp. Med.* **203**(4), 961–971.

Stille, C. J., Thomas, L. J., Reyes, V. E., and Humphreys, R. E. (1987). Hydrophobic strip-of-helix algorithm for selection of T cell-presented peptides. *Mol.Immunol.* **24**, 1021–1027.

Sturniolo, T., Bono, E., Ding, J., Raddrizzani, L., Tuereci, O., Sahin, V., Braxenthaler, M., Gallazzi, F., Protti, M. P., Sinigaglia, F., and Hammer, J. (1999). Generation of tissue-specific and promiscuous HLA ligand databases using DNA microarrays and virtual HLA class II matrices. *Nat. Biotechnol.* **17**(6), 555–561.

Sylvester-Hvid, C., Kristensen, N., Blicher, T., Ferre, H., Lauemoller, S. L., Wolf, X. A., Lamberth, K., Nissen, M. H., Pedersen, L. O., and Buus, S. (2002). Establishment of a quantitative ELISA capable of determining peptide – MHC class I interaction. *Tissue Antigens* **59**(4), 251–258.

Tangri, S., Ishioka, G. Y., Huang, X., Sidney, J., Southwood, *S.*, Fikes, J., and Sette, A. (2001). Structural features of peptide analogs of human histocompatibility leukocyte antigen class I epitopes that are more potent and immunogenic than wild-type peptide. *J. Exp. Med.* **194**(6), 833–846.

Thomson, S. A., Burrows, S. R., Misko, I. S., Moss, D. J., Coupar, B. E., and Khanna, R. (1998). Targeting a polyepitope protein incorporating multiple class II-restricted viral epitopes to the secretory/endocytic pathway facilitates immune recognition by CD4 + cytotoxic T lymphocytes: a novel approach to vaccine design. *J Virol.* **72**(3), 2246–2252.

Threlkeld, S. C., Wentworth, P. A., Kalams, S. A., Wilkes, B. M., Ruhl, D. J., Keogh, E., Sidney, J., Southwood, S., Walker, B. D., and Sette, A. (1997). Degenerate and promiscuous recognition by CTL of peptides presented by the MHC class I A3-like superfamily: implications for vaccine development. *J. Immunol.* **159**(4), 1648–1657.

Tian, L., Wang, H. N., Lu, D., Zhang, Y. F., Wang, T., and Kang, R. M. (2008). The immunoreactivity of a chimeric multi-epitope DNA vaccine against IBV in chickens. *Biochem. Biophys. Res. Commun.* **377**(1), 221–225.

Tine, J. A., Lanar, D. E. *et al.* (1996). NYVAC-Pf7: a poxvirus-vectored, multiantigen, multistage vaccine candidate for Plasmodium falciparum malaria. *Infect. Immun.* **64**(9), 3833–3844.

Tobery, T. W. and Siliciano, R. F. (1997). Targeting of HIV-I antigens for rapid intracellular degradation enhances cytotoxic T lymphocyte (CTL) recognition and the induction of de novo CTL responses *in vivo* after immunization. *J. Exp. Med.* **185**(5), 909–920.

Tong, J. C., Tan, T. W., and Ranganathan, S. (2007). Methods and protocols for prediction of immunogenic epitopes. *Brief. Bioinformatics* **8**(2), 96–108.

Tourdot, S., Oukka, M., Manuguerra, J. C., Magafa, V., Vergnon, I., Riche, N., Bruley-Rosset, M., Cordopatis, P., and Kosmatopoulos, K. (1997). Chimeric peptides: a new approach to enhancing the immunogenicity of peptides with low MHC class I affinity: application in antiviral vaccination. *J. Immunol.* **159**(5), 2391–2398.

Tourdot, S., Scardino, A., Saloustrou, E., Gross, D. A, Pascolo, S., Cordopatis, P., Lemonnier, F. A., and Kosmatopoulos K. (2000). A general strategy to enhance

immunogenicity of low-affinity HLA-A2. 1-associated peptides: implication in the identification of cryptic tumor epitopes. *Eur. J. Immunol.* **30**(12), 3411–3421.
Trombetta, E. S. and Mellman, I. (2005). Cell biology of antigen processing *in vitro* and *in vivo*. *Annu. Rev. Immunol.* **23**, 975–1028.
Unanue, E. R. (1992). Cellular studies on antigen presentation by class II MHC molecules. *Curr. Opin. Immunol.* **4**(1), 63–69.
Velders, M., Weijzen, S. *et al*. (2001). Defined Flanking Spacers and Enhanced Proteolysis Is Essential for Eradication of Established Tumors by an Epitope String DNA Vaccine. *J. Immunol.* **166**(9), 5366–5373.
Vignali, D. A., Collison, L. W., and Workman, C. J. (2008). How regulatory T cells work. *Nat. Rev. Immunol.* **8**(7), 523–532.
Wahlstrom, J., Dengjel, J., Persson, B., Duyar, H., Rammensee, H. G., Stevanovic, S., Eklund, A., Weissert, R., and Grunewald, J. (2007). Identification of HLA-DR-bound peptides presented by human bronchoalveolar lavage cells in sarcoidosis. *J. Clin. Invest.* **117**(11), 3576–3582.
Wang, R., Doolan, D. L. *et al*. (1998). Induction of antigen-specific cytotoxic T lymphocytes in humans by a malaria DNA vaccine. *Science* **282**(5388), 476–480.
Welsh, R. M. and Selin, L. K. Unpublished Work.
Wentworth, P. A., Vitiello, A., Sidney, J., Keogh, E., Chestnut, R. W., Grey, H., and Sette, A. (1996). Differences and similarities in the A2.1-restricted cytotoxic T cell repertoire in humans and human leukocyte antigen-transgenic mice. *Eur. J. Immunol.* **26**(1), 97–101.
Whitton, J. L., Sheng, N., Oldstone, M. B., and McKee, T. A. (1993). A 'string-of-beads' vaccine, comprising linked minigenes, confers protection from lethal-dose virus challenge. *J Virol.* **67**(1), 348–352.
Wille-Reece, U., Flynn, B. J. *et al*. (2006). Toll-like receptor agonists influence the magnitude and quality of memory T cell responses after prime-boost immunization in nonhuman primates. *J. Exp. Med.* **203**(5), 1249–1258.
Wilson, C. C. (2003). Development of a DNA vaccine designed to induce cytotoxic T lymphocyte responses to multiple conserved epitopes in HIV-1. *J. Immunol.* **171**, 5611–5623.
Winslow, G. M., Cooper, A., Reiley, W., Chatterjee, M., and Woodland, D. L. (2008). Early T-cell responses in tuberculosis immunity. *Immunol. Rev.* **225**, 284–299.
Wu, T. C., Guarnieri, F. G., Staveley-O'Carroll, K. F., Viscidi, R. P., Levitsky, H. I., Hedrick, L., Cho, K. R., August, J. T., and Pardoll, D. M. (1995). Engineering an intracellular pathway for major histocompatibility complex class II presentation of antigens. *Proc. Natl. Acad. Sci. U.S.A* **92**(25), 11671–11675.
Yu, K., Petrovsky, N., Schonbach, C., Koh, J. Y., and Brusic, V. (2002). Methods for prediction of peptide binding to MHC molecules: a comparative study. *Mol. Med.* **8**(3), 137–148.
Zaremba, S., Barzaga, E., Zhu, M., Soares, N., Tsang, K. Y., and Schlom, J. (1997). Identification of an enhancer agonist cytotoxic T lymphocyte peptide from human carcinoembryonic antigen. *Cancer Res.* **57**(20), 4570–4577.
Zhang, C., Anderson, A., and DeLisi, C. (1998). Structural principles that govern the peptide-binding motifs of class I MHC molecules. *J. Mol. Biol.* **281**(5), 929–947.
Zhang, G. L., Bozic, I., Kwoh, C. K., August, J. T., and Brusic, V. (2007). Prediction of supertype-specific HLA class I binding peptides using support vector machines. *J. Immunol. Methods* **320**, 143–154.
Zhu, M., Terasawa, H., Gulley, J., Panicali, D., Arlen, P., Schlom, J., and Tsang, K. (2001). Enhanced activation of human T cells via avipox vector-mediated hyperexpression of a triad of costimulatory molecules in human dendritic cells. *Cancer Res.* **61**(9), 3725–3734.

4 Genetics of Susceptibility and Resistance to Infection

Aurelie Cobat[1,2], Marianna Orlova[3,4], Alexandre Alcaïs[1,2] and Erwin Schurr[3,4]

[1] Laboratory of Human Genetics of Infectious Diseases, Necker Branch, Institut National de la Santé et de la Recherche Médicale, U.550, Paris, France; [2] University Paris Descartes, Necker Medical School, Paris, France; [3] McGill Centre for the Study of Host Resistance, The Research Institute of the McGill University Health Centre, Montreal, Québec, Canada; [4] Departments of Human Genetics and Medicine, McGill University, Montreal, Québec, Canada

CONTENTS

I. INTRODUCTION

The host genetic contribution to infectious disease susceptibility has now been firmly established by a number of proof of concept investigations in several major infectious diseases (Alcais *et al.*, 2009). However, the molecular identity of the vast majority of host genetic susceptibility factors remains unknown and this will be a major area of scientific study over the next decade. Technological advances have resulted in a large drop of genotyping costs and, together with an abundance of non-profit 'fee for service' genotyping centres, this has made high throughput genotyping a commonly accessible research tool. While whole genome association studies that analyse hundreds of thousands of markers in thousands of subjects are at the forefront of current genetic studies, it is worthwhile remembering that these studies have so far added very little to our understanding of host genetic control of infectious diseases. We therefore predict that alternative or complimentary methods of genetic analysis will continue to provide important insight into the mechanisms of pathogenesis. Many studies of host genetic susceptibility in the past have used candidate gene case–control approaches, and these studies are notorious for their poor reproducibility. An important reason for the poor reproducibility of these earlier studies was the often small number of subjects

METHODS IN MICROBIOLOGY, VOLUME 37
0580-9517 DOI 10.1016/S0580-9517(10)37004-8

enrolled resulting in low power to detect even true effects. To avoid this known pitfall, it is an important part of the design phase of genetic studies to estimate by power calculations if the planned (or accessible) number of subjects is sufficient to detect a genetic effect of the expected size.

The following chapter is not dealing in any detail with issues of how to select a phenotype that is amenable for genetic study. While this is a critical first step of any genetic analysis, epidemiological and clinical features of common infectious diseases are highly trait specific and it is not easily possible to have generic rules to reflect this diversity. Very generally, phenotypes selected for study should be specific enough to reduce the likelihood of causal heterogeneity and disease misclassification while still representing a substantial proportion of patients in clinically often syndromic infectious diseases. Likewise, the phenotype classification needs to be broad enough to allow for replication studies which are key to the genetic analysis of any complex trait. This implies that the same diagnostic criteria should be accessible to clinical centres (often in regions or countries of vastly different clinical capacity) other than the original enrolment site. Since the epidemiology of an infectious disease is by the nature of an infectious illness part of the phenotype, the question of the disease setting also deserves careful consideration. The selection of the best phenotype for genetic study and the appropriate demographic and epidemiological setting of this phenotype are pivotal for the success of the genetic analysis. Yet, decisions on the phenotype are often haphazard and do not consider the need for replication in different sites.

Likewise, we will not discuss approaches and strategies that deal with the analysis of phenotype heritability. Evidence for heritability of an infectious disease is often anecdotal and can carry stiff social stigma and discrimination. This is perhaps best illustrated by leprosy where patients and their families have been marginalized and threatened for centuries. It is important for any genetic study to address the perception that a larger community may have a 'familial' (=inherited) component of an infectious disease, and this needs to be discussed with both the community and patients and their families prior to the onset of enrolment. We will not discuss the often very substantial work that is required to prepare a study site. From the scientific point of view, heritability of a trait can be determined by conducting twin and/or segregation studies. Twin studies compare concordance rates of a disease among monozygotic (=genetically identical individuals) and dizygotic twins and can be used to obtain a direct estimate for heritability of the trait. Segregation analysis can be done in the classical way by comparing observed segregation ratios with those expected under Mendelian inheritance or by performing a complex segregation analysis, which can also give maximum likelihood estimates for the parameters of the genetic models that govern trait inheritance.

In this chapter, we will assume that an appropriate phenotype has been selected, that this phenotype shows strong evidence of heritability, that the study is well powered and that all genotypings have been done by a centralized facility. We will also assume that the genetic markers used were single nucleotide polymorphisms (SNPs) which are the current markers of choice for genetic studies. Before the analysis can start both the markers employed and the DNA

Box 1. Ten quality control rules prior to analysis

Marker quality control

1 – Exclude SNPs with low call rate or differential pattern of call rates between cases and controls
The call rate of valid genotypes is an indicator of genotyping accuracy and marker performance.

2 – Exclude SNPs not in Hardy–Weinberg Equilibrium
In well-designed studies, departure from Hardy–Weinberg equilibrium (HWE) is an indicator of a high genotyping error rate.

3 – Identify SNPs with very rare alleles
Clustering-based genotype calling algorithms tend to perform not well for SNPs with rare alleles. Unless study is targeted to rare variants, exclude SNPs with very low minor allele frequency (MAF).

4 – Exclude SNPs with high Mendelian inheritance error rates in family-based designs
Given sufficient pedigree data, inconsistencies of specific SNP genotypes with Mendelian inheritance indicate genotyping errors.

5 – Exclude SNPs with low concordance rate in duplicate samples

Sample quality control

6 – Exclude individuals with low call rate
High proportion of missing genotypes per sample is an indicator of poor DNA quality.

7 – Exclude samples with outlier genome-wide heterozygosity
Genome-wide excess heterozygosity may indicate DNA cross-contamination.

8 – Check for pedigree errors and exclude samples with Mendelian inconsistencies
Samples with excess of non-Mendelian inheritance indicate incorrect pedigree information. Pedigree errors can lead to an inflation of type I error rate and reduced power in genetic analysis.

9 – Compare gender from subject record against X chromosome heterozygosity and exclude samples with gender inconsistencies

10 – Check for duplicates/related samples
Unrecognized relatedness can lead to an inflated type I error rate or a loss of power in genetic studies.

samples used need to undergo a number of quality control steps which are summarized in Box 1.

♦♦♦♦♦♦ II. LINKAGE METHODS

In the analysis of complex traits such as infectious diseases, linkage studies are used to locate chromosomal regions containing the gene(s) of interest by either focusing on a few candidate regions or using a genome-wide search. The main interest of the whole genome approach is to ensure that all major loci involved in the control of a phenotype are identified. This implies the opportunity to discover new major genes, and consequently physiopathological pathways, that were not previously suspected of contributing to the phenotype under study. Unfortunately, unlike the analysis of simple monogenic diseases, a fine mapping of the gene(s) of interest cannot be expected from linkage studies of complex infectious phenotypes. When successful, linkage analyses generally identify a region of about 10–20 cM (~10,000 to 20,000 kb) which may still contain hundreds of genes. As detailed in the association studies section, the next step is to test the role of polymorphisms of candidate genes located within the identified region. The general principle of linkage analysis is to seek for chromosomal regions that segregate non-randomly with the phenotype of interest within families. According to what is known about the mode of inheritance of the phenotype, linkage analysis methods are usually classified as model-based or model-free. Although the terms parametric and non-parametric are sometimes used, they should be avoided since all model-free (non-parametric) approaches are actually parametric in the sense that they necessitate, more or less explicitly, the estimation of at least one parameter.

A. Model-Based Analyses

1. Principle

Model-based linkage analysis by the classical lod score method (Morton, 1955) requires to define the model specifying the relationship between the phenotype and factors that may influence its expression, mainly a putative gene with two alleles (d, D) and other relevant risk factors, often referred to as the genetic (or phenotype/genotype) model. In the context of a binary phenotype (e.g. affected/unaffected, seronegative/seropositive), this genetic model should specify, in addition to the frequency of the susceptibility allele denoted as D, the penetrance vector, i.e. the probability for an individual to be affected given a genotype (dd, Dd or DD) and a subject-specific set of relevant covariates such as age or intensity of exposure to an infectious agent. In the context of a quantitative phenotype (e.g. infection levels), the complete specification of the genetic model includes, in addition to the frequency of the allele predisposing to high values of the trait denoted as D, the three genotype-specific means and variances which may also be influenced by some individual covariates. Given the genotype, the distribution of the phenotype is assumed to be normal so that the overall distribution is a mixture of three normal distributions.

The genetic model is generally provided and estimated by segregation analysis which is the first step to determine from family data the mode of inheritance of a given phenotype. The aim of segregation analysis is to discriminate between the different factors causing familial resemblance, with the main goal to test for the existence of a single gene, called a major gene. The major gene term does not mean

that it is the only gene involved in the expression of the phenotype, but that, among the set of involved genes, there is at least one gene with an effect important enough to be distinguished from the others. For a binary phenotype, this effect can be expressed in terms of relative risks, e.g. the ratio of the probability for a subject to be affected given a 'DD' genotype to the same probability given a 'dd' genotype. For a quantitative phenotype, this effect is measured by the proportion of the phenotypic variance explained by the major gene (also denoted as the heritability). An elegant way to express this phenotype/genotype model is to use a regressive approach for binary (Bonney, 1986) as well as for quantitative (Bonney, 1984) traits. A detailed review of the pros and cons of segregation analysis can be found in Jarvik (1998). Note that in linkage studies the expression 'major gene' is used for any gene that underlies a significant linkage peak.

When there is evidence for a major gene by segregation analysis, model-based linkage analysis allows to confirm and to locate this gene, denoted below as the phenotype locus. Model-based linkage analysis tests in families whether the phenotype locus co-segregates with genetic markers of known chromosomal location and provides an estimate of the recombination rate between these two loci (Ott, 1999) (see Box 2). Linkage with the phenotype locus can be tested marker by marker (two-point analysis) or considering a set of linked markers (multipoint analysis).

Box 2. Model-based linkage analysis

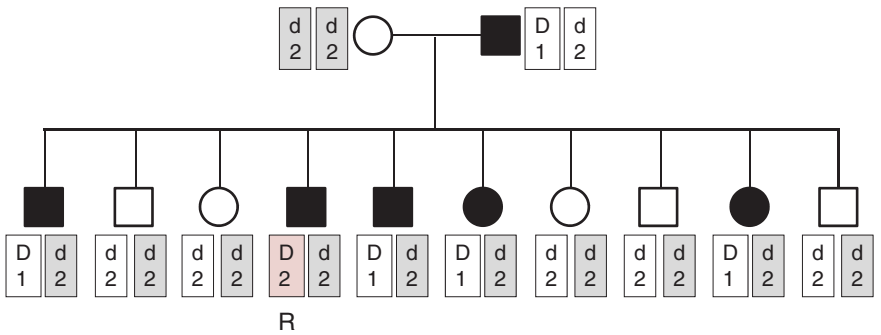

Principle:

Model-based linkage analysis tests in families whether the trait locus co-segregates with genetic markers of known chromosomal location. The method is based on the estimation of a single parameter, the recombination fraction (denoted θ) between the trait locus and a given genetic marker. The linkage test is a likelihood ratio test comparing the likelihood under the null hypothesis of no linkage ($\theta_0 = 0.5$), L_{H0}, to the likelihood under the alternative hypothesis of linkage ($\theta_1 < 0.5$), L_{H1}. The linkage statistic is classically expressed as a lod score, $Z(\theta) = \log_{10}(L_{H1}/L_{H0})$. The classical critical values to declare significant linkage and to exclude linkage are lod score ≥3 (which corresponds to a p-value of 10^{-4}) and lod score <–2, respectively (Morton, 1955).

Example:

The pedigree above shows the segregation of a rare autosomal dominant trait locus (D/d, where D is the causal allele) with complete penetrance and absence of phenocopies (i.e. individuals carrying the genotypes Dd or DD are affected and individuals carrying the genotype dd are unaffected) and an informative marker (1/2). The mother is not informative for linkage. As the phase is known, we can count the number of recombinants k (which is 1 and denoted R) out of $n = 10$ meioses. The working likelihood of the pedigree is $L(\theta) = \theta^k (1-\theta)^{n-k} = \theta(1-\theta)^9$. The likelihood of the pedigree under the null hypothesis is $L(0.5) = (0.5)^{10}$. The maximum likelihood estimate of θ is easy to compute as $k/n = 1/10$ and the lod score is $\text{lod} = \log_{10}(0.1(1–0.1)^9/0.5^{10}) = 1.6$. Results of model-based linkage analysis are presented in lod score tables where the lod scores are tabulated for a series of recombination fractions from 0 to 0.5.

Weakness:

Model-based linkage analysis requires to define the genetic model that describes the relationship between the phenotype and the genotype, i.e. the disease allele frequency, the mode of inheritance (dominant, recessive or additive) and the pattern of penetrances (i.e. the probability of being affected given the genotype status) need to be specified to infer the disease locus genotype of all individuals from their phenotype. Those parameters are generally estimated by complex segregation analyses.

Strength:

The lod score approach is the most powerful linkage method when the assumed genetic model is the true model. This approach gives a maximum likelihood estimate of the genetic distance (θ) between the genetic marker and the disease trait locus.

Popular Software:

LINKAGE (Lathrop *et al*., 1984), FASTLINK (Cottingham *et al*., 1993), MERLIN (Abecasis *et al*., 2002)

A list of genetic analysis software is available at http://linkage.rockefeller.edu/soft

In this analysis, as in segregation analysis, all the inferences for individual genotypes at the phenotype locus are made from the individual phenotypes and the specified phenotype/genotype model. For quantitative phenotypes, the probability that an individual carries genotype dd, dD or DD at the phenotype locus will be computed from the mixture of the three normal distributions described above for which means and variances have been estimated through segregation analysis.

The lod score approach is certainly the most powerful linkage method when the assumed genetic model is (close enough to) the true model. This is the case in a situation of monogenic inheritance where a simple genetic model can be assumed. However, a misspecification of the genetic model can lead to both severe loss of power to detect linkage (and therefore to false exclusion of the region containing the phenotype locus) and bias in the estimation of the recombination fraction (i.e. the genetic distance) between the phenotype locus and the marker locus (Clerget-Darpoux *et al.*, 1986). Nevertheless, such a misspecification does not affect the robustness of the method, i.e. it does not lead to false conclusions in favour of linkage, as long as only one phenotype/genotype model is tested. When there is some knowledge about the prevalence of the disease under study and the level of familial aggregation, a common procedure to reduce the risk of misspecification is to generate a limited number of realistic genetic models to use in lod score analysis. However, when performing the analysis under a number of different genetic models, one needs to introduce a correction for multiple testing and adjust the significance level of the lod score (MacLean *et al.*, 1993). The same issue occurs when several markers are tested, and guidelines have been proposed to adapt lod score thresholds to the context of a genome-wide search. Widely accepted thresholds are the ones proposed by Lander and Kruglyak (1995). Based on complex analytic calculations these authors defined the *p*-values that should be used to claim suggestive or significant linkage as 1.7×10^{-3} and 4.9×10^{-5} (corresponding to a lod score of 1.9 and 3.3, respectively) (Lander and Kruglyak, 1995). Another problem arises when marker data are missing for some family members. In this case, linkage analysis also depends on marker allele frequencies and misspecification of these frequencies can affect both the power and the robustness of the method. This is an important issue because it means that one should be very cautious when reporting suggestive or significant linkage in the context of a sample with many missing parents. Note that the two latter problems (multiple marker testing and misspecification of marker allele frequencies) are also common to model-free methods.

2. Examples

As mentioned earlier, model-based linkage analysis is very sensitive to the genetic model used and misspecification of a model parameter can result in significant loss of power to detect linkage. On the other hand, if the parameters are specified correctly, model-based linkage analysis is not only more powerful than model-free approaches but can also provide insight into mechanisms of pathogenesis that cannot be provided by model-free approaches. Model-based approaches can be applied to candidate genes/regions or used for genome-wide scanning.

Model-based linkage analysis is particularly suited for monogenic diseases. A nice illustration of parametric approaches in the context of monogenic traits is provided by the genetic analysis of the syndrome of Mendelian susceptibility to mycobacterial disease (MSMD). MSMD, first mentioned in clinical descriptions in 1951, became the subject of increased interest of clinical geneticists in the mid-1990s and has been thoroughly studied ever since (Mimouni, 1951; Jouanguy *et al.*, 1996; Newport *et al.*, 1996). In contrast to conventional primary immunodeficiencies (PIDs) which predispose to multiple infections, MSMD is considered an example

of a 'pathogen-specific' PID (Casanova and Abel, 2007). Mostly caused by weakly virulent non-tuberculosis environmental mycobacteria and BCG vaccine (Casanova *et al*., 1995), MSMD is characterized by disseminated or localized recurrent disease. A mutation in *IFNGR1* resulting in complete deficiency of the interferon (IFN)-γ receptor ligand-binding chain was the first described genetic aetiology for MSMD (Jouanguy *et al*., 1996; Newport *et al*., 1996). The *INFGR1* gene was identified by homozygosity mapping (Lander and Botstein, 1987). The core assumption of homozygosity mapping is that a region containing the disease locus will be homozygous by descent in children from consanguineous marriages affected by a rare recessive disease. Interestingly, homozygosity mapping in consanguineous kindreds employing genome-wide (Newport *et al*., 1996) or candidate gene approaches (Jouanguy *et al*., 1996) led to same results and provided cross confirmation for the validity of the finding. So far, five autosomal genes, *IFNGR1* (Jouanguy *et al*., 1996; Newport *et al*., 1996), *IFNGR2* (Dorman and Holland, 1998), *IL12B* (Altare *et al*., 1998b), *IL12RB1* (Altare *et al*., 1998a; de Jong *et al*., 1998) and *STAT1* (Dupuis *et al*., 2001), and one X-linked gene, *NEMO* (Filipe-Santos *et al*., 2006b), all involved in the IL12/23-dependent IFNγ production pathway, have been implicated in MSMD. For more information, interested readers may consult detailed reviews on this subject (Filipe-Santos *et al*., 2006a; Al-Muhsen and Casanova, 2008).

A different example for a candidate gene-based parametric linkage analysis is provided by the study of the primary tuberculosis outbreak in a large aboriginal family in Northern Alberta (Greenwood *et al*., 2000). Based on results obtained in a mouse model (Vidal *et al*., 1993) and earlier human studies of genetic susceptibility to tuberculosis (Bellamy *et al*., 1998) and leprosy (Abel *et al*., 1998b), *NRAMP1* (alias *SLC11A1*) was selected as a candidate gene. During the outbreak, 24 tuberculosis patients were identified based on clinical symptoms and microbiological testing among 81 family members (Greenwood *et al*., 2000). All patients were diagnosed within 6 months of the index case. In such a setting of a large extended multigenerational family, model-free approaches have only limited power for linkage detection and the authors decided on a model-based approach. However, for a model-based linkage analysis the authors needed to obtain estimated values for the penetrance and the frequency of a putative susceptibility allele.

Since parameter estimates for the genetic model were not available from a complex segregation analysis, estimates were based on epidemiological, clinical and population historical data. An important first step was the decision by the authors to introduce varying penetrances of the putative susceptibility allele depending on the history of mycobacterial exposure of individual patients. This resulted in the definition of four liability classes. The first liability class was represented by individuals who became tuberculin skin test (TST) positive (induration > 10 mm) during the outbreak strongly suggesting a new infection with *Mycobacterium tuberculosis*. For individuals in this liability class, the penetrance of a putative tuberculosis susceptibility gene was assumed to be 85%. Individuals with documented BCG vaccination records, previous successfully treated disease, or positive TST prior to the outbreak were assigned to the second liability class. Under the assumption that these documented exposures generated protective immunity against tuberculosis disease, the penetrance of the high-risk

genotype in this liability group was set to 37%. This choice was motivated by previous studies of the protective effect of BCG vaccination in Aboriginal Canadians which demonstrated a decrease of the disease by 57% in the vaccinated group (Houston *et al.*, 1990). All individuals who were TST negative before and during the outbreak were included in the third liability group. The penetrance of their susceptibility allele was set to 10% based on the known TST false discovery rate. Finally, all family members who were <2 years or >65 years of age were considered at high risk of tuberculosis due to constitutive age-related deficiencies in their anti-mycobacterial immunity (Greenwood *et al.*, 2000). The ratio of the high-risk to the low-risk genotype was assumed to be 10 and the susceptibility allele frequency was assumed to be 20% under an additive and 5% under a dominant model. Under the given liability classes these susceptibility allele frequencies resulted in prevalence estimates that were in keeping with historical records of TB rates in this ethnic population.

The above genetic model with four liability classes was used for a two-point lod score analysis with *NRAMP1* polymorphisms and microsatellite genetic markers in close proximity to *NRAMP1*. Under a dominant mode of inheritance there was highly significant evidence of linkage of an *NRAMP1* haplotype (lod score = 3.36) and the *D2S426* microsatellite marker in close proximity to *NRAMP1* (lod score = 3.81) with tuberculosis disease. When *NRAMP1* haplotype and the *D2S426* microsatellite were combined in a multipoint parametric linkage analysis, the evidence for a tuberculosis susceptibility locus at the chromosomal position of was very strong (lod score = 4.25). Hence, in summary, this parametric linkage analysis provided highly significant evidence for a very strong (relative risk = 10) tuberculosis susceptibility locus that was indistinguishable from *NRAMP1*. Perhaps even more strikingly was the observation that when exposure history (i.e. gene–environment interactions) were not modelled by omitting liability classes from the model, the evidence for linkage became non-significant (Greenwood *et al.*, 2000). This latter observation directly demonstrated how even very strong genetic risk factors can be missed if the epidemiological setting in which a disease occurs is neglected in the genetic analysis.

A final example of parametric linkage analysis is given by a genome-wide linkage scan for susceptibility to schistosomiasis (Marquet *et al.*, 1996). Schistosomiasis, a disease caused by parasitic helminths of the genus *Schistosoma*, globally results in nearly 200,000 deaths each year. In endemic areas, where infected snails shed free-swimming larval forms that infect humans, the extent of contact with water is an important risk factor for infection. Several studies have provided evidence for the role of genetic factors in both susceptibility to and severity of schistosomiasis (Butterworth *et al.*, 1985; Hagan *et al.*, 1987; Abel and Dessein, 1991; Abel *et al.*, 1991). A complex segregation analysis of 20 Brazilian families from an endemic region in northeast Brazil detected a major co-dominant acting gene controlling infection intensities (Abel *et al.*, 1991). Infection intensity was described by helminth egg counts in the stools of subjects and provides a typical example for a quantitative phenotype. All egg counts were adjusted on extent of contact with *Schistosoma*-infected water. By further adjusting the egg count residuals on sex and age and taking into account the presence of a major co-dominant egg count (=susceptibility) gene, a complex segregation analysis provided the critical parameters for a parametric analysis. The frequency of the allele

predisposing to high egg counts was estimated at 16% and the egg count means for the three genotype classes were estimated together with the residual egg count variance (Marquet *et al*., 1996).

The adjusted egg count susceptibility genotypes of family members were then used in a linkage analysis. To localize the chromosomal regions regulating the intensity of schistosomiasis, 142 individuals from 11 informative families were screened for 246 microsatellite markers spread throughout the genome. In this initial scan, a single linkage peak was observed on chromosome region 5q31–q33. Two adjacent markers, *D5S393* and *D5S410*, demonstrated evidence for linkage by providing two-point lod scores above 1.9. Eleven additional markers genotyped in this region provided more detailed information on the borders of the linkage peak. Two markers, *D5S636* and *CSF1R* (located in the colony stimulation factor-1 receptor gene), were highly significantly linked to the adjusted egg counts with lod scores of 4.74 and 4.52, respectively, and three other markers, including the ones observed in initial scan, displayed lod scores between 3 and 3.3. In multipoint analysis, five markers spread across the 5q31–q33 region revealed a linkage peak near *CSF1R* with maximum lod score above 6. A refined six-point linkage analysis of makers flanking the peak area confirmed that the locus controlling the intensity of *Schistosoma mansoni* infection lies very close to the *CSF1R* marker (Marquet *et al*., 1996). Although the identified chromosomal fragment contains a number of immunological candidate genes (e.g. *CSF1R, IL-4, IL-5, IL-13*), the causal variant has not yet been identified. The latter shows one of the disadvantages of model-based linkage analysis in a small number of families with highly adjusted phenotypes. The number of meioses in such a small familial sample is not sufficient to molecularly pinpoint the susceptibility lesion while the generation of corresponding susceptibility traits with similar phenotypic accuracy is very difficult to accomplish in larger population samples.

B. Model-Free Linkage Analysis

1. Principle

Model-free linkage approaches (allele sharing methods such as sib-pair studies) allow locating the genetic factors influencing a phenotype without specifying the phenotype/genotype model. Therefore, they are strongly recommended when little is known about this model (i.e. no segregation analysis has been performed or no clear major gene model can be inferred from segregation analysis). The general principle of model-free linkage analyses is to test if relatives who share the same phenotype (e.g. affected relatives) share more marker alleles inherited from a same ancestor, i.e. alleles identical by descent (IBD), than expected due to their familial relationship. The most commonly used model-free linkage analysis approach is the sib-pair method. As shown in Box 3, two sibs can share 0, 1 or 2 parental alleles IBD at any locus, and the respective proportions of this IBD sharing under random segregation are simply 0.25, 0.5 and 0.25. Stated differently, overall, two sibs are expected to share 50% of their alleles in common.

For binary phenotypes (e.g. affected/unaffected), the sib-pair method tests if *affected* sib-pairs share more alleles IBD at the marker(s) of interest than expected

Box 3. Model-free linkage analysis

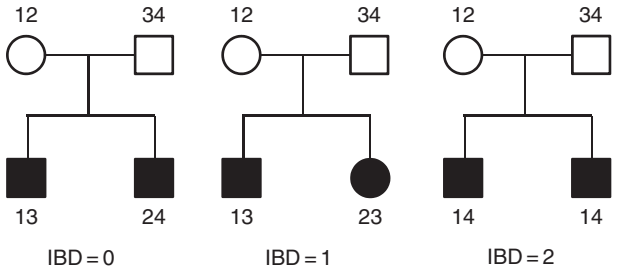

Principle:

The general principle of model-free linkage methods is to test if phenotypically similar relatives (e.g. affected relatives) share more markers alleles inherited from the same ancestor. Alleles derived from the same ancestor are called identical by descent (IBD). The most commonly used approach is the sib-pair approach. As shown in the figure above, two sibs can share 0, 1 or 2 alleles IBD at any locus with the respective probability of 0.25, 0.5 and 0.25 under the null hypothesis of no linkage (i.e. under random marker allele segregation). Under the alternative hypothesis of linkage, affected sib-pairs share more IBD alleles at the marker of interest than expected by chance. This excess can be evaluated by a simple χ^2 test with 2 degrees of freedom (df), in particular when the IBD status can be determined unambiguously.

Example:

Let us consider a sample of 100 affected sib-pairs and a fully informative genetic marker genotyped in all individuals. Of the 100 sib-pairs, 15 share 0 marker alleles IBD, 50 share 1 marker allele IBD and 35 share 2 marker alleles IBD. Under the null hypothesis of no linkage, the expected distribution is 0.25×100, 0.50×100 and 0.25×100 (1:2:1) sib-pairs sharing 0, 1 and 2 alleles IBD, respectively (see the table below).

	IBD = 0	IBD = I	IBD = 2
Observed	15	50	35
Expected	$0.25 \times 100 = 25$	$0.50 \times 100 = 50$	$0.25 \times 100 = 25$

The χ^2 statistic is $\chi^2_{ASP} = \sum(O–E)^2/E = (15–25)^2/25 + (50–50)^2/50 + (35–25)^2/25 = 8$. This corresponds to $p = 0.018$ using the χ^2 distribution with 2 df.

Weakness:

Model-free linkage methods provide no estimate of the genetic distance between the marker and the disease trait locus.

Model-free linkage methods are less powerful than the lod score approach when the assumed genetic model is the true model.

Strength:

No specification of a phenotype/genotype model is required.

Popular software:

GENEHUNTER (Kruglyak *et al.*, 1996), ALLEGRO (Gudbjartsson *et al.*, 2000), MERLIN (Abecasis *et al.*, 2002), MLBGH (Abel and Muller-Myhsok, 1998b; Alcais and Abel, 1999)

A list of genetic analysis software is available at http://linkage.rockefeller.edu/soft

according to their familial relationship. The significance of excess allele sharing can be assessed by a simple χ^2 test, in particular when all parental marker data are known (Box 3). The rationale for focusing on affected rather than unaffected subjects is that they are more informative and robust since their phenotypes are fixed while we do not know if an unaffected subject will develop the disease at a later time. In situations where unaffected status is less ambiguous (especially by using additional information provided by relevant covariates), it has been shown that incorporating unaffected individuals into the analysis can increase power (Alcais and Abel, 2001). Maximum likelihood methods have been developed to analyse affected sib-pair data, e.g. the maximum likelihood score (MLS) (Risch, 1990) and the maximum likelihood binomial (MLB) approach (Abel and Muller-Myhsok, 1998b; Abel *et al.*, 1998a). Compared to χ^2 tests, these analytical approaches may be more powerful to detect linkage. The MLB method, which relies on the idea of binomial distributions of parental alleles among offspring, is of particular interest when the sample includes families with more than two affected sibs since it does not need to decompose the sibship into its constitutive sib-pairs. This latter strategy of decomposition can lead to a large inflation of type I errors (i.e. false conclusions in favour of linkage) due to the non-independence of the resulting pairs (Abel *et al.*, 1998a; Holmans, 2001).

When the phenotype under study is quantitative, the general idea of the approach consists in testing whether sibs having close phenotype values share more alleles IBD than sibs having more distant values. Most of the methods differ only in the way that they quantify the phenotypic resemblance. The widely used regression-based approach proposed 30 years ago by Haseman and Elston regresses the squared difference of the sib-pair phenotypes on the expected proportion of alleles shared IBD by the sib-pair (Haseman and Elston, 1972).

Numerous developments have been performed on this method to account for multipoint analysis (Olson, 1995) or large pedigrees (Amos and Elston, 1989). More recent approaches have proposed to use the cross-product of the sib-pair phenotypes in addition to their difference [for an excellent review see (Feingold, 2002)]. As a regression-based approach, the Haseman–Elston method relies on specific assumptions about the residuals (i.e. normal distribution, homoscedasticity and independence). Violation of these assumptions can significantly impact on power and robustness of the method. Another way of assessing the phenotypic resemblance of sibs is by means of the covariance and this is the core of the variance components methodology that has gained increasing popularity (Goldgar, 1990; Amos, 1994; Almasy and Blangero, 1998). In essence, this method involves first estimating IBD sharing for relative pairs, and then estimating co-variances between relatives that are a function of the IBD sharing. Estimates and test statistics are obtained under the assumption of a multivariate normal distribution of the trait within families, and violation of this assumption [e.g. by ascertainment on the trait values as proposed in (Risch and Zhang, 1995) to increase the power of analysis] has been shown to inflate the type I error rate (Allison *et al*., 1999b). By contrast, extension of the MLB approach to quantitative traits, denoted as MLB-QTL (Alcais and Abel, 1999), is insensitive to non-normal phenotypic distribution whatever the mechanism underlying this non-normality (Alcais and Abel, 2000a) and can be used to analyse sibships of any size (Alcais and Abel, 2000b). Some of these methods are implemented in popular packages such as MERLIN (Abecasis *et al*., 2002), SOLAR (Almasy and Blangero, 1998) or MLBGH (Abel and Muller-Myhsok, 1998b; Alcais and Abel, 1999).

As mentioned previously, model-free methods share some potential problems with model-based linkage analysis, regarding missing parental marker data and testing with multiple markers. In particular, the significance levels of the tests should be adapted to the number of comparisons that are made, and replication studies are required to confirm suggestive linkage. Moreover, it should be noted that the distinction between model-free and model-based approaches may not be so clear. As an example, in the affected sib-pairs method all calculations are carried out on marker alleles and clearly this method does not require specification of a disease inheritance model. However, this method *implies* an inheritance model as shown in Knapp *et al*. (1994) since the affected sib-pair approach is equivalent to a model-based linkage analysis assuming a recessive inheritance with complete penetrance, no sporadic cases and unknown parental phenotypes. This latter point ('assuming unknown parental phenotypes') underlines the important feature that model-free approaches do not consider parental phenotypes, i.e. they assume that both parents are potentially informative for linkage. For this reason, affected sib-pairs methods are less powerful for dominant-like than for recessive-like traits.

Although it is clear that there is no unique answer to the question of whether to use model-free or model-based approach, it is possible to propose some practical guidelines (Goldgar, 2001). When there is some knowledge about the prevalence of the disease under study and the level of familial aggregation, it is possible to generate a limited number of realistic genetic models to use in lod score analysis (with appropriate correction for the number of models tested). Conversely, when there is a lack of reliable epidemiological information so that consistent models

cannot be generated, model-free approaches should be preferentially used. Also, investigators should be aware of the multiple testing issues when using several methods of analysis unless they carefully account for it when computing the significance criterion.

Finally, another key point when performing a linkage analysis is whether to choose a candidate gene strategy or to decide for a whole genome search. From a statistical point of view, this has striking consequences. The 'candidate gene by hypothesis' approach is motivated by what is known about the trait biologically and can be understood as a classical *hypothesis testing strategy* where the type I (i.e. false positive) and type II (i.e. false negative) errors have their standard definitions and interpretations. By contrast, the 'genome scan' strategy is applied without prior knowledge of the biological basis of the disease and therefore aims at *generating hypothesis*. In this context, the central parameter becomes the type II error, whereas the interpretation of type I errors is more difficult and controversial. The debate is still open to decide between (unrealistically) increasing the sample size to allow for both acceptable type I and II error rates and using less stringent nominal significance levels than those proposed by Lander and Kruglyak (1995) that were based on complex analytic calculations under very particular assumptions rather than practical considerations (Elston, 1998; Morton, 1998). In the paper by Lander and Kruglyak (1995), the *p*-values associated to 'suggestive/significant linkage' were defined as $1.7 \times 10^{-3}/4.9 \times 10^{-5}$ (corresponding to a lod score of 1.9/3.3) and $7.4 \times 10^{-4}/2.2 \times 10^{-5}$ (2.2/3.6) for model-based and model-free approaches, respectively. Contrary to the initial fear that has led to the definition of such rigorous thresholds, it seems that genome scans are rather flooded by false negative than by false positive results and several authors now advocate new criteria for significance of linkage (Sawcer *et al.*, 1997; Elston, 1998; Rao, 1998). Although there is little doubt that improvements in statistical methods will increase the power of linkage analysis, it is our feeling that the most efficient way to achieve detection of disease loci by linkage is to increase the correlation between the marker locus and the phenotype either theoretically, e.g. by focusing on Mendelian-like phenotypes, or experimentally, e.g. by using larger pedigrees and more homogeneous samples.

2. Examples

In most complex diseases, a model-based linkage analysis is not possible due to absence of parameter estimates for the genetic model. Still, by employing techniques and analytical approaches discussed, it is possible to conduct genome-wide linkage scans by analyzing extent of allele sharing among affected pairs of siblings. Since unaffected siblings are generally not considered in this approach this precludes its application to diseases where familial clustering is uncommon (e.g. HIV/AIDS). In infectious diseases, model-free genome-wide linkage scanning has been used successfully for mycobacterial diseases, i.e. tuberculosis and leprosy. As in model-based scans, microsatellite-based model-free scans are done in two steps. First, the entire genome is scanned with a panel of equally spaced markers (usually around 400 microsatellites). Once regions with lod scores >1 are identified, the corresponding chromosomal intervals are saturated with higher marker density,

the so-called fine mappings stage. More recently, microsatellites have been replaced by a large number of SNPs where due to the high information content achieved in the initial scan, fine mapping is no longer necessary [e.g. (Cobat *et al.*, 2009b)].

In leprosy, genome-wide linkage scans were done on Brazilian, Indian and Vietnamese multiplex families, i.e. families with more than one leprosy patient (Siddiqui *et al.*, 2001; Mira *et al.*, 2003; Miller *et al.*, 2004). The first scan performed with Indian leprosy families followed a classical design. In the first microsatellite-based low-resolution scan 84 of 93 families represented true sib-pair families, i.e. families with only two affected children (Siddiqui *et al.*, 2001). Consequently, the authors opted for the MLS score method of analysis. Chromosomal regions with an MLS lod score >1 were selected for additional fine mapping in 142 families, 120 of which were single sib-pair families. Only one region on chromosome 10p13 showed significant evidence (multipoint MLS lod score=4.09) for linkage (Siddiqui *et al.*, 2001). A second region on chromosome 20p12 was subsequently found to show suggestive evidence for linkage to leprosy (multipoint MLS lod score = 3.16) in a subset of South Indian leprosy families (Tosh *et al.*, 2002). An important aspect of the Indian study was that the vast majority of cases belonged to the paucibacillary subtype of leprosy. Hence, a decision if chromosome region 10p13 and possibly chromosome region 20p12 harboured leprosy *per se* or paucibacillary leprosy susceptibility loci was not possible.

To avoid such ambiguity a second genome-wide linkage study in Vietnamese multi-case families took care to enrol approximately equal proportions of pauci- and multibacillary forms of leprosy. Compared to the Indian sample, the Vietnamese sample contained a higher proportion of families with more than two affected children (Mira *et al.*, 2003). To accommodate extended families without a loss of power, the authors opted for the MLB approach of genetic analysis (Abel *et al.*, 1998a). A first low-resolution, microsatellite-based scan identified 11 chromosomal regions with some evidence of linkage (multipoint MLB lod score >1) to leprosy (Mira *et al.*, 2003). Subsequent fine mapping of these regions detected suggestive evidence for linkage of leprosy to chromosome region 6p21 (multipoint MLB lod score = 2.62) and highly significant evidence for linkage to chromosome region 6q25–q27 (multipoint MLB lod score = 4.31). Surprisingly, no significant evidence was detected for linkage to chromosome region 10p13. When leprosy families were stratified by leprosy subtype it was possible to show that only paucibacillary cases were linked to the 10p13 region (multipoint MLB lod score = 1.98), while multibacillary cases were not. By contrast, evidence for linkage of chromosome region 6q25–q27 was independent of subtype status. These results demonstrated the need for prudent phenotype selection and provided strong evidence that the locus on chromosome region 6q25–q27 is critical for leprosy *per se* susceptibility while the 10p13 region locus impacts only on susceptibility to paucibacillary leprosy (Mira *et al.*, 2003).

A third genome-wide linkage scan was conducted among Brazilian leprosy families (Miller *et al.*, 2004). The family sample in this scan comprised extended two and three generational multi-case pedigrees (Shaw *et al.*, 2001). Due to the complex family structure, the authors opted for the ALLEGRO program which allows model-free linkage analysis in such a setting. As in the Indian and

Vietnamese studies, the authors followed the same two-stage design of low-resolution mapping followed by high-resolution fine mapping of regions with evidence for linkage in the low-resolution scan. Some evidence for linkage was detected for the *HLA-DQA* gene (lod score = 3.23), chromosome region 17q22 (lod score = 2.38) and chromosome region 20p13 (lod score = 1.51), the latter in close proximity to the region detected in the subset of South Indian leprosy families (Miller *et al.*, 2004). However, while in the Indian families the 20p12 region hit was observed in paucibacillary cases, in the Brazilian families it were mainly multibacillary cases that contributed to the linkage peak. For this reason it is difficult to state with confidence that a replication of the Indian peak was accomplished in the Brazilian families.

An instructive example for the confluence of model-based and model-free analyses is given by a genome-wide linkage scan for tuberculosis susceptibility in Moroccan multiplex families (Baghdadi *et al.*, 2006). The study population was made up of 96 multiplex tuberculosis families with 227 tuberculosis affected offspring. Approximately, one third of the families had more than two affected offspring and 23% of the parents were also affected by tuberculosis. The results of the microsatellite low-resolution genome-wide scan in 48 families were analysed by the MLB method and identified five chromosomal regions with MLB lod scores > 1.17 ($p < 0.01$). These regions were fine mapped with 72 additional microsatellite markers in all 96 families. Chromosomal region 8q12–q13, which provided the strongest evidence for linkage (lod score = 1.98) in the primary scan, was the only interval with significant evidence for linkage to tuberculosis (multipoint MLB score = 3.49). For further investigation of the 8q12–q13 region a model-based linkage analysis was performed. A model similar to the one used for the study of the tuberculosis outbreak in Northern Alberta (Greenwood *et al.*, 2000) was applied, except that no liability classes were used. The model-based linkage analysis provided a maximum multipoint lod score of 3.38. This result strongly suggested dominant inheritance of the tuberculosis susceptibility gene. To test this hypothesis, the 96 multiplex families were subdivided into a group of 39 families with at least one affected parent and 57 families with unaffected parents. A maximum multipoint MLB lod score of 0.79 was obtained in the families without affected parents and lod score of 3.94 in the families with at least one affected parent. Moreover, significant heterogeneity of linkage was observed between the two subgroups ($p < 0.03$). Hence, a combination of model-free and model-based linkage analysis helped to identify a dominant acting major tuberculosis susceptibility gene. A dominant acting susceptibility gene was an unexpected observation but provided a credible explanation for the suspected very strong selection against genetic susceptibility in exposed populations (Baghdadi *et al.*, 2006).

♦♦♦♦♦♦ III. ASSOCIATION METHODS

When successful, linkage analyses generally identify a region of about 10 Mb which may still contain hundreds of genes. In the context of Mendelian genetics where rare mutations with a strong molecular impact are expected to be the cause

of the trait, the next step usually consists in sequencing the coding regions of the genes located under the linkage signal. This strategy has implicated several genes in the control of several infectious diseases [reviewed in (Alcais *et al*., 2009)] and Section II.A.1. In the context of complex traits, however, the most popular paradigm is that we expect to identify common variants with subtle molecular effects. Consequently, the genetic dissection of a linkage peak is usually done by association studies. In classical epidemiological studies, an association is defined as the occurrence in the same individual of two characteristics more often than would be expected by chance. In the context of genetic epidemiology studies, these two characteristics are a phenotype (e.g. a disease or a quantitative measure) and a specific allele at a genetic marker. This latter point holds the key to understanding the difference between linkage and association: linkage looks at a transmission of a locus with a phenotype, whereas association focuses co-occurrence of an allele with a phenotype, hence the popular mnemonic '*L*inkage is with *L*oci and *A*ssociation is with *A*lleles' (Ziegler and Koenig, 2006). To investigate the association between a marker allele and a phenotype, two study designs can be used. Population-based designs use data from unrelated individuals and are similar to case–control studies in classical epidemiology. The idea is to compare the count of a given marker allele, or the counts of genotypes, between unrelated affected (cases) and unaffected (controls). Because the choice of controls can be particularly problematic in the context of genetic studies, family-based designs have been developed such as the transmission disequilibrium test (TDT) that tests for the non-random transmission of a given allele from heterozygote parents to affected sibs (Spielman *et al*., 1993). The sequential strategy – fine mapping by association studies follows a successful localization by linkage – has been challenged in the last few years with the rising use of genome-wide association studies (GWAS) that bypass the linkage step and directly perform association studies on hundreds of thousands of SNPs across the genome.

A. Population-Based Association Studies

Population-based case–control studies compare the frequency of a specific allele at a genetic marker, denoted as M_1, between unrelated affected (cases) and unaffected (controls) subjects (Khoury *et al*., 1993; Lander and Schork, 1994) and it strongly resembles classical epidemiological studies. A first approach considers the allele frequency *per se*, and since each individual has two alleles at any autosomal locus, there will be twice as many alleles as people. A second approach considers genotypes, i.e. the differences in disease risk between individuals who do not carry M_1, those who have a single copy and those who are homozygous for M_1. In an appealing paper, Sasieni (1997) analytically established that both the odds ratio (OR) and the χ^2 statistic computed from the first allelic approach are appropriate provided that the population from which the cases and controls are sampled is in Hardy–Weinberg (HW) equilibrium, i.e. in practice, HW must hold in the *combined* sample (Sasieni, 1997). While some methodological developments have been proposed to overcome this problem (Schaid and Jacobsen, 1999), the interpretation in terms of relative risk of disease remains

questionable when using the allelic analysis. Therefore the use of the genotypic approach should be preferred whenever possible since it also provides the opportunity of testing some specific allelic effects (dominant/recessive) (Box 4). An understated statistical issue is the number of degrees of freedom of the test based on genotypic distribution. Three cases must be distinguished: (a) assuming a multiplicative model (i.e. the risk of M1M1 vs. M2M2 is the square of the risk between M1M2 vs. M2M2), inference about the null hypothesis of no association

Box 4. Population-based association analysis

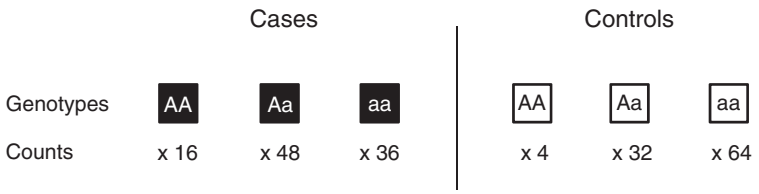

Principle:

In a population-based association design, the idea is to compare the count of a given marker allele, or the counts of genotypes, between unrelated affected (cases) and unaffected (controls) subjects. Under the null hypothesis of no association, the frequency of a given allele, or the genotype distribution, is the same between cases and controls. Under the alternative hypothesis of association, the frequency of a given allele, or the genotype distribution, differs between cases and controls. The allelic and genotypic tests are based on a 2×2 table or a 2×3 table and are asymptotically distributed as a χ^2 with 1 and 2 df, respectively. Although allelic association tests are popular, it should be remembered that humans usually do not carry alleles but genotypes.

Example:

A total of 100 cases and 100 controls are enrolled in a case–control study and genotyped for a di-allelic marker (A/a). The observed distributions of genotypes among cases and controls are summarized in the figure above. Under the null hypothesis of no association between marker and disease the expected distribution of the genotypes is:

Expected counts	AA	Aa	aa	Total
Cases	10	40	50	100
Control	10	40	50	100
Total	20	80	100	200

The χ^2 statistic is
$\chi^2_g = (16–10)^2/10 + (4–10)^2/10 + (48 – 40)^2/40 + (32–40)^2/40 + (36–50)^2/50 + (64–50)^2/50 = 18.24$ and the respective p-value from the χ^2 distribution with 2 df is 0.0001.

Weakness:

Population admixture can lead to fallacious association between a marker and a phenotype if the disease frequency and the allele frequency differ in the subpopulations. Undetected population stratification can have the same effect. Haplotypic analyses are not straightforward.

Strength:

Cost-efficient. Effect size easy to compute. Ease of accommodation of covariates.

Popular software:

Statistical analysis software such SAS (SAS institute, Cary, NC), the R software (The R project software, http://www.r-project.org/), STATA (StataCorp LP, College Station, TX) or SPSS (Chicago, IL).

between the disease and the gene is based on Armitage's trend test (Armitage, 1955) which is asymptotically distributed as a χ^2 with 1 df; (b) assuming no overdominance effect (i.e. the risk of M1M2 vs. M2M2 lies within the range bounded by 1 and the risk of M1M1 vs. M2M2) the test statistic is distributed as a mixture of χ^2 distributions with 1 and 2 df [see for example (Chiano and Clayton, 1998)]; (c) when both previous assumptions are regarded as undesirable, then a traditional χ^2 with 2 df may be used.

A statistically significant association between a given polymorphism and a given phenotype has several possible explanations: (a) random, i.e. the association has occurred just by chance (type I error); (b) the phenotype causes variation in the marker genotype. However, as noted in Allison *et al*. (1999a), this point can be ruled out *a priori* 'as being logically impossible because genotype precedes phenotype in time and because it is a fundamental axiom of causality that cause must precede effect'; (c) the allelic variation causes variation in the phenotype, i.e. it is the functional variant (direct association); (d) the marker allele under study is in linkage disequilibrium (LD) with the allele causing variation in the phenotype (indirect association); and (e) population stratification. In the context of gene identification, we are interested only in associations due to points 3 and 4.

For further explanations, we will consider a situation with two SNPs denoted as G and M. G has two alleles G_1 and G_2, and G_1 is the functional polymorphism increasing the risk of disease (G_1 may be understood as the susceptibility

allele D described previously). M has also two alleles M_1 and M_2 and corresponds to the SNP which has been genotyped and will be tested as the marker. The simplest reason that explains association is that allele M_1 is the functional polymorphism G_1 itself (M and G are identical). A more likely explanation is that M_1 has no direct biological impact on the phenotype but is in LD with allele G_1. LD implies two conditions: (a) linkage between M and G (generally tight linkage and in particular M and G can be within the same gene) *and* (b) allele M_1 is preferentially associated with allele G_1, i.e. the M_1–G_1 haplotype is more frequent than expected by the respective frequencies of M_1 and G_1. This can be interpreted that (many) cases are caused by the ancestral G_1 allele and that the ancestor who transmitted this allele was bearing the M_1–G_1 haplotype. It should be noted that linkage alone (only the first condition is fulfilled), even very close, does not lead to association. Therefore, absence of association does not exclude linkage. These two mechanistic explanations for a positive association (direct vs. indirect) have an impact on the strategy that one will use when performing an association study. Studies that rely on the assumption of direct causality will focus on a gene or a group of functionally related genes (i.e. a pathway) that are thought to be directly relevant to the phenotype under study. Without any prior knowledge on such genes or pathways, one has to rely on indirect association, i.e. genotyping a huge numbers of markers with the hope that one of them will be in strong enough LD with the causal variant to see an indirect yet significant linkage signal. The recent development of several sets of markers that efficiently take advantage of the LD structure observed in the human genome (such sets can capture as much as 90% of all common variants in the Caucasian population) has been a major reason for the large number of GWAS in many diseases over the last 2 years.

Unfortunately, there is one additional, and potentially frequent, situation which can lead to fallacious association between a marker and a phenotype: population stratification also called confounding by ethnicity. For example, a case–control study conducted in a population which is a mixture of two subpopulations in which one has a higher disease frequency and a higher M_1 frequency than the other will observe a positive association of allele M_1 with the disease. A classical example has been given by Knowler *et al*. (1988). In a study on Pima Amerindians, a significant association was reported between type 2 diabetes and the *Gm* locus (Knowler *et al*., 1988). However, type 2 diabetes is more frequent in Pima Amerindians than in Caucasians while the supposedly protective allele at the Gm locus is less frequent in Pima Amerindians than in Caucasians. Because a genetically heterogeneous group of Pima Amerindians was included in the study, i.e. the case and the control groups differed in their degree of Caucasian ancestry, this association was finally shown to be caused by this population stratification bias. Because of the prominence of this potential bias, several statistical methods have been proposed to handle it such as genomic controls (Devlin and Roeder, 1999), structured association (Pritchard *et al*., 2000) and principal component analysis (Patterson *et al*., 2006; Price *et al*., 2006). Another way to avoid this problem of population stratification is to condition on parental genotypes at the marker locus. This is the rationale for the development of family-based association methods that are described in Section III.B

1. Population-based association studies – example

Population-based association studies, also called case–control studies, are a popular design in epidemiology to determine the effect of 'exposure' to a factor under study on an 'outcome', often a disease. The design has been adapted to genetic studies where genotypes are considered as exposure factors. Despite its roots in epidemiology, this design has become the most common choice for candidate gene and GWAS in complex trait genetics. Especially for GWAS there were great hopes that these investigations would hold the key to the riddle of complex trait genetics. So far, however, GWAS have unravelled a relatively small number of loci that generally explain only a small proportion of overall heritability of complex traits. The reasons are unknown and hotly debated. A complex disease where GWAS have been relatively successful in pinpointing susceptibility genes is Crohn's Disease (CD), an idiopathic inflammatory bowel disease with very high heritability (Yang *et al*., 1993). The reason CD can now be give as example in a chapter focused on infectious diseases is a direct result of the susceptibility loci identified. These loci strongly imply an infectious aetiology for at least a proportion of CD patients. In this respect, GWAS in CD are somewhat atypical since the susceptibility genes found have markedly improved our understanding of disease pathogenesis (Mathew, 2008). Still, it is estimated that all known susceptibility variants combined explain less than 25% of the overall genetic variance of Crohn's disease risk.

CD has been extensively analysed in several GWAS (Duerr *et al*., 2006; Hampe *et al*., 2007; Libioulle *et al*., 2007; Rioux *et al*., 2007; The Wellcome Trust Case Control Consortium, 2007) as well as in a number of candidate gene-based experiments (Oliver *et al*., 2007; Villani *et al*., 2009). To address the possibility that current sample sizes are not of sufficient size to detect small genetic effects that might explain the 'missing' heritability, a meta-analysis of three GWAS in populations of European ancestry was conducted (Barrett *et al*., 2008). Since different genotyping platforms had been used in these studies a first challenge was to assemble the same set of genetic markers across all three samples. This was achieved by using so-called genotype 'imputing' methods (Li *et al*., 2009). Imputing relies on the known LD and haplotype pattern in reference individuals to derive genotypes (with defined statistical uncertainty) at missing SNP loci. For the meta-analysis, each sample was analysed independently for SNPs and corrected by the use of genomic controls. Genomic controls allow statistical adjustment for population substructure and other case–control mismatches by analysing the distribution of control alleles in the case and control groups. Such controls are an important tool to avoid an inflated type I error in case–control phenotype–genotype association studies. The individual results (not the cases and control genotypes) from each of the three samples were then combined in the meta-analysis.

The combined results of the CD-control samples had power of 74% to detect common alleles with OR as low as 1.2. A total of 526 SNPs from 74 distinct loci that showed evidence of association with CD were considered to merit additional study ($p < 5 \times 10^{-5}$) (Barrett *et al*., 2008). Among the 74 loci, 11 had already been reported as CD risk factors in previous studies (i.e. *NOD2, IBD5, IL23R, ATG16L1, IRGM, TNFSF15, PTPN2*). The remaining 63 putative CD susceptibility genes were further studied in replication samples including 2325 CD cases and 1809 controls, as well

as 1339 simplex families. From all regions tested 21 new associations were identified. While fine mapping is needed to identify susceptibility genes, it is of interest that a number of genes that are part of the IL12/IL23 signalling cascade are tagged by the associated SNPs. An alternative approach to meta-analysis for the tracking of small but true genetic effects in GWAS is so-called 'pathway' mapping (Wang *et al*., 2009). Here, the global evidence for overrepresentation of genes that encode proteins which are part of the same cellular pathway is evaluated. The usefulness of this approach for the full exploitation of GWAS data still needs to be confirmed. Finally, it is possible that rare variants with very strong genetic effects underlie a significant proportion of genetic variance in complex traits. This would imply extensive genetic heterogeneity due to rare alleles that are essentially not detectable by case–control studies.

B. Family-Based Association Studies

As already stated in Section III.A, one drawback with the use of population-based designs in testing the association between a marker and a phenotype is the possibility of population stratification. Beside elegant statistical methods, one straightforward way to avoid this problem is to condition on parental genotypes at the marker locus. This is the rationale for the development of family-based association methods, such as the TDT (Spielman *et al*., 1993). The sampling unit in the classical TDT consists of two parents with one affected child, and parental alleles non-transmitted to affected children are used as control alleles. More specifically, the TDT considers affected children born from parents heterozygous for M_1, i.e. M_1M_2 parents, and simply tests whether these children have received M_1 with a probability different from 0.5, the value expected under random segregation (Box 5). Subsequently, methods have been developed to handle families with missing parental data by either using unaffected sibs as controls (Sib-TDT) (Spielman and Ewens, 1998) or reconstructing parental genotypes from children (RC-TDT) (Knapp, 1999). The FBAT software allows efficient analysis of family data by combining these different approaches (Lake *et al*., 2000; Horvath *et al*., 2001). In addition to being robust against inflated type I errors due to population stratification or case–control mismatches, family-based designs offer several well-recognized additional advantages over population-based designs such as the inference of marker phase, i.e. the unambiguous reconstruction of haplotypes, the analysis of imprinting effects and the inference of missing genotypes. Moreover, marker imputation in a family setting has been shown to be more efficient than in case–control designs. Finally, by comparing genotypes among parents that are discordant for disease status (a parent only case–control design), family-based designs carry a build-in replication test for SNPs with significant distortion of transmission ratios. The realization that population-based and family-based methods are complementary rather than mutually exclusive has led to the recent development of hybrid approaches that accommodate both designs into a single analysis. Large-scaled association studies are still needed to assess the statistical performances of such methods but preliminary results are encouraging [for an elegant description of these methods see Infante-Rivard *et al*. (2009)].

Box 5. Family-based association analysis

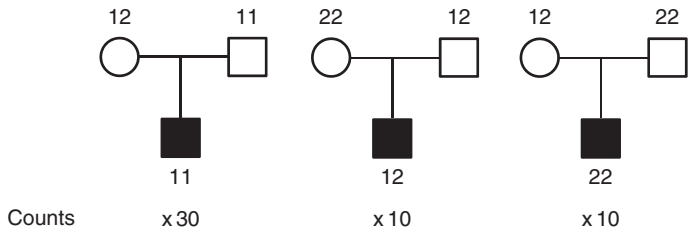

Principle:

Family-based association designs aim to avoid the problem of population admixture by conditioning on parental genotypes at the marker loci. The most commonly used test is TDT. The sampling unit in the classical TDT consists of two parents with one affected child (trio, see figure above), and parental alleles non-transmitted to affected children are used as control alleles. Under the null hypothesis of no association, affected children receive marker alleles from a heterozygous parent with equal probability. Under the alternative hypothesis, an allele that increases risk of the disease is more often transmitted to affected children than expected by chance. In informative (=heterozygous) parents, the deviation from a 1:1 allele transmission ratio of a bi-allelic marker to an affected child can be test by the McNemar χ^2 statistic. Extensions to multi-allelic markers are possible.

Example:

Fifty trios were genotyped for a di-allelic genetic marker with alleles 1 and 2. The observed genotypes are summarized in the figure above and the transmissions can be summarized in the following contingency table:

	Non-transmitted allele		
Transmitted allele	1	2	Total
1	$n_{11} = 30$	$n_{12} = 30 + 10$	70
2	$n_{21} = 10$	$n_{22} = 10 + 10$	30
Total	40	60	100

The McNemar test statistic is $\chi^2_{TDT} = (n_{21} - n_{12})^2/(n_{21} + n_{12}) = (10 - 40)^2/(10 + 40) = 18$, and the corresponding p-value from the χ^2 distribution with 1 df is <0.0001.

Weakness:

Three individuals to genotype instead of two in case–control design.

Parents of affected cases are needed, which can be difficult in late-onset disease.

Strength:

Avoids the problem of population admixture. More easy to establish phase and to conduct haplotypic analyses.

Popular software:

FBAT (Laird *et al*., 2000), TRANSMIT (Clayton and Jones, 1999), PDT (Martin *et al*., 2000)

Although association studies mostly focus on binary traits (affected/unaffected), numerous developments have been recently performed for the analysis of quantitative phenotypes that rely either on regression [e.g. (George *et al*., 1999; Waldman *et al*., 1999; Monks and Kaplan, 2000)] or variance component [e.g. (Fulker *et al*., 1999; Abecasis *et al*., 2000; Sham *et al*., 2000)] techniques that are implemented in the popular QTDT software (Abecasis *et al*., 2000). Regression and variance component techniques are closely related and therefore display similar limitations. First, they intrinsically assume multivariate normality of the phenotypic distribution, and violation of this hypothesis can lead to a large inflation of the type I error rate when compared to the asymptotic expectations. The use of very large samples would relax this assumption by allowing reliance on the central limit theorem. However, in some cases (e.g. in the context of extremely selected samples) neither the normality assumption nor the use of a large sample can be achieved. Therefore, the analysis of such data would usually require the use of additional procedures such as the transformation of the data to handle the non-normality or the computation of empirical *p*-values. Furthermore, it is clear that both approaches derive information from phenotypic variability. Consequently, as mentioned in Abecasis *et al*. (2001) these methods may have low power to detect LD under some extreme selection schemes (e.g. one-tailed selection). However, when their assumptions are verified, these approaches can be very powerful and their flexibility may allow valuable insight into the genetic mechanisms underlying the studied trait.

Association studies (population-based or family-based) are expected to be very efficient to detect the effect of allele M_1 when M_1 is the functional polymorphism G_1 itself (Risch and Merikangas, 1996). Under this latter hypothesis, Risch and Merikangas demonstrated that the TDT was more powerful than the sib-pair method even in the context of a genome-wide search involving 500,000 di-allelic polymorphisms. However, in the more common situation where M_1 is different from G_1, the power of TDT (as is true for all indirect association studies) is highly dependent on both the respective frequencies of M_1 and G_1 and the strength of LD

between M_1 and G_1 (Muller-Myhsok and Abel, 1997; Abel and Muller-Myhsok, 1998a). To a large extent, the utility of genome-wide association testing depends on the existence of marker alleles strongly associated with the disease-causing polymorphisms. Because the extent of LD is not uniformly distributed among populations, in particular being much lower in African populations (Jallow *et al.*, 2009), the optimal strategy of analysis may vary from one disease to another according to its ethno-geographical distribution. A textbook example for the impact of the LD pattern on the power of a study is the recent publication of a GWAS on severe malaria in The Gambia (Jallow *et al.*, 2009). The initial GWAS scan included 2500 children genotyped for 500,000 SNPs. First and not surprisingly, the authors found considerable population stratification. Second, signals of association at known malaria resistance loci were greatly attenuated owing to weak LD. Finally, no novel variant was convincingly identified although the sample size was large and the phenotype rather severe. These results clearly indicate that there is no universal optimal design and that linkage methods still have value in the identification of genes involved in infectious diseases.

I. Family-based association studies – example

Here, we provide two examples for LD scans of linkage peaks from the Vietnamese linkage study of leprosy susceptibility discussed above. The overall approach is similar to a GWAS except that genotyped SNPs are focused to a target region defined by the linkage peak. The linkage analysis had identified a peak on chromosome 6q25–q27. The 90% confidence interval for the location of the gene that underlies such a linkage peak is approximately the segment that is located within a 1 lod support interval. In this case the linkage peak showed a maximum lod score of 4.31 and the 1 lod interval is the segment surrounding the peak that shows evidence for linkage with lod score >3.31. The 1 lod interval spanned for 6.4 Mb of chromosomal DNA and was targeted for an association in 197 simplex (i.e. one affected child and both parents) leprosy families from Vietnam. Six markers showed significant association with leprosy ($p < 0.05$), four of which were clustered in the shared, bi-directional promoter region of the *PARK2* and *PACRG* genes (Mira *et al.*, 2004). This region was further saturated with markers and 19 SNPs were found significantly associated with leprosy. Multivariate logistic regression analysis demonstrated that two SNPs, *PARK2*_e01(–2599) and rs1040079, were sufficient to capture all association information (Mira *et al.*, 2004). Interestingly, the genetic effect (OR = 5.28 [95% CI 2.06–13.5]) determined by conditional logistic regression was very strong in the context of a complex trait. To confirm the obtained associations an independent sample of 587 leprosy cases and 388 unaffected controls from Brazil was enrolled. Out of 13 SNPs genotyped, *PARK2*_e01(–2599) and rs1040079, were among the three most associated with leprosy SNPs in this Brazilian sample under the same genetic model with the same alleles as in the initial Vietnamese family sample. These studies established *PARK2*_e01(–2599) and rs1040079 as a major leprosy risk factor in two distinct populations (Mira *et al.*, 2004).

In the next example, we want to illustrate the importance of LD pattern for a successful replication of a true genotype–phenotype association. In high-density

association scans, closely spaced SNPs usually segregate not independently of each other. Rather certain SNP alleles are correlated and due to this correlation there is a degree of redundancy among SNP segregation. This is a reflection of LD among SNPs and underlies the genotype imputing approaches discussed above. A common measure of LD is the correlation coefficient r^2 which varies from zero to unity. It is common practice to define so-called 'SNP bins' where at least one SNP is correlated with all other SNPs at $r^2 = 0.8$. Such SNPs are called tag SNPs and can be used in the first round of association studies to represent all the other SNPs in the bin. The important point is that LD between SNPs, and hence SNP bins, is often population specific as is illustrated by the limited power of the GWAS of severe malaria that used Caucasian SNP sets for the study of an African population.

The LD scanning strategy used to identify the *PARK2/PACRG* leprosy risk factors in the 6q25–q26 chromosomal interval was also applied to dissect the linkage peak on chromosome region 6p21 (Alcais *et al.*, 2007). The association scan employing the FBAT program as analysis tool quickly identified a bin of seven SNPs that was associated with leprosy in 198 simplex families. The most significantly associated SNP was *LTA-293* located in the *LTA* gene regulatory region. The association of the *LTA-293* bin with leprosy was successfully confirmed in the second sample of 104 Vietnamese simplex families. To validate the Vietnamese replication, a total of six *LTA* SNPs were tested in a sample of 364 leprosy cases and 371 unrelated controls from Northern India. Only the *LTA-294* SNP showed significant evidence for association with leprosy, a SNP that was not associated in the Vietnamese families (Alcais *et al.*, 2007). However, when conducting multivariate analysis, i.e. when adjusting on the *LTA-294* genotypes, members of the Vietnamese *LTA-293* SNP bin also showed evidence for association while SNP *LTA-293* itself was not associated. Obviously the LD pattern has changed in the North Indian population and the Vietnamese *LTA-293* bin is not maintained in the North Indian population. Likewise, SNP *LTA-294* in the North Indians is part of a bin that contains an additional unknown leprosy risk factor but this bin is not maintained in the Vietnamese population where *LTA-294* is not associated with leprosy. Together, these findings exclude *LTA-294* and *LTA-293* as causal leprosy risk factors.

Among the SNPs that are consistently associated with leprosy in both the Vietnamese and North Indian samples is *LTA+80*. This SNP had previously been shown to be a regulatory SNP due to preferential binding of the ABF transcriptional repressor to one of the *LTA+80* SNP alleles (Knight *et al.*, 2004). This SNP was therefore considered as likely candidate for a leprosy susceptibility factor. However, when trying to replicate the *LTA+80* susceptibility factor in a case–control sample of 209 leprosy cases and 192 controls from Brazil, *LTA+80* failed to provide significant evidence for association. At first glance this suggested *LTA+80* as an example for genetic heterogeneity of leprosy susceptibility. However, more close inspection of demographic covariates of the three different samples revealed a strong bias for younger patients. This bias is a direct result of the requirement for both parents being available for enrolment in the study. As a result, the median age at diagnosis of patients was 16 years in Vietnam, 31 years in India and 38 years in Brazil. Stratification by age showed a very strong effect of the *LTA+80* risk allele in Vietnamese patients less than 16 years at diagnosis ($p = 0.00004$, OR = 5.76; 95% CI 2.25–14.78) and absence of association in older cases. Likewise, the strongest

evidence for association in the Indian sample was found for the youngest patients ($p = 0.006$, OR = 2.95; 95% CI 1.32–6.58). The same observation was made for the Brazilian cases where the youngest age group (16–25 years) showed a clear enrichment of the *LTA+80*_A risk allele ($p = 0.07$). These results indicated a strong age-dependent effect of *LTA+80*_A in leprosy susceptibility. This result underlined the importance of age as critical covariate in the analysis of genotype–phenotype associations (Alcais *et al.*, 2007).

♦♦♦♦♦♦ IV. CONCLUSION

In this chapter, we have focused on the description of the genetic analysis of binary traits (affected/unaffected) and provided only a glimpse on the study of quantitative traits. While in the past the vast majority of genetic studies have focused on the affected status, there is a solid body of evidence suggesting that genetic investigation of quantitative traits will be a worthwhile line of future research. For example, recall responses to PPD-triggered cytokine production show very significant heritability with estimates varying from 40 to 58% for IFNγ production (Wiart *et al.*, 2004; Cobat *et al.*, 2009a), 70% for Mantoux delayed type hypersensitivity skin reaction (Jepson *et al.*, 2001) and 30–68% for TNFα production (Stein *et al.*, 2003; Cobat *et al.*, 2009a). An advantage of studying quantitative immune phenotypes is that quantitative traits can provide significantly higher power for gene mapping than disease alone (Duggirala *et al.*, 1997) assuming the trait under study has a substantial genetic component. Consequently, first reports have appeared that successfully identified loci impacting on granulomatous forming capacity in response to *Mycobacterium leprae* (Alcais *et al.*, 2000; Ranque *et al.*, 2005) or on extent of TST reactivity (Cobat *et al.*, 2009b). Taken together these findings suggest that quantitative trait analysis will be one of the frontiers of human genetics of infectious diseases in the next decade.

References

Abecasis, G. R., Cardon, L. R. and Cookson, W. O. (2000). A general test of association for quantitative traits in nuclear families. *Am. J. Hum. Genet.* **66**, 279–292.

Abecasis, G. R., Cherny, S. S., Cookson, W. O. and Cardon, L. R. (2002). Merlin–rapid analysis of dense genetic maps using sparse gene flow trees. *Nat. Genet.* **30**, 97–101.

Abecasis, G. R., Cookson, W. O. and Cardon, L. R. (2001). The power to detect linkage disequilibrium with quantitative traits in selected samples. *Am. J. Hum. Genet.* **68**, 1463–1474.

Abel, L., Alcais, A. and Mallet, A. (1998a). Comparison of four sib-pair linkage methods for analyzing sibships with more than two affecteds: interest of the binomial maximum likelihood approach. *Genet. Epidemiol.* **15**, 371–390.

Abel, L., Demenais, F., Prata, A., Souza, A. E. and Dessein, A. (1991). Evidence for the segregation of a major gene in human susceptibility/resistance to infection by Schistosoma mansoni. *Am. J. Hum. Genet.* **48**, 959–970.

Abel, L. and Dessein, A. (1991). Genetic predisposition to high infections in an endemic area of Schistosoma mansoni. *Rev. Soc. Bras. Med. Trop.* **24**, 1–3.

Abel, L. and Muller-Myhsok, B. (1998a). Maximum-likelihood expression of the transmission/disequilibrium test and power considerations. *Am. J. Hum. Genet.* **63**, 664–667.
Abel, L. and Muller-Myhsok, B. (1998b). Robustness and power of the maximum-likelihood-binomial and maximum-likelihood-score methods, in multipoint linkage analysis of affected-sibship data. *Am. J. Hum. Genet.* **63**, 638–647.
Abel, L., Sanchez, F. O., Oberti, J., Thuc, N. V., Hoa, L. V., Lap, V. D., Skamene, E., Lagrange, P. H. and Schurr, E. (1998b). Susceptibility to leprosy is linked to the human NRAMP1 gene. *J. Infect. Dis.* **177**, 133–145.
Al-Muhsen, S. and Casanova, J. L. (2008). The genetic heterogeneity of Mendelian susceptibility to mycobacterial diseases. *J. Allergy Clin. Immunol.* **122**, 1043–1051.
Alcais, A. and Abel, L. (1999). Maximum-Likelihood-Binomial method for genetic model-free linkage analysis of quantitative traits in sibships. *Genet. Epidemiol.* **17**, 102–117.
Alcais, A. and Abel, L. (2000a). Robustness of the Maximum-Likelihood-Binomial approach for linkage analysis of quantitative trait loci with non-normal phenotypic data. *Genescreen* **1**, 47–50.
Alcais, A. and Abel, L. (2000b). Linkage analysis of quantitative trait loci: sib pairs or sibships? *Hum. Hered.* **50**, 251–256.
Alcais, A. and Abel, L. (2001). Incorporation of covariates in multipoint model-free linkage analysis of binary traits: how important are unaffecteds? *Eur. J. Hum. Genet.* **9**, 613–620.
Alcais, A., Abel, L. and Casanova, J. L. (2009). Human genetics of infectious diseases: between proof of principle and paradigm. *J. Clin. Invest.* **119**, 2506–2514.
Alcais, A., Alter, A., Antoni, G., Orlova, M., Nguyen, V. T., Singh, M., Vanderborght, P. R., Katoch, K., Mira, M. T., Vu, H. T. *et al*. (2007). Stepwise replication identifies a low-producing lymphotoxin-alpha allele as a major risk factor for early-onset leprosy. *Nat. Genet.* **39**, 517–522.
Alcais, A., Sanchez, F. O., Thuc, N. V., Lap, V. D., Oberti, J., Lagrange, P. H., Schurr, E. and Abel, L. (2000). Granulomatous reaction to intradermal injection of lepromin (Mitsuda reaction) is linked to the human NRAMP1 gene in Vietnamese leprosy sibships. *J. Infect. Dis.* **181**, 302–308.
Allison, D. B., Heo, M., Kaplan, N. and Martin, E. R. (1999a). Sibling-based tests of linkage and association for quantitative traits. *Am. J. Hum. Genet.* **64**, 1754–1763.
Allison, D. B., Neale, M. C., Zannolli, R., Schork, N. J., Amos, C. I. and Blangero, J. (1999b). Testing the robustness of the likelihood-ratio test in a variance-component quantitative-trait loci-mapping procedure. *Am. J. Hum. Genet.* **65**, 531–544.
Almasy, L. and Blangero, J. (1998). Multipoint quantitative-trait linkage analysis in general pedigrees. *Am. J. Hum. Genet.* **62**, 1198–1211.
Altare, F., Durandy, A., Lammas, D., Emile, J. F., Lamhamedi, S., Le, D. F., Drysdale, P., Jouanguy, E., Doffinger, R., Bernaudin, F. *et al*. (1998a). Impairment of mycobacterial immunity in human interleukin-12 receptor deficiency. *Science* **280**, 1432–1435.
Altare, F., Lammas, D., Revy, P., Jouanguy, E., Doffinger, R., Lamhamedi, S., Drysdale, P., Scheel-Toellner, D., Girdlestone, J., Darbyshire, P. *et al*. (1998b). Inherited interleukin 12 deficiency in a child with bacille Calmette-Guerin and Salmonella enteritidis disseminated infection. *J. Clin. Invest.* **102**, 2035–2040.
Amos, C. I. (1994). Robust variance-components approach for assessing genetic linkage in pedigrees. *Am. J. Hum. Genet.* **54**, 535–543.
Amos, C. I. and Elston, R. C. (1989). Robust methods for the detection of genetic linkage for quantitative data from pedigrees. *Genet. Epidemiol.* **6**, 349–360.
Armitage, P. (1955). Test for linear trend in proportions and frequencies. *Biometrics*, 375–386.
Baghdadi, J. E., Orlova, M., Alter, A., Ranque, B., Chentoufi, M., Lazrak, F., Archane, M. I., Casanova, J. L., Benslimane, A., Schurr, E. *et al*. (2006). An autosomal dominant major gene confers predisposition to pulmonary tuberculosis in adults. *J. Exp. Med.* **203**, 1679–1684.

Barrett, J. C., Hansoul, S., Nicolae, D. L., Cho, J. H., Duerr, R. H., Rioux, J. D., Brant, S. R., Silverberg, M. S., Taylor, K. D., Barmada, M. M. *et al*. (2008). Genome-wide association defines more than 30 distinct susceptibility loci for Crohn's disease. *Nat. Genet.* **40**, 955–962.

Bellamy, R., Ruwende, C., Corrah, T., McAdam, K. P., Whittle, H. C. and Hill, A. V. (1998). Variations in the NRAMP1 gene and susceptibility to tuberculosis in West Africans. *N. Engl. J. Med.* **338**, 640–644.

Bonney, G. E. (1984). On the statistical determination of major gene mechanisms in continuous human traits: regressive models. *Am. J. Med. Genet.* **18**, 731–749.

Bonney, G. E. (1986). Regressive logistic models for familial disease and other binary traits. *Biometrics* **42**, 611–625.

Butterworth, A. E., Capron, M., Cordingley, J. S., Dalton, P. R., Dunne, D. W., Kariuki, H. C., Kimani, G., Koech, D., Mugambi, M. and Ouma, J. H. (1985). Immunity after treatment of human schistosomiasis mansoni. II. Identification of resistant individuals, and analysis of their immune responses. *Trans. R. Soc. Trop. Med. Hyg.* **79**, 393–408.

Casanova, J. L. and Abel, L. (2007). Primary immunodeficiencies: a field in its infancy. *Science* **317**, 617–619.

Casanova, J. L., Jouanguy, E., Lamhamedi, S., Blanche, S. and Fischer, A. (1995). Immunological conditions of children with BCG disseminated infection. *Lancet* **346**, 581.

Chiano, M. N. and Clayton, D. G. (1998). Genotypic relative risks under ordered restriction. *Genet. Epidemiol.* **15**, 135–146.

Clayton, D. and Jones, H. (1999). Transmission/disequilibrium tests for extended marker haplotypes. *Am. J. Hum. Genet.* **65**.

Clerget-Darpoux, F., Bonaiti-Pellie, C. and Hochez, J. (1986). Effects of misspecifying genetic parameters in lod score analysis. *Biometrics* **42**, 393–399.

Cobat, A., Gallant, C. J., Simkin, L., Black, G. F., Stanley, K., Hughes, J., Doherty, T. M., Hanekom, W. A., Eley, B., Beyers, N. *et al*. (2009a). High heritability of anti-mycobacterial immunity in a hyperendemic area for tuberculosis disease. *J. Infect. Dis.* (In Press.).

Cobat, A., Gallant, C. J., Simkin, L., Black, G. F., Stanley, K., Hughes, J., Doherty, T. M., Hanekom, W. A., Eley, B., Jais, J. P. *et al*. (2009b). Two loci control tuberculin skin test reactivity in an area hyperendemic for tuberculosis. *J. Exp. Med.* (In Press).

Cottingham, R. W. Jr., Idury, R. M. and Schaffer, A. A. (1993). Faster sequential genetic linkage computations. *Am. J. Hum. Genet.* **53**.

de Jong, R., Altare, F., Haagen, I. A., Elferink, D. G., Boer, T., van Breda Vriesman Kabel, P. J., Draaisma, J. M., van Dissel, J. T., Kroon, F. P., Casanova, J. L. *et al*. (1998). Severe mycobacterial and Salmonella infections in interleukin-12 receptor-deficient patients. *Science* **280**, 1435–1438.

Devlin, B. and Roeder, K. (1999). Genomic control for association studies. *Biometrics* **55**.

Dorman, S. E. and Holland, S. M. (1998). Mutation in the signal-transducing chain of the interferon-gamma receptor and susceptibility to mycobacterial infection. *J. Clin. Invest.* **101**, 2364–2369.

Duerr, R. H., Taylor, K. D., Brant, S. R., Rioux, J. D., Silverberg, M. S., Daly, M. J., Steinhart, A. H., Abraham, C., Regueiro, M., Griffiths, A. *et al*. (2006). A genome-wide association study identifies IL23R as an inflammatory bowel disease gene. *Science* **314**, 1461–1463.

Duggirala, R., Williams, J. T., Williams-Blangero, S. and Blangero, J. (1997). A variance component approach to dichotomous trait linkage analysis using a threshold model. *Genet. Epidemiol.* **14**, 987–992.

Dupuis, S., Dargemont, C., Fieschi, C., Thomassin, N., Rosenzweig, S., Harris, J., Holland, S. M., Schreiber, R. D. and Casanova, J. L. (2001). Impairment of mycobacterial but not viral immunity by a germline human STAT1 mutation. *Science* **293**, 300–303.

Elston, R. C. (1998). Methods of linkage analysis–and the assumptions underlying them [see comment]. *Am. J. Hum. Genet.* **63**, 931–934.

Feingold, E. (2002). Regression-based quantitative-trait-locus mapping in the 21st century. *Am. J. Hum. Genet.* **71**, 217–222.

Filipe-Santos, O., Bustamante, J., Chapgier, A., Vogt, G., de, B. L., Feinberg, J., Jouanguy, E., Boisson-Dupuis, S., Fieschi, C., Picard, C. *et al*. (2006a). Inborn errors of IL-12/23- and IFN-gamma-mediated immunity: molecular, cellular, and clinical features. *Semin. Immunol.* **18**, 347–361.

Filipe-Santos, O., Bustamante, J., Haverkamp, M. H., Vinolo, E., Ku, C. L., Puel, A., Frucht, D. M., Christel, K., von, B. H., Jouanguy, E. *et al*. (2006b). X-linked susceptibility to mycobacteria is caused by mutations in NEMO impairing CD40-dependent IL-12 production. *J. Exp. Med.* **203**, 1745–1759.

Fulker, D. W., Cherny, S. S., Sham, P. C. and Hewitt, J. K. (1999). Combined linkage and association sib-pair analysis for quantitative traits. *Am. J. Hum. Genet.* **64**, 259–267.

George, V., Tiwari, H. K., Zhu, X. and Elston, R. C. (1999). A test of transmission/ disequilibrium for quantitative traits in pedigree data, by multiple regression. *Am. J. Hum. Genet.* **65**, 236–245.

Goldgar, D. E. (1990). Multipoint analysis of human quantitative genetic variation. *Am. J. Hum. Genet.* **47**, 957–967.

Goldgar, D. E. (2001). Major strengths and weaknesses of model-free methods. *Adv. Genet.* **42**, 241–251.

Greenwood, C. M., Fujiwara, T. M., Boothroyd, L. J., Miller, M. A., Frappier, D., Fanning, E. A., Schurr, E. and Morgan, K. (2000). Linkage of tuberculosis to chromosome 2q35 loci, including NRAMP1, in a large aboriginal Canadian family. *Am. J. Hum. Genet.* **67**, 405–416.

Gudbjartsson, D. F., Jonasson, K., Frigge, M. L. and Kong, A. (2000). Allegro, a new computer program for multipoint linkage analysis. *Nat. Genet.* **25**.

Hagan, P., Blumenthal, U. J., Chaudri, M., Greenwood, B. M., Hayes, R. J., Hodgson, I., Kelly, C., Knight, M., Simpson, A. J. and Smithers, S. R. (1987). Resistance to reinfection with Schistosoma haematobium in Gambian children: analysis of their immune responses. *Trans. R. Soc. Trop. Med. Hyg.* **81**, 938–946.

Hampe, J., Franke, A., Rosenstiel, P., Till, A., Teuber, M., Huse, K., Albrecht, M., Mayr, G., De La Vega, F. M., Briggs, J. *et al*. (2007). A genome-wide association scan of nonsynonymous SNPs identifies a susceptibility variant for Crohn disease in ATG16L1. *Nat. Genet.* **39**, 207–211.

Haseman, J. K. and Elston, R. C. (1972). The investigation of linkage between a quantitative trait and a marker locus. *Behav. Genet.* **2**, 3–19.

Holmans, P. (2001). Likelihood-ratio affected sib-pair tests applied to multiply affected sibships: issues of power and type I error rate. *Genet. Epidemiol.* **20**, 44–56.

Horvath, S., Xu, X. and Laird, N. M. (2001). The family based association test method: strategies for studying general genotype–phenotype associations. *Eur. J. Hum. Genet.* **9**, 301–306.

Houston, S., Fanning, A., Soskolne, C. L. and Fraser, N. (1990). The effectiveness of bacillus Calmette-Guerin (BCG) vaccination against tuberculosis. A case-control study in Treaty Indians, Alberta, Canada. *Am. J. Epidemiol.* **131**, 340–348.

Infante-Rivard, C., Mirea, L. and Bull, S. B. (2009). Combining case-control and case-trio data from the same population in genetic association analyses: overview of approaches and illustration with a candidate gene study. *Am. J. Epidemiol.* **170**, 657–664.

Jallow, M., Teo, Y. Y., Small, K. S., Rockett, K. A., Deloukas, P., Clark, T. G., Kivinen, K., Bojang, K. A., Conway, D. J., Pinder, M. *et al*. (2009). Genome-wide and fine-resolution association analysis of malaria in West Africa. *Nat. Genet.*.

Jarvik, G. P. (1998). Complex segregation analyses: uses and limitations. *Am. J. Hum. Genet.* **63**, 942–946.

Jepson, A., Fowler, A., Banya, W., Singh, M., Bennett, S., Whittle, H. and Hill, A. V. (2001). Genetic regulation of acquired immune responses to antigens of Mycobacterium tuberculosis: a study of twins in West Africa. *Infect. Immun.* **69**, 3989–3994.

Jouanguy, E., Altare, F., Lamhamedi, S., Revy, P., Emile, J. F., Newport, M., Levin, M., Blanche, S., Seboun, E., Fischer, A. *et al*. (1996). Interferon-gamma-receptor deficiency in an infant with fatal bacille Calmette-Guerin infection. *N. Engl. J. Med.* **335**, 1956–1961.

Khoury, M. J., Beaty, T. H. and Cohen, B. H. (1993). *Fundamentals of Genetic Epidemiology (Monographs in Epidemiology and Biostatistics)*, Vol. 19, p. 383. Oxford Univeristy Press, New York.

Knapp, M. (1999). The transmission/disequilibrium test and parental-genotype reconstruction: the reconstruction-combined transmission/ disequilibrium test. *Am. J. Hum. Genet.* **64**, 861–870.

Knapp, M., Seuchter, S. A. and Baur, M. P. (1994). Linkage analysis in nuclear families. 2: relationship between affected sib-pair tests and lod score analysis. *Hum. Hered.* **44**, 44–51.

Knight, J. C., Keating, B. J. and Kwiatkowski, D. P. (2004). Allele-specific repression of lymphotoxin-alpha by activated B cell factor-1. *Nat. Genet.* **36**, 394–399.

Knowler, W. C., Williams, R. C., Pettitt, D. J. and Steinberg, A. G. (1988). Gm3;5,13,14 and type 2 diabetes mellitus: an association in American Indians with genetic admixture. *Am. J. Hum. Genet.* **43**, 520–526.

Kruglyak, L., Daly, M. J., Reeve-Daly, M. P. and Lander, E. S. (1996). Parametric and nonparametric linkage analysis: a unified multipoint approach. *Am. J. Hum. Genet.* **58**.

Laird, N. M., Horvath, S. and Xu, X. (2000). Implementing a unified approach to family-based tests of association. *Genet. Epidemiol.* **19**(Suppl. 1).

Lake, S. L., Blacker, D. and Laird, N. M. (2000). Family-based tests of association in the presence of linkage. *Am. J. Hum. Genet.* **67**, 1515–1525.

Lander, E. S. and Botstein, D. (1987). Homozygosity mapping: a way to map human recessive traits with the DNA of inbred children. *Science* **236**, 1567–1570.

Lander, E. and Kruglyak, L. (1995). Genetic dissection of complex traits: guidelines for interpreting and reporting linkage results. *Nat. Genet.* **11**, 241–247.

Lander, E. S. and Schork, N. J. (1994). Genetic dissection of complex traits. *Science* **265**, 2037–2048.

Lathrop, G. M., Lalouel, J. M., Julier, C. and Ott, J. (1984). Strategies for multilocus linkage analysis in humans. *Proc. Natl. Acad. Sci. U.S.A* **81**.

Li, Y., Willer, C., Sanna, S. and Abecasis, G. (2009). Genotype imputation. *Annu. Rev. Genomics Hum. Genet.* **10**, 387–406.

Libioulle, C., Louis, E., Hansoul, S., Sandor, C., Farnir, F., Franchimont, D., Vermeire, S., Dewit, O., de, V. M., Dixon, A. *et al*. (2007). Novel Crohn disease locus identified by genome-wide association maps to a gene desert on 5p13.1 and modulates expression of PTGER4. *PLoS Genet.* **3**, e58.

MacLean, C. J., Bishop, D. T., Sherman, S. L. and Diehl, S. R. (1993). Distribution of lod scores under uncertain mode of inheritance. *Am. J. Hum. Genet.* **52**, 354–361.

Marquet, S., Abel, L., Hillaire, D., Dessein, H., Kalil, J., Feingold, J., Weissenbach, J. and Dessein, A. J. (1996). Genetic localization of a locus controlling the intensity of infection by Schistosoma mansoni on chromosome 5q31-q33. *Nat. Genet.* **14**, 181–184.

Martin, E. R., Monks, S. A., Warren, L. L. and Kaplan, N. L. (2000). A test for linkage and association in general pedigrees: the pedigree disequilibrium test. *Am. J. Hum. Genet.* **67**.

Mathew, C. G. (2008). New links to the pathogenesis of Crohn disease provided by genome-wide association scans. *Nat. Rev. Genet.* **9**, 9–14.

Miller, E. N., Jamieson, S. E., Joberty, C., Fakiola, M., Hudson, D., Peacock, C. S., Cordell, H. J., Shaw, M. A., Lins-Lainson, Z., Shaw, J. J. *et al*. (2004). Genome-wide scans for leprosy and tuberculosis susceptibility genes in Brazilians. *Genes Immun.* **5**, 63–67.

Mimouni, J. (1951). Our experiences in 3 years of BCG vaccination at the center of the O.P.H.S. at Constantine; study of observed cases (25 cases of complications from BCG vaccination). *Alger Medicale* **55**, 1138–1147.
Mira, M. T., Alcais, A., Nguyen, V. T., Moraes, M. O., Di, F. C., Vu, H. T., Mai, C. P., Nguyen, T. H., Nguyen, N. B., Pham, X. K. *et al*. (2004). Susceptibility to leprosy is associated with PARK2 and PACRG. *Nature* **427**, 636–640.
Mira, M. T., Alcais, A., Van, T. N., Thai, V. H., Huong, N. T., Ba, N. N., Verner, A., Hudson, T. J., Abel, L. and Schurr, E. (2003). Chromosome 6q25 is linked to susceptibility to leprosy in a Vietnamese population. *Nat. Genet.* **33**, 412–415.
Monks, S. A. and Kaplan, N. L. (2000). Removing the sampling restrictions from family-based tests of association for a quantitative-trait locus. *Am. J. Hum. Genet.* **66**, 576–592.
Morton, N. E. (1955). Sequential tests for the detection of linkage. *Am. J. Hum. Genet.* **7**, 277–318.
Morton, N. E. (1998). Significance levels in complex inheritance. *Am. J. Hum. Genet.* **62**, 690–697.
Muller-Myhsok, B. and Abel, L. (1997). Genetic analysis of complex diseases. *Science* **275**, 1328–9.
Newport, M. J., Huxley, C. M., Huston, S., Hawrylowicz, C. M., Oostra, B. A., Williamson, R. and Levin, M. (1996). A mutation in the interferon-gamma-receptor gene and susceptibility to mycobacterial infection. *N. Engl. J. Med.* **335**, 1941–1949.
Oliver, J., Rueda, B., Lopez-Nevot, M. A., Gomez-Garcia, M. and Martin, J. (2007). Replication of an association between IL23R gene polymorphism with inflammatory bowel disease. *Clin. Gastroenterol. Hepatol.* **5**(977-81), 981.
Olson, J. M. (1995). Robust multipoint linkage analysis: an extension of the Haseman-Elston method. *Genet. Epidemiol.* **12**, 177–193.
Ott, J. (1999). *Analysis of Human Genetic Linkage*. Johns Hopkins University Press, Baltimore.
Patterson, N., Price, A. L. and Reich, D. (2006). Population structure and Eigenanalysis. *PLoS Genet.* **2**.
Price, A. L., Patterson, N. J., Plenge, R. M., Weinblatt, M. E., Shadick, N. A. and Reich, D. (2006). Principal components analysis corrects for stratification in genome-wide association studies. *Nat. Genet.* **38**.
Pritchard, J. K., Stephens, M., Rosenberg, N. A. and Donnelly, P. (2000). Association mapping in structured populations. *Am. J. Hum. Genet.* **67**.
Ranque, B., Alcais, A., Thuc, N. V., Woynard, S., Thai, V. H., Huong, N. T., Ba, N. N., Khoa, P. X., Schurr, E. and Abel, L. (2005). A recessive major gene controls the mitsuda reaction in a region endemic for leprosy. *J. Infect. Dis.* **192**, 1475–1482.
Rao, D. C. (1998). CAT scans, PET scans, and genomic scans. *Genet. Epidemiol.* **15**, 1–18.
Rioux, J. D., Xavier, R. J., Taylor, K. D., Silverberg, M. S., Goyette, P., Huett, A., Green, T., Kuballa, P., Barmada, M. M., Datta, L. W. *et al*. (2007). Genome-wide association study identifies new susceptibility loci for Crohn disease and implicates autophagy in disease pathogenesis. *Nat. Genet.* **39**, 596–604.
Risch, N. (1990). Linkage strategies for genetically complex traits. III. The effect of marker polymorphism on analysis of affected relative pairs. *Am. J. Hum. Genet.* **46**, 242–253.
Risch, N. and Merikangas, K. (1996). The future of genetic studies of complex human diseases. *Science* **273**, 1516–7.
Risch, N. and Zhang, H. (1995). Extreme discordant sib pairs for mapping quantitative trait loci in humans. *Science* **268**, 1584–1589.
Sasieni, P. D. (1997). From genotypes to genes: doubling the sample size. *Biometrics* **53**, 1253–1261.
Sawcer, S., Jones, H. B., Judge, D., Visser, F., Compston, A., Goodfellow, P. N. and Clayton, D. (1997). Empirical genomewide significance levels established by whole genome simulations. *Genet. Epidemiol.* **14**, 223–229.

Schaid, D. J. and Jacobsen, S. J. (1999). Biased tests of association: comparisons of allele frequencies when departing from Hardy-Weinberg proportions. *Am. J. Epidemiol.* **149**, 706–711.

Sham, P. C., Cherny, S. S., Purcell, S. and Hewitt, J. K. (2000). Power of linkage versus association analysis of quantitative traits, by use of variance-components models, for sibship data. *Am. J. Hum. Genet.* **66**, 1616–1630.

Shaw, M. A., Donaldson, I. J., Collins, A., Peacock, C. S., Lins-Lainson, Z., Shaw, J. J., Ramos, F., Silveira, F. and Blackwell, J. M. (2001). Association and linkage of leprosy phenotypes with HLA class II and tumour necrosis factor genes. *Genes Immun.* **2**, 196–204.

Siddiqui, M. R., Meisner, S., Tosh, K., Balakrishnan, K., Ghei, S., Fisher, S. E., Golding, M., Shanker Narayan, N. P., Sitaraman, T., Sengupta, U. *et al*. (2001). A major susceptibility locus for leprosy in India maps to chromosome 10p13. *Nat. Genet.* **27**, 439–441.

Spielman, R. S. and Ewens, W. J. (1998). A sibship test for linkage in the presence of association: the sib transmission/disequilibrium test. *Am. J. Hum. Genet.* **62**, 450–458.

Spielman, R. S., McGinnis, R. E. and Ewens, W. J. (1993). Transmission test for linkage disequilibrium: the insulin gene region and insulin-dependent diabetes mellitus (IDDM). *Am. J. Hum. Genet.* **52**, 506–516.

Stein, C. M., Guwatudde, D., Nakakeeto, M., Peters, P., Elston, R. C., Tiwari, H. K., Mugerwa, R. and Whalen, C. C. (2003). Heritability analysis of cytokines as intermediate phenotypes of tuberculosis. *J. Infect. Dis.* **187**, 1679–1685.

The Wellcome Trust Case Control Consortium (2007). Genome-wide association study of 14,000 cases of seven common diseases and 3,000 shared controls. *Nature* **447**, 661–678.

Tosh, K., Meisner, S., Siddiqui, M. R., Balakrishnan, K., Ghei, S., Golding, M., Sengupta, U., Pitchappan, R. M. and Hill, A. V. (2002). A region of chromosome 20 is linked to leprosy susceptibility in a South Indian population. *J. Infect. Dis.* **186**, 1190–1193.

Vidal, S. M., Malo, D., Vogan, K., Skamene, E. and Gros, P. (1993). Natural resistance to infection with intracellular parasites: isolation of a candidate for Bcg. *Cell* **73**, 469–485.

Villani, A. C., Lemire, M., Fortin, G., Louis, E., Silverberg, M. S., Collette, C., Baba, N., Libioulle, C., Belaiche, J., Bitton, A. *et al*. (2009). Common variants in the NLRP3 region contribute to Crohn's disease susceptibility. *Nat. Genet.* **41**, 71–76.

Waldman, I. D., Robinson, B. F. and Rowe, D. C. (1999). A logistic regression based extension of the TDT for continuous and categorical traits. *Ann. Hum. Genet.* **63**, 329–340.

Wang, K., Zhang, H., Kugathasan, S., Annese, V., Bradfield, J. P., Russell, R. K., Sleiman, P. M., Imielinski, M., Glessner, J., Hou, C. *et al*. (2009). Diverse genome-wide association studies associate the IL12/IL23 pathway with Crohn Disease. *Am. J. Hum. Genet.* **84**, 399–405.

Wiart, A., Jepson, A., Banya, W., Bennett, S., Whittle, H., Martin, N. G. and Hill, A. V. (2004). Quantitative association tests of immune responses to antigens of Mycobacterium tuberculosis: a study of twins in West Africa. *Twin. Res.* **7**, 578–588.

Yang, H., McElree, C., Roth, M. P., Shanahan, F., Targan, S. R. and Rotter, J. I. (1993). Familial empirical risks for inflammatory bowel disease: differences between Jews and non-Jews. *Gut* **34**, 517–524.

Ziegler, A. and Koenig, I. R. (2006). *A Statistical Approach to Genetic Epidemiology: Concepts and Applications*. Wiley-VCH, Weinheim.

5 Proteomic Approaches to Study Immunity in Infection

Gustavo A de Souza and Harald G Wiker
The Gade Institute, Section for Microbiology and Immunology, University of Bergen, Bergen, Norway

CONTENTS

I. INTRODUCTION

Proteomic approaches for the large-scale analysis of complex protein extracts from tissues, cells, organelles or body fluids have improved considerably over the last 3–4 years. Many will characterize the technical development as a revolution. By using traditional two-dimensional electrophoresis (2DE)-based approaches, it was possible to identify a few hundred proteins in a single sample. Recent literature now often reports several thousand protein identifications by tandem mass spectrometry (MS) in a single experiment. Much of this advance is a result of development and improvement of MS-based approaches (Aebersold and Mann, 2003), which operate independent of 2DE-based fractionation. 2DE has its limitations, but for a long period 2DE was the most widely applied proteomic method around the globe, due to its pattern recognition feature and quantitative nature. The implementation of new applications for MS-based approaches for labelling of samples has provided the needed boost to develop one of the most powerful high-throughput methods for qualitative analysis to also be versatile for quantitative and comparative proteomics.

This chapter discusses recent proteomic advances with a focus on high-resolution instruments having a mass accuracy in the range of <2–3 parts per million (ppm) and the application of such instruments for the analysis of metabolically or chemically labelled samples. Sample preparation methods for MS-based approaches are also given. Finally, this chapter will discuss recent data available in the literature that show how proteomics have been applied to contribute to our understanding of microbiology and immunology.

METHODS IN MICROBIOLOGY, VOLUME 37
0580-9517 DOI 10.1016/S0580-9517(10)37005-X

♦♦♦♦♦♦ II. QUANTITATIVE PROTEOMICS – STABLE ISOTOPE LABELLING

Proteomic approaches were facilitated 35 years ago with the invention of the 2DE technology (O'Farrell, 1975), a method that allowed high-resolution separation and visualization of individual protein entities from complex mixtures. In this method, protein mixtures are separated by isoelectric focusing in the first dimension followed by separation by molecular mass using SDS-PAGE. Quantitative information can be obtained by analyzing spot size, shape and staining intensity, while protein identity is based on relative spot position. This is the basis for image analysis softwares nowadays used to compare related samples by 2DE.

While 2DE methods are excellent for quantitative proteomics, this approach has been shown to possess many limitations. For example, while 2DE gel maps can reveal thousands of protein spots in a gel, MS analysis have demonstrated that the number of different proteins is far less because each protein is often separated into many spots. Therefore the number of different proteins revealed by 2DE is usually limited to a couple of hundred different proteins, generally the most abundant ones, such as cytoskeletal proteins (Fountoulakis *et al.*, 2004). Repeated characterization of the most abundant proteins is a well-recognized problem in proteomics. Many studies from very different cell systems or models have characterized very similar protein sets over and over (Petrak *et al.*, 2008).

In MS-based approaches, the analysis is done following digestion of protein samples using a proteolytic enzyme. Trypsin is by far the most widely used enzyme for this purpose, but other enzymes with different cleavage site specificities are also applicable. This treatment creates quite complex peptide mixtures (and not protein mixtures) that can be efficiently separated with the help of a chromatographic column directly coupled to the mass spectrometer (LC-MS/MS).

The MS instrument itself is not a quantitative tool due to variations in signal intensities in the mass detector over time and also variations in ionization yields and other factors. This made 2DE approaches superior for quantitative proteomics previously. However, MS-based approaches have now been developed that utilize a compound containing a heavy stable isotope, e.g. N^{15} or O^{18}. By using the compound with its normal isotope for reference, similar samples can be quantitatively compared when pooled together and analysed side by side in the same run by MS. The use of the different isotopes would not result in differences in ionization yields. Most importantly, since there is a mass difference between the light and the heavy compounds, two samples generated with one or the other can be mixed and injected in the instrument simultaneously which eliminates the impact of detector variation. Figure 1 shows how the mass difference between labelled peptides originating from the two samples can be quantitatively compared.

Currently, stable isotope labelling is divided into two groups, i.e. chemical and metabolic labelling. In chemical labelling, a compound containing the isotope is covalently linked to a functional group of an amino acid residue in the protein. This is done *in vitro*, after extraction of protein from the cell or sample model. For metabolic labelling, cells are grown in enriched media with the compound containing the isotope. The labelled compound would preferentially be an essential amino acid in order to assure that it is incorporated in all proteins. In this case the labelled compound is incorporated in the proteome while the cells grow.

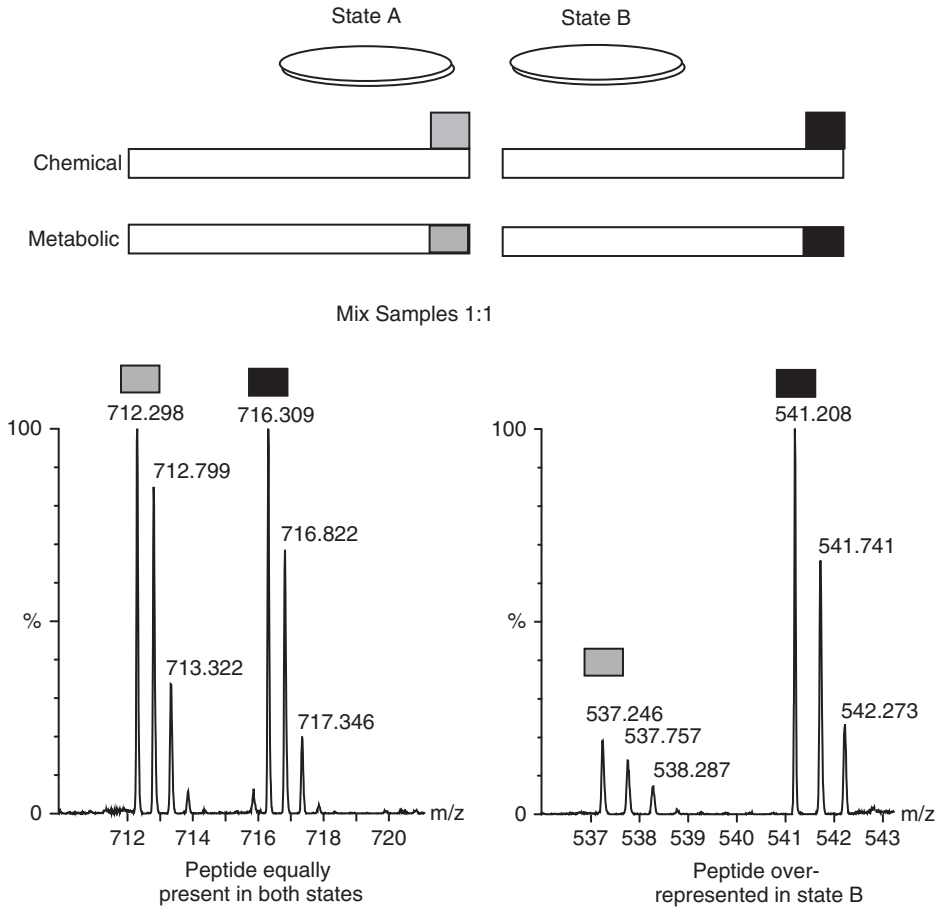

Figure 1. An illustrative example of a labelling analysis. Two populations of the same cell are submitted to two different experimental conditions. For example, state A represents a macrophage cell line in control conditions and state B represents the same cell line after infection with a pathogen. In chemical labelling, an isotope tag is covalently linked to the peptide after protein extraction and *in solution* digestion (gray box for a light isotope, black box for a heavy isotope), while in metabolic labelling the isotopic forms are incorporated in the peptides during translation. For quantitative analysis, proteins are mixed 1:1 prior to fractionation. If one ore more peptides of a protein are identified in a 1:1 ratio in the MS scan (graph to the left), it means that such a protein is equally observed in both conditions and does not respond to the infection. If peptides are under- or over-represented (graph to the right) in cell state B, it means its gene expression, protein translation or degradation is altered in response to infection. The MS scans shown in this figure were extracted from samples labelled with normal arginine or an isotopic arginine containing six C^{13} and two N^{15}. Mass differences between light and heavy peptides will depend on the type of label used.

The first of the chemical labelling methods to be developed specifically for proteomics was called *I*sotope-Coded *A*ffinity *T*ags (ICAT) (Gygi *et al.*, 1999), where an isotopic compound was covalently linked to proteins containing a thiol group (-SH). A clear disadvantage was the requirement of a cysteine, which is an uncommon amino acid in proteins, and consequently very few peptides of a protein, if any (those containing the cysteine), would actually be analysed by MS,

limiting protein identification and quantitation to very few subjects. In addition, this approach required an affinity purification step. While ICAT reagents have been improved to overcome some of the initial weaknesses, probably one of the best choices for chemical labelling available now is the *i*sobaric *T*ag for *R*elative and *A*bsolute *Q*uantitation (iTRAQ) which is a trademark of Applied Biosystems (Ross *et al*., 2004). This chemical reacts with free amino groups, i.e. the peptide N-terminal and the side chains of arginine and lysine. This method is therefore particularly adapted for using trypsin in order to cleave proteins into peptides. In theory, tryptic peptides generated from a digested sample will usually contain one labelled tag. Commercial formats are now sold with up to eight different isotopes, allowing comparison of eight different samples simultaneously.

It has been argued that the yield of the reaction in chemical labelling may be variable and cause variation among the samples to be compared. This limitation would be avoided by metabolic labelling, where cells are kept in an environment enriched with the isotope, and almost full labelling of the cells could be obtained while the cells are growing in the culture. The most refined method using this approach is probably *S*table *I*sotope *L*abelling of *A*mino acids in *C*ulture (SILAC) (Box 1) (Ong *et al*., 2002). In this case, cells are grown in custom-modified media lacking an essential amino acid (leucine, arginine, lysine, or any combination of those), and labelled or normal amino acids would then be added to the media. The cells would use these free amino acids in the media for its protein expression machinery, and each new protein copy would contain the labelled amino acid. It has been shown that, by keeping the cells in logarithmic growth (i.e. not letting them reach culture confluence for a longer period), 5–6 doubling periods are enough to guarantee almost full incorporation of the label in the proteins of the culture. Most importantly, Ong *et al*. (2002) showed that the phenotype and differentiation capacity of the cells was unaffected by the heavy isotope media.

While metabolic labelling seems to be superior to chemical labelling in terms of labelling yield, it still possess a very important practical limitation which resides in the need to be performed in cell models and systems that can be maintained in culture. Metabolic labelling is not an alternative for biological fluids or cellular extracts obtained from humans or from animal models and is not ideal for cells with a poor growth rate in culture which is often the case with primary cultures. In addition, some cells may not adapt well to dialyzed fetal bovine serum (FBS). Normal FBS contain free amino acids that can interfere with the labelling and should be avoided.

The following cell culture protocol exemplifies a typical SILAC labelling procedure. It is important to note that, while the SILAC name was later licensed as a trademark of Applied Biosystems, the method was originally described by the authors cited above, and performing this protocol is fully possible using reagents from other companies.

Box 1. SILAC labelling (Ong *et al.*, 2002)

1. Prepare stock solutions of the amino acid used for labelling. Dissolve the amino acid in PBS to make a stock solution at 1000× of final concentration in the media. Final amino acid concentrations should be taken from the specific formulation of the medium to be used. Store at 4°C.

2. The medium of choice should be acquired as a custom formulation, i.e. without the amino acid to be used for labelling. Reconstitute the media in water according to the instructions from the manufacturer; add glutamine, streptavidin/penicillin and the labelled or unlabelled amino acid. Filter the media using 0.22 μm filter to obtain sterile medium deficient only in FBS.
3. Add *dialyzed* FBS at desired concentration. The use of dialyzed FBS is recommended to avoid free amino acids.
4. During labelling, keep the cells in small bottles/petri dishes to save medium usage. Grow the cells for at least five doubling periods and split cells 3–4 times in fresh medium to guarantee full labelling.
5. After the labelling period is over, separate a small aliquot of labelled cells for protein extraction and check if adequate labelling (>95%) was obtained using MS.
6. Mix labelled and unlabelled material in a 1:1 ratio. This can be done based on total number of cells used for protein extraction or directly based on protein amount.

♦♦♦♦♦♦ III. IMPROVED RESOLUTION IN MS

As stated above, MS-based approaches rely on chromatographic separation of very complex peptide mixtures. Since peptides with similar mass-to-charge ratios (m/z) may co-elute, instruments with low resolution will not be able to distinguish them during ion detection. Poorly resolved ion peaks will result in deficient mass measurements, as well as less reliable quantitation. Until recently, available MS instruments could be divided between (a) fast, highly sensitive but low-resolution ion traps and (b) time-of-flight (TOF) instruments with good resolving power but low sensitivity.

Recent advances in MS technology have, however, increased proteomic fidelity and reliability by several fold (Mann and Kelleher, 2008), in particular high-resolution instruments such as the linear ion trap (LTQ) Fourier transformer (FT) hybrid mass spectrometers. The LTQ-FT-ICR and LTQ-FT-Orbitrap (Thermo Scientific) deserve special mention (Hu *et al.*, 2005; Makarov *et al.*, 2006; Scigelova and Makarov, 2006), and the recently developed high-resolution Q-TOF instruments from Agilent or Bruker Daltonics are all able to reach sub-ppm accuracy. In these instruments high speed and high sensitivity have been combined with high resolving power.

These improvements led to a welcome boost for MS-based protein analysis approaches. The higher mass accuracy achieved by better resolution results in high-quality data sets. High mass accuracy is an important feature of the MS data, and this is taken advantage of in the operational way a peptide identification engine tool works (Clauser *et al.*, 1999). In principle, the MS/MS peak list of an ion is not compared to the whole database itself. The identification tool initially scans the *in silico* digestion of the whole database and then selects only the peptides with theoretical masses equal to the observed mass in the experiment while taking into consideration the mass variation of the instrument. This basically means that the chance of random (i.e. incorrect) MS/MS peak list association with an incorrect (but with close m/z value) peptide is much smaller

when the search engine tool selects within a narrow mass range. These features and strategies have virtually eliminated the problem of false-positive peptide identifications in proteomics.

Together with the use of concatenated databases [i.e. a database that also contains reversed sequences of all proteins in order to set a cut-off for possible false-positive identifications (McCormack *et al*., 1997)], several groups have been reporting results with false-positive rates below 0.1% for protein identification (Brunner *et al*., 2007; Graumann *et al*., 2008; Schenk *et al*., 2008). These technologies have also paved the way for more in-depth analysis of complex proteomes.

♦♦♦♦♦♦ IV. SAMPLE HANDLING

The following example illustrates a typical Gel-LC-MS/MS experiment. In this case, proteins are separated initially by SDS-PAGE. Trypsin digestion is performed *in situ* (Box 2) in fractions separated from the electrophoretic run, and peptides extracted from the gel after digestion are submitted to further fractionation by reverse-phase liquid chromatography directly coupled to a mass spectrometer. This Gel-LC-MS/MS approach was shown to be superior to two-dimensional liquid chromatography approaches (de Godoy *et al*., 2006) due to the fact that it can identify more peptide sequences (i.e. improved sequence coverage) while using less starting material. However, for quantitative proteomics, this method is more suitable for SILAC-labelled samples. Samples labelled for ICAT or iTRAQ should in principle be fractionated by gel-free methods such as ion-exchange chromatography followed by LC-MS/MS.

Box 2. ***In situ*** **trypsin digestion (de Godoy *et al*., 2006)**

1. Prepare 2–3 replicates of 50 μg of sample to be submitted to SDS-PAGE separation. The gel concentration can be made according to user preferences. We recommend using pre-cast gels to avoid keratin contamination and a 4–12% polyacrylamide gradient. It is also recommended to use a commercial sample buffer (Invitrogen).
2. After run, visualize protein bands using a staining method that does not modify the proteins. Since sensitivity is not an issue, colloidal Coomassie blue R-250 is the most appropriate choice and is most friendly for *in situ* trypsin digestion.
3. Slice the gel lane with the sample in, e.g., 15 fractions. Cut each slice in smaller pieces (approximately 1 mm each) and place them in a 1.0 ml plastic sample tube.

   Important: Contamination of the sample with polyethylene glycol from plastic containers is a common problem in proteomics. Avoid using low-quality plastic material. In all of the following steps, use enough volume to cover the gel pieces. In addition, use HPLC-grade water in all solutions to avoid contaminants. Keep all washing solutions in glass vials (no plastic). All washing steps are done under agitation.

4. Wash the bands with 50% acetonitrile in water for 30 min, discard the solution and repeat it 2–3 times or until the Coomassie dye is removed (for intensely stained bands, a more extensive washing is required).
5. Reduce the proteins in the bands with 10 mM DTT in water at 58°C for 1 h. Remove the DTT and add 55 mM iodoacetamide for 45 min at room temperature in the dark for methylation of the -SH groups. Discard the iodoacetamide solution.
6. Wash the bands in 100 mM ammonium bicarbonate, pH 8.0 (AmBic), for 20 min. Discard the solution. Repeat this step two times.
7. Add 100% acetonitrile for 10 min to dehydrate the gel slice. Remove solution and dry the gel bands in a vacuum concentrator for 3 min (at this moment, gel slices should be white and with a rock-like appearance).
8. Prepare the trypsin in AmBic for the digestion. Use 0.125–0.2 μg of trypsin per gel slice. Use just enough volume of Ambic to cover the gel. For example, if you have 20 fractions and 20 μl will cover the gel pieces in each, prepare 4 μg of trypsin in 400 μl AmBic.
9. Add the desired volume of AmBic-containing trypsin to each dehydrated band and wait 5–10 min. Most of (or all) the trypsin should be absorbed by the gel. Remove the excess if some AmBic-containing trypsin solution remains after the gel is fully rehydrated.
10. Add extra AmBic 100 mM (without trypsin) to cover the bands and place the tubes in a 37°C dry incubator for 16 h.
11. Collect the solutions from each tube and transfer to new tubes.
12. To improve peptide recovery, add 50% acetonitrile in water and wash the bands for 20 min. Collect the solution and pool it with the solution from the previous step. Repeat one more time.

    Important: Be careful not to mix peptide extractions from different fractions.
13. Add 100% acetonitrile for 10 min to further dehydrate the gel, collect the solution and pool it with solutions from steps 11 and 12. Discard the bands. Vacuum concentrate the pooled solutions to a final volume of 50 μl.
14. De-salt the sample using pipette tips containing C18 resin, like Zip-Tips (Agilent) or STAGE-Tips (Rappsilber *et al.*, 2003).

♦♦♦♦♦♦ V. DATA HANDLING

After the samples have been processed in the mass spectrometer, data format and specific handling steps may vary depending on the type of equipment used, type of acquisition performed and so on. The protocol below (Box 3) only gives an overview of the steps required. In general, it starts by converting the file obtained from the MS instrument to a format that is readable by bioinformatic tools for peptide identification (Figure 2). In addition, most peptide validations are done using bioinformatic scripts developed elsewhere or with software supplied by the MS manufacturer. Once again, different laboratory setups may result in very different approaches for data handling.

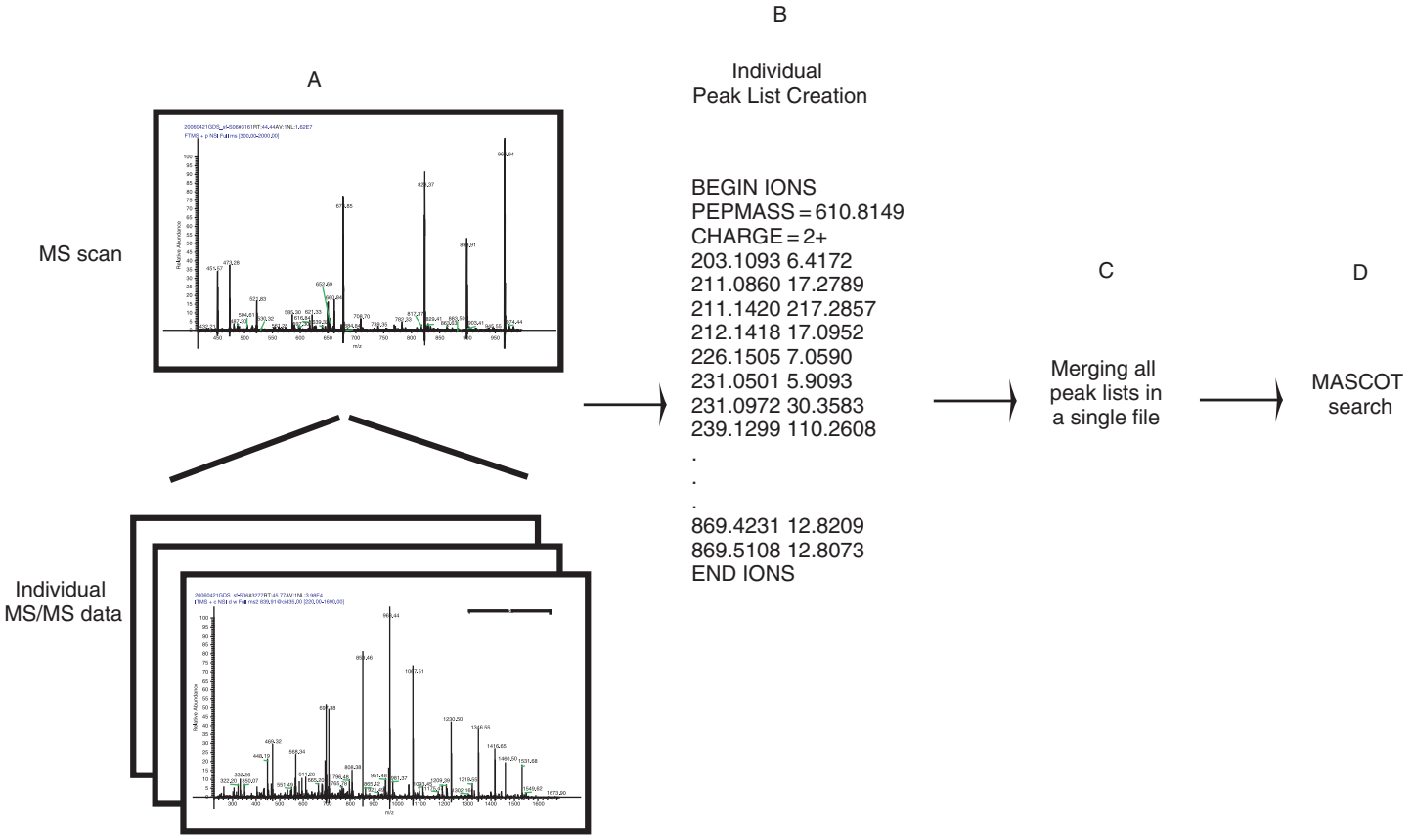

Figure 2. MS data processing. Typical data-dependent acquisition analysis in MS can be described as an initial MS scan, where peptide ions have their m/z measured, followed by MS/MS sequencing of the same peptide ions detected in the first scan and selected for fragmentation in a collision cell (A). Individual MS/MS data are transformed to a peak list format (B), containing ion mass and charge information in the header, plus the mass and intensity of the observable peaks in the MS/MS scan. All peak lists obtained from a LC-MS/MS run are then merged in a single file (C) which is subjected to a database search for peptide identifications (D) (represented by Mascot in this example).

Box 3. MS output and data handling

1. The acquisition file is converted to a format containing peak lists of individual MS/MS data, plus information regarding mass and charge state of the corresponding parent ion.
2. Peak lists for each sample (i.e. band fraction) can be submitted to peptide identification individually, or all fractions can be merged to a single file. This choice is based on the type of experiment performed and if the user has enough hardware to handle the search (e.g. if the tool engine is installed on a local server). For users doing overall proteomic analysis and have local bioinformatic tools, the data from the individual fractions can be merged.
3. Peptide identification searches can be performed using engine tools such as Mascot and X! Tandem. Select a protein database corresponding to the organism in question (SWISS-PROT, NCBInr, International Protein Index, MSMS pdbb, etc.) and select appropriate search parameters. The following parameters are frequently used: cysteine carbamidomethylation as fixed modification (sample alkylation); oxidation of methionine, protein N-terminal acetylation and pyrrolidone carboxylic acid formation in glutamine and glutamic acid (pyro-glu) as variable modifications; two or three allowed miscleavage sites; and allowed mass error according to the instrument used (below 7–15 ppm for high-resolution instruments).
4. Data from search results should be saved. The original acquisition file should be parsed to the peptide identification result through a bioinformatic tool and quantitative information can be retrieved.
5. Peptide and protein validation. In general, proteins with two peptides above the analysis threshold provided by the engine tool (for Mascot, e.g., the probability score) are automatically validated as a true identification. Proteins reported with one peptide only ('one-hit wonders') demand manual validation, applying very high score values.

♦♦♦♦♦♦ VI. WHAT HAS BEEN ACHIEVED SO FAR IN IMMUNOLOGY USING MS-BASED PROTEOMICS

The impact of proteomics in immunology and in biology and medical research in general is a result of certain types of experiments: Firstly, an in-depth analysis of the proteomes of cell lines, subcellular structures, organelles, pathogenic bacterial strains and so forth have provided better knowledge about which protein components are part of these systems. Inventories or collections of data are available in repositories with information about the localization of proteins in cells and tissues (Andersen and Mann, 2006). Secondly, information about structure and organization of protein complexes and the functional characterization of protein/signalling pathways has been obtained. Finally,

high-throughput analysis combined with quantitative approaches applied on biological models such as cell differentiation or cell infection experiments has demonstrated certain components of importance for the effect under investigation. While it is impossible to summarize all developments from so many research areas, the following paragraphs will focus on a few examples where proteomics was used successfully.

MS-based proteomics and immunology have a close link. The method which is today considered to be the basis of LC-MS/MS experiments was first used to characterize peptides associated with MHC class I molecules (Hunt *et al*., 1992). This was achieved by immuno-affinity purification of MHC molecules after detergent extraction of cancer cells. The MHC molecules were denaturated and the associated peptides were separated from the large MHC subunits by ultrafiltration and then purified by reverse-phase HPLC. Furthermore, peptides in each fraction were also tested for their ability to stimulate T cells. Active fractions were then analysed by LC-MS/MS. Identification of MHC-associated peptides is of interest because they could be further tested as potential vaccine candidates. During the last decade several papers have described MHC-associated peptides from cancer cells in culture, murine and human tumours, MHC peptides of microbial origin derived from viral and bacterial infections as well as MHC-associated peptides from autoimmune diseases. For a review see Admon *et al*. (2003) and Purcell and Gorman (2004).

The search for tumour-related antigens and pathogen-derived antigens has boosted many fields. The above-mentioned characterization of MHC-associated peptides has helped to elucidate common structural features shared by them which has been a basis for bioinformatic screening approaches used to predict potential antigens and vaccine candidates present in the genomes of microbial pathogens (Doytchinova and Flower, 2006; Liu *et al*., 2007). However, a limitation of such predictions is that they are mainly performed on gene predictions where there is little factual information about protein expression. This is particularly important for pathogenic organisms where more than half of the predicted genes code for purely hypothetical proteins. With the recent advances in MS-based proteomics described in this chapter, a majority of the genes of organisms with a few thousand predicted genes were confirmed by proteomics. For example, *Mycobacterium leprae* had 67% of its predicted proteome confirmed recently (de Souza *et al*., 2009). While such overviews are not directly applicable to immunology, this type of data can be further used as a reference for follow-up research involving antigen testing or drug design.

Similarly, creating protein inventories for cells relevant for immunology can also bring new insight about their capacities. Information of functional importance can be obtained from proteomic characterization of subcelllular fractions and isolated organelles. For example, in a recent study on neutrophils isolated from healthy donors 1118 proteins were identified in the plasma membrane and secretory vesicle membranes (Uriarte *et al*., 2008). While a good number of these proteins were not necessarily membrane components, this type of study is typical for how the application of new MS-based methods help increase the current proteomic knowledge from a couple of hundred proteins to over a thousand different proteins.

Finally, isotope labelling has helped to elucidate the function and participation of many molecules of the immune system. Examples are molecular changes in the toll-like receptor pathway and characterization of structural microdomains. Protein–protein interactions of key players in signalling pathways have been revealed. Using LPS-stimulated macrophages to induce toll-like receptor signalling, new interactions for the protein MyD88 was achieved using iTRAQ (Dai *et al.*, 2009). To validate these findings, the authors also tested the receptor modulation capacity of MyD88 partners. A similar experiment using SILAC-labelled THP1 cells infected or not with the human immunodeficiency virus showed that the infected cells had a substantial decrease in a protein named IRAK-4, which impaired toll-like receptor 2. These results were confirmed in macrophages isolated from blood donors (Pathak *et al.*, 2009).

Another example involves lipid rafts, a plasma membrane microdomain very resistant to detergent extraction, which is believed to activate T-cell proliferation pathways. The existence of these rafts was a subject of debate. Critics thought they could be artefacts from detergent extraction. Many microscopical studies confirmed their existence; however, it was proteomic studies using SILAC that demonstrated highly specific lipid raft proteins, not originating as contaminants co-purified from normal membrane regions (Foster *et al.*, 2003). By using an experimental design similar to the one depicted in Figure 1 of this chapter, Foster *et al*. compared HeLa cells treated or not with a cholesterol disrupting agent which would destroy the lipid raft. Proteins present in both extracts in a 1:1 ratio were obviously co-purified contaminants, but proteins over-represented in cells not treated with the cholesterol disrupting agent should be specific proteins present in intact rafts. Many signalling receptors were identified as lipid raft specific.

♦♦♦♦♦♦ VII. FINAL REMARKS

While it is undeniable that technological developments have had a major impact in biological areas such as immunology, the proteomic field still poses certain limitations which should be mentioned. An important technical limitation concerns the problems with identification of low-abundant proteins in a sample. This is also known as the dynamic range limitation, i.e. the difference between the most and the least abundant proteins in a mixture and the inherent masking effect that the dominant proteins have on the minor proteins. Biologists will however be more concerned with the limitations of analysis and validation of extremely large data sets. Recent work addressing reproducibility of the output from proteomic laboratories using test samples raised questions about the quality of curation of protein identifications due to many false-positive reports (Bell *et al.*, 2009). However, as high-resolution instruments have become more accessible to the general scientific community, many of these problems are expected to decrease. These issues have already been taken quite seriously by the proteomic field, and most (if not all) of the specialized publications are now quality assured by very strict criteria, and only high-quality presentations of data are accepted.

♦♦♦♦♦♦ VIII. COMMERCIAL SUPPLIERS

A. Isotopic Labelling

Custom media, dialyzed FBS and labelled amino acids for SILAC can be acquired from Sigma. Delivery time for custom media is approximately 8–12 weeks. Applied Biosystems also have a SILAC™ kit with ready-to-go media as well as reagents for iTRAQ.

B. *In situ* Digestion

We currently perform SDS-PAGE separation using NuPAGE 4–12% gels and Coomassie Staining kits from Invitrogen. HPLC-grade water, methanol and sequence-grade acetonitrile are acquired from Sigma-Aldrich. MS-grade trypsin is acquired from Promega. Filter containing C18 resin for STAGE-TIP cleaning (Rappsilber *et al*., 2003) is acquired from M3. All plastic tubes are acquired from Eppendorf.

C. Data Acquisition and Handling

While there are many good alternatives for MS, only a few machines have well documented high-resolution and sub-ppm mass accuracies. Those are high-resolution Q-TOFs from Agilent or Bruker Daltonics and linear ion traps (LTQ) FT hybrids from Thermo-Scientific. Waters is releasing a new Q-TOF instrument by the end of 2009. We use and recommend the LTQ-FT-Orbitrap XL from Thermo-Scientific. For peptide identifications we use the Mascot search engine (MatrixScience). All data handling is performed using a package named MSQuant developed by Peter Mortensen and Matthias Mann at the University of Southern Denmark, freely available at the link http://msquant.sourceforge.net/. MSQuant is compatible to most of the MS file formats, but it requires the search to be performed using the Mascot search engine.

References

Admon, A., Barnea, E. and Ziv, T. (2003). Tumor antigens and proteomics from the point of view of the major histocompatibility complex peptides. *Mol. Cell Proteomics* **2**, 388–398.

Aebersold, R. and Mann, M. (2003). Mass spectrometry-based proteomics. *Nature* **422**, 198–207.

Andersen, J. S. and Mann, M. (2006). Organellar proteomics: turning inventories into insights. *EMBO Rep.* **7**, 874–879.

Bell, A. W., Deutsch, E. W., Au, C. E., Kearney, R. E., Beavis, R., Sechi, S., Nilsson, T., Bergeron, J. J., Beardslee, T. A., Chappell, T. *et al*. (2009). A HUPO test sample study reveals common problems in mass spectrometry-based proteomics. *Nat. Methods* **6**, 411–412.

Brunner, E., Ahrens, C. H., Mohanty, S., Baetschmann, H., Loevenich, S., Potthast, F., Deutsch, E. W., Panse, C., de Lichtenberg, U., Rinner, O. *et al*. (2007). A high-quality catalog of the *Drosophila c* proteome. *Nat. Biotechnol.* **25**, 576–583.

Clauser, K. R., Baker, P. and Burlingame, A. L. (1999). Role of accurate mass measurement (+/-10 ppm) in protein identification strategies employing MS or MS/MS and database searching. *Anal. Chem.* **71**, 2871–2882.

Dai, P., Jeong, S. Y., Yu, Y., Leng, T., Wu, W., Xie, L. and Chen, X. (2009). Modulation of TLR signaling by multiple MyD88-interacting partners including leucine-rich repeat Fli-I-interacting proteins. *J. Immunol.* **182**, 3450–3460.

de Godoy, L. M., Olsen, J. V., de Souza, G. A., Li, G., Mortensen, P. and Mann, M. (2006). Status of complete proteome analysis by mass spectrometry: SILAC labeled yeast as a model system. *Genome Biol.* **7**, R50.

de Souza, G. A., Softeland, T., Koehler, C. J., Thiede, B. and Wiker, H. G. (2009). Validating divergent ORF annotation of the Mycobacterium leprae genome through a full translation data set and peptide identification by tandem mass spectrometry. *Proteomics* **9**, 3233–3243.

Doytchinova, I. A. and Flower, D. R. (2006). Class I T-cell epitope prediction: improvements using a combination of proteasome cleavage, TAP affinity, and MHC binding. *Mol. Immunol.* **43**, 2037–2044.

Foster, L. J., De Hoog, C. L. and Mann, M. (2003). Unbiased quantitative proteomics of lipid rafts reveals high specificity for signaling factors. *Proc. Natl. Acad. Sci. U. S.A* **100**, 5813–5818.

Fountoulakis, M., Tsangaris, G., Oh, J. E., Maris, A. and Lubec, G. (2004). Protein profile of the HeLa cell line. *J. Chromatogr. A* **1038**, 247–265.

Graumann, J., Hubner, N. C., Kim, J. B., Ko, K., Moser, M., Kumar, C., Cox, J., Scholer, H. and Mann, M. (2008). Stable isotope labeling by amino acids in cell culture (SILAC) and proteome quantitation of mouse embryonic stem cells to a depth of 5111 proteins. *Mol. Cell Proteomics* **7**, 672–683.

Gygi, S. P., Rist, B., Gerber, S. A., Turecek, F., Gelb, M. H. and Aebersold, R. (1999). Quantitative analysis of complex protein mixtures using isotope-coded affinity tags. *Nat. Biotechnol.* **17**, 994–999.

Hu, Q., Noll, R. J., Li, H., Makarov, A., Hardman, M. and Graham Cooks, R. (2005). The Orbitrap: a new mass spectrometer. *J. Mass Spectrom.* **40**, 430–443.

Hunt, D. F., Henderson, R. A., Shabanowitz, J., Sakaguchi, K., Michel, H., Sevilir, N., Cox, A. L., Appella, E. and Engelhard, V. H. (1992). Characterization of peptides bound to the class I MHC molecule HLA-A2.1 by mass spectrometry. *Science* **255**, 1261–1263.

Liu, W., Wan, J., Meng, X., Flower, D. R. and Li, T. (2007). In silico prediction of peptide-MHC binding affinity using SVRMHC. *Methods Mol. Biol.* **409**, 283–291.

Makarov, A., Denisov, E., Lange, O. and Horning, S. (2006). Dynamic range of mass accuracy in LTQ Orbitrap hybrid mass spectrometer. *J. Am. Soc. Mass Spectrom.* **17**, 977–982.

Mann, M. and Kelleher, N. L. (2008). Precision proteomics: the case for high resolution and high mass accuracy. *Proc. Natl. Acad. Sci. U.S.A* **105**, 18132–18138.

McCormack, A. L., Schieltz, D. M., Goode, B., Yang, S., Barnes, G., Drubin, D. and Yates, J. R. 3rd, (1997). Direct analysis and identification of proteins in mixtures by LC/MS/MS and database searching at the low-femtomole level. *Anal. Chem.* **69**, 767–776.

O'Farrell, P. H. (1975). High resolution two-dimensional electrophoresis of proteins. *J. Biol. Chem.* **250**, 4007–4021.

Ong, S. E., Blagoev, B., Kratchmarova, I., Kristensen, D. B., Steen, H., Pandey, A. and Mann, M. (2002). Stable isotope labeling by amino acids in cell culture, SILAC, as a simple and accurate approach to expression proteomics. *Mol. Cell Proteomics* **1**, 376–386.

Pathak, S., de Souza, G.A., Salte, T., Wiker, H.G. and Asjo, B. (in press). HIV impairs toll-like receptor signalling by down-regulating IRAK-4 an induces an up-regulation of the antibiotic peptide dermicidin in monocytic THP-1 cells. *Scand. J. Immunol.* **70**, 264–276.

Petrak, J., Ivanek, R., Toman, O., Cmejla, R., Cmejlova, J., Vyoral, D., Zivny, J. and Vulpe, C. D. (2008). Deja vu in proteomics. A hit parade of repeatedly identified differentially expressed proteins. *Proteomics* **8**, 1744–1749.

Purcell, A. W. and Gorman, J. J. (2004). Immunoproteomics: Mass spectrometry-based methods to study the targets of the immune response. *Mol. Cell Proteomics* **3**, 193–208.

Rappsilber, J., Ishihama, Y. and Mann, M. (2003). Stop and go extraction tips for matrix-assisted laser desorption/ionization, nanoelectrospray, and LC/MS sample pretreatment in proteomics. *Anal. Chem.* **75**, 663–670.

Ross, P. L., Huang, Y. N., Marchese, J. N., Williamson, B., Parker, K., Hattan, S., Khainovski, N., Pillai, S., Dey, S., Daniels, S. *et al*. (2004). Multiplexed protein quantitation in Saccharomyces cerevisiae using amine-reactive isobaric tagging reagents. *Mol. Cell Proteomics* **3**, 1154–1169.

Schenk, S., Schoenhals, G. J., de Souza, G. and Mann, M. (2008). A high confidence, manually validated human blood plasma protein reference set. *BMC Med. Genomics* **1**, 41.

Scigelova, M. and Makarov, A. (2006). Orbitrap mass analyzer–overview and applications in proteomics. *Proteomics* **6**(Suppl. 2), 16–21.

Uriarte, S. M., Powell, D. W., Luerman, G. C., Merchant, M. L., Cummins, T. D., Jog, N. R., Ward, R. A. and McLeish, K. R. (2008). Comparison of proteins expressed on secretory vesicle membranes and plasma membranes of human neutrophils. *J. Immunol.* **180**, 5575–5581.

6 Isolation and Characterization of Human Epithelial Antimicrobial Peptides and Proteins

Jens-M Schröder
Department of Dermatology, University Hospital Schleswig-Holstein, Kiel, Germany

CONTENTS

I. INTRODUCTION

Depending on the location, human skin contains various numbers (10^2–10^6) of microbes per cm^2, but is rarely infected. Although for long time it has been suggested that the physical barrier (stratum corneum [SC] and incorporated lipids) and a slightly acidic pH protect us from infection by both commensal bacteria and pathogens, there is now substantial evidence that both healthy and inflamed skin produce a number of antimicrobial peptides and proteins (AMPs). These are in part present at the surface, within the uppermost dead layers of the skin, the SC, or within the uppermost living areas of the skin,

METHODS IN MICROBIOLOGY, VOLUME 37
0580-9517 DOI 10.1016/S0580-9517(10)37006-1

keratinocytes of the stratum granulosum. Thus, skin is a rich source of human epithelia-derived AMPs, which can be isolated using special procedures described below. The investigator needs to decide whether the purpose of the study is to characterize identified antimicrobial activity biochemically or to obtain sufficient amounts of a particular, usually abundant natural AMP for further use, e.g. psoriasin (Gläser *et al.*, 2005) or RNase-7 from human skin (Harder and Schröder, 2002).

When the investigator is not experienced in working with AMPs, several aspects need to be considered, as outlined elsewhere in detail (Steinberg and Lehrer, 1997):

1. Tissue material for purification mostly will be available in only limited amounts.
2. The AMPs to be purified are usually only minor components.
3. Some of the bystander molecules, such as mucins or nucleic acids, may bind AMPs and mask their antimicrobial activity in crude extracts. Furthermore, many AMPs show in the presence of these molecules anomalous behaviour during size exclusion chromatography or ultrafiltration.
4. Crude low pH extracts of cells and tissues may contain potently antimicrobial components such as histones or RNA-binding proteins.
5. Some AMPs have a relatively narrow spectrum. Therefore, the choice of the target organisms is important.
6. The activity of some antimicrobial peptides will vary at different pH or at the presence of divalent cations or at increased concentration of monovalent cations.

♦♦♦♦♦♦ II. SKIN AS SOURCE OF ANTIMICROBIAL PEPTIDES AND PROTEINS

Although human skin contains a huge number of different AMPs (for review, see Schröder and Harder, 2006), only a few can be recovered in sufficient amounts for further studies (e.g. as 'gold standard', when no recombinant proteins are available or natural AMPs are posttranslationally modified forms), when purified to homogeneity. Many AMPs contain high numbers of cysteines, forming in a defined manner disulphide bridges. Recombinant expression of AMPs (e.g. defensins) often generates mixtures of AMPs with different connectivities of the disulphide bridges. For hBD-3, all variants with different cysteine bridges show antimicrobial activity (Chandrababu *et al.*, 2009). But only the hBD-3 variant, which shows the connectivity of natural hBD-3, is able to act receptor-dependent as chemotactic and activating factor (Wu *et al.*, 2003). Thus, in this case the natural AMP will serve as positive control.

In skin, nearly all AMPs are produced in the uppermost, fully differentiated epidermal layers (stratum granulosum), where they are stored or secreted. The uppermost epidermal cells are subject to cornification, and at the end these

form the SC (a layer of flattened, dead epidermal cells). Thus, the SC, which is easily available in sufficient amounts from the heel (we have often used pooled material obtained from pedicure) revealed to be one of the best sources of human (epithelial) AMPs. Healthy person's derived heel SC is a good source for constitutively produced human AMPs.

Human AMPs, which are inducible and absent in healthy skin, are difficult to identify. Therefore, lesional scales of inflamed skin – such as in psoriasis – could be a good source of inflammation-induced AMPs. One of the most intriguing examples is hBD-2, which has been discovered and purified from lesional scale material (Harder *et al.*, 1997).

Also hBD-3 is inducible and is nearly absent in healthy skin (Harder *et al.*, 2001), but is inducible upon wounding (Sørensen *et al.*, 2005).

When the investigator is planning to purify an AMP from human skin material, it is important for him or her to know that skin may contain broad-spectrum AMPs, narrow-spectrum AMPs and target-specific AMPs. This is shown in Figure 1, in which screening of a reversed phase high-performance liquid chromatography (RP-HPLC) separation of lesional psoriatic scale extract results in target-specific elution patterns of antimicrobial activity.

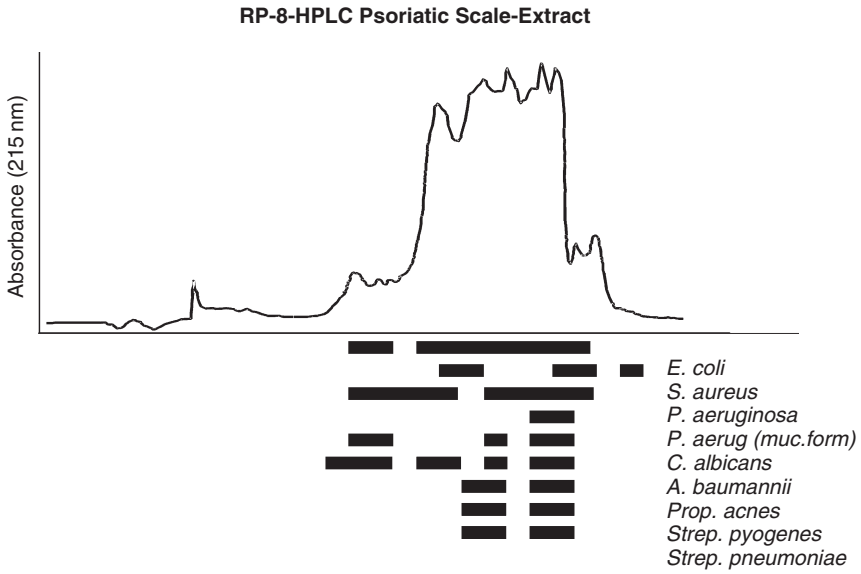

Figure 1. Microorganism-dependent antimicrobial activity of psoriatic scale extracts. Extracts were applied to a heparin-affinity column, and the bound material was further separated by RP-8. Bound proteins were eluted using a linear gradient of increasing acetonitrile concentrations and recorded at 215 nm. The resulting chromatogram is shown. Aliquots (30 µl) of HPLC fractions were tested against the indicated microorganisms in a microdilution assay system. HPLC fractions with antimicrobial activity are indicated by the bars. *S. aureus, Staphylococcus aureus; P. aeruginosa* and *P. aerug., Pseudomonas aeruginosa; C. albicans, Candida albicans; A. baumannii, Acinetobacter baumannii; Prop. acnes, Propionibacterium acnes; Strep. pyogenes, Streptococcus pyogenes; Strep. pneumoniae, Streptococcus pneumoniae*. Reproduced with courtesy of Harder and Schröder (2005).

♦♦♦♦♦♦ III. EXTRACTION OF AMPs FROM TISSUE

Skin and mucosa tissues are rich sources of AMPs. Because the majority of AMPs originate from epithelial cells and/or infiltrating phagocytes, it is important for tissue extraction to prepare prior to extraction, whenever possible, epithelial sheets of the skin or mucosa tissue samples by mechanical techniques using forceps and scissors. Because such tissues specimens are mostly available only in small amounts, these will often allow only purification of minute amounts of AMPs. The richest source of human AMPs, however, is the SC, which is generated from keratinocytes of the uppermost living epidermis layers (stratum granulosum), where most of skin AMPs are synthesized.

The majority of the AMPs are highly cationic, amphipathic molecules, which need special extraction methods to get them out of the tissue. Usually, acidic conditions and the presence of water-soluble organic solvents are necessary to allow good AMP recoveries. The acidic pH and organic solvents are believed to reduce high binding of sticky AMPs to the tissue matrix. When the investigator is planning to determine antimicrobial activity in crude extracts, it might be important for him or her to use volatile acids (i.e. formic acid or HCl) and buffers (ammonium salts) to avoid false-negative results, because antimicrobial activity of several AMPs is salt sensitive.

Specific procedures that can be used to extract AMPs from human SC are described below.

A. Mechanical Disruption and Extraction Media

The use of a homogenizer (e.g. Ultraturrax®) is recommended. The material should have been cut into convenient sized pieces and then disrupted as suspension in a small volume of appropriate buffers. Many investigators are using 70% (v/v) aqueous acetonitrile containing trifluoroacetic acid (TFA) at 0.1–1% (v/v). Others are using 1% formic acid instead of TFA or citric acid buffers at low (<3) pH. The use of TFA is recommended when the first separation step is RP-HPLC.

Under these conditions most of the high molecular weight (MW) proteins are precipitated and therefore will not cause problems upon RP-HPLC. When samples have to be analysed by electrospray ionization mass spectrometry (ESI-MS), formic acid should be used instead of TFA, because TFA can cause quenching effects.

Homogenization (usually 10–30 min) should be performed with ice/water cooling. The investigators should be also aware that acetonitrile is very toxic; therefore, it is recommended to perform homogenization under a hood. To prevent proteolytic digestion of some AMPs, the investigator can add protease inhibitors. However, the author's 15 years' experience with preparative analyses of SC extracts in the absence of exogenous protease inhibitors indicates that there seems to be no major digestion of AMPs. Even the most vulnerable AMPs, such as psoriasin and RNase 7, have been isolated as full length proteins – in the absence of major truncated proteins! It is suggested that high concentrations of endogenous protease inhibitors are present, as it has been proven (Gläser *et al.*, 2005; Harder and Schröder, 2002).

After homogenization SC suspensions are centrifuged at high speed to eliminate fines as much as possible. The nearly clear (sometimes opalescent) supernatant is then completely evaporated when it contains organic solvents (acetonitrile, ethanol) and the first purification step is RP-HPLC. When the material is rich in fat, it is recommended to treat it prior to extraction with a non-polar organic solvent (e.g. ethyl acetate) to enhance AMP recovery.

When tissue samples like nasal mucosa (e.g. nasal polyps) or gut specimens are analysed, it often happens that after centrifugation supernatants are highly viscose or gel-like. In this case the investigator should add solid NaCl until viscosity is low and apply the material directly to an RP-HPLC column (when it does not contain acetonitrile) or concentrate it using an ultrafiltration chamber and filters (cut-off: 3 kDa).

1. Collect human SC from the heel (possible source: pedicure) and homogenize (e.g. with an Ultraturrax®) 100 mg in 1 ml of aqueous acetonitrile (70 vol-%) containing 1% (v/v) TFA in a glass vial (acetonitrile dissolves some plastic material!) for 20 min under cooling with ice/water. About 12 g of heel SC (source: pooled pedicure material) is homogenized in 75 ml of citric acid (2.5% [w/v]), which contains 25% (v/v) ethanol (with heptane, denaturated ethanol can be used).
2. Centrifuge the material in a glass vial for 10 min at >3000 × *g*.
3. Collect the supernatant and evaporate it (using a SpeedVac® vacuum concentrator or via lyophilization when small tissue amounts are extracted) or concentrate it via ultrafiltration chambers (cut-off: 3 kDa) to a volume of 1–3 ml.
4. Dissolve the residues of small tissue sample extracts in 100 µl of 0.1% aqueous TFA (for RP-HPLC) or 10 mM NH_4-formate buffer, pH 4 (for cation-exchange HPLC), when HPLC analyses will be done the same day. If HPLC analyses follow the next day, freeze the sample at –20°C. For long-term storage, freeze below –70°C. Concentrated extracts of SC obtained from heel can be directly applied to a preparative RP-HPLC column or stored frozen (–20°C) until HPLC analyses.

♦♦♦♦♦♦ IV. ANTIMICROBIAL TEST SYSTEMS

Antimicrobial activity of tissue extracts or HPLC fractions can be tested with designer assays (Steinberg and Lehrer, 1997). These assays are intended for use during the discovery stages of research and differ distinctly from assays designed for routine application. Several assay systems have been optimized for the detection of AMPs (Steinberg and Lehrer, 1997). For routine testing of HPLC fractions, mostly the radial diffusion assay (RDA) is used because it is highly sensitive and consumes minimal amounts of the preparations being tested. This test system uses microbial target cells that were grown to nearly mid log phase before being included within a thin agarose gel. Instead of agar, which is used in routine antibiotic testing, the RDA gel contains low electroendosmose agarose to avoid

electrostatic interactions between AMPs (most of them are highly cationic and amphipathic) and the polyanionic components of standard agar.

Test samples are introduced into small (e.g. 3 mm diameter) wells, from which a free radial diffusion is possible. In the thin underlay agarose gel, which is prepared in diluted trypticase soy broth, only six to eight bacterial doublings are allowed. After 3 h incubation time, a nutrient-rich top agarose is poured on the thin agarose gel, so that additional colony development can occur.

Alternatively, the microbroth dilution assay (MDA) for susceptibility testing can be used. It offers some advantages over the RDA, e.g. the use of larger numbers of samples, but unfortunately, however, the method requires 10 times more peptide than the RDA. A key step of the MDA is combining microorganisms and peptide in a defined, minimal nutrient buffer system that minimizes interference with the peptide's biological activity.

Due to the requirement of relative high amounts of AMPs, this test system is rarely used for screening of HPLC fractions.

When samples are tested for the presence of AMPs, the investigator should define the target microbe, because many AMPs have a more or less narrow antibiotic spectrum. This is obvious when HPLC fractions are tested for antimicrobial activity using different targets (Figure 1). It is the author's experience that *Escherichia coli* (also K12) is very sensitive towards most AMPs and because most of the human AMPs are *E. coli*-cidal, it can be used for AMP testing. Human lysozyme can be used as AMP control. In the RDA assay we observed for *E. coli, Staphylococcus aureus* and *Candida albicans* a clearing zone of 6–9 mm with 2.5 μg of human lysozyme.

For testing aliquots of HPLC fractions (up to 5%) for antimicrobial activity, they can be stored in round-bottomed microtitre plates, in which 10 μl of 0.1% (w/v) bovine serum albumin (BSA) in water has been added to the test samples. These mixtures are stored frozen (–20°C) and lyophilized immediately prior to testing. The remaining residues are dissolved in 6–10 μl of 0.01% acetic acid and usually 5 μl is transferred into the punched holes of the RDA gel.

When micro-HPLC analyses are performed, small aliquots of HPLC fractions can be directly tested in the RDA system. In this case a solvent control (e.g. a fraction eluting close to the peptide peak, when only single HPLC peak fractions are tested) should be included.

The following protocol has been reported for a designer RDA (Steinberg and Lehrer, 1997).

1. Prepare organisms for the assay: a single colony is picked and transferred to a bottle that contains 50 ml of TSB, and incubated at 37°C in a shaking water bath for 18–24 h.
2. An aliquot (50 μl of *E. coli*) of the resulting stationary phase culture is transferred to fresh TSB and incubated for 2.5 h at 37°C in a shaking water bath.
3. This subculture is centrifuged and the bacterial pellet is washed with cold sterile 10 mM sodium phosphate buffer (pH 7.4) and resuspended in 5 ml of the same cold buffer.

4. One millilitre is removed to measure its optical density at 620 nm. From this information, the concentration of bacteria in the remaining 4 ml is calculated from the following formula, which is applicable to either organism: CFU/ml = $OD_{620} \times 2.5 \times 10^8$. From this calculation, the volume of washed bacterial suspension that contains 4×10^6 CFU (the inoculum used for each underlay) can be determined.
5. A 10-ml aliquot of the sterile, molten underlay agar (maintained at 42°C) is transferred to a plastic centrifuge tube, inoculated with 4×10^6 CFU of washed bacteria, vortexed vigorously for 15 s and then poured into a $10 \times 10 \times 1.5$ cm square dish on a levelling table (very important!), where it gels in less than 2 min.
6. After the underlay gel has set, the plates are placed over a graph paper template and a 4×4 or 5×5 array of wells is punched. The central plugs are removed by suction, using a Pasteur pipet attached to a bleach trap.
7. Five-microlitre aliquots of the various samples to be tested are added to each well in turn. The plates are covered, turned gel-side up and incubated for 3 h in a 37°C incubator.
8. Next, each underlay gel is covered with a 10-ml overlay of nutrient-rich overlay agar. As soon as the overlay gel solidifies, the plates are recovered, placed gel-side up and incubated at 37°C overnight.
9. The following morning, the plates are removed, and 10 ml of a disinfecting solution is applied to the agar surfaces for at least 20 min before the zone diameters are measured and recorded.

♦♦♦♦♦♦ V. SDS-PAGE ANALYSES OF AMPs

Most of the AMPs are highly cationic, amphipathic peptides, which show a tendency to form multimers at physiologic conditions. Its unusual biochemical properties can make it difficult to get information about its MW upon use of standard SDS-PAGE analyses. Indeed, for purity assessment acid urea (AU)-PAGE has been used. We introduced the Tricine-SDS-PAGE method, which has been originally described by Schägger and Von Jagow (1987) for the analysis of peptides down to 1 kDa size, to analyse chemokines (Schröder, 1997) and later also antimicrobial peptides such as hBD-2 (Harder *et al.*, 2000) and hBD-3 (Harder *et al.*, 2001). The presence of low amounts of AMPs in tissue extracts requires a sensitive method to stain the AMPs on the gel. We successfully used the silver staining method originally described by Heukeshoven and Dernick (1988), which is able to detect low nanogram amounts of peptides. The inclusion of urea in the gel is recommended. We found that in the absence of urea, lysozyme (MW: 14 k) and hBD-2 (4 k) showed nearly identical mobilities in a Tricine gel, whereas in the presence of 6 M urea, hBD-2 migrated like a 4 k peptide (Harder *et al.*, 2000).

When using silver staining for detection of AMP, the investigator should also take care on the colour of the band. For example, we observed for the bands of psoriasin a dark-brown, for lysozyme a middle-brown, for hBD-2, hBD-3 and

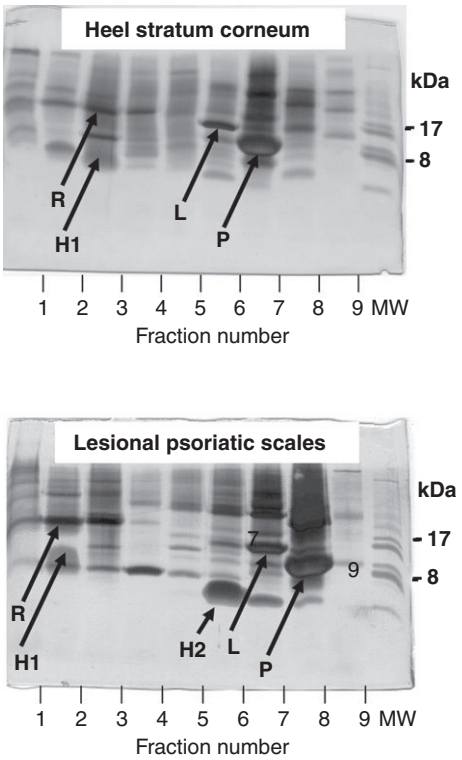

Figure 2. SDS-PAGE analyses of proteins in extracts of stratum corneum and psoriatic scales, after RP-HPLC. Ten-microlitre aliquots of HPLC fractions (as shown in Figures 1 and 2) were analysed in a Tricine/SDS/urea-PAGE system, and proteins and peptides were silver stained. Note in healthy pooled stratum corneum extract (upper panel) psoriasin (P), RNase 7 (R) and lysozyme (L) as predominant antimicrobial proteins, confirmed by ESI-MS analyses (data not shown). In psoriatic scale extracts (lower panel), psoriasin (P) represents again the principle antimicrobial protein. The second most abundant antimicrobial peptide is HBD-2 (H2), followed by lysozyme (L) and RNase 7 (R). Reproduced with courtesy of Schröder and Harder (2006).

RNase-7 a grey-anthracite and for elafin a yellow-beige colour. It is therefore interesting to note that an HPLC fraction, which contains both lysozyme and hBD-2, reveals in the absence of urea a broadened band at 15 k, which stains in its upper parts rather brownish (lysozyme) and in its lower parts rather greyish (hBD-2).

For estimation of quantities of AMPs in HPLC fractions as well as the estimation of contaminating proteins, the investigator should perform SDS-PAGE analyses in parallel to antimicrobial assays.

An example for healthy person's heel SC and, for comparison of lesional psoriatic scales, is shown in Figure 2 (Harder and Schröder, 2005). It is obvious that only under inflammatory conditions inducible AMPs represent the predominating cationic peptides.

For routine SDS-PAGE analyses of HPLC fractions, we used the following protocol:

1. Prepare a gel (dimension 130 × 100 × 1 mm) according to Schägger and Von Jagow (1987) in a Tricine buffer, without reducing agents (mercaptoethanol or dithiothreitol).
2. Mix HPLC fractions (30 µl of preparative HPLC, 2 µl of micro-HPLC) with 10 µl of sample buffer (50 mM Tris–HCl, 4% [w/v] SDS, 12% [w/v] glycerol, pH 6.8, which contains 8 M urea) and boil for 10 min.
3. Load sample on the stacking gel and run the electrophoresis with Tricine buffer without reducing agents at 10 mA current and 30 V power (power limit: 10 W) at room temperature. Using these conditions, we were able to separate the different 77, 72 and 69 residues containing forms of IL-8 (Schröder, 1997).
4. Perform fixation of the peptides for 30 min with aqueous 2-propanol (30% [v/v] containing 10% [v/v] acetic acid) and 0.3% (v/v) glutaraldehyde. In the original description (Schägger and Von Jagow, 1987) formaldehyde is used for fixation. We observed that the use of glutaraldehyde is compelling when low amounts (<10 ng AMP per lane) are expected.
5. Wash the gel with deionized water.
6. Stain peptides with 0.03% (w/v) silver nitrate in deionized water followed by developing with a solution of 10% saturated Na_2CO_3 solution containing 0.1% (v/v) of saturated aqueous formaldehyde (40% [v/v]).
7. To terminate development, remove developing solution and add acetic acid (3% [v/v] in water).

♦♦♦♦♦♦ VI. IMMUNOBLOT ANALYSES OF HUMAN AMPs

For some human AMPs antibodies are commercially available, which make it possible to monitor HPLC fractions for AMP immunoreactivity. Immunodot blot analyses can be used for initial screening and western blot analyses. When using AMP immunoassays as read out system for AMP screening in HPLC fractions, it is important to know about the molecular structure of the antigen used for immunization. Many AMPs are rich in cysteines and have knotted, globular structures as naturally occurring peptides. Thus, when antibodies have been generated against partial AMP structures or against linearized AMPs, it could happen that these antibodies only weakly recognize or do not recognize the native AMP. It is therefore important to test first whether the AMP antibody recognizes the native AMP at non-denaturating as well as denaturating (reducing) conditions.

When performing dot blot analyses with RP-HPLC fractions, the investigator should take into account that acetonitrile is dissolving the often used nitrocellulose membranes. Thus, either polyvinylidene fluoride (PVDF) membranes should be used or, alternatively, the samples should be evaporated and dissolved in 0.1% aqueous TFA before dot blot analysis.

Depending on the antibody's reactivity, upon western blot analysis electrophoresis of AMPs should be performed in the absence or presence of reducing agents. Electrophoretic AMP separation is recommended in the presence of 8 M urea with the Tricine-containing system as described above. In this system hBD-2 gives a

single band at 4 kDa (Harder *et al.*, 2000). Even with this system, cationic peptides sometimes show abnormal migration, e.g. hBD-3 (MW: 5155) migrates like a 10 kDa peptide (Harder *et al.*, 2001), and in other cases show extra bands of multimeric forms as well as complexes with other molecules.

It should be taken into account that most of the AMPs are cationic peptides, reaching sometimes isoelectric points up to 12. Thus, standard conditions (even in the presence of SDS) for transfer to the blotting membrane are often not sufficient. In several cases we observed a significant transfer to the cathode instead of the anode. Therefore, the investigator should use in the beginning of AMP-western blot experiments two blot membranes, at the anode as well as at the cathode, and optimize the conditions for transfer solely to the anode by increasing the pH of the transfer buffer.

In the following protocol western blot conditions are described, which in our hands are optimal for anodal transfer of hBD-2, giving a single 4 kDa band for natural hBD-2:

1. Separate the peptide mixture in a Tricine/urea gel according to the conditions described above.
2. Prepare the transfer buffer freshly. Stock solution: 10× transfer buffer contains 0.1 M $NaHCO_3$ and 0.03 M Na_2CO_3. Transfer buffer: 100 ml of stock solution, 200 ml of denaturated ethanol (we have successfully replaced the toxic methanol, which is commonly used in transfer buffers), 700 ml of deionized water.
3. Perform blotting with Blot Filter paper (Bio-Rad Laboratories GmbH, München, FRG, Cat.-N. 1620118) and nitrocellulose membrane (Protran BA83; Whatman GmbH, Dassel, FRG).
4. Use two nitrocellulose sheets for anodal as well as cathodal transfer and indicate these with A (for anodal transfer) and C (for cathodal transfer).
5. Incubate the blot with appropriate antibodies at optimized dilutions.
6. Block non-specific binding with low-fat milk (prepared from milk powder obtained from a health food store).
7. Incubate the blot with enzyme-labelled secondary antibodies.
8. Develop the blot with appropriate enzyme substrates (e.g. Sigma-Aldrich Chemie GmbH, Munich, FRG, Cat.-N, CPS 1120-1KT) and analyse.

♦♦♦♦♦♦ VII. ELECTROSPRAY IONIZATION MASS SPECTROMETRY (ESI-MS)

With modern mass spectrometers we are able to determine the accurate mass of AMPs. Today, two different methods are mainly used for biochemical analyses: electrospray ionization mass spectrometry (ESI-MS) and matrix-assisted laser desorption/ionization mass spectrometry (MALDI-MS) (for a most recent description of MS analyses of AMPs, see Stegemann and Hoffmann, 2008). Data from MALDI-MS are easier to interpret and, due to the higher sensitivity of this method, MALDI-MS allows the determination of the exact mass of very low (down to attomoles!)

AMP amounts as well as sequence information after appropriate derivatization of the AMP. MALDI-MS is also suitable for high-throughput analyses. This might be of advantage, when high numbers of HPLC fractions need to be analysed. In some cases, we experienced with a failure of MALDI-MS analyses to detect AMPs. Although exact reasons are not clear, the high positive charge of most AMPs and the formation of multimers and multiple charged species could have caused it.

We are analysing HPLC fractions containing AMPs with a quadrupole time-of-flight ESI hybrid mass spectrometer (QTof^{TM}II, Waters Micromass, Milford, MA). The mild ionization upon ESI-MS analyses also allows the detection of AMPs, which often are forming complexes with other molecules. Thus, with this method an AMP, which is not antimicrobially active due to formation of AMP complexes, can be detected in HPLC fractions.

Due to the presence of multiple positively charged species, AMPs show mass spectra in the positive ionization modus with signals of 4–15-fold positive charged species (AMP-dependent and specific for each AMP, when identical conditions are used for measurement).

A characteristic raw spectrum as well as the deconvoluted spectrum of an HPLC fraction, which contains HNP-1, -2 and -3, a major AMP in specimens extracted from neutrophils-containing inflammatory tissue (e.g. lesional psoriatic scales), is shown in the work of Harder and Schröder (2005).

ESI-MS analyses are sensitive towards several contaminating compounds, which often are used upon purification of peptides and proteins: for example TFA can quench signals, and high salt contents influence sensitivity and can form peptide-salt cluster. In this case it is recommended to desalt samples with Zip-Tip^{TR} (Waters) or with self-prepared reversed phase μ-columns using constricted Gel-Loader tips (Eppendorf, Wesseling-Berzdorf, Germany) packed with a 2:1 mixture of Poros®50R2 and Oligo R3 reversed phase medium (Applied Biosystems, Forster city, CA). Due to the formation of huge numbers of aggregates and micelles, detergents bind AMPs and thus completely inhibit formation of a single, defined mass (after deconvolution of the signals). Therefore, the use of detergents for purification of AMPs should be avoided.

When nanogram or low microgram amounts of AMPs are expected or mass mapping/sequencing experiments are needed, nanospray ESI-MS is recommended as described below:

1. Evaporate HPLC fractions. Dissolve the residues in 20 μl of 5% (v/v) aqueous formic acid and apply it to a Poros® or Zip-Tip^{TR}-μ-column (see above).
2. Wash the column two times with 5% (v/v) aqueous formic acid.
3. Elute bound AMPs with 1–3 μl of 60% (v/v) aqueous methanol/5% (v/v) formic acid and directly load it on the nanospray needle.
4. For mass mapping experiments (mass fingerprint), reduce cysteine residues and alkylate in the gas phase using tributyl phosphine and vinylpyridine (Amons, 1987).

5. Bring at the bottom of a wide-necked glass bottle a napkin or filter paper and add at different places 10 µl each of tributyl phosphine (Sigma), vinyl-pyridine (Sigma), pyridine (Sigma) and water.
6. Then put the opened sample vial, which contains the salt-free and dried sample, into the bottle, seal it and incubate it at 37°C for 3 h.
7. Dissolve the ethyl-pyridylated AMPs in 1–2 µl of acetonitrile and then add 20 µl of 10 mM ammonium bicarbonate.
8. Digest with appropriate enzymes (e.g. trypsin): for obtaining tryptic digests, add 1 µl of trypsin (100 ng/µl, preactivated with 1% [v/v)] aqueous acetic acid, sequencing grade, modified for MS analyses [Roche, Mannheim, FRG]) and incubate for at least 4 h at 37°C.
9. Add 10 µl of 5% (v/v) aqueous formic acid, trap the digest using a Poros® µ-column and analyse the bound material by nano-ESI-MS.

For routine ESI-MS analyses of AMPs the following protocol can be used:

1. For routine ESI-MS analyses, dilute aliquots (2–20 µl, depending on the HPLC column used) of sample-containing HPLC fractions with 100 µl of carrier (50:50 acetonitrile : water, containing 0.2% [v/v] formic acid) and infuse it into the electrospray source at a rate of 10–20 µl/min.
2. Use sodium iodide for mass calibration for a calibration range of *m*/*z* 100–2000.
3. Set the capillary potential to 3.5 or 4 kV and cone voltage between 25 and 75 V.
4. Set the cone temperature to 80°C and the desolvation temperature to 150°C.
5. Scan the charge-to-mass ratio of ions within the range of 280–2000.
6. Deconvolute the raw data with the MaxEnt-1 program.

♦♦♦♦♦♦ VIII. AMP ENRICHMENT BY HEPARIN-AFFINITY CHROMATOGRAPHY

The presence of large amounts of neutral and anionic proteins and glycosaminoglycans in tissue extracts may lead to problems in purifying human AMPs by preparative RP-HPLC. We therefore enriched cationic AMPs of tissue extracts by heparin-affinity chromatography prior to RP-HPLC.

It is important that tissue extracts do not contain much salt, because this may cause less AMP binding to the affinity column and therefore recovery losses.

Therefore, it is recommended to use volatile acids (like formic acid or TFA) for tissue extraction (see above) and then diafiltrate the extract against 10 mM $NaHCO_3$. Elution of most AMPs from the heparin-affinity column can be done with high molar salt. Some AMPs, however, cannot be efficiently eluted under these conditions. We made the experience that remarkable amounts of hBD-3

remained on the column, when 2 M NaCl was used for elution. To strip it from the column, it was necessary to use 0.1 M glycine–HCl buffer, pH 2.0.

The second AMP, which could not be eluted efficiently with 2 M NaCl, is HNP-(1–3). Although we could increase its elution with acidic glycine buffer, the majority of HNP-(1–3) was eluted when the column was subsequently washed with 0.1 M NaOH. The reason might be lectin-like properties which have been found in some defensins (Lehrer, 2004), which may lead – apart from heparin binding – to binding to sugars of the sepharose matrix.

The heparin-affinity chromatography is only useful when extracts are available from gram amounts of tissue.

The following protocol was used for heparin-affinity enrichment of AMPs:

1. Diafiltrate the acidic tissue extract against 10 mM $NaHCO_3$, pH 8.0, using an ultrafiltration equipment (Amicon Ultra-15 Centrifugal Filter Unit, Millipore GmbH, Schwalbach/Ts., FRG) with a molecular weight cut-off of 3 kDa and concentrate to a volume of 1–2 ml. Alternatively, when salt concentration is low, adjust the pH to pH 8.0 with 1 M NaOH.
2. Centrifuge the diafiltrate (3000 × *g*) or alternatively the pH-adjusted extract.
3. Apply the diafiltrated or pH-adjusted extract to a heparin sepharose cartridge (Hi Trap, 10 × 5 mm, 1 ml volume, GE Healthcare, Freiburg, FRG), when extracts of up to 5 g tissue are used. With higher amounts of tissue, use a 5 ml heparin sepharose cartridge.
4. Wash the loaded heparin cartridge with 2 ml of 10 mM $NaHCO_3$, pH 8.0.
5. Elute with 2 M NaCl in 10 mM $NaHCO_3$, pH 8.0, and adjust the pH of the eluted material to 2–3 by adding TFA.
6. Elute the remaining material, when the investigator is interested in hBD-3 or HNP-(1–3), with ice-cold 0.1 M glycine/HCl buffer, pH 2.0.
7. Wash the column with 0.1 M NaOH, when HNP-(1–3) is of interest.
8. Immediately reconstitute the pH of the heparin column to 7–8.

Repeated elution at acidic pH may reduce the capacity of the heparin column to bind AMPs. Therefore, this step should only be used when hBD-3 or HNP-(1–3) is of interest. We were able to use the same heparin sepharose cartridge after four times of acid treatment without capacity problems, when ice-cold acidic buffers were used and the pH in the heparin cartridge has been reconstituted to neutral pH immediately after acid elution.

♦♦♦♦♦♦ IX. AMP SEPARATION BY PREPARATIVE RP-HPLC

Any HPLC or fast protein liquid chromatography (FPLC) machine containing a pump, gradient mixer, UV detector and fraction collector can be used. UV detection should be done at 215 nm, 280 nm or both. Use solvents that do not show absorbance at 215 nm (e.g. acetonitrile, water and TFA).

When the investigator intends to use preparative, analytical and micro (not nano!)-HPLC columns, it is important that the HPLC system allows flow rates between a few µl and 3 ml.

As first step to separate AMPs in tissue extracts, preparative RP-HPLC (for tissue amounts between 500 mg and 10 g) can be used. When HPLC columns are chosen, it is important to use 'wide-pore' (200 or 300 Å) columns. Furthermore, remaining free silanol groups at the surface of silica-based HPLC columns (most of the columns are based on silica) could affect the peak shape of basic peptides (most of the AMPs are cationic) and may decrease recovery dramatically due to binding to acidic silanol groups. Therefore, HPLC columns with 'endcapping', where silanol groups are derivatized, are preferred for AMP purification.

Samples should contain only low amounts – if any – of organic solvents. Therefore, it may be necessary to evaporate the sample, e.g. in a SpeedVac® vacuum concentrator. Prior to HPLC analyses, it is important to acidify the samples, preferably with TFA.

Usually the extract volumes (several ml) have to be injected. Although one could concentrate the sample by a SpeedVac® vacuum concentrator, this is not necessary when the HPLC system contains a 2 ml-volume injection loop. This will allow the injection of higher volumes (we injected sometimes 10 ml by five times filling the 2 ml-injection loop and injecting after each filling circle without starting the gradient).

The following protocol can be used for preparative RP-8-HPLC:

1. Equilibrate the preparative RP-HPLC column (C8 Nucleosil with endcapping, 250 × 12.6 mm, 7 mm particle size, and a precolumn [50 × 12.6 mm], filled with the same material [Macherey & Nagel, Düren, Germany] as well as particle filter with HPLC-grade H_2O containing 0.1% [v/v] TFA).
2. Centrifuge (or filtrate through a 0.1-µm filter) the sample before injection.
3. Inject and start the gradient of eluent A (0.1% [v/v] TFA in H_2O) and B (0.1% [v/v] TFA in acetonitrile) (time 0 min: 100% A; time 5 min: 100% A; time 30 min: 40% A, 60% B; time 31 min: 20% A, 80% B) at a flow rate of 3 ml/min.
4. Separate peaks – when possible – manually according to the appearance of UV (215 nm)-absorbing peaks and shoulders. Take several fractions from broad peaks.
5. Place fractions immediately in the refrigerator.
6. Take an aliquot of each fraction for the bioassay or immunoassay, SDS-PAGE analyses or ESI-MS analyses in round-bottomed microtitre plates. Use for each assay a separate plate to avoid repeated freezing and thawing and then store it frozen (–20°C).

Figure 3 shows a typical RP-89 HPLC chromatogram obtained from heparin-bound peptides and proteins present in the extract of 10 g pooled healthy person's heel SC. *E. coli*-killing activity (tested in 20-µl aliquots of each HPLC fraction) was present in most of the HPLC fractions. Note the presence of peak activity (RDA assay) in fractions corresponding to psoriasin, lysozyme and RNase-7, which were found to be the quantitatively dominating AMPs (Schröder and Harder, 2006). Figure 4 shows a typical RP-8-HPLC chromatogram obtained

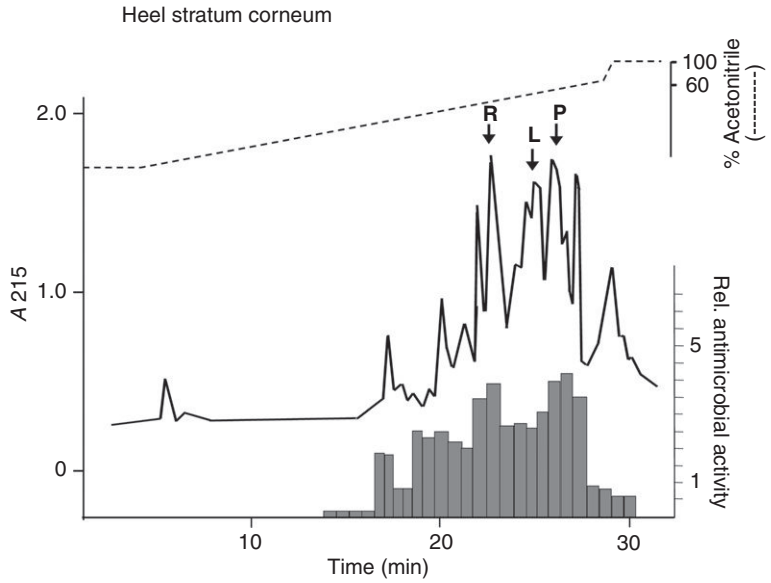

Figure 3. RP-HPLC of a healthy stratum corneum extract. Heparin-bound material of an extract obtained from 100 g of pooled healthy stratum corneum was separated by preparative wide-pore RP-8-HPLC and 10-µl aliquots of each fraction were tested for *E. coli*-cidal activity in the radial diffusion assay (RDA) system. Bars represent the diameter of the clearing zone in the assay system. L, lysozyme; P, psoriasin; R, RNase7. Reproduced with courtesy of Schröder and Harder (2006).

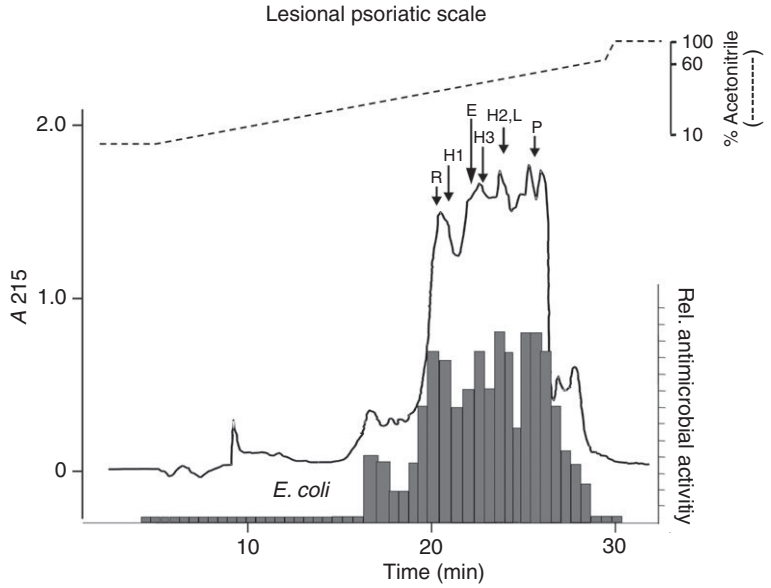

Figure 4. RP-HPLC of a healthy stratum corneum extract. Heparin-bound material of an extract obtained from 7 g of pooled lesional psoriatic scales was separated by preparative wide-pore RP-8-HPLC and 10-µl aliquots of each fraction were tested for *E. coli*-cidal activity in the radial diffusion assay (RDA) system. Bars represent the diameter of the clearing zone in the assay system. Note the difference in the antimicrobial activity pattern and the increased activity in psoriatic scale extracts compared with healthy person's stratum corneum extracts, despite the use of 14-fold less amounts of material. H2, hBD-2; H3, hBD-3; L, lysozyme; P, psoriasin; R, RNase7. Reproduced with courtesy of Schröder and Harder (2006).

from heparin-bound peptides and proteins present in the extract of 10 g pooled lesional psoriatic scales. Note the presence of hBD-2 and hBD-3 as inflammation-induced AMPs.

♦♦♦♦♦♦ X. MICRO-CATION-EXCHANGE HPLC OF AMPs

Selected fractions of preparative RP-8-HPLC should be subjected to micro-cation-exchange HPLC, when necessary. We have used in our studies a Smart® MonoS® strong cation-exchange micro-column. When only small amounts of protein are present in the selected RP-8-HPLC fractions, it may be more favourable to use a Smart® MiniS®-column instead of a Smart® MonoS®. This change may reduce losses during purification.

In general, losses of material by cation-exchange HPLC are high, when the ratio of column bed volume/applied protein is inappropriate. Furthermore, if a cation-exchange HPLC separation is necessary to eliminate major RP-8-HPLC-coeluting impurities and the AMP is only a trace component, the purification strategy should be changed and the Smart® MonoS®-HPLC should be used as first step after heparin-affinity enrichment of AMPs.

For separation of cationic AMPs, low pH conditions for cation-exchange HPLC are recommended. Although such conditions contradict textbook knowledge, these have been successfully used to separate several cationic peptides from tissue or cell culture supernatants, such as the chemokines IL-8, Gro-α, RANTES and eotaxin (Mochizuki *et al.*, 1998), AMPs like hBD-2 (Harder *et al.*, 1997), hBD-3 (Harder *et al.*, 2001), RNase-7 (Harder and Schröder, 2002) and psoriasin (Gläser *et al.*, 2005) and cationic protease inhibitors like LEKTI-2 (Meyer-Hoffert *et al.*, 2009).

Bactericidal activity of many cationic AMPs is inhibited by high salt concentrations (Goldman *et al.*, 1997). Therefore, analyses of antimicrobial activity in ion-exchange HPLC fractions may generate false-negative results for peptides, which elute with increased salt concentrations. When only a few fractions need to be tested for AMP activity, the investigator may use RP cartridges (e.g. ZIP-TIP^{TR} or Poros®, as described for MS analyses) to eliminate salt with the following protocol:

1. Take 2–10 µl of micro-cation-exchange HPLC fraction and dry it (to eliminate acetonitrile).
2. Dissolve the residue in 5 µl of 0.1% (v/v) aqueous TFA.
3. Subject it to an RP cartridge (e.g. ZIP-TIP^{TR} or Poros®), which has been already equilibrated with 0.1% TFA.
4. Elute the peptide with 5 µl of 80% (v/v) aqueous acetonitrile.
5. Evaporate the acetonitrile and dissolve the residue in 5 µl of 0.01% (v/v) aqueous acetic acid and use it immediately for testing antimicrobial activity in the RDA.

Alternatively, the investigator may use volatile salts, which can be removed by lyophilization. We have successfully used 20 mM ammonium formate/formic acid buffer, pH 4, for equilibrating the cation-exchange HPLC column and eluting with an increasing gradient of 1 M ammonium formate (without adjusting the pH to 4.0). The elution pattern was found to be similar as seen with NaCl.

Lyophilization of volatile buffer-containing samples needs particular attention. When aliquots of HPLC fractions have been taken into microtitre plates, increased amounts of salts will be seen in wells containing late eluting fractions after lyophilization. Because volatile salts will only be able to lyophilize in the presence of water, it is necessary to add water (10 µl) to salt-containing wells and lyophilize again. This process needs to be repeated until no salt is visible in these wells.

The following protocol can be used for micro-cation-exchange HPLC:

1. Equilibrate a micro-MonoS®-HPLC column (GE Healthcare) with 20 mM aqueous ammonium formate/formic acid buffer, pH 4.0, which contains 25% (v/v) acetonitrile at a flow rate of 100 µl/min. Record absorbance at 215 and 280 nm.
2. Dissolve the residues of lyophilized RP-8-HPLC fractions that have been chosen for cation-exchange HPLC, in equilibration buffer. In the case that salt-containing HPLC fractions or extracts are subjected to cation-exchange HPLC, diafiltrate the samples against the starting buffer and take care that pH and ion strength are identical with those of the equilibration buffer.
3. Centrifuge the sample and inject it.
4. Start the elution with a linear gradient (0–20 min) of increasing concentrations of NaCl (0–1 M) in 20 mM aqueous ammonium formate/formic acid buffer, pH 4.0, which contains 25% (v/v) acetonitrile.
5. Collect all fractions according to elution time. This is important to avoid losses of peptides, which do not absorb at 280 nm. These will show apparently very weak absorbance at 215 nm due to the very high background absorbance of the buffer and thus can be easily overseen.

Micro-MonoS®-HPLC has been found to represent the critical step to purify RNase-7 from lesional psoriatic scale or healthy person's SC extracts. Although it elutes as a major peak upon preparative RP-8-HPLC, a major contaminant is HNP-(1–3). As shown in Figure 5, RNase-7 elutes with 0.80 M NaCl as the last, single symmetric peak from the cation-exchange column, when the protocol described above was used. The defensin HNP-(1–3), which most likely originates from neutrophils that have been migrated into the lesional psoriasis skin, elutes already with 0.41 M NaCl at these conditions.

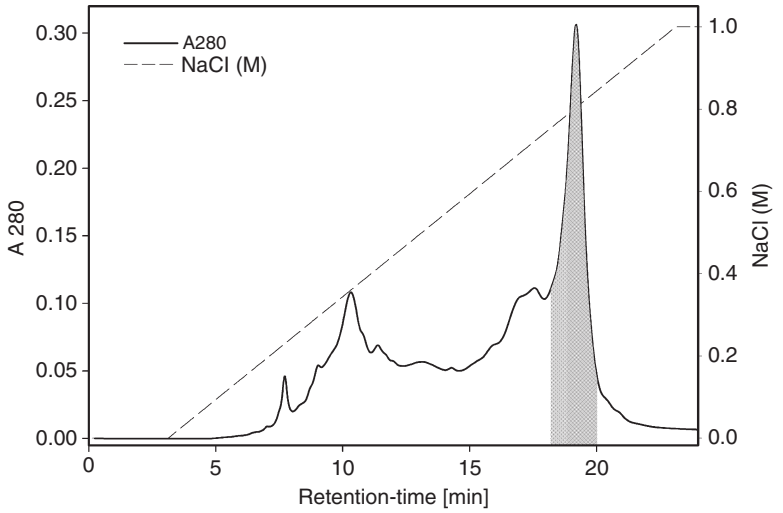

Figure 5. Micro-MonoS®-HPLC purification of RNase-7. Preparative RP-8-HPLC fractions containing RNase-7 were separated by micro-MonoS®-HPLC at acidic conditions (ammonium formate buffer) as described above in detail. RNase-7 was eluted with a gradient of NaCl as the last, most prominent UV-absorbing peak (hatched area), which usually contained >95% pure RNase-7.

♦♦♦♦♦♦ XI. MICRO-C2/C18 RP-HPLC

Final purification of human AMPs (and desalting) can be done with a micro-C2/C18 RP-HPLC. Due to its unique properties, this HPLC column allows the complete separation of hBD-2 from lysozyme, which can be a major contaminant in hBD-2 preparations separated by preparative RP-8-HPLC or by micro-cation-exchange HPLC. A typical chromatogram is shown in Figure 6. hBD-2 is eluting at 46% acetonitrile.

When hBD-3 (obtained from lesional psoriatic scale extracts) is separated using this C2/C18 RP-HPLC column, it shows a unique peak profile, starting with a small, sharp peak, followed by broadened overlapping peaks and then the principle peak (Figure 7).

♦♦♦♦♦♦ XII. EXAMPLE 1: PURIFICATION OF PSORIASIN FROM HEALTHY SKIN

Psoriasin is the most abundant antimicrobial protein in healthy skin (Gläser *et al.*, 2005). It also represents the principal protein in skin-washing fluid (Gläser *et al.*, 2005). We identified SC of the heel as the best natural psoriasin source. This material is easily available, also in gram amounts as pooled material from pedicure.

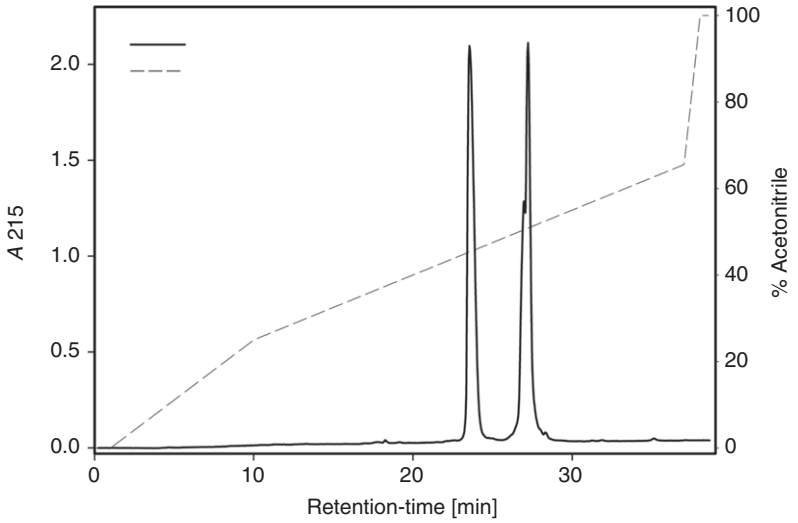

Figure 6. Micro-C2/C18-RP-HPLC of a crude, lysozyme-containing hBD-2 preparation. Due to its unique properties, this HPLC column allows the complete separation of hBD-2 from lysozyme, which often is a major contaminant in hBD-2 preparations separated by preparative RP-8-HPLC or by micro-cation-exchange HPLC. hBD-2 is eluting at 46% acetonitrile.

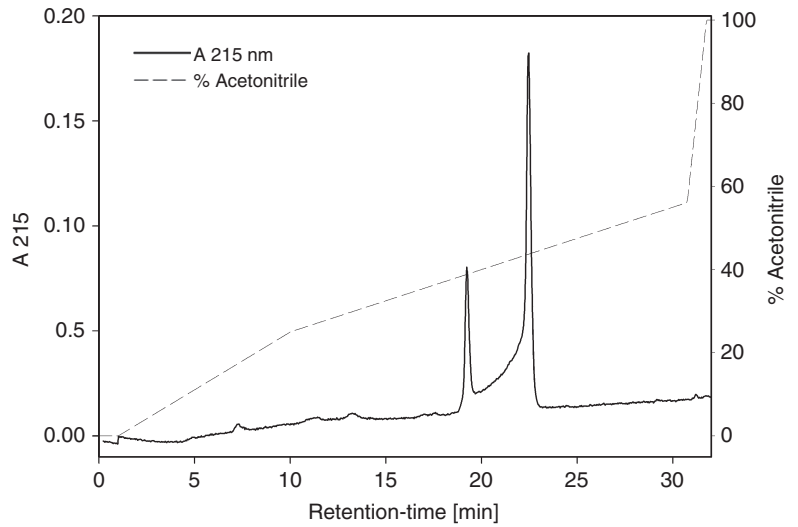

Figure 7. Micro-C2/C18-RP-HPLC of hBD-3. hBD-3 obtained from lesional psoriatic scale extracts is separated using a C2/C18-RP-HPLC column. A unique peak profile is visible with both natural and recombinant or synthetic hBD-3, starting with a small, sharp peak, followed by broadened overlapping peaks and then the principle peak. ESI-MS analyses revealed for all fractions the same mass at 5155 Da.

Due to its high abundance, psoriasin can be purified from SC extracts in a single RP-HPLC step. Depending upon the amounts the investigator needs for further studies, preparative or analytical RP-HPLC columns should be used. Psoriasin usually elutes as one of the last major peaks indicating it as a highly hydrophobic protein. Sometimes – when resolution of the HPLC column is low – other S100-proteins, in particular S100-A8 and -A9 as well as cystatin A, could be contaminants.

Psoriasin can be identified by SDS-PAGE giving a 10-kDa band (Gläser *et al.*, 2005). Mass determination by MALDI or ESI-MS will give an exact mass of 11,366 Da, which is different from the sequence calculated mass. Indeed, the natural psoriasin is N-terminally acetylated, missing the N-terminal Met (Gläser *et al.*, 2005). When the investigator is using a single RP-HPLC step for purification of natural psoriasin, the preparation will show an additional signal at 11,382, which comes from an oxidized (methionine-sulphoxide) psoriasin. Furthermore, there are often many different signals of psoriasin variants and/or oxidized forms present. This is markedly demonstrated by a MonoS®-HPLC of a preparative RP-8-purified psoriasin preparation, where several psoriasin variants can be identified (Figure 8). This cation-exchange HPLC purification step should be included, when a pure 11,366 Da form of psoriasin is required. This elutes at 0.51 M NaCl and represents the principal peak. A subsequent C2/C18 RP-HPLC will desalt the preparation and always gives a single peak of psoriasin.

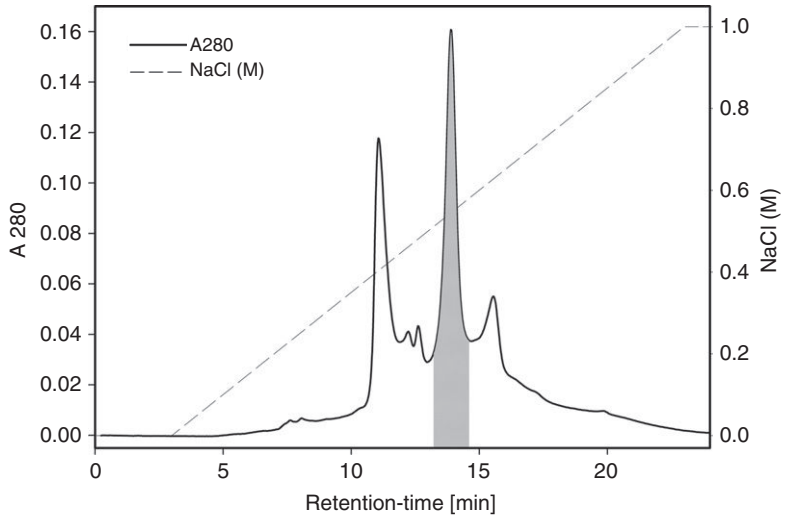

Figure 8. Micro-MonoS®-HPLC purification of Psoriasin (S100A7). Preparative RP-8-HPLC fractions containing Psoriasin were separated by micro-MonoS®-HPLC at acidic conditions (ammonium formate buffer) as described above in detail. Elution with a gradient of NaCl revealed heterogeneity of psoriasin with the principal psoriasin 11.366 kDa form eluting as the most prominent UV-absorbing peak (hatched area). The other peaks contain both post-translationally modified psoriasin forms and psoriasin variants. In some cases, unrelated contaminants such as lysozyme and/or hBD-2 may be also present.

To obtain 200–600 μg psoriasin from 5 g heel SC, we used the following protocol according to the procedures described above:

1. Extract 5 g of pooled heel SC (source: pedicure) with aqueous citric acid (2.5% [w/v]), which contains 25% denaturated (heptane) ethanol.
2. Centrifuge the sample and collect the supernatant.
3. Evaporate the supernatant in a SpeedVac® vacuum concentrator or lyophilize it. Alternatively, adjust the pH to 8 by adding 1 M NaOH and apply to a 5 ml heparin sepharose cartridge and elute with 2 M NaCl, as described above in the protocol.
4. Dissolve the evaporated residues in 2 ml of 0.1% aqueous TFA or, alternatively, adjust the pH with TFA to 2–3. Centrifuge or filtrate both samples through a 0.1-μm filter.
5. Apply the sample to a preparative wide-pore RP-8-HPLC column (Nucleosil C8-RP column, see above), which has been equilibrated with 0.1% aqueous TFA.
6. Elute with the acetonitrile gradient shown in the protocol for RP-8-HPLC (see above) and test aliquots of late eluting the major protein-containing HPLC fractions for 10 kDa proteins.
7. Lyophilize psoriasin-containing HPLC fractions (usually eluting at ~45% acetonitrile) and dissolve these in 100 μl MonoS®-HPLC equilibration buffer.
8. Apply the sample to the MonoS®-HPLC column and elute with a gradient of increasing concentration of NaCl in acidic ammonium formate buffer, as described above. Screen the fractions for a 10 kDa protein (see above). Psoriasin$_{11,366}$ elutes as the principal protein (see Figure 8) with 0.51 M NaCl. The other peaks may contain, apart from traces of other psoriasin variants, three post-translationally modified forms, hBD-2 and lysozyme as major impurities.
9. Add to psoriasin$_{11,366}$-containing MonoS®-HPLC fractions 1 μl TFA and apply to an RP-HPLC column (micro-C2/C18, analytical C4, C8 or C18 column). Psoriasin$_{11,366}$ elutes as a single peak.

♦♦♦♦♦♦ XIII. EXAMPLE 2: PURIFICATION OF RNASE-7

RNase-7 is the most efficient *Enterococcus*-killing antimicrobial protein in healthy skin (Harder and Schröder, 2002). It also represents one of the secreted AMPs, which can be found in skin-washing fluid (Köten *et al.*, 2009). We identified SC of the heel as the best natural RNase-7 source. This material is easily available, also in gram amounts as pooled material from pedicure.

Due to its relative high abundance, RNase-7 can be purified from SC extracts in three steps by HPLC of heparin-bound material. Depending upon the amounts the investigator needs for further studies, preparative or analytical RP-HPLC columns should be used. RNase-7 usually elutes as one of the early major peaks indicating it as a rather polar protein. As major contaminant in this system (depending on the source of the SC) we have found HNP-(1–3), which elutes from a preparative RP-8-HPLC column at similar retention time.

RNase-7 can be identified by SDS-PAGE giving a 19-kDa band (instead of a 14.5-kDa band as predicted) (Harder and Schröder, 2002). Mass determination by MALDI or ESI-MS will give an exact mass of 14,546 Da, calculated from the characteristic, multiple charged species. The preparations will show additional signals at 14,562 and 14,578 Da, which originate from oxidized (methionine-sulphoxide) RNase-7. We observed that air oxidation of the sample rather than the presence of oxidized protein in the extract causes these extra peaks. Separation of contaminating peptides and proteins is optimal when MonoS®-HPLC is performed at acidic conditions with ammonium formate-containing eluent (see above). RNase-7 will elute as the last and principal UV-absorbing peak (Figure 5). This material can be used after desalting or can be finally purified (we identified only very few contaminants!) by C2/C18 RP-HPLC.

To obtain 50–300 µg of psoriasin from 5 g of heel SC, we used the following protocol according to the procedures described above:

1. Extract 5 g of pooled heel SC (source: pedicure) with aqueous citric acid (2.5% [w/v]), which contains 25% denaturated (e.g. with *n*-heptane) ethanol.
2. Centrifuge the sample and collect the supernatant.
3. Adjust the pH to 8 by adding 1 M NaOH and apply to a 5ml heparin sepharose cartridge and elute with 2 M NaCl, as described above in the protocol.
4. Adjust the pH with TFA to 2–3. Centrifuge or filtrate the sample through a 0.1-µm filter.
5. Apply the sample to a preparative wide-pore RP-8-HPLC column (Nucleosil C8-RP column, see above), which has been equilibrated with 0.1% aqueous TFA.
6. Elute with the acetonitrile gradient shown in the protocol for RP-8-HPLC (see above).
7. Screen HPLC fractions for 14.5 kDa antimicrobial proteins by SDS-PAGE (here the investigator should look for a 19-kDa band, which stains grey [and not brownish]). RNase-7 elutes with ~38% acetonitrile. Lysozyme (a 15 kDa protein, which elutes at higher acetonitrile concentration than RNase-7) shows a band exactly with the predicted size. This, however, stains brownish with silver. When *S. aureus* killing is used as read-out system, RNase-7 should elute as one of the AMPs in early eluting fractions. Staphylocidal activity may be not as high as expected in the RDA assay, possibly due to impaired diffusion of RNase-7 in the agarose.
8. Lyophilize RNase-7-containing HPLC fractions and dissolve these in 100 µl MonoS®-HPLC equilibration buffer.
9. Apply the sample to the MonoS®-HPLC column and elute with a gradient of increasing concentration of NaCl in ammonium formate buffer as described above. Screen the late eluting fractions for a 14.5 kDa protein (see above). RNase-7 elutes as the principal protein with 0.80 M NaCl.
10. Add to RNase-7-containing MonoS®-HPLC fractions 1 µl TFA and apply to an RP-HPLC column (micro-C2/C18, analytical C4, C8 or C18 column). RNase-7 elutes as a single peak.

Acknowledgement

This work has been supported by Deutsche Forschungsgemeinschaft (SFB 617). I would like to thank J. Bartels for editorial help.

References

Amons, R. (1987). Vapor-phase modification of sulfhydryl groups in proteins. *FEBS Lett.* **212**, 68–72.

Chandrababu, K. B., Ho, B. and Yang, D. (2009). Structure, dynamics, and activity of an all-cysteine mutated human beta defensin-3 peptide analogue. *Biochemistry* **48**, 6052–6061.

Gläser, R., Harder, J., Lange, H., Bartels, J., Christophers, E. and Schröder, J.-M. (2005). Antimicrobial psoriasin (S100A7) protects human skin from Escherichia coli infection. *Nat. Immunol.* **6**, 57–64.

Goldman, M. J., Anderson, G. M., Stolzenberg, E. D., Kari, U. P., Zasloff, M. and Wilson, J. M. (1997). Human beta-defensin-1 is a salt-sensitive antibiotic in lung that is inactivated in cystic fibrosis. *Cell* **88**, 553–560.

Harder, J., Bartels, J., Christophers, E. and Schröder, J.-M. (1997). A peptide antibiotic from human skin. *Nature* **387**, 861.

Harder, J., Bartels, J., Christophers, E. and Schröder, J.-M. (2001). Isolation and characterization of human beta-defensin-3, a novel human inducible peptide antibiotic. *J. Biol. Chem.* **276**, 5707–5713.

Harder, J., Meyer-Hoffert, U., Teran, L. M., Schwichtenberg, L., Bartels, J., Maune, S. *et al.* (2000). Mucoid Pseudomonas aeruginosa, TNF-alpha, and IL-1beta, but not IL-6, induce human beta-defensin-2 in respiratory epithelia. *Am. J. Respir. Cell Mol. Biol.* **22**, 714–721.

Harder, J. and Schröder, J.-M. (2002). RNase 7: a novel innate immune defense antimicrobial protein of healthy human skin. *J. Biol. Chem.* **277**, 46779–46784.

Harder, J. and Schröder, J.-M. (2005). Psoriatic scales: a promising source for the isolation of human skin-derived antimicrobial proteins. *J. Leukoc. Biol.* **77**, 476–486.

Heukeshoven, J. and Dernick, R. (1988). Improved silver staining procedure for fast staining in PhastSystem Development Unit. I. Staining of sodium dodecyl sulfate gels. *Electrophoresis* **9**, 28–32.

Köten, B., Simanski, M., Gläser, R., Podschun, R., Schröder, J.-M. and Harder, J. (2009). RNase 7 contributes to the cutaneous defense against Enterococcus faecium. PLo S One **4**, e6424.

Lehrer, R. I. (2004). Primate defensins. *Nat. Rev. Microbiol.* **2**, 727–738.

Meyer-Hoffert, U., Wu, Z. and Schröder, J.-M. (2009). Identification of lympho-epithelial Kazal-type inhibitor 2 in human skin as a kallikrein-related peptidase 5-specific protease inhibitor. *PLoS ONE* **4**, e4372.

Mochizuki, M., Bartels, J., Mallet, A. I., Christophers, E. and Schröder, J.-M. (1998). IL-4 induces eotaxin: a possible mechanism of selective eosinophil recruitment in helminth infection and atopy. *J. Immunol.* **160**, 60–68.

Schägger, H. and Von Jagow, G. (1987). Tricine-sodium dodecyl sulfate-polyacrylamide gel electrophoresis for the separation of proteins in the range from 1 to 100 kDa. *Anal. Biochem.* **166**, 368–379.

Schröder, J.-M. (1997). Identification and structural characterization of chemokines in lesional skin material of patients with inflammatory skin disease. *Methods Enzymol.* **288**, 266–297.

Schröder, J.-M. and Harder, J. (2006). Antimicrobial skin peptides and proteins. *Cell Mol. Life Sci.* **63**, 469–486.

Sørensen, O. E., Thapa, D. R., Rosenthal, A., Liu, L., Roberts, A. A. and Ganz, T. (2005). Differential regulation of beta-defensin expression in human skin by microbial stimuli. *J. Immunol.* **174**, 4870–4879.

Stegemann, C. and Hoffmann, R. (2008). Sequence analysis of antimicrobial peptides by tandem mass spectrometry. *Methods Mol. Biol.* **494**, 31–46.

Steinberg, D. A. and Lehrer, R. I. (1997). Designer assays for antimicrobial peptides. Disputing the 'one-size-fits-all' theory. *Methods Mol. Biol.* **78**, 169–186.

Wu, Z., Hoover, D. M., Yang, D., Boulegue, C., Santamaria, F., Oppenheim, J. J. *et al*. (2003). Engineering disulfide bridges to dissect antimicrobial and chemotactic activities of human beta-defensin 3. *Proc. Natl. Acad. Sci. USA* **100**, 8880–8885.

7 Visualization and Functional Evaluation of Phagocyte Extracellular Traps

Maren von Köckritz-Blickwede[1,2], Ohn Chow[1], Mariam Ghochani[3] and Victor Nizet[1,4,5]

[1] Department of Pediatrics, University of California, San Diego School of Medicine, La Jolla, CA, USA; [2] Department of Physiological Chemistry, University of Veterinary Medicine Hannover, Germany; [3] Department of Physics and Biology, San Diego State University, San Diego, CA, USA; [4] Skaggs School of Pharmacy and Pharmaceutical Science, University of California San Diego, La Jolla, CA, USA; [5] Rady Children's Hospital, San Diego, CA, USA

CONTENTS

I. INTRODUCTION

In 2004, Brinkmann *et al.* (2004) discovered that neutrophils can produce extracellular traps (ETs) as a mechanism for bacterial clearance. This novel phenomenon has forced a reappraisal of the principal means by which granulocytes function in innate immune defence. ETs are DNA-based net like fibres that mediate an antimicrobial function outside the cell. These structures bind microorganisms, preventing their spread and ensuring a high local concentration of antimicrobial agents capable of inhibiting or killing the invading pathogens extracellularly [reviewed by von Köckritz-Blickwede and Nizet (2009)]. ETs are complexes of nuclear or mitochondrial DNA (Brinkmann *et al.*, 2004; Yousefi *et al.*, 2009) together with proteins such as histones, cell-specific enzymes (e.g. myeloperoxidase or elastase) and antimicrobial peptides (e.g. cathelicidins). DNA is the

METHODS IN MICROBIOLOGY, VOLUME 37
0580-9517 DOI 10.1016/S0580-9517(10)37007-3

major structural component of ETs, since treatment of cells with nucleases leads to their dissolution (Fuchs *et al.*, 2007). However, the DNA itself is not antimicrobial, and it is the host proteins bound to the DNA scaffold that give ETs their antimicrobial activity. Using a proteomic approach, Urban *et al.* (2009) identified a total of 24 ET-associated proteins in neutrophils (Urban *et al.*, 2009).

The cellular processes that lead to the formation of ETs are not completely understood. It has been shown that the production of reactive oxygen species (ROS), such as superoxide (O_2^-) or H_2O_2, are essential signalling molecules leading to the induction of a unique cell death program and the elaboration of ETs (Fuchs *et al.*, 2007). Interference with ROS generation using diphenyleneiodonium (DPI), an inhibitor of NADPH-oxidase enzymes, blocks the formation of ETs. Since this cell death process is morphologically distinct from the classical cell death processes of apoptosis and necrosis, it was named 'ETosis' (Wartha and Henriques-Normark, 2008). In ETosis, global chromatin decondensation and disintegration of the nuclear membrane occur concomitantly with cytoplasmic granule dissolution, allowing the ET components to mix in the cytoplasm prior to their extracellular release.

Formation of ETs was first thought to be restricted to neutrophils, as stimulation of peripheral blood mononuclear cells did not induce the release of similar DNA-based structures (Fuchs *et al.*, 2007). However, confocal fluorescent and scanning electron microscopic studies have also demonstrated the formation of ETs by mast cells (von Köckritz-Blickwede *et al.*, 2008) and eosinophils (Yousefi *et al.*, 2008) in response to bacteria or proinflammatory stimuli. It still remains to be shown whether ET formation by additional cell types might also be detected using techniques which are specifically aimed to analyse this novel immune function.

Here we present methods that facilitate the visualization and/or quantification of ETs. These methods comprise different *in vitro* cell culture techniques as well as *in vivo* histological techniques. Furthermore, we discuss techniques that can be used to evaluate the antimicrobial function of ETs against bacterial pathogens. *Staphylococcus aureus* and *Streptococcus pyogenes* are used as examples. Both are important human pathogens responsible for a wide spectrum of localized and invasive disease conditions. Each pathogen can produce infections in essentially every human organ or tissue, including severe life-threatening conditions such as necrotizing fasciitis, endocarditis, sepsis and toxic shock syndrome. The propensities of *S. aureus* and *S. pyogenes* to produce systemic infections, often in otherwise healthy children and adults, define a capacity of each pathogen to resist host innate immune clearance mechanisms that normally function to prevent microbial dissemination beyond epithelial surface [reviewed in Nizet (2007)]. The innate defences overcome by an invasive pathogen are now known to include antimicrobial ETs.

♦♦♦♦♦♦ II. PREPARATION OF NEUTROPHILS AND BACTERIA

This chapter describes techniques based on use of human blood-derived neutrophils as a prototype. Similar techniques can be used and have already been

proven to be fruitful for other cell types, including human or murine bone-marrow derived mast cells (von Köckritz-Blickwede *et al.*, 2008) and eosinophils (Yousefi *et al.*, 2008). However, efficiency of ET induction may vary depending on the cell type, source or differentiation status of the cells (Martinelli *et al.*, 2004). For example, a longer period of stimulation with Phorbol myristate acetate (PMA) is necessary to induce similar amounts of ETs from murine bone-marrow-derived neutrophils compared to human blood-derived neutrophils (Ermert *et al.*, 2008a). Furthermore, neutrophils derived from several individual mouse strains produce neutrophil ETs (NETs) at different rates (Ermert *et al.*, 2008a).

A. Isolation of Neutrophils

Human neutrophils are isolated and purified from venous blood by density gradient centrifugation using the Polymorphprep™ system (Axis-Shield, Fisher Scientific, #AN1114683). Twenty millilitre of whole blood is sufficient to isolate approximately $2–4 \times 10^7$ neutrophils according to the following protocol:

1. Draw 20 ml venous blood using a 30 ml heparinized syringe (100 µl heparin in a 30 ml syringe).
2. Slowly layer 20 ml blood on top of 20 ml Polymorphprep™ in a 50 ml Falcon tube, taking care to avoid mixing.
3. Centrifuge at $512 \times g$ (without brake) for 30 min at room temperature (Figure 1).
4. Aspirate 5 ml plasma and mononuclear cells from the top layer (This plasma can be used as medium supplement during the assays. Therefore it needs to be heat inactivated at 56°C (to inhibit complement) or 70°C (to completely inhibit serum nucleases) for 30 min and centrifuged at $3000 \times g$ for 10 min to remove remaining proteins).

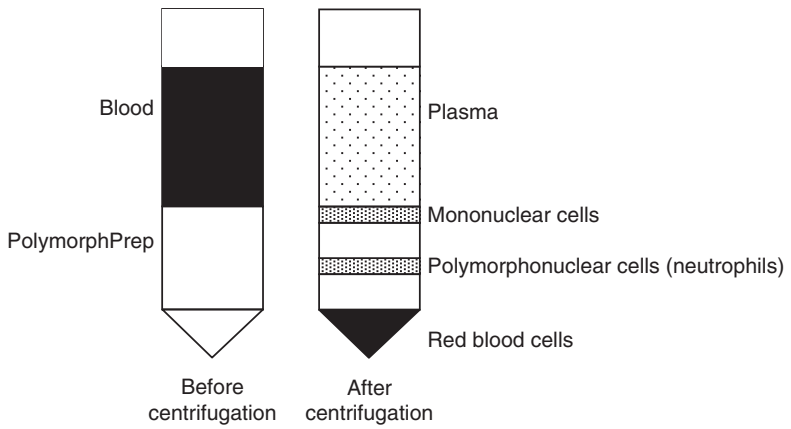

Figure 1. Density gradient before and after centrifugation of Polymorphprep™ with blood.

5. Collect the neutrophil layer (~5–10 ml) into a 50 ml Falcon tube.
6. Add sterile phosphate-buffered saline (PBS, Mediatech, #21-031-CV) to a volume of 50 ml and spin at 512 × *g* for 10 min.
7. Remove the supernatant, add 5 ml of sterile molecular grade water (Cellgro, #46-000-CM) and mix by pipetting up and down for 5 s to lyse erythrocytes.
8. Immediately add 45 ml of PBS and spin at 512 × *g* for 10 min.
9. Repeat the above step once again until complete lysis of erythrocytes. The neutrophil pellet should be white in colour.
10. After the final wash, discard supernatant and resuspend the neutrophils in 1000 µl PBS.
11. For the haemocytometer count, dilute neutrophils 1:100 with 0.4% trypan blue (Invitrogen, #15250) and count at least 100 cells. Score for both blue (dead) cells and the total number of cells. Calculate the percentage of dead cells and the total number of cells present. Neutrophils should have >95% viability when used in the following assays.
12. Finally, the cells are resuspended in RPMI-1640 (Invitrogen, #11875) containing desired serum supplements (e.g. autologous heat-inactivated human plasma, foetal calf serum (FCS) or serum albumin). Since serum has been shown to block the formation of ETs based on its antioxidant properties and the presence of serum nucleases, a maximum of 2% serum should be added to the medium. See the following *Note* for further information about the presence of nucleases in serum.

Note: Degradation of ETs by serum nucleases!

We previously showed that serum contains heat-stable nucleases that can degrade non-fixed or paraformaldehyde-fixed neutrophil-derived ETs (von Köckritz-Blickwede *et al.*, 2009). Serum nucleases can be inhibited by heat inactivation of serum for 30 min above 66°C (Segal *et al.*, 1992). Nuclease activity has also been shown to be present in aged solution of bovine plasma albumin Fraction V (Anai *et al.*, 1972), which is widely used in culture experiments as an alternative to FCS.

The presence of serum nucleases should be avoided and can simply be tested by a functional DNA-degradation assay: 7.5 µl of calf thymus DNA (1 mg/ml, Sigma, #D3664), 40 µl Tris-buffer (5 mM $MgCl_2$, 5 mM $CaCl_2$, 300 mM Tris; pH 7.4) and 10 µl serum are mixed and incubated for 18 h at 37°C. Then, 12.5 µl or 0.33 M EDTA (pH 8.0) is added to stop the reaction. After addition of 12.5 µl of 6× loading dye, the DNA degradation can be visualized by agarose gel electrophoresis (100 mV for 30 min) using a 1% agarose gel containing 0.5 µg/ml ethidium bromide (Figure 2).

B. *Staphylococcus aureus* and *Streptococcus pyogenes*

S. aureus and *S. pyogenes* are both Gram-positive, non-motile, non-spore-forming cocci, 0.6–1.0 µm in diameter. However, the arrangement of cells is different

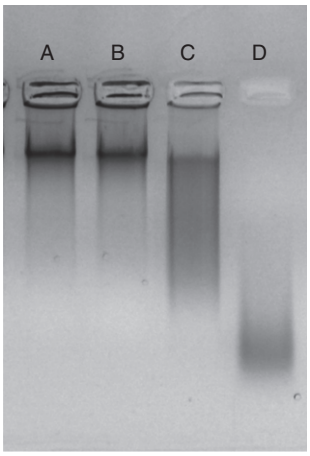

Figure 2. Representative agarose gel demonstrating nuclease activity in different serum charges. (A) DNA control, (B) nuclease-free serum, (C) nuclease-containing serum, (D) micrococcal nuclease as positive control.

between those two organisms due to a different pattern of binary fission: streptococci form a chain of round cells as a result of their linear division, whereas staphylococci divide in various directions forming grape-like clusters. Both are facultative anaerobes that grow by aerobic respiration or by fermentation that mainly yields lactic acid. However, in contrast to *S. pyogenes, S. aureus* shows more robust growth under aerobic than anaerobic conditions due to its catalase activity. Therefore *S. aureus* is grown under shaking conditions (at 180 rpm).

Before starting the assay, dilute overnight cultures of the bacteria 1:50 in fresh Todd–Hewitt broth and grow to the logarithmic phase [$OD_{600\,nm} = 0.4$ corresponding to ~2×10^8 colony forming units (cfu)/ml]. Centrifuge the bacteria at $512 \times g$ for 10 min and wash with PBS to remove released toxins, proteases and nucleases. Finally, resuspend the bacteria in their respective cell culture media at the desired concentration.

C. ET-Inducing Agents to Serve as Positive Controls

Various agents have been shown to induce the formation of ETs in neutrophils or other cell types. Table 1 resumes those agents that can be used as positive controls for induction of ETs.

♦♦♦♦♦♦ III. *IN VITRO* VISUALIZATION OF ETs

Different techniques can be used to visualize and quantify the formation of ETs in response to a bacterial infection *in vitro* by fluorescence microscopy. Since DNA is

Table 1. Factors inducing formation of ETs in neutrophils

Factor	Concentration	Reference
Phorbol myristate acetate	25 nM (30–240 min)	Brinkmann *et al.* (2004)
H_2O_2-producing glucose oxidase	100 mU/ml (30–60 min)	Fuchs *et al*. (2007)
Interleukin 8	100 ng/ml (30–60 min)	Brinkmann *et al.* (2004); Fuchs *et al*. (2007)
Lipopolysaccharide (LPS)	100 ng/ml	Brinkmann *et al.* (2004)
Interferon (IFN) α + C5a	500 units/ml (30 min) IFNα + 10^{-7} M C5a (10 min)	Martinelli *et al*. (2004)
GM-CSF + LPS	25 ng/ml (20 min) GM-CSF + 0.3 μg/ml LPS (15 min)	Yousefi *et al.* (2009)
GM-CSF + C5a	25 ng/ml (20 min) GM-CSF + 10^{-7} M C5a (15 min)	Yousefi *et al*. (2009)

the major backbone of ETs, different DNA-intercalating dyes are sufficient to visualize ETs. However, since cell-specific enzymes, such as neutrophil-specific myeloperoxidase in NETs and mast cell-specific tryptase in mast cell ETs, have been shown to be present at high amounts within ETs, additional immunostaining of those enzymes can help to visualize ETs.

For all staining techniques, neutrophils are seeded onto poly-L-lysine-coated glass coverslides using the following protocol:

1. Place one glass coverslide per well into non-treated suspension culture plates (Cellstar, Greiner Bioone, #677102). Use 12 mm glass slides (Fisherbrand microscope cover glass 1.5 thickness, Fisher Scientific, #12-545-81) for a 24-well plate and 8 mm glass slides (Electron Microscopy Research, #72296-08) for a 48-well plate. In contrast to tissue culture-treated plates, non-treated (suspension culture) plates prevent unspecific attachment of bacteria to the bottom of the plates.
2. To coat the glass slides, add 100 μl (12 mm) and 50 μl (8 mm) of 0.01% poly-L-lysine (Sigma, #P4707) to the centre of each cover slide. Be careful not to put poly-L-lysine to close to the border of the glass slide. Do not allow the poly-L-lysine to run beside or below the glass slide. Otherwise cells may attach below the glass slide! Incubate for 10–30 min at room temperature.
3. Wash the wells twice with PBS to remove excessive poly-L-lysine.
4. Immediately add the cells to the wells. Seed 5×10^5 cells/well in 24-well plates (with 12 mm glass slides) or 2×10^5 cell/well in 48-well plates (with 8 mm glass slides) with 500 or 250 μl medium per well, respectively.
5. Add bacteria at a multiplicity of infection (MOI) of 0.1. Higher MOIs (1, 2, 5, 10, 25) can be used to analyse concentration-dependent ET induction. Always include a negative control of unstimulated cells to detect unspecific

ET formation that may be induced spontaneously during the procedure or that may occur due to fixation artefacts.
6. Centrifuge the plates for 10 min at 800 rpm and further incubate at 37°C and 5% CO_2 for 30 min to 3 h before visualization of ETs.

A. Staining of ETs with DNA-Intercalating Dyes

Different DNA-intercalating dyes can be used for the visualization of extracellular DNA. The cells can be stained with the cell-permeable fluorescent DNA-staining dye SYTO 13 (0.5 μM, Invitrogen, #S7575) and/or with a fluorescent dye unable to enter intact cells (Sytox Orange, 5 μM, Invitrogen, #S11368). A combination of both dyes can be used to distinguish between ETs released by living or dead cells (Yousefi *et al.*, 2009). After staining the cells (for 10 min at room temperature in the dark), washing with PBS can reduce unspecific background staining. (Make sure to never let the slides dry out during washing steps to avoid undesired unspecific background fluorescence. After soaking off the supernatant, immediately add back respective buffers. This is also important during immunostaining of paraformaldehyde-fixed cells or tissue.)

A successfully used alternative to these dyes is the usage of the LIVE/DEAD® Viability/Cytotoxicity Assay Kit for mammalian cells (Invitrogen, #L3224). This kit provides a two-colour fluorescence cell viability assay that is based on the simultaneous determination of live and dead cells with the two probes calcein acetoxymethyl (AM) and ethidium homodimer (EthD-1) that measure recognized parameters of cell viability (intracellular esterase activity) and plasma membrane integrity. Background fluorescence levels are inherently low with this assay technique, since the dyes are virtually non-fluorescent before interacting with cells. Live cells are distinguished by the presence of ubiquitous intracellular esterase activity, determined by the enzymatic conversion of the virtually non-fluorescent cell-permeant calcein AM to the intensely fluorescent calcein. The polyanionic dye calcein is well retained within live cells, producing an intense uniform green fluorescence in live cells (ex/em ~495 nm/~515 nm). EthD-1 enters cells with damaged membranes and undergoes a 40-fold enhancement of fluorescence upon binding to nucleic acids, thereby not only producing a bright red fluorescence in dead cells (ex/em ~495 nm/~635 nm) but also staining the formation of ETs. EthD-1 is excluded by the intact plasma membrane of live cells.

LIVE/DEAD® Viability/Cytotoxicity Assay Kit for mammalian cells (Invitrogen)

1. Prepare the dye solution provided within the kit: 20 μl of component B + 1 μl of component A in 10 ml PBS (for cells on poly-L-lysine-coated glass slides). If glass-bottom-plates are used, only ⅓ of the amount of both dye components should be used.
2. Before starting the staining procedure, wash the cells twice with PBS.
3. Add 150 μl of the preliminary prepared dye solution to each well.

4. Incubate for approximately 30 min in the dark.
5. Visualize the samples immediately without fixation by adding 10 µl of staining solution to a microscope slide and placing the glass cover slide with attached cells 'face down' into the staining solution.
6. This staining needs to be visualized immediately. Staining characteristics are lost after paraformaldehyde fixation. Thus, immediately after staining take $n = 5$ representative images of each sample. Subsequently count the total amount of cells (green), the amount of dead cells (red) and the amount of ET-forming cells.

Using the above-mentioned method for ET visualization and quantification, an individual bacterial protein, the surface anchored and soluble M1 protein of *S. pyogenes*, was recently found to induce ET formation by neutrophils and mast cells (Lauth *et al.*, 2008). The authors show that ET induction was significantly reduced with an isogenic M1 protein-deficient mutant strain compared to the wild-type *S. pyogenes* parent strain. Furthermore, complementation of the mutant strain with a plasmid expressing M1 protein restored the ET formation (Figure 3).

B. Immunostaining of ETs

Since DNA is not the only ET component, immunostaining of specific additional ET elements may help to better visualize these unique structures and characterized possible antimicrobial factors that are embedded within them. Furthermore,

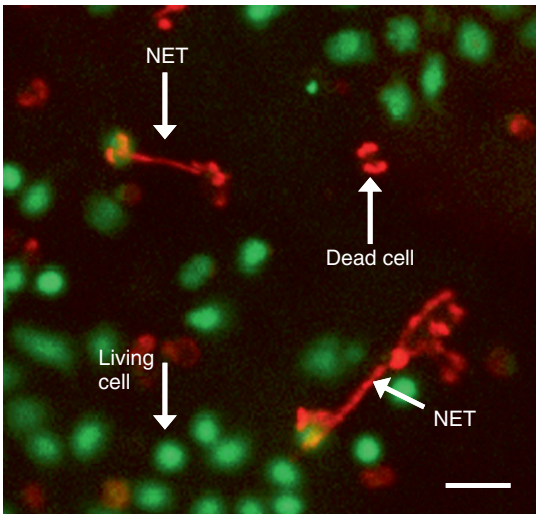

Figure 3. Representative fluorescent image of ETs stained with Live/dead viability/cytotoxicity kit for mammalian cells (Cytoplasm of viable cells is stained in green and dead cells and extracellular DNA are stained in red). Bar 10 µm. Unfixed samples were recorded using a Zeiss Axiolab microscope (Zeiss 20×/0.5 Plan-Neofluor objective) with an attached Sony Digital Photo Camera DKC-5000 at calibrated magnifications. (See color plate section).

immunostaining techniques offer the possibility of using fixed cells and/or tissue that can be kept cool for up to 6 months.

For immunostainings, fix stimulated/infected cells by adding 16% paraformaldehyde (Electron Microscopy Science, #15710) to each well at a final concentration of 4% PFA for 10 min at room temperature. After that, the slides can be kept at 4°C before starting the immunostaining. For storage, wrap parafilm around the plate to avoid evaporation.

Use the following protocol for myeloperoxidase staining of fixed samples:

1. Wash the fixed glass slides three times with PBS.
2. Block by adding 2% BSA–PBS+2% goat serum for 45 min at room temperature. (To additionally visualize intracellular protein expression, the blocking step can be combined with the permeabilization of the cells by adding 0.25% Triton X-100 to the blocking buffer.)
3. Wash three times with PBS.
4. Add rabbit anti-human MPO (Dako, #A0398) 1:300 diluted in 2% PBS–BSA for 1 h at room temperature.
5. Wash three times with PBS.
6. Add the secondary antibody Alexa fluor 488 goat anti-rabbit IgG (Invitrogen, #A11070) 1:500 diluted in 2% BSA–PBS for 45 min at room temperature in dark.
7. Wash three times with PBS and embed the samples in 5 µl ProlongGold antifade + Dapi (Invitrogen, #P36931). For embedding, add 5 µl of the ProlongGold to a microscope slide, and place the glass cover slide with attached cells 'face down' into the embedding solution. Let it dry in the dark at room temperature over night. The following day, seal the border with nail polish to avoid evaporation. Keep at 4°C in dark.
8. Take $n = 5$ representative images per sample and count the number of ET-releasing cells versus non-ET-forming cells (Figure 4).

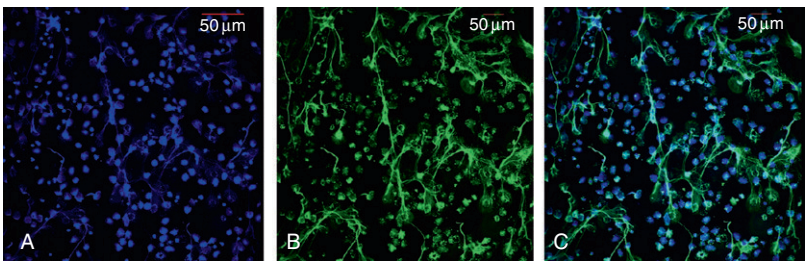

Figure 4. Representative immunofluorescence micrograph of neutrophils ETs (NETs) after stimulation for 3 h with 25 nM PMA. NETs were visualized using a rabbit anti-myeloperoxidase-antibody followed by a secondary goat anti-rabbit Alexa 488 antibody; samples were embedded in ProlongGold+Dapi to counterstain DNA in blue. A) DNA (blue), B) myeloperoxidase (green), c) overlay. Mounted samples were examined using an inverted confocal laser scanning 2-photon microscope Olympus Fluoview FV1000 with Fluoview TM Spectral Scanning Technology (Olympus) and a 20×/0.75 UPlanSApo Olympus objective. (See color plate section).

For the identification of a new component within ETs, a similar protocol can be used. The following controls need to be included to validate the specificity of respective antibodies:

1. Cells that are known to be positive for the respective target (positive control).
2. Cells that do not express the protein of interest (negative control).
3. Isotype control antibody or pre-immune serum, which is used instead of the primary antibody to exclude possible unspecific binding of the antibodies.

Using an antibody against histone–DNA complexes (Losman *et al.*, 1992), different stages of NET-formation can be identified based on characteristic morphological changes of the nucleus upon stimulation and before release of ETs. The process that leads to ET formation has been shown to be neither apoptosis nor necrosis, but rather a new form of cell death termed 'ETosis'. During this process, disintegration of the nuclear membrane occurs concomitantly with cytoplasmic granule dissolution, allowing NET components to mix in the cytoplasm. The normal lobulated nuclear structure is then broken and a delobulated nuclear form can be found in those cells that are in the early stages of Etosis (Figure 5).

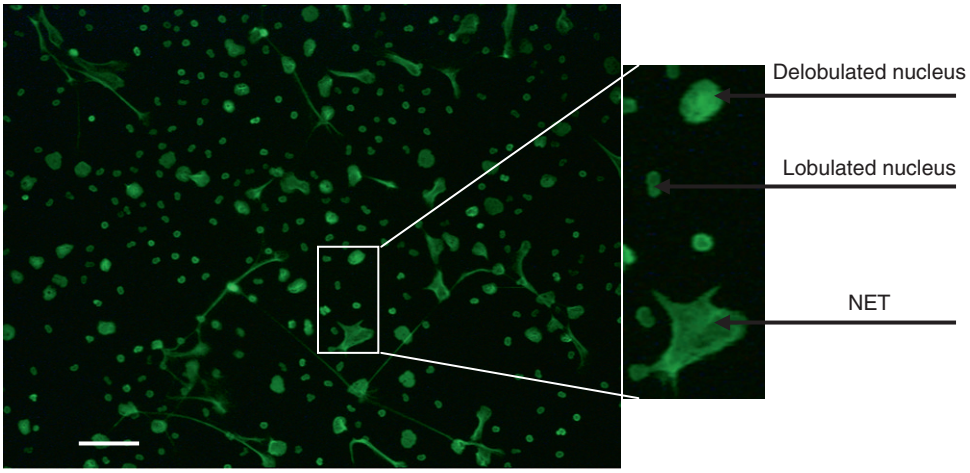

Figure 5. Representative immunofluorescence micrograph of neutrophils ETs (NETs) after stimulation for 2 h with 25 nM PMA. NETs were visualized using a mouse anti-H2A–H2B–DNA complex antibody (Losman *et al.*, 1992) followed by a secondary goat anti-mouse Alexa 488 antibody (Invitrogen). Samples were embedded in ProlongGold+Dapi (Invitrogen) to counterstain DNA in blue. Bar 30 μm. Mounted samples were examined using an inverted confocal laser scanning 2-photon microscope Olympus Fluoview FV1000 with Fluoview TM Spectral Scanning Technology (Olympus) and a 20×/0.75 UPlanSApo Olympus objective. (See color plate section).

Use the following protocol for staining H2A–H2B–DNA complexes:

1. Wash the glass slides three times with PBS.
2. Block and permeabilise the cells by adding 2% BSA–PBS +2% rabbit + 0.2% Triton X-100 (MP-Biomedicals, #807423) for 45 min at room temperature.
3. Wash three times with PBS.
4. Add mouse monoclonal anti-H2A–H2B–DNA complex (1 μg/ml; Losman *et al.*, 1992) diluted in 2% PBS–BSA + 0.2% Triton X-100 overnight at 4°C. Isotype control: mouse IgG2b (Thermo Scientific, # NC1391)
5. Wash three times with PBS.
6. Add the secondary antibody Alexa fluor 488 goat anti-mouse IgG (Invitrogen, #A11017) 1:500 diluted in 2% BSA–PBS + 0.2% Triton X-100 for 45 min at room temperature in dark.
7. Wash three times with PBS and embed in 5 μl ProlongGold antifade + Dapi (Invitrogen, #P36931).

C. Quantification of ETs

In addition to the visual assessment of ET formation by fluorescence microscopy, another spectrofluorometric method can be used to quantify ETs. This method is based on the fact that DNA is the major backbone of ETs. Micrococcal nuclease is used to disrupt the ETs and to release the DNA of ETs into the supernatant. The amount of extracellular DNA can then be quantified in the supernatant of cells by using the Quant-iT^{TM} Picogreen$^{®}$-dsDNA kit (Invitrogen, #P11496). The percentage of ET-DNA is calculated using total cell DNA as 100%.

Although this kit is an ultrasensitive fluorescent nucleic stain for quantifying double-stranded DNA (dsDNA) in solution, the Picogreen assay is not sensitive enough to detect a relatively small amount of cells (<than 20% within 1 h after stimulation) that are releasing ETs. In this case, the microscopic evaluation of ET release is more sensitive. However, the Picogreen assay is a useful tool to investigate the formation of ETs in a high-throughput format. Nevertheless, a microscopic confirmation of the results is always necessary to exclude necrotic release of cellular DNA and to thus confirm specificity of the assay (Figure 6).

Spectro-(fluoro)-metric quantification of ETs

1. Seed 2×10^5 cells per well (each sample in triplicate) into a 96-well tissue culture plate (BD Bioscience, #353072) in RPMI without Phenol red (Mediatech, #17-105-CV).
2. Stimulate with selected ET inducer as positive control (see Table 1) or with different MOIs of bacteria in 200 μl volume. Use untreated cells as background control.
3. Incubate for 1–4 h.
4. Add 500 mU/ml micrococcal nuclease in a volume of 50 μl per well (stock: 50 kU/ml, dilute 1:20.000; Worthington, #NFCP) for 10 min at 37°C.
5. Stop with 5 mM EDTA (stock: 0.33M pH 8).
6. Centrifuge at $200 \times g$ for 8 min.

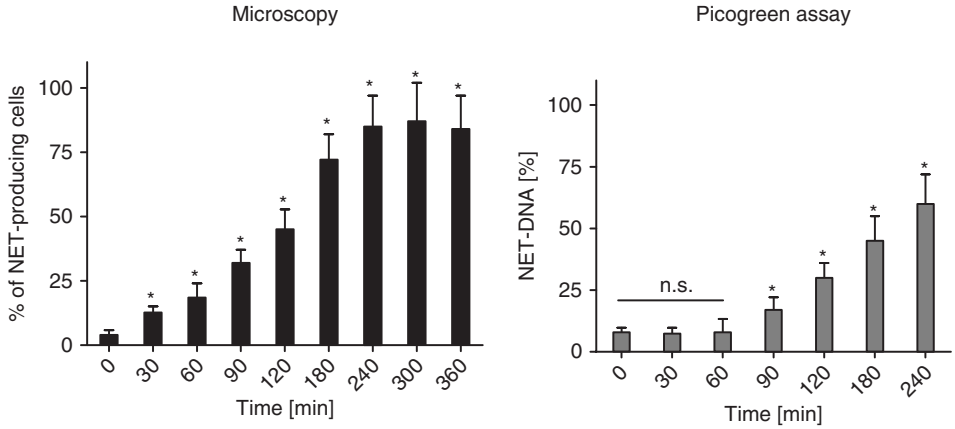

Figure 6. Determination of percentage (%) of NET-release by human blood-derived neutrophils after stimulation with 25 nM PMA (incubated in RPMI without serum supplements) using two different methods: microscopic evaluation versus spectrofluorometric quantification with the Quant-iT^{TM} Picogreen$^{®}$-dsDNA assay. Comparison of zero-time point with later time points was made by use of Student's *t*-test. *P* values of .05 or less were considered significant. Note that the microscopic evaluation is more sensitive to detect significant difference at 30 and 60 min upon stimulation.

7. Transfer 100 µl supernatant to a separate 96-well plates (flat bottom) for Quant-iT Picogreen (Invitrogen, #P11496) assay.
8. Dilute Picogreen reagent 1:200 in TE buffer (freshly made).
9. Mix reagent 1:1 with samples (add 100 µl working solution to 100 µl samples in 96-well plate).
10. Incubate 2–5 min at room temperature in dark.
11. Measure excitation 480 nm, emission 520 nm (fluorescein).
12. Quantify the amount of extracellular DNA in respect to a Lambda DNA standard curve (10–0.1 µg/ml).
13. Calculate the percentage compared to total DNA of 2×10^5 cells.

Isolation of total DNA as 100% control:

1. Add 250 µl DNazol (MRS, #DN127) +2.5 µl Polyacryl Carrier (Molecular Research Center, #PC152) to 2×10^5 cells and lyse cells by pipetting up and down.
2. Centrifugate 10 min at 10,000 × *g*.
3. Transfer viscous supernatant to a new tube.
4. Add 125 µl of 100% ethanol.
5. Mix samples by inverting the tube five to eight times and incubate at room temperature for 1–3 min.
6. Centrifuge 5000 × *g* for 5 min.
7. Wash pellet twice with 75% ethanol by inverting the tubes three to six times.
8. Centrifuge 1000 × *g* for 1–2 min.
9. Resuspend the DNA in water.

D. Electron Microscopy

Several different electron microscopy protocols have been used to understand the formation of ETs. Whereas scanning electron microscopy (SEM) can be used to visualize the overall release of ETs and its three-dimensional structure, transmission electron microscopy (TEM) can be used to visualize the morphological changes within a cell.

Thus, high-resolution SEM showed that ETs contain smooth stretches with a diameter of 15–17 nm and globular domains of around 25 nm that aggregates into larger threads with diameters of up to 50 nm (Brinkmann *et al.*, 2004). Analysis of cross-sections of the ETs by TEM additionally revealed that ETs are not surrounded by membranes. Furthermore, TEM analysis was used to identify the morphological changes that lead to the formation of ETs: first, the nuclei start to lose their lobules, and the chromatin begins to decondense. The space between the inner and outer nuclear membrane dilates and the nuclear envelope finally completely disintegrates. With the loss of nuclear and granule membranes, the decondensed chromatin comes into contact with cytoplasmic and granule components (Fuchs *et al.*, 2007).

Here, selected methods for SEM as well as TEM will be presented. For both processes, 2×10^7 neutrophils are incubated with bacteria (MOI of 1) in 250 µl HBSS + Ca/Mg (Invitrogen, #14065) in a 1.5 ml Eppendorf tube under constant rotation at 37°C for 20 min. Then the cells are centrifuged for 10 min at $512 \times g$ and washed twice with PBS before fixation (Figure 7).

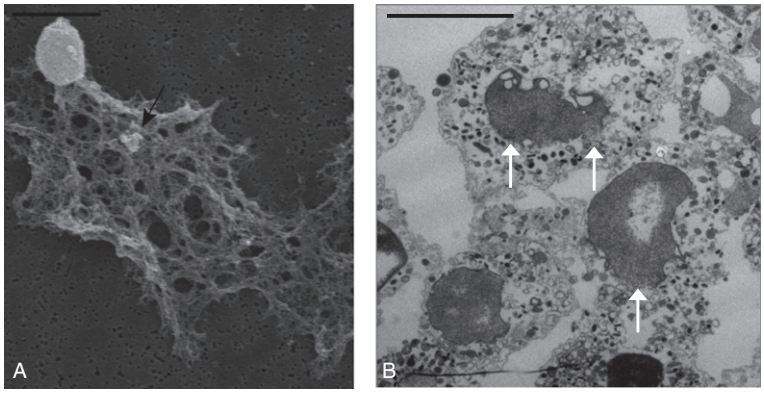

Figure 7. Electron micrograph showing neutrophils that are releasing extracellular DNA-traps in response to *S. pyogenes* infection. (A) Scanning electron micrograph using a Hitachi S-2700 scanning electron microscope in a 60:60 ratio at an accelerating voltage of 10 kV. Note the bacterium entrapped within the ET (black arrow). Bar, 10 µm. (B) Transmission electron micrograph (TEM) using an FEI Tecnai 12 transmission electron microscope operated at 120 kV. Bar, 5 µm. Images were recorded on a Tietz 214 CCD camera after which images were assembled in Adobe Photoshop CS version 8 with only linear adjustments in brightness and contrast. Note the disintegration of the nuclear membrane with subsequent release of nuclear DNA and mixing with cytoplasm (white arrow).

Transmission electron microscopy

1. After incubation, the cells are immediately fixed with 3.0% formaldehyde (Ted Pella, #18505) + 1.5% glutaraldehyde (Ted Pella, #18420) + 0.1 M sodium cacodylate trihydrate (Sigma-Aldrich, #C0250) + 5 mM calcium chloride (J.T. Baker, #1-1332) + 2.5% sucrose (Sigma-Aldrich, #24761-8) at pH 7.4 for 1 h at room temperature.
2. Cells are then washed three times for 10 min each in ice-cold 0.1 M sodium cacodylate buffer containing 2.5% sucrose.
3. In accordance with the general procedure of Perkins and McCaffery (2007), the primary fixed cells are then incubated with 1% osmium tetroxide (Ted Pella, #18463) + 0.02 N hydrochloric acid (J.T. Baker, #6011) in 0.056 M acetate-veronal solution (0.028 M sodium acetate anhydrous (J.T. Baker, #1-3470) + 0.028 M sodium barbital (Merck, #6921)) for 1 h on ice in the dark.
4. Wash with 0.056 M acetate-veronal solution-0.028 N hydrochloric acid three times for 10 min each.
5. Fixed cells are stained and stabilized en bloc with 0.5% uranyl acetate (Ted Pella, #19481) + 0.056 M acetate-veronal solution + 0.028 N hydrochloric acid solution, pH 6, over night at room temperature in the dark.
6. After one rinse with ddH_2O and one rinse with 50% ethanol (4°C), the cells are dehydrated at 4°C through a series of 70, 95 and 100% ethanol successively for 15 min each.
7. Wash three times for 15 min each in fresh 100% ethanol (Pharmco-AAPER, #E200) at room temperature.
8. Cells are then infiltrated in well-mixed Epon (Ted Pella, #18010)-ethanol resin series of 33% for 7 h, 66% for 7 h followed by 100% at least overnight with agitation at room temperature.
9. The samples are allowed to polymerize in 100% Epon blocks at 60°C for 24 h.
10. For conventional electron microscopy, 70-nm sections are cut using a Diatome diamond knife on a Leica EM UC6 ultramicrotome.
11. Mount the samples on 100 mesh copper grids (Ted Pella, #12414-CU).
12. Stain the cells with 2% uranyl acetate and Reynolds lead citrate before examination.

Scanning electron microscopy

1. Cells are immediately fixed with 3.0% formaldehyde (Ted Pella, # 18505) + 1.5% glutaraldehyde (Ted Pella, #18420) + 0.1 M sodium cacodylate trihydrate (Sigma-Aldrich, #C0250) + 5 mM calcium chloride (J.T. Baker, #1-1332) + 2.5% sucrose (Aldrich Chem. Comp., #24761-8) at pH 7.4, for 1 h at room temperature.

2. Cells are washed three times for 10 min each in ice-cold 0.1 M sodium cacodylate buffer containing 2.5% sucrose.
3. To post-fix the cells with Palade's OsO_4 (Palade, 1952), they are then incubated with 1% osmium tetroxide (Ted Pella, #18463) + 0.02 N hydrochloric acid (J.T. Baker, #6011) in 0.056 M acetate-veronal solution [0.028 M sodium acetate anhydrous (J.T. Baker, #1-3470) + 0.028 M sodium barbital (Merck, #6921)] for 30 min on ice in the dark.
4. Wash three times with 0.056 M acetate-veronal solution-0.028 N hydrochloric acid for 10 min each.
5. The cells are then filtered through 0.4 μm HTTP Isopore membrane filters (Millipore, #HTTP01300).
6. Wash with ddH_2O and dehydrate in graded series of ethanol (30, 50, 70, 95 and 100%) (Pharmco-AAPER, #E200) for 15 min each at room temperature.
7. The cells in the filter are then critical-point dried with liquid CO_2 in a Tousimis Samdri 790 drier.
8. Mount the cells with an adhesive carbon conductive tab onto an aluminium sample stub (Ted Pella) and coat with Au-Pd (60:40w/w) film on a Denton Desk II sputter coater before examination in a SEM.

♦♦♦♦♦♦ IV. *IN VIVO* VISUALIZATION OF ETs

Most of the antibodies in Table 2 that have been used for the visualization of ETs *in vitro* can also be used to identify ETs *in vivo* by using formalin-fixed and paraffin-embedded tissue sections. The most commonly used fixatives are 10% buffered formalin (Fisher Scientific, #SF93-4) or 4% paraformaldehyde. However, it must be noted that the fixative penetrates into the tissue very slowly (approximately 1 mm per hour). Thus, the tissue needs to remain in the fixative for approximately 24 h. Note that the lung morphology is best examined after perfusion of fixative through the trachea to inflate all lobes. After fixation and subsequent paraffin embedding, 3–7 μm thick sections should be used for subsequent immunostaining using the following described protocol. Besides, haematoxylin-eosin-staining can be useful to detect additional pathological changes within the tissue (Figure 8).

Immunostaining of paraffin-embedded tissue

1. Deparafinize sample with xylene (three times 10 min; Fisher Scientific, #X3P-1GAL), 1000% alcohol (two times, 5 min each; Fisher Scientific, #A962P-4), 95% alcohol (two times, 5 min each), 70% alcohol (two times, 5 min each).
2. Wash with PBS (three times 10 dips).

3. Microwave (high level) the sections for 2 × 5 min in target retrieval solution, citrate buffer pH 6 (Dako, #S2369), with lid to break cross-links formed during formalin fixation.
4. Let stand for 20 min in citrate buffer solution without lid at room temperature.
5. Wash with PBS three times with 10 dips/wash.
6. Block with 2% BSA–PBS + 2% goat serum for 45 min at room temperature. [Since paraffin sections are usually very thin (3–7 μm), most of antigens/epitopes are already exposed, making detergent-permeabilization unnecessary.]
7. Add the primary antibody (rabbit anti-mouse CRAMP; Dorschner *et al.*, 2001) in the presence of 2% BSA–PBS covered with parafilm, overnight at 4°C in humid chamber.
8. Wash with PBS four times.
9. Add the secondary antibody (Alexa 488 goat anti-rabbit, Invitrogen #A11070) 1:500 and incubate for 45 min at room temperature, in humid chamber covered with parafilm.
10. Wash with PBS four times.
11. Put on coverslides using ProlongGold+Dapi (Invitrogen, #P36931) as embedding solution.

Table 2. Antibodies for visualization of ETs

Target protein	Antibody	Target tissue/cells	Reference
Myeloperoxidase	Rabbit anti-human MPO (Dako, # A0398)	Murine and human neutrophils	Ermert *et al.* (2008a); Von Köckritz-Blickwede *et al.* (2009)
H2A–H2B–DNA complex	Mouse anti-H2A–H2B–DNA complex (Losman *et al.*, 1992)	Murine and human neutrophils	Brinkmann *et al.* (2004); Ermert *et al.* (2008a)
Histone H4cit3	Rabbit anti-H4cit3 (Millipore, #07-596)	HL-60 cells	Wang *et al.* (2009)
Cathelicidins (CRAMP)	Rabbit anti-CRAMP (Dorschner *et al.*, 2001)	Mouse lung tissue	See this chapter '*In vivo* visualization of ETs'
Elastase	Urban *et al.* (2006)	Human neutrophils	Urban *et al.* (2006)
Tryptase	Mouse anti-human tryptase (clone 4A1, Dako, #M7052)	Mast cells (HMC-1)	Von Köckritz-Blickwede *et al.* (2008)
Calprotectin	Urban *et al.* (2009)	Human neutrophils, mouse lung tissue	Urban *et al.* (2009)

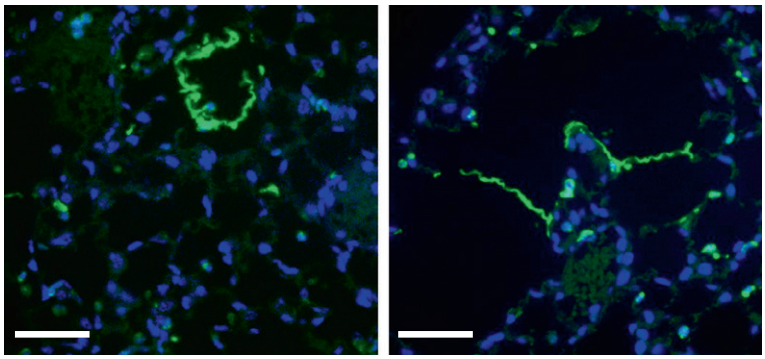

Figure 8. Representative fluorescent images of extracellular trap formation (visualized by Alexa 488 (green)-labelled CRAMP production and counterstained with Dapi; see protocol on the next page) in 3 µm thick paraffin-embedded lung sections of mice intranasally infected with 2×10^8 cfu of *S. aureus* strain Newman for 48 h. Bars represent 25 µm. Images were recorded using an Olympus Spinning Disc Confocal IX81 microscope (40×/1.0 oil UPlanApo objective) with a Xenon DG5 illumination source driven by SlideBook software (Intelligent Imaging Innovations). (See color plate section).

♦♦♦♦♦♦ V. FUNCTIONAL ASSAYS

ETs have been discovered to exhibit an important antimicrobial role during host immune defence by entrapment of an invading pathogen to (a) prevent its further spread and/or (b) to directly kill the pathogen. Ermert *et al.* (2008b) described methods that can be used to measure killing of microbes by ETs and further to differentiate whether phagocyte killing is occurring through ETs, phagocytosis or granule extracts. The methods are based on quantification of surviving cfu as parameter for the calculated antimicrobial activities. Here we present additional fluorescence-based methods that can be used to quantify entrapment and to visualize killing of bacteria within ETs.

A. Quantification of Bacterial Entrapment by ETs

For the quantification of bacterial entrapment, the bacteria are labelled with fluoresceinisothiocyanat (FITC) and then added to neutrophils, which have been stimulated for 4 h with PMA for maximal ET formation and abolishment of phagocytic activity (Fuchs *et al.*, 2007). Finally the entrapment of fluorescent bacteria can be measured spectrofluorometrically. The following protocol can be used:

1. Seed 2×10^5 neutrophils per well in 96-well plate (each sample in triplicate) in RPMI without Phenol red (100 µl per well). Use similar amounts of respective control wells without cells.
2. Stimulate cells with 25 nM PMA (Sigma, #P1585) for 4 h at 37°C + 5% CO_2.
3. Meanwhile incubate logarithmic phase bacteria with 0.2 mg/ml FITC (stock 10 mg/ml in DMSO, Invitrogen, #F1906) for 30 min on ice in the dark (Goldmann *et al.*, 2004).

4. After incubation, centrifuge the bacteria at 3000 × *g* for 10 min and wash twice with PBS to remove unbound FITC.
5. Infect the PMA-stimulated neutrophils with FITC-labelled bacteria at an MOI of 10, 25, 50 and 100 (by adding 100 µl medium). Include control wells without bacteria.
6. Include control wells without neutrophils for bacterial-FITC standard curve.
7. Centrifuge at 512 × *g* for 10 min.
8. Incubate for 30 min at 37°C.
9. Wash cells carefully two times with 200 µl RPMI (without Phenol red).
10. Measure green fluorescence at 485/538 nm (SpectraMax® Gemini XS Spectrofluorometer (Molecular Devices).
11. Percent entrapment of GAS can be calculated as ([A485/538 nm experimental well]/[A485/538 nm control well without neutrophils]) × 100%.
12. Control wells containing serial dilutions of FITC-labelled bacteria are used for standard curve construction and subsequent quantification of entrapped bacteria.

B. Visualization of Bacterial Killing by ETs

To visualize the bacterial killing by ETs, the LIVE/DEAD® BacLight™ Bacterial Viability Kit (Invitrogen, #L7012) can be used in combination with Dapi Prolong-Gold. The kit utilizes a mixture of Syto 9-green fluorescent nucleic acid stain and the red-fluorescent nucleic acid stain propidium iodide. These stains differ both in their spectral characteristics and in their ability to penetrate healthy bacterial cells. Syto 9 stain generally labels all bacteria in a population – those with intact membranes and those with damaged membranes. In contrast, propidium iodide penetrates only bacteria with damaged membranes, causing a reduction in the Syto 9 stain fluorescence. Thus, with an appropriate mixture of the Syto 9 and propidium iodide stains, living bacteria stain fluorescent green, whereas dead bacteria stain red.

1. Seed neutrophils at cell density of 5×10^5 cells per 500 µl in RPMI in a 24-well plate with poly-L-lysine-coated glass cover slides (as described above).
2. Add bacteria at an MOI of at least 2.
3. Centrifuge for 10 min at 512 × *g*.
4. Incubate at 37°C, 5% CO_2 for 20 min.
5. After incubation, wash attached cells twice with PBS (to remove serum which may interfere with the staining).
6. Add 150 µl of the dye components A + B (each 1.5 µl in 1 ml PBS) to each well.
7. Incubate for 15 min in the dark.
8. Wash three times with PBS to remove unbound dye.
9. Fixation with 1% paraformaldehyde for 5 min at room temperature.
10. Wash three times with PBS.
11. Embedding in 5 µl ProlongGold + Dapi.
12. Let it dry in the dark at room temperature over night. Then seal the border with clear nail gloss to avoid evaporation and drying of the samples. Keep samples at 4°C in dark (Figure 9).

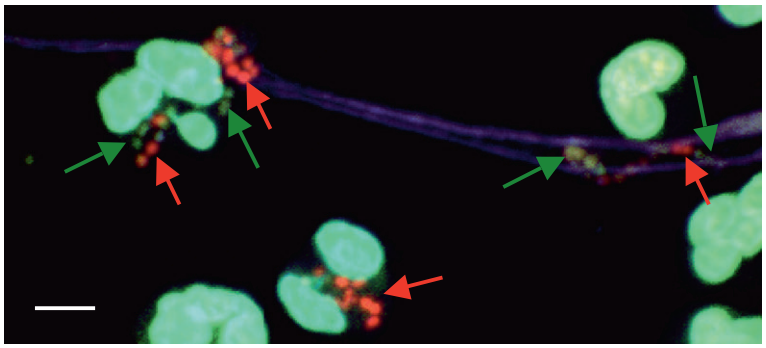

Figure 9. Representative immunofluorescence image of viable (green) versus dead (red) bacteria entrapped by NETs or phagocytosed by neutrophils. Samples were embedded in ProlongGold+Dapi to counterstain DNA and visualize ETs in blue. Mounted samples were examined using an inverted confocal laser scanning 2-photon microscope Olympus Fluoview FV1000 with Fluoview TM Spectral Scanning Technology (Olympus) and a 60×/1.42 PlanApo Olympus objective. (See color plate section).

♦♦♦♦♦♦ VI. COMMERCIAL SUPPLIERS

- BD Biosciences, 2350 Qume Drive, San Jose, CA 95131, USA
  Phone: 877-232-8995
  Fax: 410-316-4770
  Website: http://www.bdbiosciences.com/home.jsp
  E-Mail: Industrial_CS@bd.com
- Dako Denmark A/S
  Produktionsvej 42, DK-2600 Glostrup, Denmark
  Phone: +45-44-859500
  Fax: +45-44-859595
  Website: www.dako.com
  E-mail: contact@dako.com
- Electron Microscopy Science, P.O. Box 550, 1560 Industry Road, Hatfield, PA 19440, USA
  Phone: 800-523-5874
  Fax: 215-412-8450
  Website: http://www.emsdiasum.com
  E-Mail: sgkcck@aol.com
- Fisher Scientific, 2000 Park Lane Drive, Pittsburgh, PA 15275, USA
  Phone: 800-766-7000
  Fax: 800-926-1166
  Website: http://www.fishersci.com
  E-Mail: Access via Website
- Greiner Bio-One North America Inc., 4238 Capital Drive, Monroe, NC 28110, USA
  Phone: 1-800-884-4703
  Fax: 1-800-726-0052

Website: http://www.greinerbioone.com
E-Mail: info@us.gbo.com

- Invitrogen Corporation, 5791 Van Allen Way, PO Box 6482, Carlsbad, CA 92008, USA
  Phone: 760-603-7200
  Fax: 760-602-6500
  Website: http://www.invitrogen.com
  E-mail: catalog@invitrogen.com
- J.T. Baker, Mallinckrodt Baker, Inc., 222 Red School Lane, Phillipsburg, NJ 08865, USA
  Phone: 908-859-2151
  Fax: 908-859-9318
  Website: http://www.solvitcenter.com
  E-Mail: Access via Website
- MatTek Corporation, 200 Homer Avenue, Ashland, MA 01721, USA
  Phone: 800-634-9018
  Fax: 508-879-1532
  Website: http://www.mattek.com
  E-Mail: information@mattek.com
- Mediatech, Inc., 9345 Discovery Blvd., Manassas, VA 20109, USA
  Phone: 800-235-5476
  Fax: 703-471-0363
  Website: http://www.cellgro.com/shop/customer/home.php
  E-Mail: custserv@cellgro.com
- Merck & Co., One Merck Drive, P.O. Box 100, Whitehouse Station, NJ 08889, USA
  Phone: 908-423-1000
  Website: http://www.merck.com/
- Millipore, 290 Concord Road, Billerica, MA 01821, USA
  Phone: 800-645-5476
  Website: http://www.millipore.com
  E-Mail: Access via Website
- Molecular Research Center, Inc. (MRC), 5645 Montgomery Road, Cincinnati, OH 45212, USA
  Phone: 800-462-9868
  Fax: 513-841-0080
  Website: http://www.mrcgene.com/
  E-Mail: mrc@mrcgene.com
- MP-Biomedicals, 29525 Fountain Pkwy., Solon, OH 44139, USA
  Phone: 800-854-0530
  Fax: 800-334-6999
  Website: http://www.mpbio.com/
  E-Mail: Access via Website
- Pharmaco-AAPER, 58 Vale Road, Brookfield, CT 06804, USA
  Phone: 800-243-5360
  Fax: 203-740-3481
  Website: http://www.pharmco-prod.com

E-Mail: j.perez@pharmcoaaper.com
- Sigma-Aldrich, P.O. Box 14508, St. Louis, MO 63178, USA
  Phone: 800-325-3010
  Fax: 800-325-5052
  Website: http://www.sigmaaldrich.com/united-states.html
  E-Mail: OC_DOM_HC@sial.com
- Ted Pella Inc., P.O. Box 492477, Redding, CA 96049, USA
  Phone: 530-243-2200
  Fax: 530-243-3761
  Website: http://www.tedpella.com/
  Email: sales@tedpella.com
- Thermo Scientific, Thermo Fisher Scientific, 120 Bishops Way, Brookfield, WI 53008, USA
  Phone: 800-532-4752
  Website: http://www.thermo.com
  E-Mail: Access via Website

Acknowledgements

The authors wish to thank San Diego State University Electron Microscopy Facility and the UCSD Microscopy Facility (UCSD Neuroscience Microscopy Shared Facility Grant P30NS047101) for support and facilities and Steve Barlow as well as Dr. Terry Frey for their advice with electron microscopy.

This work was supported by NIH Grant AI077780 to Victor Nizet. Ohn Chow was funded in part by the UCSD Genetics Training Program (T32 GM008666). Maren von Köckritz-Blickwede was supported through a fellowship from the Deutsche Akademie der Naturforscher Leopoldina (BMBF-LPD 9901/8-187).

References

Anai, M., Haraguchi, H. and Takagi, Y. (1972). An endonuclease associated with bovine plasma albumin fraction. *J. Biol. Chem.* **247**, 199–203.

Brinkmann, V., Reichard, U., Goosmann, C., Fauler, B., Uhlemann, Y., Weiss, D. S., Weinrauch, Y. and Zychlinsky, A. (2004). Neutrophil extracellular traps kill bacteria. *Science* **303**, 1532–1535.

Dorschner, R. A., Pestonjamasp, V. K., Tamakuwala, S., Ohtake, T., Rudisill, J., Nizet, V., Agerberth, B., Gudmundsson, G. H. and Gallo, R. L. (2001). Cutaneous injury induces the release of cathelicidin anti-microbial peptides active against group A *Streptococcus*. *J. Invest. Dermatol.* **117**, 91–97.

Ermert, D., Urban, C. F., Laube, B., Goosmann, C., Zychlinsky, A. and Brinkmann, V. (2008a). Mouse neutrophil extracellular traps in microbial infections. *J. Innate Immun.* **1**, 181–193.

Ermert, D., Zychlinsky, A. and Urban, C. (2008b). Fungal and bacterial killing by neutrophils. *Methods. Mol. Biol.* **470**, 293–312.

Fuchs, T. A., Abed, U., Goosmann, C., Hurwitz, R., Schulze, I., Wahn, V., Weinrauch, Y., Brinkmann, V. and Zychlinsky, A. (2007). Novel cell death program leads to neutrophil extracellular traps. *J. Cell Biol.* **176**, 231–241.

Goldmann, O., Rohde, M., Chhatwal, G. S. and Medina, E. (2004). Role of macrophages in resistance to group A streptococci. *Infect. Immun.* **72**, 2956–2963.

Lauth, X., von Köckritz-Blickwede, M., McNamara, C. W., Myskowski, S., Zinkernagel, A. S., Beall, B., Ghosh, P., Gallo, R. L. and Nizet, V. (2008). M1 protein allows group A streptococcal survival in phagocyte extracellular traps through cathelicidin inhibition. *J. Innate Immun.* **1**, 202–214.

Losman, M. J., Fasy, T. M., Novick, K. E. and Monestier, M. (1992). Monoclonal autoantibodies to subnucleosomes from a MRLP/Mp-+/+ mouse. *J. Immunol.* **148**, 1561–1569.

Martinelli, S., Urosevic, M., Daryadel, A., Oberholzer, P. A., Baumann, C., Fey, M. F., Dummer, R., Simon, H. U. and Yousefi, S. (2004). Induction of genes mediating interferon-dependent extracellular trap formation during neutrophil differentiation. *J. Biol. Chem.* **279**, 44123–44132.

Nizet, V. (2007). Understanding how leading bacterial pathogens subvert innate immunity to reveal novel therapeutic targets. *J. Allergy Clin. Immunol.* **120**, 13–22.

Palade, G. E. (1952). The Fine Structure of Mitochondria. *Anat. Rec.* ***114***, 427–451.

Perkins, E. M. and McCaffery, J. M. (2007). Conventional and immunoelectron microscopy of mitochondria. *Methods. Mol. Biol.* **372**, 467–483.

Segal, G. M., Smith, T. D., Heinrich, M. C., Ey, F. S. and Bagby, G. C. (1992). Specific repression of granulocyte-macrophage and granulocyte colony-stimulating factor gene expression in interleukin-1-stimulated endothelial cells with antisense oligodeoxynucleotides. *Blood* **80**, 609–616.

Urban, C. F., Ermert, D., Schmid, M., Abu-Abed, U., Goosmann, C., Nacken, W., Brinkmann, V., Jungblut, P. R. and Zychlinsky, A. (2009). Neutrophil extracellular traps contain calprotectin, a cytosolic protein complex involved in host defense against candida albicans. *PLoS Pathog.* **5**, e1000639.

Urban, C. F., Reichard, U., Brinkmann, V. and Zychlinsky, A. (2006). Neutrophil extracellular traps capture and kill Candida albicans yeast and hyphal forms. *Cell. Microbiol.* **8**, 668–676.

von Köckritz-Blickwede, M., Chow, O. and Nizet, V. (2009). Fetal calf serum contains heat-stable nucleases that degrade neutrophil extracellular traps. *Blood* **114**, 5245–5246.

von Köckritz-Blickwede, M. and Nizet, V. (2009). Innate immunity turned inside-out: antimicrobial defense by phagocyte extracellular traps. *J. Mol. Med.* **87**, 775–783.

Wang, Y., Li, M., Stadler, S., Correll, S., Li, P., Wang, D., Hayama, R., Leonelli, L., Han, H., Grigoryev, S. A. *et al*. (2009). Histone hypercitrullination mediates chromatin decondensation and neutrophil extracellular trap formation. *J. Cell Biol.* **184**, 205–213.

Wartha, F. and Henriques-Normark, B. (2008). ETosis: a novel cell death pathway. *Sci. Signal.* **1**, pe25.

Yousefi, S., Gold, J. A., Andina, N., Lee, J. J., Kelly, A. M., Kozlowski, E., Schmid, I., Straumann, A., Reichenbach, J., Gleich, G. J. *et al*. (2008). Catapult-like release of mitochondrial DNA by eosinophils contributes to antibacterial defense. *Nat. Med.* **14**, 949–953.

Yousefi, S., Mihalache, C., Kozlowski, E., Schmid, I. and Simon, H. U. (2009). Viable neutrophils release mitochondrial DNA to form neutrophil extracellular traps. *Cell. Death. Differ.* **16**, 1438–1444.

von Köckritz-Blickwede, M., Goldmann, O., Thulin, P., Heinemann, K., Norrby-Teglund, A., Rohde, M. and Medina, E. (2008). Phagocytosis-independent antimicrobial activity of mast cells by means of extracellular trap formation. *Blood* **111**, 3070–3080.

8 Killer Cell Assays

Patricia Graef, Veit R Buchholz and Dirk H Busch
Institute for Medical Microbiology, Immunology, and Hygiene, Technische Universität München, Munich, Germany

CONTENTS

♦♦♦♦♦♦ I. INTRODUCTION

Cell-mediated cytotoxicity plays an important role in the host immune defence against pathogens localized within cells (Pamer, 1993). Intracellular pathogens escape antibody, complement and neutrophil-mediated defences. Infected cells must therefore be specifically identified and destroyed in order for the infection to be cleared, a role fulfilled by $CD8^+$ cytolytic T lymphocytes (CTLs). CTLs recognize epitopes presented on the cell surface by MHC class I molecules (Zinkernagel and Doherty, 1974). Pathogen-derived proteins are first degraded into small peptides (8–10 residues), which are translocated via the transporter associated with antigen processing (TAP) into the endoplasmic reticulum (ER) (Pamer and Cresswell, 1998). Peptides with sufficient affinity for the MHC class I peptide-binding groove stabilize the newly synthesized molecules, forming MHC/peptide complexes that are transported to the cell surface. $CD8^+$ CTLs detect pathogen-derived peptides presented by MHC class I molecules with their specific T-cell receptor, resulting in activation of different effector mechanisms that induce death of the infected cell.

Two major cytotoxic pathways utilized by CTLs have been described: (a) release of cytotoxins from secretory granules that directly damage the host cell membrane (perforins) leading to death by necrosis, and (b) induction of programmed cell death (apoptosis) of the target cell by secreted proteases (granzymes), interaction of tumour necrosis factor α or β (TNFα or β) with TNF-receptor 1 or direct Fas/Fas-ligand binding (Berke, 1995). The different mechanisms of CTL-induced apoptosis all culminate in the cleavage and activation of caspase 3. While TNFα/β

METHODS IN MICROBIOLOGY, VOLUME 37
0580-9517 DOI 10.1016/S0580-9517(10)37008-5

and Fas-ligand – both members of the TNF family of molecules – induce this process via ligation to transmembrane receptors, granzyme B is strongly dependent on the pore-forming action of perforin to reach and cleave its intracellular target – caspase 3 (Lieberman, 2003).

For many years our laboratory has used the murine model of *Listeria monocytogenes* infection to examine the CTL response to infection with an intracellular pathogen (Busch *et al.*, 1998, 1999). *L. monocytogenes* is a Gram-positive bacterium that survives and multiplies within the cytosol of infected cells. After phagocytosis by macrophages, *L. monocytogenes* lyses the phagolysosomal membrane by secreting listeriolysin (LLO) and enters the host cell cytosol (Bielecki *et al.*, 1990; Pamer, 2004). Immunocompetent mice infected with a sub-lethal dose of *L. monocytogenes* clear the infection within a few days and develop long-lasting protective immunity. $CD8^+$ cytotoxic lymphocytes play a major role in this rapid, extremely effective immune response (Kaufmann *et al.*, 1985).

Recently, our research has focused on analysing the functional diversification of antigen-specific CTL populations *in vivo* and *ex vivo*, and we have constantly strived to visualize this process with increasing resolution. Ultimately, these efforts merged in monitoring the fate of differentiation of single precursor cells *in vivo* (Stemberger *et al.*, 2007). Parallel to these exciting technical developments, new methods allowing to analyse T-cell function on the single cell level directly *ex vivo* or *in situ* are urgently needed.

In this chapter, we discuss the currently available methods to characterize the cytotoxic activity of CTLs. Sections II and III focus on *in vitro* and *ex vivo* detection of CTL activity. The chromium release assay (CRA), which is still the gold standard of cytotoxicity assays, is described in detail (Section II) and compared to a selection of novel assays that promise to circumvent some of the caveats of chromium release (Section III). Section IV highlights the importance and advantages of *in vivo* CTL analysis and provides a straight forward protocol for evaluating cytotoxicity *in vivo*. Although parts of our methodological descriptions employ the *L. monocytogenes* infection model, the methods described can easily be modified for the detailed study of CTL responses to other intracellular pathogens or CTL-inducing vaccination protocols.

♦♦♦♦♦♦ II. CHROMIUM RELEASE ASSAY

The standard CRA was one of the first assays established to detect and quantify CTL-mediated target cell lysis (Brunner *et al.*, 1968; refined by Ostler *et al.*, 2001) and is still widely used because of its high sensitivity and specificity. To investigate cytotoxic activity of effector cells *in vitro*, the release of radioactive ^{51}chromium (^{51}Cr) out of labelled target cells is used as indicative value proportional to target cell lysis. If cells are exposed to medium supplemented with high concentrations of $Na_2^{51}CrO_4$, most cell types efficiently take up the radioactive agent. The spontaneous release of ^{51}Cr is very low, so viable cells can be stably labelled. In order to generate target cells for CTLs, ^{51}Cr-labelled cells can be

infected with a pathogen or an antigen-expressing vector, as well as coated with antigenic peptide epitopes. Co-cultures of target cells and epitope-specific effector cells enable antigen recognition and initiation of cytotoxic activity of CTLs. The induction of cell death and damage of the cell membrane of target cells results in an increased release of ^{51}Cr into the culture medium. Consequently, the ratio of released to cell-associated ^{51}Cr is proportional to the degree of cell lysis.

A. Chromium Release Assay Using Infected Target Cells

As previously mentioned, the infection of ^{51}Cr-labelled cells with an intracellular pathogen converts such cells into target cells that can be tested for specific lysis by CTLs recognizing epitopes associated to the respective pathogen (Kaufmann *et al.*, 1986). Effector cells generated in different infection settings can be recovered *ex vivo* and assayed for cytolysis, thus providing a measure for the CTL priming capacity of a certain infection setting. Furthermore, epitope-specific T-cell clones or T-cell lines can be utilized for the characterization of epitope presentation by actively infected cells. For this assay to be interpretable the vast majority of labelled cells have to be infected and hence the range of utilizable target cell types might be limited by a narrow cell tropism of the pathogen. In the case of *L. monocytogenes,* an infection efficiency of nearly 100% can be reproducibly achieved in both primary bone marrow macrophages and tumour cell lines. When studying *Listeria*-specific CTL responses in mice of the $H2^d$ haplotype (e.g. BALB/c), the $H2^d$-expressing macrophage tumour cell line J774 (ATCC TIB 67) can be used as a convenient source of target cells (Pamer *et al.*, 1991). J774 cells are readily infected with *L. monocytogenes*, and bacteria enter the cytosol and multiply intracytoplasmatically. The J774 cell line is grown in conventional culture medium, without the addition of supplementary growth factors, resulting in nearly unlimited quantities of target cells – the homogeneity of which makes this system highly reproducible.

The following section describes a typical protocol to test *Listeria*-specific CTL lines for specific lysis of J774 cells infected with live *L. monocytogenes*.

1. Reagents and equipment

- Antibiotic-free culture medium (RP10–): 1× RPMI 1640 supplemented with L-glutamine plus 10% (v/v) FCS
- Gentamicin sulphate
- 0.5% Triton X-100
- 96-well V-bottom microtitre plates
- J774 macrophage cell line (ATCC TIB 67), cultured in RP10–
- Bacterial culture: virulent *L. monocytogenes* (e.g. ATCC 43251) grown in trypticase soy broth (TSB)
- Gamma counter
- Effector cells: *Listeria*-specific T-cell line

2. Labelling target cells with Chromium 51

J774 cells are radioactively labelled by short incubation in the presence of high concentrations of 51Cr. 51Cr has a relatively short half-life (28 days) and is less hazardous to work with than most other isotopes. Nevertheless, work with 51Cr must be performed following the appropriate radiation safety guidelines.

- Pellet 5×10^5 J774 cells (1500 rpm, 7 min, 4°C)
- Resuspend cells in 100 µl $RP10^-$
- Add 100 µCi [^{51}Cr] sodium chromate (usually equivalent to 100 µl fresh ^{51}Cr, calculate the actual activity considering a half-life of 28 days)
- Incubate for 1 h at 37°C
- Wash cells two times in 10 ml $RP10^-$
- Resuspend cells in 12.5 ml $RP10^-$ (=4×10^4 cells/ml)
- Add 100 µl (=4×10^3 cells) per well in a 96-well plate and allow macrophages to adhere for 30 min at 37°C

3. Infecting labelled cells with intracellular bacteria

^{51}Cr-labelled macrophages are infected by the direct addition of *L. monocytogenes* from a mid log-phase culture. After incubation, the medium is replaced by $RP10^-$ containing gentamicin, a membrane-impermeable antibiotic, to kill extracellular but not intracellular bacteria.

- Grow *L. monocytogenes* in TSB to early/mid log phase ($A_{600} = 0.1$); at this density, there are approximately 2×10^8 bacteria per ml present (for highest accuracy we recommend performing a calibration of A_{600}/bacterial number fit to your laboratory equipment and culture conditions)
- Add 6 µl bacteria (=1.2×10^6) to wells with ^{51}Cr-labelled J774 cells designated as infected target cells
- Add 6 µl TSB to ^{51}Cr-labelled J774 macrophages to be used as uninfected controls
- Incubate for 25 min at 37°C
- Carefully remove 80 µl of medium from each well, add 80 µl RP10– containing 10 µg/ml gentamicin

4. Assaying for specific lysis by CTLs using different effector to target ratios

To assay for specific lysis, $CD8^+$ T cells are incubated together with the prepared target cells. The more antigen-specific T cells/effector cells (E) are added to the assay, the greater the expected extent of specific target cell (T) lysis. However, high E:T ratios are often accompanied by high non-specific target cell lysis. Antigen-specific lysis is determined by comparison of the chromium release in parallel incubations of effector cells with infected and uninfected target cells. The optimal E:T ratio is difficult to predict, so it is advisable to test for specific lysis at several E:T ratios. Titration of the E:T ratio is usually achieved by changing the number of

effector cells, keeping the number of target cells constant (here 4×10^3 cells). Titration of the E:T ratio is achieved by adding different dilutions of effector cells.

- Pellet target cells and resuspend in 50 µl $RP10^-$ containing 10 µg/ml gentamicin

A typical CTL assay contains the following controls and titrations:

Spontaneous release: Infected and uninfected labelled target cells are incubated in the absence of effector cells to control for the spontaneous release of chromium.

- Add 50 µl $RP10^-$ to 4 wells each of uninfected and infected target cells

Maximum release: A detergent is added lysing all target cells in order to determine the maximum radioactivity that can be released.

- Add 50 µl 0.5% Triton X-100 to 4 wells

CTLs plus infected or uninfected target cells: CTLs added to uninfected and infected ^{51}Cr labelled target cells at various E:T ratios to determine specific and background lysis.

- Add 50 µl of effector cells (in $RP10^-$) to infected and uninfected target cells. Make several dilutions of effector cells to achieve E:T ratios of 100:1, 50:1, 25:1, 12:1, 6:1, 3:1 and 0.3:1
- The final volume in all wells should be 100 µl
- Incubate the cells for 3 h at 37°C in a 5% CO_2 incubator
- Pellet the cells in the 96-well plate by gentle centrifugation at 1500 rpm, 7 min, 4°C
- Carefully harvest 50 µl of supernatant from each well with a multichannel pipettor and count the released ^{51}Cr with a gamma counter

5. Determining % specific lysis

Specific lysis is calculated by accounting for spontaneous chromium release (sr) and maximum release (mr) using the formula:

$$\% \text{ Specific lysis} = \left[\frac{\text{counts per minute [cpm] sample} - \text{cpm sr}}{\text{cpm mr} - \text{cpm sr}} \right] \times 100$$

Lysis specifically related to the presence of the pathogen can be estimated by comparing lysis in response to infected versus uninfected target cells at the same E:T ratios. A difference of greater than 10–20% between lysis against infected and uninfected cells can be interpreted as antigen-specific lysis (Figure 1).

6. Limitations of direct CTL assays

Using target cells infected with intracellular pathogens as CTL targets has certain disadvantages that can limit the utility of these assays. For example, the pathogen will continue to multiply inside the infected target cells. Pathogens with a high intracellular growth rate might simply burst the infected cell within a relatively short time period, resulting in a rapid increase of spontaneous ^{51}Cr-release. Alternatively, some intracellular pathogens release lytic proteins that can cause high degrees of spontaneous lysis in the absence of CTL. If the spontaneous release of

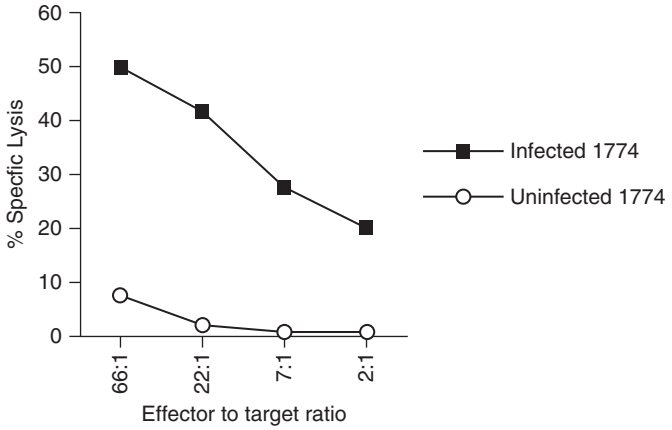

Figure 1. CTLs derived from *L. monocytogenes* immunized mice specifically lyse infected J774 cells. Spleens cells from *L. monocytogenes* immunized BALB/c mice were re-stimulated *in vitro* with infected J774 cells. Five days following *in vitro* re-stimulation, CTLs were assayed for specificity using *L. monocytogenes* infected or uninfected ^{51}Cr labelled J774 cells, as described in the text. The % specific lysis was determined 3 h after addition of different CTL numbers to 10,000 target cells.

^{51}Cr exceeds 30–40% of maximum release values, then the specific lysis values become very difficult to interpret.

Although the incubation time for CTL assays can be shortened to prevent exceedingly high spontaneous release values, there is a certain delay until specific target cell lysis is detectable; a minimum incubation time of 2–3 h is needed. Possible explanations for the delayed onset of specific lysis are that specific CTLs need time to find their target cells and to induce cell death, and that target cells may not immediately release all ^{51}Cr upon encounter with a specific CTL.

B. Chromium Release Assay Using Target Cells Coated with Peptide

Several years ago, Rammensee and colleagues (Roetzschke *et al.*, 1990) exploited the ability to acid elute and HPLC purify MHC-associated peptides from infected cells, subsequently transferring the isolated peptides to uninfected cells in an assay for antigen-specific, CTL-mediated lysis. The characterization of peptide epitopes of a huge range of antigens enables the synthesis of highly concentrated and purified peptide stocks that can be used to coat target cells for CRAs. The application of peptide epitopes, eluted from infected cells or produced synthetically, is particularly useful when the pathogen in question does not infect CRA target cells or spontaneously lyses them within the time frame of a conventional CRA (see also Section II.A.6). Even when direct CTL assays with infected cells are feasible, the alternative of peptide extraction or peptide synthesis has several advantages. For example, the sensitivity of the assay is increased when epitopes can be added in relatively high concentrations to target cells. When using peptides, it is also possible to choose target cells that further optimize sensitivity (i.e. cells with high ^{51}Cr uptake, low spontaneous release, and a high capacity to bind exogenously added peptides) and give

highly reproducible results. HPLC fractionation of antigenic epitopes allows to estimate the complexity of the CTL response, assuming that most CTL epitopes will elute in different fractions. When fractionated or synthesized peptides are loaded onto partially MHC-mismatched target cells, the MHC-restriction for individual epitopes can be determined. Finally, purified peptides can be sequenced to obtain more detailed information about the structure and origin of the epitopes. We have performed CRAs with peptide-loaded or untreated naïve syngeneic splenocytes from C57BL/6 mice to investigate CTL responses during *L. monocytogenes* infection or after vaccination (Heit *et al.*, 2007; Huster *et al.*, 2004).

1. Reagents and equipment (see also Section II.A.1)

- Complete culture medium (RP10+): 1× RPMI 1640 supplemented with 10% (v/v) FCS and 5% (v/v) SC^+
- Supplement complete (SC^+): 1 ml β-mercaptoethanol, 20 ml gentamicin, 23.83 g HEPES, 4 g L-glutamine, 200 ml penicillin/streptomycin
- Target cells: usually a tumour cell line expressing the appropriate MHC class I molecules (e.g. $H2^d$ positive mastocytoma cell line P815/ATCC TIB64)
- Peptide: synthetic listeriolysin ($LLO_{91–909}$) peptide stock [1 μg/μl in dimethyl sulfoxide (DMSO)]

  OR

  fraction from acid-eluted infected cells

2. Peptide loading of target cells

Lyophilized acid-eluted or synthesized peptides should be resuspended in DMSO to obtain a proper solubilization of hydrophobic peptides. In order to minimize DMSO addition to the assay cultures, peptide stocks are kept at high concentration (e.g. 1 μg/μl) at –20°C. To estimate proper spontaneous release rates, same amounts of DMSO have to be added to unpulsed cells. Usually peptide fractions of 100 million extracted cells are resuspended in 200 μl DMSO or PBS buffer.

Most tumour cell lines express well-characterized MHC class I molecules, and many of them are excellent candidates for chromium labelling. Thus, a wide range of possible target cells for different animal models and MHC haplotypes are available. In our system, we use the mouse mastocytoma cell line P815 (ATCC TIB 64) to test for H2-Kd-restricted epitope presentation.

For detailed information, see Section II.A

Peptide loading or target cells:

- Label P815 cells with ^{51}Cr, pellet and resuspend in $RP10^+$ containing 1 μM synthetic peptide at final concentration of 4×10^4 cells/ml
- Add 100 μl (4×10^3 cells) to wells of a 96-well plate
- Incubate at 37°C for 2 h
- Wash three times with $RP10^+$ and resuspend in 50 μl $RP10^+$

OR

- Label P815 cells with ^{51}Cr and place 4×10^3 cells (in 25 µl $RP10^+$) in wells of a 96-well plate
- Resuspend HPLC fractions in 200 µl of PBS and add 25 µl of each sample to a designated well of target cells
- Incubate for 45–60 min at 30°C

CTL assay using peptide-loaded target cells:

- Add CTLs at a constant E:T ratio in a volume of 50 µl $RP10^+$ medium per well (to determine an optimal E:T ratio, different effector cell dilutions should be tested in advance)
- Incubate plates for 4–6 h at 37°C and harvest supernatants as described

♦♦♦♦♦♦ III. ALTERNATIVES TO THE CHROMIUM RELEASE ASSAY

The CRA has long been viewed as *the* optimal assay for detection of cytotoxicity – praised for its sensitivity and simplicity. In recent years, however, the advent of improved flow cytometry-based methods has challenged this status and highlighted some disadvantages of the traditionally used assay:

First, CRA measures CTL activity in bulk cultures, without accounting for target cell death at the single cell level. Second, relatively high effector and target cell numbers are required to generate sufficient ^{51}Cr release for detection by a gamma counter. Third, effector cell characteristics apart from cytotoxicity cannot be monitored in parallel to chromium release. Fourth, during longer periods of incubation the spontaneous release of ^{51}Cr from target cells becomes problematic. And fifth, the radioactive material needed for CRA, potentially alters effector cell behaviour, requires special licensing and handling and poses a considerable health risk to the researcher.

In order to circumvent some of the limitations and hazards of the conventional CRA, other methods have been established to quantify CTL-mediated lysis of infected or peptide-pulsed target cells. In the following sections, we briefly outline some of these methods and refer the reader to appropriate references for more detailed protocols.

A. Assays for Measuring Degranulation

Activated CTLs release cytotoxins and proteases from secretory granules in order to induce death of the target cells. One of these cytolytic proteases, the enzyme serine esterase, can be detected in the culture medium upon its release from CTLs (Taffs and Sikovsky, 1994). Enzyme activity in the supernatant correlates with the extent of CTL activation in the presence of epitope-presenting target cells. The detection of serine esterases is based on hydrolysis of Na-benzyloxycarbonyl-L-lysine thiobenzyl ester, which is detected in a standard colorimetric assay using dithio-*bis*(2-nitrobenzoic acid). In this assay, the amount of enzymatically active

serine esterase released by antigen stimulation is compared to release in the absence of antigen and the maximal release obtained with a mild detergent.

A similar assay detects the enzymatic activity of granzyme B, an aspartase released from cytotoxic granules upon degranulation (McElhaney *et al.*, 1996). The enzymatic activity of granzyme B is measured using its unique substrate, *tert*-butyloxycarbonyl-Ala-Ala-Asp-thiobenzyl ester (BAADT). Cleavage of BAADT is detected in a colorimetric assay analogous to that mentioned above.

To evaluate degranulation on the single cell level two different types of ELISPOT assays detecting either the exocytosis of perforin (Zuber *et al.*, 2005) or that of granzyme B (Rininsland *et al.*, 2000) have been developed. Both utilize perforin- and granzyme B-specific monoclonal antibodies to capture and detect the substrate in question.

Monoclonal antibodies for direct intracellular staining and flow cytometric evaluation (Pala *et al.*, 2000) of perforin and granzyme B are available from many providers and have become standard tools for determining cytotoxic capacity. Since intracellular staining is intrinsically limited to the time point before degranulation, these assays are not capable to determine the true cytotoxic activity of CTLs.

A flow cytometric assay detecting the presence of CD107a (LAMP-1) or CD107b (LAMP-2) on the CTL's surface has solved this dilemma (Betts *et al.*, 2003). Both molecules are present in the cytotoxic granular membrane and are thought to prevent content leakage. Upon degranulation they are exposed on the CTL's plasma membrane and become accessible to detection via fluorochrome-conjugated monoclonal antibody. The assay requires CTLs to be exposed to their cognate antigen in a brief *in vitro* re-stimulation period of 5–6 h. Exposure of CD107a and b during this period is highly dynamic and is followed by rapid re-internalization and re-transfer to the acidic lysosomal compartment. To allow efficient antibody labelling of CD107a and b despite their only transient accessibility, the presence of target-specific monoclonal antibody is required throughout the course of re-stimulation. Additionally, cultures have to be supplemented with monensin, an agent that inhibits acidification of lysosomes and thus ensures the stability of pH sensitive fluorochromes after antibody binding and shuttling to lysosomes.

Most of the assays mentioned above generate an estimate of cytotoxicity similar to that provided by CRA. However, none of them measures target cell lysis and death directly.

B. Assays for Measuring Target Cell Death

In recent years two main fluorometric, non-radioactive approaches were developed to measure target cell lysis or death. The first is constructed in analogy to the principle of chromium release and utilizes labelling agents retained within live but released from dead or dying cells. The second follows the inverse principle of selectively labelling dead cells. Some assays combine the two approaches.

A very simple assay adhering to the first approach utilizes an intrinsic labelling agent, namely the enzyme lactate dehydrogenase (LDH), which is present in all

mammalian cells (Korzeniewski and Callewaert, 1983; Weidmann *et al.*, 1995). Release of LDH from dead cells into the supernatant is detected via a colorimetric reaction. While being inexpensive and simple, this assay holds substantial disadvantage due to the background noise created by LDH release from CTLs, the restriction to bulk analysis and the impossibility to simultaneously acquire additional parameters of CTL function.

An assay that provides target cells with a unique label detects its lysis-dependent release on the single cell level and allows for detection of at least one more component of CTL function is the Lysispot assay (Snyder *et al.*, 2003). Here, a herpes simplex amplicon vector is used to express *Escherichia coli* β-galactosidase in mouse or human target cells. The release of β-galactosidase from killed target cells is then detected via ELISPOT. The additional combination with a cytokine ELISPOT – in a 'one well two-colour assay' – is able to yield unique one to one information on the relation of cytotoxicity and cytokine secretion activity of CTLs. Using such a two-colour Lysispot, the developers of this assay were able to confirm the separate regulation of IFNγ secretion and cytotoxicity.

A flow cytometry-based killing assay is the so-called FATAL (fluorometric assessment of T lymphocyte antigen-specific lysis) assay (Sheehy *et al.*, 2001). Here, target cells are labelled with PKH26 and 5- (and 6-) carboxyfluorescein diacetate succinimidyl ester (CFSE). PKH-26 is a lipid associating dye that stably labels cell membranes of live *and* dead cells. CFSE is an uncharged fluorescent dye, taken up by living cells and enzymatically cleaved to produce its charged membrane impermeable form. When membrane integrity of target cells is compromised, PKH-26 staining remains intact while CFSE staining is lost. Percent of antigen-specific cytotoxicity can then be calculated by comparing CFSE loss from antigen-pulsed versus unpulsed target cells.

Another assay, proposed by Lecoeur *et al.*, uses CFSE to stain CTLs and relies solely on 7-aminoactinomycin D (7-AAD), an intercalating dye, in conjunction with measurements of cell size and granularity, to flow cytometrically define target cell death (Lecoeur *et al.*, 2001). The absence of a specific target cell label makes the assay's ability of discriminating dead target cells from dead CTLs questionable. Especially if one takes into account that upon disruption of membrane integrity CTLs will lose their CFSE staining and acquire positivity for 7-AAD, thus becoming indistinguishable from dead target cells.

This problem is resolved by the fluorolysis assay, an assay using peptide-pulsed target cell lines stably transfected with a plasmid expressing the enhanced green fluorescent protein (EGFP) gene (Kienzle *et al.*, 2002). The degree of target cell death is measured here by staining with another intercalating dye, propidium iodide (PI), and flow cytometrically counting the percentage of viable PI^- $EGFP^+$ cells. By simultaneously measuring the loss of one fluorescent intracellular label and the acquisition of another, this assay is the first to utilize both approaches of death detection. By using a constitutively expressed fluorescent label, this assay also circumvents the problem of unspecific label leakage during prolonged incubation times, which both the CRA and the CFSE release assays face. Due to the high sensitivity and precision of the flow cytometry-based death detection used in this assay, the number of target cells needed for cytotoxicity detection could be lowered to as few as 200–800 cells. Thus, creating high effector to target cell ratios with

fewer antigen-specific CTLs. This aspect in combination with the possibility of prolonging incubation times to up to 2 days lets the fluorolysis assay reach sensitivities that are up to 30-fold higher than those of the traditional CRA. In fact, the presence of as few as 25 antigen-specific CTLs can be detected. However, a major restriction of the fluorolysis assay is the use of a transfected cell line for providing labelled target cells. The feasibility of stable EGFP transfection for various primary target cell types remains in question and poses a limitation to a broader applicability of this assay.

The Live Count assay takes a similar approach as described by Lecoeur *et al.* but focuses on *surviving* target cells, improves on target detection as well as antigen specificity and provides a novel measure of *specific cytolytic activity* by simultaneously taking into account degranulation of CTLs and death of target cells (Devêvre *et al.*, 2006). For the Live Count assay, specific and irrelevant target cells are labelled with different concentrations of CMTMR, a fluorescent chloromethyl derivate that freely enters through the membrane of living cells and reacts with intracellular components hindering its release through an intact plasma membrane. After co-incubation with antigen-specific CTLs staining with 4′-6-diamidino-2-phenylindole (DAPI), a dye selectively labelling dead cells, is performed and $DAPI^+$ cells are excluded from analysis. $DAPI^-$ $CMTMR^{high}$ and $DAPI^-$ $CMTMR^{low}$ cells can easily be distinguished via flow cytometry creating an internal control for specific overall lysis by comparing the number of surviving specific ($DAPI^-$ $CMTMR^{high}$) to irrelevant ($DAPI^-$ $CMTMR^{low}$) target cells. The additional staining for CD107a as a parameter for degranulation provides a novel measure of *specific cytolytic activity* when related to overall specific lysis determined by $CMTMR^{high}$/$CMTMR^{low}$ cell counts. The strengths of the Live count assay, besides introducing a novel parameter, are the sufficiency of extremely low target cell numbers of as few as 125 cells for performing the assay and the almost unrestricted choice of possible target and control cell types for labelling with CMTMR.

The VITAL assay, as indicated by its name, also focuses on enumeration of remaining live cells (Hermans *et al.*, 2004). Here, no additional agent for labelling dead cells is used and the measure for target cell death is reduced to loss of the intracellular dyes CMTMR and CFSE. As in the Live Count assay, different concentrations of theses dyes are used to label specific and irrelevant target cells. Specific lysis is calculated as the number of live specific target cells versus live irrelevant targets. This approach is derived from experiences with flow cytometry-based *in vivo* cytotoxicity assays, highlighted in Section III of this chapter, and is itself applicable to *in vitro, ex vivo* and *in vivo* settings. The major novelty of the VITAL assay is its ability to measure specific cytolysis against multiple antigenically distinct target populations. This is made possible by an elegant combination of different labelling concentrations and varying combinations of the two dyes CMTMR and CFSE for labelling target cells. One concentration of CMTMR and three of CFSE used in conjunction to label one type of target cell (e.g. mouse splenocytes) unfold a matrix that enables the simultaneous monitoring of specific cytolysis of six distinctly labelled and one irrelevant or control target population. While the amount of target and effector cells needed clearly exceeds that employed in the fluorolysis or Live Count assay, the option of multiple specific assays in one well and the transferability to *in vivo* settings makes this assay a valuable experimental tool.

While all the assays mentioned above have added their share of experimental advances for measuring the cytolytic action of CTLs, the visualization of this process in real time has been realized most convincingly by the Flow Cytometry Caspase assay: Using cell-permeable fluorogenic substrates of various caspases, Lui *et al.* establish an assay that allows enumeration of specific versus non-specific target cell apoptosis using flow cytometry or imaging techniques. Cytotoxic activity of CTLs is accompanied by apoptosis induction and activation of caspase cascades in the early phases of CTL-mediated killing. Target cells can be loaded with a fluorescent caspase substrate, usually peptides containing caspase cleavage sites linked to fluorophores. The uncleaved fluorophores form 'silent' dimers. Due to the activation of caspase enzymes, the 'silent' substrates are cleaved and start to emit fluorescence [(Liu *et al.*, 2002; reviewed by Chahroudi *et al.* (2003)].

A high-throughput assay for determining CTL-mediated cytotoxicity against a multitude of different antigenic targets is demonstrated in a proof of principle report by Rong *et al.* (2007). Here, reverse transfection microarray technology is used to allow individual cDNA and thus antigen expression at defined locations in a cell monolayer. CTL-mediated target cell death is then visualized by staining with a fluorochrome-labelled inhibitor of active caspases (FLICA) that specifically binds active caspases within target cells. The position of fluorescence emission on the microarray is then traced back to a specific cDNA and the antigen encoded by it. This technique holds potential for rapidly defining useful target antigens for immunotherapy and cancer vaccines.

♦♦♦♦♦♦ IV. *IN VIVO* CYTOTOXICITY ASSAY

The previous section discussed CRA as an *in vitro* cytotoxicity assay that reflects effector cell presence within cultured leukocyte populations or *ex vivo* taken cell specimens. However, the evaluation of CTL responses by CRA is limited by its semi-quantitative read-out. Furthermore, the specific lysis of target cells *in vitro* is difficult to compare to conditions *in vivo*. CRA uses co-cultures of effector and target cells that have to be available as cell lines or have to be purified *ex vivo*. But the number of effector cells that can be recovered *ex vivo* might be limited, especially at time points other then the peak of antigen-driven expansion. Additionally, the need for *in vitro* re-stimulation hinders the distinction of effector cells with immediate cytolytic activity, memory cells that re-acquire effector functions or even naive T cells that may become activated during culture. Therefore, visualization of antigen-specific cytotoxic activity directly *in vivo* is required to make correct estimates about the size, functional activity and kinetics of CTL responses. The fluorescent labelling of target cells such as peptide-loaded splenocytes followed by adoptive transfer into mice harbouring peptide-specific CD8 T cells provides a tool to test for target cell lysis *in vivo* [(Aichele *et al.*, 1997; Barchet *et al.*, 2000; Coles *et al.*, 2002; Hermans *et al.*, 2004; Oehen *et al.*, 1997; Oehen and Brduscha-Riem, 1998; reviewed by Ingulli (2007)]. The transferred cells migrate spontaneously to the draining lymph nodes and

persist for several days. In the presence of effector cells, splenocytes loaded with specific antigen indeed serve as target cells and disappear rapidly from the draining LNs with kinetics that parallel the known kinetics of CD8 T cell differentiation up to the point of acquisition of effector function (Hermans *et al.*, 2000; Coles *et al.*, 2002). The disappearance of labelled target cells is proportional to the extent of CTL responses in individual recipients (Oehen and Brduscha-Riem, 1998; Ritchie *et al.*, 2009). In order to study CTL responses against pathogens without known peptide epitopes or against complex antigens, splenocytes out of acutely infected or immunized mice can be labelled and used as target cells (Aichele *et al.*, 1997).

A. *In Vivo* Cytotoxicity Assay Using Peptide-Pulsed Splenocytes as Target Cells

Splenocytes can easily be isolated out of naïve MHC-matched or -mismatched mice. For the use as target cells for *in vivo* cytotoxicity assays such cell suspensions are loaded with synthetic peptide antigen and labelled by carboxyfluorescein succinimidyl ester (CFSE), a fluorescent dye also used for proliferation assays. In case of *L. monocytogenes* immune responses, the immunodominant listeriolysin O (LLO) peptide 91-99 is recognized by MHC class 1 molecules of the H-2^d background of BALB/c mice. Furthermore, genetically engineered strains of *L. monocytogenes* expressing model antigens are available, for example *L. monocytogenes-OVA* expressing Ovalbumin (*L.m.-OVA*) (Shen *et al.*, 1995).

SIINFEKL is a well-characterized epitope of Ovalbumin ($OVA_{257–264}$) presented on MHC class I molecules of the H-2^b haplotype of C57BL/6 mice for which multimer staining and TCR-transgenic mouse lines are established. For the example shown, we used splenocytes that were either pulsed with SIINFEKL or left unpulsed, mixed at a 1:1 ratio and subsequently transferred into *L.m.-OVA* infected mice or mice that had received vaccination with *Modified Vaccinia Virus Ankara* expressing Ovalbumin (*MVA-OVA*) or Ovalbumin plus adjuvant (Hamm *et al.*, 2007; Heit *et al.*, 2007; Huster *et al.*, 2009). For several infection systems transgenic pathogen strains are available that express model antigens.

1. Reagents and equipment

- Complete culture medium (RP10+): 1× RPMI 1640 supplemented with 10% (v/v) FCS and 5% (v/v) SC^+
- Supplement complete (SC^+): 1 ml β-mercaptoethanol, 20 ml gentamicin, 23.83 g HEPES, 4 g L-glutamine, 200 ml penicillin/streptomycin
- Target cells: naïve C57BL/6 (syngeneic) and BALB/c splenocytes (allogeneic)
- Cell strainer (70 µm)
- Ammonium chloride-Tris (ACT): 0.17 M NH_4Cl, 0.3 M Tris–HCl pH 7.5
- Peptide: synthetic SIINFEKL ($OVA_{257–264}$) peptide stock (1 µg/µl in DMSO)
- PBS buffer
- CFSE
- Recipient mice: 5×10^3 cfu *L. monocytogenes-OVA* infected C57BL/6 mice, day 12 and naïve C57BL/6 mice

2. Preparation and peptide loading of splenocytes for *in vivo* cytotoxicity assay

Spleens are isolated out of naïve mice from the same or different MHC haplotype compared to the recipient. Spleens are homogenized to single cell suspensions and loaded with synthetic SIINFEKL peptide by short-term incubation in medium containing the peptide.

- Remove spleen and strain through cell strainer in 5 ml $RP10^+$ in a culture plate
- Rinse cell strainer and culture plate with the cell suspension
- Rinse cell strainer and culture plate with fresh 5 ml $RP10^+$ and pool medium
- Harvest and pellet splenocytes (1500 rpm, 7 min, 4°C)
- Resuspend in 5 ml ACT and incubate at room temperature for 5 min to lyse erythrocytes
- Stop erythrocyte lysis by adding 5 ml ice-cold $RP10^+$
- Pellet splenocytes (1500 rpm, 7 min, 4°C) and wash in two times in 10 ml PBS buffer
- Resuspend at 1×10^6 cells/ml in $RP10^+$ containing 1 μM SIINFEKL
- Incubate at 37°C for 30 min
- Wash three times with $RP10^+$

3. CFSE-labelling of target cells

Covalent binding to intracellular molecules via its succinimidyl group causes the strong and stable fluorescent labelling of cells by CFSE. Consequently, cytotoxic side effects of CFSE labelling may arise at higher staining concentrations and/or longer incubation times. Therefore, CFSE staining is performed with relatively low concentrations in short-term incubation.

- Pellet target cells (1500 rpm, 7 min, 4°C) and resuspend at 5×10^6 cells/ml in PBS containing 0.5 μM (low fluorescence intensity) or 5 μM (high fluorescence intensity) CFSE
- Incubate at 37°C for 10 min
- Wash one time in 5 vol ice-cold PBS
- Wash two times in 5 vol $RP10^+$

4. Adoptive transfer of labelled target cells

In vivo cytotoxicity can be compared between mice that received different treatments, for example varying infection dose or vaccination strategies. Administration of labelled target cells into chosen recipients may either be systemically by intravenous (i.v.) injection or locally, for example, by subcutaneous (s.c.) or intranasal (i.n.) injection.

- Pellet target cells (1500 rpm, 7 min, 4°C), wash three times in PBS and resuspend 1×10^6 cells in 200 μl PBS for i.v. injection or 50 μl PBS for s.c. or i.n. injection
- Injection into recipients

5. Assaying for specific lysis using adoptive co-transfer of peptide-loaded and untreated splenocytes

To make estimates about the extent of specific lysis of transferred target cells, the *ex vivo* recovery of peptide-loaded splenocytes has to be compared to that of untreated splenocytes. Due to variations in transfer and recovery efficiency, adoptive transfer of peptide-loaded and untreated splenocytes into individual recipients has several difficulties. For the same reasons the comparison of different routes of administration is hindered. Adoptive co-transfer of peptide-loaded and untreated splenocytes can overcome those problems and allow to accurately evaluate the disappearance of target cells, irrespective of varying injection sites, transferred number of cells and other parameters. Labelling with different amounts of CFSE enables the distinction of both populations by FACS analysis.

A typical *in vivo* cytotoxicity assay contains the following mixtures of target cells and controls:

Peptide-loaded (see Section IV.A.2) and untreated splenocytes are labelled with different amounts of CFSE (see Section IV.A.3) and mixed at a 1:1 ratio in the final volume for administration.

- Pellet labelled target cells (1500 rpm, 7 min, 4°C), wash three times in PBS and resuspend 1×10^6 peptide-loaded (high fluorescence intensity) and 1×10^6 untreated (low fluorescence intensity) splenocytes at a 1:1 ratio in a final volume of 200 µl for i.v. injection or 50 µl for s.c. or i.n. injection

The mix of peptide-loaded and untreated splenocytes is injected into recipient mice. At different time points or over a time frame after adoptive transfer, blood, draining LNs and other organs can be analysed by FACS. Data are expressed as the mean percentage of CFSE high and CFSE low cells found for each experimental group. CTL-mediated elimination of antigen-loaded splenocytes is expressed as a ratio of target cells loaded with antigen (high fluorescence intensity) over splenocytes without antigen (low fluorescence intensity). The time point for analysis has to be chosen depending on the immune status of mice. In settings where CTL frequencies are high, cytotoxicity is often visible in peripheral blood specimens or draining LNs as early as 20 h after adoptive transfer. In contrast, analysis in situations where CTL frequencies are expected to be relatively low should be delayed until 48–72 h after adoptive transfer (Hermans *et al.*, 2000).

6. Determining % specific lysis

The adoptive co-transfer of peptide-loaded and untreated splenocytes into naïve mice enables the comparison of transfer and recovery efficiency evaluation to the survival of the two target cell populations. Out of naïve mice equal proportions of both target cell populations can be recovered and thus the ratio of the differently fluorescent-labelled cells is constant at about 1 (unprimed). Adoptive co-transfer into mice harbouring peptide-specific effector cells is accompanied by a selective elimination of peptide-loaded target cells and a recovery of untreated splenocytes comparable to control naïve mice. Consequently, the ratio of the differently fluorescent-labelled cells approximates 0 (primed). Comparable numbers of recovered untreated splenocytes out of naïve or antigen-experienced mice ensure that the loss

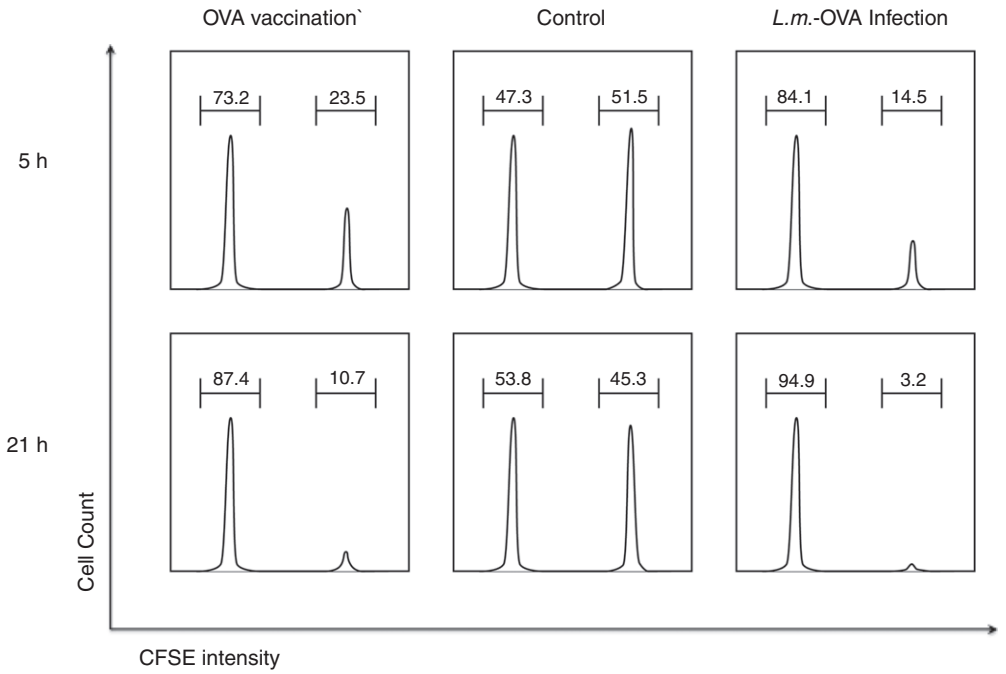

Figure 2. Schematic representation: Antigen-specific elimination of peptide-loaded splenocytes in OVA-immunized and *L.m.-OVA*-primed mice. Splenocytes were loaded with SIINFEKL peptide ($OVA_{257–264}$) or left untreated and labelled with high or low concentrations of CFSE, respectively. This resulted in two cell populations of different CFSE intensities. Splenocytes were mixed 1:1 and 2×10^6 cells were transferred intravenously into the differently primed mice that had received treatment 7 days before or into control mice (as indicated on top of the histogram panels). Cytotoxic activity was detected 5 h (top row) and 21 h (bottom row) after adoptive co-transfer by flow cytometry.

of target cells in infected animals is not due to pathogen-induced cytopathy or dilution of splenocyte numbers by inflammation-driven leukocyte influx.

To calculate % specific lysis, the following formula is used (Figure 2):

$$\text{Ratio} = \frac{\text{Mean percentage of CFSE high}}{\text{Mean percentage of CFSE low}}$$

$$\%\ \text{Specific lysis} = \left[1 - \frac{\text{ratio primed}}{\text{ratio unprimed}}\right] \times 100$$

7. Limitations of *in vivo* cytotoxicity assays

Analyses like the shown example for the use of *in vivo* cytotoxicity assays have the limitation that they are restricted to antigens characterized in form of peptide epitopes. But the vast majority of antigens are of complex nature and until now not well characterized. The phagocytic and pinocytic activities of

macrophages and dendritic cells may enable the uptake and presentation of complex antigens and thereby allow this method to evaluate cytotoxic activities against a huge range of antigens. Additionally, antigen-presenting cells may be loaded with antigen by different methods like viral transfection or uptake of RNA. Furthermore, whole splenocyte populations out of acutely infected or immunized mice can be labelled and used as target cells compared to control splenocyte preparations out of naïve mice or mice that were immunized with an unrelated antigen or infected with a different pathogen (Aichele *et al.*, 1997, see Section IV.B). A problematic issue is the possibility to induce primary immune responses by administration of peptide-loaded antigen-presenting cells (Hermans *et al.*, 1997, 1999). Therefore, the time point of analysis is critical to be able to neglect such *de novo* responses, as they are usually not observable within the first 3 days after immunization. Due to the high precursor frequency of CTL in models using adoptive transfer of TCR-transgenic T cells, the time frame for analysis may have to be shortened to 42 h after immunization (Hermans *et al.*, 2000). The risk of inducing *de novo* responses can be minimized by assaying for target depletion at earlier time points (24–36 h post-infection) sufficient for target cells to reach draining LNs but not for naïve T cells to acquire effector function. Another problem is active migration of target cells during the assay. To ensure the accurate measurement of effector cells in the organs investigated, the time frame for the assay can further be shortened to about 4 h (Coles *et al.*, 2002). However, the calculation of percent specific lysis in this short-term kill assay is a semi-quantitative read-out. That makes is difficult to compare efficiencies of CTL responses to different agents. There have been attempts to calculate death rates or half-life times of target cells out of *in vivo* cytotoxicity assay data, even the number of target cells killed on average by one CD8 T cell per day can be estimated (Barchet *et al.*, 2000; Regoes *et al.*, 2007; Yates *et al.*, 2007; Ganusov and de Boer, 2008), but the meaning of these results has to be regarded with caution because of their complex nature.

B. *In Vivo* Cytotoxicity Assay Using Splenocytes of Antigen-Experienced Mice as Target Cells

As mentioned above, the complex nature of most antigens limits an extensive characterization of all MHC class I-presented peptide epitopes. Additionally, for certain studies it is less important to evaluate single epitope-specific CTL responses than bulk CTL responses induced by a certain pathogen or vaccination strategy. For that reasons the application of whole splenocyte populations out of infected or immunized mice as target cells for the *in vivo* cytotoxicity assay might be an interesting alternative to the use of peptide-loaded splenocytes (Aichele *et al.*, 1997). A corresponding protocol is provided below.

1. Reagents and equipment (see also Section IV.A.1)

- Splenocytes donors: 2×10^6 cfu *L. monocytogenes-OVA* infected C57BL/6 mice, day 2 and naïve C57BL/6 mice

2. Preparation of splenocytes for *in vivo* cytotoxicity assay

Depending on the treatment that mice received the time point for spleen removal for optimal antigen presentation may vary. For infections with very high *L. monocytogenes* dose best epitope presentation is achieved 48 h post-infection.

For detailed information see Section IV.A

- Spleen is removed, single cell suspension is prepared and erythrocyte lysis follows
- Stop erythrocyte lysis by adding 5 ml ice-cold $RP10^+$
- Pellet splenocytes (1500 rpm, 7 min, 4°C) and wash two times in 10 ml PBS
- Pellet splenocytes (1500 rpm, 7 min, 4°C) and resuspend at 2×10^7 cells/ml
- Label antigen-experienced splenocytes with CFSE high and splenocytes out of naïve mice with CFSE low
- Transfer CFSE high and low splenocytes into recipients

The evaluation of % specific lysis is analogous to Section IV.A.6.

References

Aichele, P., Brduscha-Riem, K., Oehen, S., Odermatt, B., Zinkelnagel, R. M., Hengartner, H. and Pircher, H. (1997). Peptide antigen treatment of naive and virus-immune mice: antigen-specific tolerance versus immunopathology. *Immunity* **6**(5), 519–529.

Barchet, W., Oehen, S., Klenerman, P., Wodarz, D., Bocharov, G., Lloyd, A. L., Nowak, M. A., Hengartner, H., Zinkernagel, R. M. and Ehl, S. (2000). Direct quantitation of rapid elimination of viral antigen-positive lymphocytes by antiviral CD8(+) T cells *in vivo*. *Eur. J. Immunol.* **30**, 1356–1363.

Berke, G. (1995). The CTL's kiss of death. *Cell* **81**, 9–12.

Betts, M. R., Brenchley, J. M., Price, D. A., De Rosa, S. C., Douek, D. C., Roederer, M. and Koup, R. A. (2003). Sensitive and viable identification of antigen-specific CD8+ T cells by a flow cytometric assay for degranulation. *J. Immunol. Methods* **281**, 65–78.

Bielecki, J., Youngman, P., Connelly, P. and Portnoy, D. A. (1990). Bacillus subtilis expressing a haemolysin gene from *Listeria monocytogenes* can grow in mammalian cells. *Nature* **345**, 175–6.

Brunner, K. T., Mauel, J., Cerottini, J.-C. and Chapuis, B. (1968). Quantitative assay of the lytic action of immune lymphoid cells on 51Cr labeled allogeneic target cells *in vitro*: inhibition by isoantibody and by drugs. *Immunology* **14**, 181–196.

Busch, D. H., Kerksiek, K. M. and Pamer, E. G. (1999). Processing of *Listeria monocytogenes* antigens and the *in vivo* T-cell response to bacterial infection. *Immunol. Rev.* **172**, 163–169.

Busch, D. H., Pilip, I. M., Vijh, S. and Pamer, E. G. (1998). Coordinate regulation of complex T cell populations responding to bacterial infection. *Immunity* **8**, 353–362.

Chahroudi, A., Silvestri, G. and Feinberg, M. B. (2003). Measuring T cell-mediated cytotoxicity using fluorogenic caspase substrates. *Methods* **31**(2), 120–126.

Coles, R. M., Mueller, S. N., Heath, W. R., Carbone, F. R. and Brooks, A. G. (2002). Progression of armed CTL from draining lymph node to spleen shortly after localized infection with herpes simplex virus 1. *J. Immunol.* **168**(2), 834–838.

Devêvre, E., Romero, P. and Mahnke, Y. D. (2006). LiveCount Assay: concomitant measurement of cytolytic activity and phenotypic characterisation of CD8(+) T-cells by flow cytometry. *J. Immunol. Methods* **311**, 31–46.

Ganusov, V. V. and de Boer, R. J. (2008). Estimating *in vivo* death rates of targets due to CD8 T-cell-mediated killing. *J Virol.* **82**(23), 11749–11757.

Hamm, S., Heit, A., Koffler, M., Huster, K. M., Akira, S., Busch, D. H., Wagner, H. and Bauer, S. (2007). Immunostimulatory RNA is a potent inducer of antigen-specific cytotoxic and humoral immune response *in vivo*. *Int. Immunol.* **19**(3), 297–330.

Heit, A., Schmitz, F., Haas, T., Busch, D. H. and Wagner, H. (2007). Antigen co-encapsulated with adjuvants efficiently drive protective T cell immunity. *Eur. J. Immunol.* **37**(8), 2063–2074.

Hermans, I. F., Daish, A., Moroni-Rawson, P. and Ronchese, F. (1997). Tumor-peptide-pulsed dendritic cells isolated from spleen or cultured *in vitro* from bone marrow precursors can provide protection against tumor challenge. *Cancer Immunol. Immunother.* **44**, 341.

Hermans, I. F., Ritchie, D. S., Daish, A., Yang, J., Kehry, M. R. and Ronchese, F. (1999). Impaired ability of MHC class $II^{-/-}$ dendritic cells to provide tumor protection is rescued by CD40 ligation. *J. Immunol.* **163**, 77.

Hermans, I. F., Ritchie, D. S., Yang, J., Roberts, J. M. and Ronchese, F. (2000). CD8+ T cell-dependent elimination of dendritic cells *in vivo* limits the induction of antitumor immunity. *J. Immunol.* **164**, 3095.

Hermans, I., Silk, J., Yang, J., Palmowski, M., Gileadi, U., McCarthy, C., Salio, M., Ronchese, F. and Cerundolo, V. (2004). The VITAL assay: a versatile fluorometric technique for assessing CTL and NKT-mediated cytotoxicity against multiple targets *in vitro* and *in vivo*. *J. Immunol. Methods* **285**, 25–40.

Huster, K. M., Busch, V., Schiemann, M., Linkemann, K., Kerksiek, K. M., Wagner, H. and Busch, D. H. (2004). Selective expression of IL-7 receptor on memory T cells identifies early CD40L-dependent generation of distinct CD8+ memory T cell subsets. *Proc. Natl. Acad. Sci. U.S.A.* **101**, 5610–5615.

Huster, K. M., Stemberger, C., Gasteiger, G., Kastenmüller, W., Drexler, I. and Busch, D. H. (2009). Cutting edge: memory CD8 T cell compartment grows in size with immunological experience but nevertheless can lose function. *J. Immunol.* **183**(11**)**, 6898–6902.

Ingulli, E. (2007). Tracing tolerance and immunity *in vivo* by CFSE-labeling of administered cells. *Methods Mol. Biol.* **380**, 365–376.

Kaufmann, S., Hug, E. and De Libero, G. (1986). *Listeria monocytogenes*-reactive T lymphocyte clones with cytolytic activity against infected target cells. *J. Exp. Med.* **164**, 363–368.

Kaufmann, S. H., Hug, E., Vaeth, U. and Mueller, I. (1985). Effective protection against *Listeria monocytogenes* and delayed-type hypersensitivity to listerial antigens depend on cooperation between specific L3T4+ and Lyt-2+ T-cells. *Infect. Immun.* **48**, 273–278.

Kienzle, N., Olver, S., Buttigieg, K. and Kelso, A. (2002). The fluorolysis assay, a highly sensitive method for measuring the cytolytic activity of T cells at very low numbers. *J. Immunol. Methods* **267**, 99–108.

Korzeniewski, C. and Callewaert, D. M. (1983). An enzyme-release assay for natural cytotoxicity. *Immunol. Methods* **64**(3), 313–320.

Lecoeur, H., Fevrier, M., Garcia, S., Riviere, Y. and Gougeon, M. L. (2001). A novel flow cytometric assay for quantitation and multi-parametric characterization of cell-mediated cytotoxicity. *J. Immunol. Methods* **253**, 177–187.

Lieberman, J. (2003). The ABCs of granule-mediated cytotoxicity: new weapons in the arsenal. *Nat. Rev. Immunol.* **3**, 361–370.

Liu, L., Chahroudi, A., Silvestri, G., Wernett, M. E., Kaiser, W. J., Safrit, J. T., Komoriya, A., Altman, J. D., Packard, B. Z. and Feinberg, M. B. (2002). Visualization and quantification of T cell-mediated cytotoxicity using cell-permeable fluorogenic caspase substrates. *Nat. Med.* **8**, 185–189.

McElhaney, J. E., Pinkoski, M. J., Upshaw, C. M. and Bleackley, R. C. (1996). The cell-mediated cytotoxic response to influenza vaccination using an assay for granzyme B activity. *J. Immunol. Methods* **190**, 11–20.

Oehen, S. and Brduscha-Riem, K. (1998). Differentiation of naive CTL to effector and memory CTL: correlation of effector function with phenotype and cell division. *J. Immunol.* **161**(10), 5338–5346.
Oehen, S., Brduscha-Riem, K., Oxenius, A. and Odermatt, B. (1997). A simple method for evaluating the rejection of grafted spleen cells by flow cytometry and tracing adoptively transferred cells by light microscopy. *J. Immunol. Methods* **207**, 33–42.
Ostler, T., Schamel, K., Hussell, T., Openshaw, P., Hausmann, J. and Ehl, S. (2001). An improved protocol for measuring cytotoxic T cell activity in anatomic compartments with low cell numbers. *J. Immunol. Methods* **257**, 155–161.
Pala, P., Hussell, T. and Openshaw, P. J. (2000). Flow cytometric measurement of intracellular cytokines. *J. Immunol. Methods* **243**, 107–124.
Pamer, E. G. (1993). Cellular immunity to intracellular bacteria. *Curr. Opin. Immunol.* **5**, 492–496.
Pamer, E. (2004). Immune responses to Listeria monocytogenes. *Nat. Rev. Immunol.* **4**, 812–822.
Pamer, E. G. and Cresswell, P. (1998). Mechanisms of MHC class I–restricted antigen processing. *Annu. Rev. Immunol.* **16**, 323–358.
Pamer, E. G., Harty, J. T. and Bevan, M. (1991). Precise prediction of dominant class I MHC-restricted epitope of *Listeria monocytogenes*. *Nature* **353**, 853–855.
Regoes, R., Barber, D., Ahmed, R. and Antia, R. (2007). Estimation of the rate of killing by cytotoxic T lymphocytes *in vivo*. *Proc. Natl. Acad. Sci. U.S.A.* **104**, 1599–1603.
Rininsland, F. H., Helms, T., Asaad, R. J., Boehm, B. O. and Tary-Lehmann, M. (2000). Granzyme B ELISPOT assay for ex vivo measurements of T cell immunity. *J. Immunol. Methods* **240**, 143–155.
Ritchie, D. S., Hermans, I. F., Lumsden, J. M., Scanga, C. B., Roberts, J. M., Yang, J., Kemp, R. A. and Ronchese, F. (2009). Dendritic cell elimination as an assay of cytotoxic T lymphocyte activity *in vivo*. *J. Immunol. Methods* **246**(1–2), 109–117.
Roetzschke, O., Falk, K., Deres, K., Schild, H., Norda, M., Metzger, J., Jung, G. and Rammensee, H. G. (1990). Isolation and analysis of naturally processed viral peptides as recognized by cytotoxic T cells. *Nature* **348**, 252–254.
Rong, J., Chris Bleackley, R. and Kane, K. P. (2007). Direct detection of cytolytic T lymphocyte-mediated cytotoxicity on antigen-transfected cell microarray. *J. Immunol. Methods* **326**, 1–9.
Sheehy, M. E., McDermott, A. B., Furlan, S. N., Klenerman, P. and Nixon, D. F. (2001). A novel technique for the fluorometric assessment of T lymphocyte antigen specific lysis. *J. Immunol. Methods* **249**, 99–110.
Shen, H., Slifka, M., Matloubian, M., Jensen, E., Ahmed, R. and Miller, J. F. (1995). Recombinant Listeria monocytogenes as a live vaccine vehicle for the induction of protective anti-viral cell-mediated immunity. *Proc. Natl. Acad. Sci. U.S.A.* **99**, 3987–3991.
Snyder, J. E., Bowers, W. J., Livingstone, A. M., Lee, F.E.-H., Federoff, H. J. and Mosmann, T. R. (2003). Measuring the frequency of mouse and human cytotoxic T cells by the Lysispot assay: independent regulation of cytokine secretion and short-term killing. *Nat. Med.* **9**, 231–235.
Stemberger, C., Huster, K. M., Koffler, M., Anderl, F., Schiemann, M., Wagner, H. and Busch, D. H. (2007). A single naive CD8+ T cell precursor can develop into diverse effector and memory subsets. *Immunity* **27**, 985–997.
Taffs, R. E. and Sitovsky, M. V. (1994). Granule enzyme exocytosis assay for CTL activation. In: *Current Protocols in Immunology.* Coligan, J. E., Kruisbeek, A. M., Margulies, D. H., Shevach, E. M., Strober, W. eds., John Wiley and Sons, Inc., unit 3.16.
Weidmann, E., Brieger, J., Jahn, B., Hoelzer, D., Bergmann, L. and Mitrou, P. S. (1995). Lactat dehydrogenase-release assay: a reliable, nonradioactive technique for analysis of

cytotoxic lymphocyte-mediated lytic activity against blasts from acute myelocytic leukemia. *Ann. Hematol.* **70**(3), 153–158.
Yates, A., Graw, F., Barber, D. L., Ahmed, R., Regoes, R. R. and Antia, R. (2007). Revisiting estimates of CTL killing rates *in vivo*. *PLoS ONE* **2**, e1301.
Zinkernagel, R. M. and Doherty, P. C. (1974). Restriction of in vitro T cell-mediated cytotoxicity in lymphocytic choriomeningitis within a syngeneic or semiallogeneic system. *Nature* **248**, 701–702.
Zuber, B., Levitsky, V., Jönsson, G., Paulie, S., Samarina, A., Grundström, S., Metkar, S., Norell, H., Callender, G. G., Froelich, C. *et al*. (2005). Detection of human perforin by ELISpot and ELISA: ex vivo identification of virus-specific cells. *J. Immunol. Methods* **302**, 13–25.

9 Analysis of Intestinal T Cell Populations and Cytokine Productions

Jun Kunisawa and Hiroshi Kiyono
Division of Mucosal Immunology, Department of Microbiology and Immunology, The Institute of Medical Science, The University of Tokyo, Minato-ku, Tokyo, Japan

♦♦

CONTENTS

♦♦♦♦♦♦ I. INTRODUCTION

Intestinal tissues act as the frontlines of the host defense against large numbers of antigens and microorganisms at the most harsh environment in our body. To achieve immunosurveillance and immunological homeostasis in the gut, intestines establish the unique mucosal immune system tightly regulating a state of opposing but harmonized immune activation and quiescence (Kiyono *et al.*, 2008). Accumulating evidence has revealed that numerous types of immunocompetent cells are involved in the maintenance of an appropriate immunological environment of the mucosal immune system. Although the intestinal immune system shared some common immunological features with the systemic immune system, they also show distinct and unique immunological features (Kunisawa *et al.*, 2008).

Among various immunocompetent cells presented at the intestinal tissues, $CD4^+$ T cells play a key role in the regulation of harmonized mucosal immune responses. Classically, $CD4^+$ T cells are divided into two subsets, namely Th1 and Th2 cells, according to their distinct cytokine production profiles which account for two major functions (e.g. cell-mediated immunity [CMI] and humoral-mediated immunity in host immune responses, respectively) (Mosmann and Coffman, 1989; Street and Mosmann, 1991). It is well established that Th1 cells secrete interleukin (IL)-2, interferon (IFN)-γ and tumor necrosis factor (TNF)-α and function in CMI for protection against intracellular bacteria and viruses. In this regard, it has been shown that $CD8^+$ T cells, through their production of IFN-γ, are closely related to

METHODS IN MICROBIOLOGY, VOLUME 37
0580-9517 DOI 10.1016/S0580-9517(10)37009-7

and play a central role in their cytotoxic functions (Mosmann and Coffman, 1989; Street and Mosmann, 1991). Furthermore, Th1 cells also provide limited help for B cell responses where IFN-γ supports μ to γ2a switches and IgG2a synthesis in mice (Mosmann and Coffman, 1989; Street and Mosmann, 1991). By contrast, the Th2 cells preferentially secrete IL-4, IL-5, IL-6, IL-10 and IL-13 and provide effective help for B cell responses, in particular for IgG1 (and IgG2b), IgE and IgA antibody synthesis (Coffman *et al*., 1987; Beagley *et al*., 1988, 1989; Harriman *et al*., 1988). Thus, numerous numbers of Th2 cells are observed in the mucosal tissues for the preferential induction and regulation of IgA B cell responses.

In addition to classical Th1/Th2 paradigm, recent studies have discovered novel T cell subsets involving in the pro- and anti-inflammatory responses. One subset is $CD4^+$ T cells producing IL-17 and is known as Th17 cells (Harrington *et al*., 2005; Littman and Rudensky, 2010; Weaver *et al*., 2007). Like Th1 and Th2 cells, Th17 cells act as effector cells to exclude pathogens by inflammatory responses. On the other hand, it has been shown that $CD4^+$ $CD25^+$ $Foxp3^+$ T cells (known as regulatory T [Treg] cells) play a critical role in the down-regulation of immune responses by IL-10 production and cell–cell interaction (Hand and Belkaid, 2010; Littman and Rudensky, 2010; Sakaguchi *et al*., 2008). Another regulatory T cell population is known as Tr1 cells, which also produce IL-10 but lack the expression of Foxp3 (Groux *et al*., 1997; Asseman and Powrie, 1998). It should be noted that these novel types of T cells are preferentially observed in the mucosal tissues, especially in the intestine. Therefore, it is essential to examine cytokine responses in order to characterize the nature of immune responses induced at different stages of host–pathogen interactions or inflammatory responses in the intestine.

Several important cytokines influence the process of generation and development of these T cell subsets. For example, IL-12 and IL-4 direct $CD4^+$ T cells to

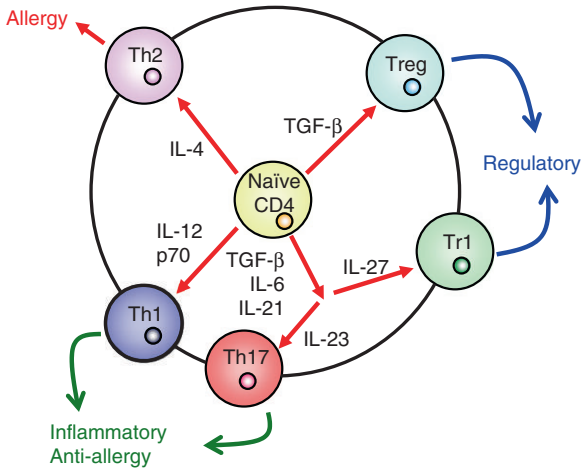

Figure 1. Versatile T cell network in the intestine. Naïve $CD4^+$ T cells activated in the presence of TGF-β differentiate into Treg cells. IL-10-producing Tr1 cells is another type of regulatory T cell induced by TGF-β and IL-6, 21 and 27. On the other hand, IL-23 and IL-12 p70 are involved in the induction of Th17 and Th1 cells, respectively. Th2 cells, a major T cell population in the development of allergic responses, require IL-4.

the differentiation into Th1 and Th2 cells, respectively, while later in development IFN-γ and IL-10 (together with IL-4) can reinforce Th1 or Th2 phenotype expansion (Seder and Paul, 1994). Transforming growth factor (TGF)-β and IL-2 promote the differentiation of Foxp3$^+$ Treg cells (Chen *et al.*, 2003). Although TGF-β is also a prerequisite factor for the differentiation of Th17 and Tr1 cells, IL-6 and IL-23 are additionally required for Th17 cell development (Bettelli *et al.*, 2006; Zhou *et al.*, 2007), whereas IL-6 and IL-27 enhance the Tr1 cell differentiation (Stumhofer *et al.*, 2007) (Figure 1).

♦♦♦♦♦♦ II. CELL ISOLATION FROM INTESTINAL TISSUES

A. Background

Intestinal tissues are generally and functionally divided into two sites. One is organized lymphoid organs and acts as the inductive site for the initiation of antigen-specific immune responses. Peyer's patches (PPs) are representative lymphoid organs in the intestine and known as a member of gut-associated lymphoid tissues (GALTs) (Kunisawa *et al.*, 2008) (Figure 2A). PPs show the features of

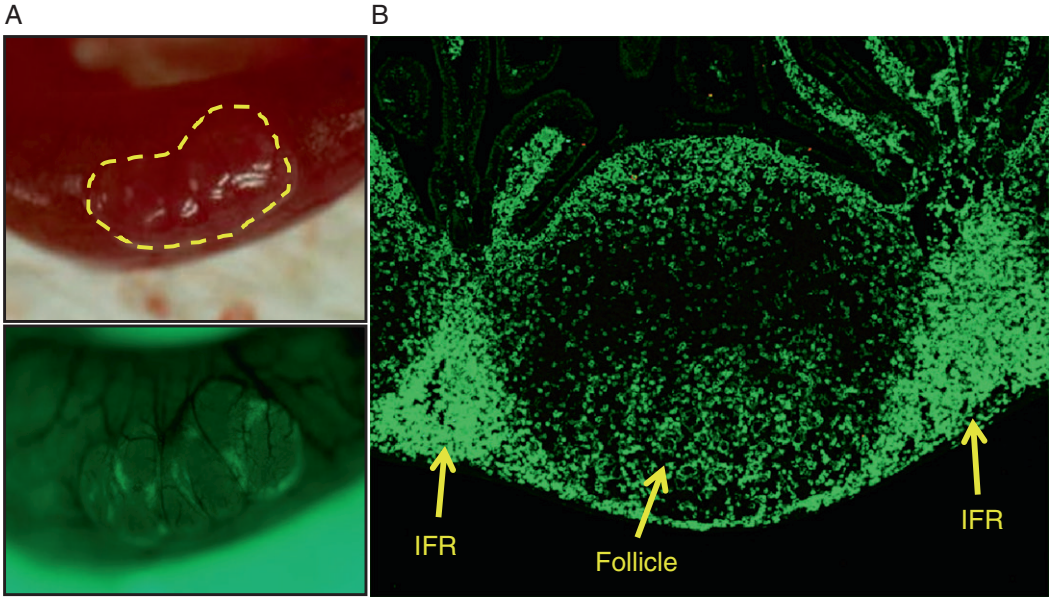

Figure 2. Macroscopic and histological views of Peyer's patches. (A) Mice were adoptively transferred with green fluorescent dye (carboxyfluorescein succinimidyl ester)-labelled naïve T cells. Sixteen hours later, small intestine was observed by conventional (upper) and fluorescent (bottom) stereomicroscopy. Yellow line in upper picture indicates the place of Peyer's patch. (B) Immunohistochemical data on Peyer's patch are shown. CD4$^+$ T cells (green) are present mainly in the intrafollicular regions (IFRs) and follicle. (See color plate section).

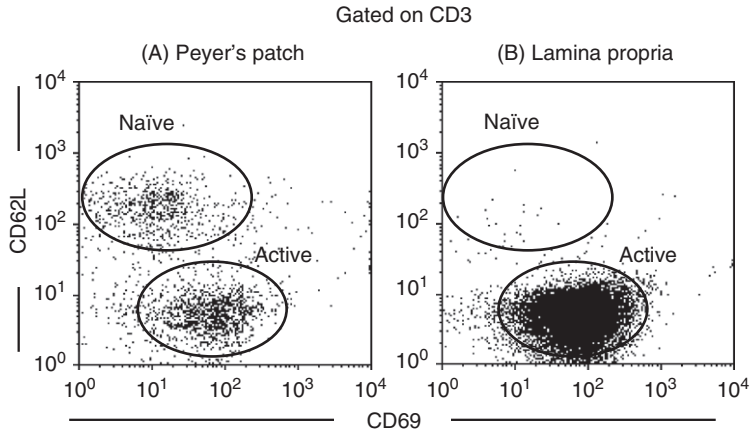

Figure 3. Immunological phenotypes of intestinal T cells. Cells were isolated from the Peyer's patches (A) and intestinal lamina propria (B), and stained with fluorescent-labelled antibodies for CD3, CD62L and CD69. The figures show the naïve ($CD62L^{hi}$ $CD69^{-}$) and activated ($CD62L^{-}$ $CD69^{+}$) cells in $CD3^{+}$ T cells.

secondary lymphoid organs and thus contain naïve T cells, especially at the interfollicular region (IFR: Figures 2B and 3A). In the IFR, naïve T cells recognize antigen presented by dendritic cells and subsequently differentiate into activated Th1- or Th2-type T cells in the follicle (Figures 2B and 3A). The other part is lamina propria region containing various types of T cells such as Th1, Th2, Th17, Tr1 and Treg cells for the execution of different effector functions including active and quiescent immune responses and thus known as the effector site. Under the epithelium, T cells exist diffusely with IgA^{+} plasma cells (Figure 4) and show activated phenotype mainly (Figure 3B).

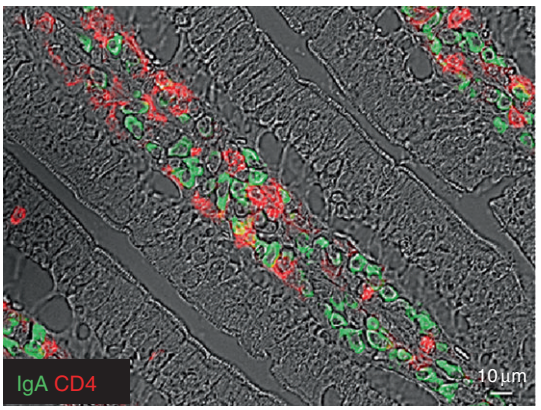

Figure 4. Distribution of immunocompetent cells in the intestinal lamina propria. Immunohistochemical data on intestinal lamina propria are shown. $CD4^{+}$ T cells (red) and IgA^{+} plasma cells (green) are diffusely present in the lamina propria region of small intestine. (See color plate section).

B. Isolation Lymphocytes from the Peyer's Patches (PPs)

1. Isolate the intestines and remove the PPs carefully using scissors.
2. Cut into small pieces as possible by scissors.
3. Incubate the pieces in 15 ml of pre-warmed RPMI1640 medium containing 2% foetal calf serum (FCS) plus 0.5 mg/ml of collagenase (available from many companies, but activity is different among companies and their lot. Therefore, it is necessary to check the activity and determine the optimal concentration). Stir the intestine for 20 min at 37°C.
4. Collect the supernatants in a fresh 50-ml tube and centrifuge for 5 min at 500 × *g* at 4°C. Suspend pellet with RPMI1640 containing 2% FCS.
5. Repeat twice steps 3 and 4.
6. Combine all cells and pass the cells through a 80-μm cell strainer. Centrifuge for 5 min at 500 × *g* at 4°C.
7. Suspend the cells with appropriate solution for further analysis.

C. Isolation Lymphocytes from the Intestinal Lamina Propria

1. Isolate the intestines and remove the PPs.
2. Open the intestine longitudinally, and wash it with ice-cold RPMI1640 medium (no FCS). Place the intestine in ice-cold RPMI1640 medium containing 2% FCS.
3. Cut the intestine into 2–3 cm pieces by scissors and incubate the pieces in 25 ml of pre-warmed (37°C) RPMI1640 medium containing 2% FCS and 0.5 mM ethylenediaminetetraacetic acid (EDTA). Stir the intestine in conical flask for 20 min at 37°C.
4. Remove the solution by passing the intestine through stainless mesh (e.g. a tea strainer). Put the intestine in a 50-ml tube containing 20 ml of plain RPMI1640 medium and shake them vigorously (~15 s).
5. Repeat step 4 once again.
6. Incubate the pieces in 25 ml of pre-warmed RPMI1640 medium containing 2% FCS. Stir the intestine in conical flask for 20 min at 37°C.
7. Repeat step 4 twice.
8. Cut into small pieces by scissors.
9. Incubate the pieces in 15 ml of pre-warmed (37°C) RPMI1640 medium containing 2% FCS plus 0.5 (small intestine) or 1.0 (large intestine) mg/ml of collagenase (concentration is dependent on the lot). Stir the intestinal pieces for 20 min at 37°C.
10. Collect the cell suspensions in a fresh 50-ml conical tube and centrifuge for 5 min at 500 × *g* at 4°C. Suspend pellet with RPMI1640 containing 2% FCS and pass the cell suspensions through a 100-μm cell strainer.
11. Repeat steps 9 and 10 twice.
12. Combine all cells and pass them through a 80-μm cell strainer. Centrifuge for 5 min at 500 × *g* at 4°C.
13. Suspend the pellet with 40% Percoll solution and overlay the cell suspension on 75% Percoll solution (Figure 5). Centrifuge for 20 min at 900 × *g* at 20°C without brakes.

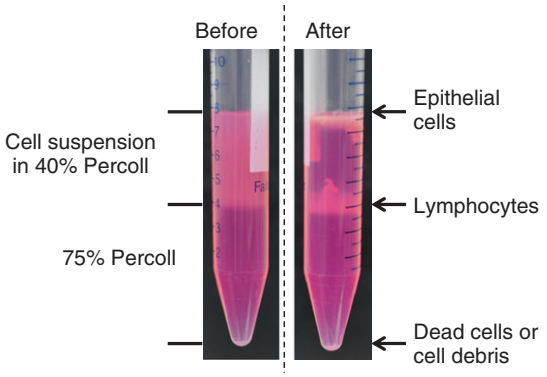

Figure 5. Cell purification using Percoll gradient centrifugation. To remove the epithelial cells, cell debris and dead cells, Percoll gradient centrifugation was performed. Initially, cells were suspended in the 40% of Percoll solution and put on the 75% of Percoll solution (before). After the centrifugation, lymphocytes were observed at the interphase between 40 and 75% Percoll solution. Epithelial cells and dead cells plus cell debris are observed at the top of layer and the bottom of the tube, respectively.

14. Collect cells at the interphase between 40 and 75% Percoll solutions (some epithelial cells are observed at the top of layer and debris and dead cells are at the bottom of the tube) (Figure 5).
15. Wash cells with 30 ml of RPMI1640 plus 2% FCS and centrifuge the cell suspension for 5 min at 500×g at 4°C.
16. Suspend the cells with appropriate solution and use for analysis.

♦♦♦♦♦♦ III. MEASURING CYTOKINE PRODUCTION FROM INTESTINAL T CELLS

A. Background

Cytokines are important biological molecules regulating distinct functions of different immunocompetent cells. As indicated above, T cells can be divided into several populations by the cytokine productions. Various techniques for the detection of cytokine production and/or expression have proven to be valuable for studies of T cell-mediated immune responses and examine the outcome of vaccine- and immune therapy-induced responses. We describe here three of these commonly used techniques to detect murine cytokines productions at protein levels and show some representative data on various cytokine productions by intestinal T cells. First, enzyme-linked immunosorbent assay (ELISA) assay can enumerate the amounts of produced cytokines from T cells. Second, ELISPOT assay is used to quantify the numbers of T cells producing particular cytokines (Czerkinsky *et al.*, 1988). Third, Intracellular cytokine staining assay can determine the T cell subsets and frequencies producing the specific cytokines when the cell were simultaneously stained with subset-specific markers.

B. Cytokine-Specific ELISA

For the analysis of murine cytokines, various kinds of ELISA kits are currently available from many companies. In addition, wide-ranging cytokine assays such as cytokine bead array (BD Biosciences, San Jose, CA) and Bio-plex system (Bio-rad, Richmond, CA) are currently available. Therefore, we summarize here the basic protocol by cytokine-specific ELISA system. We also show the example of cytokine production of small intestinal $CD4^+$ T cells (Figure 6).

1. Dilute the capture antibody in phosphate-buffered saline (PBS) and add 100 µl to the wells of 96-well microtitre plates (e.g. Immulon [Thermo Fisher Scientific, Rochester, NY]). Incubate the plates overnight at 4°C.
2. Remove the antibody solution from wells and block the coated antibody with PBS containing 1% BSA for 1 h at room temperature.
3. Wash the plates three times with PBS.
4. Prepare the standard curves using recombinant cytokines (e.g. two-fold serial dilutions in PBS containing 0.5% Tween 20 [PBS-T]).
5. To obtain the T cell culture supernatant, $2–10 \times 10^4$ purified T cells were stimulated with immobilized anti-CD3 antibody (clone: 145-2C11; 1–5 µg/ml in PBS) plus 1 µg/ml of anti-CD28 antibody (clone: 37.51) for 72–96 h at 37°C. Alternatively, antigen-primed T cells ($2–10 \times 10^4$ cells) are stimulated with appropriate antigen plus antigen-presenting cells (e.g. irradiated splenocytes) for 96 h at 37°C.
6. Add 100 µl of cytokine standards or appropriately diluted T cell culture supernatants and incubate the plates overnight at 4°C.
7. Wash the plates four times with PBS-T.
8. Add 100 µl of appropriate biotinylated capture antibody diluted in PBS-T with 1% BSA. Incubate the plates overnight at 4°C.
9. Repeat step 7.
10. Add 100 µl of peroxidase-labelled anti-biotin antibody and incubate the plates for 1 h at room temperature.

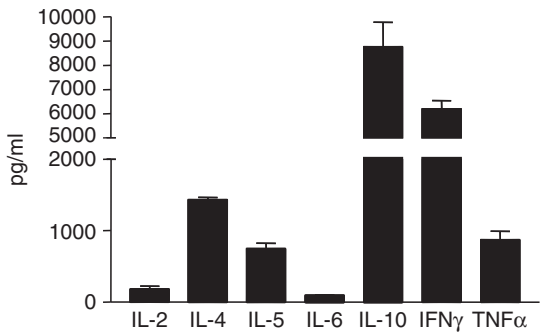

Figure 6. Cytokine productions by activated intestinal $CD4^+$ T cells. Lymphocytes were isolated from the small intestine and applied to the FACS cell sorting to purify the $CD4^+$ T cells. For the stimulation of T cells, 2×10^4 purified $CD4^+$ T cells were cultured with immobilized anti-CD3 antibody plus 1 µg/ml of anti-CD28 antibody for 96 h at 37°C. Cytokine production in the culture supernatant was determined by cytokine-specific ELISA.

11. Repeat step 7.
12. Develop the colour with appropriate chromogenic substrates (e.g. TMB microwell peroxidase substrate system [KPL, Gaithersburg, MD]) and read the absorbance.
13. Calculate the concentrations of samples by reference to the liner portion of the standard curve.

C. Cytokine-Specific ELISPOT

Like cytokine ELISA assay, several ELISPOT kits are commercially available. Thus, we summarize here a basic protocol of cytokine ELISPOT assay.

1. Dilute the capture antibody in PBS and add 100 μl to the wells of 96-well nitrocellulose-backed microtitre plate (e.g. Millititer-HA [Millipore, Billerica, MA]). Place the plates in a humidified chamber or carefully wrap the plate in saran wrap and incubate overnight at 4°C.
2. Remove the antibody solution from wells and block the immobilized antibody with culture medium (e.g. RPMI1640 medium containing 10% FCS) for 1 h at 37°C.
3. Rinse the plate three times with PBS.
4. Prepare the five-fold dilutions of purified T cells in culture medium starting at $1–10\times10^6$ cells/ml. Immediately add 100 μl of cells and incubate them for 12–16 h at 37°C. The time required for T cell purification significantly reduces the numbers of detectable cytokine-producing cells. Therefore, it is important to prepare the cells in a prompt manner.

   For the assessment of cytokine productions by antigen-specific T cells, purified T cells should be re-stimulated with the same antigens in the presence of irradiated antigen-presenting cells. Between 1 and 6 days after antigen stimulation, T cells are harvested and immediately added to the capture antibody-coated plates as described above.
5. Wash the plates three times with PBS followed by three times washes with PBS-T.
6. Add 100 μl of appropriate biotinylated capture antibody diluted in PBS-T with 1% BSA. Incubate the plates overnight at 4°C.
7. Wash the plates six times with PBS-T.
8. Add 100 μl of peroxidase-labelled anti-biotin antibody and incubate the plates for 1 h at room temperature.
9. Wash the plates four times with PBS.
10. Develop the colour with appropriate chromogenic substrates (e.g. AEC [BD Biosciences]) and count red spots by stereomicroscope or automated ELISPOT readers (e.g. KS ELISPOT [Carl Zeiss, Oberkochen, Germany]).

D. Intracellular Cytokine Staining

Using intracellular cytokine staining method, the frequency of cytokine-producing cells and their phenotypes can be determined by flow cytometer. By using subset-

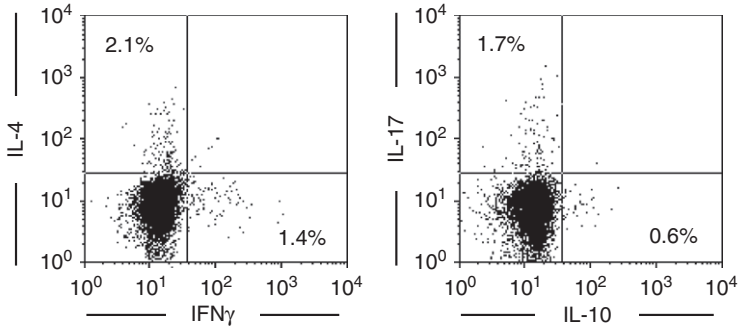

Figure 7. Intracellular cytokine staining of small intestinal T cells. Lymphocytes were isolated from the small intestine and cultured with 50 ng/ml PMA, 5 μM calcium ionophore A23187 and golgistop (BD Biosciences) for 4 h at 37°C. Cells were stained with anti-CD3 antibody followed by the fixation and permeabilization of cell membrane by Cytofix/Cytoperm kit (BD Biosciences). The permeable cells were further stained with antibodies specific for each cytokine and analysed by flow cytometry.

specific antibody, we do not need to purify the T cells. As example, we show here the data on cytokine-producing $CD4^+$ T cells isolated from small intestines (Figure 7).

1. Incubate lymphocytes in culture medium with 50 ng/ml PMA, 5 μM calcium ionophore A23187 and golgistop (BD Biosciences) for 4 h at 37°C.
2. Harvest the cells and stain cells with a corresponding cocktail of fluorescently labelled antibodies for 30 min at 4°C.
3. Wash the cells twice with PBS plus 2% FCS (PBS-F).
4. Fix the stained cells with 250 μl of Cytofix/Cytoperm solution (BD Biosciences) or 2% paraformaldehyde for 20 min at 4°C.
5. Wash cells twice with 1 ml of Perm/Wash buffer (BD Biosciences).
6. Incubate cells with fluorescently labelled cytokine-specific antibodies for 20 min at 4°C.
7. Repeat step 5 and suspend cells with PBS-T.
8. Analyse with Flow cytometer.

♦♦♦♦♦♦ IV. CONCLUSION

In this chapter, we have described the protocol for the analysis of T cell population in the intestine and their cytokine productions. For the cytokine production assay, we show three different methods: ELISA, ELISPOT and intracellular cytokine staining. These three assay systems allow the detection of different stages of cytokine production. Although each assay has unique advantages for the detection of T cell cytokines, the use of individual assays in a separate manner may often not

be sufficient for a thorough and accurate determination of the T cell cytokine profiles. Additionally, recent advances in the imaging technologies allow us to observe the cytokine-producing cells *in vivo* (Kamanaka *et al*., 2006). Thus, combining traditional technologies with the modern and novel technologies will lead to the better understanding of T cell responses in the intestine.

Acknowledgements

This work was supported by grants from the Ministry of Education, Science, Sports, and Culture of Japan; the Ministry of Health and Welfare of Japan; the Global Center of Excellence (COE) program on Center of Education and Research for the Advanced Genome-based Medicine; and Yakult Bio-Science Foundation.

References

Asseman, C. and Powrie, F. (1998). Interleukin 10 is a growth factor for a population of regulatory T cells. *Gut* **42**, 157–158.

Beagley, K. W., Eldridge, J. H., Kiyono, H., Everson, M. P., Koopman, W. J., Honjo, T. and McGhee, J. R. (1988). Recombinant murine IL-5 induces high rate IgA synthesis in cycling IgA-positive Peyer's patch B cells. *J. Immunol.* **141**, 2035–2042.

Beagley, K. W., Eldridge, J. H., Lee, F., Kiyono, H., Everson, M. P., Koopman, W. J., Hirano, T., Kishimoto, T. and McGhee, J. R. (1989). Interleukins and IgA synthesis. Human and murine interleukin 6 induce high rate IgA secretion in IgA-committed B cells. *J. Exp. Med.* **169**, 2133–2148.

Bettelli, E., Carrier, Y., Gao, W., Korn, T., Strom, T. B., Oukka, M., Weiner, H. L. and Kuchroo, V. K. (2006). Reciprocal developmental pathways for the generation of pathogenic effector TH17 and regulatory T cells. *Nature* **441**, 235–238.

Chen, W., Jin, W., Hardegen, N., Lei, K. J., Li, L., Marinos, N., McGrady, G. and Wahl, S. M. (2003). Conversion of peripheral $CD4^+CD25^-$ naive T cells to CD4+CD25+ regulatory T cells by TGFβ induction of transcription factor Foxp3. *J. Exp. Med.* **198**, 1875–1886.

Coffman, R. L., Shrader, B., Carty, J., Mosmann, T. R. and Bond, M. W. (1987). A mouse T cell product that preferentially enhances IgA production. I. Biologic characterization. *J. Immunol.* **139**, 3685–3690.

Czerkinsky, C., Andersson, G., Ekre, H. P., Nilsson, L. A., Klareskog, L. and Ouchterlony, O. (1988). Reverse ELISPOT assay for clonal analysis of cytokine production. I. Enumeration of gamma-interferon-secreting cells. *J. Immunol. Methods* **110**, 29–36.

Groux, H., O'Garra, A., Bigler, M., Rouleau, M., Antonenko, S., de Vries, J. E. and Roncarolo, M. G. (1997). A $CD4^+$ T-cell subset inhibits antigen-specific T-cell responses and prevents colitis. *Nature* **389**, 737–742.

Hand, T. and Belkaid, Y. (2010). Microbial control of regulatory and effector T cell responses in the gut. *Curr. Opin. Immunol.* **22**, 63–72.

Harriman, G. R., Kunimoto, D. Y., Elliott, J. F., Paetkau, V. and Strober, W. (1988). The role of IL-5 in IgA B cell differentiation. *J. Immunol.* **140**, 3033–3039.

Harrington, L. E., Hatton, R. D., Mangan, P. R., Turner, H., Murphy, T. L., Murphy, K. M. and Weaver, C. T. (2005). Interleukin 17-producing $CD4^+$ effector T cells develop via a lineage distinct from the T helper type 1 and 2 lineages. *Nat. Immunol.* **6**, 1123–1132.

Kamanaka, M., Kim, S. T., Wan, Y. Y., Sutterwala, F. S., Lara-Tejero, M., Galan, J. E., Harhaj, E. and Flavell, R. A. (2006). Expression of interleukin-10 in intestinal lymphocytes detected by an interleukin-10 reporter knockin tiger mouse. *Immunity* **25**, 941–952.

Kiyono, H., Kunisawa, J., McGhee, J. R. and Mestecky, J. (2008). The mucosal immune system. In: *Fundamental Immunology* (W. E. Paul, ed.), pp. 983–1030. Lippincott-Raven, Philadelphia.

Kunisawa, J., Nochi, T. and Kiyono, H. (2008). Immunological commonalities and distinctions between airway and digestive immunity. *Trends Immunol.* **29**, 505–513.

Littman, D.R. and Rudensky, A.Y. (2010). Th17 and regulatory T cells in mediating and restraining inflammation. *Cell* **140**, 845–858.

Mosmann, T. R. and Coffman, R. L. (1989). Th1 and Th2 cells: different patterns of lymphokine secretion lead to different functional properties. *Annu. Rev. Immunol.* **7**, 145–173.

Sakaguchi, S., Yamaguchi, T., Nomura, T. and Ono, M. (2008). Regulatory T cells and immune tolerance. *Cell* **133**, 775–787.

Seder, R. A. and Paul, W. E. (1994). Acquisition of lymphokine-producing phenotype by CD4+ T cells. *Annu. Rev. Immunol.* **12**, 635–673.

Street, N. E. and Mosmann, T. R. (1991). Functional diversity of T lymphocytes due to secretion of different cytokine patterns. *FASEB J.* **5**, 171–177.

Stumhofer, J. S., Silver, J. S., Laurence, A., Porrett, P. M., Harris, T. H., Turka, L. A., Ernst, M., Saris, C. J., O'Shea, J. J. and Hunter, C. A. (2007). Interleukins 27 and 6 induce STAT3-mediated T cell production of interleukin 10. *Nat. Immunol.* **8**, 1363–1371.

Weaver, C. T., Hatton, R. D., Mangan, P. R. and Harrington, L. E. (2007). IL-17 family cytokines and the expanding diversity of effector T cell lineages. *Annu. Rev. Immunol.* **25**, 821–852.

Zhou, L., Ivanov, I. I., Spolski, R., Min, R., Shenderov, K., Egawa, T., Levy, D. E., Leonard, W. J. and Littman, D. R. (2007). IL-6 programs Th17 cell differentiation by promoting sequential engagement of the IL-21 and IL-23 pathways. *Nat. Immunol.* **8**, 967–974.

10 Isolation and Measuring the Function of Professional Phagocytes: Murine Macrophages

Leanne Peiser[1], Subhankar Mukhopadhyay[2], Richard Haworth[3] and Siamon Gordon[2]
[1] Amgen Inc., Seattle, WA, USA; [2] Sir William Dunn School of Pathology, University of Oxford, Oxford, UK;
[3] Department of Pathology, Safety Assessment, Glaxosmithkline Research and Development, Park Road, Ware, Herts., UK

CONTENTS

List of Abbreviations

BCG	Bacille Calmette–Guérin
BGMϕ	Biogel-elicited peritoneal macrophages
BMMϕ	Bone marrow culture-derived macrophages
BP	Bacteriologic plastic
c.f.u.	Colony-forming units
CR3	Complement receptor type 3
DC	Dendritic cell
ECM	Extracellular matrix
EDTA	Ethylenediamine tetraacetic acid
FCS	Foetal calf serum
g	gravity
HBSS	Hank's buffered salt solution
IFN-γ	Interferon-gamma
IgG	Immunoglobulin gamma
IL	Interleukin
LCM	L929 cell conditioned medium
LPS	Lipopolysaccharide
LTA	Lipoteichoic acid
Mϕ	Macrophage(s)
mAb	Monoclonal antibody

METHODS IN MICROBIOLOGY, VOLUME 37
0580-9517 DOI 10.1016/S0580-9517(10)37010-3

M-CSF	Macrophage colony-stimulating factor
MHC	Major histocompatibility complex
NO	Nitric oxide
PBMC	Peripheral blood mononuclear cells
PBS	Phosphate-buffered saline
PMN	Polymorphonuclear neutrophils
RBMMϕ	Resident bone marrow-derived macrophages
SR-A	Scavenger receptor class A
TBAC	Tris-buffered ammonium chloride
TCP	Tissue culture plastic
TPMϕ	Thioglycollate broth-elicited peritoneal macrophage
Tris	Tri(hydroxymethyl)aminomethane

♦♦♦♦♦♦ I. INTRODUCTION

Professional phagocytes can be divided into macrophages (Mϕ) and polymorphonuclear leucocytes (PMNs) (Gordon, 2001, 2009; Russell and Gordon, 2009). Monocytes and Mϕ are cells of the mononuclear phagocyte system and are detected in most tissues throughout the body. Mϕ are sometimes referred to as the 'dustbins' of the body because of their efficiency at recognizing and removing foreign and host-derived debris. However, Mϕ are more than a vehicle for the elimination of waste and play a pivotal role in diverse processes including tissue homeostasis, inflammation and development. Mϕ are also key cells in immunity as they are essential in innate protection against pathogens and can regulate the acquired immune system through interactions with B and T cells.

When investigating Mϕ function, it is important to remember that as a population of cells they are extremely heterogeneous (Gordon and Taylor, 2005). Membrane receptor expression, biosynthesis and metabolic responses vary greatly between populations and during migration and maturation (Taylor *et al.*, 2005; Martinez *et al.*, 2006). Indeed, this variety of Mϕ phenotype has provided obstacles to the use of Mϕ as targets for drug delivery (Gordon and Rabinowitz, 1989). However, there are studies that have looked at targeting of cell surface receptors expressed by most Mϕ as possible avenues for delivering therapeutics (Szabó *et al.*, 2005).

Mϕ may also become activated, which modifies their effector function and adds to their heterogeneity (Gordon and Taylor, 2005; Mosser and Edwards, 2008). Activation is a dynamic process and each stimulus can induce unique changes in gene and protein expression; however, activated Mϕ can be broadly grouped based on similarities with changes in effector function and marker expression. These groups are as follows: classical activation, induced by a combination of Toll-like receptor (TLR) ligands such as lipopolysaccharide (LPS) and interferon-γ (IFN-γ); microbial activation by bacterial products in the absence of IFN-γ; alternative activation by interleukin 4 (IL-4) and IL-13 and deactivated Mϕ by stimulation with anti-inflammatory cytokines (IL-10 and transforming growth factor-β) or by ligating inhibitory receptors such as CD200R (Gordon and Taylor, 2005; Martinez *et al.*, 2006; Martinez *et al.*, 2009).

In this chapter, we will discuss *in vitro* methods for the measurement of Mϕ functions such as phagocytosis and cytokine production. Those seeking information on PMNs are referred to elsewhere (Leijh *et al.*, 1986), though protocols reported here are easily adapted for use on neutrophils. A wide range of techniques are available for assessing the role of Mϕ *in vivo*, and some of these are described elsewhere in this volume. We will focus on the acquisition and handling of different murine Mϕ populations; indeed the mouse provides an invaluable tool for studying these cells due to the accessibility of primary Mϕ from a number of different tissues. The murine system also offers the possibility of isolating or generating large numbers of primary cells for well-powered *in vitro* experiments through recruitment of primed Mϕ to the peritoneal cavity or by generating bone marrow culture-derived resident-type Mϕ.

♦♦♦♦♦♦ II. ISOLATION OF Mϕ

The different Mϕ populations that are readily isolated from mice along with the ability to maintain them in culture and activate them *in vitro* with various stimuli have greatly advanced our understanding of the biology of the cell. With the advent of array technology, our understanding has progressed further (Hume *et al.*, 2010). RNA from all the different culture conditions and Mϕ populations described below can be easily isolated for such purposes. RNA isolation using traditional methodology will not be described here, but has been widely employed to understand Mϕ heterogeneity (Antoni *et al.*, 2009). All animals should be treated and handled according to the guidelines dictated by the relevant home office.

A. Peritoneal Mϕ

The mouse peritoneal cavity is a convenient source of primary Mϕ. This site provides high yields of cell from which Mϕ can be purified via adhesion. In addition, different phenotypes of Mϕ can be isolated depending on the activation status and the stimulus used, if any, to recruit the cells. The populations that can be isolated can be divided phenotypically into resident, elicited or activated cells and are collected following peritoneal lavage.

1. Resident peritoneal Mϕ

Resident peritoneal Mϕ are an easy acquirable source of normal, non-activated tissue Mϕ. However, each mouse typically yields only $1–2 \times 10^6$ Mϕ per animal, which is useful for phenotypic studies, but not for experiments requiring many cells. Researchers should consider applying other methods that yield larger numbers of cells, such as bone marrow culture-derived Mϕ (BMMϕ) or elicited peritoneal Mϕ, for any analysis requiring more cells.

Isolation of resident peritoneal Mϕ

1. Sacrifice the mice using carbon dioxide inhalation and then pin them down with their ventral surface uppermost.
2. Sterilize the skin with 70% ethanol in water, and using fine scissors, make a lateral cut in the skin over the abdomen. Do not break the body wall at this stage.
3. Pull the skin back from the incision to reveal the shiny surface of the body wall. (It is important to keep this area sterile during the whole procedure.)
4. Using a 23-gauge needle, inject approximately 10 ml of sterile saline into the peritoneal cavity. The needle should be injected bevel uppermost into the caudal half of the cavity and care should be exercised not to puncture any organs. As the needle is removed, there may be a small leakage of fluid, but omental fat will usually block further leakage.
5. Agitate the filled cavity by rubbing the tube of a sterile 19-gauge needle over the external body wall a few times.
6. Remove the fluid using a 23-gauge needle attached to a 10-ml syringe. The needle should be inserted bevel downwards into the cranial half of the cavity to avoid fat blockage during aspiration. It is unlikely that the whole 10 ml of fluid will be recovered, and if the cavity fills up with blood, the animal should be discarded as it may contaminate the resident population.
7. Pellet the cells via centrifugation and culture in bacteriologic plastic (BP) or tissue culture plastic (TCP) vessels as appropriate.

2. Thioglycollate broth-elicited Mϕ

Intraperitoneal injection of sterile inflammatory agents is a useful method for isolating large numbers of Mϕ for *in vitro* assays. Thioglycollate-elicited peritoneal Mϕ (TPMϕ) are recruited to the peritoneal cavity following injection of 1 ml of Brewer's complete thioglycollate broth (BD Biosciences, Franklin Lakes, NJ) (Johnson *et al*., 1978). The cells are harvested, as described above for resident cells, 4–5 days following injection. TPMϕ ingest large amounts of the inflammatory agent (agar), but retain active endocytic and phagocytic capabilities upon isolation. The use of protease peptone as a stimulant produces cells with a phenotype similar to that of TPMϕ, but with fewer vacuoles and lower cell yields. An important consideration when analysing Mϕ function using TPMϕ is that the thioglycollate often contains small amounts of LPS (0.5 ng/ml), which may alter Mϕ responsiveness in the subsequent assays.

3. Biogel polyacrylamide beads-elicited Mϕ

The need to obtain large numbers of elicited Mϕ has resulted in the testing of other inflammatory stimuli. The first reported use of polyacrylamide beads for this purpose was by Fauve *et al*. (1983). They injected beads into subcutaneous pouches created in the dorsal skin of mice. In this model, 10^7 phagocytic cells (60% Mϕ and

40% PMNs) could be recovered from the resulting 'granuloma'. In our laboratory, Biogel beads have been successfully used to elicit a high yield (10^7 cells per animal) of peritoneal Mϕ. The most suitable size of bead is P100 (hydrated size 45–90 nm), which Mϕ are unable to ingest or extracellularly digest.

Preparation of BPMϕ

1. Wash Biogel polyacrylamide beads (Biogel P-100 [fine], Bio-Rad laboratories, Hercules, CA) in phosphate-buffered saline (PBS) by repeated centrifugation and autoclave before use. Remember to use pyrogen-free laboratory equipment and endotoxin-free PBS to prevent LPS contamination.
2. Inject 1 ml of a 2% (v/v) suspension of Biogel into the peritoneal cavity of the animal.
3. Isolate the Mϕ from the peritoneal cavity as described above for resident cells 4–5 days following the injection of Biogel.
4. To purify the Mϕ via adherence, plate the cells in medium at the appropriate density (Table 1) on TCP or BP.
5. After incubation at 37°C for 60–90 min when plated on TCP or 24 h on BP, remove the non-adherent cells by washing the culture dishes five times with PBS. Under these condition, the adherent monolayers consist of >90% Mϕ, and viability is usually >97% by phase microscopy and trypan blue exclusion.

Biogel-elicited peritoneal Mϕ (BPMϕ) have a number of features that distinguish them phenotypically from TPMϕ. For example, following incubation overnight in serum-containing medium on TCP, 50% of BPMϕ will have become completely non-adherent and the remainder will have rounded up. By contrast, TPMϕ will remain completely flattened and tightly adherent to the substratum (M. Stein, unpublished observations). In addition, the culture medium selected and the presence of serum

Table 1. The phenotype of different macrophages isolated from the peritoneal cavity

	Resident	Thioglycollate	Biogel	BCG
Approximate total cellular yield per mouse ($\times 10^6$)	7	21	17	10
% Mϕ	40	86	59	62
Adherence to TCP at 24 h	+	+	±	+
F4/80 expression	++	+	+	+
Mannose receptor expression	++	++	++	+
Macrosialin expression	+	++	+	+
MHCII	–	+	+	+++
Respiratory burst	–	+	+	+
Constitutive NO production	–	–	–	+

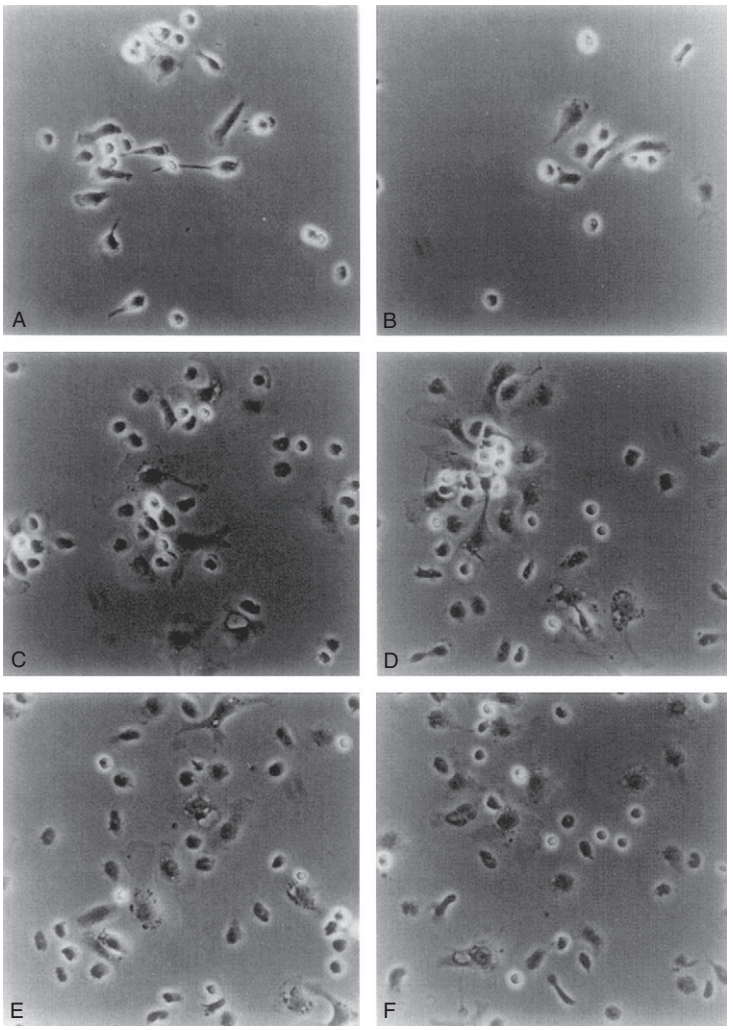

Figure 1. The effect of culture medium are on BPMϕ cultured on glass coverslips. Cells were harvested as described and allowed to adhere for 30 min in RPMI containing 10% FCS (A,B), in RPMI alone (C,D) or in Optimem (E,F). Cells were fixed in 2% paraformaldehyde and photographed under phase contrast. (A,C,E) Wild-type cells; (B,D,F) cells from mice lacking SR-A. BPMϕ spread more rapidly on this surface in media lacking serum (Optimem or RPMI). There is no discernible difference in the spreading morphology of wild-type cells and SR-A$^{-/-}$Mϕ. original magnification ×400.

have profound effects on the degree of spreading by BPMϕ (Figure 1). Some differences in phenotype between these elicited and other Mϕ populations are listed in Table 2.

One of the most useful markers of murine Mϕ is defined by the monoclonal antibody (mAb) F4/80, which recognizes a 160 kDa glycoprotein on the surface of most mouse Mϕ populations (Austyn and Gordon, 1981; McKnight *et al.*, 1996). F4/80 is a member of a growing family of epidermal growth factor (EGF) seven-transmembrane

Table 2. Membrane antigens and the corresponding antibodies that can be used to define Mϕ distribution and heterogeneity in murine tissues

Marker	Tissue distribution	Clone	Supplier
Macrosialin	Mϕ and DC endosome membrane	FA-11	AbD Serotec
CD11b (CR3)	PMN, Mϕ, B1 B cells and NK cells	5C6	AbD Serotec
CD14	PMN, monocytes and Mϕ	rmC5-3	BD Biosciences
F4/80	Mature macrophages, DCs, eosinophils	F4/80	AbD Serotec
FcR	Mϕ, DC and B cells	2.4G2	BD Biosciences
SR-A	Mature Mϕ, DC and hepatic endothelium	2F8	AbD Serotec
MHCII	Activated Mϕ	Tib120	ATCC
Sialoadhesin/ CD169/Siglec-1	Stromal Mϕ and marginal zone metallophilic Mϕ	3D6.112/ MOMA1	AbD Serotec
MARCO	Resident peritoneal macrophages, Activated and marginal zone Mϕ	ED31	AbD Serotec

molecules (Stacey *et al.*, 2000) and has been suggested to play a role in peripheral tolerance (Lin *et al.*, 2005). F4/80 expression is known to be down-regulated by INF-γ and in response to Bacille Calmette–Guérin (BCG) infection (Ezekowitz *et al.*, 1981; Ezekowitz and Gordon, 1982) (Table 2).

The FA11 mAb recognizes macrosialin, the murine homologue of CD68, which is an endosomal marker for Mϕ and dendritic cells (DCs) (Rabinowitz and Gordon, 1991). CD68/macrosialin expression is a useful indicator of endocytic activity, and the data suggest that BPMϕ are less endocytic than TPMϕ. Therefore, BPMϕ may be useful in studies examining the entry and replication of facultative pathogens (e.g. *Mycobacterium tuberculosis* and *Leishmania donovani*) within endosomal compartments. *In vivo*, elicited BPMϕ, largely unstimulated by lymphokines, are permissive host cells for the above-mentioned pathogens (Gordon, 1986). Therefore, BPMϕ, or other foreign body-elicited Mϕ, may resemble cells recruited early to a focus of infection, and maybe appropriate populations for studies examining the regulation of Mϕ microbicidal activity. In addition, these cells respond well to cytokines *in vitro*, e.g. IL-4 and INF-γ (Stein *et al.*, 1992). If sepharose, polystyrene or smaller polyacrylamide beads are used, then a higher percentage of PMNs will be recruited. Zymosan and other β-glucan particles may also be used for recruitment of peritoneal Mϕ (Rosas *et al.*, 2008).

4. BCG-recruited Mϕ

BCG organisms (e.g. Pasteur strain) provide a suitable stimulus to recruit immunologically activated Mϕ to the peritoneal cavity. BCG stocks are stored at –80°C and thawed immediately prior to use. The BCG organisms are resuspended in PBS and sonicated before use. Mice are inoculated with approximately 10^7 colony-forming units (c.f.u.) in 0.2 ml of PBS by intraperitoneal injection. Peritoneal Mϕ are harvested by lavage, as described above, 4–6 days post injection. Percoll gradients can be used at this stage in order to enrich the population for Mϕ (Pertoft and Laurent, 1977).

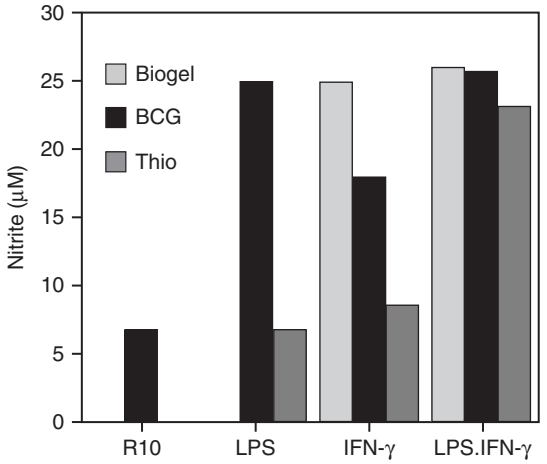

Figure 2. NO production by different peritoneal Mϕ *in vitro*. TPMϕ (thio), BPMϕ (Biogel) and BCG-recruited cells were harvested as described in the text, and plated at 2×10^5 cells per well and treated with medium (R_{10}) alone, LPS (20 ngml^{-1}) or IFN-γ (100 units ml^{-1}) overnight. Nitrite levels were measured using the Griess reaction, as described in the text. All values shown are NMMA inhibitale.

These Mϕ become activated *in vivo* under the influence of T cell products, such as INF-γ, and express high levels of cell surface major histocompatibility complex class II (MHC-II). In addition, they produce nitric oxide (NO) in serum-containing media in the absence of further stimulation, in contrast to the other elicited Mϕ populations described above (Figure 2). These cells are useful for investigating the activated Mϕ response to bacterial cell products such as LPS and lipoteichoic acid (LTA), which can be added to the cells in culture.

5. *Corynebacterium parvum*-recruited cells

The use of inactivated *C. parvum* (also known as *Propionibacterium acnes*) provides a convenient, alternative method of recruiting activated Mϕ. The use of this organism to recruit Mϕ to the liver resulted in the cloning of IL-18, which induces the production of INF-γ by T cells (Okamura *et al.*, 1995). The use of *C. parvum* avoids the need for using viable pathogenic organisms. Inactivated *C. parvum* is washed in non-pyrogenic saline twice, resuspended in PBS and sonicated before use. Mice are inoculated with 500 μg in 0.2 ml of PBS by intraperitoneal injection. Peritoneal Mϕ are harvested by lavage 4–5 days post injection.

B. Tissue Mϕ

Resident Mϕ can be isolated from a range of tissues and activated cells can be isolated from infected or inflamed organs using the enzymatic methods described below.

1. Spleen and Thymus

Mϕ can be isolated from the spleen and thymus using enzymatic digestion. Most researchers use mechanical disruption for the isolation of lymphocytes. While this protocol is good for isolating lymphocytes, it is not optimal for monocyte and Mϕ isolation and should be avoided.

To isolate Mϕ, the organs are removed intact from the mice and placed on ice in PBS until use. The organs are subject to enzymatic digestion and gentle mechanical disruption to release the cells and the Mϕ purified via adhesion as described for BPMϕ or via flow cytometry. It is critical to note that in order to maintain Mϕ cell integrity, it is important that sufficient digestion has taken place before mechanical disruption is used. The yield of Mϕ greatly diminishes if the protocol below is not followed precisely. The protocol below is optimized for the spleen, but is readily adapted for isolating thymic Mϕ. It is worth noting that the Mϕ in the spleen represent a heterogenous population, and different approaches may be used to isolate the subpopulations, such as via flow cytometry.

Isolation of splenic Mϕ

1. Prepare the digestion mixture[a] consisting of 6 ml of RPMI 1640 culture medium, 3 ml of collagenase D (Roche) and 1 ml of DNAse-1 (Roche) and place at 37°C.
2. Prepare the Stop Solution consisting of RPMI 1640 containing 20% foetal calf serum (FCS) and place at 4°C.
3. Sacrifice the mice and harvest the spleen into culture medium that does not contain serum[b] and place on ice. It is important to make sure that the spleen is kept intact as any nicks at this stage can dramatically reduce Mϕ yield. Also remove as much connective tissue as possible.
4. Fill a 5-ml syringe with the digestion mixture and attach a 26-gauge needle. Inject each spleen so that it gently swells with liquid and appears lighter in colour.
5. Place the spleens at 37°C for 15 min.
6. Place 5 ml of Stop Solution into a tube and place on ice.
7. After 15 min incubation gently tease apart the spleen with the flat end of a bent needle. Harvest the released cells with a Pasteur pipette and place in the Stop Solution on ice. Be careful not to remove any remaining clumps of spleen.
8. Add more digestion mixture to the remaining clumps of spleen and incubate at 37°C for a further 15 min.
9. Tease apart the spleen once again to release the cells and place them in the Stop Solution.
10. Add more digestion mixture to the remaining clumps of spleen; incubate for 15 min at 37°C.
11. Tease apart the pieces of spleen one last time, discard the cell debris and harvest the remaining cells into the Stop Solution.

12. Centrifuge the cells at 365 × *g* for 10 min at 4°C.
13. Discard the supernatant and lyse the red blood cells using commercial cell lysis solutions such as RBC lysing buffer (Sigma, St. Louis, MO).
14. Centrifuge the cells and resuspend in culture medium. The Mϕ can be harvested by adherence or sorted from the other cells using flow cytometry.

[a] Use 10 ml of digestion mixture per three spleens.
[b] Serum inactivates the collagenase D.

2. Bone marrow

Both resident bone marrow culture-derived (RBMMϕ) and bone marrow culture-derived (BMMϕ) Mϕ can be obtained from this tissue.

(a) Resident bone marrow Mϕ

Isolation of RBMMϕ

1. Sacrifice the mice and sterilize the abdomen and hind legs with 70% ethanol in water.
2. Dissect the skin away from the abdomen and hind legs following a transverse cut through the skin of the abdomen.
3. Remove the muscles attaching the hind limb to the pelvis and those attaching the femur to the tibia using a pair of fine scissors.
4. Only when the femur is well exposed, cut through the tibia just below the knee joint using strong scissors, and free the femur from the mouse by cutting through the pelvis bone close to the hip joint.
5. Store the femur in RPMI 1640 on ice until all the femurs are collected. Place the bones in a petri dish of 70% ethanol for 1 min to maintain sterility, before washing twice with PBS.
6. Next, hold each femur firmly with forceps and, in a single motion, cut off the expanded ends (epiphyses) using strong scissors.
7. Using a 5-ml syringe attached to a 25-gauge needle, flush out the bone marrow by forcing an RPMI solution containing 0.05% collagenase and 0.001% DNAse down the central cavity. The bone will become white when all the marrow is expelled.
8. Resuspend the bone marrow plugs from two femurs in 10 ml of the same enzyme solution mentioned above and digest at 37°C with shaking for 1 h.
9. Add FCS to a final concentration of 1% (v/v) to stop the digestion. At this stage the marrow plug fragments should no longer be visible, and a homogenous suspension is obtained. Harvest and culture as appropriate.
10. Enrich clusters of cells by gravity sedimentation in RPMI containing 30% FCS or by use of a Ficoll-Hypaque cushion (Crocker and Gordon, 1985).
11. Wash purified cell clusters twice in RPMI by centrifugation at 100 × *g* for 10 min, suspended in RPMI containing 10% (v/v) FCS (R_{10}) and added to glass coverslips in TCP plates.

12. After 3 h incubation at 37°C, wash off non-adherent cells with PBS, resulting in a population of adherent cells with the characteristic morphology of RBMMϕ but contaminated with a varying population of monocytes and neutrophils.

(b) Bone marrow-derived Mϕ

The manufacture of BMMϕ is a simple method to obtain large numbers of primary non-activated Mϕ. Typically, one animal yields up $2–6 \times 10^7$ Mϕ. To obtain BMMϕ, femurs are flushed with PBS, with no enzymes added. The marrow plugs are mechanically disrupted by passage through a 19-gauge needle prior to centrifugation at $160 \times g$ for 5 min. The cells are then resuspended in RPMI 1640 containing 10 mM HEPES (*N*-[2-hydroxyethyl]piperazine-N^1-[2-ethanesulphonic acid]), 10% FCS and 15% (v/v) L cell conditioned media (LCM) (Hume and Gordon, 1983) and plated into 15 cm BP dishes (two dishes per animal). Alternatively, 100 ng/ml recombinant Mϕ colony-stimulating factor (M-CSF) can replace the LCM. Fresh culture medium is added to the Mϕ on day 3, and at day 6 all the medium is replaced with fresh R_{10} and 15% LCM. Maintain the culture in the presence of the LCM or M-CSF continually. The cultures are routinely confluent after 7 days incubation, and cells can be harvested by incubating them with PBS containing 10 mM ethylenediaminetetraacetic acid (EDTA) and 4 mg/ml Lidocaine–HCl for 10 min before removal of the loosened cells by pipetting. Although these cells represent mature Mϕ, they are proliferating as long as CSF is present, but can be used in a wide range of assays from phagocytic to Mϕ response investigations. The cells can be used in colony assays in agar to assess changes in Mϕ differentiation from progenitors in response to different stimuli (Cooper and Broxmeyer, 2001).

As long as the bone marrow is handled correctly, BMMϕ are readily generated from bones from animals that have been sacrificed some time prior to the start of culture. This allows for the shipping of bones/whole legs, which is particularly useful for obtaining cells from different strains without having to import the live animal. To ship the bones, sacrifice the animals and place the bones or the whole leg, detached from the hip, into a complete culture medium, such as RPMI supplemented with 10% FCS. Ship/store the legs on ice until they are ready for use, making sure that at no time the bone marrow is allowed to freeze. Isolate the bone marrow and place in culture as soon as possible so overnight shipping is recommended. BMMϕ are also readily immortalized by transformation for the generation of cell lines (see below).

C. Foetal Liver

The foetal liver contains the richest source of Mϕ in the developing mouse. $F4/80^+$ membrane processes of these cells interact extensively with developing haemopoietic cells, forming cell clusters *in vivo*. To investigate the interactions between erythroid cells and stromal Mϕ, isolation of haemopoietic cell clusters is recommended (Morris *et al*., 1988).

D. Lamina Propria Mϕ

Isolation of lamina propria Mϕ

1. Sacrifice the mice and remove the colon.
2. Cut the colon lengthwise and gently scrape with scissors to remove the faeces and mucus.
3. Without letting the colon dry out, chop into ~0.5-cm pieces with a blade and transfer to a tube containing 10 ml of PBS supplemented with 0.1% bovine serum albumin (BSA).
4. Wash the colon by inverting the tube several times and allowing the pieces of colon to sediment before aspirating off the PBS.
5. Add 10 ml of pre-warmed RPMI 1640 supplemented with 10% FCS and 5mM EDTA to the colon pieces and incubate for 15 min at 37°C shaking.
6. Allow the colon pieces to sediment before aspirating the supernatant and repeat this washing twice more.
7. After removal of the culture medium from the last wash step, add 15 ml of RPMI 1640 culture medium supplemented with 15 mM HEPES.
8. Incubate the colon pieces at room temperature for 10 min before allowing the pieces to sediment and discarding the supernatant.
9. Next, add 10 ml of fresh RPMI 1640 supplemented with 15 mM HEPES and 0.2 mg/ml type VIII collagenase (Sigma) to the pieces of colon and incubate shaking at 37°C.
10. After 1 h, harvest the released cells by passing the culture medium through a cell strainer.
11. Pellet the cells by centrifuging the strained culture supernatant.
12. Resuspend the cell pellet with ice-cold RPMI 1640 supplemented with 5 mM EDTA and 10% FCS to inactivate the collagenase.
13. Repeat digestion described above with the remaining pieces of colon and add the released cells to those from the first digestion.
14. Next, prepare dilutions for the Percoll gradient. First, mix nine parts Percoll with one part PBS to make Percoll-100. Dilute Percoll-100 with RPMI 1640 to make Percoll-40 (40% Percoll-100 and 60% RPMI), and with PBS supplemented with 0.1% BSA (w/v) to make Percoll-75 (75% Percoll-100 and 25% PBS/BSA) and Percoll-30 (30% Percoll-100 and 70% PBS/BSA)
15. Harvest the cells by centrifugation and resuspend the pellet in 3 ml of Percoll-30 solution.
16. Create a gradient with the Percoll solutions mentioned above by adding 3 ml of Percoll-75 to a 15-ml tube and overlaying it with 4 ml of Percoll-40.
17. Overlay the cells diluted in the Percoll-30 over the gradient created above and centrifuge for 20 min at 526 × g at 10°C. Turn off the centrifuge brake for this step.
18. Aspirate the Percoll-30 and Percoll-40 layers which contain the epithelial cells and collect the leucocytes at the Percoll-40–Percoll-75 interface.

19. Wash the cells with cold PBS supplemented with 0.1% BSA before harvesting via centrifugation.
20. Resuspend the leucocytes in culture medium. The Mϕ can be separated using an adherence step or via cell sorting as required by the researcher.

E. Peripheral Blood Mononuclear Cells

To obtain peripheral blood mononuclear cells (PBMCs), mice are killed and bled by cardiac puncture into a heparinized syringe with a 25-gauge needle. The blood is diluted by adding an equal volume of 0.9% saline, and layered over a Nycoprep 1.077 Animal cushion (Nycomed Pharma AS, Zurich, Switzerland). Cells are centrifuged at $586 \times g$ (no brake) for 15 min. Mononuclear cells can then be collected from the interface between the plasma and the Nycoprep cushion. These cells are then resuspended in Tris-buffered ammonium chloride (TBAC) lysis buffer, which is made by mixing 0.15 M ammonium chloride and 0.17 M Tris at a ratio of 9:1 before adjusting the pH to 7.2 and filter sterilization. The red blood cells are lysed following 5 min incubation in TBAC buffer for 5 min at room temperature followed by three washes in RPMI 1640. The PBMCs are then resuspended in R_{10} before use.

F. Use of Cell Lines

A number of different cell lines can be used in assays for investigating the function of professional phagocytes (Ralph, 1986). Murine Mϕ-like cell lines include the widely available RAW 264 (Raschke *et al.*, 1978), J774 (Ralph *et al.*, 1975) and P388D1 (Koren *et al.*, 1975). These cells can be cultured in RPMI 1640 on either BP or TCP surfaces. Also, see below for the generation of new Mϕ cell lines using viral transduction of primary cells. Care should be taken when using cell lines as although they are Mϕ-like they are not true Mϕ and may vary functionally from their primary cell counterparts (Peiser *et al.*, 2000), and so wherever possible, confirming results with primary cells are recommended.

♦♦♦♦♦♦ III. CULTURE OF Mϕ

Following the isolation of primary Mϕ as outlined above, it is important to maintain the cells in culture under appropriate conditions, which will vary according to the functional tests required. For example, the substratum on which the cells are cultured may be important if adhesion studies are planned.

A. Substratum

Mϕ can be cultured in suspension using tissue culture vessels with a Teflon-coated surface (Thermo Fisher Scientific). By contrast, Mϕ adhere firmly to TCP and BP. On BP, adherence is mediated via integrins, especially CR3 (complement receptor

type 3), and can be readily detached using Lidocaine–HCl and EDTA as mentioned above for BMMϕ. However, on TCP, adherence is mediated via integrins and SR-A (Mϕ class A scavenger receptor), which is EDTA resistant; thus, the cells are more difficult to detach and the viability of the Mϕ should be examined after lifting. Incubation with Lidocaine–HCl and EDTA at 37°C for 10–30 min is effective in most cases (Rabinovitch and deStefano, 1976), but in some instances Pronase may be used to remove the cells. Note that Lidocaine may be added directly to the culture medium as it is able to function in the presence of serum. Trypsin is ineffective at removing Mϕ from TCP. All cells should be centrifuged and washed thoroughly with fresh medium before use.

B. Media and Sera

Mϕ are plastic cells and vary functionally depending on the culture conditions in which they are maintained, and so these are important considerations for researchers who are isolating Mϕ for functional studies. The addition of cytokines is further able to skew their phenotype (Martinez *et al.*, 2006); for example, culturing the Mϕ in the presence of LPS and IFN-γ results in a fully activated cell that is able to effectively kill intracellular pathogens – while the addition of IL-4 and IL-13 results in an alternatively activated cell with increased endocytic capability.

Mϕ are routinely cultured in a wide range of media in our laboratory, including RPMI 1640, modified Eagle's medium (MEM) and Dulbecco's modified Eagle's medium (DMEM) (Invitrogen). These media are supplemented with 2 mM glutamine, 50 IU/ml penicillin and 50 μg/ml streptomycin (Invitrogen). RPMI 1640 is also supplemented with 10 mM HEPES (pH 7.3). FCS (Sigma) is heat inactivated at 56°C for 30 min, filter sterilized through a 0.22 M filter prior to use and used at 10% (v/v).

Primary Mϕ can be cultured for a variable time under serum-free conditions. Specifically, in endocytic and phagocytic assays the use of OPTIMEM (Invitrogen), which is a proprietary serum-free medium, has proven successful. However, it should be borne in mind that Mϕ adhere to substrata under serum-free conditions by way of molecules that have not been fully identified, which may result in practical problems in harvesting the cells from the substrata prior to their use in assays.

1. Transfection and gene expression

Traditionally transfection of Mϕ was difficult and limited only to a few cell lines. The advent of nucleofection® and transduction using viruses has opened up a world of possibilities for manipulating Mϕ gene expression, using RNAi technology (Wiese *et al.*, 2010), and for generating immortalized cell lines (Rosas *et al.*, 2008). BMMϕ are particularly useful for generating Mϕ lines from various knockout animals. Retroviruses containing a gene fusion of the *estrogen receptor* with the *Hoxa9* genes have proven particularly successful for immortalizing primary Mϕ (Wang *et al.*, 2006; Rosas *et al.*, 2008). Viral transduction of cell lines is also a useful method of generating stable transfectants overexpressing your gene of choice. One thing to note is that Mϕ are able to repress translation of genes containing a cytomegalovirus (CMV) promoter with in a few days of transfection so it is

advisable to use alternative promoters, e.g. the *elongation factor* promoter region, when trying to generate stable lines (Gough *et al*., 2001).

♦♦♦♦♦♦ IV. MEASURING Mϕ FUNCTION

A. Adhesion Phenotype

One of the key functions of a professional phagocyte is the ability to adhere both to other cells and to the extracellular matrix (ECM). In order to explore the cell surface molecules involved in this interaction, *in vitro* assays of adhesion of Mϕ to artificial substrata (e.g. TCP) have been developed. These have provided a useful strategy for purifying Mϕ from a mixed population (see above) and also for isolating reagents that interfere with this adhesion. For example, murine Mϕ adhere to BP in the presence of serum in a divalent-cation-dependent fashion. Used as a screening strategy to develop novel mAbs, the ability of a hybridoma supernatant to inhibit this adhesion produced the 5C6 mAb (Rosen and Gordon, 1987). This antibody recognizes CR3, a leucocyte integrin. Subsequent studies have shown that this mAb has an *in vivo* role in adhesion, since 5C6 is able to block the adhesion of Mϕ to inflamed endothelium and recruitment to immunologically non-specific stimuli (Rosen and Law, 1989; Rosen *et al*., 1989; Rosen, 1990).

In order to use this strategy to identify further molecules involved in adhesion, the investigator can vary (a) the phenotype of the Mϕ added, (b) the presence or absence of chelators or other chemicals or (c) the character of the substratum. For example, Mϕ adhere to TCP in the absence of divalent cations (Figure 3). The use of an adhesion assay, as outlined below, allowed the identification of SR-A (Fraser *et al*., 1993), which had no known adhesive function prior to these studies.

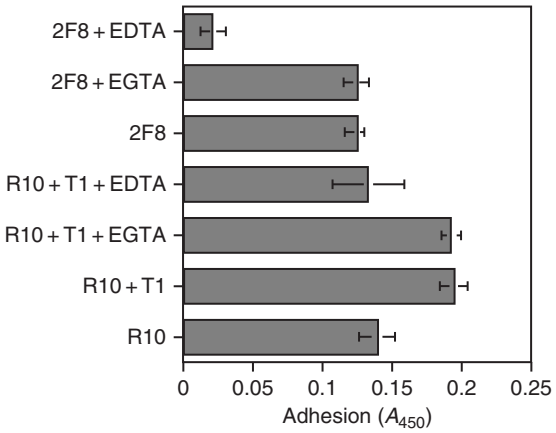

Figure 3. Adhesion phenotype of BPMϕ. Adhesion of BPMϕ to FCS coated TCP. Cells were plated at 3×10^5 Mϕ per well of a 96-well plate in the presence of various mAb and/or chelators. Adhesion (mean ± SD) is represented as the absorbence at 450 nm (A_{450}), and is the result of quadruplicate wells. Significant adhesion occurs in the presence of an isotype matched control andtibody (T1) in the presence of EDTA. By contrast, in the presence of 2F8, which blocks adhesion via SR-A, significant inhibition of adhesion occurs. Note that EDTA needs to be present to observe this activity, since other mechanisms of adhesion (integrins) need to be inactivated.

Adhesion assay

1. Plate Mϕ at a density of 3×10^5 cells per well of a 96-well plate in the presence of various mAbs and chelators.
2. Incubate the plates at 4°C for 30 min, then at 37°C for 90 min before washing to remove non-adherent cells.
3. Fix the remaining adherent cells in methanol, and stain with 40% giemsa for 1 h.
4. Quantify the level of adhesion by solubilizing the dye in methanol and reading the optical density (OD) at 450 nm.

B. Antigen Expression

Changes in levels of expression of either cell surface or intracellular antigens (Table 2) can provide useful information regarding activation status or endocytic activity of Mϕ. A highly sensitive method of analysis of individual cells is provided by immunostaining and flow cytometry (Figures 4 and 5). Immunohistochemistry is described elsewhere in this volume, and can be applied with success to defining resident and recruited Mϕ populations *in vivo*.

Indirect immunofluorescent staining of cultured Mϕ

1. Detach adherent cells from the culture dishes, if required, and fix the cells in 4% (w/v) paraformaldehyde[a,b] in PBS buffered to pH 7.0 with 1 M HEPES for 10 min on ice. Approximately, 1×10^6 cells should be stained in analysing results by flow cytometry.
2. Harvest the cells by centrifugation and resuspend in a blocking solution containing 10% normal serum[b,c] of the species of secondary antibody[c] diluted in PBS. If staining an intracellular antigen, add permeabilization agents (0.25% [w/v] saponin or 0.1% [v/v] Triton in PBS) at this point to the blocking solution and keep them present in all subsequent incubation steps.
3. After 30 min, resuspend the cells in blocking solution containing the correct dilution of primary antibody. Use antibodies at the manufacturer's recommended concentration or at 10 μg/ml. Incubate for 1 h.
4. Wash the cells three times with blocking solution before labelling with the secondary antibody diluted in the blocking solution.
5. After washing the cells three times with PBS, analyse on a flow cytometer or by microscopy if the cells were plated on a coverslip.

[a] Other fixatives, like acetone, may be used for microscopic analysis, but we recommend paraformaldehyde. Paraformaldehyde is best to use for flow cytometry.

[b] If staining unfixed cells, then perform the staining at 4°C and begin the protocol from step 2.

[c] This is to block non-specific IgG-binding sites.

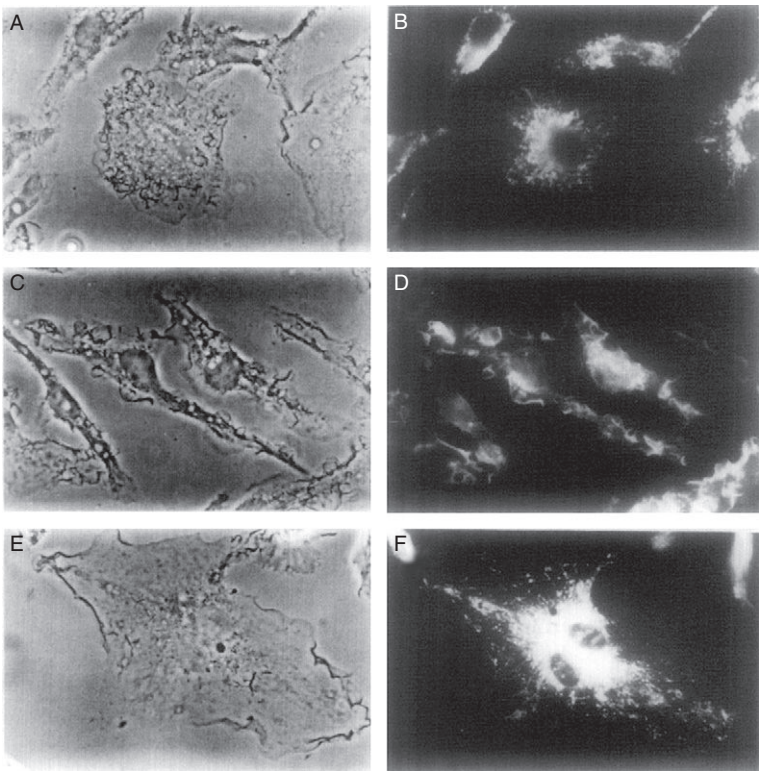

Figure 4. Immunofluorescent staining and DiI-AcLDL labelling of murine BMMϕ. Murine BMMϕ were plated in a 24-well plate containing 13 mm glass coverslips at a density of 2×10^5 cells per well. (A–D) Cells were fixed in 4% paraformaldehyde, permeabilized and stained with anti-macrosialin (FA-11) (A+B) or anti F4/80 (F4/80) (C+D) followed by FITC-conjugated goat anti-rat IgG. Cells were viewed by fluorescence microscopy and photographs of the same field taken under phase contrast (A+C) or fluorescence (B+D). The staining highlights the predominantly intracellular localization of macrosialin compared to the cell surface expression of the F4/80 antigen. (E–F) Cells were labelled by incubation with DiI-AcLDL at a concentration of 5 μg ml for 3 h at 37°C, washed four times with PBS and subsequently fixed in 4% paraformaldehyde. Coverslips were viewed by fluorescence microscopy and photographs taken under phase contrast (E) and fluorescent (F) illumination.

C. Endocytosis

Endocytosis in Mϕ can be mediated by ubiquitously expressed receptors, such as the transferrin receptor, or Mϕ-restricted receptors including the mannose receptor (MR) and SR-A (Table 3, Figure 4). The expression of many Mϕ-specific receptors is regulated by the stage of differentiation of the Mϕ and its activation state. Regulation may affect the levels of receptor expression, in addition to the rate of receptor trafficking and its processing in the endocytic pathway. Ubiquitously expressed receptors, like the transferrin receptor, may give information on the basal rate of endocytosis. When testing the endocytic function of Mϕ, choose a well-documented receptor, like the transferrin and LDL receptor or MR. If testing the capabilities

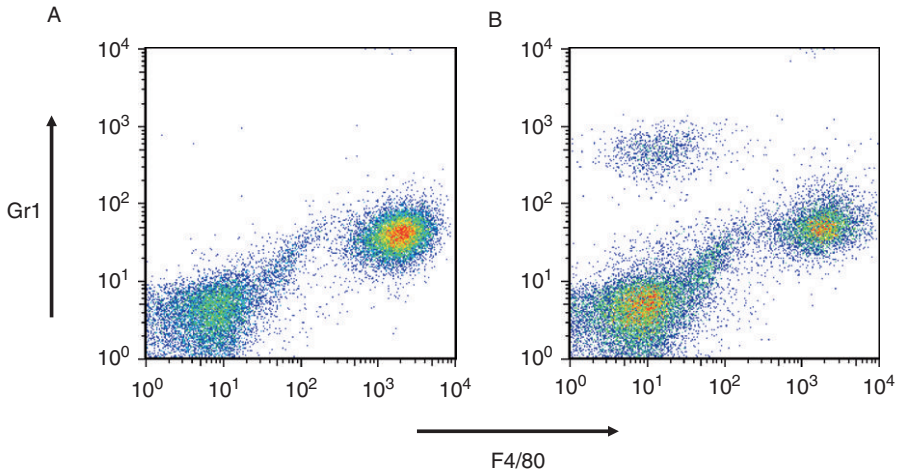

Figure 5. Peritoneal macrophages. Mice were injected with PBS (A) or bacteria (B) IP before being sacrificed and cells harvested by lavage after 4 h. The cells were fixed and stained with F4/80-APC and Gr1-PE. Note that the resident macrophages are F4/80^{hi} and Gr1^{low}, while the recruited PMN are Gr1^{hi} and F4/80$^{low/neg}$. (See color plate section).

Table 3. Commonly used endocytic tracers and phagocytic particles

Probe	Receptor	Supplier
Texas Red Dextran (MW 70000)	Unknown	Invitrogen
FITC-holo-transferrin	Transferrin receptor	Invitrogen
DiI-AcLDL	SR-A, CD36, MARCO	Invitrogen
DiI-LDL	LDL receptor	Invitrogen
HRP	Mannose receptor on macrophages or fluid phase in other cell types	Sigma
Lucifer yellow	Fluid phase	Sigma
Mannosylated BSA	Mannose receptor	E-Y labs
Latex beads (polystyrene with or without carboxylation and/or fluorescent tracers)	Unknown	Polysciences
Sheep erythrocytes	CR3 if coated with complement, FcR if coated with IgG	Diamedix Miami, FL
E. coli bioparticles	Multiple	Invitrogen
S. aureus bioparticles	Multiple	Invitrogen
Zymosan	B-glucan receptor	Invitrogen

of a novel receptor, comparison with known receptors can give a wealth of information. Assays can be readily adapted to measure binding, internalization and degradation of ligand. Receptor-specific binding will be saturable, i.e. reaches a plateau, when background is subtracted.

When investigating a particular receptor, the appropriate cognate ligand must be chosen. There are a large number of commercially available labelled ligands (Table 3), but coupling of fluorochromes to proteins is quick and easy (see protocol

below). Specificity can be shown by competition with saturating amounts of unlabelled ligand, which controls for alterations caused by the labelling procedure. A suitable ligand should not be degraded too quickly once internalized, especially when loading the late endosomes and lysosomes. Dextran is a good marker as its poly-(α-D-1-6-glucose) linkages make it resistant to degradation. See Table 3 for examples of commonly used ligands for analysis of the endocytic pathway. Suitable ligands for measuring pinocytosis, such as lucifer yellow, must not be recognized by any Mϕ receptors. Horseradish peroxidase (HRP) is commonly used as a pinocytic marker; however, it is not ideal for Mϕ as it has mannose residues which are recognized by the MR. Selected fluorochromes undergo pH-dependent shifts in their excitation and/or emission spectra so the acidification of endocytic compartments can be monitored.

Fluorescent labelling of proteins or particles

Coupling fluorescein isothiocyanate (FITC)[a] to proteins

1. Mix 5.8 ml of 5.3% Na_2CO_3 with 10 ml of 4.2% $NaHCO_3$.
2. Make the bicarbonate buffer by adding one volume of the mixture mentioned above to one volume of 0.15 M NaCl and adjust the pH to 9.5.
3. In separate tubes, dissolve the FITC and the protein[b,c] to be labelled in the bicarbonate buffer, at final concentrations of 1 and 5 mg/ml, respectively.
4. Mix the protein and FITC together at 0.3 ml FITC for each ml of protein.
5. Incubate in the dark for 2 h at room temperature.
6. Equilibrate a G-50 or G-25 sephadex column (Sigma) with PBS and run the FITC/protein mixture over the column.
7. Elute the FITC-conjugated protein with PBS.
8. Determine the OD of the conjugated protein fractions at 280 and 495 nm. The ratio of OD_{495}/OD_{280} should be approximately 1.
9. Determine the conjugated protein concentration using the following formula:

$$\text{Protein concentration (mg/ml)} = \frac{OD_{280} - (OD_{495} \times 0.35)}{1.4}$$

Coupling of Texas Red[a] to proteins

1. Prepare the bicarbonate buffer as above except adjust the pH to 9.
2. Dissolve the protein in the bicarbonate as above and add 1 mg Texas Red sulphonyl chloride (Invitrogen) for every 10 mg protein in one drop of dimethylformamide.
3. Incubate for 1 h in the dark at room temperature.

4. Separate the conjugated protein on a sepharose column. Determine the OD of the pooled fraction at 596 and 280 nm. The ratio of OD_{596}/OD_{280} should be approximately 0.8.

[a] There are many FITC and Texas Red derivatives available; use the derivatives most suitable for the individual requirements of the assay.

[b] Dialyse or exchange buffer by running a desalting column.

[c] Use zymosan at 10^9 particles per ml and live bacteria at 10^7 particles per ml.

Quantitation of Mϕ endocytic function[a]

Loading Mϕ with a single tracer

1. Remove the culture medium from the cells and wash them twice in PBS.
2. Add OPTIMEM-I containing 100 μg/ml fluorescently labelled tracer to the wells.
3. Incubate the Mϕ for 1 h at 37°C. Keep a control sample on ice[b].
4. Stop the endocytic uptake by placing the Mϕ on ice and wash the Mϕ at least four times in ice-cold PBS.
5. If measuring the amount for uptake by flow cytometer, detach and fix the cells, or if measuring the fluorescence on a fluorimetric plate reader, follow the steps below.
6. Lyse the cells with 1% Trition-X100 in 10 mM Tris buffer (pH 7.5). Incubate on ice for 30 min.
7. Scrape the Mϕ from the bottom of the dish and transfer the lysed cells to an appropriate vessel to read on a plate reader.
8. Remove an aliquot of supernatant to determine the protein concentration and express the result as a function of the protein concentration or number of cells depending on analysis.

Dual endocytic tracer loading of Mϕ

1. Perform steps 1–3.
2. Remove the first tracer and wash the cells well in warmed RPMI (or the usual culture medium for the Mϕ).
3. Chase the tracer into lysosomes, by incubating the Mϕ overnight at 37°C.
4. Remove the culture medium and wash the Mϕ twice in PBS.
5. Add culture medium containing 100 μg/ml of the second fluorescent-labelled tracer[c]. Place a control sample on ice.
6. Load the early endocytic compartments by incubating the Mϕ at 37°C for 10–15 min[d].
7. Remove the second tracer and cool the Mϕ quickly by placing them on ice before washing with ice-cold PBS.

8. Follow steps 5–8 above remembering to take fluorometric readings for both the fluorochromes.

[a] This assay is easily adapted for analysis by flow cytometry, microscopy or a plate reader.

[b] This controls for the non-specific sticking of the tracer to the extracellular surface of the cells and the tissue culture dishes. Subtract this value, after analysis, for a correct measurement of total endocytic uptake.

[c] This tracer should be labelled with a fluorochrome different from that used for the first tracer.

[d] Mϕ are very endocytic cells so incubation for longer times will start to load later endocytic compartments as well as the earlier ones.

D. Phagocytosis

Traditional phagocytic assays involve the addition of particles to Mϕ followed by microscopic analysis of the number of particles bound and internalized by a cell. This type of analysis is time consuming as large numbers of cells have to be counted manually to obtain statistically significant results. Therefore, we suggest adapting the assays so that the results may be analysed on a plate reader or flow cytometer which can collect information on large numbers of cells (Figure 6).

There are two types of basic assay: the first determines the number of particles associated with the Mϕ, while the other monitors decreasing numbers of particles in the extracellular medium. Either assay is acceptable, but we will only discuss the former. Uptake assays can be adapted to measure cellular responses, such as the respiratory burst, by appropriate bulk or single cell methods (Baorto *et al*., 1997) and to determine the survival or killing of ingested live organisms (see below). Appropriate safety precautions must be taken in handling living micro-organisms, in all procedures.

The ligands expressed on a chosen particle will determine the receptors used for ingestion of that particle so ligands must be appropriately chosen if investigating a particular receptor. Complex ligands, like bacteria, may be recognized

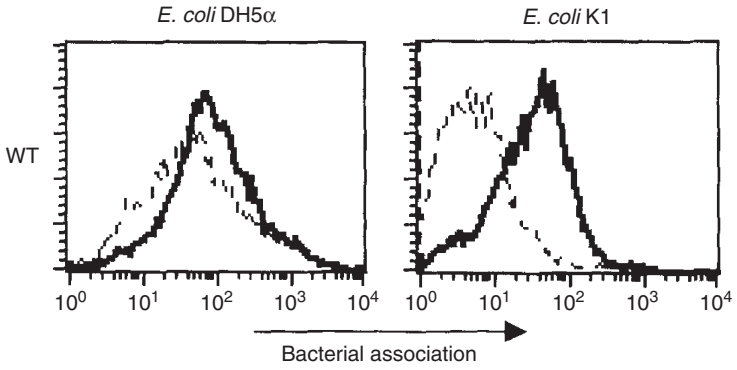

Figure 6. The measurement of *E. coli* association with BMMϕ by flow cytometry. BMMϕ were incubated with paraformaldehyde-fixed fluorescently labelled *E. coli* DH5α or *E. coli* K1 (60 bacteria per Mϕ) in the presence or absence of Poly I.—,depicts the fluorescence obtained by flow cytometry for the Mϕ populations incubated with *E. coli*; – – – –, Mϕ populations incubated with *E. coli* in the presence of Poly I, a scavenger receptor inhibitor.

by more than one receptor. Bacteria are easily fluoresceinated (see above) or some are available commercially (see Table 3). If not investigating phagocytosis mediated by a particular receptor, then complex ligands can be used. Latex beads, the receptors for which are unknown, are readily taken up and are suitable particles for phagocytosis. They are available in a wide range of sizes and can be coated by absorption or, in the case of carboxylated polystyrene latex beads, can be coupled directly to protein ligands to target them to specific receptors; some examples used previously are mannose BSA and lipoarabinomannan. However, even apparently single ligands may also be recognized by multiple receptors.

Besides latex beads, zymosan, derived from the cell wall of *Saccharomyces cerevisiae*, is a commonly used particle. It is highly mannosylated and is recognized by a number of receptors including MR, β-glucan receptor (Brown and Gordon, 2001) and CR3, with or without opsonization. (It readily activates the alternative pathway of complement.) It is commercially available, though easy to prepare and label with fluorochromes. Zymosan should be boiled before use to destroy contaminating phospholipases. Erythrocytes coated with opsonins are widely used to analyse the function of opsonic receptors. Smaller particles may be taken up by macropinocytosis, so when using latex beads, ensure that the size used is larger than 1 μm in diameter and test the ability of phagocytic inhibitors on particle uptake. Inhibitors on ingestion, like cytochalasin B and D, and inhibitors that block ligand binding should always be used as controls for phagocytosis. Recently, phagocytosis has been used to track Mϕ *in vivo*. Nanoparticles have been used effectively *in vivo* to follow Mϕ trafficking (Turner *et al*., 2009) as they are phagocytosed by the cells and are visualized using MRI (Elias and Tsourkas, 2009).

Some ligands require opsonization by complement and antibodies. Mϕ themselves may also produce opsonins like complement and fibronectin that could potentially influence uptake. The presence of serum can opsonize particles, so unless analysing general phagocytosis, use a serum-free protein-containing medium. If analysing specific opsonic receptors, coat the particles with the opsonin before the assay. Bacteria are easily opsonized by incubating them in an appropriate serum for 30 min at 37°C. Complement is only present in fresh serum and is destroyed by heat inactivation. Specific IgM and complement target CR3, but beware of IgG contamination of the IgM. IgG coating targets the Fc receptors. Polyclonal antibodies can be raised, or where available, monoclonal antibodies against erythrocyte antigens or hapten, for example, can be used with an appropriate isotype matched antibody control.

The differentiation of intracellular particles and those bound to the extracellular surface is crucial in any phagocytic assay, and there are numerous modifications to existing methods available for this purpose. Firstly, fluorescence on any extracellular particles can be quenched with appropriate agents such as ethidium bromide, crystal violet and trypan blue. It is not easy to control for total quenching of the extracellular fluorescence. In addition, the quenching agent must not be cell permeable. An alternative approach is to cleave or lyse the bacteria from the extracellular surface; for example, lysostaphin can lyse *S. aureus* and lysozyme can lyse *Micrococcus lysodeikticus*. Erythrocytes are easily lysed by brief osmotic shock (water or

hypotonic solutions). Lastly, immunofluorescent techniques can be used to distinguish intra- and extracellular bacteria, with only external bacteria detected by antibodies. The distribution of the bacteria, with respect to the numbers found inside and bound to the cell, can be obtained by comparison between antibody staining of permeabilized and unpermeabilized cells.

Mϕ are highly professional phagocytic cells and particle ingestion occurs rapidly. Generally, incubation times range between 10 min and 1 h. However, the kinetics of uptake should be determined by performing a time course experiment before embarking on these assays. At time zero there should be no uptake and also at 4°C as the membrane is not fluid enough to mediate uptake. Following any uptake assay, the Mϕ should be quickly cooled to 4°C to stop any further internalization by the cell, and ideally, the rest of the protocol should be performed in the cold. The optimal dose of particles should always be determined, especially when using live and virulent bacteria as too many bacteria may lyse or kill the Mϕ. An initial particle to Mϕ ratio of between 1:1 and 20:1 is recommended. The rate of ingestion should reach zero-order kinetics with increasing dose and is an important test of any assay method.

Particle contact with the Mϕ may be enhanced by centrifuging them directly onto the cells, in special holders available commercially. If performing the assay on non-adherent cells, tumble the bacteria and Mϕ together for optimal contact. The protocols detailed below are for adherent populations, though they are easily adapted for non-adherent assays.

Phagocytic uptake of dead bacteria or inert particles by Mϕ

1. Remove the culture medium from the cells and wash twice in PBS to remove any non-adherent cells.
2. Add culture medium to the cells containing the phagocytic particle at the appropriate dose.
3. Centifuge the particle onto the Mϕ and incubate the cells at 37°C for 1 h.
4. Wash the cells well in ice-cold PBS to remove as many extracellular particles as possible before detaching and fixing the cells in 4% paraformaldehyde in PBS buffered to pH 7 using 1 m HEPES.
5. Stain the extracellular particles with the anti-particle antibody[a] and analyse the cells by microscopy or flow cytometry.

[a] Remember not to permeabilize the Mϕ.

1. Ingestion of live bacteria

The association and ingestion of bacteria by Mϕ is readily measured by colony assay. Important considerations are the 'stickiness' of the bacteria to the plastic surface, the cytotoxic effects of the organism on the Mϕ, the ability of the cells to control the infection and the growth of the bacteria during the assay. All these factors must be controlled during the assay.

Measurement of bacterial association with Mϕ using a colony assay

1. Seed Mϕ onto 96-well plates at a density of 1×10^5 Mϕ per well.
2. Wash the cells three times in Hank's buffered salt solution (HBSS) before use and add the appropriate culture medium with or without serum depending on particular assay conditions.
3. Harvest the bacteria from the agar plates or broth and resuspend in PBS. To remove large aggregates, centrifuge the bacteria at $85 \times g$ for 1 min Determine the concentration of bacteria and confirm by plating aliquots on solid media and counting the number of c.f.u.
4. Add the organisms to the cells and incubate at 37°C for a predetermined period. Remember to include the following controls: (a) for each assay condition, some wells containing bacteria and culture medium in the absence of Mϕ are required to control for bacterial adhesion to the plastic; and (b) Mϕ and bacteria are incubated together for the length of the assay before lysing the total contents of the well with saponin (1% final concentration) to control for Mϕ killing and bacterial growth.
5. Following the incubation, wash all the wells, except for the bacterial growth controls, four times in HBSS to remove all organisms not associated with the cells.
6. Lyse the cells with saponin (1% final concentration). It is important to test that the bacteria are resistant to treatment with 1% saponin.
7. Estimate the total c.f.u. associated with the cells by making dilutions of the bacteria using PBS and count at least three dilutions for each well. The number of cell-associated bacteria can be determined after correction for attachment to exposed plastic by subtraction of the bacterial adhesion control wells from the experimental association wells, as described previously (Virji *et al*., 1991).

The number of internalized bacteria can be determined by including antibiotics to kill extracellular bacteria. Gentamicin is commonly used as it is considered to be impermeable; however, it has been suggested that it may be able to enter Mϕ, and the antibiotic may not kill extracellular bacteria that are in close association with the cells. To measure internalized organisms only, incubate the Mϕ as above with the bacteria and then wash the cells to remove most extracellular organisms. Culture medium containing 200 μg/ml gentamicin is then added to each well for 05–1.5 h to eliminate remaining extracellular bacteria. A control for gentamicin killing of bacteria must be included in each assay by incubating bacteria alone with the antibiotic. Following gentamicin treatment, the Mϕ are washed in HBSS and lysed with saponin and the c.f.u. estimated as before. In some cases, lysis of the cells can be achieved using the endogenous bacterial lysins, such as in the case of *Listeria monocytogenes*, which express listerolysin O (Dancz *et al*., 2002). Adapting this assay to include a time course can give information on intracellular Mϕ killing.

The assays above are useful for studying specific Mϕ receptors if the ligands are known. In some instances, before the above assays can be performed, the researcher may want to identify new ligands for a known cell surface receptor or, if

the receptor is a novel molecule, screen for ligands that can bind. A simple solid-phase assay can be used for rapid screening for ligands of any cell surface receptor without the requirement of many research tools (Pluddemann *et al*., 2008; Neyen *et al*., 2009). Basically, enzyme-linked immunosorbent assay (ELISA) plates are coated with purified ligands overnight. After blocking, as per a usual ELISA protocol, the wells are overlayed with post-nuclear supernatant derived from Mϕ or transfected cells that express the cell surface receptor under investigation or a control supernatant derived from knockout Mϕ for the receptor or untransfected cells that do not express the molecule. After washing the wells thoroughly, the receptor binding to the coated ligands is detected by staining the wells with antibodies against the receptor coupled to HRP directly or through inclusion of a secondary antibody step and visualized using TMB reagent according to manufacturer's instructions. Ligands that bind will be positive only in wells that were overlayed with supernatant containing the receptor, but not when control supernatant was used. Ligands that bind the receptor can then be examined under more physiological conditions using the endocytic and phagocytic assays described above (Neyen *et al*., 2009).

E. Secreted Products

An important functional characteristic of Mϕ is their conversion, under appropriate stimulation, from the resting to the activated state. Activated Mϕ have increased numbers of lysosomal granules, more mitochondria and a greater capacity to phagocytose opsonized particles. In addition, the activated cell produces higher levels of certain cytokines (e.g. TNF-α) and has an increased capacity to generate superoxide anions. Assays for measuring superoxide, NO and cytokines *in vitro* are described below.

1. Superoxide

This assay provides an easy an convenient method for estimating microbicidal and cytocidal potential. Other assays of the respiratory burst include hydrogen peroxide release, chemiluminescence and fluorescence, which are detailed elsewhere (Root *et al*., 1975; Thrush *et al*., 1978). The release of superoxide from murine Mϕ is tightly regulated, and therefore freshly isolated cells produce negligible levels of superoxide in the absence of further stimulation, and in our experience BMMϕ do not release superoxide even after phorbol 12-myristate 13-acetate (PMA) stimulation.

Measurement of superoxide release

1. Plate Mϕ in 24-well dishes. Suitable negative controls include a cell-free blank and wells containing superoxide dismutate at 30 μg/ml. Positive controls should include wells containing elicited cells stimulated with PMA (Sigma) at 10–100 ng/ml or zymosan at 100 μg/ml.
2. Wash the adherent cells with PBS and incubate with 450 μl of reaction mixture (HBSS, 80 μM ferricytochrome C [Sigma type IV], 2 mM sodium azide and 10 mM sodium phosphate buffer, pH 7.4) for 5 min at 37°C.

3. Add 50 µl of HBSS containing the stimulant and incubate at 37°C for 1 h.
4. Remove 100 µl of the supernatant from each well and read the A_{550} against a reaction mix cell blank.

2. Nitric oxide

NO is a highly reactive molecule that mediated cytotoxic effects on micro-organisms and tumour cells (Saito and Nakano, 1996). NO is an important player in innate immunity as a mediator of Mϕ cytotoxicity against intracellular pathogens (Nathan and Shiloh, 2000). For example, the induction of NO production following BCG infection has been known for some time (Stuehr and Marletta, 1987). Because NO is rapidly converted to nitrite in the presence of oxygen, the secretory activity of cells can be estimated by determining nitrite concentrations by the colorimetric Griess reaction.

Colorimetric Griess reaction

1. Seed Mϕ in 96-well BP plates at 1×10^5 cells per well and wash twice with PBS before use.
2. Add stimuli, e.g. LPS with or without INF-γ at 50–100 U/ml (AbD Serotec, Oxford, UK). For each stimulus, set up a negative control with *N*-monomethyl arginine (NMMA) (Sigma) at the same time.
3. After incubating at 37°C, remove 50 µl of culture supernatant and add it to 50 µl of Griess reagent (a 1:1 dilution of 1% [w/v] naphthylethylenediamine diHCl [Sigma] in distilled water and 1% [w/v] sulphanilamide in 5% [v/v] phosphoric acid [Sigma]). Set up sodium nitrite doubling dilutions for a standard curve starting with 1 mM nitrite.
4. Measure the absorbance at 550 nm and express the results as NMMA inhibitable accumulation of nitrite per 10^6 cells.

3. Cytokines

Murine Mϕ secrete a wide range of cytokines *in vitro* and *in vivo*. It is possible to assay cytokine concentrations both from serum and from culture supernatant. Cytokines may be assayed by use of bioassay, by ELISA or by intracellular cytokine staining and flow cytometry. ELISA and intracellular cytokine assays are described elsewhere in this volume and in detail on BD Biosciences web site (http://www.bdbiosciences.com/support/resources/cytokines/index.jsp#search=intracellular cytokine assays). A protocol for the measurement of bioactive TNF-α is given below as an example of a bioassay, where L929 cells are target cells susceptible to lysis when TNF-α reaches a critical concentration.

TNF-α bioassay

L929 cell culture

1. Grow L929 cells in Eagle's minimum essential medium (EMEM) or DMEM containing 24 mM HEPES <5% FCS at pH 7.4. It is important to split cultures frequently from a non-confluent status and change the medium every 3–4 days.
2. Use PBS to wash the cultures and incubate with 0.01% trypsin at 10 mM EDTA in PBS to detach the cells before harvesting using centrifugation.

L929 cytotoxic assay

1. Detach the L929 cells from a semi-confluent status and resuspend in assay medium at 4×10^4 cells in 100 µl medium in all wells of a 96-well plate except row 1, A–D (blanks). Incubate the cells for 18–20 h at 35°C in 5% CO_2.
2. Aspirate the culture medium and replace it in all wells with 100 µl assay medium, which contains culture medium supplemented with penicillin and streptomycin. Also include 1 µg/ml actinomycin D.
3. In wells A2–A11, add 50 µl of the samples to be tested and 50 µl of medium containing 2 µg/ml actinomycin D. Add 50 µl of recombinant TNF-α 10 ng/ml (AbD Serotec) to well A12. Double dilute down the plate with an eight-channel pipette from row A to H and discard the last 100 µl.

F. Fusion Assays

The fusion of Mϕ lead to the formation of multinucleated giant cells and osteoclasts (Helming and Gordon, 2009). The molecular mechanisms of fusion are poorly understood, though recent advances have shown roles for RANKL, M-CSF, CD36, DAP12 and STAT6 signalling (Helming and Gordon, 2007, 2008; Helming *et al.*, 2009). A simple fluorescent microscopic method has been developed to quantify Mϕ fusion. Basically, Mϕ that have been labelled with one of two different colours of fluorescent tracers, e.g. PKH26 and CFSE, are co-incubated in the presence or absence of cytokines known to promote fusion, such as IL-4. The level of fusion can then be measured microscopically by counting the number of cells where the two tracers colocalize (Helming and Gordon 2007).

♦♦♦♦♦♦ V. CONCLUSION

The assays described here will enable investigators to isolate various Mϕ populations from the mouse and measure their functions in a range of simple assays. The choice of populations is an important part of the experimental design. Table 1 shows that the cellular phenotype can vary widely according to stimulus, even when the cells are isolated from the same site. Cell surface receptors expressed on

different Mϕ populations can be recognized using a variety of different surface markers (Table 2). The mouse represents an important source of primary cells for use in studying the cellular response to micro-organisms. The development of transgenic and gene knockout mice has provided new tools for the study of the role of, for example, cell surface receptors or cytokines in the binding, uptake and killing of microbial pathogens. In addition, rapid progress is now being made in elucidating the molecular biology underlying many aspects of function. Further investigation using new tools will hopefully enhance our understanding and characterization of the host–pathogen relationship.

♦♦♦♦♦♦ VI. SUPPLIERS

AbD Serotech Ltd
MorphoSys UK Ltd, Endeavour House, Langford Business Park, Langford Lane, Kidlington, Oxford, OX5 1GE, UK
Tel: +44-1865-852-700
Fax: +44-1865-852-739
Primary antibodies

BD Biosciences
1 Becton Drive, Franklin Lakes, New Jersey 07417, USA
Tel: +1-201-847-6800
Antibodies, ELlSA kits, other imrnunochemical reagents, thiogiycollate broth, LPS and bacterial culture medium

Bio-Rad Laboratories
2000 Alfred Nobel Drive, Hercules, CA 94547, USA
Tel: +1-510-741-1000
Fax: +1-510-741-5800
Biogel polyacrylamide beads

E-Y Laboratories
107 N. Amphlett Blvd, San Mateo, CA 94401 USA
Tel. +1-650-342-3296
Fax. +1-650-342-2648
Mannosylated ligands

Invitrogen
1600 Faraday Avenue, PO Box 6482, Carlsbad, California 92008
Tel: +1-760-603-7200
Fax: +1-760-602-6500
Fluorescent tracers and culture medium

Jackson Immunoresearch Laboratories
872 West Baltimore Pike, PO Box 9, West Grove, PA 19390, USA
Tel: +1-215-367-5296
Fax: +1-215-869-0171
Secondary antibodies

Nycomed Pharma
Leutschenbachstr. 95, CH-8050 Zurich, Switzerland
Tel: +41-44-555-1000
Nycoprep for PBMC preparation

Ribi lmmunochem Research
553 Old Corvalis Road, Hamilton, MT 59840, USA
Tel: + 1-406-363-6214
Fax: + 1-406-363-6129
Bacterial products (C. *parvum)*

Sigma-Aldrich
St. Louis, MO, USA
Phone: +1-314-771-5765
Fax: +1-314-771-5757
General chemicals

Thermo Fisher Scientific
75 Panorama Creek Drive, Rochester, NY 14625, USA
Phone: + 1-800-625-4327
Fax: + 1-585-586-8987
Plasticware

Vector Laboratories
30 lngold Road, Burlinghame, CA 940 10, USA
Tel: + 1-415-697-3600
Fax: + 1-415-697-0339
lrnmunohistochemical reagents

References

Antoni, A., Graham, L. H., Rauch, J. and Levine, J. S. (2009). Altered cell-cell and cell-matrix interactions in the development of systemic autoimmunity. *Autoimmunity* **42**, 278–281.

Austyn, J. M. and Gordon, S. (1981). F4/80, a monoclonal antibody directed specifically against mouse macrophages. *Eur. J. Immunol.* **11**, 805–815.

Baorto, D. M., Gao, Z., Malaviya, R., Dustin, M. L. *et al*. (1997). Survival of FimH-expressing enterobacteria in macrophages relies on glycolipid traffic. *Nature* **389**, 636–639.

Brown, G. and Gordon, S. (2001). A new receptor for β-glucans. *Nature* **413**, 36–37.

Cooper, S. H. and Broxmeyer, H. E. (2001). Measurement of interleukin 3 and other hematopoietic cytokines, such as GM-CSF, G-CSF, M-CSF, erythropoietin, steel factor, and Flt-3 ligand. *Curr. Protoc. Immunol.* Chapter 6:Unit 6.4.

Crocker, P. R. and Gordon, S. (1985). Isolation and characterisation of resident stromal macrophages and hematopoietic cell clusters from mouse bone marrow. *J. Exp. Med.* **162**, 993–1014.

Dancz, C. E., Haraga, A., Portnoy, D. A. and Higgins, D. E. (2002). Inducible control of virulence gene expression in Listeria monocytogenes: temporal requirement of listeriolysin O during intracellular infection. *J. Bacteriol.* **184**, 5935–5945.

Elias, A. and Tsourkas, A. (2009). Imaging circulating cells and lymphoid tissues with iron oxide nanoparticles. *Hematology Am. Soc. Hematol. Educ. Program.*, 720–726.

Ezekowitz, R. A. B., Austyn, J., Stahl, P. and Gordon, S. (1981). Surface properties of Bacillus-Calmette-Gugrin-activated mouse macrophages. Reduced expression of mannose-specific endocytosis, Fc receptors, and antigen F4/80 accompanies induction of Ia. *J. Exp. Med.* **154**, 60–75.

Ezekowitz, R. A. B. and Gordon, S. (1982). Down regulation of mannosy receptor mediated endocytosis and antigen F4/80 in Bacillus-Calmett-Guerin-activated mouse macrophages. Role of T lymphocytes and cytokines. *J. Exp. Med.* **155**, 1623–1637.

Fauve, R. M., Jusforgues, H. and Hevin, B. (1983). Maintenance of granuloma macrophages in serum-free medium. *J. Immunol. Methods* **64**, 345–351.

Fraser, I., Hughes, D. and Gordon, S. (1993). Divalent cation-independent macrophage adhesion inhibited by monoclonal antibody to murine scavenger receptor. *Nature* **364**, 343–346.

Gordon, S. (1986). Biology of macrophages. *J. Cell Sci. Suppl.* **4**, 267–286.

Gordon, S. (2001). Mononuclear phagocytes in immune defence. In: *Immunology* (I. Roitt, J. Brostoff, and D. Male eds), Chapter 9, pp. 1–13. Mosby, London.

Gordon, S. (2009). Monocyte/macrophages in innate immunity. In: *Innate Immunity: Host Recognition and Response in Health and Disease, The Biomedical & Life Sciences Collection* (S. Gordon ed), Henry Stewart Talks Ltd, London, (online at http://www.hstalks.com/?t=BL0612130-Gordon).

Gordon, S. and Rabinowitz, S. (1989). Macrophages as targets for drug delivery. *Adv. Drug Deliv. Rev.* **4**, 27–47.

Gordon, S. and Taylor, P. R. (2005). Monocyte and macrophage heterogeneity. *Nat. Rev. Immunol.* **5**, 953–964.

Gough, P. J., Gordon, S. and Greaves, D. R. (2001). The use of human CD68 transcriptional regulatory sequences to direct high-level expression of class A scavenger receptor in macrophages *in vitro* and *in vivo*. *Immunology* **103**, 351–361.

Helming, L. and Gordon, S. (2007). Macrophage fusion induced by IL-4 alternative activation is a multistage process involving multiple target molecules. *Eur. J. Immunol.* **37**, 33–42.

Helming, L. and Gordon, S. (2009). Molecular mediators of macrophage fusion. *Trends. Cell Biol.* **19**, 514–522.

Helming, L., Tomasello, E., Kyriakides, T. R., Martinez, F. O., Takai, T., Gordon, S. and Vivier, E. (2008). Essential role of DAP12 signaling in macrophage programming into a fusion-competent state. *Sci. Signal.* **1**, ra11.

Helming, L., Winter, J. and Gordon, S. (2009). The scavenger receptor CD36 plays a role in cytokine-induced macrophage fusion. *J. Cell. Sci.* **122**, 453–459.

Hume, D. A. and Gordon, S. (1983). Optimal conditions for proliferation of bone marrow-derived mouse macrophages in culture: the roles of CSF-I, serum, Ca2+, and adherence. *J. Cell. Physiol.* **117**, 189–194.

Hume, D. A., Summers, K.M., Raza, S., Baillie, J. K. and Freeman, T. C. (2010). Functional clustering and lineage markers: insights into cellular differentiation and gene function from large-scale microarray studies of purified primary cell populations. *Genomics*. **95**, 328–338.

Johnson, R. B. J., Godzik, C. A. and Cohn, Z. A. (1978). Increased superoxide anion production by immunologically activated and chemically elicited macrophages. *J. Exp. Med.* **148**, 115–127.

Koren, H. S., Handwerger, B. S. and Wunderlich, J. R. (1975). Identification of macrophage-like characteristics in a cultured murine tumor line. *J. Immunol.* **114**, 894–897.

Leijh, P. C. J., Van Furth, R. and Van Zwet, T. L. (1986). *In vitro* determination of phagocytosis and intracellular killing by polymorphonuclear and mononuclear phagocytes. In: *Handbook of Experimental Immunology* (D. M. Weir, ed), pp. 46.1–46.21. Blackwell Scientific, Oxford.

Lin, H. H., Faunce, D. E., Stacey, M., Terajewicz, A., Nakamura, T., Zhang-Hoover, J., Kerley, M., Mucenski, M. L., Gordon, S. and Stein-Streilein, J. (2005). The macrophage F4/80 receptor is required for the induction of antigen-specific efferent regulatory T cells in peripheral tolerance. *J. Exp. Med.* **201**, 1615–1625.
Martinez, F. O., Gordon, S., Locati, M. and Mantovani, A. (2006). Transcriptional profiling of the human monocyte-to-macrophage differentiation and polarization: new molecules and patterns of gene expression. *J. Immunol.* **177**, 7303–7311.
Martinez, F. O., Helming, L. and Gordon, S. (2009). Alternative Activation of Macrophages: an Immunologic Functional Perspective. *Annu. Rev. Immunol.* **27**, 451–483.
McKnight, A. J., MacFarlane, A. J., Dri, P., Turley, L. and Gordon, S. (1996). Molecular cloning of F4/80, a murine macrophage-restricted cell-surface glycoprotein with homology to the G-protein linked transmembrane 7 hormone receptor family. *J. Biol. Chem.* **271**, 486–489.
Morris, L., Crocker, P. R. and Gordon, S. (1988). Murine fetal liver macrophages bind developing erythroblasts by a divalent cation-dependent hemagglutinin. *J. Cell Biol.* **106**, 649–656.
Mosser, D. M. and Edwards, J. P. (2008). Exploring the full spectrum of macrophage activation. *Nat. Rev. Immunol.* **8**, 958–969.
Nathan, C. and Shiloh, C. U. (2000). Reactive oxygen and nitrogen intermediates in their relationship between mammalian hosts and microbial pathogens. *Proc. Natl. Acad. Sci. U.S.A.* **97**, 8841–8848.
Neyen, C., Plüddemann, A., Roversi, P., Thomas, B., Cai, L., van der Westhuyzen, D. R., Sim, R. B. and Gordon, S. (2009). Macrophage scavenger receptor A mediates adhesion to apolipoproteins A-I and E. *Biochemistry* **48**, 11858–11871.
Okamura, H., Tsutsui, H., Komatsu, T. and Kurimoto, M. (1995). Cloning of a new cytokine that induces INF-γ production by T-cells. *Nature* **378**, 88–91.
Peiser, L., Gough, P. J., Kodama, T. and Gordon, S. (2000). Macrophage class A scavenger receptor-mediated phagocytosis of Escherichia coli: role of cell heterogeneity, microbial strain, and culture conditions *in vitro*. *Infect. Immun.* **68**, 1953–1963.
Pertoft, H. and Laurent, T. C. (1977). Isopycnic separation of cells and cell organelles by centrifugation in modified colloidal silica gradients. In: *Methods of Cell Separation* (N. Catsimpoolas, ed), p. 25. Plenum Press, New York.
Plüddemann, A., Neyen, C., Gordon, S. and Peiser, L. (2008). A sensitive solid-phase assay for identification of class A macrophage scavenger receptor ligands using cell lysate. *J. Immunol. Methods* **329**, 167–175.
Rabinovitch, M. and de Stefano, M. J. (1976). Cell shape changes induced by cationic anesthetics. *J. Exp. Med.* **143**, 290–304.
Rabinowitz, S. and Gordon, S. (1991). Macrosialin, a macrophage-restricted membrane sialoprotein differentially glycosylated in response to inflammation stimuli. *J. Exp. Med.* **174**, 827–836.
Ralph, P. (1986). Macrophage cell lines. In: *Handbook of Experimental lmmunology* (D. M. Weir, ed), pp. 45.1–45.16. Blackwell Scientific, Oxford.
Ralph, P., Prichard, J. and Cohn, M. (1975). Reticulum cell sarcoma: an effector in antibody-dependent cell-mediated immunity. *J. Immunol.* **114**, 898–905.
Raschke, W. C., Baird, S., Ralph, P. and Nakoinz, I. (1978). Functional macrophage cell lines transformed by Abelson leukemia virus. *Cell* **15**, 261–267.
Root, R. K., Metcalf, J., Oshino, N. and Chance, B. (1975). Hydrogen peroxide release from human granulocytes during phagocytosis. (I) Documentation, quantitation, and some regulating factors. *J. Clin. Invest.* **55**, 945–955.
Rosas, M., Liddiard, K., Kimberg, M., Faro-Trindade, I., McDonald, J. U., Williams, D. L., Brown, G. D. and Taylor, P. R. (2008). The induction of inflammation by dectin-1 *in vivo* is

dependent on myeloid cell programming and the progression of phagocytosis. *J. Immunol.* **181**, 3549–3557.
Rosen, H. (1990). Role of CR3 in induced myelomonocytic recruitment: insights from *in vivo* monoclonal antibody studies in the mouse. *J. Leukoc. Biol.* **48**, 465–4.
Rosen, H. and Gordon, S. (1987). Monoclonal antibody to the murine type 3 complement receptor inhibits adhesion of myelomonocytic cells *in vitro* and inflammatory cell recruitment *in vivo*. *J. Exp. Med.* **166**, 1685–1701.
Rosen, H. and Law, S. K. A. (1989). The leukocyte cell surface receptor(s) for the iC3b product of complement. *Curr. Top. Microbiol. Immunol.* **153**, 99–122.
Rosen, H., Milon, G. and Gordon, S. (1989). Antibody to the murine type 3 complement receptor inhibits T lymphocyte-dependent recruitment of myelomonocytic cells *in vivo*. *J. Exp. Med.* **169**, 535–548.
Russell, D. and Gordon, S. (2009). *Phagocyte-Pathogen Interactions: Macrophages and the Host Response to Infection*, ASM Press, Washington, DC.
Saito, S. and Nakano, M. (1996). Nitric oxide production by peritoneal macrophages of *Mycobacterium bovis* BCG infected or non-infected mice: regulatory roles of T lymphocytes and cytokines. *J. Leukoc. Biol.* **59**, 908–915.
Stacey, M., Lin, H. H., Gordon, S. and McKnight, A. J. (2000). LNB-TM7, a group of seven-transmembrane proteins related to family-B G-protein-coupled receptors. *Trends Biochem. Sci.* **25**, 284–289.
Stein, M., Keshav, S., Harris, N. and Gordon, S. (1992). Interleukin 4 potently enhances murine macrophage mannose receptor activity: a marker of alternative immunologic macrophage activation. *J. Exp. Med.* **127**, 287–292.
Stuehr, D. J. and Marletta, M. A. (1987). Induction of nitrite/nitrate synthesis in murine macrophages by BCG infection, lymphokines or gamma interferon. *J. Immunol.* **139**, 518–525.
Szabó, R., Peiser, L., Plüddemann, A., Bösze, S., Heinsbroek, S., Gordon, S. and Hudecz, F. (2005). Uptake of branched polypeptides with poly[L-lys] backbone by bone-marrow culture-derived murine macrophages: the role of the class a scavenger receptor. *Bioconjug. Chem.* **16**, 1442–1450.
Taylor, P. R., Martinez-Pomares, L., Stacey, M., Lin, H. H., Brown, G. D. and Gordon, S. (2005). Macrophage receptors and immune recognition. *Annu. Rev. Immunol.* **23**, 901–944.
Thrush, M. A., Wilson, M. E. and van Dyke, K. (1978). The generation of chemiluminescence by phagocytic cells. *Methods Enzymol.* **57**, 462.
Turner, G. H., Olzinski, A. R., Bernard, R. E., Aravindhan, K., Boyle, R. J., Newman, M. J., Gardner, S. D., Willette, R. N., Gough, P. J. and Jucker, B. M. (2009). Assessment of macrophage infiltration in a murine model of abdominal aortic aneurysm. *J. Magn. Reson. Imaging* **30**, 455–460.
Virji, M., Kayhty, H., Ferguson, D. J., Alexandrescu, C. *et al*. (1991). Interactions of *Haemophilus influenzae* with cultured human endothelial cells. *Microb. Pathog.* **10**, 231–245.
Wang, G. G., Calvo, K. R., Pasillas, M. P., Sykes, D. B., Häcker, H. and Kamps, M. P. (2006). Quantitative production of macrophages or neutrophils ex vivo using conditional Hoxb8. *Nat. Methods* **3**, 287–293.
Wiese, M., Castiglione, K., Hensel, M., Schleicher, U., Bogdan, C. and Jantsch, J. (2010). Small interfering RNA (siRNA) delivery into murine bone marrow-derived macrophages by electroporation. *J. Immunol. Methods* **353**, 102–110.

11 Measuring Immune Responses *In Vivo*

Stefan Ehlers[1], Norbert Reiling[2], Christoph Hölscher[3] and Sahar Aly[4]

[1] Molecular Inflammation Medicine, University of Kiel, Kiel, Germany; [2] Microbial Interface Biology, Research Center Borstel, Borstel, Germany; [3] Infection Immunology, Research Center Borstel, Borstel, Germany; [4] Microbial Inflammation Research, Research Center Borstel, Borstel, Germany

♦♦♦

CONTENTS

♦♦♦♦♦♦ I. INTRODUCTION

When analysing the immune response during infection in human patients or in experimentally infected mice, there are two major goals: (a) to detect differences in the kinetics and magnitude of, for instance, mediator or receptor expression in individual tissues or experimental groups and (b) to define the cellular localization of this response.

The most sensitive methods involve amplification strategies of reverse-transcribed mRNAs, e.g. cytokines and chemokines [qualitative or semi-quantitative reverse transcription and polymerase chain reaction (RT-PCR)], in tissue biopsies. In some cases, it is also possible to directly measure soluble mediators in tissue homogenates by enzyme-linked immunosorbent assay (ELISA)-based systems or other cell-associated molecules by immunoblotting. These methods have the distinct disadvantage that the individual cells expressing the mRNA or protein cannot be directly identified.

Intracellular or surface fluorescence staining and flow cytometric analysis of single cell suspensions isolated from infected tissues may be used to obtain that information but is often not sensitive enough and requires *in vitro* polyclonal or

METHODS IN MICROBIOLOGY, VOLUME 37
0580-9517 DOI 10.1016/S0580-9517(10)37011-5

antigen-specific restimulation of *ex vivo* isolated cell populations to boost protein expression.

The standard procedure to allow detection of molecules associated with individual cells within structurally intact tissue is immunohistochemistry which may also be employed to gather information on the physiology of the tissue environment (e.g. hypoxia).

Most often, a combination of the approaches outlined in this chapter will lead to a more complete picture of the nature of the infection-induced immune response.

♦♦♦♦♦♦ II. *EX VIVO* mRNA ANALYSIS BY REAL-TIME PCR

A. General Precautions

When working with RNA, every attempt should be made to keep reagents and utensils RNAse-free. This involves making buffers and stock reagents with diethylpyrocarbonate (DEPC)-treated water, double-autoclaving all utensils and using disposable articles wherever possible. Gloves must be worn at all times and should be frequently changed. As long as you work with RNA, keep all solutions, tubes, etc., on ice. It is useful to clean bench surfaces routinely with bleach solutions or commercial RNAse destroying agents such as RNAse off (TaKaRa).

Harvesting tissues

1. Remove tissues to be analysed under aseptic conditions. In kinetic studies, it is useful to always sample the same part of the organ, e.g. upper right liver lobe, lower left lung lobe. The size of the removed tissue should be roughly the same throughout the course of the experiment.
2. Place samples immediately into chilled lysis buffer (approx. 1 ml per 10–100 mg of tissue):
   - 4 M Guanidine isothiocyanate (Merck)
   - 25 mM Sodium citrate (pH 7)
   - 0.5% *N*-Lauroylsarcosine (Sigma)
   - 100 mM 2-Mercaptoethanol

   Alternatively, commercially available lysis buffers may be used, e.g. Trizol (Invitrogen) or TriFast FL (PeqLab).
3. Samples can now be snap frozen on liquid nitrogen and stored at –70°C until homogenization.
4. Alternatively, samples can now be homogenized using either an ultra-turrax at full speed or teflon pestles and tight-fitting glass tubes. Use appropriate biosafety hoods when homogenizing infectious tissue. If you must reuse homogenizing tools, rinse at full speed (a) for 10 s in a beaker

containing a large volume of distilled water, (b) for 10 s in a beaker containing a large volume of 95% ethanol, (c) in lysis buffer, before additional tissue is homogenized.
5. After homogenization, store 500 µl aliquots in Eppendorf tubes for multiple work-ups. Mark tubes with indelible ink writers. Homogenized tissues in lysis buffer can be stored at –70°C indefinitely.

An alternative to commercially available RNA isolation kits (e.g. High Pure RNA Tissue Kit, Roche Applied Science) is the following procedure.

Preparation of RNA

1. Add 100 µl of chloroform to the tissue homogenates in lysis buffer (TriFast, 500 ml).
2. Vortex for 15 s. Allow to sit at room temperature for 3–10 min.
3. Centrifuge at 12,000 × *g* for 5 min at 4°C.
4. In steps of 100 µl each, remove aqueous supernatant to another labelled tube; take care not to disturb the interface.
5. Add an equal volume of redistilled, in TE buffer, equilibrated phenol: chloroform: isoamyl alcohol (25:24:1, pH 7.5–8.0; e.g. Roti®-Phenol/ Chloroform/Isoamyl alcohol, Carl Roth KG) and vortex.
6. Centrifuge at 12,000 × *g* for 10 min at 4°C.
7. Repeat steps 4, 5 and 6 once.
8. Add 250 µl chilled isopropanol per 500 µl TriFast, vortex and incubate for 5–15 min at room temperature.
9. Centrifuge at 12,000 × *g* for 10 min at 4°C.
10. The RNA pellet should be white–translucent.
11. Remove isopropanol and wash pellet with 1 ml 75% ethanol.
12. Centrifuge at 12,000 × *g* for 10 min at 4°C.
13. Repeat steps 11 and 12 once.
14. Remove ethanol entirely and let the pellet dry shortly for 5–10 min. Resuspend in 100 µl DEPC-treated water.
15. Store RNA at –80°C.
16. To determine the concentration of nucleic acid in your sample, measure O.D. 260/280 ratio in a 1:100 dilution. 1 mg RNA has an O.D. reading of 1.0 at 260 nm. (To calculate the concentration of RNA in µg/ml: O.D. reading × dilution factor × 40.) You may wish to check the integrity of your RNA on a formaldehyde gel at this point. Alternatively, RNA concentration and quality can be determined using a specific spectrophotometer (NanoDrop ND-1000, PEQLAB).

♦♦♦♦♦♦ III. *EX VIVO* REVERSE TRANSCRIPTION OF mRNA AND POLYMERASE CHAIN REACTION USING CYTOKINE-SPECIFIC PRIMERS

A. General Precautions

Cross-contamination is the biggest problem in all PCR procedures, and great care should be taken to avoid contamination of test samples with extraneous sources of DNA. Therefore, only use aerosol-resistant pipette tips, keep separate pipetors for reagents and stock solutions and use separate pipetors for PCR and RNA work. It helps to aliquot source reagents in a room far away from where RNA extraction and PCR are performed, and RNA work-up and PCR pipetting should be performed in separate rooms as well. Most importantly, pipetting amplicons (i.e. for electrophoresis) should be carried out with a set of altogether different pipetors (preferably old and used ones, so that nobody else uses them) and in a completely different room from the rest. If contamination has occurred, it helps to clean surfaces and pipetors with a solution of 0.1 N HCl.

For RT of RNA, commercial RT-Kits (e.g. Transcriptor High Fidelity cDNA Synthesis Kit, Roche Applied Science) give reliable results, but a cost-effective alternative is the following protocol.

Reverse transcription

1. Add 1–5 μg of RNA to an Eppendorf tube, add 1 μl (0.2 μg) of Random hexamer primer (100 μM, Fermentas) and fill up the volume to 12.5 μl with RNAse-free water. Be careful not to use too much RNA in the RT reaction.
2. Denature the mixture at 65°C for 5 min, then place on ice.
3. Prepare RT mix as follows (per reaction). Prepare mix for $n+2$ samples):
   - 5× reaction buffer 4 μl
   - dNTPs (10 mM) 2 μl
   - RiboLock Ribonuclease Inhibitor (40 U/μl, Fermentas) 0.5 μl
   - RevertAid H Minus M-MuLV Reverse Transcriptase (200 U/μl, Fermentas) 1 μl
4. Add 7.5 μl of the RT mix to the RNA-Random hexamer mixture, vortex, spin down and incubate for 10 min at 25°C. Subsequently incubate at 42°C for 1 h.
5. Stop the reaction by incubating at 70°C for 10 min. Add 180 μl DEPC-treated water. cDNA may be stored at –20°C indefinitely or for up to 2 weeks at 4°C.

B. Qualitative PCR

For PCR primer selection, remember that primers should be complementary to sequences in separate exons or should span exon–exon boundaries to be mRNA/

cDNA specific. Primers should be checked for unique complementarity using a computer-assisted search (Lasergene, DNAStar); for most purposes, annealing temperatures around or higher than 60°C will guarantee specificity. The 'Universal Probe Library Assay Design Center' of 'Roche Applied Science' is a very helpful web-based tool to select intron-spanning primers in different species. It is in particular useful for real-time PCR primers (see below).

Polymerase Chain Reaction

1. For each PCR, add to one tube:
   - dNTPs (10 mM) 0.5 µl
   - $MgCl_2$ (50 mM) 1.25 µl
   - Water 10.75 µl
   - 10× buffer 2.5 µl
   - Taq polymerase (5 U/ml; preferably HotStart) 0.1 µl
   - Primers (mix of sense and anti-sense), (1 µM) 5 µl
   - cDNA 5 µl
2. It is best to first put 5 µl of each primer mix to the bottom of the tube, then make a mix of the other PCR reagents for all reactions and vortex thoroughly. Add 20 µl of this reaction mix to the side of each tube.
3. If you wish to perform a PCR for different cDNA samples at the same time, first put 5 µl of primer mix to the PCR tubes, then make PCR mix leaving out the cDNA, add 20 µl of the reaction mix to one side of the tube and 5 µl of the cDNA to the other side. After closing and numbering the tubes, spin briefly to make sure all reagents mix at the bottom of the tube.
4. Prepare a chart to identify tube numbers with primer and cDNA contents.

A typical protocol consists of 25–30 cycles
- 95°C for 45 s (to denature dsDNA)
- 60°C for 45 s (to let cDNA and primer sets anneal)
- 72°C for 30 s (to allow for elongation of strands by the Taq polymerase)

Electrophoresis and detection of PCR products

1. Prepare 1.5% agarose gel in 0.5× TBE buffer. (You may add 0.5 µl/ml ethidium bromide at this point to visualize amplicons on a UV tray during electrophoresis, but a more even staining of the gel is obtained when soaking the gel after electrophoresis in 0.5× TBE containing 0.5 µl/ml ethidium bromide.)
2. Add 5 µl of 5× loading buffer to each well of a microtitre plate.
3. Remove 15–20 µl of PCR solution, mix with loading buffer in the wells and add to individual slots in the gel. (You may use less PCR solution if you want to perform additional studies on your amplicon. A suitable control for the specificity of your amplicon involves a restriction enzyme digest of the

PCR product resulting in the predicted pattern of bands after electrophoresis.)
4. Add molecular weight markers to first and last rows. If you have many samples, it is useful to double-comb the gels.
5. Run at 120 V for approx. 2–3 h, until dye front reaches bottom end of the gel.
6. Use any form of photodocumentation to visualize bands on a UV transilluminator (Figure 1).

C. Semi-quantitative PCR

The purpose of semi-quantitative RT-PCR is to compare RNA samples from different sources for their relative content of specific mRNAs. Since no absolute quantitation is involved, no 'absolute' calibration using *in vitro* synthesized RNA is necessary. However, only cDNAs normalized for content of housekeeping genes [i.e. β2-microglobulin or hypoxanthine phosphoribosyltransferase (HPRT)] may be directly compared with one another.

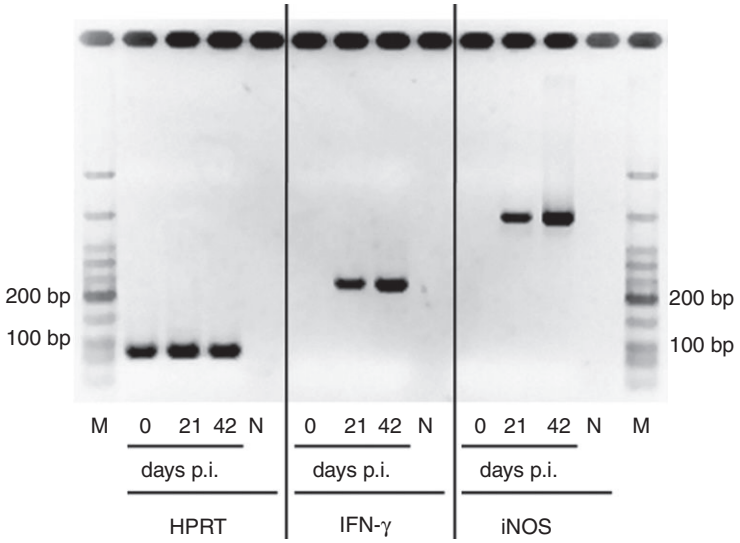

Figure 1. Qualitative analysis of IFN-γ-, iNOS- and HPRT mRNA expression levels in lung homogenates of *Mycobacterium tuberculosis (Mtb)*-infected mice. RNA was isolated from lung homogenates of *Mtb*-infected mice on day 21 (d21) and 42 (d42) post-infection and compared to uninfected mice (d0) according to the protocol. After RT mRNA expression of IFN-γ and iNOS were analysed. A PCR for HPRT was done to analyse a constitutively expressed housekeeping gene. The PCR was performed using a Hot-start–Taq using a SYBR Green master mix using the following conditions. 95°C (10 s), 60°C (10 s), 72°C (12 s) for 35 cycles on the LightCycler 480 II System. Subsequently aliquots of the PCR reaction were mixed with 5× loading buffer and loaded on a 2% agarose gel and run for 90 min. M = Molecular weight maker (Low Molecular Weight DNA Ladder, New England Biolabs). Whereas comparable levels of HPRT are detectable in all samples, IFN-γ and iNOS transcripts are only detectable after infection with *Mtb*. This approach allows a rough estimate of whether a gene is highly expressed or not.

D. Real-Time PCR

There are a number of instruments on the market capable of performing real-time PCR. These machines monitor the fluorescence emitted during the reaction as an indicator of amplicon production during each PCR cycle as opposed to the end point detection in conventional quantitative PCR protocols, such as by gel electrophoresis. The real-time RT-PCR does not detect the size of the amplicon and thus does not allow the differentiation between DNA (e.g. primer–dimer) and cDNA amplification. Real-time PCR quantification eliminates post-PCR processing of PCR products which helps to increase throughput and reduce the potential for 'carryover contamination'. In comparison to conventional RT-PCR, real-time PCR offers a much wider dynamic range of up to 10^7-fold compared with 1000-fold in conventional RT-PCR.

The real-time PCR is based on the detection and quantification of a fluorescent reporter. The signal increases in direct proportion to the amount of PCR product in a reaction. By recording the amount of fluorescence emission (by means of a CCD camera or a photomultiplier) at the end of each cycle, it is possible to monitor the PCR reaction online during the exponential phase. Quantification is based on the threshold cycle (C_t), defined as the cycle number at which the fluorescence (and thus the PCR product) becomes first detectable above background noise. The C_t value can then be translated into a quantitative result by constructing a standard curve. Standard curves using fluorescence are easily generated due to the linear response over a wide dynamic range. The standard curve of a gene 'A' (e.g. a cytokine gene) is generated by plotting individual C_t values of a series of dilutions of an equivalent mixture of the different samples (i.e. *X* and *Y*) against the logarithm of the corresponding volumes. The ratio of expression between the two samples *X* and *Y* is then calculated from the linear regression of that standard curve. The same calculations as for 'A' must be performed for a housekeeping gene (e.g. HPRT) in order to normalize for differences in the amount of total RNA starting material. (Most proprietary softwares that can be obtained for commercial real-time PCR instruments will perform these calculations automatically; see example in Figure 2.) Our own experience studying gene expression in both murine and human immune cells (B and T lymphocytes, monocytes and epithelial cells) shows that the use of HPRT as housekeeping gene is particularly suitable when normalizing for RNA content in these cell types.

There are two general methods for the quantitative detection of the amplicon: fluorescence probes (TaqMan probes, molecular beacons) and DNA-binding agents (SYBR Green). TaqMan probes make use of labelled oligonucleotide probes and a 5′ nuclease PCR assay to generate a fluorescent signal during PCR. In this approach, a specific oligo probe is used with a reporter and a quencher dye attached. During the PCR reaction, the probe is cleaved by the 5′ nuclease activity of the Taq DNA polymerase, separating the reporter dye from the quencher dye. This generates a sequence-specific fluorescent signal that increases with each cycle.

Molecular beacons also contain fluorescent and quenching dyes at either end, but they are designed to adopt a hairpin structure while free in solution to bring the

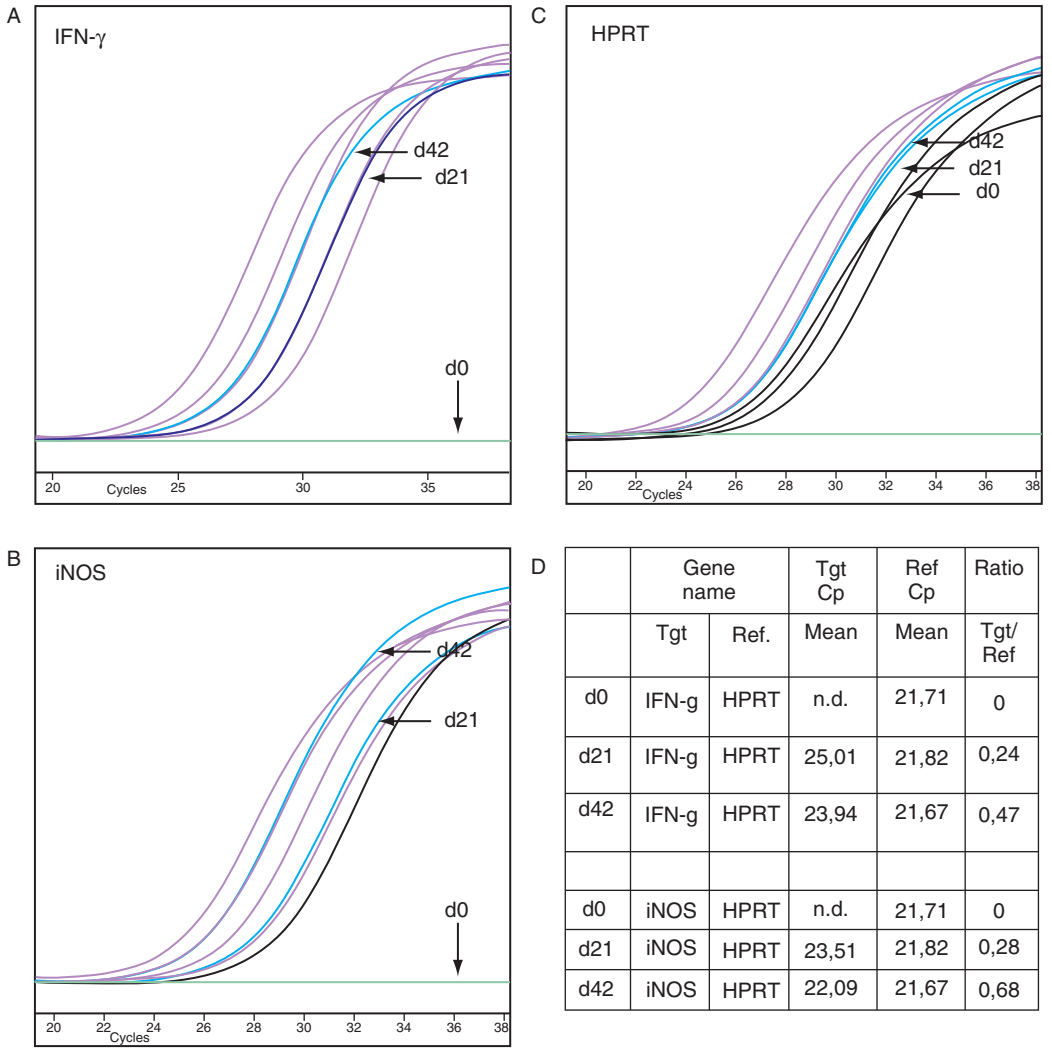

D

	Gene name		Tgt Cp	Ref Cp	Ratio
	Tgt	Ref.	Mean	Mean	Tgt/ Ref
d0	IFN-g	HPRT	n.d.	21,71	0
d21	IFN-g	HPRT	25,01	21,82	0,24
d42	IFN-g	HPRT	23,94	21,67	0,47
d0	iNOS	HPRT	n.d.	21,71	0
d21	iNOS	HPRT	23,51	21,82	0,28
d42	iNOS	HPRT	22,09	21,67	0,68

Figure 2. Analysis of mRNA expression of IFN-γ-, iNOS- and HPRT mRNA expression levels in lung homogenates of *Mtb*-infected mice using quantitative real-time PCR. The formation of the PCR products shown in Figure 1 was analysed online during the run using the LightCycler 480 II System [IFN-γ (A), iNOS (B) and HPRT (C)] using the LC480 software (Release 1.5.0). For quantification, serial dilutions of a lung homogenate from *Mtb*-infected mice served as a standard (red lines) and were run in parallel. The amplification curves for IFN-γ, iNOS and HPRT on day 0, 21 and 42 of the samples are depicted in blue. Quantifiable data of the PCR are shown in (D). The software calculates the ratio of the target and the reference gene from the C_p values of the distinct curves. Based on the standard curve for all three genes the relative expression levels of IFN-γ and iNOS were related to HPRT. Interpretation: iNOS and IFN-γ levels show an approximate twofold increase between d21 and d42. Since no IFN-γ and iNOS were detectable on day 0, the massive increase from d0 to d21 cannot be quantified. (See color plate section).

fluorescent dye and the quencher into close proximity. The close proximity of the reporter and the quencher in this hairpin configuration suppresses reporter fluorescence. When the beacon (specific oligo probe) hybridizes to the target during the

annealing step, the reporter dye is separated from the quencher and the reporter fluoresces. Molecular beacons remain intact during PCR and must rebind to their target every cycle for fluorescence emission. Both TaqMan probes and molecular beacons allow detection of multiple DNAs ('multiplex PCR') by use of different reporter dyes on different probes/beacons.

DNA dye-binding assays are the cheapest option for performing real-time RT-PCR assays, as they do not require an amplicon-specific probe (which can make gene expression profiling experiments in immunology very costly). SYBR Green is a minor groove binding dye which does not bind single-stranded DNA. The major problem with SYBR Green is that non-specific amplicons cannot be distinguished from specific ones. The primers shown in Table 1 (left side) have therefore been extensively tested for non-specific amplification and primer–dimer complex formation and are suitable for a broad range of applications in immunology of infection.

The Universal ProbeLibrary (UPL; www.universalprobelibrary.com) combines the flexibility, availability and convenience of SYBR Green I assays with the specificity of hydrolysis probe assays. The unique combination of online available assay design software and 165 pre-validated, real-time PCR probes allows quantitation of virtually any mRNA in the transcriptomes of a large number of organisms. The UPL-based real-time PCR assay (*Taq*Man® assay, Roche Applied Science) uses chemically modified probes composed of eight to nine nucleotides [locked nucleic acids (LNA)] to guarantee the specificity of the PCR reaction (see examples in Table 1, right side). These LNA probes contain two labels, a fluorescence reporter and a fluorescence quencher, in close proximity to each other and are used along with gene-specific primers. The assay is based on the principle that an LNA probe specifically bound to template DNA is cleaved through 5′ nuclease activity of the *Taq*Man® DNA polymerase during PCR amplification. When excited, cleaved fluorescence reporter-labelled nucleotides of the LNA probe emit a fluorescent signal that which is quantified.

E. Primers for SYBR Green Real-Time RT-PCR

When searching primers on the computer (several software packages are commercially available which provide reasonable results), the following parameters are recommended:

- Primer length: 17–24 bp
- Primer melting temperature: 52–65°C
- 'Optimal' annealing temperature: 54, 58 or 60°C

F. Product Length

The optimal amplicon length is less than 100 bp. It is recommended to generate amplicons no longer than 90–150 bp, but a product length of up to 250 bp may give good results. Shorter amplicons amplify more efficiently than longer ones and are more robust towards reaction conditions.

Table 1. Primers validated for SYBR Green- and UPL- Probe based real-time PCR

SYBR Green based RT-PCR				UPL-Probe-based RT-PCR			
5′ primer	3′primer	bp	Gene	5′ primer	3′primer	bp	UPL No.
gca gca gcc tcc tag cct ttg tgg	ttg gca tgg ggt ttc gag ttc ctg	273	**EBI-3**	tct ctg atg ggt cac taa ctc g	gct tag agc cac gag agc tg	131	#21
gca gta cag ccc caa aat gg	aac aaa gtc tgg cct gta tcc aa	84	**HPRT**	tcc tcc tca gac cgc ttt t	cct ggt tca tca tcg cta atc	90	#95
caa cca aca agt gat att ctc cat g	gat cca cac tct cca gct gca	151	**IL-1β**				
			IL-2	tac agc gga agc aca gca	atc ctg ggg agt ttc agg tt	129	#1
cat cgg cat ttt gaa cga g	acg ttt ggc aca tcc atc tc	85	**IL-4**	cat cgg cat ttt gaa cga g	cga gct cac tct ctg tgg tg	104	#2
gca aaa caa cgg gat gca ga	tgt gac cta caa gga acc ca	216	**IL-4R**	gag tgg agt cct agc atc acg	cag tgg aag gcg ctg tat c	66	#11
aca ttg acc gcc aaa aag ag	atc cag gaa ctg cct cgt c	62	**IL-5**				
gag gat acc act ccc aac aga cc	aag tgc atc atc gtt gtt cat aca	141	**IL-6**	tct aat tca tat ctt caa cca aga gg	tgg tcc tta gcc act cct tc	119	#78
cct ggc tca gca ctg cta t	gct ctt att ttc aca ggg gag aa	404	**IL10**	cag agc cac atg ctc cta ga	tgt cca gct ggt cct ttg tt	79	#41
cct ctg acc ctt aag gag ctt at	cgt tgc aca ggg gag tct	70	**IL-13**	cct ctg acc ctt aag gag ctt at	cgt tgc aca ggg gag tct	70	#17
act ggc tat tct ttg gag ata aaa gt	aac caa gta atc cag gat cca a	73	**IL-13Rα2**				
gat gac atg gtg aag acg gcc	gga ggt ttc tgg cgc aga gt	400	**IL-12p35**	cca tca gca gat cat tct aga caa	cgc cat tat gat tca gag act g	77	#49
ctg gcc agt aca cct gcc ac	gtg ctt cca acg cca gtt ca	384	**IL-12p40**	atc gtt ttg ctg gtg tct cc	gga gtc cag tcc acc tct aca	80	#78
			IL-12Rβ1	ccc cag cgc ttt agc ttt	gcc aat gta tcc gag act gc	108	#101
ctg cac cca ctc aca tta ac	cag ttg gct ttg ccc tgt gg	652	**IL-12Rβ2**	tgt ggg gtg gag atc tca gt	tct cct tcc tgg aca cat ga	71	#12

gct cca gaa ggc cct cag a	agc ttt ccc tcc gca ttg a	142	**IL-17**				
			IL-21	gac att cat cat tga cct cgt g	tca cag gaa ggg cat tta gc	99	#27
ttt cct gac caa act cag ca	tct gga tgt tct ggt cgt ca	68	**IL-22**	ttt cct gac caa act cag ca	ctg gat gtt ctg gtc gtc ac	67	#17
tgc tgg att gca gag cag taa	gca tgc aga gat tcc gag aga	122	**IL-23 p19**				
			IL-27	gat tgc cag gag tga acc tg	cga gga agc aga gtc tct cag	114	#51
			IL-27p28	cat ggc atc acc tct ctg ac	aag ggc cga agt gtg gta	61	#38
gct ctg aga caa tga acg ct	aaa gag ata atc tgg ctc tgc	229	**IFN-γ**	atc tgg agg aac tgg caa aa	ttc aag act tca aag agt ctg agg ta	89	#21
agc tcc tcc cag gac cac ac	acg ctg agt acc tca ttg gc	482	**iNOS**	ctt tgc cac gga cga gac	tca ttg tac tct gag ggc tga c	66	#13
ctg tag ccc acg tcg tag c	ttg aga tcc atg ccg ttg	97	**TNFα**	ctg tag ccc acg tcg tag c	ttg aga tcc atg ccg ttg	97	#102
cgc ccg ggt tgt gtt ggt tgt ag	aac cgg ccc ttc ctg ctc ctc at	288	**TGFβ**	agc caa cca tgc tca act tc	ggc ttt tca gaa att agt tcc att	76	#67
tct cat cag ttc tat ggc cc	ggg agt aga caa ggt aca ac	211	**TNFα**				

G. Annealing Temperature

In order to optimize throughput, primers should be designed that give optimal results with one out of three annealing temperatures that match most of the primers used. In case sufficient amounts of product at the annealing temperature suggested by the software cannot be generated, a gradient PCR to find the most suitable temperature should be performed.

H. 5′–3′ Relation

For the SYBR Green method it is crucial not to generate non-specific PCR products (see above). To avoid these non-specific products every primer pair has to be optimized regarding its concentration. For this purpose, a so-called primer-matrix is performed in which three different concentrations (900, 300 and 50 mM) for every 5′-primer with the corresponding concentrations from the 3′-primer with and without template are tested. The appearance of non-specific amplification products in the presence and absence of template is monitored by plotting the first derivative of the melting curve. By doing this crucial optimization step, one can raise the efficiency of the reaction, which increases the difference in threshold (C_t) between the specific and non-specific amplicons.

I. Exon–Intron

One should aim to identify primers that bind to separate exons to avoid false-positive results arising from amplification of contaminating genomic DNA. Unfortunately, the genomic sequence is not known for all mRNAs. Moreover, sometimes targeting of an intron-less gene is desired. In this case the RNA may be treated with RNAse-free DNAse (DNAse I, Roche Applied Science).

J. Real-Time PCR Protocols

The methodology described here has been developed for use within a carousel-based LightCycler System and the Roche LightCycler 480 System, a high-throughput system. Both systems have a typical run time from 45 to 90 min. The formation of PCR products is monitored fluorometrically via the incorporation of SYBR Green and the hydrolysis of UPL probes, which uses chemically modified probes composed of eight to nine nucleotides (LNA).

Non–hot start, conventional SYBR Green PCR

1. This protocol makes use of a conventional, non-hot start Taq polymerase, thus it is critical to work on ice at all times. For beginners, do not use too many samples when establishing the system. Pipetting of 20–30 samples takes a long time. Due to the basal activity of the enzyme at 4°C and room

temperature unspecific amplifications are likely to occur, which may interfere with a proper PCR reaction. Open the program and have the protocol ready prior to the preparation to the PCR mix to ensure an immediate start, as soon as the cDNA has been added.

2. For a standard reaction, prepare PCR mix as follows (per reaction). Prepare mix for $n+2$ samples:

DEPC-treated water	4.60 µl
10× PCR buffer (New England Biolabs)	1.4 µl
$MgCl_2$ (50 mM)	0.7 µl
dNTP (100 mM)	0.5 µl
BSA (100 mM)	0.6 µl
5′ Primer 6.25 µM	0.4 µl
3′ Primer 6.25 µM	0.4 µl
SYBR Green 1 mM	0.2 µl
Taq DNA polymerase (New England Biolabs)	0.2 µl

3. Transfer 9 µl of the PCR mix into each capillary of the rotor or well of the 96-well plate.
4. Pipet 1 µl of the cDNA template into PCR mix.
5. Close the capillaries (or seal the plate with the foil and remove foil edges); keep the surface of the plate clean, do not touch the surface with your fingers!
6. Spin down the mixture in a centrifuge (e.g. 1200 rpm, 1 min).
7. Load the plate into LightCycler System and start run.
   PCR protocol:

[t]	[T]		
15 s	95°C	Initial denaturation	
5 s	95°C		25-30 cycles
10 s	x_1°C	Annealing	
x_2 s	72°C	Elongation	
1 s	x_3°C	Analysis	
0 s	95°C	Denaturation	
15 s	72°C	Final Elongation	
65°C to 95°C		Melting Curve	
at 0.1°C/s		(constant analysis)	

8. The x variables in the PCR protocol need to be defined as follows: x_1 depends on the primer set used (see Table 1); x_2 depends on the length of the estimated product (calculate a *Taq* synthesis rate of approx. 25 bp/s); x_3 is the temperature to quantify the product. At this temperature all potential primer–dimers, which can be seen during melting curve analysis, should have melted.

Although this protocol has led to very reproducible results, home-made mixes often work less well, as they are often not as sensitive and robust. Thus,

it is recommended to use an easy-to-use hot start reaction mix for PCR (e.g. LightCycler® 480 SYBR Green I Master, Roche). Although the costs of commercially available master mix kits are higher at first sight, the reproducibility of the experiments is substantially better and does not depend on the technical skills of single individuals (pipetting speed, temperature control).

Hot start SYBR Green PCR and UPL-Probe PCR

1. It is not necessary to work on ice. The prepared PCR mix in the plate or the capillary is stable for 24 h at room temperature. However, do protect from light.
2. For a standard reaction, prepare PCR mix as follows (per reaction). Prepare mix for $n+2$ samples (for primers see left or right side of Table 1):
   a. Hot Start *SYBR Green* PCR:
      - DEPC-treated water 2 µl
      - 5′ Primer 6.25 µM 1 µl
      - 3′ Primer 6.25 µM 1 µl
      - LC 480 SYBR Green Master (2× conc.) 5 µl

   b. Hot start *UPL Probes* PCR
      - DEPC-treated water 1.9 µl
      - 5′ Primer 6.25 µM 1 µl
      - 3′ Primer 6.25 µM 1 µl
      - LC 480 Probes Master (2× conc.) 5 µl
      - UPL probe 0.1 µl
3. Transfer 9 µl of the PCR mix into each well of the 96-well plate.
4. Pipet 1 µl of the cDNA template into PCR mix.
5. Seal the plate with the foil and remove foil edges; keep the surface of the plate clean, do not touch the surface with your fingers!
6. Spin down the mixture in a plate centrifuge (e.g. 1200 rpm, 1 min).
7. Load the plate into the LC480 System and start run.

The amounts of template (see below) and primers depend on the abundance of the gene of interest in the sample and the primer matrix. Based on the annealing temperature of selected primer pairs a parallel analysis of several genes of interest in one single run is possible. When using UPL assays, all PCRs are run with the same temperature protocol (see below).

Typical PCR Protocol: SYBR Green/UPL Probes

1. Program Name: Act (Activation of the thermostable Taq polymerase)
   Cycles: 1
   Analysis mode: None

	Target °C °C	Acquisition Mode	Hold (hh:mm:ss)	Ramp/Rate (°C/s)
SYBR/UPL	95	None	00:05:00	4.40

2. Program Name: Ampli
   Cycles: 45 (minimum)
   Analysis mode: Quantification

	Target °C	Acquisition Mode	Hold (hh:mm:ss)	Ramp/Rate (°C/s)
SYBR/UPL	95	None	00:00:10	4.40
SYBR Green	see Table 1	None	00:00:20	2.20
UPL probes	60	None	00:00:20	2.20
SYBR/UPL	72	Single	00:00:01	4.40

3. Program Name: Cool
   Cycles: 1
   Analysis mode: None

	Target °C °C	Acquisition Mode	Hold (hh:mm:ss)	Ramp/Rate (°C/s)
SYBR/UPL	40	None	00:00:30	2.20

Both protocols are identical, only the annealing temperature needs to be adapted in SYBR Green PCR reactions. It is also possible to use a two-step protocol (no extension step) with primer-specific annealing temperatures and the initial activating step only. The ramp rate specifies the rate at which the instrument heats up or cools down to the target temperature. If you transfer a protocol from a conventional PCR machine to a LightCycler, there is optimization potential by reducing the hold times and increasing the temperature ramp rates. Current technologies have significantly shortened the ramp times using electronically controlled heating blocks or fan-forced heated air flows to moderate the reaction temperature. A typical example of quantitative real-time PCR is shown in Figure 2.

Quantitation

1. Produce a standard by mixing equivalent amounts of cDNA from samples *X* and *Y*.
2. Run a real-time PCR for the cytokine gene and for the housekeeping gene HPRT with serial dilutions from the 'standard', corresponding to, e.g., 1.0–0.01 µl of the mix. Generate a standard curve by plotting C_t values obtained against the logarithm of the corresponding volume.
3. Run a real-time PCR with primers for the cytokine gene and the housekeeping gene (e.g. HPRT) for samples X and Y, always performing duplicates (better triplicates).
4. The obtained C_t values from samples X and Y for the cytokine gene and for the housekeeping gene are used to calculate a 'volume' based on the corresponding standard curve by linear regression. Normalize by dividing the 'volume' for the cytokine gene of sample X by the 'volume' of the housekeeping gene of X. Do the same for sample Y.
5. The ratio of cytokine gene expression between samples X and Y is calculated by dividing the normalized values from X and Y.

♦♦♦♦♦♦ IV. LIMITATIONS

A. Points to Remember

- Be careful to isolate sufficient amounts of good-quality RNA.
- Use a stepper for the master mix.
- Make sure that the C_t values of the samples are in the linear range of the corresponding standard.
- Always check for the presence of non-specific products (perform melting curve analysis after the PCR is complete).

Any RT-PCR measures steady-state mRNA levels, i.e. quantitative differences may only be found when there is induced/repressed transcription of mRNA or increased/repressed turnover of mRNA. Whenever the amount of cytokine secreted is highly regulated by translational modifications (as is for example the case with TNF-α and TGF-β) it may be difficult to measure mRNA differences, although at the protein level major differences are observed. It is, however, true that where there is no mRNA, there usually is no protein; thus, RT-PCR always is a good indicator what cytokine *not* to look for by ELISA in tissue homogenates or by immunohistochemical analyses.

Remember that the kinetics of induction for mRNA species vary tremendously and always precede peaks of protein production; therefore, a detailed kinetic study is often warranted to define where to best look for differences when comparing experimental settings. Always be aware that these procedures allow for the relative quantitation of mRNA for any given cytokine but do not allow for comparison of mRNA levels between different cytokines.

♦♦♦♦♦♦ V. DETERMINATION OF CYTOKINES BY CYTOMETRIC BEAD ARRAYS

Because gene expression analysis does not always reveal the bioactive form of cytokines, a quantification of protein production in serum or organ homogenates is often preferable. However, standard ELISA techniques to measure cytokine concentrations require high sample volumes and are fraught with high background noise in organ homogenates already in uninfected animals. In contrast, determining cytokine production in organ homogenates from uninfected and infected mice by a cytometric bead array (CBA) reliably yields cleaner results.

In a bead assay, one or more bead populations with discrete and distinct fluorescence intensities are used to simultaneously detect multiple cytokines in a small sample volume. The beads capture and quantify soluble analytes such as cytokines through a sandwich format. A particular analyte in the sample binds to a corresponding bead with a given fluorescence characteristic. The bead is coated with capture antibodies specific for a cytokine. A reporter antibody (different from the capture antibody) binds to the analyte. The reporter antibody is conjugated with fluorescent molecules (different colour from those used to distinguish beads). Excess reporter antibodies and cytokines are eliminated by washing.

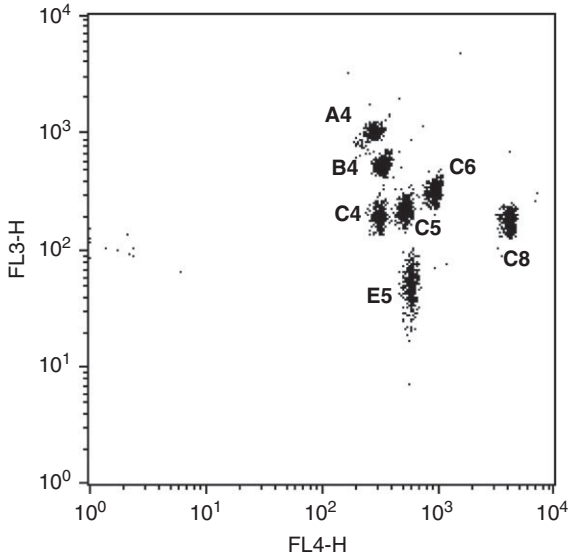

Figure 3. Cytokine-specific bead populations are distinguished by gating bead clusters. Dual-colour beads enable an accurately analysis of a maximum of 30 beads using a grid on the FL4/FL3 dotplot (A4 to E9) (an example of measuring seven cytokines is depicted). Position A4 = IFN-γ, B4 = IL-6, C4 = IL-10, C5 = IL-17A, C6 = IL-12/IL-23p40, C8 = TNF, E5 = IL-1β.

Samples are acquired with a flow cytometer and cytokine-specific bead populations are distinguished by gating bead clusters (Figure 3). By measuring the intensity of the reporter antibody fluorescence, the amount of cytokine in a given sample may be quantified when compared to standards of known concentrations.

CBA assays have the following advantages over standard ELISA techniques: low amount of sample required, multiplex analysis of many cytokines simultaneously, fast procedure, low background signals. One disadvantage is the limited choice of and high price of commercially available ready-to-use cytokine BD CBA Flex Sets™ and corresponding buffer systems. However, the development of so-called BD Functional Beads™ offers the possibility to generate an unlimited set of cytokine-coated beads in the lab.

Harvesting and processing of tissue

Materials

- Serum separator tubes (BD Bioscience)
- Proteinase Inhibitor Cocktail (Roche Applied Science)
- Ultra-turrax or glass dounce homogenizer equipped with teflon pestles and tight-fitting glass tubes

Serum preparation

For preparation of serum, collect blood from anesthetized animals, place in serum separator tube, centrifuge at 4000 × *g* for 10 min at 4°C and store at –80°C. Serum separator tubes allow for immediate processing of samples and prevent protein degradation.

Tissue homogenates

1. To assay the cytokine content in organ homogenates, remove tissue to be analysed. Weigh and place tissue in a small volume of phosphate-buffered saline (PBS) containing a proteinase inhibitor cocktail. Marginal cytokine concentrations may be detectable only in a small volume.
2. Homogenize samples in an ultra-turrax or using teflon pestles and tight-fitting glass tubes at full speed under appropriate biosafety hoods when homogenizing infectious tissue. Distribute homogenates into Eppendorf tubes.
3. Centrifuge samples at 10,000 × *g* for 5 min at 4°C.
4. Collect supernatants and store 100 µl aliquots in marked Eppendorf tubes at –80°C.

A. Preparation of Functional Beads (adapted from BD Bioscience)

1. Choosing the right antibody pair

To develop a bead-based immunoassay for cytokine detection, a matched pair of antibodies recognizing different epitopes is needed. A good starting point is to use a pair of antibodies that work in an ELISA.

It is difficult to predict which antibody out of the pair will function best as the capture antibody. If a known ELISA pair is being used, generally the capture antibody for the ELISA works best as the capture antibody with the functional beads. However, this is not always the case and some of the available antibody pairs do not work at all. Therefore, different pairs of ELISA antibodies from various suppliers should be tested. Table 2 shows already validated matched antibody pairs for the detection of cytokines using functional beads. Commercially available antibody pairs usually come with a biotinylated secondary antibody, the below introduced staining procedure is adapted to the use of biotinylated detector antibodies in a multiplex assay of functional beads.

2. Coating of functional beads with primary antibodies

In this procedure monoclonal antibodies specific for distinct cytokines are covalently linked to the surface of colour-coded functional beads using sulfo-SMCC chemistry. The presence of stabilizing proteins such as BSA or other stabilizing additives, glycine or Tris, may affect the performance of the beads after conjugation. The conjugation method will activate and bind any free

Table 2. List of validated matched antibody pairs for CBA

Cytokine	First antibody (cat #)	Second antibody (cat #)	Supplier
IFN-γ	BD OptEia Set Mouse IFN-γ (551866)		BD Bioscience
IL-4	BD OptEia Set Mouse IL-4 (551866)		BD Bioscience
IL-6	BD OptEia Set Mouse IL-6 (551866)		BD Bioscience
IL-12/IL-23p40	Purified rat-anti-mouse IL-12/IL-23p40 (551219)	Biotinylated rat-anti-mouse IL-12/IL-23p40 (554476)	BD Bioscience
IL-10	BD OptEia Set Mouse IL-10 (551866)		BD Bioscience
IL-13	BD OptEia Set Mouse IL-13 (551866)		BD Bioscience
IL-17A	Purified rat-anti-mouse IL-17A (555068)	Biotinylated rat-anti-mouse IL-17A (555067)	BD Bioscience
TGFβ	Purified rat-anti-mouse TGFβ1 (555052)	Biotinylated rat-anti-mouse TGFβ1 (555053)	BD Bioscience
TNF	BD OptEia Set Mouse TNF (558874)		BD Bioscience

amino group in the sample to the beads. For a successful conjugation, the protein needs to be suspended in PBS, pH 7.2 ± 0.2. The procedure to conjugate antibodies to functional beads described below is designed for 1000 tests and requires roughly 3.5 h.

Conjugating antibodies to beads

Materials

- Functional beads (BD Bioscience; see Table 2)
- Functional Bead Conjugation Buffer Set (BD Bioscience; coupling buffer, storage buffer)
- Purified rat anti-mouse cytokine antibody (see Table 2)
- Bio-Spin 30 Tris-Columns (Bio-Rad)
- 1M Dithiothreitol (DTT; 1.54 g DDT/ml ddH_2O, freeze aliquots at –20°C)
- Sulfosuccinimidyl 4-*N*-Maleimidomethyl cyclohexane 1-carboxylate (Sulfo-SMCC; 2 mg/ml ddH_2O, prepare always freshly and use immediately)
- *N*-Ethylmaleimide (NEM; 2 mg/ml in DMSO, freeze aliquots at –20°C)
- FACS tubes (12 × 75 mm), ultrasonic bath, orbital shaker
- Mouse/Rat Soluble Protein Master Buffer Kit
  - From BD bioscience (assay diluent, capture bead diluent, detection reagent diluent, wash buffer)
  - Self-made (assay diluent: PBS (Mg^{2+} and Ca^{2+} free), 10% heat-inactivated FCS, 0.15% Proclin-150 (Sigma); capture bead and detection reagent diluent: PBS (Mg^{2+} and Ca^{2+} free), 3% heat-inactivated FCS, 0.1% NaN_3; wash buffer: PBS (Mg^{2+} and Ca^{2+} free), 0.05% Tween-20
- Setup Beads
- PE goat anti-Rat Ig Detector (BD Bioscience)

Bead preparation

1. Vortex original vial with beads for 30 s, transfer 150 µl into screw-capped Eppendorf tubes and cover with aluminium foil.
2. Sonicate for 1 min, add 3.8 µl 1 M DTT, vortex for 5 s and incubate for 1 h at room temperature on an orbital shaker.
3. Add 1 ml coupling buffer and vortex for 5 s.
4. Centrifuge at 900 × *g* for 3 min, discard supernatants and repeat steps 3 and 4 twice.
5. Resuspend beads in 40 µl coupling buffer for 1000 tests.

Protein activation

1. Transfer 180 µg coating antibody into screw-capped Eppendorf tube wrapped in aluminium foil.
2. Prepare Sulfo-SMCC in ddH_2O at 2 mg/ml, add 4 µl to antibody, vortex for 5 s and incubate for a maximum of 1 h on an orbital shaker.

Buffer exchange in spin columns

1. Place column into FACS tube, fill with coupling buffer and let buffer completely run through; repeat twice.
2. Put column into new FACS tube and centrifuge at 1000 × *g* for 2 min.
3. Position column in new FACS tube, add the antibody Sulfo-SMCC preparation and centrifuge at 1000 × *g* for 2 min and 15 s.
4. Discard column and immediately proceed with the antibody conjugation.

Antibody conjugation

1. Transfer activated antibodies to beads, vortex for 5 s and incubate for 1 h at room temperature on an orbital shaker.
2. Add 4 µl NEM, vortex for 5 s and incubate for 15 min at room temperature on an orbital shaker.
3. Add 1 ml storage buffer and vortex for 5 s.
4. Centrifuge at 900 × *g* for 3 min, discard supernatant and repeat steps 3 and 4 three times.
5. Resuspend beads in 1 ml storage buffer and keep away from light at 4°C; conjugated beads may be stored for up to 1 year.
6. Before first use, store at least overnight at 4°C to reduce background.

3. Validation of antibody conjugation

Before using the conjugated beads in an assay, the success of the conjugation procedure should be confirmed using a FACSCalibur and a PE anti-Ig antibody that binds specifically to the antibody conjugated to the bead. A successful

conjugation normally gives a PE signal greater than 500 mean fluorescence intensity (MFI).

1. Label 3 FACS tubes with tube 1 (beads dilution), tube 2 (negative control), tube 3 (sample).
2. Vortex beads for 5 s, add 245 µl wash buffer and 5 µl beads in tube 1, and vortex 5 s.
3. Transfer 50 µl bead dilution in tube 2 and tube 3, discard tube 1.
4. Add 50 µl wash buffer to tube 2 and 50 µl PE anti-Ig antibody to tube 3.
5. Vortex for 5 s and incubate both tubes for 30 min at room temperature in the dark.
6. Add 1 ml wash buffer to each tube, centrifuge at 1000 × *g* for 5 min and discard supernatants.
7. Resuspend beads in wash buffer and measure PE intensity in a flow cytometer.
8. A MFI of the conjugated beads in tube 3 that is 500 times increased over the negative control indicates a sufficient antibody conjugation to the beads.

4. Validation of specificity

The conjugated functional beads and detector need to be tested against a standard, such as a recombinant cytokine, and against samples that contain the cytokine. It is important that your assay measures the particular molecule of interest in the same range that occurs physiologically. For most cytokine assays, the likely range of detection will be from 5000 pg/ml down to 20 pg/ml or lower.

5. Validation of linearity

Another important consideration is the linearity of the standard curve. In particular, the standard curve and the sample titration curve must be parallel to each other. This will ensure that values read at the top of the standard curve will be comparable to values read at the end. If the curves are not parallel, the results obtained for sample dilutions will not be the same across the standard curve range.

6. Multiplexing with functional beads

It is critical to confirm that functional beads perform the same way in a single bead assay as they do in a mixture. The following tests are recommended:

1. Make a mixture of all of the beads and all of the detectors. The standards for each assay are then added individually to different wells. A signal should only be seen with the correct bead.
2. A standard curve and a titration of a positive test sample should be tested with a single bead assay and with a multiplex of bead assays. The quantitation of the

test sample should be the same regardless of which other assays are being run with it.

The following protocol may be used for both, CBA Flex Sets and Functional Beads.

B. Performing a CBA

Materials

- Mouse/Rat Soluble Protein Master Buffer Kit
  - From BD bioscience (assay diluent, capture bead diluent, detection reagent diluent, wash buffer)
  - Self-made (assay diluent: PBS (Mg^{2+} and Ca^{2+} free), 10% heat-inactivated FCS, 0.15% Proclin-150 (Sigma); capture bead and detection reagent diluent: PBS (Mg^{2+} and Ca^{2+} free), 3% heat-inactivated FCS (0.1% NaN_3); wash buffer: PBS (Mg^{2+} and Ca^{2+} free), 0.05% Tween-20
- Bead sets (depending on whether commercially available CBA Flex Sets or self-made Functional Bead sets are required)
  - CBA Flex Sets (BD Bioscience)
  - Functional Bead Sets (antibody-coated Functional Beads, biotinylated rat anti-mouse cytokine, streptavidin-PE, recombinant mouse cytokine)
- 96-well U-bottomed plate

Standards

1. To prepare serial dilutions of appropriate cytokines standards, add 500 µl assay diluent into 10 Eppendorf tubes per cytokine and label tubes from 2 to 12.
2. In one additional Eppendorf tube (tube 1), prepare 1 ml recombinant cytokine standard in assay diluent at an optimal concentration ranging from 5 ng/ml to 10 ng/ml and vortex.
3. Transfer 500 µl cytokine standard from tube 1 into tube 2, vortex and prepare 1:2 dilutions.
4. Add 500 µl assay diluent into an additional tube 12 (negative control).

Bead master mix

1. Calculate the required amount of beads: number of unknown samples +12 standards and control + 2 = number of samples (e.g. for 1 plate 84 unknown samples + 12 standards and control + 2 = 98 samples).
2. Per sample, resuspend 1 µl beads that have been vortexed for 15 s in 49 µl bead dilution buffer (e.g. for 98 samples 49.00 µl beads and 4802.00 µl bead dilution buffer) and vortex.

Staining – 1st step

1. Pipet 50 µl bead master mix per sample in wells of 96-well U-bottom plate.
2. Add 50 µl standard dilutions, control and samples.
3. Mix by gentle scraping the bottom of the plate and incubate for 1 h at room temperature in the dark.

For Functional Beads: Preparation of the biotin-streptavidin PE mixes

a. Calculate the required amount of the biotin-streptavidin PE mixes: number of unknown samples +12 standards and control +2 = number of samples (e.g. for 1 plate 84 unknown samples + 12 standards and control +2 = 98 samples).
b. Per sample, resuspend 0.2 µl biotinylated secondary antibody and 0.33 µl streptavidin PE and vortex (e.g. for 1 plate = 96 + 2 samples: 19.6 µl + 32.34 µl).
c. Per sample, fill up with assay diluent to a total volume of 50 µl divided by the number of analytes and vortex (e.g. for 1 plate and 5 analytes = 96 + 2 samples: 51.94 µl biotinylated secondary antibody and streptavidin PE + 928.06 µl assay diluent).
d. Incubate for 1 h at 4°C in the dark.

Staining – 2nd step

1. Proceed with the addition of biotin-streptavidin PE mixes (for functional beads) or secondary PE-labelled AB (for Flex Sets).

   For Functional Beads: incubation of the biotin-streptavidin PE mixes

   a. Add 50 µl biotin-streptavidin PE mix to each well, mix by gentle scraping the bottom of the plate and incubate for 1 h at room temperature in the dark.

   For BD Flex Sets: incubation of the PE detection reagents mix

   a. Calculate the required amount of the PE detection reagent: number of unknown samples +12 standards and control +2 = number of samples (e.g. for 1 plate 84 unknown samples +12 standards and control +2 = 98 samples).
   b. Per sample, resuspend 1 µl PE detection reagent in assay diluent to a total volume of 50 µl divided by the number of analytes and vortex (e.g. for 1 plate and 5 analytes = 96 +2 samples: 98 µl PE detection reagent and streptavidin PE + 882 µl assay diluent).
   c. Add 50 µl PE detection reagent mix to each well, mix by gentle scraping the bottom of the plate and incubate for 1 h at room temperature in the dark.
3. Centrifuge plate at 300 × *g* for 5 min.
4. Carefully decant supernatants, add 200 µl wash buffer and centrifuge plate at 300 × *g* for 5 min.
5. Carefully decant supernatants and repeat step 3.
6. Add 150 µl wash buffer.
7. Measure samples. If acquisition cannot be performed on a flow cytometer equipped with a plate loader, samples have to be transferred to FACS tubes.

C. Acquisition, Analysis and Calculation

1. Materials

- Flow cytometer that can detect and distinguish fluorescence emissions at 576, 670 and >680 nm (e.g. BD FACSArray™ bioanalyzer or BD FACSCalibur™; BD Bioscience).
- Software (BD FCAP Array™, BD FACSComp™ and BD CellQuest™; BD Bioscience).

2. Acquisition

The BD FACSArray bioanalyzer has been designed for simple setup and acquisition of CBA assays. Although CBA assays are optimized for digital flow cytometers, they are compatible with virtually all dual-laser flow cytometers capable of detecting and distinguishing fluorescence emissions at 576, 670 and >680 nm. Among these, the widely used BD FACSCalibur can also be applied to acquire CBA assays. This cytometer can accurately distinguish the dual-colour CBA beads in the 30-plex comprised of the beads between A4 and E9 (see Figure 3). However, due to the inherent properties of the dyes used in the beads, the CBA assay reporter, PE and the instrument optics, the actual distinguishable plex size may be less than 30. This lower number of distinguishable bead populations is because one of the dyes used to index the beads and PE are both excited by the blue (488 nm) laser. Thus, compensation between the bead channel (FL3) and the reporter channel (FL2) must be established. In instances where the PE signal is high (e.g. high cytokine concentrations) the PE signal spills over into the FL3 channel, causing an increase in MFI. This increase in MFI can lead to bead clusters merging and possible misidentification by the BD FCAP Array software. Additionally, background in large multiplexes and instrument performance issues can cause the FL3 intensity of the beads in the D and E rows to fluctuate, which results in populations merging or having increased peak CV that can cause similar bead clustering issues. If clustering fails for any reason, the entire data file is excluded from analysis by FCAP Array software. Therefore, samples should be diluted in order to keep PE signals within an acceptable range. This may cause samples with low analyte concentrations to become undetectable. When designing multiplex experiments, it may be necessary to analyse beads that are spatially close to each other in separate tubes, to prevent merging of adjacent clusters. This is most important with the beads in the D and E rows but it can extend to any bead that corresponds to an analyte that might be overly abundant in a particular sample. The BD FACSComp software is useful for setting up the flow cytometer and the BD CellQuest software is required for acquiring samples. However, the FCAP Array software is required for subsequent data analysis of the CBA assays.

After performing an instrument setup using FACSComp software and BD Calibrite™ beads, samples may be acquired using the CellQuest software. Create a template as shown in Figure 4.

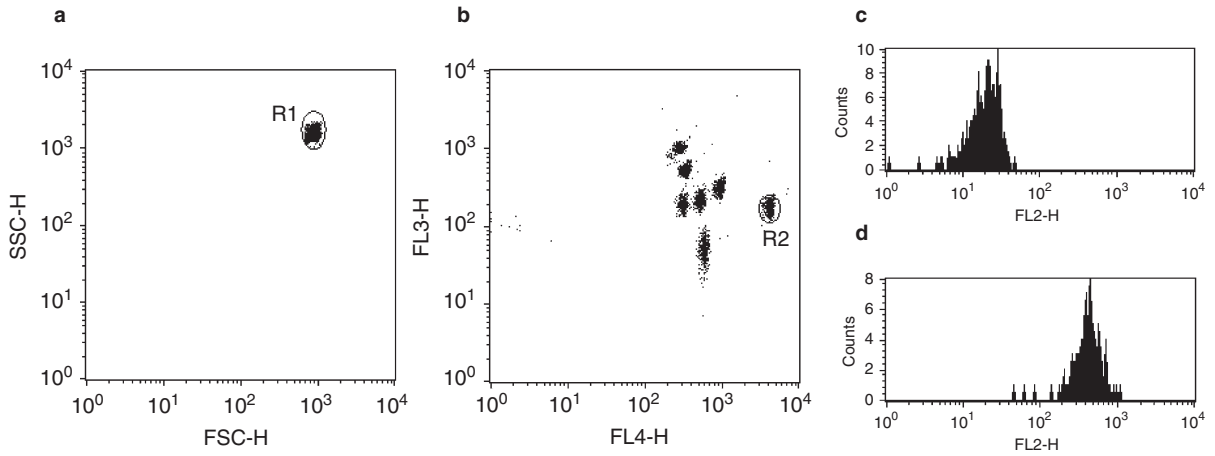

Figure 4. A CBA acquired on a FACSCalibur flow cytometer. During acquisition and analysis, the singlet bead population has to be adjusted and gated according to its FSC/SSC profile (A). Gated on the R1 population, it is possible to find seven different positioned beads within an FL4/FL3 dotplot – differentiating different cytokines as shown in Figure 1(B). Analysing these different singlets (R2 in B) within the reporter channel (FL2) gives sensitive information about the amount of the measured cytokine (low concentration in C, high concentration in D).

1. Set acquisition mode.
2. In the acquisition and storage window, set the acquisition gate to accept G1=R1 events (this will allow for only the events that fall into R1 to be saved).
3. Set the collection criteria for acquisition to stop at 300× the size of the CBA plex (e.g. 300 × 6 = 1800 events for a 6 plex). This ensures that the sample file contains approximately 300 events of each bead population. Do not acquire more than 300 beads per population.
4. To facilitate analysis of data files using the FCAP Array software and to avoid confusion, add a numeric suffix to each file that corresponds to the assay tube number (e.g. tube 1 containing 0 pg/ml could be saved as CBA090721.001). The file name must be alphanumeric (i.e. contain at least one letter). In setup mode, run a first tube and using the FSC vs. SSC dot plot, place the R1 region gate around the singlet bead population (Figure 4).
5. Start sample acquisition with the flow rate set to low. Using the lowest flow rate can improve resolution of the individual bead populations in the bead plex.

D. Analysis

Data may be easily analysed using the FCAP Array software as instructed by the manufacturer. The software can read any legal FCS file versions 1 or 2, and it also reads most of the non-standard FCS files, thus supporting the analysis of data acquired on most commercial flow cytometers. For analysis with the FCAP software, FCS files have to be imported when samples were acquired with a flow cytometer different from the FACS array. Alternatively, MFIs of the PE reporter fluorescence of a given bead population in standard and unknown samples may be analysed.

For quantification of cytokine concentrations in organ homogenates, the amount of cytokines are calculated by the measured concentration in the samples, the volume in which the tissue was homogenized, the weight of the homogenized tissue and the weight of the whole organ.

♦♦♦♦♦♦ VI. IMMUNODETECTION OF PROTEINS BY WESTERN BLOT

A. Immunodetection of Proteins by Western Blot

When ELISA- or CBA-based systems are not available, it may be helpful to monitor the presence and quantity of a given protein (e.g. inducible nitric oxide synthase) on a whole organ level, e.g. during a defined window of the infection process. To do this sodium dodecyl sulphate (SDS)–polyacrylamide gel electrophoresis (PAGE), Western Blot and immunodetection are uncomplicated approaches to obtain fast results. (for an example see Figure 5)

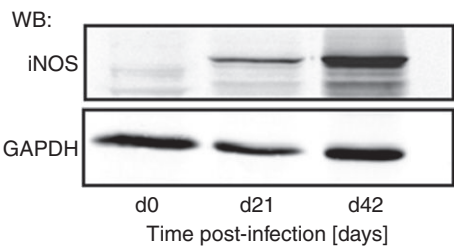

Figure 5. Western blot analysis of iNOS and GAPDH levels in lung homogenates of *Mtb*-infected mice. Analysis was performed on day 21 and 42 post-infection and compared to uninfected mice (d0). Equal amounts of lung homogenates of five infected mice were pooled, subsequently aliquots were separated by SDS-PAGE, and proteins transferred onto nitrocellulose membrane. Detection was performed by incubation with primary antibodies against iNOS (rabbit anti-mouse, Upstate, 1:1000) and GAPDH (mouse anti-mouse, Hytest) 1:4000). The blots were washed three times for 15 min in T-TBS and incubated with secondary antibody (goat-anti-rabbit-IRDye700 (Rockland) and goat anti-mouse AlexaFluor680 (Invitrogen) at an appropriate dilution in T-TBS containing 1% (v/v) Roti-ImmunoBlock for 1 h at 25°C. The signal was detected using the Odyssey Infrared imaging system (Ver. 2.1, Li-Cor Biotechnology, Lincoln, NE) at the following settings: resolution 84 μm, intensity 2–3, grey scale image, automatic sensitivity detection, brightness and contrast were adjusted equally from the automated image.

Protein extraction and electrophoresis

1. Mix 400 µl or organ homogenates with 100 µl of fivefold Laemmli buffer, heat to 95°C for 5 min. Store samples at –20°C.
2. Prior to electrophoresis thaw the samples at room temperature and denature the samples for 5 min at 95°C in a heating block or a water bath. Subsequently put them on ice and centrifuge the samples for 5 min at 10,000 × *g*. The supernatant is then ready to be used in SDS– PAGE.
3. SDS-PAGE. A simple and easy format to perform SDS-PAGE and Western Blot Analysis is the use of Minigels (e.g. the Mini-Protean Tetra Electrophoresis System (Bio-Rad). One may use commercially available precast gels; however, the preparation of home-made SDS gels is a lot cheaper, very easy to perform and described below. To perform a one-dimensional gel electrophoresis using a discontinuous gel system as described by Laemmli, the following steps need to be done.
4. Attention: Wear nitrile gloves and protect your eyes, when handling acrylamide solutions.
5. Clean the glass plates with 70% ethanol in order to removed grease spots that can disturb the polymerization of the gel. Prepare the resolving gel (sufficient for 2 gels) as described in Table 3. Mix the components in the order they are listed. Add the TEMED and the APS to the gel solution immediately prior to casting the gel. Mix the gel solution gently.
6. Fill 7.5 ml of the unpolymerized resolving gel mixture into the 1.5 mm space between two clean glass plates that were fixed in a casting stand (e.g. Bio-Rad) using a 1 ml pipette. Add 500 µl 2-propanol on top of the gel to remove air bubbles and prevent extensive drying of the gel.
7. After 45–60 min (at room temperature) the gel should be polymerized. Remove the 2-propanol completely, e.g. use Whatman filter paper for absorption.
8. Prepare the stacking gel (sufficient for two gels) as described in Table 3. Again add the APS to the gel solution immediately prior to casting the gel and mix the gel solution gently.
9. Fill up the remaining space to the edge, and carefully insert a 10- or 15-well comb into the gel to form the sample slots. Wait approximately 45 min for polymerization. The gels may be stored at this step at 4°C, if kept in a humidified atmosphere (plastic bags).
10. Remove the gels with the inserted combs from the casting stand and clamp them into the electrophoresis chamber. Fill the chamber with electrophoresis running buffer and remove the combs carefully. Remove any air bubbles from the slots and from the lower glass plate edge, e.g. by using a pipette.
11. Load at both ends (in the first slot) of the gel 5 µl of pre-stained molecular weight marker (e.g. 6.5–175 kDa, New England Biolabs).
12. Load equal volumes of the prepared protein lysates into the loading slots (15–40 µl). Do not overload the slots!
13. Start the electrophoresis at 70 V for the first 15 min to focus the protein onto the resolving gel and continue the electrophoresis at 200 V until the

visible bands formed by bromophenol blue in the sample buffer have moved to the end of the gel.

14. Prepare the Western blot buffers and filters during the time needed for electrophoresis and store the buffer at 4°C until use. It is best to immediately continue with the blotting of the proteins. Blotting buffer should be made freshly on the day the blot is performed.

Western blotting

15. Wet blot systems (e.g. Mini Trans-Blot Electrophoretic Transfer Cell, Bio-Rad) are widely used for the transfer of proteins onto a given membrane. This membrane can consist of nitrocellulose (e.g. Whatman Protran; pore size 0.45 µm) or polyvinylidene fluoride.
16. Wear nitrile gloves in all subsequent steps to prevent protein contamination of the membrane!
17. Remove the gels from the electrophoresis chamber and carefully remove the upper glass plate, e.g. by lifting a corner with a plastic spacer. Cut the stripline between stacking and resolving gel with the plastic spacer and remove the stacking gel carefully.
18. Prior to mounting the blotting sandwich equilibrate two fibre pads, four sheets of Whatman filter paper and one nitrocellulose membrane (approx. 4 × 10 cm) for each prepared gel in blotting buffer.
19. Prepare the blotting sandwich as follows: Place the first fibre pad on the opened gel holder cassette. Put two wet sheets of Whatman filter paper of the gel size onto the first fibre pad. Position the gel on top of the Whatman paper. Place the wet nitrocellulose membrane on the gel. Put again two wet sheets of Whatman filter paper on top of the membrane. Remove air bubbles from the sandwich. Add the second fibre pad and close the sandwich.
20. With the membrane facing towards the anode, place the cassette into an electrode module within an ice cooled buffer tank filled with 750 ml blotting buffer (4°C). Keep the blotting chamber at 4°C when transferring the negatively charged protein from the gel onto the nitrocellulose membrane at 75 V, 0.16 A/cm^2 for 90 min. To monitor the quality of the protein transfer, stain the membrane in Ponceau S solution (Thermo Scientific) for 1 min at room temperature. By washing two times for 5 min in T-TBS using an orbital shaker at 100 rpm (IKA), the red staining is completely removed.

Immunodetection of protein

21. Prior to the specific detection of protein the blots need to be blocked at room temperature in T-TBS containing 5% low-fat dried milk for 60 min. Alternatively 5% (w/v) BSA/T-TBS can be used.
22. Wash the membrane three times in T-TBS (15 min, 25°C).

23. Incubate with the primary antibody diluted in 10% Roti block (ROTI, Carl Roth KG) or 5% low-fat dry milk/T-TBS overnight at 4°C on a 3D tumbling shaker at 25 rpm. A good starting concentration is a 1:1000 dilution. Note: Each antibody needs to be titrated to reach optimal results. To do this, run an SDS-PAGE using a long lane comb with a lysate which is positive for your protein of interest. Blot the membrane as described, block it and cut it into 0.4-mm wide strips and place each strip into an individual well with a distinct concentration of the primary antibody of an 8-well reservoir (Labsystems, Finland).
24. Be sure that the blot membrane does not fall dry during incubation.
25. Wash the blot the next day three times as described above and incubate at room temperature with the fluorochrome (see 26.)- or enzyme (see 27.)-conjugate-labelled secondary antibody, diluted in 10% Roti block or 5% low-fat dry milk/T-TBS for 60 min and shaking at 100 rpm.
26. Remove the secondary antibody and wash the blot again three times. Maintain the blot in T-TBS and scan the blot using an Odyssey infrared imaging system (Ver. 2.1, LI-COR) at the following settings: resolution 84 μm, intensity 2–3, grey scale image, automatic sensitivity detection.
27. A cheap but very sensitive alternative is the use of horseradish peroxidase (HRP)-coupled secondary antibodies (e.g. from Jackson ImmunoResearch Laboratories) and the subsequent use of a chemiluminescence detection system (e.g. Amersham™ ECL™ detection systems). This requires a light sensitive film (Hyperfilm, Amersham), a autoradiography cassette (Hypercassette, Amersham) and a conventional X-ray film developing unit. Work in a dark room when handling light sensitive films.
28. Once you have detected your protein of interest, you need to be sure that a comparable amount of protein has been analysed in the samples. To do this you can check the presence of a constitutively expressed housekeeping molecule [e.g. glyceraldehyde 3-phosphate dehydrogenase (GAPDH)].
29. You may use one gel for the protein of interest and the other one for incubating with an antibody against a housekeeping protein and process them in parallel. Alternatively the blot can be cleared off immunoglobulins by incubating the membrane for 30 min in stripping solution (Restore ™ Western Blot Stripping Buffer, Thermo Scientific) as recommended by the manufacturer. Subsequently the blot can be reprobed with the second antibody, e.g. against GAPDH, as described above.

♦♦♦♦♦♦ VII. FLOW CYTOMETRIC APPROACHES

A. Detection of Intracellular Cytokines

Staining for intracellular cytokines, followed by flow cytometry analysis, can provide qualitative and quantitative information about the cellular source of a given cytokine that one cannot obtain from quantitative real-time PCR, CBA or western blot.

Table 3. Reagents and solutions for SDS-PAGE and Western Blot Analysis.

Reagents	12% Resolving gel (pH 8.8)	4% Stacking gel (pH 6.8)
Aqua bidest	3.75 ml	3.08 ml
Resolving gel buffer	2.13 ml	
Stacking gel buffer		1.25 ml
40% (w/v) acrylamide/bis solution, 37.5:1 (Serva)	2.55 ml	0.63 ml
10% (w/v) SDS solution	85 µl	50 µl
1 M N,N,N′,N′-Tetramethylethylenediamine (TEMED)	5 µl	5 µl
10% (w/v) Ammonium persulfate (APS)	25 µl	25 µl
Required Solutions:		
Resolving gel buffer (1.5M Tris/HCl)	*Stacking gel buffer (0.5M Tris/HCl)*	
18.1 g Tris	6.1 g Tris	
Add 60 ml bidest	Add 60 ml bidest	
HCl ad pH 8.8	HCl ad pH 6.8	
Add 100 ml bidest	Add 100 ml bidest	
Store 4°C	Store 4°C	
10% SDS	*10% APS*	
10 g SDS pellets	10 g APS	
Dissolve in 100 ml bidest	Dissolve in 100 ml bidest	
Store at RT	Store –20°C	
5x Electrophoresis running buffer	*Blot buffer*	
15 g Tris	2.25 g Tris	
72 g Glycine	10.8 g Glycine	
5 g SDS	Add 600 ml bidest	
Add 1000 ml bidest	150 ml MeOH	
	Add 750 ml bidest	
5% Low-fat dry milk	*10x TBS*	
5 g Low-fat dry milk powder	24.2 g Tris	
Dissolve in 100 ml T-TBS	80 g NaCl	
	1 M HCl at pH 7.6	
	Add 1000 ml bidest	
T-TBS		
1x TBS		
0.1% Tween-20		

Materials

- Medium (e.g. RPMI supplemented with 10% FCS, 1% Penicillin/Streptomycin, 1% L-Glutamine)

- Red cell removing buffer (RCRB; 8.34 g/l NH_4Cl, 0.037 g/l EDTA, 1.0 g/l $NaHCO_3$)
- Stimuli
  - Anti-mouse CD3 mAb (clone 145-2C11; e.g. from BD Bioscience) and anti-mouse CD28 mAb (clone 37/51; e.g. from BD Bioscience); coat wells of a 24-well plate with 300 µl of a anti-CD3/CD28 suspension at a final concentration of 1 mg/ml
  - Phorbol myristate acetate (PMA) (Sigma; final concentration of 10 ng/ml, prepare freshly)
  - Ionomycin (Sigma; final concentration of 1 pM, prepare freshly)
  - LPS (final concentration 10 pg/ml)
  - Recombinant murine IFN-γ (e.g. from BD Bioscience; final concentration 100 U/ml)
- Golgi transport inhibitor [e.g. BD GolgiPlug™ (BD Bioscience) or alternatively freshly prepared Brefeldin A (Sigma; 10 mg/ml)]
- FACS buffer [PBS (Mg^{2+} and Ca^{2+} free), 3% heat-inactivated FCS, 0.1% NaN_3]
- Blocking reagent [purified anti-mouse CD16/CD32 (clone 2.4.G2; e.g. from BD Bioscience), mouse serum, rat serum 1:40 in FACS buffer]
- Antibodies against surface markers optimally diluted in FACS buffer
- Fixation/permeabilization reagent [e.g. BD CytofixCytoperm™ (BD Bioscience) or 4× permeabilization solution and permeabilization diluent (eBioscience)]
- Permeabilization buffer [e.g. BD PermWash™ buffer (BD Bioscience) or 10× permeabilization buffer (eBioscience)]
- Antibodies against intracellular cytokines diluted in 1× PermWash buffer
- Paraformaldehyde [1% PFA; resuspend 0.1 g PFA (wear mask) to 0.5 ml PBS (Mg^{2+} and Ca^{2+} free), add 1 drop 0.5–1 M NaOH and dissolve suspension at 60–80°C in shaking water bath; add PBS, adjust pH to 7.2–7.4 with HCl and fill up to 10 ml with PBS; store aliquots at –20°C]

Cell preparation

1. Kill mouse and isolate the organ of interest aseptically.
2. Prepare single cell suspensions in medium, centrifuge at 320 × *g* for 8 min at 4°C and discard supernatants.
3. If necessary, red blood cells could be removed by resuspending cells RCRB.
   a. Add 5 ml RCRB, resuspend and incubate suspension for less than 3 min.
   b. Fill up with medium to dilute RCRB.
   c. Centrifuge at 320 × *g* for 8 min at 4°C and discard supernatants.
4. Resuspend cells in medium and adjust concentration to 2×10^6 cells/ml.

Restimulation

To stain for T-cell-derived cytokines (e.g. IFN-γ, IL-17) induced during infection in vivo, single cell populations from infected organs should be

restimulated with PMA and ionomycin or with plate-bound anti-mouse CD3 and anti-mouse CD28. For measurement of intracellular cytokines in monocytes/macrophages (e.g. IL-6, IL-10, IL-12/IL-23p40, TNF), the cells may be restimulated with LPS or with LPS and IFN-γ.

1. Calculate the amount of wells that are required per sample. One well with 2×10^6 cells will be sufficient for two sets of stainings.
2. Stimulation.
   a. For restimulation with plate-bound anti-CD3/CD28 in a 24-well plate, take of antibody solution and add 1 ml cell suspension.
   b. For restimulation with soluble PMA/ionomycin, LPS and/or cytokines, transfer 1 ml cell suspension per well of a 24-well plate and add stimuli.
   c. As a control, leave 1 ml cell suspension unstimulated.
3. Golgi transport inhibitor.
   d. Add 1 µl GolgiPlug or 20 µl 10 mg/ml Brefeldin A to each well.
   e. Incubate for at least 4 h at 37°C and 5% CO_2; incubation for longer than 12 h will affect cell viability.

Harvesting of cells

1. Prepare FACS tubes (2 tubes per well = 2 sets of stainings).
2. Transfer cell suspensions in first tube.
3. Wash wells 2× with 1 ml FACS buffer.
4. Resuspend cell suspension, centrifuge at 320 × *g* for 8 min at 4°C and discard supernatants.
5. Resuspend cells in 1 ml FACS buffer and transfer 500 µl into second tube.
6. Add 1 ml FACS buffer, centrifuge at 320 × *g* for 8 min at 4°C and discard supernatants.

Staining of surface markers

1. Block unspecific binding sites with 50 µl blocking reagent per tube.
2. Incubate for 30 min at 4°C.
3. Add 1 ml FACS buffer, centrifuge at 320 × *g* for 8 min at 4°C, discard supernatants and shortly disperse cells.
4. For staining of surface markers, add appropriate antibodies (e.g. CD4-FITC and CD44-APC) in an optimal dilution.
5. Incubate for 30 min at 4°C in the dark.
6. Add 1 ml FACS buffer and centrifuge at 320 × *g* for 8 min at 4°C.

Fixation and permeabilization

1. Discard supernatants, shortly disperse cells and add 250 µl fixation/permeabilization reagent per tube.
2. Incubate for 20 min at 4°C in the dark.
3. Add 750 µl 1× permeabilization buffer (from this step on, do not use FACS buffer!).

4. Centrifuge at 320 × *g* for 8 min at 4°C, discard supernatants and add 1 ml 1× permeabilization buffer.
5. Centrifuge at 320 × *g* for 8 min at 4°C.

Staining of intracellular cytokines

1. Discard supernatants and shortly disperse cells.
2. For intracellular staining of cytokines, add appropriate antibodies (e.g. IFN-γ- and IL-17-PE) 1:100 diluted in 1 ml 1× permeabilization buffer (do not use FACS buffer!).
3. Incubate for 30 min at 4°C in the dark.
4. Add 1 ml permeabilization buffer and centrifuge at 320*g* for 8 min at 4°C.
5. Take of supernatants and add 300 µl of 1% PFA.
6. Incubate at 4°C overnight.

Analysis

1. Perform acquisition and analysis on a flow cytometer (e.g. BD FACSCalibur™ using the software BD CellQuest™).
2. Staining of CD4, CD44, IFN-γ and IL-17 allows the discrimination of TH1 and TH17 cells (Figure 6).

♦♦♦♦♦♦ VIII. IMMUNOHISTOCHEMISTRY

In order to directly visualize localized or cell-specific protein expression within the context of tissues or entire organs, detection by immunhistochemical techniques is the method of choice. Paraffin-embedded tissues show a nicer morphology than

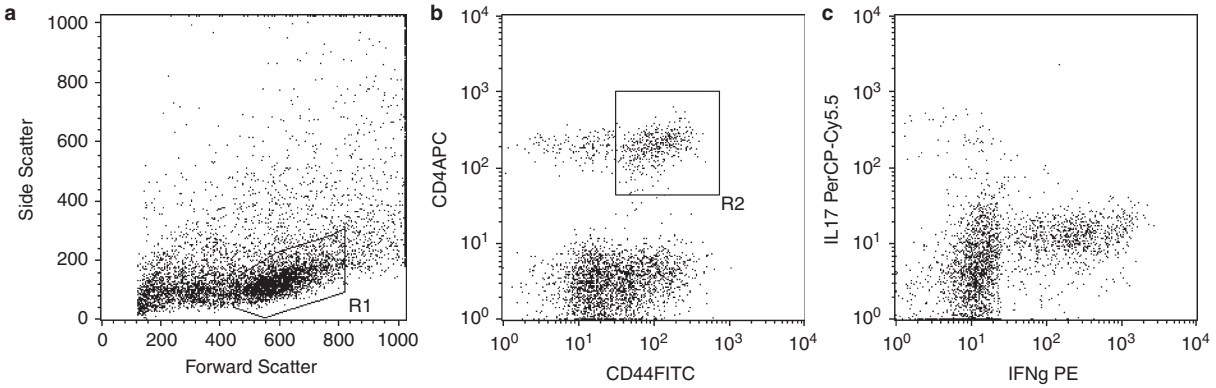

Figure 6. Intracellular staining of IFN-γ and IL-17A in activated $CD4^+$ T cells. Lung cells from *Mycobacterium tuberculosis*-infected mice were restimulated with anti-CD3/CD28 in the presence of GolgiPlug for 4 h. Cells were first stained with anti-mouse CD4-APC and CD44-FITC. After fixation and permeabilization cytokines were intracellularly stained with anti-mouse IL-17-PerCP-Cy5.5 and IFN-γ-PE. Cells in the lymphocyte gate (R1 in A) and in the CD44/CD4 gate (R2 in B) were used for analysing intracellular cytokine expression (C).

frozen tissues, as the tissue structure is better preserved. Infected tissues containing BSL2–BSL4 microorganisms are often sterilized by formaldehyde fixation (fresh 4% formaldehyde in PBS, pH 7.4, for 24 h or overnight), followed by embedding in paraffin. This will denature most proteins, making them inaccessible to many immunological staining reagents. For some antigens, it is, however, possible to use the antigen retrieval procedures outlined below.

Tissue preparation

Frozen tissues

1. Remove tissues and place into a flat-bottomed cylindrical sealable plastic tube filled with sterile PBS or normal saline to fully cover the tissue sample. Antigenicity is best preserved under these conditions, although some researchers prefer commercial embedding media (e.g. Tissue freezing medium, Leica Instruments).
2. With a long forceps, immediately place the sealed container in an up-right position into liquid nitrogen until frozen. It is important to snap freeze fresh specimens to prevent the formation of ice crystals in the tissue. These will appear as slits or fracture lines and give rise to artifactual staining. Containers may be stored at –70°C indefinitely. Tissues should always be maintained in the frozen state. If they are allowed to thaw, refreezing will result in extensive damage to the tissue as well as loss of antigenicity.
3. Prepare cryostat sections of 4–5 μm thickness.
4. Air dry sections for at least 15 min, or up to 24 h. Fix for 15–30 min in acetone followed by 15–30 min in chloroform. (If the cryostat sections are not meant to be stained the following day, it is also advised to air dry them for 4–24 h, to fix them for 10 min in acetone and store them at –70°C. When needed, thaw the sections covered with a paper towel in order to prevent water condensation on the frozen slides, and fix in acetone and chloroform as detailed above.)
5. For some staining procedures (particularly to detect cytokines), fixing of specimens with PFA/saponin is preferred. For this purpose, fix the air-dried slides for 15 min in 4% PFA in PBS without NaCl (pH 7.4–7.6), followed by a 15-min treatment in 0.1% saponin/PBS to remove cholesterol from the membranes. Wash thoroughly with PBS before immunostaining.

Paraffin-embedded tissues

1. Prepare sections from paraffin blocks onto pre-cleaned, grease-free slides. (Cut 2 μm sections, stretch them in a cold then in a 37°C warm water bath and mount them on glass slides. Leave sections to dry at least for 2 h at 37°C on a slide-drying bench.)
2. Dewax routinely processed paraffin sections by submerging them for 10 min in xylene followed by 10 min in acetone and 10 min in a 1:1 mixture

of acetone and Tris-buffered saline (TBS: 50 mM Tris, 150 mM NaCl, pH 7.5). Keep the sections in TBS until staining.
3. Deparaffinate the sections for 2 × 10 min in xylene and rehydrate them in a series of alcohols at 5-min intervals (100, 95, 80%). Rinse in PBS 10 mM (pH 7.2) and keep until staining.

Procedures for antigen retrieval

Microwave pre-treatment

1. Transfer the slides to a plastic staining jar filled with 100 mM sodium citrate buffer (pH 6).
2. Place the plastic staining jars into a microwave oven and heat for several 5 min at 500 W. After 5 min it is essential that the staining jar be refilled with buffer to prevent the specimens from drying out. The frequency of the heating steps depends on the embedding procedure performed previously and must be optimized for each laboratory individually. Thus, the time of formalin fixation and the quality of the paraffin may influence antigen retrieval. In most instances, heating the sections four to six times for 5 min will be sufficient to give good results.
3. After microwaving, let the slides cool down in the staining jar for approximately 15–20 min at room temperature and rinse briefly in PBS before proceeding with immunostaining.

Pressure cooker pre-treatment

1. Fill a normal household pressure cooker with enough 100 mM sodium citrate buffer to cover the slides (approx. 1.5–2.0 l). Bring the buffer to a boil at maximum temperature, reduce the heating temperature to a medium temperature before submerging the slides, close the lid and boil the sections 35–45 min. As with microwaving, the boiling time must he optimized depending on the embedding procedure used, because variables such as time of formalin fixation, quality of paraffin and section thickness may influence antigen retrieval.
2. Cool the pressure cooker under running cold water. (Take extreme care when performing this step and absolutely follow the manufacturer's instructions for opening the cooker.)
3. Open the cooker and let the water run slowly into the hot buffer, until the buffer becomes lukewarm, transfer the sections into PBS, rinse once and wash three times for 5 min in PBS before proceeding with immunostaining.

Pronase pre-treatment

1. Apply approximately 200 µl of Pronase (Fisher Scientific; ready to use) on the deparaffinized tissues.

2. Cover slides while ensuring that specimens are generously covered by (slide covers should be rather swimming on the surface of the solution and should not be fixed, in order to prevent drying out).
3. Leave for 40 min at 40°C.
4. Transfer the sections into PBS, rinse once and wash three times for 5 min in PBS before proceeding with immunostaining.

A. Staining Procedure

For a more detailed outline of various immunoenzymatic and fluorescent detection methods, please refer to Chapter 17. When working with mouse tissue, the primary antibody is most likely a rat monoclonal antibody or a rabbit polyclonal antiserum. Below is a description of primary and secondary reagents necessary for the HRP method which should be a useful guideline when adapting other protocols for use in animal tissues. Table 4 summarizes examples of modified protocols that work well in mouse tissues.

All incubations with antibodies are performed in a level humid chamber at room temperature, using approximately 200 µl of antibody solution. Excess humidity should be avoided since water condensation on the slides will interfere with the staining reaction. On the other hand, insufficient humidity will dry out the antibody on the sections, resulting in false-positive staining. Drying is usually most apparent at the edge of the sections (rim effect). Between incubations, rinse the slides once and wash three times for 5 min in PBS in staining jars and drain off excess fluid by capillary action using a paper towel.

Peroxidase method

1. Always include negative controls without primary antibody and with an irrelevant primary antibody of the same immunoglobulin class (or with pre-immune serum). The specificity of the primary antibody can be analysed by neutralization experiments in which blocking of antibody binding results in negative staining. For this purpose, pre-incubate the antibody with recombinant or purified antigen for 30 min at 37°C before applying it to the slides.
2. Before incubating the slides with primary antibody, block endogenous peroxidase activity in the tissue by pre-incubating the slides for 30–35 min in a light-protected staining jar with 3% H_2O_2.
3. Block non-specific binding by incubating the slides for 50–70 min with 5% FCS in PBS, after incubation drain off without rinsing.
4. Add the rabbit primary antiserum or rat monoclonal antibody in the appropriate dilution in PBS containing 5% FCS. (To find the appropriate concentration of primary antibody, perform threefold serial dilutions to optimize the ratio of background and specific staining.) Incubate for 70–90 min.
5. As the secondary antibody add the appropriate biotin-SP-F(ab')$_2$ fragment (Dianova; diluted 1:500 in 5% FCS/PBS). The optimal concentration of secondary reagents is usually indicated by the manufacturers.
6. Incubate for 35–45 min.

Table 4. Examples of validated, modified staining procedures

Antigen	Retrieval	Blocking	Primary	Dilution	Secondary	Dilution
iNOS	Citrate buffer	5% FCS/PBS	Rabbit, Upstate, 06-295	1:800 in 5% FCS/PBS	Goat-α-Rabbit, Dianova, 111-066-003	1:500 in 5% FCS/PBS
Mac-3	Citrate buffer	5% FCS/PBS	Rat, Pharmingen, 550292	1:10 in 5% FCS/PBS	Goat-α-Rat, Dianova, 112-066-003	1:500 in 5% FCS/PBS
CD3	Citrate buffer	5% FCS/PBS	Rat, Serotec, MCA 1477	1:200 in 5% FCS/PBS	Goat-α-Rat, Dianova, 112-066-003	1:500 in 5% FCS/PBS
CD45R/ B220	Not required	5% FCS/PBS	Rat, Pharmingen, 550286	1:50 in 5% FCS/PBS	Goat-α-Rat, Dianova, 112-066-003	1:500 in 5% FCS/PBS
Hypoxia-modified proteins	Pronase	Protein blocker	Mouse, Chemicon, HP-100	1:50 in 0.2% Brij/PBS with 1 drop/ml protein blocker	Rabbit-α-Mouse Dianova 315-066-045	1:500 in 0.2% Brij/PBS with 1 drop/ml protein blocker
HIF-1 alpha	Citrate buffer	5% FCS/PBS	Mouse, Novus-Biologicals, NB 100-123	1:100 in 5% FCS/PBS	Rabbit-α-Mouse, Dianova, 315-066-045	1:500 in 5% FCS/PBS
HIF-2 alpha	Citrate buffer	5% FCS/PBS	Rabbit, Novus-Biologicals, NB 100-122	1:1000 in 5% FCS/PBS	Goat-α-Rabbit, Dianova, 111-066-003	1:500 in 5% FCS/PBS
FDC	Citrate buffer	5% FCS/PBS	Rat, Pharmingen, 551320	1:10 in 5% FCS/PBS	Goat-α-Rat, Dianova, 112-066-003	1:500 in 5% FCS/PBS
Ki-67	Citrate buffer	5% FCS/PBS	Rabbit, Spring Bioscience, 05491576001	1:200 in 5% FCS/PBS	Goat-α-Rabbit, Dianova, 111-066-003	1:500 in 5% FCS/PBS

(*Continued*)

Table 4. (*Continued*)

Antigen	Retrieval	Blocking	Primary	Dilution	Secondary	Dilution
IL-4	Citrate buffer	PBS+0.05% Tween-20+3% BSA	Goat, Santa Cruz, Sc-1260	1:50 in PBS+0.05% Tween-20+3% BSA	Rabbit-α-Goat, Dako, E0466	1:200 in PBS+0.05% Tween-20+3% BSA
IL-13	Citrate buffer	PBS+0.05% Tween-20+3% BSA	Goat, Santa Cruz, Sc-1776	1:50 in PBS+0.05% Tween-20+3% BSA	Rabbit-α-Goat, Dako, E0466	1:200 in PBS+0.05% Tween-20+3% BSA
IFN-γ	Citrate buffer	PBS+0.05% Tween-20+3% BSA	Goat, Santa Cruz, Sc-1377	1:45 in PBS+0.05% Tween-20+3% BSA	Rabbit-α-Goat, Dako, E0466	1:200 in PBS+0.05% Tween-20+3% BSA
IL-12	Citrate buffer	PBS+0.05% Tween-20+3% BSA	Goat, Santa Cruz, Sc-1283	1:45 in PBS+0.05% Tween-20+3% BSA	Rabbit-α-Goat, Dako, E0466	1:200 in PBS+0.05% Tween-20+3% BSA

Note: Hypoxia is recommended with Dako ARK peroxidase kit. HIF-1 alpha is recommended with Dako ARK peroxidase kit. FDC is recommended with diluted haematoxylin and overnight incubation at 4°C with primary antibody. IL-4, IL-13, IFN-γ, IL-12 are recommended with overnight incubation at 4°C with primary antibody.

7. Add streptavidin peroxidase (Dako; ready to use) and incubate for 35–45 min.
8. Prepare the developing buffer by dissolving 1 tablet of 3,3′-diaminobenzidine and 1 tablet of Urea H_2O_2 (Sigma) in 5 ml distilled water. Mix well (should be prepare ahead in a light-protected tube, as it does not dissolve easily).
9. Incubate the slides with developing buffer in the dark in the humid chamber for up to 50 min. The degree of development can be checked microscopically and is terminated at the desired point. Rinse in distilled water and wash three times for 5 min in distilled water.
10. Counterstain with haematoxylin for 30 s. Haematoxylin stock solution is prepared from 6 g haematoxylin (Merck), 0.6 g sodium iodate (Merck), 52.8 g aluminium sulphate (Sigma) in 690 ml tap water, then add 250 ml ethylene glycol (Sigma) and 60 ml glacial acetic acid (Merck). Before staining, pass the solution through a sterile filter. Haematoxylin solution may be reused a few times.
11. Rinse the slides in running tap water and leave in tap water for 5 min before mounting with pre-warmed (40°C) Kaiser's glycerol-gelatine.

B. Detecting Tissue Pathophysiology

In addition to ascribing protein expression to specific cells by immunohistology, it is often possible to obtain useful information on the pathophysiological environment of infected sites when oxidative or nitrosative stress-related products are generated or when hypoxia-associated protein modifications take place.

For detection of hypoxia, inject mice intravenously with the hypoxia marker pimonidazole hydrochloride at a dose of 60 mg/kg weight of mouse between 1.5 and 3 h prior to necropsy. Pimonidazole derivatives are known to develop under conditions of severe hypoxia. A specific antibody is used for detection that binds to pimonidazole derivatives developing in tissues with an oxygen concentration below 14 μM (which is equivalent to a partial oxygen pressure of 10 mmHg or less).

Staining for hypoxia

1. Perform antigen retrieval for hypoxia on deparaffinized tissues with pronase for 40 min at 40°C.
2. Reduce endogenous peroxidase activity with 0.03% hydrogen peroxide (Dako ARK peroxidase) for 5 (±1) min at room temperature.
3. The anti-hypoxia antibody Hypoxyprobe-1mAb1 (Chemicon) is labelled with a biotinylation reagent (Dako ARK peroxidase), followed by incubation with a blocking reagent (Dako ARK peroxidase) in order to block non-specific binding. (Biotinylated antibodies containing blocking reagent should be used within 1 day of preparation. If storage of biotinylated antibodies is desired, do not add blocking reagent until the day of use. Biotinylated antibodies not containing blocking reagent are stable for at least 2 weeks at 2–8°C.)

4. Add the biotinylated antibody in the appropriate dilution in 0.2% Brij35/PBS with 1 drop/ml protein blocker (Dako). Incubate for 15 (±1) min at room temperature.
5. The reaction is visualized using streptavidin conjugated to HRP (Dako ARK peroxidase) followed by its substrate 3,3′-diaminobenzidine (Dako ARK peroxidase).
6. Add streptavidin peroxidase and incubate for 15 (±1) min.
7. Prepare the developing buffer by transferring enough 1 ml aliquots of buffered substrate (Dako ARK peroxidase) into a test tube (the preparation of 1 ml of the substrate chromogen is sufficient for up to 10 tissue sections or up to five cell smears).
8. Depending on the number of slides to be stained, for each 1 ml of buffer, add one drop (20 µl) from 3,3′-diaminobenzidine chromogen solution (Dako ARK peroxidase). Mix immediately and apply to tissue sections. (The prepared substrate chromogen is stable approximately 5 days when stored at 2–8°C. This reagent should be mixed thoroughly prior to use. Any precipitate developing in the reagent does not affect staining quality.)
9. Incubate the slides with developing buffer in the dark in the humid chamber for 5 (±1) min. The degree of development can be checked microscopically and is terminated at the desired point. Rinse in distilled water and wash three times for 5 min in distilled water.
10. Counterstain with haematoxylin for 30 s.
11. Rinse the slides in running tap water and leave in tap water for 5 min before mounting with pre-warmed (40°C) Kaiser's glycerol-gelatine.

An example of tumour and infection-associated hypoxia is shown in Figure 7.

♦♦♦♦♦♦ FURTHER READING AND TYPICAL EXAMPLES FOR THE DESCRIBED PROCEDURES

Quantitative Real-Time PCR

Smith, C. J. and Osborn, A. M. (2009). Advantages and limitations of quantitative PCR (Q-PCR)-based approaches in microbial ecology. *FEMS Microbiol. Ecol.* **67**(1), 6–20, Review.

Giulietti, A., Overbergh, L., Valckx, D., Decallonne, B., Bouillon, R. and Mathieu, C. (2001). AN overview of real-time quantitative PCR: applications to quantify cytokine gene expression. *Methods* **25**(4), 386–401, Review.

Kubista, M., Andrade, J. M., Bengtsson, M., Forootan, A., Jonák, J., Lind, K., Sindelka, R., Sjöback, R., Sjögreen, B., Strömbom, L. et al. (2006). The real-time polymerase chain reaction. *Mol. Aspects Med.* **27**(2–3), 95–125, Review.

Bustin, S. A. and Nolan, T. (2004). Pitfalls of quantitative real-time reverse-transcription polymerase chain reaction. *J. Biomol. Tech.* **15**(3), 155–166, Review.

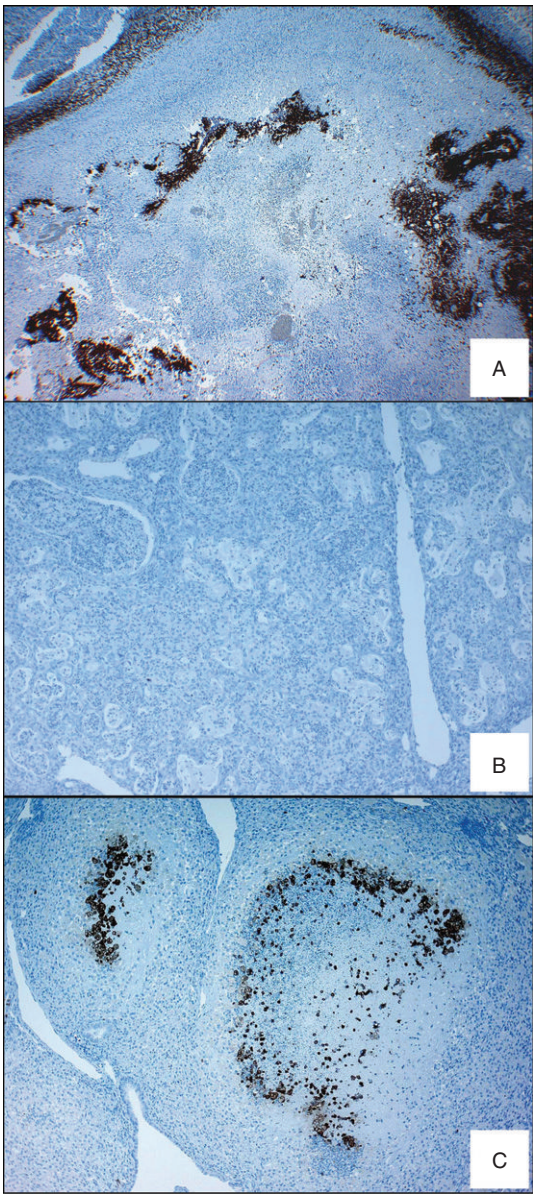

Figure 7. Staining for hypoxia in infected tissues. (A) C57BL/6 mice were subcutaneously injected with 1×10^5 tumour cells (MB49). After becoming necrotic (5 weeks), the tumour was dissected from killed mice. Note hypoxic regions around necrotic areas. (B) C57BL/6 mice were infected with *M. tuberculosis* (H37Rv, 100 CFU/mouse) by aerosol and the lungs were removed from killed mice at day 404 after infection. Note complete absence of hypoxia. (C) C57BL/6 mice were infected with *M. avium* (TMC724, 10^5 CFU/mouse) by aerosol and 18 weeks after infection the lungs were removed from killed mice. Note zone of hypoxic cells around central granuloma necrosis. All mice were injected with pimonidazole 1.5 h before killing. Staining was performed as described in this chapter. (See color plate section).

Cytokine Bead Arrays and Intracellular Cytokine Staining

Letsch, A. and Scheibenbogen, C. (2003). Quantification and characterization of specific T-cells by antigen-specific cytokine production using ELISPOT assay or intracellular cytokine staining. *Methods* **31**(2), 143–149, Review.

Ahmad, S. F., Pandey, A., Kour, K. and Bani, S. (2010). Downregulation of pro-inflammatory cytokines by lupeol measured using cytometric bead array immunoassay. *Phytother. Res*. **24**, 9–13.

Hölscher, C., Reiling, N., Schaible, U. E., Hölscher, A., Bathmann, C., Korbel, D., Lenz, I., Sonntag, T., Kröger, S., Akira, S. et al. (2008). Containment of aerogenic *Mycobacterium tuberculosis* infection does not require MyD88 adaptor function for TLR 2, 4 and 9. *Eur. J. Immunol.* **38**, 680–694.

Immunohistology

Shi, S. R., Cote, R. J. and Taylor, C. R. (2001). Antigen retrieval techniques: current perspectives. *J. Histochem. Cytochem.* **49**(8), 931–937, Review.

Schreiber, T., Ehlers, S., Aly, S., Hölscher, A., Hartmann, S., Lipp, M., Lowe, J. B. and Hölscher, C. (2006). Selectin ligand-independent priming and maintenance of T cell immunity during airborne tuberculosis. *J. Immunol.* **176**(2), 1131–1140.

Higgins, D. M., Sanchez-Campillo, J., Rosas-Taraco, A. G., Higgins, J. R., Lee, E. J., Orme, I. M. and Relative, G. -J. M. (2008). levels of M-CSF and GM-CSF influence the specific generation of macrophage populations during infection with *Mycobacterium tuberculosis*. *J. Immunol.* **180**(7), 4892–4900.

Aly, S., Wagner, K., Keller, C., Malm, S., Malzan, A., Brandau, S., Bange, F. C. and Ehlers, S. (2006). Oxygen status of lung granulomas in *Mycobacterium tuberculosis*-infected mice. *J. Pathol.* **210**(3), 298–305.

Suppliers of Unique Reagents

Amersham	http://www5.gelifesciences.com/
BD Biosciences	http://www.bdbiosciences.com
Biochrom	http:// www.biochrom.de
Bio-Rad	http://www.bio-rad.com/
Carl Roth	http://www.carl-roth.de/
Chemicon	http://millipore.com
Dianova	http://www.dianova.com
Fermentas	http://www.fermentas.com
IKA	http://www.ika.de/
Invitrogen	http://www.invitrogen.com/
Jackson ImmunoResearch	http://www.jacksonimmuno.com/

Laboratories

Labsystems	http://www.thermo.com/
Leica Instruments	http://www.leica.com

Li-Cor	http://www.licor.com/
Merck Co.	http://www.merck.com
New England Biolabs	http://www.neb.com/
Peqlab Erlangen	http://www.peqlab.de
Promega	http://www.promega.com
Roche Applied Science	https://www.roche-applied-science.com/
Santa Cruz Biotech.	https://scbt.com
Serva	http://www.serva.de
Sigma Chemical Co.	http://www.sigma-aldrich.com
TaKaRa	http://www.takarabioeurope.com
Upstate	http://www.millipore.com/
Universal probe library	http://www.universalprobelibrary.com
Whatman	http://www.whatman.com/

12 Murine and Guinea Pig Models of Tuberculosis

Diane J Ordway and Ian M Orme
Mycobacteria Research Laboratories, Department of Microbiology, Immunology and Pathology, Colorado State University, Fort Collins, CO, USA

♦♦

CONTENTS

♦♦♦♦♦♦ I. HANDLING AND CULTIVATION OF MYCOBACTERIA

A. Introduction

The isolation and cultivation of *Mycobacterium tuberculosis* in both the clinical and the research laboratory setting has been well described in numerous publications and books (Vestal, 1975; Youmans, 1979; Kubica and Wayne, 1984; Sambrook *et al*., 1989; Bloom, 1994; Rom and Garay, 1995). The methods described in many of these references have been in use for many years and have changed very little. For example, many laboratories routinely cultivate *M. tuberculosis* cultures in Proskauer and Beck (PB) liquid medium which is a modified medium first developed by Youmans and Karlson (1947). However, this chapter will not attempt to outline all of the well-established methodologies which have been used by various investigators, but instead will concentrate on those utilized in our own laboratory for the cultivation of *M. tuberculosis* for research purposes.

A wide variety of animal models have been used to test new vaccines and drugs (Orme, 1988; McMurray *et al*., 2005; Orme, 2005, 2006; Lenaerts *et al*.,

METHODS IN MICROBIOLOGY, VOLUME 37
0580-9517 DOI 10.1016/S0580-9517(10)37012-7

2008). Mice are the most widely used small animal model because of the broad availability of immunological reagents, relatively low cost and the availability of inbred and genetically engineered strains with well-defined genotypes. The one notable disadvantage of the mouse model is that the pulmonary and extrapulmonary pathology following aerosol challenge lacks important morphologic features that are commonly seen in humans with untreated tuberculosis. To model these aspects the guinea pig low-dose aerosol infection model has been developed since it shares these clinical features with the human disease (McMurray, 2003; Basaraba *et al*., 2008).

In this laboratory we routinely cultivate strains of *M. tuberculosis* for use in the following activities: (a) the *in vivo* determination of disease host response and pathogenesis, primarily using the murine and guinea pig airborne infection models; (b) the *in vivo* determination of bactericidal effectiveness of novel immunotherapy, vaccination, post-exposure vaccination or chemotherapy using both models; (c) the *in vivo* determination of bacterial virulence of clinical strains and (d) the *in vitro* testing of potential chemotherapeutic agents using a murine bone marrow-derived macrophage infection model. Each of these procedures requires the cultivation of 'laboratory strains' (Erdman and H37Rv) as well as newly acquired clinical isolates of *M. tuberculosis.*

Every inoculum of *M. tuberculosis* should be handled in an appropriate 'Class II' biosafety cabinet, which requires stringent biosafety level 3 (BSL-3) biosafety conditions. Recommended 'minimum requirements' are a facility with shower in/shower out protocols (which also avoids transmission of mouse viruses), a safety cabinet, a glove box, room air filtered both in and out through high-efficiency particulate air (HEPA) filters and a graduated airflow handling system. (An electrical generator backup system is also recommended as a fail-safe.) Animals should be kept in HEPA-filtered cages and in separate rooms away from equipment because of animal bedding dust. Personnel should wear protective surgical scrubs, socks, hairnets, N95 masks (Sigma) and facilities shoes and should be tuberculin (Mantoux) skin tested every 6 months. Because various procedures, such as injections, tissue homogenization and plating, can all potentially create significant aerosols, the use of additional battery-charged HEPA-filtered respirators to be worn when performing the above procedures is strongly recommended.

Each BSL-3 should have an Exposure Control Plan in place before starting operation, and all personnel should be familiar with this. In our experience accidents are very rare, but when they do occur often as not it is due to some mental preoccupation instead of some technical lapse. In other words, only work under BSL-3 conditions when your mind can be kept completely on the task at hand.

Wherever possible BSL-3 laboratories should be stand alone or part of a larger animal facility. If there are regular open laboratories on floors above the BSL-3 then the air-handling systems should be very carefully checked on regular occasions (however, we do not recommend this type of architectural arrangement). If the facility includes any form of aerosol generation device, this should be kept separately in a room under the lowest air pressure relative to the rest of the BSL-3 facility.

B. Receiving New Cultures

The cultivation of *M. tuberculosis* often begins with the receipt of clinical isolates from other research institutions/hospitals. When shipments arrive the shipping container should be examined to make sure that it has not been damaged while in transit. All agents such as *M. tuberculosis* need to be shipped (within the USA) in accordance with the interstate quarantine regulations (Federal Register, Title 42, Chapter 1, part 72, revised 30 July 1972). The shipping container should consist of an outer heavy cardboard shipping box with adequate packing to absorb any crushing. Inside this box should be a leak-proof canister (such as heavy polypropylene biocontainment canisters with rubber seals) with absorbent packing material inside. Within this canister there should reside an additional canister with more absorbent material and the tubes containing the tuberculosis isolate on Lowenstein-Jensen slants. The outside of the shipping container should have all appropriate biohazardous materials markings as well as addresses/phone numbers for the shipper and recipient. The shipping box should also contain appropriate documentation describing the contents as per strains included and (if known) drug susceptibility data.

Upon receipt and initial inspection of the package it should be taken to an appropriate BSL-3 containment facility. The technician wearing appropriate facility-specific clothing and protective respirators as stated above should open the package within a biological safety cabinet. The package is carefully opened and examined for any damage or spillage onto the absorbent materials. If leakage has occurred the materials are thoroughly soaked with disinfectant (5% Lysol) and allowed to let stand for 30 min before proceeding. If the interior tubes are damaged it is best carefully to bag all materials in autoclave bags and autoclave immediately. Wipe down all work surfaces with disinfectant and notify sender of the condition of the shipment. If the contents of the package are intact, check the inventory against the documentation that came with the package.

C. Cultivation

It is essential that stock cultures of *M. tuberculosis* used in research experiments should be standardized in terms of the culture medium as well as the cultural conditions (initial inocula, temperature, aeration, agitation, subculture times and so on). This is important because it assures that each individual isolate has been cultivated under similar physiological conditions during growth, which is critical if you plan to compare data between strains and experiments.

Each laboratory has its own favourite broth mediums; we prefer PB (Youmans and Karlson, 1947) or glycine alanine salts (GAS) broth. Both of these liquid mediums are simple minimal salt solutions with glycerol as a carbon source. Our approach limits the amount of extraneous additives in our cultures found in other broth mediums, such as 7H9 broth, which requires enrichment with Oleic Acid–Albumin–Dextrose Complex (OADC). This is particularly important when trying to isolate secreted proteins or metabolites from a mycobacterial culture so as to avoid contaminating proteins from the culture medium. Mycobacteria in general, and *M. tuberculosis* in particular, have the tendency to clump or raft when

cultivated in liquid broth media. This is a problem which is overcome by the addition of the detergent Tween 80 to the culture which disperses the bacilli and provides a smooth even suspension. When cultures are grown in Tween-containing media there can be a more accurate determination of the true number of viable bacilli by optical absorbance or serial dilution plating on solid media such as 7H11 agar.

There has been some discussion as to the merits of adding detergents to the culture medium as it may affect the pathogenicity or viability of the bacilli (Davis and Dubos, 1948; Dubos and Middlebrook, 1948; Dubos, 1950; Collins *et al*., 1974). We recognize this concern but feel that in order to achieve dispersed cultures free from large clumps, Tween is a necessary evil. For example, the necessity for smooth and evenly dispersed cultures is critical for the accurate delivery of bacilli for *in vivo* studies when the infection is given by aerosol. The aerosol device utilizes a glass venturi system to form tiny droplets containing the bacilli which are then delivered to a chamber containing the test animals over a specified period of time. If inocula from different isolates with different degrees of clumping were to be used, the data we would generate would be meaningless because of the wide variation in uptake, as well as the variation in particle size (i.e. size of rafts). On the other hand, with smooth evenly dispersed cultures the uptake parameters are highly reproducible. In fact we have demonstrated that aerosol infection results in an even distribution of bacilli in lungs using magnetic resonance imaging (Kraft *et al*., 2004).

Another critical parameter is that all cultures used in biological experiments should be harvested at the same phase of growth. We like to harvest broth cultures when they are still in the log growth phase but before the culture enters into the late-log growth/stationary phase. At this point the culture is at its optimum concentration and viability. Cultures harvested at this time routinely have colony-forming unit (cfu) counts at 5×10^7 up to a maximum of 10^9 colonies/ml of broth. Higher concentrations are not recommended; when the culture gets in the range of 10^9 cfu/ml there is more clumping of the bacilli and many bacilli are probably dead. If necessary, the presence of non-viable bacilli in cultures can be detected by the presence of autolytic enzymes such as isocitrate dehydrogenase.

As described above, all manipulations with *M. tuberculosis* should be performed in a biological safety cabinet (Class II) within a BSL-3 facility. The establishment of a primary seed culture collection or repository is essential in maintaining the integrity of the individual clinical isolates as they are received. Proper documentation as to the source, date received, accession number, strain name, history of isolate, drug susceptibility, drug resistance and virulence data should be maintained in a database. When a clinical isolate is received and unpacked it first needs to be evaluated as to whether there is sufficient growth for immediate subculture. In most instances clinical isolates of *M. tuberculosis* arrive in the research laboratory on Lowenstein-Jensen (LJ) slants (Jensen, 1932), but there are occasions when samples arrive in sealed serum vials containing broth cultures (1.0–2.0 ml).

If cultures arrive on LJ slants they have usually been incubated prior to shipment and have sufficient colony growth to allow immediate subculture into broth. On occasion there is very little visible growth and these slants should be further incubated at 37°C for 1–2 weeks to establish visible colonies. With samples which

have been shipped as broth cultures, they are usually at a high bacterial density and can be subcultured directly into broth media. It is generally more desirable to ship LJ slants because of the reduced risk of leakage while the package is in transit.

The first step in subculture of clinical isolates is the preparation of the work area in the biological safety cabinet. The cabinet is turned on and allowed to run for at least 30 min to allow the blower motors to reach optimum operating speed and allow the air balance to be achieved. The interior work surfaces are then disinfected prior to use with 5% Lysol™ solution followed by 70% ethanol. All cleaning materials are deposited into a small autoclave bag which is then taped to the inside wall of the cabinet. This bag is used as a waste bag for soiled gloves, Kimwipes, etc., while working in the cabinet and is closed and removed when work is complete. The work surface within the cabinet is covered with bench blotters (i.e. plastic-backed paper towelling). A heat-resistant plastic pipette boat with 2–3 cm of 5% Lysol™ is placed in a convenient working location for the technician (usually in the centre towards the back, but not too close or over the air returns of the cabinet). All materials which will be needed for manipulations, such as sterile pipettes, inoculation loops, sterile tubes, flasks and extra gloves, should be located close to the cabinet on a bench or laboratory cart. When all materials are assembled work can then proceed. To establish, broth seed cultures we use sterile 150 × 25 mm screw-capped culture tubes which have been prefilled with 20 ml of either PB or GAS liquid medium supplemented with 0.05% Tween 80. Each tube contains a very small plastic-coated magnetic stir bar for culture aeration and agitation. Using a sterile disposable inoculating loop, a sample from the LJ slant is inoculated into the broth within the tube. It is important only to inoculate one loop; if you seed the culture with an overly heavy amount of bacilli the clumps will not dissipate and you have the potential of having a larger amount of dead bacilli in your seed stock upon harvest. The inoculation loop is then discarded carefully into the pipette boat containing the Lysol™. The reason for using plastic disposable loops is that you minimize the potential aerosol hazard which may occur with flaming a metal inoculation loop. Metal loops can be used, but should be first speared into a 70% ethanol sand bath to remove any remaining material before being flamed in an electric loop incinerator. With broth samples, the top of the vial is first swabbed with 70% ethanol and then flamed with a Bunsen burner to sterilize. A 1 cc tuberculin syringe fitted with a 26 G needle is then used carefully to remove 1.0–2.0 ml of the inoculum from the vial. The inoculum is then carefully injected down the side of the culture tube, taking care not to create an aerosol. The inoculated tubes are each labelled with the following information: Species (*M. tuberculosis*), Strain, Media, Date, Technician, Drug Resistance (Yes/No).

The seeded culture tubes are carefully placed into a plastic test tube rack which has been secured on top of a magnetic stir plate within a 37°C incubator. The original LJ slants are deposited in a 4°C refrigerator within the biosafety laboratory and retained. All instruments during subculture are wiped down with disinfectant prior to removal from the cabinet. All waste materials are double bagged in autoclave bags and removed immediately for sterilization in a steam autoclave (121°C at 15 lbs/in 2 for 40 min). The interior surfaces of the biological safety cabinet are thoroughly disinfected with 5% Lysol followed by 70% ethanol.

The seeded cultures are checked twice a week for growth and possible contamination. Usually the cultures reach a density of 5×10^7 to 5×10^8 within 1–2 weeks after initial seeding. With experience a trained technician can visually estimate the approximate cfu growth within a tube of broth. Generally a tube less than 10^6 cfu/ml is clear and growth cannot be visually detected. At 10^7 cfu/ml there is a discernible cloudiness which can be visually seen. When the culture reaches 10^8 cfu/ml there is a very hazy growth and printed text can be detected when placed behind the tube but individual letters cannot be visualized. A culture which has reached 10^9 cfu/ml or greater is very turbid/milky and some clumping or 'stringy' growth may be detected (resulting from the Tween being metabolized by the bacilli).

An optical density measurement at A580 can also be made to determine the relative concentration. When the cultures reach mid-late-log growth, approximately 10^8 cfu/ml, they are then subcultured into 150 ml of fresh broth in disposable 250 ml polycarbonate Erlenmeyer flasks with screw-type closures (Coming 25600). The flasks are labelled as above and incubated at 37°C on orbital shakers (slow speed with gentle agitation), or stationary with gentle swirling twice weekly for an additional 1–2 weeks. When the density has once again reached approximately $1–5 \times l0^8$ cfu/ml the culture is removed from the incubator to be aliquoted into serum vials for laboratory seed cultures. The mycobacterial culture is aliquoted in volumes of 1.5 ml into 2 ml sterile serum vials which are fitted with sterile butyl rubber stoppers, which are then crimped into place with sterile aluminium seals (Wheaton Glass). The vials are disinfected by immersion in 70% ethanol and then allowed to air dry. Each vial is then labelled with small Avery™ labels printed with information as to the species, strain, date (lot), media and technician. The vials are then placed in labelled storage boxes which are then placed in a –70°C freezer for long-term storage.

After the vials have been frozen, a random sampling of vials from the storage box is taken out the following day for the determination of the viability of the lot. The vials are thawed, vortexed vigorously and the butyl rubber septum disinfected with 70% ethanol followed by flaming with the Bunsen burner. A sterile 24-well tissue culture plate is set up with 0.9 ml of sterile Tween-saline (0.05% Tween 80 in 0.85% NaC1 solution) in each well. With a 1 ml sterile tuberculin syringe, the suspension of bacilli is removed from the serum vial via the butyl stopper. A 0.5 ml sample of this suspension is plated onto a Trypticase Soy or Blood Agar plate to check sterility. Into the first column of the 24-well plate, 100 µl of sample is deposited. With a P-200 Gilson™ Pipetman set at a 100 µl volume, and fitted with a barrier-type pipette tip, the samples are serially diluted through a series of 10-fold dilutions starting at column 1 and ending at column 6. Column 1 corresponds to a 1:10 dilution of the original vial as column 6 in the series corresponds to a 1:1,000,000 dilution. A volume of 100 µl is removed from each dilution well and plated onto quadrant-type petri plates containing Middlebrook 7Hll agar. The plates are bagged in polypropylene zip lock sandwich bags (four plates per bag) and incubated in the dark at 37°C for 3 weeks. Colonies are then counted and the cfu of the mycobacterial frozen seed lot determined.

Once the cfu has been established for each seed culture lot, these data are entered into the culture collection log, notebook or database. For each particular strain approximately 25–30 vials are retained as 'primary' seeds and not used except for subculture to establish more working stock. The repetitive or continuous subculture of any strain of *M. tuberculosis* should be discouraged as this may cause physiological changes in the strain over time and reduce its virulence.

If a strain needs to be subcultured or expanded it is advisable to start from one of the 'primary' seeds in the culture collection or if available from the original LJ slant (Note: LJ slants can be maintained at 4°C and subcultured onto fresh LJ for maintenance of cultures). The additional 70 vials or so from each initial subculture are then used as your working stocks.

D. Liquid Media

1. PB liquid medium

Into 1 l of distilled water add each of the following ingredients in the order listed, making certain that each salt is dissolved before the next is added: KH_2PO 45.0 g; asparagine 5.0 g; $MgSO_4 \cdot 7H_2O$ 0.6 g; magnesium citrate 2.5 g; glycerol 20 ml.; Tween 80 0.5 ml (optional for dispersed cultures, 0.05% final concentration). The pH is then adjusted to 7.8 by the addition of 3–5 ml 40% NaOH. The medium is then autoclaved at 121°C for 15 min on slow exhaust, after which the pH should be 7.4. On occasion there is a precipitate which forms after autoclaving; if so, the media should be allowed to cool and the precipitate removed by filtration. The media is then autoclaved once again at 121°C for 15 rain [or can be sterile filtered through a 0.2 gm filter unit/cartridge (Gelman)].

2. Glycerol Alanine Salts

To prepare GAS, each of the following ingredients is dissolved in the following order into 990 ml of distilled water: Bacto Casitone [Pancreatic Digest of Casein (Difco)] 0.3 g; ferric ammonium citrate 0.05 g; K_2HPO_4 4.0 g; citric acid (anhydrous) 2.0 g; L-alanine 1.0 g; $MgC1_2o6H_2O$ 1.2 g; K_2SO_4 0.6 g; NH_4C1 2.0 g; glycerol 10 ml. The pH is adjusted to 6.6 by the addition of 1.8 ml 40% NaOH. The GAS media is then autoclaved at 121°C for 15 min on slow exhaust.

E. Solid Media

1. Middlebrook 7H I 0 and 7H I I Agar (Difco)

Both 7H10 and 7Hll agar media are routinely used for the cultivation and enumeration of *M. tuberculosis* by limiting dilution plating. The 7H11 agar contains a pancreatic digest in the base, whereas 7H10 does not; this additive seems to enhance the growth of many strains of mycobacteria and hence is the preferred medium in our laboratory. Both formulations, however, produce acceptable colony growth over a 3 week incubation at 37°C. To prepare 1 l of 7Hll or 7H10, place the

following ingredients into a 2 1 Erlenmeyer flask: 7Hll (or 7H10) agar base 21 g; asparagine 1.0 g; glycerol 5.0 ml; distilled water 900 ml. All of the ingredients are thoroughly dissolved and the flask is capped with heavy aluminium foil which is then secured into place with autoclave tape. The agar is then autoclaved for 15 min at 15 psi, and 121°C on slow exhaust cycle.

Remove the flasks from the autoclave and check the colour of the agar. The agar should be an emerald green, if, however, it appears to be olive drab or brown, discard this batch of agar as it may have been 'overcooked' during autoclaving and the malachite green has degraded. (The breakdown of malachite green produces compounds which inhibit the growth of mycobacteria.) After checking the colour of the agar, place the flask into a 57°C water bath and allow the agar to equilibrate for at least 45 min. While the agar is cooling, set up the following materials in a sterile media prep bench:

- One sterile 10 ml Cornwall Syringe set to dispense 5.0 ml aliquots (if dispensing into X-plates; if using non-divided plates, disregard the Cornwall Syringe).
- 60 #1009 X-plate petri dishes for each litre of agar.
- One wire basket to support the 2 l flask.
- Sharpies to code plates as to possible drug additives.
- 100 ml of OADC enrichment media per litre of agar (described below).

When the agar has equilibrated to 57°C, remove the flask from the water bath and place it in the wire basket in the bench. Carefully remove the foil and aseptically pour 100 ml of the OADC enrichment media into the litre of agar. Gently swirl the flask to mix the OADC throughout the agar. At this time, drugs such as 2-Thiophenecarboxylic acid hydrazide (TCH) or isoniazid (INH) can be added by filter sterilization. Carefully unwrap the Cornwall syringe from its foil envelope and aseptically place the tubing into the flask. Prime the syringe and proceed to dispense the agar into the petri dishes with strict aseptic technique. Dispense 5.0 ml of agar per quadrant per plate, or pour approximately 20 ml of agar into a non-divided plate. After dispensing the media, allow the plates to stand at room temperature for at least 2 h. This is sufficient time to allow the agar to solidify. Cover the plates with a dark plastic bag or aluminium foil to protect the media from the light.

When the agar has solidified put the plates into plastic storage trays and place these trays in a dry 37°C incubator for 24–48 h. This is a 'curing' step in which the excess moisture is removed from the agar and allows an opportunity for any contaminants to become apparent. After the incubation of the plates is accomplished they are placed into zip lock polypropylene bags (five plates/bag) and labelled as to type of agar, drugs, date and name. If the plates are not to be used immediately, they are stored at 4°C until use. Plates can be stored for up to 1 month; use after this time is not recommended.

F. Middlebrook Oleic Acid–Dextrose Complex

To prepare 4.0 l of OADC the following ingredients need to be dissolved in 3.8 l of distilled water in the following order: NaC1 32.4 g; bovine albumin fraction V 200 g; dextrose (D-glucose) 80 g. The pH of the mixture is then adjusted to 7.0 with 4% NaOH when everything is in solution.

To this mixture a sodium oleate solution is then added. This solution is prepared with the following ingredients: distilled water 120 ml; 6 M NaOH 2.4 ml; oleic acid 2.4 ml. Once the sodium oleate solution is prepared it is warmed in a 56°C water bath until the solution is clear. The complete OADC enrichment media is then filter sterilized through 1.0 μm and then 0.2 μm cartridge filters (Gelman) using a peristaltic pump system. The media are dispensed in a laminar flow tissue culture hood into sterile 100 ml bottles which are capped, heated in a 56°C water bath for 1 h and then incubated at 37°C overnight. The heating and incubation is then repeated the following day. After inspecting the OADC media for contamination, the bottles are stored at 4°C for up to 2 months.

G. Adding Drugs to Media

1. Acriflavine

- Working Concentration: 100 μg/ml = 100 mg/l
- Preparation: Dissolve 100 mg of acriflavine in 10 ml of *sterile distilled* water and filter sterilize. Add all 10 ml to 1 l of agar.

2. Isoniazid

- Working Concentration: 0.2 μg/ml = 200 mg/l = 0.2 mg/l
- Preparation: Dissolve 20 mg of INH in 10 ml of *sterile distilled* water. Dilute this 1:10 in *sterile distilled* water to give a final concentration of 200 μg/ml and filter sterilize. Add 1 ml of the 200 μg/ml stock to 1 l of agar.

3. 2-Thiophenecarboxylic acid hydrazide

- Working Concentration: 1 μg/ml = 1 mg/l
- Preparation: Dissolve 10 mg of TCH in 10 ml of *sterile distilled* water and filter sterilize. Add 1 ml of this stock to 1 l of agar.

♦♦♦♦♦♦ II. PROPAGATION METHODS FOR THE ISOLATION OF IMMUNOLOGICALLY REACTIVE PROTEIN FRACTIONS

A. Equipment and Reagents

The growth of *M. tuberculosis* described in this section is for 500–1000 ml cultures, i.e. much higher volumes than for infecting inocula, because of this some growth conditions are different from above. The equipment required includes a roller-bottle apparatus or platform shaker for gentle agitation of cultures and a class II biological safety cabinet. *M. tuberculosis* is a class III pathogen and its propagation must be performed in a certified BSL-3 laboratory (Centers for Disease Control, 1993).

Several types of broth media are available for the growth of *M. tuberculosis*; however, media containing supplemental proteins such as BSA or yeast extract should be avoided. We generally use GAS broth (see above). This media allows for ample growth of the tubercle bacilli and is easily prepared.

B. Growth of *M. tuberculosis*

For initial growth of *M. tuberculosis* a 1ml aliquot from frozen stock is inoculated on a Middlebrook 7Hll agar plate and incubated at 37°C for 2–3 weeks. Once colonies are visible a liberal inoculum of cells is scraped from the plate and placed in GAS broth (20 ml). This is allowed to incubate at 37°C with gentle shaking for 2 weeks. An aliquot (10 ml) of this seed culture is transferred to 100 ml of GAS broth. Following 2 weeks of incubation, the entire 100 ml culture is used to inoculate 1 l or is split for 500 ml GAS broth cultures. These cultures are incubated in roller bottles or fernbach flasks with gentle agitation for 2 weeks. It is our experience that 2 weeks of incubation provides cultures that are in a mid- to late-logarithmic phase of growth (Sonnenberg and Belisle, 1997).

C. Harvesting Culture Filtrate Proteins and Preparation of Subcellular Fractions

1. Equipment and reagents

The separation of the cells and the culture supernatant is performed in a Class II biological safety cabinet in a BSL-3 laboratory. The supernatant is harvested using 0.2 mm ZapCap filters (Schleicher and Schuell, Keene, NH, USA). Vacuum for this procedure is provided by a vacuum pump (maximum vacuum 26 in mmHg) with an in-line 0.2 mm filter (Gelman, Ann Arbor, MI, USA, catalogue #4251) placed between the ZapCap and the vacuum pump. Concentration of the filtrate is accomplished with an Amicon apparatus (Beverly, MA, USA). Harvesting of the cells requires a table top centrifuge such as a Sorvall RT-6000 with sealed buckets for containment of potential aerosols. Lysis of the cells requires a French press or probe sonicator.

2. Breaking buffer

- 10 mM Tris-Cl, pH 7.4
- 150 mM NaCl
- 10 mM EDTA
- 100 mg/ml DNase
- 100 mg/ml RNase
- proteinase inhibitors.

3. Harvesting of CFPs

The bacilli in 500 or 1000 ml cultures are allowed to settle and the supernatant is filtered through a 0.2 mm ZapCap filter into 4-1 bottles. To minimize plugging of

the filter it is important to use ZapCap with a prefilter and decant a minimal amount of cells along with the supernatant. Sodium azide is added to the filtrate to a final concentration of 0.04% w/v and this material is stored at 4°C. After filtration, the culture supernatant is considered sterile. Nevertheless, before further use, a 1 ml aliquot of this filtrate is plated on Middlebrook 7Hll agar and incubated for 3 weeks to ensure the absence of viable bacilli. The filtrate is concentrated to approximately 2% of its original volume using an Amicon apparatus with a low protein binding, 10 kDa molecular weight cut off membrane. This concentrate is dialysed extensively against 10 mM ammonium bicarbonate and the protein concentration estimated by the BCA protein assay (Pierce, Rockford, IL, USA). The final culture filtrate protein (CFP) preparation is aliquoted and stored at –70°C. Typically, 4–5 mg of CFPs is obtained from 1 l of a 2 week culture of *M. tuberculosis.*

4. Isolation of subcellular fractions of *M. tuberculosis*

The cells from which the culture supernatant has been decanted are collected by centrifugation at 3000 g. The cell pellet is washed with sterile H_2O and inactivated. To preserve the integrity of proteins 7-irradiation is recommended for the killing of *M. tuberculosis.* A radiation dose of 2.4 megaRad renders all exposed bacilli non-viable whilst not affecting the large majority of the enzymatic functions of the cells (Hutchinson and Pollard, 1961). Alternatively, *M. tuberculosis* cells can be killed by heating at 80°C for 1 h. This is best done in an autoclave with the capacity to perform low-temperature isothermal cycles. However, heat killing is much more damaging to the integrity of the *M. tuberculosis* proteins. As with the CFP preparations the lack of viable bacilli should be checked before cells are removed from containment facilities.

Several techniques for the generation of *M. tuberculosis* subcellular fractions have been reported (Hirschfield *et al*., 1990; Lee *et al*., 1992; Trias *et al*., 1992; Wheeler *et al*., 1993). Although some of these protocols may result in cleaner separation of subcellular fractions, we have found that the methods used by Hirschfield *et al*. (1990) and Lee *et al.* (1992) provide a rapid and simple means by which to obtain crude fractions of cell wall, membrane and cytosol. Lysis of *M. tuberculosis* cells is accomplished by suspending the cell pellet at a concentration of 2 g of cells/ml of breaking buffer and passing this suspension through a French press at 1500 psi, 5–7 times. The lysate is diluted with 1 volume of the breaking buffer and unbroken cells are removed by centrifugation at 3000 g for 15 min. Cell wall material is harvested from the supernatant of the low speed spin by centrifugation at 27,000 g for 30 min. The cell wall pellet is washed with 10 mM ammonium bicarbonate, dialysed against the same, aliquoted and stored at –70°C. Supernatant from the 27,000 g spin is further separated into cytosolic and membrane fractions by centrifugation at 100,000 g for 1 h. The membrane pellet is washed, suspended in 10 mM ammonium bicarbonate and stored at –70°C. The cytosolic fraction is dialysed against 10 mM ammonium bicarbonate, aliquoted and stored. Extraction of proteins from the cell wall or membrane fraction may be performed using a number of detergent or chaotropic agents that are easily removed prior to use of the proteins in immunological assays (Hjelemeland, 1990; Thomas and McNamee, 1990; Scopes, 1994).

♦♦♦♦♦♦ III. ANIMAL INFECTION PROTOCOLS

A. Intravenous Infection of Mice

The proper handling and restraining techniques for mice should be mastered prior to any attempt at intravenous inoculation with virulent strains of *M. tuberculosis.* The technician should seek proper training which is provided by most institutional animal facilities in order to assure the safety of both the technician and the laboratory animal. Proper humane methods for handling laboratory mice should be learned by the technician and a certain degree of skill and confidence achieved prior to performing any work involving the use of *M. tuberculosis* in an animal model. The technician needs to be fully aware of the risks of accidental infection via a bite wound, scratch, accidental needle stick or aerosol exposure when restraining and inoculating mice with *M. tuberculosis.* Because of this, it is extremely important that the technician develop a methodical approach when performing such techniques.

All infections of laboratory animals with *M. tuberculosis* should be done in an appropriate Animal Biosafety Level-3 laboratory (ABL-3) with the technician wearing appropriate facility clothing and personal protective equipment. Double disposable surgical gloves should be worn when handling mice to prevent accidental exposure due to tearing of the outer glove (mice can bite through the outer glove, but rarely through both). To infect mice intravenously the technician will require a preparation of *M. tuberculosis* from a stock of known cfu ml. Working under BSL-3 conditions, the bacilli are thawed and carefully removed from the vial via a 1 ml tuberculin syringe fitted with a 26 G needle. The bacteria should then be diluted in normal saline or buffered saline saline (PBS) to achieve the required cfu concentration per millilitre for intravenous challenge. When the mycobacterial suspension is dispensed from the tuberculin syringe into the dilution tube it is done in a manner in which the suspension is slowly dispensed down the inside wall of the tube. This is done in order to minimize the possibility of the creation of an aerosol from the needle. After dispensing the mycobacterial suspension, the syringe is carefully placed in an appropriate 'sharps' container for disposal.

The mycobacterial suspension is serially diluted and a sample plated on 7Hll agar to verify the concentration. Pipetting operations during the serial dilution process are carried out with extreme care in order to prevent aerosol generation. Any small spills or drops during the pipetting process should be immediately disinfected with 5% Lysol™. All pipettes and other materials used serially to dilute the mycobacteria are placed in a pipette boat containing 5% Lysol™ solution. The biological containment hood is disinfected after use. The culture tubes, stock vials and pipette boat are double bagged in autoclave bags and taped with heat-sensitive autoclave tape. These materials are then placed in a large autoclave pan located near the ABL-3 autoclave for subsequent sterilization.

In our laboratory, the standard intravenous challenge dose is 10^5 cfu per mouse. This dose was chosen because it is sub-lethal and allows the mouse to make a very strong cellular response. This is delivered intravenously in a volume of 0.2 ml from a working concentration of 5×10^5 cfu/ml suspended in normal saline or PBS. The injectate is loaded into a 1 ml tuberculin syringe fitted with a 26 G needle with the needle bevel at the same orientation as the syringe graduations.

All intravenous infections with *M. tuberculosis* should be performed in an appropriate 'Class II' biosafety cabinet. Prior to injecting mice a full-face shield should be put on to prevent accidental exposure from injectate inadvertently spraying back during injection (a common, and scary event, to the novice). Although a simple shield is probably sufficient, the operator should consider wearing a RACAL AC-3 (Racal Health and Safety) respirator which consists of a belt with a blower unit fitted with a HEPA filter which delivers sterile air to a helmet face shield. This unit provides clear visibility and does not fog up, unlike traditional face respirators. Once sufficient syringes have been prepared, a cage of mice is placed under a heat lamp to warm the mice gently and increase their venous circulation. It is essential that the worker pay close attention that the mice are warmed but are not heat stressed while under this lamp. While the mice are warming, a mouse restrainer device is set up. We use a metal cone type of restrainer which bolts to the edge of the laboratory bench. When the mice are sufficiently warm, one mouse is removed from the cage by gently grasping the tail. It is then placed into the restrainer with the tail sliding through the slot in the top of the restrainer. While holding the tail, swab the area to be injected with a 70% ethanol-soaked gauze sponge or swab. Allow the ethanol to air dry. Identify a lateral tail vein and keeping the needle bevel up gently insert the needle parallel to the vein 2–4 mm into the lumen closer to the end of the tail.

Once you are sure you are in the vein, inject the *M. tuberculosis* suspension slowly. No bleb should be visible if the needle was properly inserted into the lumen of the vein; if a bleb appears, indicating failure to locate the vein, additional attempts may be made proximally. It is desirable to make the first attempt at injection as close to the tip of the tail as possible. NEVER force the syringe if you miss the vein as spray back will occur, or the needle hub may dislodge from the syringe or tail and cause a subsequent aerosol of *M. tuberculosis.* When finished, withdraw the needle slowly and apply pressure at the injection site with gauze if necessary to achieve hemostasis. It is strongly advised to practice the intravenous infection of mice with saline on multiple occasions prior to using *M. tuberculosis*.

B. Aerosol Infection of Mice

Because the natural route of tuberculosis infection in humans is the lung, the most precise animal models try to mimic this route. Intranasal or intratracheal inoculation of mice can give rise to pulmonary infection, but the most reproducible technique is to generate an aerosol that is inhaled by the animal.

Aerosol devices are available in two main types: one is the sealed cabinet system pioneered by Middlebrook and the other a newer device that fits over the nose of the animal. Whatever your choice, the device must be kept under stringent ABL-3 conditions due to the very high aerosol danger. Our preference is the Middlebrook Airborne Infection apparatus which has been used for this specific purpose for the past 30 years. This instrument is currently manufactured by Glas-Col, Inc., of Terre Haute, Indiana, and has changed very little in configuration since the original design. The instrument consists of a large circular tank (aerosol chamber) which

contains a circular basket/cage with five pie-shaped compartments in which animals are placed. Each of the compartments can accommodate as many as 25 mice, two 500 g guinea pigs or one rabbit. The aerosol chamber has a heavy acrylic lid with four locking handles that lock tightly against a heavy-duty rubber gasket. The lid also has two ultraviolet lamps on its underside and these lamps are turned on during the decontamination cycle of instrument operation.

The technician will require a preparation of *M. tuberculosis* from a stock of known cfu/ml. Working under BSL-3 conditions, the bacilli are thawed and carefully removed from the vial via a 1 ml tuberculin syringe fitted with a 26 G needle. The bacteria should then be diluted in normal saline or PBS to achieve the required cfu concentration per millilitre for aerosol challenge. The technician puts on the appropriate safety equipment [a RACAL safety helmet with HEPA filters is recommended (Orme and Collins, 1994)]. When the mycobacterial suspension is properly diluted it is sucked up with a 10 ml syringe and placed in a closed plastic box, transported to the aerosol room and slowly placed into the nebulization chamber (place needle against the glass wall slowly dispensing the liquid without creating aerosols).

The front of the instrument consists of a control panel, which allows the machine to be programmed; two airflow meters; two air-control knobs and a series of switches which control power. Also, on the front of the instrument are three tygon hoses with hose clamps for attaching the glass venturi unit (nebulizer) which is fitted in a holding bracket and filled with the bacterial suspension. When the instrument is in operation, compressed air flows through the nebulizer and produces a very fine mist of the bacterial suspension, which is then carried by a larger volume of air flowing into the aerosol chamber. The airflow then exits the chamber through two HEPA filters and a super-heated exhaust stack wherein it is incinerated. The program, controlled via the control panel, is used to determine the duration of the various cycles involved in the 'aerosol' process. The first parameter to be entered is the length of the 'pre-heat' cycle; this cycle allows the incinerator to attain suitable temperature prior to nebulization. The second parameter is the length of time required for the nebulization cycle; this cycle does not engage until the pre-heat cycle is complete. During nebulization the compressed air comes on and is routed through the venturi of the nebulizer to create the fine bacterial mist. The third parameter to be entered is the time required for the 'cloud decay' cycle and it is during this cycle that the aerosol chamber is purged with fresh air and the bacterial mist dissipated. The final parameter is the length of the 'ultraviolet cycle', in which the UV lamps are switched on and decontaminate the top surfaces of the basket. The length of time suggested for the incinerator warm up and the UV decontamination cycles is 15 min each. The time required for the cloud decay cycle is 40 min. The time required for the nebulizing cycle should be determined empirically for each animal type.

Once all cycles are complete the instrument is carefully examined to make sure hoses and gaskets are still in place. The technician, wearing appropriate safety equipment [a RACAL safety helmet with HEPA filters is recommended (Orme and Collins, 1994)], then opens the chamber lid and removes the animals. The basket is carefully removed, wrapped in autoclave bags and autoclaved to sterilize. The interior of the chamber is then disinfected with 5% LysoV M followed by 70%

ethanol. The glass venture nebulizer is carefully removed and placed in a stainless steel pan containing 5% Lysol, covered with a lid, wrapped in an autoclave bag and sterilized via autoclaving. All disinfecting materials are likewise double bagged and autoclaved.

C. Aerosol Infection of Guinea Pig

Pulmonary tuberculosis in guinea pigs has multiple similarities to the disease in humans. It has long been considered the gold standard small animal model for vaccine testing, and it beginning to be used to evaluate chemotherapy (Lenaerts *et al*., 2008; Ordway *et al*., 2008; Williams *et al*., 2009).

Exposure of guinea pigs to aerosols of *M. tuberculosis* can be performed under stringent ABL-3 conditions using a Madison (Generation III) infection chamber manufactured by the University of Wisconsin. This chamber has undergone very little configuration since the original design in 1970 and there are currently 40–50 chambers in worldwide use today (Selecting the Most Suitable Aerosolization Equipment, Tradeline, Inc., 2007). The aerosol chamber consists of a large cylindrical tank which holds a metal aerosol infection basket that contains 18 small individual compartments, each compartment able to house a single guinea pig. The aerosol basket is loaded with guinea pigs and then placed into the Madison aerosol chamber using a cart. The aerosol chamber door is then locked shut with eight latches that secure the door tightly against the machine, preventing airflow from leaking.

The front of the instrument consists of the control panel. This is the power supply chamber system which consists of the power switch, cycle start and stop knobs, emergency shut off button, fan test button and photohelic unit. The control panel can be opened to check that the time delay relay 1 (TD1) and the second time delay (TD2) are properly set. The TD1 controls the total time of an exposure cycle and should be set to 900 sec/*on delay*. The TD2 controls the time that the nebulizer is on and should be set to 300 sec/*interval delay*. After the door is closed and latched the photohelic unit should read between 9 and 13 in. of water to ensure that the proper amount of vacuum is maintained. If the vacuum pressure is lower than 9 in. the exposure cycle will not start. If during a cycle the vacuum pressure exceeds 13 in. then there is a blockage of incoming secondary air. This will sound the alarm and activate the *end cycle light*. If this occurs the fans will shut off but the nebulizer will continue to work. The cycle can be stopped by pressing the RESET button.

The flow panel is located on the right side of the chamber and contains two flow meters. The right flow meter controls the secondary airflow. This is the air being pumped through the system by the vacuum/compressor unit through a series of two HEPA filters at a rate of ~45 l/min. The left flow meter indicates the primary airflow. This is the air being channelled through the nebulizer unit and is determined by the pressure regulator located at the centre of the flow panel. When the instrument is in operation, compressed air flows through the nebulizer at ~4 l/min and produces a very fine mist of the bacterial suspension, which is then carried by a larger volume of air flowing into the aerosol chamber. The airflow then exits the chamber through two HEPA filters.

A test cycle is run prior to an aerosol infection to be sure that the machine is running properly. During this test cycle no animals are loaded into the chamber. Fifteen millilitres of sterilized water in a 20 cc syringe with an 18 G 1½ needle is loaded into a sterile nebulizer jar by unscrewing the plug screw located on the top of the collision nebulizer unit and dispensing the water through the orifice. After dispensing the water into the nebulizer jar re-fasten the plug screw. Once all doors are properly latched check to see that the proper amount of secondary airflow is ~45 l/min and the proper amount of vacuum is maintained. The test run can then be initiated by pressing the *cycle start* button. After starting the cycle check to see that the nebulizer probe is properly functioning. A spray mist coming from three jets will be observed.

If the test cycle runs with no errors then an aerosol infection run can be performed. A new sterilized nebulizer jar is placed on the collision nebulizer unit while the water run nebulizer jar is placed in 5% Lysol. Ten millilitres of inoculum containing 1.0×10^6 cfu/ml of *M. tuberculosis* suspended in sterile saline is added to the nebulizer jar the same way as the sterile water. A metal square spacer is placed at the back of the chamber to prevent the aerosol basket from hitting the fans. The aerosol basket that contains the animals is then loaded into the chamber. The doors are latched, the proper airflow and vacuum pressure gauges are checked and the CYCLE START button is pressed to initiate the infection run. A cycle will last for 15 min. Please note that all interior surfaces of the chamber from the nebulizer to the exit of the HEPA filters are exposed to *M. tuberculosis* during an exposure cycle. When the cycle is complete press the *end cycle* button on the control panel, unlatch the door to unload the aerosol basket containing the animals, then re-latch the door. Finally, carefully unscrew the nebulizer jar containing remnants of the infectious inoculum and place the jar in 5% Lysol solution. The animals are then carefully unloaded from the basket and placed back into their correct cage. If more that one infectious aerosol cycle needs to be performed repeat the above process.

Once all infectious cycles are complete a final water run is performed. This is similar to the initial water run except prior to adding a new sterile nebulizer jar the probe is carefully dabbed with a Wypal soaked with 5% Lysol followed with a Wypal soaked with 70% ethanol. Also, 20 ml of sterile water is added to the nebulizer jar instead of 15 ml. During this water run the aerosol basket can be loaded into an autoclave bag to be sterilized by autoclaving. The cart that holds the aerosol basket is then properly wiped down with first a 5% Lysol solution followed with a 70% ethanol solution.

On completion of the final water run the machine is turned off and the chamber is thoroughly cleaned with 5% Lysol then 70% ethanol. This includes the jets at the back of the machine and on the door, the spacer, the entire inside of the chamber and another wipe down of the probe. A new nebulizer jar is then placed on the probe and the doors are latched to the chamber once the ethanol has evaporated. The nebulizer jars are autoclaved out in the 5% Lysol solution. During the whole procedure donning of proper PPE is required. This includes surgical scrubs, facility shoes, hairnet, N95 respirators, double gloves, tyvec suit and a RACAL safety helmet with HEPA filters.

♦♦♦♦♦♦ IV. CULTURING AND INFECTING MACROPHAGES

A. Establishing Macrophage Cultures *In Vitro*

The establishment of primary cell cultures of murine bone marrow-derived macrophages is an important *in vitro* technique, which is easy to perform. These macrophages can be used for numerous types of studies ranging from responses to infection (nitric oxide or chemokine production for example), to evaluating the ability of drugs to prevent intracellular replication and to identifying protein targets of IFNγ secreting T-cell subsets.

Bone marrow macrophage cultures are established by first euthanizing mice in accordance with the methods approved by your institutional animal care and use committee. We recommend placing mice in a 100% CO_2 which is gradually introduced to result in replacement of 20% chamber volume per minute to produce a loss of consciousness without apparent distress. Following the induction of unconsciousness, the rate can be raised to 3–4 times the initial flow rate to accelerate the process and after apparent clinical death of the animal, gas flow should be maintained for at least one minute. Death should be verified via cervical dislocation or bilateral thoracotomy. Once the animals have been euthanized they are placed on a clean dissection board and saturated with 70% ethanol. The skin at the mid back is clipped with sterile scissors and then pealed back to expose the lower part of the body including the hind legs. The knee is then dislocated by holding the thigh with one hand and the shin with the other. Dislocation is accomplished by firmly pulling apart the knee joint. When this is done bend the knee back, holding the leg on the shin. Clip the muscle under the knee and bend the knee in the direction it normally would not bend. Pull down on the shin, and the femur will emerge through the muscle. Clip the femur from the hip, removing the excess muscle and place it in a tube containing ice-cold, sterile media (see below). Clip the foot off and place the sharp edge of the scissors between the tibia and the fibula and slide the scissors up the shin, cutting the muscle. Peel the tibia out of the muscle and clip it from the knee, removing the excess muscle. The tibia is also placed in the tube containing ice-cold media.

The tube containing the bones is then taken to the tissue culture area of the laboratory and placed in a laminar flow biological containment cabinet for the extraction of the bone marrow. The tube containing the bones and media is carefully emptied into a large sterile petri dish. Sterile forceps and scissors are used to pick up the bones, remove any excess muscle tissue, and to clip the ends to expose the marrow. Using a 10 ml syringe filled with media and fitted with a 26 G needle, rinse the bone marrow out of both ends of the bones into a 50 ml conical tube which contains 5–10 ml of media. Rinse with about 4 ml of media per bone to ensure complete removal of all bone marrow cells.

A 10 ml pipette is then used gently to mix the marrow suspension up and down until all the clumps have been broken up. The bone marrow cells are then pelleted by centrifugation (150 g/7 min/4°C). The supernatant is decanted and the cells resuspended (use 2 ml media per animal harvested). Pass the cells through 100 tim sterile cell strainer to break up cell clumps. Count the cells in 3% acetic acid/PBS (to lyse red cells) and then adjust the cell suspension to a concentration of

Table 1. Bone marrow macrophage culture[a]

Tissue culture system	Seed density (nucleated cells/ml)	Volume required (ml)
75 cm TC flasks	5.0×10^5	30.0
150 mm TC flasks	1.0×10^6	20.0
100 mm TC flasks	1.0×10^6	12.0
12-well TC flasks	1.0×10^6	2.0
24-well TC flasks	1.0×10^6	1.0
96-well TC flasks	1.0×10^6	0.20

[a] TC flasks, tissue culture flasks that have a 75 cm:' culture area; TC, tissue culture.

2×10^6 nucleated cells/ml of medium. Each mouse should provide $1–2 \times 10^7$ bone marrow cells. These are then plated onto petri dishes, flasks or well-type tissue culture plates as shown in Table 1.

The bone marrow cell cultures are then placed in a 37°C incubator which is supplemented to 95% humidified air with 5–7% CO_2. The media in the cultures are changed at 48 h post-seeding and then again changed at day 4–5. The macrophages should have differentiated and formed a confluent monolayer by day 7–9. At this point the macrophages are mature and ready for use in experiments. If these bone marrow macrophages are to be used for infection with *M. tuberculosis* the media needs to be changed to antibiotic-free media 48 h prior to the experiment.

B. Bone Marrow Medium

- Complete DMEM (Sigma #D5530) supplemented with FCS (Intergen) and 10% L-929 conditioned medium
- HEPES buffer (Sigma #H0887)
- L-glutamine (Sigma #G7513) MEM Non-essential #M7145)
- Penicillin/streptomycin (Sigma #P-078 I) (omit for Antibiotic-Free Bone Marrow Media)
- 10% heat-inactivated amino acids (Sigma)

C. L-929 Conditioned Medium

- L-929 cells from ATCC are grown up at 4.7×10^5 cells total in a 75 cm^2 tissue culture (TC) flask with 55 ml of DMEM (Sigma)
- 10% FCS (Intergen)

1. Allow cells to grow for 7 days or until confluent.
2. On day 7 collect the supernatant, filter through a 0.45 μm Nalgene filter and freeze at –20°C in 40 ml aliquots. The use of fetal calf serum in these cultures requires that each new batch be assessed prior to purchase. The characteristics of the macrophages can differ depending on the constituents of the FCS.

D. Infecting Macrophage Cultures

The *in vitro* infection of murine bone marrow-derived macrophages is routinely used in our laboratory to evaluate the macrophage response to different clinical isolates (Park *et al.*, 2006) and also to determine the efficacy of various novel antibiotic compounds on the intracellular growth of *M. tuberculosis* (Furney *et al.*, 1995). In such studies, the macrophage monolayers are washed once with sterile PBS and then supplemented with fresh antibiotic-free bone marrow macrophage medium as described above. The cultures are then allowed to incubate for 48 h prior to infection with *M. tuberculosis.* If the protocol involves cytokine treatment of the cells, these are added at this time.

The resulting macrophage monolayer contains approximately 1.0×10^7 cells after 8–10 days of incubation (24-well plate method). On the day of infection the media are removed from the macrophage monolayer and immediately replaced with 200 µl of antibiotic-free media containing 1.0×10^6 cfu (5.0×10^6 cfu/ml) of *M. tuberculosis.* The plates are returned to the 37°C humidified air-CO_2 incubator for 4 h. After this incubation period, the monolayers are washed gently four times with 1 ml sterile PBS to remove any bacilli that were not phagocytosed. (Great care should be taken not to generate aerosols during this procedure.)

The cells are now ready for further use. Production of oxygen or nitrogen radicals can be measured by colorimetric assays, and supernatants can be collected to measure the secretion of chemokines or cytokines by enzyme-linked immunospot assay (ELISPOT), Enzyme-Linked Immunosorbent Assay (ELISA) and cytometric bead array (CBA). The cells can be lysed in Ultraspec (Biotecx) and processed for the presence of mRNA for molecules of interest. Alternatively, growth of the bacteria can be followed by plating lysates (distilled water plus 0.05% Tween 80, then diluted in PBS) and plotting cfus versus time.

It has been claimed that such cultures can be taken out for as long as a month. Certainly the cultures can look good under phase-contrast microscopy for up to 2 weeks in our hands, but even then some detached macrophages are seen ('floaters') which can make the bacterial numbers appear lower than they really are. For this reason, we do not go further than 8 days in these assays. The user will also note, if monitoring cfu versus time, that there is a 'lag phase' of 3–4 days in this assay before florid growth of the infection is observed.

There is a similar caveat with regard to using radioactive uracil as opposed to counting cfu in macrophage cultures. In our hands reduction in uracil uptake usually only reflects bacteriostasis, not bactericidal activity, so any claims that a reduction in uracil counts equals killing should be backed up by showing a reduction in cfu counts (Rhoades and Orme, 1997).

♦♦♦♦♦♦ V. IDENTIFYING KEY PROTEINS RECOGNIZED BY IMMUNE T CELLS

The bone marrow-derived macrophage system can also be utilized in immunological assays involving antigen-processing and presentation to T cells. In our laboratory we have had quite variable results based on cell proliferation assays,

and so, given our demonstration of protective T cells as cells that secrete IFNγ (Orme *et al*., 1992; Cooper *et al*., 1993), we developed the following assay to detect the presence of these cells and to obtain a picture of the proteins they are recognizing. Details of these results are published elsewhere (Roberts *et al*., 1995).

The system uses bone marrow-derived macrophages to present antigen to T cells (or subsets thereof) harvested from syngeneic mice which have been infected with *M. tuberculosis*. This type of assay can be used to determine the kinetics against time of the response to a given antigen (Orme and Collins, 1994). Adequate numbers of T cells can be harvested from the spleen or the lung, as described below, and used in the T-cell overlay method.

Tissue culture plates (96 well) are seeded with 2×10^5 bone marrow cells and left for 7 days. Samples of individual proteins or protein fractions are dissolved in sterile pyrogen-free water to a concentration of 1 mg/ml. The medium in the bone marrow macrophage cultures is carefully removed and replaced with fresh medium. For pulsing macrophage cultures the stock protein samples must be diluted to a working concentration of 10 μg/ml. Ovalbumin is used as an irrelevant negative control (there is some background IFNγ secretion, usually in the picogram range). The macrophage cultures are then incubated overnight at 37°C and 6% CO_2 to allow processing and presentation of the test antigens.

The following day infected mice are euthanized and spleen (or lung, see below) cell suspensions prepared. These are then incubated at 37°C in 5% CO_2 for 1 h in plastic flasks to allow macrophages to adhere. After incubation, the plate is removed from the incubator and gently rocked/swirled to resuspend the non-adherent spleen cell population. The non-adherent cells are gently pipetted off into a sterile 50 ml conical tube and centrifuged at 200 g for 7 rain. The supernatant is gently decanted and the cell pellet is resuspended with 5 ml of Gey's lysing buffer (see below) per spleen in order to remove red blood cells from the non-adherent spleen cell population. The cells are incubated for 5 min at room temperature with occasional shaking. (Note: Gey's lysing buffer needs to be used at room temperature in order to work properly.) After the Gey's incubation is complete, the tube is filled to 45 ml with tissue culture medium and again centrifuged for 7 min. This wash process is then repeated one additional time. After the last wash the supernatant is decanted and the cell pellet is resuspended with monoclonal antibody supernatant preparations from clones TIB-210 (clone 2.43 anti-CD8.2) and TIB-183 (clone J11d.2 anti-B-cell, granulocyte, immature T-cell supernatant).

The exact working dilutions need to be determined for each lot of antibody supernatants. After incubation at 37°C for 30 min Cederlane™ Low-Tox-M Rabbit Complement (1:16 Final Concentration) is added to the cell suspension and incubated for a further 1 h. The cells are then centrifuged at 200 g for 7 min, and repeated twice. These cells should be an enriched population containing predominantly CD4 T cells, which can be checked by flow cytometric analysis.

Alternatively, CD4 or CD8 T cells can be purified using MACS cell separation beads (Miltenyi Biotec) and by following the manufacturer's protocol. Briefly, cells are incubated with MACS beads specific for CD4 or CD8 for 15 min at 4°C, washed and passed over a cell separation column (Miltenyi Biotec). Eluted cells are then collected, counted and resuspended 1×10^6 cells/ml in media containing 20 units of

IL-2 per millilitre to maintain T-cell viability. The T cells are then added in volumes of 0.1 ml to the wells containing the macrophages and incubated for 72 h at 37°C in 5% CO_2. Supernatants are then removed and assayed for IFNγ by ELISA.

A. Gey's Lysing Buffer

1. 4.15 g NH_4Cl
2. 0.5 g $KHCO_3$
3. Add 500 ml H_2O and adjust pH to 7.2–7.4 with 1N HCl
5. Filter sterilize through 0.2 ftm filter and store at room temperature

B. Complete Tissue Culture Medium

- Complete DMEM (Sigma #D5530) supplemented with 10% heat-inactivated FCS (Intergen)
- HEPES buffer (Sigma #H0887)
- L-glutamine (Sigma #G7513) MEM non-essential amino acids (Sigma #M7145)
- Penicillin/streptomycin (Sigma #P-0781)

♦♦♦♦♦♦ VI. FOLLOWING THE COURSE OF INFECTION

A. Mouse Infections

Following the course of the tuberculosis infection by plating tissues and counting bacterial colonies can provide valuable information about the kinetics of expression of the host response (Orme, 1995; Ordway *et al.*, 2007a,b). You should also be aware, however, that the assay is rather crude, with a counting error of about 20%. Because of this variance one cannot read too much into small changes in numbers; as an example, late stages of the infection often appear to be 'chronic', i.e. flat-line. The infection may truly be chronic, but could also be increasing and waning over a small range; there is simply no way to tell. Similar care should be taken in the case of drug therapy, in which bacterial numbers can reach very low numbers. Either way, given the biological variation in this system, a statistical difference is not seen unless the mean values differ by about 0.5–0.7 log.

Simple statistic power calculations show that five mice per group is the minimum number that should be used for *in vivo* determination of bacterial growth. Thus to follow the course of infection, one should harvest five mice at each time point.

We place organs in individual industrial-strength homogenizing tubes with a very tight pestle (keep on dry ice before using so the pestle does not expand) and grind for 30–40 s. Do not worry about the high shearing forces; these are needed to disrupt all the cells and disperse the bacteria. Then make serial dilutions and plate 100 µl of each dilution on quadrants of petri dishes containing 7Hll agar. Keep the homogenates on ice at all times.

Incubate the plates in a 37°C cabinet containing a tray of water to keep the air humid to prevent the plates drying. Resist the temptation to count colonies when they are still small (you will undercount). Count the quadrant in which there are between 10 and 100 colonies, but also make sure the other quadrants correlate, i.e. if you have about 40 colonies, there should be about 400 on the one above and about 3–5 on the next dilution down. Then apply dilution factors and the original homogenate volume to calculate total bacteria per organ.

If you see no colonies at the 0 or –1 dilutions of the liver tissues, but there are some at higher dilutions, do not worry. The liver contains enzymes that inhibit bacterial growth; as these are diluted out the colonies start to grow. We generally do not use the liver to quantify bacteria because of this reason.

A further 'quality control' is to do a day 1 viable count, i.e. 24 h after infection. The numbers you obtain here can tell you if the infectious dose required was obtained. After i.v. infection expect about a 90/10/2% distribution in uptake in the liver, spleen, and lungs. Look especially at the lung counts; if your uptake was 25–50% in the lungs instead of a few per cent, then your inoculum was clumped (and the rafts got stuck in the lungs). The sensitivity of the assay is about 1.7 logs; below this we usually designate as ND (not detected). In fact, low numbers, or zero colonies, can sometimes be a problem; if you are using a computer program, do not incorporate a zero as this will undercount your values. In the same vein, be careful about very high values; a common mistake made by beginners is not to change pipettes between dilutions. As a result bacteria are 'carried over' from one dilution to the next, which can escalate the count as much as 3–4 logs. Use common sense; if the bacterial load in wet weight is larger than the weight of the mouse, you did something wrong!

For aerosol infection studies, the uptake in the lungs should be in the 100–200 range. Lower uptakes can be achieved, but greater variance between groups is also seen.

B. Bacterial Numbers in Infected Guinea Pigs

Counting bacterial colonies in guinea pig organs can provide valuable information about the virulence of the bacterial strain (Ordway *et al.*, 2007c; Palanisamy *et al.*, 2008), the efficacy of vaccines (Horwitz and Harth, 2003; McMurray *et al.*, 2005; Henao-Tamayo, 2009; Ordway *et al.*, 2008) and the effects of drug treatment (Hoff *et al.*, 2008).

As in the mouse, simple power calculations show that five guinea pigs per group is the minimum number that should be used for *in vivo* determination of bacterial growth. Thus to follow the course of infection, one should harvest five guinea pigs at each time point.

Organs are placed in individual industrial-strength homogenizing tubes (Glas-Col, LLC. Terre Haute, IN) filled with 9.0 ml of sterile saline. The organs are then homogenized with a hand-held tissue tearor (BioSpec Products, Inc., Bartlesville, OK) with a probe diameter of 14 mm and a probe length of 13.2 cm. Complete homogenization of tissues is usually achieved in 30–40 s. The high shearing forces are required to disrupt all the cells and disperse the bacteria. One millilitre of the homogenate is then diluted three times 1:10-fold for vaccine studies and six times

1:5-fold for chemotherapy studies. One hundred microlitres of each dilution is plated on a quadrant petri plate filled with 4.5 ml of 7H11 agar per quadrant; 4-0 dilutions for vaccine studies and 7-0 dilutions for chemotherapy studies.

The plates are incubated in a 37°C cabinet for 3–6 weeks or until waxy, cream coloured, flower-shaped colonies appear (it is important not to count colonies when they are too small or let the colonies overgrow, both could lead to undercounting). To give the most accurate cfu data, count the quadrants in which there are between 10 and 100 colonies, and also note that in a 10-fold dilution the other quadrants correlate, i.e. if you have about 40 colonies in dilution 2, there should be about 400 colonies in dilution 1 and about 3–5 colonies in dilution 3. To obtain the cfu's per organ multiply the counted colonies by $10 \text{ ^ } ^{\text{dilution}}$ (in a 10-fold dilution 10^^0 is 10, 10^^1 is 100, 10^^2 is 1000, etc.). This number is then multiplied 10 (the homogenate total volume).

Some times there are no colonies in the 0 dilutions and colonies in the consecutive 1–3 dilutions. This is usually due to too much homogenate for the colonies to grow, or can sometimes be due to enzymes in the organ that may inhibit bacterial growth. Such effects should dilute out.

C. Murine and Guinea Pig Animal Husbandry

Daily animal observation during mycobacterial infection is a necessary part of animal husbandry. When mice and guinea pigs are noted to have certain clinical symptoms indicative of morbidity (which can vary dependant on the mycobacterial strain virulence, vaccination or drug treatment procedures), a score can be given to those symptoms indicating severity of disease progression and animals under authority of the facility Veterinarian can be euthanized.

To achieve this, simple Karnovsky scales can be generated. Animals should be scored in terms of general behaviour, feeding habits and weight gain or loss. In addition, the veterinary staff should be alerted to various clinical problems such as ulcerative dermatitis (mice often fight to establish pecking orders), or tumours (sometimes a problem with certain inbred strains). Torticollis, in which the animal is actively spinning or rolling, is sometimes seen. Other symptoms may be seen depending on the nature of the study.

Clinical scores when paired with daily weights and body temperatures can provide useful information for monitoring animals. The recent invention of temperature sensitive chips which can be inserted into the animal's skin and monitored easily using a scanner (Bio Medic Data Systems, Inc., Seaford, Delaware) has made this task easy.

D. Mouse Pathology

Disease progression can be monitored by evaluating the existing organ pathology at different stages of infection. Mice are the most widely used small animal model because of the broader availability of immunological reagents and of inbred and genetically engineered strains with well-defined genotypes (Ordway *et al.*, 2007a,b; Basaraba, 2008). The pulmonary granulomatous response to *M. tuberculosis* in the

mouse is different from that in the guinea pig or human. The major difference is the lack of early central caseating necrosis in primary pulmonary lesions of immunologically intact mice. In addition, due to the smaller organ size it is difficult to discriminate between primary and secondary lesions in the organs. Generally the disease progresses in five stages (Rhoades *et al*., 1995, 1997; Rhoades and Orme, 1997) which are based on the extent of granulomatous involvement, the cell types present, the degree of lymphocyte organization and the presence of destructive sequelae such as airway epithelium erosion and airway debris. Many of these parameters can be used to give an overall group ranking or lesion score based on histopathological assessments by a qualified veterinary pathologist (Basaraba, 2008).

To obtain pathology samples during the infection the accessory lung lobe, portions of the spleen, lymph node and liver of each mouse in each group are removed surgically and infused with 10% neutral-buffered formalin (NBF). Organs are placed into 30 ml of 10% NBF for fixation prior to being embedded in wax and cut on a cryostat (Leica, CM 1850) and placed on glass slides for routine haematoxylin and eosin and acid fast bacilli staining.

E. Guinea Pig Pathology

The disease that develops in the guinea pig following aerosol exposure to *M. tuberculosis* can be divided into acute, subacute and chronic stages of infection based on the pattern of bacterial growth and dissemination, as well as patterns of pulmonary and extra-pulmonary pathology (Basaraba, 2007, Ordway *et al*., 2007c, 2008). During acute infection, there is an initial 3 day lag in bacterial growth, followed by an approximately 2 week period of rapid bacterial proliferation in the lung and draining lymph nodes. The acute stage is also characterized by progression of granulomatous inflammation and necrosis in the primary granuloma lesion of the lung and draining mediastinal lymph nodes. The subacute or bacillemia phase from 2 to 4 weeks is characterized by the emergence of a stationary phase of bacterial replication in the lung and lymph nodes. During the subacute phase, the most severe inflammation within the primary lesion begins to subside but not before it has replaced a significant proportion of the normal tissue, particularly in the draining lymph nodes (Basaraba, 2007; Ordway *et al*., 2007c). Importantly in this subacute stage, infection is established in multiple extra-pulmonary sites such as the spleen and liver by hematogenous dissemination of bacilli. Concurrent with bacillemia and exponential bacterial growth in extra-pulmonary sites, there is re-infection of the lung by the hematogenous dissemination. Finally, the chronic stage is characterized by continued bacterial replication in extra-pulmonary tissues but with either stationary or a gradual increase in bacterial numbers in the lung and lymph nodes. The morbidity and mortality of guinea pigs at this stage is due to the combined effect of progressive pulmonary and extra-pulmonary pathology.

Following euthanasia, the left pulmonary lobes are infused *in situ* with 5 ml of 10% NBF and then placed into 30 ml of 10% NBF overnight. The NBF is then replaced (the following day) with fresh 10% NBF (30 ml) and preserved until processing for histopathological assessment. At the time of processing, all tissues

are embedded in paraffin, sectioned at 5 μm, and stained with haematoxylin and eosin for histologic evaluation and subsequent photography. These should be reviewed by a veterinary pathologist; we recommend reviewing two serial sections from each guinea pig obtained from equivalent areas of the left cranial lung lobe. Our method of evaluation is to arrange sections from the least affected to the most severely affected based on lesion burden by sub-gross and microscopic examination. The sections can be further grouped into normal or mild lesions (Category 1), moderate severity lesions (Category 2) and severe lesions (Category 3). The overall ranking is then determined by ranking the number of sections that are classified as either mild or moderate or severe in each group.

♦♦♦♦♦♦ VII. MEASURING THE CELLULAR RESPONSE

Measuring the immune response to mycobacterial infections is now common place. Here we describe simple methods to detect responses by real-time polymerase chain reaction (RT-PCR), by various ELISA-based methods and by flow cytometry.

A. RT-PCR Detection and Quantification of Cytokines in the Mouse Model

Immediately following euthanasia, the tissues of interest should be placed in 1 ml of Ultraspec (a preparatory solution containing chaotropic agents and RNAse inhibitors from Biotecx TX) or directly into TRIzol reagent (Invitrogen). After the collection (and as soon as possible) the sample should then be homogenized inside a glove box and immediately frozen in liquid nitrogen. The frozen samples can be stored at –80°C until all samples from the experiment have been collected. Normal precautions for handling RNA should be observed throughout the extraction procedure. The RNA extraction should be performed following basic protocols and all samples should be treated in an identical manner. The total amount of RNA should be determined by optical density readings at 260 and 280 nm and the integrity can be determined by gel electrophoresis.

The RT-PCR procedure requires a machine capable of monitoring fluorescence signals over time. We use the ABI Prism 7700 (Applied Biosystems). The RT-PCR analysis should be performed using specifically designed primers and probes. The Applied Biosystems TaqMan Primer Express Program is a straightforward tool for generating primers for cytokines.

For this procedure RNA samples from each group and at each time point are reverse transcribed using the Reverse Transcriptase Enzyme (M-MLV RT – Invitrogen). cDNA was then amplified using the ABI Prism 7700 (Applied Biosystems) following the manufacturer's protocol. Fold induction of mRNA was determined by analyzing cycle threshold (C_T) values and normalized for 18s by ($\Delta\Delta C_T$) calculation method.

For all RT-PCR analyses, it is important to use at least five samples (i.e. five mice) per group and also to ensure that the amount of readable RNA is equivalent between samples. One major advantage to this technique is that old RNA samples

stored in the freezer can be analyzed for any newly discovered cytokine as soon as the sequence has been published.

B. Guinea Pig RT-PCR Detection and Quantification of Cytokines

For these studies, tissues of interest should be taken from a minimum of four guinea pigs euthanized at each time point. Following the sacrifice and as soon as possible after the tissue collection, the sample should be well homogenized in saline solution inside a glove box. One millilitre of homogenate is placed in 1 ml of TRIzol reagent (Invitrogen) and then immediately frozen in liquid nitrogen. The frozen samples can be stored at –80°C until all samples from the experiment have been collected. Normal precautions for handling RNA should be observed throughout the extraction procedure. The RNA extraction should be performed following basic protocols and all samples should be treated in an identical manner. The total amount of RNA should be determined by optical density readings at 260 and 280 nm and the integrity can be determined by gel electrophoresis.

The amount of RNA in each sample can be quantified by performing RT-PCR method. This procedure requires a machine capable of monitoring fluorescence signals over time and the analysis should be performed using specifically designed primers. We use the iCycler iQ 5 (BIO Rad).

For this procedure, RNA samples from each group at each time point are reverse transcribed using the reverse transcriptase enzyme (M-MLV RT – Invitrogen). cDNA is then amplified using the iQ SYBR Green Supermix (Bio-Rad) following the manufacturer's protocol on the iQ5 iCycler amplification detection system (Bio-Rad). A negative control using ultra pure Molecular Biology water as the template is run to confirm that the signals are derived from RNA and not due to contaminating genomic DNA. In order to ensure that only the correct gene is amplified, and was not the presence of primer-dimer or non-specific secondary products, a Melting Curve is performed for each run. Fold induction of mRNA is determined by analyzing cycle threshold (C_T) values normalized for HPRT (C_T) expression by ($\Delta\Delta C_T$) calculation method.

C. Organ Digestion and Cell Separation in the Mouse

To obtain cells from the lung the tissue should be perfused through the pulmonary artery with 10 ml of ice-cold PBS containing 50 U/ml of heparin (Sigma, St Louis, MO). This procedure clears the blood from the lungs and the lungs should turn white. Once clear of blood the lungs, as well as the draining lymph nodes and spleens are removed and placed in 2 ml of cold, incomplete D-MEM. It is important to keep samples on ice at all times while processing to increase cellular viability. The organs are dissected into small pieces using razor blade or scissors, then 2 ml of incomplete D-MEM containing type IV bovine pancreatic DNAse (Sigma Chemical, 30 mg/ml) and collagenase XI (Sigma Chemical, 0.7 mg/ml) is added for 30 min at 37°C on motion in the H_2O bath. Use collagenase/DNAse on all organs for routine analysis of macrophages and dendritic cells (DC); however if not, then the lung is the only organ which needs collagenase/DNAse treatment. To stop the

digestion, 10 ml of incomplete D-MEM is added and samples are placed on ice again. To obtain cells from the lung, spleen and mediastinal lymph nodes the tissue should be pushed gently through cell screens with the plunger of a 10 or 5 ml syringe. The resultant single-cell suspension contains a variety of cells including both mononuclear and polymorphonuclear cells. The cell suspension should be kept on ice to avoid loss of any macrophages, which will stick to warm plastic. The remaining erythrocytes are lysed with 2.0 ml Gey's solution (0.15 M NH_4Cl, 10 mM $KHCO_3$) and the cells are washed with Dulbecco's modified Eagle's minimal essential medium. The remaining cells are then counted and plated at 1×10^6 per well in 96-well plates. Total cell numbers are determined by flow cytometry using BD™ Liquid Counting Beads (BD PharMingen, San Jose, CA USA 95131).

Cells prepared from infected tissue can be cultured alone or, if purified cell populations, are used (prepared as described earlier), with antigen-presenting cells. For antigen-related responses 10 μg/ml of mycobacterial antigen can be added (with 2 μg/ml of the mitogen concanavalin A as a control). Cytokines accumulating in the supernatants can then be assayed; timing of sampling will depend on how fast you anticipate these will be made. One should be aware that cells other than antigen-specific lymphocytes can produce many of the cytokines of interest and appropriate controls should be included. Other controls include cells from uninfected mice and unstimulated cells from infected mice.

Specialized DC are central to the generation of acquired immunity after carriage of antigens to draining lymph nodes, where recognition by T cells then occurs. To examine their role in tuberculosis we have used the following techniques. After lung tissues are processed as above to yield a single-cell suspension the pellet is resuspended in 400 μl of PBS containing 0.5% of FBS, without calcium or magnesium. To disrupt clumps and isolated DC the cells are pipetted up and down gently and 100 μl of anti-CD11c (N418) microbeads (Miltenyi Biotec) are added. The mixture is then incubated for 15 min at 4°C, then washed in 10–15 ml of PBS/FBS and resuspended in 5 ml of PBS/FBS. This suspension is then passed over an LS+/+ separation column (Miltenyi Biotec) which binds cells that have beads attached. The column is then washed with 10 ml of PBS/FBS three times. The magnetic field is then removed and the bound cells are collected. The purity of the CD11c-positive population is assessed by flow cytometry or cytospin followed by morphometric analysis.

DC taken directly from the lung can be analysed for functional activity or they can be matured *in vitro* as follows. Cells can be cultured in RPMI containing 10% FBS and 20 ng/ml of GM-CSF (Peprotech Inc., Rocky Hill, NJ, USA). Cells should be plated at 5×10^6 cells/ml and cultured in 6-well plates or petri dishes. The cultures should be fed after 48 h and on the sixth day by replacing one-third of the original volume of media.

Cells cultured in this fashion can then be infected with bacteria. In order to infect the cells they should be cultured without antibiotics for 48 h prior to infection. To collect the cells from the culture media they are centrifuged at 300 g and washed once with PBS (lacking calcium and magnesium). The cells are then resuspended in 50 ml conical tubes at $2–4 \times 10^6$ cells/ml in RPMI containing 2% FBS. Mycobacteria can then be added at a ratio of 1, 5 or 10 cfu per cell and the mixture incubated at 37°C for 4 h. The cells are then washed twice with PBS and resuspended in culture

media lacking antibiotics and with 10% FBS. Infection rates can be checked by acid fast staining and colony counting after 4, 24 and 48 h and cellular viability by the trypan blue method.

D. Organ Digestion and Cell Separation in the Guinea Pig

To obtain cells from the lung the tissue should be perfused through the pulmonary artery with 25 ml of ice-cold PBS containing 50 U/ml of heparin (Sigma, St Louis, MO). This procedure clears the blood from the lungs and the lungs should turn white. Once clear of blood the lungs, lymph nodes and spleens are removed and placed in 4 ml of cold, incomplete D-MEM. It is important to keep samples on ice at all times while processing to increase cellular viability. Then the organs are dissected into small pieces using razor blade or scissors. Then 4 ml of incomplete D-MEM containing type IV bovine pancreatic DNAse (Sigma Chemical, 30 mg/ml) and collagenase XI (Sigma Chemical, 0.7 mg/ml) is added for 30 min at 37°C on movement in the H_2O bath. Because guinea pig lungs contain a large amount of fatty tissue always use collagenase/DNAse treatment for all the organs. To stop the digestion, 10 ml of incomplete D-MEM is added and samples are placed on ice again. To obtain cells from the lung, spleen and mediastinal lymph nodes the tissue should be pushed gently through cell screens with the plunger of a 10 or 5 ml syringe. You will note that large amounts of fat will float on top of the cell suspensions; this can be removed by placing the cells in a small agar plate and tipping the plate to remove the cellular layer while the fat clings to the bottom of the agar plate and decant the cells off. The remaining erythrocytes are lysed with 4.0 ml Gey's solution (0.15 M NH_4Cl, 10 mM $KHCO_3$) and the cells are washed with Dulbecco's modified Eagle's minimal essential medium. The remaining cells are then counted and plated at 1×10^6 per well in 96-well plates. Total cell numbers are determined by flow cytometry using BD™ Liquid Counting Beads, as described by the manufacturer (BD PharMingen, San Jose, CA USA 95131).

E. ELISA and CBA Cytokine Assay in the Mouse

To determine the level of cytokines/chemokines produced by cell cultures of organs, macrophages or dendritic macrophages or T-cell overlays of antigen-presenting cells, the supernatants are removed from the cell culture assays at different time points and can then be analyzed by ELISA or by CBA.

If you do not have a flow cytometer, simple ELISAs are the most straightforward method. Several companies produce matched antibody pairs and standards for many cytokines. Standard sandwich ELISA procedures are as follows:

1. Primary antibody at l μg/ml in coating buffer, 4°C overnight in Immulon 2 plates from Dynatech.
2. Flick out primary antibody and block the non-specific protein binding sites using 1% bovine serum albumin in PBS (0.1% Tween, PBST) for 2 h at room temperature.

3. Wash plate four times with PBST, add sample and standard diluted in cell culture medium (if samples are from infected animals this and the following steps should be performed under BSL-3 conditions). Leave at 4°C overnight.
4. Wash plate four times as above. Add biotinylated secondary antibody at 1 μg/ml in the BSA blocking solution and leave for 45 min at room temp.
5. Wash plate four times. Add avidin-peroxidase in working buffer and allow to develop.
6. Read plate.

A far superior assay is the CBA (BD Biosciences) which has the advantage of reading 5–7 cytokines/chemokines at the same time from the same sample. The BD CBA system uses the sensitivity of amplified fluorescence detection by flow cytometry to measure soluble analytes in a particle-based immunoassay. Each bead in a BD CBA Kit provides a capture surface for a specific protein and is analogous to an individually coated well in an ELISA plate. The BD CBA capture bead mixture is in suspension to allow for the detection of multiple analytes in a small sample volume (50 μl). These CBA kits allow for 100 sample analysis.

To perform, reconstitute mouse standards (15 min) in assay diluent and then dilute standards using the assay diluent. You can use small plastic 12×75 mm sample acquisition tubes for a flow cytometer (e.g. BD Falcon™ Cat. No. 352008). Then mix 10 μl/test of each mouse capture bead suspension. It is very important to vortex the tubes before aliquoting because the beads fall down to the bottom of the bottle quickly. Then transfer 50 μl of mixed beads to each assay tube and add standard dilutions and test samples to the appropriate sample tubes at 50 μl/tube. Also add PE detection reagent at 50 μl per test. All of the samples and standards now need to be wrapped with tin foil to protect them from light and incubated at room temperature for 2 h. Then wash samples with 1 ml wash buffer and centrifuge and then add 300 μl of wash buffer to each assay tube and analyze samples on a flow cytometer. A flow cytometer equipped with a 488 nm laser capable of detecting and distinguishing fluorescence emissions at 576 and 670 nm (e.g. BD FACScan™ BD FACSCalibur™ instruments) and BD CellQuest™ software is required. In addition you need to have BD CBA Software, or FCAP Array software (Cat. No. 641488).

F. Analysis of Cell Surface Expression of Markers in the Mouse by Flow Cytometry

To analyze the expression of surface markers on cells derived from tissues, cells are prepared as above and re-suspended at a concentration of 5×10^6 cells/ml in PBS containing 0.1% sodium azide. Cells are incubated in PBS containing 0.1% sodium azide on ice for at least 30 min. This incubation is an important step if one is analyzing the expression of cell surface activation molecules; this is because it is our experience that the antibody-mediated ligation of activation markers on the cell surface results in the up-regulation of several molecules that are used to determine cell activation status. For example, immediate incubation of cells with anti-CD44 and anti-CD45RB results in the cells becoming 'blast cells' (as determined by an increase in scatter by flow cytometer analysis) and in the increased expression of CD44 on the cell surface.

Once cells have been fixed, they are dispensed into 96-well plates (200 μl per well) and centrifuged to pellet the cells. The supernatant is removed by gently inverting the plate and discarding the contents into a vessel containing a 5% Lysol solution. Antibody is added to the cells at appropriate concentrations, and the plate incubated for 30 min at 4°C in the dark. Following two washes in d-RPMI the cells are analyzed on a flow cytometer.

Recommended stains include the following:

Discriminating between cell populations: FITC anti-CD19 or CD45R/B220 (B cells), PE anti-CD3e (T ells), PerCP anti-CD4 (T-cell subset), APC anti-CD8 (T-cell subset) or FITC anti-NKl.1 (NK cell), PE anti-CD3e (T cell), PerCP anti-CD4 (T-cell subset), APC anti-CD8 (T-cell subset).

Effector/memory T-cell differentiation: FITC anti-CD44 (T-cell activation), PE anti-CD62L (T-cell memory), PerCP anti-CD3e (T cell), APC anti-CD4 or CD8 (T-cell subset) or FITC anti-CD44 (T-cell activation), PE anti-CD62L (T-cell memory), PerCP anti-CCR7 (T-cell memory), APC anti-CD4 or CD8 (T-cell subset).

Regulatory T-cell evaluation: FITC anti-CD25 (T-cell activation), PE anti-Foxp3 (Treg marker), PerCP anti-CD3e (T cell), APC anti-CD4 or CD8 (T-cell subset).

Macrophage/DC evaluation: FITC anti-CD80 (cell activation), PE anti-MHC class II (cell activation), PerCP anti-CD11b (macrophage/DC differentiation), APC anti-C11c (macrophage/DC differentiation).

It is essential to include isotype controls for each individual antibody isotype that is used, in order to appreciate the contribution of non-specific binding.

G. Intracellular Staining for Cytokine Production in the Mouse

The capacity for a T cell to secrete certain cytokines can be measured using an intracellular cytokine staining protocol. Cells are harvested from the lungs and incubated with anti-CD3ε and anti-CD28 (both at 0.2 μg/10^6 cells) and monensin (3 μM) for 4 h at 37°C, 5% CO_2. Cells are harvested, washed in PBS containing 0.1% sodium azide and labelled with the outer cell surface markers as described above and then fixed and permeabilized with a solution containing paraformaldehyde and saponin (BD Pharmingen, Fix/Perm reagent). Cells are then incubated with antibody specific for the cytokine of interest for 30 min at 4°C, in the dark. Cells are then washed twice and analyzed using a flow cytometer.

Recommended stains include the following:

Th1 cytokines produced by CD4 or CD8 T cells: FITC anti-IFNγ PE anti-CD4, PerCP anti-CD8, APC anti-IL2

Th2 cytokine production by CD4 or CD8 T cells: FITC anti-IL-10 PE anti-CD4, PerCP anti-CD8, APC anti-IL-4

Th1 cytokines produced by macrophages and DC*:* FITC anti-IL-12 PE anti-TNFα, PerCP anti-CD11b, APC anti-CD11c

Th2 cytokines produced by macrophages and DC*:* FITC anti-IL-10 PE anti-TGFβ, PerCP anti-CD11b, APC anti-CD11c

The use of isotype control antibody particularly for the cytokine reagent is essential in confirming that the (sometimes low) specific signal is real.

H. Analysis of Cell Surface Expression of Markers in the Guinea Pig by Flow Cytometry

Flow cytometry in the guinea pigs to date has been difficult for various reasons, but we have recently been able to overcome most of the organ processing difficulties and gating problems and can now use these new protocols to measure the major leukocytes that accumulate in infected lungs (Ordway *et al.*, 2007c, 2008).

Regarding the previous difficulties with initial cell gating parameters, the traditional use of forward/side scatter (FSC/SSC) flow cytometric gating has proven difficult to adequately and consistently identify the distinct fractions of guinea pig leukocytes. We have now solved this by using gating based on SSC and a specific antibody [MIL4], which stains guinea pig granulocytes (heterophils/neutrophils and eosinophils) (Ordway *et al.*, 2007c, 2008). Gating out these cells allows a clean separation of the various subsets under analysis, as shown in Figure 1.

To analyze the expression of surface markers on cells derived from tissue, cells are prepared as above and re-suspended at a concentration of 5×10^6 cells/ml in PBS containing 0.1% sodium azide. Cells are incubated in the PBS containing 0.1% sodium azide on ice for at least 30 min. Once cells have been fixed, they are dispensed into 96-well plates (200 µl per well) and centrifuged to pellet the cells. The supernatant is removed by gently inverting the plate and discarding the contents into a vessel containing a 5% Lysol solution. Antibody is added to the cells at the appropriate concentration, and the plate incubated for 30 min at 4°C, in the dark. Following two washes in d-RPMI the cells are analyzed on a flow cytometer. It is recommended to incubate the secondary non-conjugated antibodies alone without adding conjugated antibodies to avoid non-specific binding.

The primary drawback of the guinea pig model is the relative lack of specific immunological reagents with which to monitor the emerging acquired immune response in infected animals. This situation is gradually improving, however, with the availability of some antibodies to T-cell markers (Serotec) and the development of PCR-based techniques (discussed above) to measure key cytokines and chemokines. Table 2 shows some currently available guinea pig-specific antibodies (Serotec).

Recommended stains include the following:

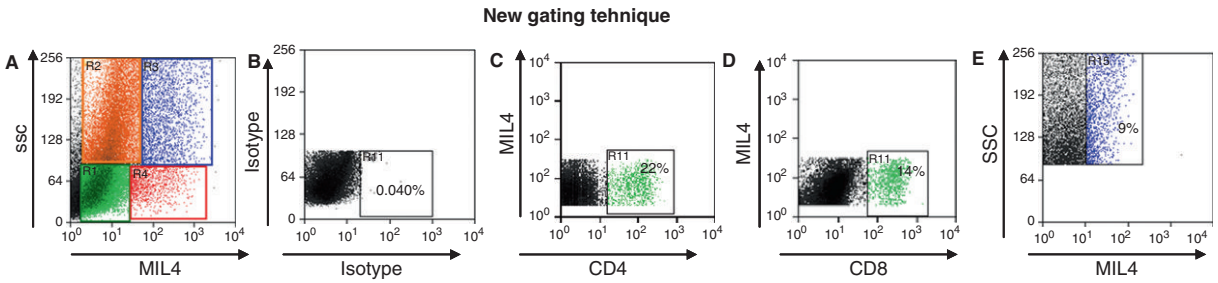

Figure 1. New flow cytometric gating techniques. Dead cells were excluded by propidium iodide and viable cell were gated. The new SSC versus MIL4 (A), gating shows lymphocytes (green), MIL4neg SSC high (orange), MIL4low SSClow monocytes (red), MIL4neg SSChigh granulocytes (blue). Further separation of R1 lymphocytes shows isotype controls (B), MIL4neg versus CD4+ (C), MIL4neg versus CD8+ (D) and further separation of the granulocytes shows SSC versus MIL4+ (E). (See color plate section).

Table 2. Panel of anti-guinea pig antribodies used for flow cytometry and immunohistochemistry[a]

Specificity	Clone	Fluorescence label
CD4	CT7	FITC
CD8	CT6	FITC
Pan T Cell	CT5	APC
CD45	ITH-1	RPE
Neutrophils eosinophils	MIL4	RPE
Macrophages	MR-1	FITC
MHC Class II	C1.13.1	RPE
B Cells	MsGP9	FITC

[a]Anti-guninea pig monoclonal antibodies were purchased from Serotec.

Discriminating between T-cell populations: FITC anti-CD4, FITC anti-CD8. APC anti-TCR.

Activated T cells: RPE anti-CD45 (T-cell activation), RPE anti-CT4 (homing receptor).

B-cell evaluation: FITC anti-B cell, RPE anti-CD45 (activation marker).

Heterophils (neutrophils) /eosinophils: FITC anti-MIL4 (heterophils/eosinophils).

Macrophages: FITC anti-MR-1 (macrophage marker), RPE anti-MHC class II (cell activation).

As with the mouse, it is essential to include isotype controls for each individual antibody isotype that is used, in order to appreciate the contribution of non-specific binding.

As yet, this model does not have the flexibility enjoyed by the mouse model. We are currently using CD45 and CT4 as 'activation markers' on guinea pig CD4 and CD8 cells, but this still requires further validation. Regularly used markers such as CD44 and CD62L are not as yet available. A cross-reactive (anti-mouse) CD62 lectin domain antibody has been described, but we do not recommend this for the simple reason that CD62L does not exist in the guinea pig genome (this animal has E-selectin and P-selectin only), so what this antibody really stains (in low cell numbers) in the guinea pig is unknown.

I. Immunohistochemical Analysis of Cells in the Lungs of Mice and Guinea Pigs

Relating flow cytometric data obtained from lung tissues to the actual location of these cells within the granuloma architecture is highly useful information and can be achieved by immunohistochemistry. We have described this technique for infected mouse lungs (Park *et al.*, 2006; Ordway *et al.*, 2006, 2007b) and more recently for the guinea pig lung (Ordway, 2007c, 2008). Figure 2 shows a representative example of analysis of guinea pig lungs stained for CD4+ and CD8+ T cells and for macrophages.

For optimum results it is very important that specimens are collected and frozen as soon as possible in order to retain the morphology of the tissue and integrity of the antigens. The lung tissue should be inflated with 30% OCT (in PBS) (Tissue-Tek, Inc., Torrance, CA, USA) and placed in a tissue embedding cassette (Peel-Away, Polysciences, Inc., PA, USA). Care should be taken to

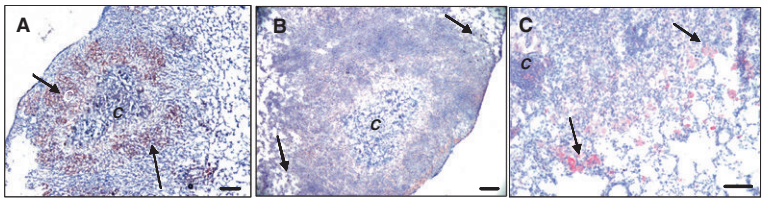

Figure 2. Immunohistochemical staining of CD4, CD8 T cells and macrophages in guinea pig lungs during the course of *M. tuberculosis infection*. Representative photomicrographs from granuloma lung sections with the central necrosis (c) show immunohistochemical staining for CD4+ (A), CD8+ (B) T cells and macrophages (C) in lung tissue sections from guinea pigs after 30 days of the infection, illustrating co-locatization of staining. Bar indicate, total magnification A, B = 4× and C = 10×. (See color plate section).

ensure that at least 1/8 of an inch of 100% OCT is above and below the specimen. The specimen should be central within the cassette. Once samples are placed correctly the cassette should be floated in liquid nitrogen until approximately two-thirds of the OCT turns white. Alternatively, the cassettes can be placed on dry ice. Once frozen, cassettes can be wrapped in foil to avoid drying and can be stored at –70°C.

Frozen blocks should be considered BSL-3 agents as freezing may not kill the bacteria. Sections should be cut under BL3 conditions. We house our cryostat in a small room, separate from the rest of the BSL-3 containment rooms. The operator should wear a protective mask and dispose of all debris as BSL-3 material.

Serial sections of 7 g are cut on a cryostat (Leica, CM 1850). A tape transfer system (Instrumedics Inc., Hackensack, NJ, USA) is particularly useful when sectioning delicate tissue such as the lung. The sections are then fixed in cold acetone for 5–10 min and air-dried. Endogenous peroxidase should be blocked with peroxidase block (Innogenex, San Ramon, CA, USA) and the sections washed in PBS containing 1% BSA (PBS-BSA) for 5 min. The sections are then incubated for 30 min at room temperature with goat serum to block non-specific binding sites (Biogenex, San Ramon, CA, USA). Primary antibody (or isotype control) diluted in PBS/BSA should be added for an overnight incubation at 4°C. Sections should be washed three times for 15–20 min each in PBS/BSA containing 0.05% Tween 20. The last wash should be carried out with PBS alone. Secondary antibody, such as Goat F(ab)2 anti-rat IgG conjugated to horseradish peroxidase (Biosource International, Camarillo, CA, USA), should then be added for 40 min. Wash as above. Antibody is then detected using aminoethylcarbazole (AEC) (Innogenex, San Ramon, CA, USA) as substrate (red colour). Counterstain for cell structure with Meyer's haematoxylin (colour blue).

As for all of the above analyses, the comparison of sections from at least five mice and guinea pigs per group will add greater weight to any conclusions made from the immunohistochemistry data.

Acknowledgements

We thank Crystal Shanley, Megan Caraway, Marisa Harton, Dr. Marcela Henao Tamayo, Dr. Shaobin Shang, Dr. Susan Kraft and Dr. Randy Basaraba and our colleagues in the Mycobacteria Research Laboratories for their contributions to the

development of the methods described here. Several of the more modern approaches were developed using funding from NIH programs AI-40488, AI-44072, AI-41922, 5 U01 AI070456, 1DP2OD006450 – 01 and the Bill & Melinda Gates Foundation, Contract #48980.

References

Basaraba, R. J. (2008). Experimental tuberculosis: the role of comparative pathology in the discovery of improved tuberculosis treatment strategies. *Tuberculosis* **88**, S35–47.

Basaraba, R. J., Bielefeldt-Ohmann, H., Eschelbach, E. K., Reisenhauer, C., Tolnay, A. E., Taraba, L. C., Shanley, C. A., Smith, E. A., Bedwell, C. L., Chlipala, E. A. *et al*. (2008). Increased expression of host iron-binding proteins precedes iron accumulation and calcification of primary lung lesions in experimental tuberculosis in the guinea pig. *Tuberculosis* **88**, 69–79.

Bloom, B. R. (1994). *Tuberculosis – Pathogenesis, Protection, and Control*, ASM Press, Washington, DC.

Centers for Disease Control (1993). *Biological Safety in Microbiological and Biomedical Laboratories*, 3rd edn. HHS publication No. (CDC) 93-8395. US Government Printing Office, Washington, DC.

Collins, F. M., Wayne, L. G. and Montalbine, V. (1974). The effect of cultural conditions on the distribution of *Mycobacterium tuberculosis* in the spleens and lungs of specific pathogen-free mice. *Am. Rev. Respir. Dis.* **110**, 147–156.

Cooper, A. M., Callahan, J. E., Griffin, J. P., Roberts, A. D. and Orme, I. M. (1995b). Old mice are able to control low-dose aerogenic infections with *Mycobacterium tuberculosis*. *Infect. Immun.* **63**, 3259–3265.

Cooper, A. M., Dalton, D. K., Stewart, T. A., Griffin, J. P., Russell, D. G. and Orme, I. M. (1993). Disseminated tuberculosis in gamma interferon gene-disrupted mice. *J. Exp. Med.* **178**, 2243–2247.

Cooper, A. M., Roberts, A. D., Rhoades, E. R., Callahan, J. E., Getzy, D. M. and Orme, I. M. (1995a). The role of interleukin-12 in acquired immunity to *Mycobacterium tuberculosis* infection. *Immunology* **84**, 423–432.

Davis, B. D. and Dubos, R. J. (1948). The inhibitory effect of lipase on the bacterial growth in media containing fatty acid esters. *J. Bacteriol.* **55**, 11–23.

Dubos, R. J. (1950). The effect of organic acids on mammalian tubercle bacilli. *J. Exp. Med.* **92**, 319–332.

Dubos, R. J. and Middlebrook, G. (1948). The effect of wetting agents on the growth of tubercle bacilli. *J. Exp. Med.* **83**, 409–423.

Furney, S. K., Skinner, P. S., Farrer, J. and Orme, I. M. (1995). Activities of rifabutin, clarithromycin, and ethambutol against two virulent strains of *Mycobacterium avium* in a mouse model. *Antimicrob. Agents Chemother.* **39**, 786–789.

Henao-Tamayo, M., Palaniswamy, G. S., Smith, E. E., Shanley, C. A., Wang, B., Orme, I. M., Basaraba, R. J., DuTeau, N. M. and Ordway, D. (2009). Post-exposure vaccination against *Mycobacterium tuberculosis*. *Tuberculosis* **89**, 142–148.

Hirschfield, G. R., McNeil, M. and Brennan, P. J. (1990). Peptidoglycan-associated polypeptides of *Mycobacterium tuberculosis*. *J. Bacteriol.* **172**, 1005–1013.

Hjelemeland, L. M. (1990). Removal of detergents from membrane proteins. *Methods Enzymol.* **182**, 277–282.

Hoff, D. R., Caraway, M. L., Brooks, E. J., Driver, E. R., Ryan, G. J., Peloquin, C. A., Orme, I. M., Basaraba, R. J. and Lenaerts, A. J. (2008). Metronidazole lacks antibacterial activity in guinea pigs infected with *Mycobacterium tuberculosis*. *Antimicrob. Agents Chemother.* **52**, 4137–4140.

Horwitz, M. A. and Harth, G. (2003). A new vaccine against tuberculosis affords greater survival after challenge than the current vaccine in the guinea pig model of pulmonary tuberculosis. *Infect. Immun.* **71**, 1672–1679.
Hutchinson, F. and Pollard, A. (1961). Target theory and radiation effects on biological molecules. In: *Mechanisms in Radiology* (M. Errara, and A. Forssberg, eds.), pp. 71–92. Academic Press, New York.
Jensen, A. (1932). Reinzuchtung und ypenbestimmung von tuberkelbacillenstammen. Eine vereinfachung der methoden fur die praxis. *Zentralbl. Bakteriol.* **125**, 222–226.
Kraft, S. L., Dailey, D., Kovach, M., Stasiak, K. L., Bennett, J., McFarland, C. T., McMurray, D. N., Izzo, A. A., Orme, I. M. and Basaraba, R. J. (2004). Magnetic resonance imaging of pulmonary lesions in guinea pigs infected with *Mycobacterium tuberculosis*. *Infect. Immun.* **72**, 5963–5971.
Kubica, G. P. and Wayne, L. G. (1984). *The Mycobacteria – a Sourcebook.* vol. 15. A&B, Marcel Dekker, Inc., New York.
Lee, B., Hefta, S. A. and Brennan, P. J. (1992). Characterization of the major membrane protein of virulent *Mycobacterium tuberculosis*. *Infect. Immun.* **60**, 2066–2074.
Lenaerts, A. J., Degroote, M. A. and Orme, I. M. (2008). Preclinical testing of new drugs for tuberculosis: current challenges. *Trends Microbiol.* **16**, 48–54.
McMurray, D. N. (2003). Hematogenous reseeding of the lung in low-dose, aerosol-infected guinea pigs: unique features of the host-pathogen interface in secondary tubercles. *Tuberculosis* **83**, 131–134.
McMurray, D. N., Allen, S. S., Jeevan, A., Lasco, T., Cho, H., Skwor, T., Yamamoto, T., McFarland, C. and Yoshimura, T. (2005). Vaccine-induced cytokine responses in a guinea pig model of pulmonary tuberculosis. *Tuberculosis* **85**, 295–301.
Ordway, D. J., Harton, M., Henao-Tamayo, M., Orme, I. M. and Gonzalez-Juarrero., M. (2006). Enhanced macrophage activity in granulomatous lesions of immune mice challenged with *Mycobacterium tuberculosis*. *J. Immunol.* **176**, 4931–4939.
Ordway, D., Henao-Tamayo, M., Harton, M., Palanisamy, G., Troudt, J., Shanley, C., Basaraba, R. J. and Orme., I. M. (2007). The hypervirulent *Mycobacterium tuberculosis* strain HN878 induces a potent TH1 response followed by rapid down-regulation. *J. Immunol.* **179**, 522–531.
Ordway, D., Henao-Tamayo, M., Shanley, C., Smith, E. E., Palanisamy, G., Wang, B., Basaraba, R. J. and Orme., I. M. (2008). The influence of BCG vaccination on the cellular immune response in immune guinea pigs infected with *Mycobacterium tuberculosis*. *Cell. Vaccine Immunol.* **15**, 1248–1258.
Ordway, D., Higgins, D. M., Sanchez-Campillo, J., Spencer, J., Henao-Tamayo, M., Harton, M., Orme, I. and Gonzalez-Juarrero., M. (2007). XCL1 (lymphotactin) chemokine produced by activated CD8 T cells during the chronic stage of infection with *Mycobacterium tuberculosis* negatively affects production of IFN-γ by CD4 T cells and participates in granuloma stability. *J Leukoc. Biol.* **82**, 1221–1229.
Ordway, D., Palanisamy, G., Henao-Tamayo, M., Smith, E., Shanley, C., Orme, I. M. and Basaraba, R. J. (2007). Cellular immune responses during *Mycobacterium tuberculosis* infection in the guinea pig. *J. Immunol.* **179**, 2532–2541.
Orme, I. M. (1988). Induction of nonspecific acquired resistance and delayed-type hypersensitivity, but not specific acquired resistance, in mice inoculated with nonliving mycobacterial vaccines. *Infect. Immun.* **56**, 3310–3312.
Orme, I. M. (1995). *Immunity to Mycobacteria*, RG Landes Company, Austin, TX.
Orme, I. M. (2005). Mouse and guinea pig models for testing new tuberculosis vaccines. *Tuberculosis* **85**, 13–17.
Orme, I. M. (2006). Safety issues regarding new vaccines for tuberculosis, with an emphasis on post exposure vaccination. *Tuberculosis* **86**, 68–73.

Orme, I. M. and Collins, F. M. (1994). Mouse model of tuberculosis. In: *Tuberculosis; Pathogenesis, Protection, and Control* (B. R. Bloom, ed.), pp. 113–134. ASM Press, Washington, DC.

Orme, I. M., Miller, E. S., Roberts, A. D., Furney, S. K., Griffin, J. P., Dobos, K. M., Chi, D., Rivoire, B. and Brennan, P. J. (1992). T lymphocytes mediating protection and cellular cytolysis during the course of *Mycobacterium tuberculosis* infection. *J. Immunol.* **148**, 189–196.

Palanisamy, G. S., Smith, E. E., Shanley, C. A., Ordway, D., Orme, I. M. and Basaraba., R. J. (2008). Disseminated disease severity as a measure of virulence of *Mycobacterium tuberculosis* in the guinea pig model. *Tuberculosis* **88**, 295–306.

Park, J. S., Henao-Tamayo, M., Gonzalez-Juarrero, M., Orme, I. M. and Ordway, D. J. (2006). Virulent clinical isolates of *Mycobacterium tuberculosis* grow rapidly and induce cellular necrosis in murine macrophages. *J Leukoc. Biol.* **79**, 1–7.

Rhoades, E., Cooper, A. M. and Orme, I. M. (1995). Chemokine response in mice infected with *Mycobacterium tuberculosis*. *Infect. lmmunol.* **63**, 3871–3877.

Rhoades, E. R., Frank, A. A. and Orme, I. M. (1997). Progression of chronic pulmonary tuberculosis in mice aerogenically infected with virulent *Mycobacterium tuberculosis*. *Tuber. Lung Dis.* **78**, 57–66.

Rhoades, E. R. and Orme, I. M. (1997). Susceptibility of a panel of virulent strains of *Mycobacterium tuberculosis* to reactive nitrogen intermediates. *Infect. Immun.* **6S**, 1189–1195.

Roberts, A. D., Sonnenberg, M. G., Ordway, D. J., Furney, S. K., Brennan, P. J., Belisle, J. T. and Orme, I. M. (1995). Characteristics of protective immunity engendered by vaccination of mice with purified culture filtrate protein antigens of *Mycobacterium tuberculosis*. *Immunology* **85**, 502–508.

Rom, W. N. and Garay, S. (1995). *Tuberculosis*, Little, Brown and Company, New York.

Sambrook, J., Fritsch, E. F. and Maniatis, T. (1989). *Molecular Cloning. A Laboratory Manual*, Cold Spring Harbor Press, Cold Spring Harbor.

Scopes, R. K. (1994). *Protein Purification: Principles and Practice*, Springer-Verlag, New York.

Sonnenberg, M. G. and Belisle, J. T. (1997). Definition of *Mycobacterium tuberculosis* culture filtrate proteins by two-dimensional polyacrylamide gel electrophoresis, N-terminal amino acid sequencing and electrospray mass septrometry. *Infect. lmmunol.* **65**, 4515–4524.

Thomas, T. C. and McNamee, M. G. (1990). Purification of membrane proteins. *Methods Enzymol.* **182**, 499–520..

Trias, J., Jariler, V. and Benz, R. (1992). Porins in the cell wall of mycobacteria. *Science* **258**, 1479–1481.

Vastal, A.L (1975). *Procedures for the Isolation and Identification of Mycobacteria*, Centers for Disease Control, Washington, DC.

Wheeler, P. R., Besra, G. S., Minnikin, D. E. and Ratledge, C. (1993). Stimulation of mycolic acid biosynthesis by incorporation of cis-tetracos-5-enoic acid in a cell wall preparation from *Mycobacterium smegmatis*. *Biochim. Biophys. Acta* **1167**, 182–188.

Williams, A., Hall, Y. and Orme, I. M. (2009). Evaluation of new vaccines for tuberculosis in the guinea pig model. *Tuberculosis*, 2009. **89**, 89–97.

Youmans, G. P. (1979). *Tuberculosis*. W.B. Saunders Co., PA.

Youmans, G. P. and Karlson, A. G. (1947). Streptomycin sensitivity of tubercle bacilli; studies on recently isolated tubercle bacilli and the development of resistance to streptomycin *in vivo*. *Am. Rev. Tuberc.* **55**, 529–534.

13 The Leishmaniasis Model

Pascale Kropf, Ulrich D Kadolsky, Matthew Rogers, Thomas E Cloke and Ingrid Müller
Imperial College London, Faculty of Medicine, Department of Immunology, London, UK

CONTENTS

I. INTRODUCTION

The leishmaniases are a group of vector-borne parasitic diseases that represent a major international public health problem; they belong to the most neglected tropical diseases, are major causes of morbidity and mortality and impede economic development especially in the developing world. The leishmaniases in humans are caused by more than 20 different species of *Leishmania* parasites. Currently the diseases affect an estimated 12 million people in 88 countries, and approximately 350 million people are at risk (http://www.who.int/leishmaniasis/en/). The leishmaniases present with a wide range of symptoms, ranging from the self-healing cutaneous disease associated with *L. major*, *Leishmania mexicana* and other cutaneous strains, to the mucocutaneous and fatal disseminated visceral leishmaniasis due to infection with parasites of the *Leishmania donovani* complex. Experimental infection of mice with *Leishmania major* have established the current paradigm of T helper subset involvement in infectious diseases. The majority of inbred strains of mice develop small cutaneous lesions that heal within a few weeks; this ability to control of infection and to resolve the cutaneous lesions has been associated with the expansion of $CD4^+$ Th1 cells, characterized by the production of IFN-γ. In contrast, a few strains of mice, such as BALB/c, develop progressive non-healing disease that has been attributed to the expansion of $CD4^+$ Th2 cells, characterized by the production of IL-4, IL-10, IL-13 and other Th2 cytokines (Sacks and Noben-Trauth, 2002). However, the regulation of immune responses against *Leishmania* parasites is more complex and Th2 dominance does not fully explain non-healing or reactivated forms

METHODS IN MICROBIOLOGY, VOLUME 37
0580-9517 DOI 10.1016/S0580-9517(10)37013-9

of disease (Noben-Trauth *et al.*, 1996; Anderson *et al.*, 2007). Indeed, a multitude of factors, including parasite and vector species, host immune responses, genetic and environmental factors influence the establishment of infection and the outcome of disease. Experimental infections with *Leishmania* spp. are widely used to study a range of different questions including basic host–parasite interactions, immune mechanisms leading to protective immunity or persistent non-healing disease as well as the efficacy of novel drugs, immunotherapy, adjuvant and vaccines.

The protozoan parasites are transmitted between hosts by the bite of infected female phlebotomine sand flies and are delivered to a host as metacyclic promastigotes along with the saliva of the sand fly (Titus and Ribeiro, 1988) and a mucin-rich gel produced by the parasites in the sand fly midgut (Rogers *et al.*, 2004, 2009; Bates, 2007). After transmission to their mammalian host by the bite of infected female sand flies *Leishmania* parasites are taken up by neutrophils and subsequently establish residence inside macrophages (Peters *et al.*, 2008) and they are obligate intracellular parasites of macrophages in their mammalian hosts. Inside the macrophages the promastigotes transform into, and multiply as a flagellate amastigotes. Macrophages are not only the host cells for *Leishmania* parasites, they also play a central role in the innate and adaptive immune response against *Leishmania* parasites. Macrophages can be instructed to kill the intracellular *Leishmania* parasites but they can also be instructed to provide a permissive environment for parasite growth. The fate of the intracellular *Leishmania* parasites depends on the balance of two inducible enzymes, nitric oxide synthase 2 (NOS2) and arginase (Iniesta *et al.*, 2002; Kropf *et al.*, 2005). These two enzymes use a common substrate, L-arginine and are competitively regulated by Th1 and Th2 cytokines (Modolell *et al.*, 1995). Th1 cytokines induce classical activation of macrophages and the induction of NOS2 that oxidizes L-arginine in a two-step process into nitric oxide (NO), a metabolite responsible for parasite killing (Wei *et al.*, 1995; Bogdan, 2001). Th2 cytokines result in the alternative activation of macrophages and the induction of arginase, which hydrolyzes L-arginine into ornithine, an amino acid that is the main intracellular source for the synthesis of polyamines which are important for parasite growth (Munder *et al.*, 1998; Roberts *et al.*, 2004; Kropf *et al.*, 2005).

Since most tests used to investigate immune responses are described in detail in other chapters and can be used for the analysis of immune responses to *Leishmania* parasites, we will focus here on the handling of *Leishmania* parasites and on methods assessing the killing and the growth of the parasites in macrophages and in infected animals. *Leishmania* is widely used in immunological research to assess the function of host genes using genetically modified mice, and genetically modified parasites are used to understand the functions of parasite genes. Until now, there is no efficient vaccine available and there is no good correlate of protection; therefore, determination of the load of viable parasites is used as a standard to assess the contribution of genes to disease outcome and to evaluate the success of intervention strategies.

♦♦♦♦♦♦ II. METHODS

A. Parasite Isolation and Maintenance

In the following paragraphs we describe in detail the materials as well as the preparative steps necessary for the handling of *Leishmania* parasites.

B. Maintenance Media

1. Promastigotes

Promastigotes of *Leishmania* spp. can be maintained in different media. The most commonly used media are Schneider's Drosophila Medium (Gibco), Grace's Insect Cell Culture Medium (Gibco) and a biphasic system, consisting of a liquid phase of Dulbecco's Modified Eagle Medium (DMEM, Gibco) over a solid layer of rabbit blood agar. In our laboratory we use the biphasic culture. The DMEM medium used to routinely maintain the parasites in culture is supplemented with the following:

- 10% complement inactivated fetal bovine serum (FBS, Gibco)
- 50 I.U. ml^{-1} penicillin (Gibco)
- 50 mg ml^{-1} streptomycin (Gibco)
- 292 mg ml^{-1} L-glutamine (Gibco)
- 4.5 mg ml^{-1} glucose (Gibco)

The same medium is used for the parasite limiting dilution assay (LDA medium).

2. Axenic amastigotes

Not all *Leishmania* spp. can be grown in culture as amastigotes without the need of a host cell (i.e. macrophage). For example, it has not been possible up to now to culture amastigotes of *L. major* in the absence of host cells. However, *L. mexicana* and members of the *L. donovani* complex can be cultured for 4–5 passages as amastigotes. Such 'axenic' amastigote cultures are best initiated from amastigotes freshly isolated from lesions of infected mice (see 'Parasite isolation'). We experience less success with amastigotes obtained from promastigote cultures allowed to transform through acidification of their media. Axenic *L. mexicana* amastigotes are grown in supplemented M199 medium acidified to pH 5.5 (Bates and Tetley, 1993):

- 20% complement-inactivated FBS
- 50 IU ml^{-1} penicillin
- 50 μg ml^{-1} streptomycin
- 1 × Basal Medium Eagle's vitamins (Gibco)

1. Wash lesion amastigotes three times with Phosphate-buffered saline (PBS).
2. Adjust parasites to 1×10^6 cells ml^{-1} in acidified M199, pre-warmed to 32°C.

3. Incubate at 32°C in a humidified incubator with an atmosphere of 5% CO_2, with flask caps slightly loosened.

Note: The pH of the media is critical to this method. Therefore, any pH meter used should be freshly calibrated before its preparation.

The FBS is necessary for optimal culture conditions. However, some batches of FBS can inhibit the parasite growth. Therefore, careful screening of the FBS is necessary.

C. Blood Agar

In order to prepare 100 ml of solid blood agar medium, the following material is necessary:

- 3.0 g nutrient agar (Difco)
- 0.6 g NaCl (Sigma)
- 100 ml nanopure H_2O
- 10 ml rabbit blood with 10% sodium citrate (Merck)
- 5 ml glucose 30% in phosphate buffer (Sigma)
- 70 ml polystyrene tissue culture flasks (Corning Costar)

1. Autoclave the mixture of agar, water and NaCl for 20 min
2. Cool the agar to about 45°C
3. Place into a prewarmed water bath (45°C)
4. Add 10 ml of rabbit blood and 5 ml of glucose 30%
5. Distribute 5 ml of agar mixture on the flat side of 70 ml polystyrene tissue culture flask
6. Let solidify and cool at room temperature
7. Tightly close the flasks
8. Keep at 4°C for up to 4 weeks

D. Parasite Counting

Promastigotes are actively moving and need to be fixed for counting. Before fixing, parasites are washed as follows:

1. Centrifuge for 5 min at 500 rpm to pellet debris
2. Transfer the supernatant in a new tube
3. Wash the supernatant twice at 3500 rpm for 10 min
4. Resuspend the parasites in the maintenance medium and fix them using one of the two solutions described here:
   - 2% formaldehyde in phosphate-buffered saline
   - Hayem's solution:
     - 0.5 g $HgCl_2$ (Sigma)
     - 1.0 g NaCl (Sigma)
     - 5.0 g Na_2SO_4 (Sigma)
     - 200 ml H_2O (Sigma)

5. After resuspending the parasites in DMEM, we usually dilute them in 2% formaldehyde in phosphate buffer and count them in a hemocytometer.

E. Parasite Isolation

Leishmania parasites are easy to handle *in vitro* and *in vivo*; however, it is important to pay attention to a few points relating to the virulence and infectivity of these organisms. Some *Leishmania* species – for example *L. amazonensis* – maintain virulence during *in vitro* culture whereas others – for example *L. major* – rapidly loose virulence *in vitro*. The maintenance of *L. major* in culture has an innate problem in that the parasite undergoes an evolution different from that in the natural environment where it is cycled through the sand fly prior to infection in a new vertebrate host. A decrease in virulence is the dominant characteristic of maintenance of *L. major* parasites *in vitro*. To be able to work with parasites with comparable virulence we regularly passage *Leishmania* parasites *in vivo* and we routinely use the first stationary phase of freshly isolated parasites to initiate experimental infections. Many strains of mice can be used for this purpose. In our laboratory, we use BALB/c mice and infect them in the hind footpad with *Leishmania* parasites in a final volume of 50 µl. Two to four weeks after infection, the mice are sacrificed and the parasites are isolated from the cutaneous lesions as follows:

1. Swab the skin of the dead mouse with 70% ethanol
2. Make an incision of the skin around the ankle
3. Cut the toes of the footpad
4. Carefully remove the skin and necrotic tissue of the infected footpad
5. Cut the footpad just above the joint
6. Place the footpad in a sterile petri dish
7. Cut the footpad in several small pieces
8. Transfer them into a sterile glass homogenizer or cell dissociation sieves
9. Gently homogenize the tissue in 5 ml medium
10. Transfer the suspension in a blood agar flask or your preferred maintenance medium
11. Incubate at 26°C, in a humid atmosphere, 5% CO_2 in air to allow transformation of amastigotes into promastigotes*
12. After 3–5 days, the suspension is washed as before
13. Resuspend the parasites in 5 ml of maintenance medium and transfer the suspension in a new flask

*the parasites can also transform and grow in tightly closed flasks in a dry incubator.

F. Parasite Maintenance

Once isolated, the parasites should be maintained for a maximum of 3–4 weeks with the minimal *in vitro* dilutions possible. Like other unicellular organisms,

L. major have lag, log and stationary phases and promastigote populations during these phases are not uniform with respect to infectivity. During the log phase, parasites are motile and dividing cells, whereas in the stationary phase the majority of parasites are stationary and not dividing. Log phase parasites are washed, counted and a new culture is started with 10^6 parasites ml^{-1} in a new blood agar flask.

G. Cryopreservation of Parasites

Leishmania promastigotes can be cryopreserved using the same techniques as for other eukaryotic cells. For successful cryopreservation, it is important to use parasites from the first *in vitro* passage after a new isolation and to freeze them in a late log phase. We cryopreserve promastigotes in the following way:

1. Wash the parasites as described before
2. Adjust them to 1×10^8 cells ml^{-1} in FBS containing 10% of dimethyl sulfoxide (Fluka) in a final volume of 1 ml per tube. The tubes are placed in a styrofoam box and immediately transferred at –70°C for 24 h and are then stored in the vapour phase of liquid nitrogen until further use.

As for eukaryotic cells, the parasites have to be thawed quickly. We thaw the vial in a water bath pre-warmed at 37°C and distribute the cells drop by drop in a tube containing medium at room temperature. The cells are washed once at 3500 rpm for 10 min, resuspended in their culture medium and transferred in a blood agar flask.

It is imperative to passage the thawed batch of parasites in a mouse. In our experience, a clear reduction in virulence was noted with the time of storage.

H. Isolation of Metacyclic Promastigotes for Infection: Peanut Agglutinin Agglutination

Metacyclic *L. major* parasites represent the infectious form of the parasite. Log phase procyclic and stationary phase metacyclic promastigotes of *L. major* differ in the composition of the repeating phosphorylated saccharide units of lipophosphoglycan (LPG). The repeat units of LPG from log phase *L. major* contain terminal β-galactose residues and these galactose residues account for the agglutination by the lectin peanut agglutinin (PNA). The repeat units of metacyclic promastigotes terminate predominantly with α-arabinose, which do not serve as ligands for the lectin (Sacks *et al*., 1985; Sacks and da Silva, 1987; Turco and Descoteaux, 1992). Metacyclic promastigotes have lost their ability to bind PNA and a technique using this differential binding has been developed by Sacks *et al*. to purify infective stages of *L. major* from cultures (Sacks *et al*., 1985).

To isolate metacyclic *L. major* parasites, the following material is necessary:

- Phosphate-buffered saline
- PNA isolated from *Arachis hypogaea* (PNA, Vector Laboratories or Sigma)

I. Isolation

1. Wash the parasites three times with PBS
2. Adjust the parasites to 1×10^8 cells ml^{-1} in PBS
3. Add an equal volume of PNA ($100\,\mu g\,ml^{-1}$) in PBS
4. Incubate 1 h at room temperature
5. To isolate the non-agglutinated parasites, two methods can be used as follows:
   a.
      - Harvest the suspension and carefully layer it on top of the same volume of PBS containing 50% of FBS
      - Incubate 30 min at room temperature
      - Carefully harvest the parasites remaining above the interphase
      - Wash three times in PBS and count.
   b.
      - Harvest the suspension and centrifuge at 600 rpm for 5 min
      - Carefully harvest the supernatant, wash three times in PBS and count.

J. Isolation of Metacyclic Promastigotes for Infection: Culture Enrichment Method

In contrast to *L. major, L. mexicana* metacyclic promastigotes cannot be isolated using PNA because the repeat units of their LPG contain glucose residues (Sacks *et al*., 1990). Instead, we have devised a culture method, which attempts to mimic the loss of parasites during blood meal digestion and defecation by the sand fly vector (Rogers *et al*., 2008). This results in a synchronous population of metacyclic-enriched parasites, which are of equal infectivity to sand fly-derived parasites (Rogers *et al*., 2004). This method also avoids biochemical or biophysical selection. The culture media used are M199 (Sigma) and Graces' insect culture medium (Invitrogen), supplemented with the following:

- 10% complement-inactivated FBS
- 50 IU ml^{-1} penicillin
- $50\,\mu g\,ml^{-1}$ streptomycin
- 1 × Basal Medium Eagle's vitamins (Gibco)

1. Wash lesion-derived amastigotes 3× with PBS.
2. Adjust parasites to 5×10^5 cells ml^{-1} in M199 adjusted to pH 7.2.
3. Incubate at 26°C until parasites transform and reach mid-Log phase of growth, typically after 2–3 days. This is characterized by a predominance of long (12–20 μm) promastigote forms known as nectomonad promastigotes.
4. Wash parasite three times with PBS.
5. Adjust parasites to 5×10^5 cells ml^{-1} in Graces' insect culture medium adjusted to pH 5.5.
6. Incubate at 26°C for 6–7 days to obtain 85–95% metacyclic promastigotes.

K. *In Vitro* and *In Vivo* Models of Infection with *Leishmania* Parasites

Macrophages activated by exposure to cytokines such as IFN-γ and TNF-α acquire microbicidal activity due to the induction of NOS2 that oxidizes L-arginine in a two-step process into NO, the major effector molecule for the destruction of the intracellular *Leishmania* (Mauel *et al*., 1991; Oswald *et al*., 1994; Wei *et al*., 1995). Macrophages activated by this pathway are called 'classically activated macrophages' or M1 macrophages.

Th2 cytokines such as IL-4 and IL-13 result in the alternative activation of macrophages – or M2 macrophages – and the induction of arginase, which hydrolyzes L-arginine into ornithine, an amino acid that is the main intracellular source for the synthesis of polyamines which are essential for parasite nutrition and growth (Kropf *et al*., 2005).

L. Generation and Activation of Primary Macrophages

Resting or activated peritoneal, splenic, air-pouch or bone marrow-derived macrophages can be used to determine the leishmanicidal activity of macrophages. Detailed methods for isolation and activation of primary macrophages of different origin are described in another chapter. We will just briefly describe the generation and use of bone marrow-derived macrophages and the recruitment and infection of macrophages *in vivo* using the air pouch model.

Bone marrow-derived macrophages (BM-MΦ) are obtained by differentiation of BM precursor cells *in vitro.* BM precursor cells are flushed from femurs and tibiae of naive mice and cultivated at a concentration of 5×10^5 cells ml^{-1} in hydrophobic Teflon bags (FEP film 100C DuPont, USA) (Munder *et al*., 1971; Kropf *et al*., 2004).

Macrophage culture medium is DMEM (as described above) supplemented with the following:

- 10% heat-inactivated FCS
- 5% horse serum
- 15% L929 supernatant

The concentration of sterile cell-free culture supernatant from L929 cells (L929 cells are available from ATCC) can vary since it needs to be determined for each new batch of L929 culture supernatant.

After 8–10 days of culture, the Teflon bags are opened with sterile scissors, the BM-MΦ are harvested, centrifuged at 4°C, washed extensively with cold DMEM and seeded in 96- or 24-well tissue culture plates at a density of 5×10^5 MΦ ml^{-1} and allowed to adhere. After adherence, BM-MΦ are infected at a ratio of 1:5 with *Leishmania* promastigotes. Six hours later, plates are washed to remove non-phagocytosed parasites and infected macrophages are activated:

M. Macrophage Activation

1. Classical activation of macrophages

IFN-γ (100 U ml^{-1}) and TNF-α (200 U ml^{-1}).

IL-4 (20 U ml^{-1}) alone or a mixture of IL-4 (20 U ml^{-1}) and IL-10 (10 U ml^{-1}).

Standard read-out systems for classically activated macrophages are NO production and the killing of intracellular parasites (see methods of evaluating parasite burden).

Standard read-out systems for alternatively activated macrophages are the induction of arginase 1 and the determination of arginase enzyme activity in macrophage lysates as well as the assessment of intracellular parasite growth (Kropf *et al*., 2005; Modolell *et al*., 2009).

After 48 h, culture supernatants are removed and the levels of cytokines and chemokines can be determined by standard techniques. NO_2^- accumulation in macrophage culture supernatants are determined as an indicator of NO production and measured by using the Griess assay. The remaining macrophages can be lysed and the survival of parasites can be determined by colorimetric quantitation (see below).

N. Griess Assay for the Determination of Nitrite

Nitrite and nitrate are breakdown products of the hydrophobic gas nitric oxide and nitrite (NO_2^-) accumulation is used as an indicator of NO production. The Griess reaction is a fast and simple colorimetric assay for nitrite. Nitrite in cell culture supernatants is measured by the method of Ding *et al*. (1988):

- Add an equal volume of Griess reagent (1% sulfanilamide and 0.1 % *n*-(1-naphthyl) ethylenediamine dihydrochloride in 5% H_3PO_4; Sigma, St. Louis, MO) to the supernatants from MΦ cultures.
- Incubate 10 min at room temperature.
- Read absorbance with a spectrophotometer at 570 nm.
- Standard curve: NO_2^- concentration is determined using $NaNO_2$ dissolved in DMEM as a standard and DMEM alone as a blank.

Nitrate does not react in the Griess reaction. In the blood nitrite is rapidly converted into nitrate by haemoglobin and this is the reason why in blood or urine sample, derived from infected mice, nitrate needs to be reduced to nitrite before breakdown products of NO can be measured.

O. Determination of Arginase Activity in Macrophage Cultures

- Centrifuge 96- or 24- well tissue culture plates
- Wash macrophages three times with PBS
- Add 200 µl of 0.1% Triton X-100/10 mM $MnCl_2$/25 mM Tris–HCl
- Incubate 15–30 min on a shaker
- Freeze at –20°C
- Thaw the lysate and transfer 50 µl in a 0.5 ml Eppendorf tube
- Activate the enzyme by heating for 10 min at 56°C
- Incubate with 50 µl of 0.5 M L-arginine (pH 9.7) at 37°C for 15–20 min to conduct arginine hydrolysis

- Stop the reaction with 400 µl of H_2SO_4 (96%)/H_3PO_4(85%)/H_2O (1/3/7 v/v/v)
- Prepare urea standards using serially diluted urea (3.5–120 µg) in PBS
- Add 20 µl of α-isonitrosopropiophenone (dissolved in 100% ethanol) to the standards and samples
- Mix well for 1 min using a vortex
- Heat 45 min at 95°C
- Cool at 4°C for 30 min
- Transfer 100 µl in a 96-well flat bottom plate
- Measure the optical density at 540 nm

Calculate the concentration of urea using a standard curve

One unit of arginase enzyme activity is defined as the amount of enzyme that catalyzes the formation of 1 µmol urea/min.

P. Macrophage Lysis for the Determination of Parasite Load

BM-MΦ infected *in vitro* are activated as described above and the survival and killing of parasites is determined (Kiderlen and Kaye, 1990; Kropf *et al.*, 2005). After incubation for 48–72 h, BM-MΦ are washed once with 37°C Hepes-buffered RPMI (RPMI 1640, Gibco) containing 0.008% w/v SDS (=lysis medium) and incubated with 100 µl fresh lysis medium for 7–20 min. During this time macrophage disintegration has to be monitored regularly with an inverted microscope. Once host cell lysis is complete, 150 µl/well Hepes-buffered RPMI containing 17% FCS is added to neutralize the SDS. The lysates are then incubated in a CO_2 incubator (5% CO_2 in air) for 48–72 h at 25°C to allow the parasites to transform to the promastigote stage.

Q. Determination of Parasite Viability by the MTT Assay

The relative number of viable *Leishmania*/well is determined by a modified version of the MTT assay (Mosmann, 1983). The test is based on the ability of viable cells to metabolize water-soluble tetrazolium salt (yellow) into a water-insoluble formazan product (purple colour). The purple formazan crystals are produced by dehydrogenases in active mitochondria in viable cells. Dead cells are unable to perform this reaction. 10 µl of a 5 mg ml^{-1} MTT (3-(4,5-dimethylthiazol-2-yl)-2,5-diphenyltetrazolium bromide, Sigma) stock solution is added to each well. For the stock solution, 5 mg MTT ml^{-1} is dissolved in PBS, passed through a 0.22 µm filter and kept at 4°C for no more than 2 weeks. The parasites are incubated at 25°C for another 8–16 h before the reaction is stopped and the insoluble formazan crystals are solubilized by adding 100 µl of 10% acidified SDS (pH 4.7 with acetate buffer) and incubated for a further 6–16 h at 37°C. The relative absorbance is determined with a spectrophotometer at a wavelength of 570 nm and a reference wavelength of 630 nm.

R. Enumeration of Macrophage Parasite Burden by Microscopy

BM-MΦ can be infected *in vitro* on glass slides, allowing the average intracellular parasite burden to be determined by microscopy. Sixteen well slides

(Lab-Tek, Nunc) allow experimentation on a smaller scale (200 µl max), which uses less reagents and is therefore particularly suited to *in vitro* drug screening. Macrophages (5×10^4) are seeded into the wells and allowed to adhere at 37°C for 1 h in a CO_2 incubator (5% CO_2 in air). After incubation, BM-MΦ are exposed to *Leishmania* at a parasite to macrophage ratio (multiplicity of infection) of five *L. major/L. mexicana* metacyclic promastigotes to one macrophage for 4 h at 37°C. This results in an intermediate level of infection, roughly 60–70%. The multiplicity of infection and duration of infection may be adjusted to achieve a desired level of initial infection, since drug studies require a near 100% infection rate to accurately measure parasite killing. Extracellular parasites are washed away with several rounds of PBS with a multichannel pipette before the infected BM-MΦ are incubated for the required amount of time. Generally, BM-MΦ do not last longer than 4 days in culture before they show signs of deterioration. The culture medium is flicked or sucked away and the cells are washed three times with PBS before they are fixed. To fix, first remove the plastic wells and silicon gasket and flood with absolute methanol for 5 min at room temperature. Staining is carried out in 10% Giemsa solution (Sigma) in Giemsa buffer (0.009 mM Na_2HPO_4, 0.074 mM $NaH_2PO_4H_2O$, pH 7.0) for 10 min followed by extensive rinsing in cold tap water. Allow the slides to air dry before transferring to a microscope for parasite counting. The average intracellular parasite load is determined by oil-immersion microscopy of at least 200 Giemsa-stained macrophages from random fields (performed in duplicate), using the formula: (#parasites/#infected cells) X (#infected cells/total#cells) X 100. Infections are expressed as the average number of intracellular parasites per 100 infected macrophages.

S. Recruitment and Infection of Macrophages in the Air-Pouch *In Vivo*

The air-pouch model can be used for *in vivo* infection of macrophages that are recruited to a local site. To inflate a dermal air-pouch, 3 ml of sterile air is injected into the backs of shaved mice with a 25-gauge needle. This separates the dermis and epidermis from the subcutaneous tissue to create a pocket of air, which can accommodate a maximum of 5 ml of fluid and can remain inflated for up to 3 weeks (and possibly beyond). Mice are shaved 24 h previously to allow any skin irritation to recede, and the skin site is swabbed with 70% ethanol to sterilize before injection. Into each air pouch parasites are inoculated in endotoxin-free PBS using a 27-gauge needle. Cells are recovered from the air pouch by injecting 5 ml ice-cold PBS cavity lavage. Filled air pouches are massaged for approximately 1 min before the fluid is withdrawn into a 50 ml centrifuge tube on ice. Following extensive washing with ice-cold PBS to remove extracellular parasites, macrophages can be separated from neutrophils by adhesion to plastic for 2 h at 37°C in DMEM medium supplemented with 20% FCS. Macrophages then are released from the plastic by incubation on ice for 30 min with gentle cell scraping and pipetting to allow them to be counted using a Neubauer improved hemocytometer. Viable intracellular parasite burdens are determined by transformation assay of liberated amastigotes from 2.5×10^5 cells using the 0.008% SDS lysis method (see below). The air-pouch technique also allows the differential quantification and

characterization of leukocyte subsets that transmigrate into the dermal cavity in response to infection. We find that as early as 12 h post-infection, enough cells can be recovered per air pouch to run fluorescent-activated cell sorting (FACS). In addition, cells can be concentrated to 0.5 ml by centrifugation (1800 rpm, 5 min) and live cells counted by diluting 1/10 in Trypan blue dye for 30 s (live cells exclude the dye and remain unstained). The cells can then be cytoadhered to glass slides using a cytospin (we use a Shandon cytospin2: 500 rpm, 5 min) and stained with 10% Giemsa solution to determine the proportions of monocytes/macrophages, neutrophils, lymphocytes, basophils and eosinophils by morphology.

T. Promastigote Transformation Growth Assay

The relative number of viable amastigotes (intracellular or axenic) can be determined using a modification of the LDA (see below), which takes advantage of their transformation into flagellated promastigote forms easily counted using a hemocytometer. This method is particularly suited to determining the burden of *in vitro* or air-pouch-derived macrophages infected for 48 h in 24-well plates with *L. major/L. mexicana*. Macrophages are lysed to release their amastigotes and grown for a further 48 h in promastigote medium. Macrophages are lysed with sterile 0.008% v/v SDS in simple DMEM medium for 4 min at room temperature. The lysis is stopped by the addition of 17% v/v FCS in simple DMEM medium and the cells mechanically ruptured with a cell scraper. Released amastigotes are concentrated on the bottom of the wells by centrifuging the plate at 3100 rpm for 10 min, followed by washing in PBS and resuspension in 200 μl M199 promastigote medium, pH 7.2. The density of viable amastigotes that transform and grow as promastigotes after 48/72 h of culture at 26°C in 96-well plates can then be counted with a hemocytometer. Air pouches infected with parasites (typically, 1×10^6 metacyclic promastigotes) are separated from neutrophils by adhesion to plastic for 2 h at 37°C in DMEM medium supplemented with 20% FCS. Viable amastigote burdens from a standard density of 2.5×10^5 cells are then determined by counting transformed promastigotes following 48/72 h incubation at 26°C in promastigote medium.

U. Fluorescent Growth Assay

A further modification of this method is the use of a fluorescent dye. Macrophage infections can be processed as per the promastigote transformation growth assay (above) except 10% v/v alamarBlue viability dye (Invitrogen) is added to the promastigote culture medium. alamarBlue is a blue non-toxic dye that when metabolized by growing cells generates a fluorescent metabolite. Fluorescence is measured (excitation wavelength = 544 nm; emission wavelength = 590 nm) 48 h following transformation and growth in promastigote culture medium using a fluorescent microplate reader (we use a Molecular Devices Gemini XPS) and recorded with Spectramaxi software. Readings are normalized by subtracting the background fluorescence of uninfected macrophages lysate, incubated in promastigote medium for the same period of time. We find that this method, although less labour-intensive and quicker, is slightly less sensitive than the general transformation assay method.

V. Assessment of Infections with *Leishmania* Parasites *In Vivo*

Experimental infection of mice with *Leishmania* parasites is widely used to investigate a broad range of different questions in basic immunology, cell biology, chemotherapy and host–parasite interaction. The outcome of infection depends on many different factors such as the immune response of the infected host (host genetics) the species of the infecting *Leishmania* parasite, the presence of vector-derived compounds, the route and dose of infection.

W. Factors Influencing the Lesion Development

Usually, high-dose s.c. infections with 1×10^6 to 1×10^7 stationary phase *L. major* promastigotes or 10^5 purified metacyclic promastigotes in a final volume of 50 µl PBS in one hind footpad results in the development of healing lesion in genetically resistant mice such CBA or C57BL/6 and in progressive disease in non-healing BALB/c mice. Initiation of infection intradermally in the ear, the rump or the footpad with low parasite doses (10^3–10^4 parasites) mimics the natural course of infection more closely but take much longer to develop.

The route of entry of the *L. major* promastigotes also influences the nature of the developing immune response. Nabors and Farrell showed that SWR mice display a non-healing response to *L. major* comparable to that of BALB/c mice when the parasites are inoculated subcutaneously at the base of the tail (Nabors and Farrell, 1994; Etges and Muller, 1998). In contrast, if infected subcutaneously in the footpad with the same number of parasites, the SWR mice were able to control their lesion.

Mouse strain	Route of parasite entry	Form of disease
SWR	s.c., base of the tail	Non-healing
SWR	s.c., footpad	Healing

The development of progressive disease is not restricted to BALB/c mice and is not exclusively determined by the genetic composition of the infected host. C57BL/6 mice, one of the prototype healer strains, can resolve cutaneous lesions developing after subcutaneous infection. However, when infected intravenously with *L. major*, mice from this strain developed non-healing disease and were unable to mount a DTH response (Scott and Farrell, 1982). Local differences in the skin temperature might influence the growth of *L. major* amastigotes and the responsiveness of macrophages to cytokines and contribute to the expression of site-specific immunity.

The dose of *L. major* parasites injected can also influence the lesion development. Indeed, resistance and susceptibility have been shown to be dose dependent (Leclerc *et al.*, 1981). In this study, it was shown that 1×10^5 parasites induced self-healing lesions in BALB/c mice and enabled them to become immune to reinfection, whereas 3.3×10^5 parasites induced progressive disease (Bretscher *et al.*, 1992; Menon and Bretscher, 1996).

X. Evaluation of Cutaneous Lesions

The most commonly used index for disease progression in *Leishmania*-infected mice as well as for the determination of the effects of drug treatment and immunotherapies is the measurement of the size of cutaneous lesions which develop at the site of parasite inoculation.

The development of cutaneous lesions at the site of infection should be monitored in regular intervals during the course of infection. After inoculation of infectious *Leishmania* parasites (in one hind footpad, the rump or the ear) the development of the infection can be followed by determining the degree of local swelling at the site of parasite inoculation. Infections into the footpads are widely used and the uninfected, contralateral footpad can be used as a control. To determine the size of the cutaneous lesions, the actual thickness of the infected and the non-infected, contralateral footpad is measured in regular intervals (for example on a weekly basis). The size of the footpads can be determined with a dial caliper (Kröplin, Schlüchtern) or a digimatic caliper (Mitutoyo, Japan) or with any other metric caliper. The lesion size is calculated by subtracting the thickness of the non-infected contralateral footpad from the thickness of the infected footpad.

An example of the lesion size during the course of *L. major* infection in healer and non-healer mice is given in Table 1 and Figure 1.

Table 1. Development of cutaneous lesions during the course of *L. major* infection in healer and nonhealer strains of mice

Weeks post infection	BALB/c footpad size ± S.E.M.	CBA footpad size ± S.E.M.
1	0.25 ± 0.08	0.30 ± 0.04
2	0.48 ± 0.07	0.91 ± 0.04
3	1.02 ± 0.06	1.10 ± 0.06
4	1.80 ± 0.30	1.09 ± 0.09
5	2.43 ± 0.13	0.68 ± 0.06
6	3.80 ± 0.10	0.50 ± 0.02
7	4.65 ± 0.75	0.32 ± 0.04

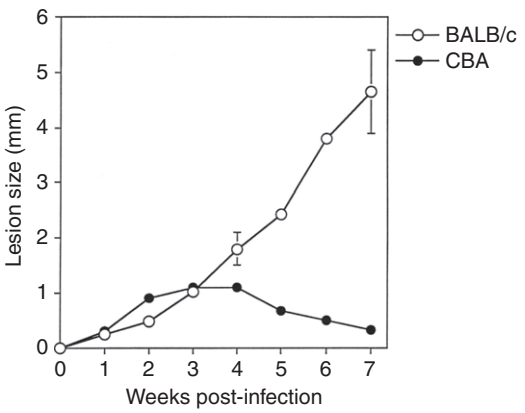

Figure 1. Lesion size development during *L. major* infection.

Y. Determination of Parasite Burden in Lesions of Infected Animals

The most stringent evaluation of the effect of vaccination, immunotherapy, chemotherapy or any other intervention on the manifestation of experimental leishmaniasis is the determination of the parasite burden. The growth of the parasites can be monitored in their main host cells, the macrophages as described above, or it can be evaluated in lesions and tissues derived from *Leishmania*-infected animals.

Z. Enumeration of Viable Parasites by LDA

The replicating parasites, inflammatory responses of the infected host and pathological changes due to infiltrating cells contribute to the expression of the lesions and to pathology (Hill *et al*., 1983; Titus *et al*., 1985). Therefore, monitoring only the increase or decrease of the cutaneous lesion may give inaccurate or even false impressions of the true progress of the disease (Hill *et al*., 1983; Vieira *et al*., 1996). Similar differences in lesion sizes can be accompanied by widely varying differences in the number of viable parasites. Lesions could be present when there are no parasites and parasites could be found when there were no lesions (Hill *et al*., 1983; Titus *et al*., 1985; Vieira *et al*., 1996; Lima *et al*., 1997).

Since the size of the cutaneous lesions does not always correlate with the number of viable parasites within the lesion (Vieira *et al*., 1996; Lima *et al*., 1997) cutaneous leishmaniasis should not only be evaluated by monitoring the lesion development but also by enumeration of the number of viable parasites present in the lesions. The combined use of monitoring the size of the cutaneous lesions and the determination of the parasite burden in the infected tissue will reflect more accurately the status of disease, the effect of vaccines and immunotherapies.

A technique was developed by Titus *et al*. (Titus *et al*., 1985; Lima *et al*., 1997) to determine parasite burden in different infected tissues. An example of an infected footpad is described here, but this same technique can be used for different organs (draining lymph nodes, spleens or ears).

For the determination of the number of viable parasites, the tissue homogenates from infected mice need to be plated on blood agar plates.

1. Prepare the blood agar as described before
2. Distribute 50 µl/well of agar mixture in a slant (see Figure 2) with a repeater pipetter (Eppendorf) in 96-well flat bottom tissue culture plates
3. Let solidify and cool at room temperature and keep in a humid box at 4°C for up to 4 weeks
4. Determine the weight of a petri dish
5. Prepare the footpad as described for the parasite isolation
6. Weigh the petri dish with the footpad
7. Calculate the weight of the footpad*
8. Cut the footpad in several small pieces
9. Transfer them into a sterile glass homogenizer

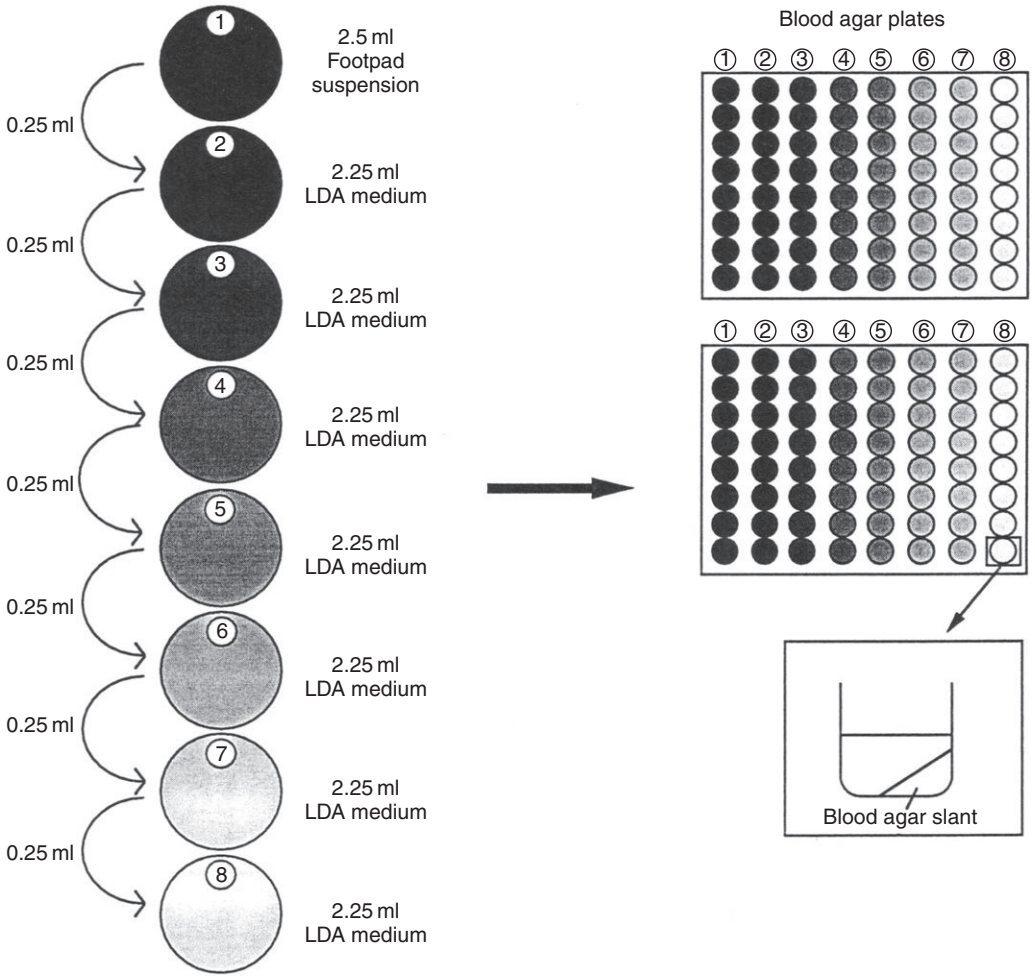

1. Carefully mix well ① with a ① ml pipet
2. Remove 0.25 ml, transfer it into well ②
3. Go back to well ① and remove 0.8 ml with the same 1 ml pipet
4. Distribute 0.1 ml into 8 replicates of one blood agar plate
5. Repeat steps 3 and 4, but distribute into the second plate
6. Change the pipet and start again with well ② and ③

Figure 2. Model for the preparation of parasite limiting dilution assays.

10. Gently homogenize the tissue in 5 ml of LDA medium (see 'maintenance media')
11. Prepare 8–12 serial 10-fold dilutions of the footpad homogenate in a final volume of 2.5 ml (see Figure 1)
12. Distribute of each dilution 100 µl/well in at least 16 replicate wells, change pipettes between each dilution (see Figure 1)

13. Incubate the plate at 26°C, in a humid atmosphere, 5% CO_2 in air to allow transformation of amastigotes into promastigotes**
14. After 10 days, the assay is read by scoring the number of positive wells (presence of motile parasites) and negative wells (absence of motile parasites). An example is illustrated in Table 1

*if the parasite load is determined in lymphoid organs, count the cells and use the number of cells instead of the ng of tissue for the frequency estimation.

**the parasites can also transform and grow in plates sealed with Parafilm in a dry incubator.

To determine the plating efficiency of the LDA, a control plate consisting of serial dilutions of a known number of parasites has to be set up. The model of dilutions depicted in Figure 1 can be used. We perform 6 serial 10-fold dilutions, starting with a concentration of 1×10^4 *L. major* per well. After 10 days, the assay is read by scoring the number of positive wells (presence of motile parasites) and negative wells (absence of motile parasites).

AA. Analysis of the Parasite LDA Results

The data obtained by the above assay can be used to estimate the frequency and total number of parasites in a given tissue. As described in Taswell (Taswell, 1981, 1984, 1987), a single-hit Poisson model is assumed to represent the distribution of parasites, and the minimum chi-squared iterative method is used to estimate the frequency of parasites. A program to calculate these values, Leishmaniasis LDA (L-LDA), is available as both a web-based program and an R-script (for offline use), at http://www.imperial.ac.uk/theoreticalimmunology/llda.

Example: Two footpads (weight 0.165 g) were homogenized, resuspended in 10 ml of LDA medium (1,650,000 ng of tissue in the first dilution) and plated as described above. After 10 days, the assay was read by scoring the number of negative wells.

The results are illustrated in Table 2, and summarized in Table 3. Groups without any negative wells (i.e. all wells were positive) and without any positive wells (i.e. all wells were negative) are termed 'responding groups' and used for the statistical analysis. In Table 3 there are two responding groups, which have been highlighted in bold.

Table 2. Results of the microscopic scoring of positive and negative wells

	1	2	3	4	5	6	7	8		1	2	3	4	5	6	7	8
A	+	+	+	+	+	+	–	–	**A**	+	+	+	+	+	+	–	–
B	+	+	+	+	+	+	–	–	**B**	+	+	+	+	+	+	–	–
C	+	+	+	+	+	–	–	–	**C**	+	+	+	+	+	+	–	–
D	+	+	+	+	+	+	–	–	**D**	+	+	+	+	+	+	–	–
E	+	+	+	+	+	+	–	–	**E**	+	+	+	+	+	+	+	–
F	+	+	+	+	+	+	–	–	**F**	+	+	+	+	+	+	–	–
G	+	+	+	+	+	+	+	–	**G**	+	+	+	+	+	+	+	–
H	+	+	+	+	+	+	–	–	**H**	+	+	+	+	+	+	–	–

Table 3. Summary of the LDA assay results

Dilutions	Number of negative wells	Tissue weight (ng)	
1/1	0	1,650,000	
1/10	0	165,000	
1/100	0	16,500	
1/1,000	0	1,650	
1/10,000	0	165	
1/100,000	**1**	**16.5**	**Responding group**
1/1,000,000	**13**	**1.65**	**Responding group**
1/10,000,000	16	0.165	

Table 4. Results from the example, using the web-based version of L-LDA

L-LDA: Parasite estimation

Summary

Estimated number of parasites in total tissue is 12,649,000, and there are 0.153 parasites per nanogram of tissue. Model fits the data and the estimated frequency is valid.

AVT

	Model 1	**Model 2**
chi-squared AVT	0.18315	0.20367
p-values of AVT	0.66868	0.65178

PEVT

Estimated frequency of parasites per nanogram	0.15332450751772
Estimated parasites per footpad	12649271.870212
chi-squared PEVT	0.21224539487103
p-value of PEVT	0.64501315034315
Estimated variance	0.0023195357342168
95% upper confidence level	0.24772116252502
95% lower confidence level	0.058927852510415
1/frequency	6.5221145411764
Nanograms of tissue	165,000,000
Number of iterations to converge	1076

AVT: assay validity test, PEVT: parasite estimate validity test.

AB. Using the L-LDA Website

To use the web-based program, open an Internet browser (e.g. Firefox, Safari, Chrome, Opera, Internet Explorer) and navigate to Leishmaniasis LDA at http://www.imperial.ac.uk/theoreticalimmunology/llda

The above example is the first example on the website, clicking on 'Click to fill form' will populate the form with the above values. To run the program and obtain the results, click 'Run L-LDA'. Results are shown in Table 4.

AC. Using the L-LDA R Script

An R script is also available from the website. This can be downloaded and used to run L-LDA locally (and when internet access is not available) using the open source software R, available for free from http://www.r-project.org. Instructions for using the R version of L-LDA are given on the website and in the script itself. Results are shown in Table 4.

AD. Interpreting the Results

Regardless of whether the website or R script version of L-LDA is used, the results will be the same and are divided into the following sections:

- Summary of results: gives the number of the parasites in the tissue, or the reason why the number of parasites could not be calculated.
- Assay validity test (AVT): checks whether the data is consistent with the model. Of note is whether the *p*-values for model 1 and model 2 are ≤0.05. If this is the case, then the single-hit Poisson model does not describe the data and the number of parasites cannot be estimated.
- Parasite estimate validity test (PEVT): calculates the number of parasites in total tissue, the frequency of parasites per nanogram of tissue (with 95% confidence levels) and the validity of the estimate. If the PEVT *p*-value is ≤0.05 then the estimate is not valid and the number of parasites cannot be estimated.

In this example, both the AVT and the PEVT are not rejected (*p*-values are greater than 0.05), so the data and the estimate is valid (Table 4). The program estimates the frequency as 0.153 parasites per nanogram of tissue, and the number of parasites in the total tissue as 12,649,000.

Leishmaniasis LDA can also be used with cell numbers instead of tissue weight. To use cells with the program, select 'cells' instead of 'tissue'. Then input the total number of cells (10^6), and when inputting the responding groups, use number of cells at each 'dilution' instead of tissue weight. There is a cell-based example on the L-LDA website to illustrate this option.

References

Anderson, C. F., Oukka, M., Kuchroo, V. J. and Sacks, D. (2007). CD4(+)CD25(–)Foxp3(–) Th1 cells are the source of IL-10-mediated immune suppression in chronic cutaneous leishmaniasis. *J. Exp. Med.* **204**, 285–297.

Bates, P. A. (2007). Transmission of Leishmania metacyclic promastigotes by phlebotomine sand flies. *Int. J. Parasitol.* **37**, 1097–1106.

Bates, P. A. and Tetley, L. (1993). Leishmania mexicana: induction of metacyclogenesis by cultivation of promastigotes at acidic pH. *Exp. Parasitol.* **76**, 412–423.

Bogdan, C. (2001). Nitric oxide and the immune response. *Nat. Immunol.* **2**, 907–916.

Bretscher, P. A., Wei, G., Menon, J. N. and Bielefeldt-Ohmann, H. (1992). Establishment of stable, cell-mediated immunity that makes 'susceptible' mice resistant to Leishmania major. *Science* **257**, 539–542.

Ding, A. H., Nathan, C. F. and Stuehr, D. J. (1988). Release of reactive nitrogen intermediates and reactive oxygen intermediates from mouse peritoneal macrophages. Comparison of activating cytokines and evidence for independent production. *J. Immunol.* **141**, 2407–2412.

Etges, R. and Muller, I. (1998). Progressive disease or protective immunity to Leishmania major infection: the result of a network of stimulatory and inhibitory interactions. *J. Mol. Med.* **76**, 372–390.

Hill, J. O., North, R. J. and Collins, F. M. (1983). Advantages of measuring changes in the number of viable parasites in murine models of experimental cutaneous leishmaniasis. *Infect. Immun.* **39**, 1087–1094.

Iniesta, V., Gomez-Nieto, L. C., Molano, I., Mohedano, A., Carcelen, J., Miron, C., Alonso, C. and Corraliza, I. (2002). Arginase I induction in macrophages, triggered by Th2-type cytokines, supports the growth of intracellular Leishmania parasites. *Parasite Immunol.* **24**, 113–118.

Kiderlen, A. F. and Kaye, P. M. (1990). A modified colorimetric assay of macrophage activation for intracellular cytotoxicity against Leishmania parasites. *J. Immunol. Methods* **127**, 11–18.

Kropf, P., Freudenberg, M. A., Modolell, M., Price, H. P., Herath, S., Antoniazi, S., Galanos, C., Smith, D. F. and Muller, I. (2004). Toll-like receptor 4 contributes to efficient control of infection with the protozoan parasite Leishmania major. *Infect. Immun.* **72**, 1920–1928.

Kropf, P., Fuentes, J. M., Fahnrich, E., Arpa, L., Herath, S., Weber, V., Soler, G., Celada, A., Modolell, M. and Muller, I. (2005). Arginase and polyamine synthesis are key factors in the regulation of experimental leishmaniasis *in vivo*. *FASEB J.* **19**, 1000–1002.

Leclerc, C., Modabber, F., Deriaud, E. and Cheddid, L. (1981). Systemic infection of Leishmania tropica (major) in various strains of mice. *Trans. R. Soc. Trop. Med. Hyg.* **75**, 851–854.

Lima, H. C., Bleyenberg, J. A. and Titus, R. G. (1997). A simple method for quantifying Leishmania in tissues of infected animals. *Parasitol. Today* **13**, 80–82.

Mauel, J., Corradin, S. B. and Buchmuller Rouiller, Y. (1991). Nitrogen and oxygen metabolites and the killing of Leishmania by activated murine macrophages. *Res. Immunol.* **142**, 577–580, discussion 593–574.

Menon, J. N. and Bretscher, P. A. (1996). Characterization of the immunological memory state generated in mice susceptible to Leishmania major following exposure to low doses of L. major and resulting in resistance to a normally pathogenic challenge. *Eur. J. Immunol.* **26**, 243–249.

Modolell, M., Choi, B. S., Ryan, R. O., Hancock, M., Titus, R. G., Abebe, T., Hailu, A., Muller, I., Rogers, M. E., Bangham, C. R., et al. (2009). Local suppression of T cell responses by arginase-induced L-arginine depletion in nonhealing leishmaniasis. *PLoS Negl. Trop. Dis.* **3**, e480.

Modolell, M., Corraliza, I. M., Link, F., Soler, G. and Eichmann, K. (1995). Reciprocal regulation of the nitric oxide synthase/arginase balance in mouse bone marrow-derived macrophages by TH1 and TH2 cytokines. *Eur. J. Immunol.* **25**, 1101–1104.

Mosmann, T. (1983). Rapid colorimetric assay for cellular growth and survival: application to proliferation and cytotoxicity assays. *J. Immunol. Methods* **65**, 55–63.

Munder, M., Eichmann, K. and Modolell, M. (1998). Alternative metabolic states in murine macrophages reflected by the nitric oxide synthase/arginase balance: competitive regulation by CD4+ T cells correlates with Th1/Th2 phenotype. *J. Immunol.* **160**, 5347–5354.

Munder, P. G., Modolell, M. and Hoelzl Wallach, D. F. (1971). Cell propagation on films of polymeric fluorocarbon as a means to regulate pericellular pH and pO(2) in cultured monolayers. *FEBS Lett.* **15**, 191–196.

Nabors, G. S. and Farrell, J. P. (1994). Site-specific immunity to Leishmania major in SWR mice: the site of infection influences susceptibility and expression of the antileishmanial immune response. *Infect. Immun.* **62**, 3655–3662.
Noben-Trauth, N., Kropf, P. and Muller, I. (1996). Susceptibility to Leishmania major infection in interleukin-4-deficient mice. *Science* **271**, 987–990.
Oswald, I. P., Wynn, T. A., Sher, A. and James, S. L. (1994). NO as an effector molecule of parasite killing: modulation of its synthesis by cytokines. *Comp. Biochem. Physiol. Pharmacol. Toxicol. Endocrinol.* **108**, 11–18.
Peters, N. C., Egen, J. G., Secundino, N., Debrabant, A., Kimblin, N., Kamhawi, S., Lawyer, P., Fay, M. P., Germain, R. N. and Sacks, D. (2008). *In vivo* imaging reveals an essential role for neutrophils in leishmaniasis transmitted by sand flies. *Science* **321**, 970–974.
Roberts, S. C., Tancer, M. J., Polinsky, M. R., Gibson, K. M., Heby, O. and Ullman, B. (2004). Arginase plays a pivotal role in polyamine precursor metabolism in Leishmania. Characterization of gene deletion mutants. *J. Biol. Chem.* **279**, 23668–23678.
Rogers, M. E., Hajmova, M., Joshi, M. B., Sadlova, J., Dwyer, D. M., Volf, P. and Bates, P. A. (2008). Leishmania chitinase facilitates colonization of sand fly vectors and enhances transmission to mice. *Cell. Microbiol.* **10**, 1363–1372.
Rogers, M. E., Ilg, T., Nikolaev, A. V., Ferguson, M. A. and Bates, P. A. (2004). Transmission of cutaneous leishmaniasis by sand flies is enhanced by regurgitation of fPPG. *Nature* **430**, 463–467.
Rogers, M., Kropf, P., Choi, B. S., Dillon, R., Podinovskaia, M., Bates, P. and Muller, I. (2009). Proteophosophoglycans regurgitated by Leishmania-infected sand flies target the L-arginine metabolism of host macrophages to promote parasite survival. *PLoS Pathog.* **5**, e1000555.
Sacks, D. L., Brodin, T. N. and Turco, S. J. (1990). Developmental modification of the lipophosphoglycan from Leishmania major promastigotes during metacyclogenesis. *Mol. Biochem. Parasitol.* **42**, 225–233.
Sacks, D. L. and da Silva, R. P. (1987). The generation of infective stage Leishmania major promastigotes is associated with the cell-surface expression and release of a developmentally regulated glycolipid. *J. Immunol.* **139**, 3099–3106.
Sacks, D. L., Hieny, S. and Sher, A. (1985). Identification of cell surface carbohydrate and antigenic changes between noninfective and infective developmental stages of Leishmania major promastigotes. *J. Immunol.* **135**, 564–569.
Sacks, D. and Noben-Trauth, N. (2002). The immunology of susceptibility and resistance to Leishmania major in mice. *Nat. Rev. Immunol.* **2**, 845–858.
Scott, P. A. and Farrell, J. P. (1982). Experimental cutaneous leishmaniasis: disseminated leishmaniasis in genetically susceptible and resistant mice. *Am. J. Trop. Med. Hyg.* **31**, 230–238.
Taswell, C. (1981). Limiting dilution assays for the determination of immunocompetent cell frequencies. I. Data analysis. *J. Immunol.* **126**, 1614–1619.
Taswell, C. (1984). Limiting dilution assays for the determination of immunocompetent cell frequencies. III. Validity tests for the single-hit Poisson model. *J. Immunol. Methods* **72**, 29–40.
Taswell, C. (1987). Limiting dilution assays for the separation, characterization, and quantification of biologically active particles and their clonal progeny. In: *Cell Separation: Methods and Selected Applications* (T. G. Pretlow and T. P. Pretlow, eds), pp. 109–145. Academic Press, London.
Titus, R. G., Marchand, M., Boon, T. and Louis, J. A. (1985). A limiting dilution assay for quantifying Leishmania major in tissues of infected mice. *Parasite Immunol.* **7**, 545–555.
Titus, R. G. and Ribeiro, J. M. (1988). Salivary gland lysates from the sand fly Lutzomyia longipalpis enhance Leishmania infectivity. *Science* **239**, 1306–1308.

Turco, S. J. and Descoteaux, A. (1992). The lipophosphoglycan of Leishmania parasites. *Annu. Rev. Microbiol.* **46**, 65–94.
Vieira, L. Q., Goldschmidt, M., Nashleanas, M., Pfeffer, K., Mak, T. and Scott, P. (1996). Mice lacking the TNF receptor p55 fail to resolve lesions caused by infection with Leishmania major, but control parasite replication. *J. Immunol.* **157**, 827–835.
Wei, X. Q., Charles, I. G., Smith, A., Ure, J., Feng, G. J., Huang, F. P., Xu, D., Muller, W., Moncada, S. and Liew, F. Y. (1995). Altered immune responses in mice lacking inducible nitric oxide synthase. *Nature* **375**, 408–411.

14 Animal Models of Mucosal *Candida* Infections

Flavia De Bernardis, Silvia Arancia and Silvia Sandini
Department of Infectious, Parasitic and Immune-mediated Diseases, Istituto Superiore di Sanità, Rome, Italy

♦♦

CONTENTS

Animal Models of Mucosal *Candida* Infections

♦♦♦♦♦♦ I. PREFACE

Candida infections are a significant clinical problem for a variety of immunocompromised patients (McNeil *et al.*, 2001; Wisplinghoff *et al.*, 2004; Nucci and Marr, 2005; Pfaller and Diekema, 2007). Defective antifungal neutrophil-mediated effector function and T cell immunity are the two major conditions that predispose to invasive and mucosal infections, respectively.

Mucosal candidiasis (oropharyngeal and vaginal) is almost invariably observed in acquired immune deficiency syndrome (AIDS) patients. Oropharyngeal candidiasis (OPC) is the most frequent opportunistic fungal infection among AIDS patients (Samaranayake, 1992). Although the incidence of OPC in human immunodeficiency virus (HIV) infection is reduced with use of highly active antiretroviral therapy, it remains a common opportunistic infection (Martins *et al.*, 1998; de Repentigny, 2004; Morris, 2006).

The prevalence of oral and vaginal candidiasis is depending on the immune status of the host, OPC is frequent in immunocompromised patients, whereas vulvovaginal candidiasis (VVC) is equally common in immunocompetent and immunocompromised women. Several epidemiological studies (Fidel and Sobel, 1996) have documented that VVC is a widespread, common disease affecting up to 75% of healthy women with some of them affected by recurrent often intractable forms of the disease (recurrent VVC – RVVC). In these cases the quality of life is

METHODS IN MICROBIOLOGY, VOLUME 37
0580-9517 DOI 10.1016/S0580-9517(10)37014-0

devastated; the associated cost of medical visits is high. Antifungal therapy is highly effective for individual symptomatic attacks but does not prevent recurrences. In fact, maintenance therapy with an efficacious anti-*Candida* drug lengthens the time to recurrence but does not provide a long-term cure (Sobel *et al.*, 2004). Furthermore, there is concern that repeated treatments might induce drug resistance, shift the spectrum of causative *Candida* species and result in an increased incidence of non-*Candida albicans*, intrinsically resistant species (Bauters *et al.*, 2002; Mardh *et al.*, 2004; Jackson *et al.*, 2005; Richter *et al.*, 2005; Cernicka and Subik, 2006; Eckert, 2006; Ringdahl, 2006; Ventolini *et al.*, 2006).

The mortality rate of the most common fungal infections such as mucosal and invasive candidiasis has remained rather stable despite the introduction of the new antifungal agents, almost all effective against *Candida* (McNeil *et al.*, 2001). Thus, there is an urgent need for novel approaches to combat *Candida* infections, among which the immunopreventive or immunotherapeutic ones deserve increased attention.

Although the majority of human *Candida* infections occur at mucosal surfaces, relatively little is known about the role of mucosal immunity in protection against *Candida.* Therefore, understanding the components of the host–fungus interaction at mucosal level can lead to a better understanding of the pathogenesis of mucosal candidiasis and result in optimization of preventive and therapeutic antifungal strategies.

Candida albicans is capable of colonizing and persisting on mucosal surface of the oral cavity and of the gastrointestinal (GI) and genitourinary tracts of healthy humans and also of stimulating mucosal responses. Odds (1998) has suggested that 40–50% of any given sample population temporarily or permanently carry this fungus in their GI tract.

The transition from asymptomatic colonization to symptomatic candidiasis occurs in the presence of factors that enhance *Candida* virulence and/or as a result of loss of defense mechanisms. Both humoral and cellular factors have been suggested to confer protection.

This review will summarize the defense mechanisms of immune response to *Candida* at mucosal level evidenced in the animal models (oral, GI and vaginal) of candidiasis. In fact, animal models have provided an important contribution to study various aspects of the nature of the host's immune response against *C. albicans* at mucosal level.

♦♦♦♦♦♦ II. MUCOSAL IMMUNE RESPONSE TO *CANDIDA*

Mucosal colonization with *C. albicans* induces both antibody and cell-mediated immunity (CMI). *Candida albicans* can persist on the mucosal surfaces of healthy individuals despite demonstrable adaptive anti-*Candida* immunity.

In the majority of healthy humans, *Candida* commensalism can be evidenced by the presence of appreciable levels of anti-*Candida* antibodies as well as by a state of T-cell-mediated delayed-type hypersensitivity (DTH) response to fungal antigens as a prototypic CMI response *in vivo*. The DTH response to *Candida* is presumed to

prevent mucosal colonization from progression to symptomatic infection (Fidel *et al.*, 1994; Romani, 1997). In fact, DTH reactivity to *Candida* antigens is often absent in immunocompromised individuals with recurrent or persistent *Candida* infections (Odds, 1988).

Candida antigens, which encounter the mucosal immune system, can initiate two types of immune response leading to the induction of immunity or tolerance (Romani, 2004; Romani and Puccetti, 2006; Bonifazi *et al.*, 2009). In fact, a successful host/*Candida* interaction that led to a commensalism requires the coordinate actions of both innate and adaptive immune systems. Thus, the sensitization to *Candida* represents the capacity of reacting to *Candida* cell wall components particularly proteins and mannoproteins released in the external milieu (Cassone and Torosantucci, 1991; Cassone *et al.*, 1998) which are potent inducers of DTH in humans.

Candida colonization of the GI tract remains localized in healthy individuals, but may be an important reservoir of this opportunistic agent, from where dissemination occurs under conditions that compromise the host immune defense system and results in a progressive disease associated with a high rate of mortality (McNeil *et al.*, 2001; Nucci and Marr, 2005). For instance, this fungus is prone to invade oropharyngeal and oesophageal mucosa in AIDS patients (Klein *et al.*, 1984; Morris, 2006) and internal organs in severely neutropenic subjects (Pfaller and Diekema, 2007).

Although the importance of T-cell-dependent immunity in chronic mucocutaneous candidiasis has been clearly established, the exact mechanisms of protection have not been clearly defined.

Clinical data and animal experiments indicate a role for $CD4^+$ T cells in resistance to mucosal candidiasis (Cantorna and Balish, 1991a,b). AIDS patients with reduced numbers of $CD4^+$ T lymphocytes are susceptible to OPC, but they seldom develop disseminated candidiasis (Cantorna and Balish, 1991a,b). These observations suggest differences in cell and cytokine requirements for antifungal resistance at mucosal or systemic levels.

Overall, resistance to candidiasis at mucosal level seems mainly mediated by $CD4^+$ T cells via the production of T-helper-type 1 (Th1) cytokines which determine mobilization and consequent activation of anticandidal effectors (Asham and Papadimitriou, 1995). These immunological mechanisms provide a prompt and effective control of infection once *Candida* has colonized the mucosal tissue.

Among the predisposition factors to mucosal *Candida* infections, there are breaches of the integrity of mucosal surfaces, secretory Ig A deficiency and primary and acquired T cell immunodeficiency (Odds, 1988; Marodi, 1997).

The transition of *C. albicans* from commensal to invasive pathogen is primarily the consequence of a defective host cellular immune response, but of some relevance can be also the virulence of *C. albicans* strains (De Bernardis *et al.*, 1990, 1995; Cutler, 1991; Greenfield, 1992; Calderone and Fonzi, 2001; De Bernardis *et al.*, 2001; Naglik *et al.*, 2003; Hube, 2004). The virulence factors of *Candida* that play a role in mucosal infections are adherence, dimorphisms with antigenic variations, enzyme production, especially proteinase secretion, and cell surface composition (Ghannoum and Abu-Elteen, 1990; Cutler, 1991; Calderone and Fonzi, 2001; Naglik *et al.*, 2003). The formal demonstration of the role in infection has been obtained for some of these factors by the use of knockout (KO) mutants and re-insertion of

relevant genes (De Bernardis *et al*., 1999, 2001; Calderone and Fonzi, 2001; Hoyer, 2001; Hube, 2004; Kumamoto and Vinces, 2005).

Adhesins play an important role in the pathogenesis of mucosal candidiasis by facilitating adherence to vaginal tissue (Hoyer, 2001; Sundstrom, 2002; Spelberg *et al*., 2006). There is a clear evidence that the capacity of *C. albicans* to develop hyphae is required for vaginal infection (Saville *et al*., 2003; Kumamoto and Vinces, 2005; Sandini *et al*., 2007). Tissue sections of animal vaginas show that hyphae strongly adhere to the keratinized surface of the vaginal epithelium with some hyphal tips slightly infiltrating the subepithelial layer (De Bernardis *et al*., 1994, 2007). Some adhesin-encoding genes are critically expressed during hyphal formation (Sundstrom, 2002; Kumamoto and Vinces, 2005; Sandini *et al*., 2007). There is a clear demonstration that each deletion of relevant genes affecting hyphal transition determines decrease or abolition of experimental pathogenicity (Calderone and Fonzi, 2001; Kumamoto and Vinces, 2005).

Enzyme secretion in particular aspartyl proteinase (Sap), a family of 10 enzymes, plays a role in vaginal candidiasis. In fact, symptomatic vaginitis in women was strongly associated with high *in vitro* Sap expression by vaginal isolates of *C. albicans*, and elevated Sap levels in the vaginal fluid (Cassone *et al*., 1987; De Bernardis *et al*., 1990). These findings have been later corroborated by the observation that mutants of *C. albicans* with Sap1-3 KO genes do not cause vaginal infection in rats and lose the capacity of damaging the reconstituted human vaginal epithelium, both pathogenic activities being regained following re-insertion of the relevant gene (De Bernardis *et al*., 1999; Schaller *et al*., 2003). No such inference could be made with Sap4-6 KO mutants, even when the triple mutant was used (De Bernardis *et al*., 1999).

Despite the redundancy of Sap proteins and the likelihood that these isoenzymes cooperate, and sequentially affect virulence expression at different times during *C. albicans* infection (Naglik *et al*., 2003; Hube, 2004), it has emerged that Sap2 protein plays a particularly consistent role in vaginal infection by *C. albicans*, probably as no other single virulence trait. In fact, Sap2 is the predominant enzyme in vaginal secretion of women and rats, and Sap2 gene was the first Sap gene that was seen to be expressed in vaginal infection (De Bernardis *et al*., 1995, 2001; Naglik *et al*., 2003). Moreover, Sap2 is the member of Sap family with the broadest substrate specificity. It is capable of hydrolysing structural host proteins, among which keratin of the skin and that lining the surface of the vaginal epithelium are quite a preferred substrate. Furthermore, practically all humoral factors of innate and adaptive immunity, including complement and immunoglobulins, are highly susceptible to Sap2 degradation (Naglik *et al*., 2003). By this combined action, Sap2 can literally derange the whole epithelial tissue, as clearly seen with the reconstituted human vaginal epithelium (Naglik *et al*., 2003).

Not surprisingly, all the virulence traits described above have been associated with the immunoescape potential of the fungus. The transition from the commensal yeast cells to the pathogenic hyphae is accompanied by genetic reprogramming ultimately leading to remarkable antigenic and structural variations in the cell wall, avoidance of phagocyte internalization and killing, and perturbation in dendritic cell (DC) function in *in vitro* and *ex vivo* experiments (Fè D'Ostiani *et al*., 2000; Torosantucci *et al*., 2004; Wheeler and Fink, 2006). Germ tubes (i.e. the precursors of

hyphal forms) are found on the vaginal epithelium of the rat vagina a few hours after intravaginal challenge and continue to overlay the epithelia without any sign of leucocyte infiltration from distant tissue. In such cases, *C. albicans* is able to modify the nature of some cell wall constituents under the selective pressure of *in vivo* growth and the need of survival in new organ environments. An example of *C. albicans* adaptation is the different expression of pH-regulated proteins in relation to the environments, and specific host tissue invasion (De Bernardis *et al.*, 1995).

These potential immunoescape mechanisms would probably be irrelevant in a normal host. However, they could enhance fungus spread in an immunocompromised host.

♦♦♦♦♦♦ III. ANIMAL MODELS OF MUCOSAL CANDIDIASIS

Animal models have been employed to study various aspects of the host immune response against *C. albicans* at mucosal level under conditions possibly mimicking human infection. Reviews of experimental animal models were published by Samaranayake and Samaranayake (2001), Naglik *et al*. (2008) and Capilla *et al*. (2007).

A. Oral Candidiasis

Experimental models of oral candidiasis have been difficult to reproduce because of the lack of a persistent and reproducible infection without significant manipulation; in fact, without some form of immunosuppression, oral *Candida* infection declines rapidly. To establish oral candidiasis in mice, a treatment with steroids is usually required, often with the addition of antibiotics such as tetracycline (Deslauriers *et al.*, 1995; Kamai *et al.*, 2001). It has been evidenced that *Candida* colonization can be initially high, especially during the first week after oral challenge, and then the number of *Candida* cells decreases after suspension of drug treatment (Deslauriers *et al.*, 1995). A complete review of experimental animal model of oral candidiasis was published by Samaranayake and Samaranayake (2001).

A role for T cells in protection against oral candidiasis was evidenced by the increased susceptibility to oral candidiasis in athymic mice (nu/nu); by contrast, mice deficient in macrophage or polymorphonuclear neutrophils (PMNs) (beige/beige) were shown to be resistant (Balish *et al.*, 1990; Cantorna and Balish, 1991a). The same authors (Balish *et al.*, 1993) suggested a role for innate cells in so far as they evidenced that SCID mice, deficient in both T and B cells, were resistant to oral infection when treated with cyclophosphamide. These studies have established that a defect in the protective $CD4^+$ T cell response to *C. albicans* results in mucosal candidiasis; the presence of α/β $CD4^+$, $CD8^+$ and γ/δ T cells was evidenced in the oral cavity of naïve immunocompetent mice and after *Candida* oral challenge; all these T cell subpopulations were shown to increase in the oral mucosa correlating with clearance of infection (Chakir *et al.*, 1994). Results obtained in an

immunodeficient murine model confirmed the role for $CD4^+$ T cells in host response against the oral infection. In fact, mice devoid of $CD4^+$ T cells were more susceptible to *Candida* infection and adoptive transfer of CD+ T cells, taken from *Candida* immune mice protected against oral *Candida* infection (Elahi *et al.*, 2001; Farah *et al*., 2002a,b, 2006).

A role for $CD8^+$ T cells in the host response against oral candidiasis in mice was evidenced by Beno and Mathews (1990) and Beno *et al*. (1995) and in a murine AIDS model (Deslauriers *et al*., 1997).

The development of oral candidiasis in transgenic mice expressing HIV gene in immune cells and with an AIDS-like disease has provided an important model of oral candidiasis that closely mimics the pathological aspects of *Candida* infection in human AIDS (Deslauriers *et al.*, 1997; de Repentigny *et al*., 2002). Recently, in this model the role of $CD8^+$ T cells in limiting chronic oral carriage and dissemination of *C. albicans* to deep organs was confirmed. Moreover, it was evidenced that PMNs were not dispensable to limit oral infection; in fact, profound depletion of PMNs did not increase oral *Candida* colonization and did not lead to systemic dissemination (Marquis *et al.*, 2006).

Rahman and collaborators (2007) have developed a murine model of concurrent oral and vaginal colonization. This model appears useful and would permit investigations of host–*Candida* interaction at both oral and vaginal levels.

B. Gastrointestinal Candidiasis

Experimental GI candidiasis has been induced in rodents, particularly mice. Establishment of GI infection is done by gavage with a suspension of yeast, allowing the animals to drink from a suspension of yeast or by feeding the fungus in pellets. The administration of immunosuppressive drugs, irradiation ray treatment and administration of broad-spectrum antibiotics are critical factors, as reviewed by Naglik *et al*. (2008) and Capilla *et al.* (2007).

Pope *et al*. (1979) were the first to describe an infant mouse model of GI.

Contribution of both innate and adaptive immune responses in the control of infection was evaluated after GI infection with *C. albicans* (Bistoni *et al.*, 1993; Cenci *et al*., 1995).

Other animal models have also focused on aspects of dissemination of *Candida* from the GI tract leading to systemic candidiasis (De Maria *et al.*, 1976; Myerowitz, 1981; Hector and Domer, 1982; Kennedy and Volz, 1985).

An infant mouse model of GI candidiasis has been employed by Cole and collaborators (Cole *et al.*, 1989). Histopathology of long-term *Candida* colonization of the GI tract and the nature of the mucosal immune and non-immune cell responses to chronic yeast infection were investigated in CFW infant mice 3 weeks post *Candida* challenge (Cole *et al.*, 1993). Histological sections of lesions of the oesophageal and gastric mucosa revealed intraepithelial abscesses associated with infection by *C. albicans*. Moreover, abundant PMNs were found in cluster within the epithelial layer and adjacent to *C. albicans* cells and comprised the majority of inflammatory cells present in the abscess; in addition, low numbers of macrophages were also evidenced in the lamina propria of the gastric mucosa of infected mice.

Cole *et al.* (1992) have also investigated GI candidiasis in mice which have concurrent *C. albicans* infection and an AIDS-related murine immunodeficiency syndrome (MAIDS) which shares many characteristics with human AIDS. Both B cell and T cell functions are abnormal in these retroviral-infected mice. These include impaired T cell proliferative response, which related to defects of $CD4^+$ T cell and not $CD8^+$ T cell, as well as phagocytosis and killing of *C. albicans* by macrophages and neutrophils in the GI tract (Cantorna and Balish, 1991a,b).

According to the authors (Cole *et al.*, 1992), chemotactic factors as well as lytic enzymes released by *Candida* caused tissue damage. Lysis of keratinocytes occurs at the squamous epithelial surface of the GI tract, which potentiates the release of interleukin-1 (IL-1), a proinflammatory cytokine for mucosal tissues. In addition to these innate host defense mechanisms, *C. albicans* antigens induce an acquired immunoprotection at the mucosal level, mediated by secretion of specific IgA and the presence of sensitized T lymphocytes. Defects of CMI associated with MAIDS exacerbate *C. albicans* infection of the gastric mucosa.

Balish and coworkers (1996) studied immune response to mucosal candidiasis in b2-microglobulin KO mice. These mice express little major histocompatibility complex class I (MHC-I) protein on their cell surface and are deficient in $CD8^+$ TCR α/β^+ T cells and show susceptibility to candidiasis in some mucosal tissues (such as oesophageal gastric tract) and, by contrast, displayed resistance to candidiasis in others, including intestine and vagina.

Rahman and Challacombe (1995) studied humoral and cellular immune response following mucosal infection by *C. albicans* given orally to gnotobiotic mice. Salivary counts of *C. albicans* were significantly reduced in orally immunized mice in comparison with controls. Anti-*Candida* salivary IgA antibodies were detected in intragastric immunized mice but not in intraperitoneal immunized mice while serum anti-*Candida* IgG antibodies were found in i.p. immunized mice but not in i.g. immunized mice.

Animals which were adoptive transferred with mesenteric lymph node cells or $CD8^+$-enriched T cells from orally immunized donors showed a significant reduction of oral *Candida* carriage compared with controls, but transfer of $CD4^+$-enriched T cells did not give the same protection. On the other hand, adoptive transfer of spleen cells, $CD4^+$ T cells or $CD8^+$ T cells from i.p. immunized donors resulted in a reduction of oral *Candida* carriage. The authors suggest that both oral and systemic immunization can protect against *Candida* colonization at mucosal surfaces with different mechanisms.

Bistoni, Romani and collaborators (Bistoni *et al.*, 1993; Cenci *et al.*, 1995) evidenced different outcome of mucosal *Candida* infections in various inbred strains of mice. In fact, a primary mucosal infection with *C. albicans* confers anti-*Candida* immuno-mediated protection in genetically resistant BALB/C and C57BL/6 mice, whereas it fails to elicit a protective response in the susceptible DBA/2 strain. A high number of yeast and filamentous form of the fungus was observed in the stomach of these mice and was associated with localized foci of mucosal involvement. Based on these findings, it was suggested as the existence of locally occurring anti-*Candida* immune mechanisms of defense.

Regarding the nature of these immune responses, impaired local Th2-associated functions were observed, as defective production of IgA, IL-4 and IL-5 by Peyer's

patches, $CD4^+$ T lymphocytes and increased numbers of interferon (IFN)-γ-producing cells were detected.

Thus, although both Th1 and Th2 responses were present in mice recovering from GI candidiasis, protective immunity was associated with the induction of a local Th1 response that would ultimately overcome the Th2 reactivity.

The development of protective anti-*Candida* Th1 responses requires the concerted actions of several cytokines such as IFN-γ, transforming growth factor (TGF)-β (Cenci *et al*., 1995, 1998), IL-6 (Bistoni *et al*., 1993), tumour necrosis factor (TNF)-α (Mencacci *et al*., 1998a,b) and IL-12 and the absence of inhibitory Th2 cytokines such as IL-4 and IL-10 in that neutralization of IL-4 and IL-10 was found to favour the development of Th1. In highly susceptible mice, however, exogenous IL-12 did not exert beneficial effects on the course and outcome of mucosal infection (Romani *et al*., 1996; Romani, 1997). Moreover, administration of IL-4 failed to convert an already established Th1 response into a Th2 response and late IL-4 depletion exacerbated chronic infection, suggesting that in this model the Th differentiation may be locked in and persist.

Studies performed in mice with distinct genes deleted including those involving cytokines, cytokine receptors, IL-1β-converting enzyme or MHC class II molecules showed that susceptibility to primary or secondary intragastric infections greatly varies in relation to the genes knocked out. In general, cytokine-deficient mice showed more extensive fungal growth in stomach and oesophagus as compared to normal mice. In particular, mice depleted of TNF-α and IL-6 were highly susceptible to primary gastric infection and did not develop innate and acquired immunity. In fact, impaired function of phagocytic cells, particularly neutrophils, and the activation of non-protective Th2 responses were observed in these animals. Gastric candidiasis improved upon administration of recombinant TNF-α, which determined the induction of antifungal Th1 responses and consequently stimulation of antifungal effector functions (Mencacci *et al*., 1998a,b). By contrast, resistance to primary and secondary infections was not impaired in the absence of IL-1β or $CD4^+$ T cells.

Susceptibility to primary and secondary gastric *C. albicans* infections in cytokine KO mice correlates with the failure to develop anti-*Candida* protective Th1 responses and with the occurrence of non-protective IL-4- and IL-10-producing Th2 cells. By contrast, the successful control of infection is the result of protective Th1-dependent immunity induced by an early release of proinflammatory cytokines such as TNF-α, IL-6 and IL-1β. IL-12 production is required for the development of Th1 cells, whose activation is IL-4- and IL-10-dependent. Thus, a finely regulated balance of cytokine levels, such as IL-4, IL-10 and IL-12, appears to be required for optimal development and maintenance of Th1 reactivity in mice with candidiasis.

Overall, Romani *et al*. (Romani *et al*., 1996; Romani, 1997; Cenci *et al*., 1998; Mencacci, 1998a,b; Del Sero *et al*., 1999) studies have contributed to understanding of cytokine-mediated regulation of Th cell development and effector functions in mucosal candidiasis and have revealed complex levels of immunoregulation that were previously unappreciated. In fact, their observations go beyond the more usual paradigm of Th1 and Th2 cytokines meaning protection or susceptibility, respectively, to infection by *Candida*. Their findings rather suggest that regulation of both Th1 and Th2 cytokines, depending on the site of infection and the amount

of the fungus challenge, is needed for effective anti-*Candida* immunoprotection, a situation likely valid in many other models of infections.

Th1 cells, by their production of IFN-γ and TNF-β, directly activate cell-mediated immune responses leading to the eradication of infection, but they may also cause pathogenic effect if their synthesis/release is dysregulated. Th2 cells, by releasing IL-4 and IL-5, activate mast cells and eosinophils and are responsible of atopy and humoral immunity.

It is also suggested that Th0 cells, which produce both Th1 and Th2 type cytokines (O'Garra, 1998), participate in eliminating *Candida* infection.

Other conditions may result in activation of both Th1 and Th2 type responses which can be pathogenic (O'Garra, 1998). Other studies (Chen *et al*., 1994; Weiner, 1997; Mason and Powrie, 1998) have provided evidence on an alternative regulatory population distinct from Th2 cells: the regulatory T (T reg) cells including Th3 and Tr-1 that can inhibit cell-mediated immune responses and/or inflammatory pathologies and are involved in the maintenance of self-tolerance. TGF-β produced by these cell populations seems essential for their suppressive activity.

Recent studies by Romani and collaborators (Montagnoli *et al*., 2002; De Luca *et al*., 2007) evidenced the ability of T reg cells to inhibit aspects of innate and adaptive immunity and their protective function in fungal infections. Mice genetically deficient for a specific pathway or Toll-like receptors were challenged intragastrically with *C. albicans* to assess the relative contributions of natural T reg (nTreg) cells and inducible or adaptive T reg (iTreg) cells to *Candida* infection. The authors found that nTreg and iTreg cells are sequentially induced in infection and have non-overlapping complementary roles. NTreg cells modulated the effector function and proinflammatory ability of PMNs and thus exerted an early control over fungal growth and local inflammation. Later, during the infection *Candida* induce Ag-specific I Treg cells and this activation led to Th17 cell antagonism and protective Th immunity. In fact, when the Th17 pathway is activated by *C. albicans*, it inhibits protective Th1 immunity and determines susceptibility to infection (Zelante *et al*., 2007). T reg cells prevent *Candida* eradication from the GI tract and excessive inflammation, but they enable memory immunity and consequent durable anti-*Candida* protection. Overall, the studies of Romani and collaborators (De Luca *et al*., 2007; Zelante *et al*., 2007) have provided new insights into the pathogenesis of chronic mucocutaneous candidiasis and may have possible therapeutic implications.

C. Experimental Vaginal Candidiasis

Animal models have been employed to study various aspects of the immune response in *Candida* vaginitis under conditions possibly mimicking human infection. In these models *Candida* infections may be established under controlled and reproducible conditions. Experimental *Candida* vaginitis has been reproduced especially in mice and rats, and a primate model has also been explored.

Corresponding to above-reported murine experimental model, a rat model, initially generated to study the efficacy of antifungal therapy (Scholer, 1960; Mc Ripley *et al*., 1979; Thienpont *et al*., 1980; Ryley *et al*., 1981; Sobel and Muller, 1983;

Kinsman *et al*., 1986; Van Cutsen *et al*., 1987; Jansen *et al*., 1991), has been adapted to investigate the immunological mechanisms of protection against *Candida* at vaginal level (Cassone *et al*., 1995; De Bernardis *et al*., 1997). The induction and the maintenance of 'pseudoestrus' in rats require oophorectomy and oestrogen administration (Kinsman and Collard, 1986). Under oestrogen administration, the vaginal epithelium is fully keratinized and *C. albicans* colonization is greatly facilitated. Germ-tube (hyphal) formation, strong adherence and secretion of aspartyl proteinase activity are also induced by the production of the keratin layer. In addition, the oestrogens reduce leucocyte infiltration, which helps fungal growth and the establishment of infection.

The hormonal dependence of *Candida* vaginitis in rats has a precise correlation in the role of oestrogen in human vaginitis. Although not exactly defined, this role can be easily inferred by the rare incidence of *Candida* vaginitis in premenarchal and post-menopausal ages, while it greatly increases and is exacerbated in the premenstrual week (Sobel and Muller, 1984).

I. Murine model

The mouse model of *Candida* vaginitis has been used by Taschdjan *et al*. (1960), Ryley and Mc Gregor (1986), Fidel *et al*. (1993a,b) and Valentin *et al*. (1993). A state of pseudoestrus is required at the time of intravaginal inoculation to obtain a persistent infection in mice.

In the mouse model, Fidel and collaborators have first evidenced that local rather than systemic CMI is an important host defense mechanism of the vaginal mucosa (Fidel, 1994; Fidel *et al*., 1995a,b,c). They have also suggested some level of immunological independence or immune compartmentalization. The authors (Fidel and Sobel, 1996) reported that vaginal T lymphocytes are phenotypically distinct from those in periphery and confirmed the previous observations by Ibraghimov *et al*. (1995). In fact, by flow cytometric analysis, Fidel *et al*. (1996) showed that although $CD4^+$ TCR α/β^+ cells are the predominant ones among the intravaginal T cells, a high percentage (15%) of TCR γ/δ^+ cells are also found (Fidel *et al*., 1996, 1997b; Fidel and Sobel, 1998). Cytofluorimetric analysis using different anti-CD4 antibodies evidenced that, on vaginal $CD4^+$ T cells, the CD4 protein is expressed in a different conformation compared to lymph node cells.

In addition, mice treated intravenously with antibodies specific for T cells were depleted of T cells in the periphery but not in the vagina, whereas the intravaginal administration of the same antibodies depleted T cells in both the vagina and the periphery (Fidel *et al*., 1997a,b). These observations further support the concept of immune compartmentalization of vaginal T cells.

Partial protection against vaginitis was observed in mice after a second intravaginal challenge with *C. albicans* following the spontaneous resolution of a primary infection (Fidel *et al*., 1995b). However, little to no changes in the percentage or phenotype of vaginal T cells were found during either primary or secondary experimental vaginal *Candida* infections when analysing the vaginal lymphocyte populations by flow cytometry, immunohistochemistry or RT-PCR (Fidel *et al*., 1999).

Jones-Carson *et al*. (1995) observed an enhanced susceptibility to *Candida* vaginitis in mice depleted of γ/δ T cells and suggested a potential role of γ/δ T cells in the protective response in the vaginal mucosa. Conversely, Wormley *et al.* (2001) observed a less severe vaginitis in δ-chain TCR KO mice with respect to wild-type mice and suggested a tolerogenic role for vaginal γ/δ T cells.

In the studies of Mulero-Marchese *et al*. (1998), protection from vaginal candidiasis was transferred to BALB/C mice by adoptive transfer of *C. albicans* immune splenic T cells. Depletion of $CD3^+$ or $CD4^+$ T cells, but not $CD8^+$ T cells before transfer, completely abrogated protection. These results demonstrate a significant role for CD4 T lymphocytes in the resistance to mucosal candidiasis.

The information on the role of $CD8^+$ T cells in resistance to mucosal candidiasis is little and somewhat controversial, although $CD8^+$ T cells are found in large numbers in most mucosal tissues. The studies by Fidel *et al.* (1995c) in mice treated with monoclonal antibodies to deplete $CD8^+$ T cells suggest that they do not play a role in the resistance to vaginal candidiasis. Ghaleb *et al*. (2003) in a murine model of vaginal candidiasis observed a significant increase in the number of $CD3^+$ T cells, with the percentage of $CD8^+$ higher than that of $CD4^+$ (10–15%), after *C. albicans* administration; the increased number of vaginal lymphocytes persisted throughout the infection period. There are also a few observations about a population of $CD8^+$ T cells capable of killing *C. albicans* hyphae upon stimulation *in vitro* with high doses of IL-2, but no *in vivo* evidence are available to substantiate this interesting finding (Beno and Mathews, 1990).

To evaluate the role of innate immunity in protection against vaginitis, Fidel and collaborators examined the effects of polymorphonuclear leucocytes in non-oestrogen and oestrogen *C. albicans*-infected mice and showed that neutrophil depletion had no effect on vaginal fungal burden under hormonal conditions (Fidel *et al*., 1999). These observations correlate with studies of Cantorna and coworkers (1990), who observed same susceptibility to *C. albicans* vaginal infection in non-oestrogenized animals that were immunodeficient in phagocytic cells (beige/beige) and indicate a lack of demonstrable effects by systemic adaptive and innate CMI against vaginitis.

Fidel and collaborators (Saavedra *et al*., 1999; Steele *et al*., 1999; Normanbhoy *et al*., 2002; Fidel, 2006) demonstrated that epithelial cells taken from the vagina of naïve mice or collected from human and primate vaginal layers inhibited the growth of *C. albicans in vitro* and produced proinflammatory cytokines (IL-1α and TNF-α). These observations correlate with studies of Hedges and collaborators (1995), which showed that epithelial cells produce cytokines and chemokines, and of Fratti *et al.* (1996), which demonstrated that endothelial cells can phagocytize *Candida*. Thus, epithelial cells may represent important innate effector cells against *C. albicans* at the vaginal mucosa.

The analysis of chemokines associated with the chemotaxis of T cells, macrophages (RANTES, MIP-1α, MCP-1) and PMNs (MIP-2) secreted during experimental vaginal candidiasis showed significant increases in MCP-1 protein and mRNA in vaginal tissue of infected mice 2 and 4 days after *Candida* infection, respectively, and persistent through 21 days. By contrast, RANTES, MIP-1α and MIP-2 were not detected in the vaginal tissue of infected mice. Furthermore, the intravaginal immunoneutralization of MCP-1 with anti MCP-1 antibodies resulted in a

significant increase in vaginal *Candida* colonization early during the infection, suggesting that MCP-1 play a role in reducing the fungal burden during vaginal infection (Steele and Fidel, 2002).

The analysis of cytokines secreted during vaginal candidiasis in mice showed high levels of TGF-β and low or undetectable levels of other cytokines (IL-2, IFN-γ, IL-12, IL-4, IL-10) (Taylor *et al.*, 2002; Fidel, 2006). These observations suggest a possible contribution of TGF-β to immunoregulation or tolerance at mucosal level.

Recently, the same authors showed that immunodeficient mice (SCID, Nude) or KO (CD4) mice had similar vaginal colonization and similar levels of vaginal Th and proinflammatory cytokines compared to wild-type mice. Their studies evidenced lack of a protective role for T cells against *C. albicans* vaginitis and support the influence of immunoregulatory mechanisms (Fidel and Sobel, 2002; Fidel, 2007).

2. Rat model

Little information exists on the role of antibodies in resistance to mucosal vaginal candidiasis, and the results are somewhat controversial.

We investigated the efficacy of antibodies in the protection against *C. albicans* vaginal infection by using a rat vaginitis model. The induction and the maintenance of 'pseudoestrus' in rats require oophorectomy and oestrogen administration (Kinsman and Collard, 1986). Under oestrogen administration, the vaginal epithelium is fully keratinized and *C. albicans* colonization is greatly facilitated. Germ-tube (hyphal) formation, adherence and secretion of aspartyl proteinase activity are also induced by the production of the keratin layer. In addition, the oestrogens reduce leucocyte infiltration, which helps fungal growth and the establishment of infection. After clearing the primary *C. albicans* infection, rats were highly resistant to a second vaginal challenge with the fungus (Cassone *et al.*, 1995). We assumed that if adherence, germ tube formation and secretion of aspartyl proteinase play a role in vaginal infection, it is conceivable that specific antibodies against these factors could be protective. Thus, we investigated the potential protective effect of specific antibodies against a well-defined immunogenic cell wall antigen (mannoprotein) and against a well-established virulence factor of *Candida* such as aspartyl proteinase (Sap). Animals receiving vaginal fluids, containing anti-mannan (MP) and anti-aspartyl proteinase (Sap) antibodies, from *C. albicans*-infected rats were significantly protected against vaginitis compared to animals given antibody-free vaginal fluid from non-infected rats. Pre-absorption of the antibody-containing fluids with either one or both proteins MP and Sap sequentially reduced or abolished, respectively, the amount of protection. A degree of protection from a vaginal infection with *C. albicans* was also conferred by post-infectious administration of anti-Sap and anti-Mp monoclonal antibodies and by intravaginal immunization with MP or Sap preparations. In order to investigate whether the protection conferred by antibody response was T cell dependent, we reproduced *Candida* vaginitis in congenitally athymic nude rats. The animals showed a primary infection not dissimilar in extent and duration to that observed in euthymic rats, but they were not protected against a secondary fungal challenge.

No anti-Mp or anti-Sap antibodies were elicited in the vaginal fluids of athymic rats during both the first and the second *Candida* infection. These results demonstrated that the induction of antibody response was T cell dependent and also evidenced a link between cell-mediated and humoral immunity in vaginal infection with *C. albicans* (De Bernardis *et al*., 1997, 2000).

Overall, the results of our studies evidenced the protective role in Candida vaginitis of specific antibodies against mannoprotein or proteinase of *C. albicans*; moreover, monoclonal antibodies against these antigens were locally protective. The recombinant forms of these antigens (65 kDa mannoprotein and Sap 2) have been investigated as active immunogens in vaginal candidiasis (De Bernardis *et al*., manuscript in preparation). The mechanisms by which anti-mannan and anti-proteinase antibodies protect against candidiasis are unclear. The hypothesis is that anti-sap antibodies act neutralizing the proteinase activity of *C. albicans* and inhibiting adherence to vaginal mucosa and consequent colonization. In addition the binding of antibodies to cell wall may facilitate phagocytosis of the fungus. Thus, more investigations were required for a clear understanding of how antibodies can help the host in resolving vaginal candidiasis; we evaluated the activity of human domain antibodies (DAbs) generated against recombinant 65-kDa mannoprotein (rMP65) or aspartyl proteinase (r-Sap), which strongly inhibited *Candida* adherence to endothelial and epithelial cells. DAbs which specifically bind Mp65 or Sap2 exerted both a marked preventive and curative effect on experimental vaginal candidiasis. In fact, both DAb families strongly accelerated clearance of *C. albicans* from rat vagina to a greater extent when they were intravaginally administered before or after *Candida* challenge and were equally effective against both azole-susceptible and azole-resistant isolates of *C. albicans* (De Bernardis *et al.*, 2007).

These results evidence a potential therapeutic use of some antibodies or their engineered derivatives in the treatment of *Candida* vaginal infections.

Undoubtedly, the use of animal models has been invaluable to investigate and understand the humoral host defense mechanisms that protect against *C. albicans* at the vaginal mucosal surface. Overall, several studies have evidenced the protective role of antibodies direct against specific immunogenic antigen of *Candida* cell wall (mannan) or against specific virulence factors of *C. albicans* (adhesins, proteinase, germ tube). Although the mechanisms by which these antibodies exert protection during vaginal infection is not completely understood (inhibition of adhesion or germ tube formation, opsonization and neutralization of proteolytic enzymes are the mechanisms hypothesized), these observations provide a valuable approach to the potential therapeutic use of some antibodies or their engineered derivatives in the treatment of *Candida* vaginal infections refractory to antimycotics.

We have also demonstrated that CMI exerts a critical regulatory role in anti-*Candida* response, as evidenced by the lack of protection induced by active *Candida* antigen immunization in congenitally athymic nude rats (De Bernardis *et al*., 1997). Thus, the study of T cell activation at vaginal level remains a key point for understanding local host immunity. The analysis of the T cell responses in immunized and protected rats demonstrated relevant changes in the $CD4^+/CD8^+$ T cell ratio, during subsequent fungal infections, regarding in particular the cells bearing the CD25 (IL-2 receptor α) activation marker. In fact, an increased number of both $CD4^+$ TCR α/β^+ and $CD4^+/CD25^+$ vaginal lymphocytes were observed after the

second and the third *Candida* challenge, as compared to oestrogenized but uninfected control rats that exhibit high numbers of $CD8^+$ cells. During a third *Candida* challenge, vaginal lymphocytes showed a dose-dependent proliferative response to stimulation with a mannoprotein fraction of *C. albicans*. No response to this antigen by mitogen-responsive blood, lymph node and spleen cells was found (De Bernardis *et al.*, 2000).

The analysis of the cytokines secreted in the vaginal fluid of *Candida*-infected rats showed high levels of IL-12 during the first, immunizing infection, followed by progressively increasing amounts of IL-2 and IFN-γ. These results constitute good evidence for induction of locally expressed *Candida*-specific antibody and cellular responses which are potentially involved in anti-*Candida* responses at the vaginal level.

We have investigated the protective roles of different lymphocytes subsets also by adoptive transfer of vaginal lymphocytes or purified $CD3^+$ T cells, $CD4^+$ or $CD8^+$ T cells or $CD3^-CD5^+$ B cells from the vagina of normal rats or rats immunized with three consecutive *C. albicans* challenge. The rank of anti-*Candida* efficacy of adoptive transfer was $CD4^+/CD3^+$ T cells > $CD3^-CD5^+$ B cells > $CD8^+$ T cells (Santoni *et al.*, 2002). These experiments demonstrated not only that $CD4^+$ Tcells were essential for protection but also that other cellular types were probably involved. To further investigate on this aspect, we evaluated the presence of DCs in the vaginal tissue. In fact, DCs are key inducers of both innate and adaptive immunity (Austyn, 1998; Banchereau and Steinman, 1998; Bacci *et al.*, 2002). Nonetheless, very little were known on the phenotype and role of vaginal DCs (VDCs) in the induction of mucosal immunity against *C. albicans* infection. We evaluated the presence of VDCs in the vaginal tissue of non-infected and *C. albicans*-infected rats by immunohistochemical analysis using the OX62 monoclonal antibody that recognizes the rat aE2 integrin chain or CD103 (Satake *et al.*, 2000; Trinitè *et al.*, 2000; De Bernardis *et al.*, 2006). $OX62^+$ VDCs were found in the vaginal mucosa on both non-infected and infected rats, after the third round of *Candida* infection, with a higher number of $OX62^+$ VDCs observed in the infected vaginal mucosa. These results were confirmed by a quantitative analysis of isolated VDC population that evidenced a significantly higher number of $OX62^+$ VDCs in the vaginal tissue from infected rats compared to those recovered from the vagina of non-infected rats (about 4.5 vs. 1.9×10^5/rat). VDCs from infected rats were capable of inducing naïve $CD4^+$ T cell proliferation and the release of high levels of IL-2, IFNγ and IL-6 and low levels of IL-10 by T cells in response to staphylococcal enterotoxin B (SEB) stimulation. By contrast, VDCs from non-infected rats stimulated neither T cell cytokine release nor cell proliferation.

Adoptive transfer of highly purified $OX62^+$ VDCs from infected rats induced a significant acceleration of *Candida* clearance from the vagina compared with that in rats receiving naïve VDCs, suggesting a protective role of VDCs in the anti-*Candida* mucosal immunity. VDC-mediated protection was associated with the ability to rapidly migrate to the vaginal mucosa and lymph nodes, as assessed by adoptive transferring of carboxyfluorescein diacetate succidimyl ester (CFSE)-labelled VDCs.

It has long been suspected that protection from vaginal candidiasis was entirely due to immune response restricted at vaginal level itself. Our studies demonstrated

that distinct vaginal lymphocyte subsets participate in the adaptive anti-*Candida* immunity at vaginal level, with the vaginal $CD4^+$ T cells and $CD5^+$ B lymphocytes probably playing a major role.

Our data emphasized the role of specific integrated cellular and humoral immunity at vaginal level and could lead to new strategies for vaccination or immunotherapy of vaginal candidiasis.

There is therefore consensus that the models described above are somewhat representative of human disease and that knowledge of virulence expression by the fungus and related immune responses in the animal models may help to understand the determinant of *Candida* infection and immunity in women. Two main aspects must, however, be considered in making a parallel between human and animal settings. First, *C. albicans* is a commensal in the vagina of most women, whereas it is not either in mouse or in rat vagina. Thus, women are 'primed' against the fungus while the animals are not. Second, experimental vaginal infection in rodents is achieved by direct, intravaginal inoculation of a rather high fungus inoculum size (usually between 10^5 and 10^6 cells) that is unlikely to be the ordinary mechanism of human infection which probably occurs by 'exacerbation' of the resident *Candida* or neo-influx of fungal cells from intestinal reservoir.

A special mention is due to the experimental vaginal infection in women performed by Fidel and collaborators (Fidel *et al.*, 2004). These authors used a live fungal challenge in volunteers with different susceptibility to vaginal infection by *C. albicans* to explore the mechanisms of pathogenesis directly in human vagina. The clinical signs of the vaginal infection caused in a percentage of predisposed subjects were all attributed to polymorphonuclear infiltration in the vaginal tissue, to an intensity correlated with the intravaginal fungus growth. Importantly, no signs of inflammation were detected in the subjects without predisposing factors who mostly resisted to the experimental infection.

Despite all the cautions, the experimental models of vaginal candidiasis have provided invaluable information about fungal pathogenicity and immune response, which may constitute the basis for immune intervention against vaginal candidiasis in women.

♦♦♦♦♦♦ IV. GENERAL CONCLUSIONS AND PERSPECTIVES

The use of animals models have been invaluable to investigate and understand host defense mechanism protecting against mucosal candidiasis. These studies have evidenced that the immune response to *Candida* is different at the various mucosal sites. Experimental animal studies and the deriving considerations summarized above do strongly suggest that local mucosal immunity is critically important as defense mechanism against *Candida* infections. Particularly, the role of $CD4^+$ T cells in resistance to mucosal candidiasis is relevant. These cells may act locally and/or be involved as critical regulators of defined-isotype antibody response by the production of Th1 cytokines.

Experimental oral candidiasis has evidenced the role of $CD4^+$ T cells and $CD8^+$ T cells together with Th1-type responses in protection against *Candida* infection.

The observations of GI candidiasis reproduced in genetically modified mice including cytokine-deficient mice have clarified the role of cytokine-mediated regulation of Th cell development. They have also revealed complex levels of immunoregulation in mucosal candidiasis.

The results obtained in experimental *Candida* vaginitis have clearly evidenced that systemic CMI is not protective against vaginitis while some form of locally acquired mucosal immunity seems to be protective. This clearly supports the current idea of immunological independence or immune compartmentalization. The local compartmentalized resistance involves both innate and adaptive immune responses.

Our results obtained in a rat model of *Candida* vaginitis have demonstrated the presence of protective antibodies against specific virulence factors of the fungus, together with the activation of T cell mucosal compartment. Distinct vaginal lymphocyte subsets participate in the adaptive anti-*Candida* immunity at vaginal level, with the $CD4^+$ T cells and $CD5^+$ B cells probably playing a major role.

These results pave the way to the use of cellular and/or antibody therapy for those subjects with recurrent, antimycotic refractory *Candida* vaginitis.

Therefore, substantial progress can be made to develop immunotherapeutic strategies to treat or prevent oral and recurrent vaginal candidiasis. Further studies of host defense mechanisms at the oral and vaginal mucosa may lead to the development of effective immunotherapy.

Acknowledgements

We would like to thank Sofia Graziani and Antonietta Girolamo for the contribution to the work described; we are grateful to Prof. Antonio Cassone for his timely support and advices and for his wisdom and unfailing enthusiasm throughout our work. We are also grateful to Dr. G. Mandarino for her valuable help in manuscript preparation.

References

Asham, R. B. and Papadimitriou, J. M. (1995). Production and function of cytokines in natural and acquired immunity to *Candida albicans* infection. *Microbiol. Rev.* **59**, 646–672.

Austyn, J. M. (1998). Dendritic cells. *Curr. Opin. Hematol.* **5**(1), 3–15. Review.

Bacci, A., Montagnoli, C., Perruccio, K., Bozza, S., Gaziano, R., Pitzurra, L., Velardi, A., d'Ostiani, C. F., Cutler, J. E. and Romani, L. (2002). Dendritic cells pulsed with fungal RNA induce protective immunity to *Candida albicans* in hematopoietic transplantation. *J. Immunol.* **168**, 2904–2913.

Balish, E., Filutowicz, H. and Oberley, T. D. (1990). Correlates of cell-mediated immunity in *Candida albicans*-colonized gnotobiotic mice. *Infect. Immun.* **58**, 107–113.

Balish, E., Jensen, J., Warner, T., Brekke, J. and Leonard, B. (1993). Mucosal and disseminated candidiasis in gnotobiotic SCID mice. *J. Med. Vet. Mycol.* **31**(2), 143–154.

Balish, E., Vazquez-Torres, A., Jones-Carson, J., Wagner, R. D. and Warner, T. (1996). Importance of β_2-microglobulin in murine resistance to mucosal and systemic candidiasis. *Infect. Immun.* **64**(*12*), 5092–5097.

Banchereau, J. and Steinman, R. M. (1998). Dendritic cells and the control of immunity. *Nature* **392**(6673), 245–252. Review.

Bauters, T. G., Dhont, M. A., Temmerman, M. I. and Nelis, H. J. (2002). Prevalence of vulvovaginal candidiasis and susceptibility to fluconazole in women. *Am. J. Obstet. Gynecol.* **187**, 569–574.
Beno, D. W. and Mathews, H. L. (1990). Growth inhibition of *Candida albicans* by interleukin-2-induced lymph node cells. *Cell. Immunol.* **128**, 89–100.
Beno, D. W., Stover, A. G. and Mathews, H. L. (1995). Growth inhibition of *Candida albicans* hyphae by CD8+ lymphocytes. *J. Immunol.* **154**(10), 5273–5281.
Bistoni, F., Cenci, E., Mencacci, A., Schiaffella, E., Mosci, P., Puccetti, P. and Romani, L. (1993). Mucosal and systemic T helper cell function after intragastric colonization of adult mice with *Candida albicans*. *J. Infect. Dis.* **168**, 1449–1457.
Bonifazi, P., Zelante, T., D'Angelo, C., De Luca, A., Moretti, S., Bozza, S., Perruccio, K., Iannitti, R. G., Giovannini, G., Volpi, C. *et al.* (2009). Balancing inflammation and tolerance *in vivo* through dendritic cells by the commensal *Candida albicans*. . *Mucosal Immunol.* **2**(4), 362–374.
Calderone, R. and Fonzi, W. (2001). Virulence factors of *Candida albicans*. . *Trends Microbiol.* **9**, 327–335.
Cantorna, M. T. and Balish, E. (1991a). Acquired immunity to systemic candidiasis in immunodeficient mice. *J. Infect. Dis.* **164**, 936–943.
Cantorna, M. T. and Balish, E. (1991b). Role of $CD4^+$ T lymphocytes in resistance to mucosal candidiasis. *Infect. Immun.* **59**, 2447–2455.
Cantorna, M. T., Mook, D. and Balsh, E. (1990). Resistance of congenitally immunodeficient gnotobiotic mice to vaginal candidiasis. *Infect. Immun.* **58**, 3813–3815.
Capilla, J., Clemons, K. V. and Stevens, D. A. (2007). Animal models: an important tool in mycology. *Med. Mycol.* **45**, 657–684.
Cassone, A., Boccanera, M., Adriani, D., Santoni, G. and De Bernardis, F. (1995). Rats clearing a vaginal infection by *Candida albicans* acquire specific, antibody-mediated resistance to vaginal reinfection. *Infect. Immun.* **63**, 2619–2624.
Cassone, A., De Bernardis, F., Ausiello, C. M., Gomez, M. J., Boccanera, M., La Valle, R. and Torosantucci, A. (1998). Immunogenic and protective *Candida albicans* costituents. *Res. Immunol.* **149**, 289–299.
Cassone, A., De Bernardis, F., Mondello, F., Ceddia, T. and Agatensi, A. (1987). Evidence for a correlation between proteinase secretion and vulvovaginal candidosis.. *J. Infect. Dis.* **156**(5), 777–783.
Cassone, A. and Torosantucci, A. (1991). Immunological moieties of the cell wall. In: *Candida Albicans* (R. Prasad ed.), Springler-Verlag, Heidelberg, Berlin.
Cenci, E., Mencacci, A., Del Sero, G., Fe' d'Ostiani, C., Mosci, P., Kopf, M. and Romani, L. (1998). IFN-γ is required for IL-12 responsiveness in mice with *Candida albicans* infection. *J. Immunol.* **1161**, 3543–3550.
Cenci, E., Mencacci, A., Spaccapelo, R., Tonnetti, L., Mosci, P., Enssle, K.-H., Puccetti, P., Romani, L. and Bistoni, F. (1995). T helper cell type 1 (Th1)- and Th2-like responses are present in mice with gastric candidiasis but protecitive immunity is associated with Th 1 development. *J. Infect. Dis.* **171**, 1279–1288.
Cernicka, J. and Subik, J. (2006). Resistance mechanisms in fluconazole resistant *Candida albicans* isolates from vaginal candidiasis. *Int. J. Antimicrob. Agents* **27**, 403–408.
Chakir, J., Côté, L., Coulombe, C. and Deslauriers, N. (1994). Differential pattern of infection and immune response during experimental oral candidiasis in BALB/c and DBA/2 (H-2d) mice. *Oral Microbiol. Immunol.* **9**(2), 88–94.
Chen, Y., Kuchroo, V. K., Inobe, J. and Hafler, D. A. (1994). Regulatory T cell clones induced by oral tolerance: suppression of autoimmune encephalomyelitis. *Science* **265**, 1237–1240.
Cole, G. T., Lynn, K. T., Seshan, K. R. and Pope, L. M. (1989). Gastrointestinal and systemic candidosis in immunocompromised mice. *J. Med. Vet. Mycol.* **27**, 363–380.

Cole, G. T., Saha, K., Seshan, K. R., Lynn, K. T., Franco, M. and Wong, P. K.Y. (1992). Retrovirus-induced immunodeficiency in mice exacerbates gastrointestinal candidiasis. *Infect. Immun.* **60**, 4168–4178.

Cole, G. T., Seshan, K. R., Lynn, K. T. and Franco, M. (1993). Gastrointestinal candidiasis: histopathology of *Candida*-host interactions in a murine model. . *Mycol. Res.* **97**, 385–408.

Cutler, J. (1991). Putative virulence factors of *Candida albicans*. *Annu. Rev. Microbiol.* **45**, 187–218.

De Bernardis, F., Agatensi, L., Ross, I. K., Emerson, G. W., Lorenzini, R., Sullivan, P. A. and Cassone, A. (1990). Evidence for a role for secreted aspartate proteinase of *Candida albicans* in vulvovaginal candidiasis. *J. Infect. Dis.* **161**, 1276–1283.

De Bernardis, F., Arancia, S., Morelli, L., Hube, B., Sanglard, D., Schafer, W. and Cassone, A. (1999). Evidence that members of the secretory aspartyl proteinases gene family (SAP), in particular SAP2, are virulence factors for Candida vaginitis. *J. Infect. Dis.* **179**, 201–208.

De Bernardis, F., Boccanera, M., Adriani, D., Spreghini, E., Santoni, G. and Cassone, A. (1997). Protective role of antimannan and anti-aspartyl proteinase antibodies in an experimental model of *Candida albicans* vaginitis in rats. *Infect. Immun.* **65**, 3399–3405.

De Bernardis, F., Cassone, A., Sturtevant, J. and Calderone, R. (1995). Expression of *Candida albicans* SAP1 and SAP2 in experimental vaginitis. *Infect. Immun.* **6**, 1887–1892.

De Bernardis, F., Liu, H., O'Mahony, R., La Valle, R., Bartollino, S., Sandini, S., Grant, S., Brewis, N., Tomlinson, I., Basset, R. C. *et al.* (2007). Human domain antibodies against virulence traits of *Candida albicans* inhibit fungus adherence to vaginal epithelium and protect against experimental vaginal candidiasis. *J. Infect. Dis.* **195**, 149–157.

De Bernardis, F., Lucciarini, R., Boccanera, M., Amantini, C., Arancia, S., Morrone, S., Mosca, M., Cassone, A. and Santoni, G. (2006). Phenotypic and functional characterization of vaginal dendritic cells in a rat model of *Candida albicans* vaginitis. *Infect. Immun.* **74**, 4282–4294.

De Bernardis, F., Molinari, A., Boccanera, M., Stringaro, A., Robert, R., Senet, J. M., Arancia, G. and Cassone, A. (1994). Modulation of cell surface-associated mannoprotein antigen expression in experimental candidal vaginitis. *Infect. Immun.* **62**, 509–519.

De Bernardis, F., Santoni, G., Boccanera, M., Spreghini, E., Adriani, D., Morelli, L. and Cassone, A. (2000). Local anticandidal immune responses in a rat model of vaginal infection by and protection, *Candida albicans*. *Infect. Immun.* **68**, 3297–3304.

De Bernardis, F., Sullivan, P. A. and Cassone, A. (2001). Aspartyl proteinases of *Candida albicans* and their role in pathogenicity. *Med. Mycol.* **39**, 303–313.

De Luca, A., Montagnoli, C., Zelante, T., Bonifazi, P., Bozza, S., Moretti, S., D'Angelo, C., Vacca, C., Boon, L., Bistoni, F. *et al.* (2007). Functional yet balanced reactivity to *Candida albicans* requires TRIF, MyD88, and IDO-dependent inhibition of Rorc. *J. Immunol.* **179**(9), 59999–60008.

Del Sero, G., Mencacci, A., Cenci, E., d'Ostiani, C. F., Montagnoli, C., Bacci, A., Mosci, P., Kopf, M. and Romani, L. (1999). Antifungal type 1 responses are upregulated in IL-10-deficient mice. *Microbes Infect.* **1**(14), 1169–1180.

De Maria, A., Buckley, H. and von Lichtensberg, F. (1976). Gastrointestinal candidiasis in rats treated with antibiotics, cortisone and azathioprine. *Infect. Immun.* **13**, 1761–1770.

de Repentigny, L. (2004). Animal models in the analysis of *Candida* host–pathogen interactions. *Curr. Opin. Microbiol.* **7**, 324–329.

de Repentigny, L., Aumont, F., Ripeau, J. S., Fiorillo, M., Kay, D. G., Hanna, Z. and Jolicoeur, P. (2002). Mucosal candidiasis in transgenic mice expressing human immunodeficiency virus type 1. *J. Infect. Dis.* **185**(8), 1103–1114.

Deslauriers, N., Côté, L., Montplaisir, S. and de Repentigny, L. (1997). Oral carriage of *Candida albicans* in murine AIDS. *Infect. Immun.* **65**(2), 661–667.

Deslauriers, N., Coulombe, C., Carre, B. and Goulet, J. P. (1995). Topical application of a corticosteroid destabilizes the host–parasite relationship in an experimental model of the oral carrier state of *Candida albicans*. *FEMS Immunol. Med. Microbiol.* **11**, 45–55.
Eckert, L. O. (2006). Acute vulvovaginitis. *N. Engl. J. Med.* **355**, 1244–1252.
Elahi, S., Pang, G., Ashman, R. B. and Clancy, R. (2001). Nitric oxide-enhanced resistance to oral candidiasis. *Immunology* **104**(4), 447–454.
Farah, C. S., Elahi, S., Drysdale, K., Pang, G., Gotjamanos, T., Seymour, G. J., Clancy, R. L. and Ashman, R. B. (2002a). Primary role for CD4(+) T lymphocytes in recovery from oropharyngeal candidiasis. *Infect. Immun.* **70**, 724–731.
Farah, C. S., Gotjamanos, T., Seymour, G. J. and Ashman, R. B. (2002b). Cytokines in the oral mucosa of mice infected with *Candida albicans*. *Oral Microbiol. Immunol.* **17**, 375–378.
Farah, C. S., Hu, Y., Riminton, S. and Ashman, R. B. (2006). Distinct roles for interleukin-12p40 and tumour necrosis factor in resistance to oral candidiasis defined by gene-targeting. *Oral Microbiol. Immunol.* **21**, 252–255.
Fè d'Ostiani, C., Del Sero, G., Bacci, A., Montagnoli, C., Spreca, A., Mencacci, A., Ricciardi-Castagnoli, P. and Romani, L. (2000). Dendritic cells discriminate between yeasts and hyphae of the fungus *Candida albicans*. Implications for initiation of T helper cell immunity *in vitro* and *in vivo*. *J. Exp. Med.* **15**(191), 1661–1674.
Fidel, P. L. Jr (1994). History and new insight into host defense against vaginal candidiasis. *Trends Microbiol.* **12**(5), 220–227.
Fidel, P. L. Jr (2006). *Candida*–host interactions in HIV disease: relationships in oropharyngeal candidiasis. *Adv. Dent. Res.* **19**, 80–84.
Fidel, P. L. Jr (2007). History and update on host defense against vaginal candidiasis. *Am. J. Reprod. Immunol.* **57**, 2–12.
Fidel, P. L., Cutright, J. L. and Sobel, J. D. (1995a). Effects of systemic cell-mediated immunity on vaginal candidiasis in mice resistant and susceptible to *Candida albicans* infections. *Infect. Immun.* **63**, 4191–4194.
Fidel, P. L., Ginsburg, K. A., Cutright, J. L., Wolf, N. A., Leaman, D., Dunlops, K. and Sobel, J. D. (1997a). Vaginal-associated immunity in women with recurrent vulvovaginal candidiasis: evidence for vaginal Th1-type responses following intravaginal challenge with Candida antigen. *J. Infect. Dis.* **176**, 728–739.
Fidel, P. L., Luo, W., Chabain, J., Wolf, N. A. and Vanburen, E. (1997b). Use of cellular depletion analysis to examine circulation of immune effector function between the vagina and the periphery. *Infect. Immun.* **65**, 3939–3943.
Fidel, P. L., Jr., Luo, W., Steele, C., Chabain, J., Baker, M. and , Wormley, F., Jr. (1999). Analysis of vaginal cell populations during experimental vaginal candidiasis. *Infect. Immun.* **67**, 3135–3140.
Fidel, P. L., Jr., Lynch, M. E., Conaway, D. H., Tait, L. and Sobel, J. D. (1995b). Mice immunized by primary vaginal *Candida albicans* infection develop acquired vaginal mucosal immunity. *Infect. Immun.* **63**, 547–553.
Fidel, P. L., Lynch, M. E. and Sobel, J. D. (1993a). Candida-specific Th1-type responsiveness in mice with experimental vaginal candidiasis. *Infect. Immun.* **61**, 4202–4207.
Fidel, P. L., Jr., Lynch, M. E. and Sobel, J. D. (1993b). Candida-specific cell-mediated immunity is demonstrable in mice with experimental vaginal candidiasis. *Infect. Immun.* **61**, 1990–1995.
Fidel, P. L., Jr., Lynch, M. E. and Sobel, J. D. (1994). Effects of pre-induced Candida-specific systemic cell-mediated immunity on experimental vaginal candidiasis. *Infect. Immun.* **62**, 1032–1038.
Fidel, P. L., Lynch, M. E. and Sobel, J. D. (1995c). Circulating CD4 and CD8 T-cells have little impact on host defence against experimental vaginal candidiasis. *Infect. Immun.* **63**, 2403–2408.

Fidel, P. L., Jr. and Sobel, J. D. (1996). Immunopathogenesis of recurrent vulvovaginal candidiasis. *Clin. Microbiol. Rev.* **9**, 335–348.
Fidel, P. L. and Sobel, J. D. (1998). Protective immunity in experimental Candida vaginitis. *Res. Immunol.* **146**, 361–373.
Fidel, P. L., Jr. and Sobel, J. D. (2002). Host defense against vaginal candidiasis. In: *Candida and Candidosis* (P. A. Calderone, ed.), pp.193–209. ASM Press, Washington, DC.
Fidel, P. L., Wolf, N. A. and Kukuruga, M. A. (1996). T lymphocytes in the murine vaginal mucosa are phenotypically distinct from those in the periphery. *Infect. Immun.* **64**, 3793–3799.
Fidel, P. L. Jr., Barousse, M., Espinosa, T., Ficarra, M., Sturtevant, J., Martin, D.H., Quayle, A. J., and Dunlap, K., (2004). An intravaginal live Candida challenge in humans leads to new hypotheses for the immunopathogenesis of vulvovaginal candidiasis. *Infect. Immun.* **72**(5), 2939–2946.
Fratti, R. A., Ghannoum, M. A., Edwards, J. E. and Filler, S. G. (1996). Gamma interferon protects endothelial cells from damage by *Candida albicans* by inhibiting endothelial cell phagocytosis. *Infect. Immun.* **64**, 4714–4718.
Ghaleb, M., Hamad, M. and Abu-Elteen, K. H. (2003). Vaginal lymphocytes population kinetics during experimental vaginal candidiasis: evidence for a possible role of CD8+T cells in protection against vaginal candidiasis. *Clin. Exp. Immunol.* **131**, 26–33.
Ghannoum, M. A. and Abu-Elteen, K. H. (1990). Pathogenicity determinant of *Candida*. *Mycoses* **33**, 265–282.
Greenfield, R. A. (1992). Host defense system interaction with Candida. *J. Med. Vet. Mycol.* **30**, 89–104.
Hector, R. H. and Domer, J. E. (1982). Mammary gland contamination as a means of establishing long-term gastrointestinal colonization of infant mice with *Candida albicans*. *Infect. Immun.* **38**, 788–790.
Hedges, S. R., Agace, W. W. and Svanborg, C. (1995). Epithelial cytokine responses and mucosal cytokine networks. *Trends Microbiol.* **3**, 266–270.
Hoyer, L. L. (2001). The ALS gene family of *Candida albicans*. *Trends Microbiol.* **9**, 176–180.
Hube, B. (2004). From commensal to pathogen: stage and tissue specific gene expression of *Candida albicans*. *Curr. Opin. Microbiol.* **7**, 336–341.
Ibraghimov, A. R., Sacco, R. E., Sandor, M., Iakanbov, L. Z. and Lynch, R. G. (1995). Resident $CD4^+$ αβ T cells of the murine female genital tract: a phenotypically distinct T-cell lineage that rapidly proliferates in response to systemic T cell activation stimuli. *Int. Immunol.* **7**, 1763–1769.
Jackson, S. T., Mullings, A. M., Rainford, L. and Miller, A. (2005). The epidemiology of mycotic vulvovaginitis and the use of antifungal agents in suspected mycotic vulvovaginitis and its implications for clinical practice. *West Indian Med. J.* **54**, 192–195.
Jansen, T. M., Van De Ven, M. A., Borgers, M. J., Odds, F. C. and Van Cutsen, J. M.P. (1991). Fungal morphology after treatment with itraconazole as a single oral dose in experimental vaginal candidosis in rats. *Am. J. Obstet. Gynecol.* **165**, 1552–1557.
Jones-Carson, J., Vazquez-Torres, A., van der Heyde, T., Warner, T., Wagner, R. D. and Balish, E. (1995). γδT cell-induced nitric oxide production enhances resistance to mucosal candidiasis. *Nat. Med.* **6**, 552–557.
Kamai, Y., Kubota, M., Kamai, Y., Hosokawa, T., Fukuoka, T. and Filler, S. G. (2001). New model of oropharyngeal candidiasis in mice. *Antimicrob. Agents Chemother.* **45**, 3195–3197.
Kennedy, M. J. and Volz, P. A. (1985). Ecology of *Candida albicans* colonization and dissemination from the gastrointestinal tract by bacterial antagonism. *Infect. Immun.* **49**, 654–663.
Kinsman, O. S. and Collard, A. E. (1986). Hormonal factors in vaginal candidiasis in rats. *Infect. Immun.* **53**, 498–504.
Kinsman, O. S., Collard, A. E. and Savage, T. J. (1986). Ketoconazole in experimental vaginal candidosis in rats. *Antimicrob. Agents Chemother.* **30**, 771–773.

Klein, R. S., Harris, C. A., Small, C. B., Moll, B., Lesser, M. and Friedland, G. H. (1984). Oral candidiasis in high-risk patients as the initial manifestation of the acquired immunodeficiency syndrome. *N. Engl. J. Med.* **311**, 354–358.
Kumamoto, C. A. and Vinces, M. D. (2005). Contribution of hyphae and hypha-co-regulated genes to *Candida albicans* virulence. *Cell. Microbiol.* **7**, 1546–1554.
Mardh, P. A., Wagstrom, J., Landgren, M. and Holmen, J. (2004). Usage of antifungal drugs for therapy of genital *Candida* infections, purchased as over-the-counter products or by prescription. I. Analyses of a unique database. *Infect. Dis. Obstet. Gynecol.* **12**, 91–97.
Marodi, L. (1997). Local and systemic host defence mechanisms against *Candida*: immunopathology of candidal infections. *Pediatr. Infect. Dis.* **16**, 795–801.
Marquis, M., Lewandowski, D., Dugas, V., Aumont, F., Sénéchal, S., Jolicoeur, P., Hanna, Z. and de Repentigny, L. (2006). CD8+ T cells but not polymorphonuclear leukocytes are required to limit chronic oral carriage of *Candida albicans* in transgenic mice expressing human immunodeficiency virus type 1. *Infect. Immun.* **74**(4), 2382–2391.
Martins, M. D., Lozano-Chiu, M. and Rex, J. H. (1998). Declining rates of oropharyngeal candidiasis and carriage of *Candida albicans* associated with trends toward reduced rates of carriage of fluconazole-resistant *C. albicans* in human immunodeficiency virus-infected patients. *Clin. Infect. Dis.* **27**(5), 1291–1294.
Mason, D. and Powrie, F. (1998). Control of immune pathology by regulatory T cells. *Curr. Opin. Immunol.* **10**, 649–655.
McNeil, M. M., Nash, S. L., Hajjeh, R. A., Phelan, M. A., Conn, L. A., Plikaytis, B. D. and Warnock, D. W. (2001). Trends in mortality due to invasive mycotic diseases in the United States, 1980–1997. *Clin. Infect. Dis.* **33**(5), 641–647.
Mc Ripley, R. J., Schwind, R. A., Erhard, P. J. and Whitney, R. R. (1979). Evaluation of vaginal antifungous formulations *in vivo*. *Postgrad. Med. J.* **55**, 648–652.
Mencacci, A., Cenci, E., Bistoni, F., Bacci, A., Del Sero, G., Montagnoli, C., Fè d'Ostiani, C. and Romani, L. (1998a). Specific and non-specific immunity to *Candida albicans*: a lesson from a genetically modified animals. . *Res. Immunol.* **149**, 352–360.
Mencacci, A., Cenci, E., Del Sero, G., Fè d'Ostiani, C., Mosci, P., Montagnoli, C., Bacci, A., Bistoni, F., Quesniaux, V. F.J., Ryffel, B. *et al.* (1998b). Defective co-stimulation and impaired Th 1 development in tumor necrosis factor/lymphotoxin-α double-deficient mice infected with *Candida albicans*. *Int. Immunol.* **10**, 37–48.
Montagnoli, C., Bacci, A., Bozza, S., Gaziano, R., Mosci, P., Sharpe, A. H. and Romani, L. (2002). B7/CD28-dependent CD4+CD25+ regulatory T cells are essential components of the memory-protective immunity to *Candida albicans*. *J. Immunol.* **169**(11), 6298–6308.
Morris, A. H. (2006). Extracorporeal support and patient outcome: credible causality remains elusive. *Crit. Care Med.* **34**(5), 1551–1552.
Mulero-Marchese, R. D., Blank, K. J. and Siek, T. G. (1998). Genetic basis for protection against experimental vaginal candidiasis by peripheral immunization. *J. Infect. Dis.* **178**, 227–234.
Myerowitz, R. L. (1981). Gastrointestinal and disseminated candidiasis. *Arch. Pathol. Lab. Med.* **105**, 138–143.
Naglik, J. R., Challacombe, S. J. and Hube, B. (2003). *Candida albicans* secreted aspartyl proteinases in virulence and pathogenesis. *Microbiol. Mol. Biol. Rev.* **67**, 400–428.
Naglik, J. R., Fidel, P. L. Jr, and Odds, F. C. (2008). Animal models of mucosal Candida infection. *FEMS Microbiol Lett*. **283**(2), 129–139. Review.
Normanbhoy, F., Steele, C., Yano, J. and Fidel, P. L., Jr. (2002). Vaginal and oral epithelial cell anti-candida activity. *Infect. Immun.* **70**, 7081–7088.
Nucci, M. and Marr, K. A. (2005). Emerging Fungal Diseases. *Clin. Infect. Dis.* **41**, 521–526.

Odds, F. C. (1988). Chronic mucocutaneous candidosis. *Candida and Candidosis*, pp. 104–110. University Park Press, Baltimore, MD.
Odds, F. C. (1998). Should resistance to azole antifungals *in vitro* be interpreted as predicting clinical non-response? *Drug Resist. Updat.* **1**(1), 11–15.
O'Garra, A. (1998). Cytokines induce the development of functionally heterogenous T helper cell subsets. *Immunology* **8**, 275–283.
Pfaller, M. A. and Diekema, D. J. (2007). Epidemiology of invasive candidiasis: a persistent public health problem. *Clin. Microbiol. Rev.* **20**(1), 133–163.
Pope, L. M., Cole, G. T., Guentzel, M. N. and Berry, L. J. (1979). Systemic and gastrointestinal candidiasis of infant mice after intragastric challenge. *Infect. Immun.* **25**, 702–701.
Rahman, D. and Challacombe, S. J. (1995). Oral immunization against mucosal candidiasis in a mouse model. *Advances in Mucosal Immunity.* Plenum Press, New York.
Rahman, D., Mistry, M., Thavaraj, S., Challacombe, S. J. and Naglik, J. R. (2007). Murine model of concurrent oral and vaginal *Candida albicans* colonization to study epithelial host–pathogen interactions. *Microbes Infect.* **9**, 615–622.
Richter, S. S., Galask, R. P., Messer, S. A., Hollis, R. J., Diekema, D. J. and Pfaller, M. A. (2005). Antifungal susceptibilities of *Candida* species causing vulvovaginitis and epidemiology of recurrent cases. *J. Clin. Microbiol.* **43**, 2155–2162.
Ringdahl, E. N. (2006). Recurrent vulvovaginal candidiasis. *Mol. Med.* **103**, 165–168.
Romani, L. (1997). The T cell response to fungi. *Curr. Opin. Immunol.* **9**, 484–490.
Romani, L. (2004). Immunity to fungal infections. *Nat. Rev. Immunol.* **4**(1), 1–23.
Romani, L., Bistoni, F., Mencacci, A., Cenci, E., Spaccapelo, R. and Puccetti, P. (1996). IL 12 in *Candida albicans*. infections. *Res. Immunol.* **146**, 532–538.
Romani, L. and Puccetti, P. (2006). Protective tolerance to fungi: the role of IL-10 and tryptophan catabolism. *Trends Microbiol.* **14**(4), 183–189.
Ryley, J. F. and Mc Gregor, S. (1986). Quantification of vaginal *Candida albicans* infections in rodents. *J. Med.Vet. Mycol.* **24**, 455–460.
Ryley, J. F., Wilson, R. G., Gravestock, M. B. and Poyser, J. P. (1981). Experimental approaches to antifungal chemotherapy. *Adv. Pharmcol. Chemother.* **18**, 49–176.
Saavedra, M., Taylor, B., Lukacs, N. and Fidel, P. L., Jr. (1999). Local production of chemokines during experimental vaginal candidiasis. *Infect. Immun.* **67**, 5820–5826.
Samaranayake, L. P. (1992). Oral mycoses in HIV infection. *Oral Surg. Oral Med. Oral Pathol.* **73**(2), 171–180. Review.
Samaranayake, Y. H. and Samaranayake, L. P. (2001). Experimental oral candidiasis in animal models. *Clin. Microbiol. Rev.* **14**(2), 398–429.
Sandini, S., La Valle, R., De Bernardis, F., Macrı', C. and Cassone, A. (2007). The 65-kilodalton mannoprotein gene of *Candida albicans* encodes a putative glucanase adhesin required for hyphal morphogenesis and experimental pathogenicity. *Cell. Microbiol.* **9**, 1223–1238.
Santoni, G., Boccanera, M., Adriani, D., Lucciarini, R., Amantini, C., Morrone, S., Cassone, A. and De Bernardis, F. (2002). Immune cell-mediated protection against vaginal candidiasis: evidence for a mayor role of vaginal $CD4^+$ T cells and possible participation of other local lymphocyte effectors. *Infect. Immun.* **70**, 4791–4797.
Satake, Y., Akiba, H., Takeda, K., Atsuta, M., Yagita, H. and Okumura, K. (2000). Characterization of rata OX40 Ligand by monoclonal antibody. *Biochem. Biophys. Res. Comm.* **270**, 1041–1048.
Saville, S. P., Lazell, A. L., Monteagudo, C. and Lopez-Ribot, J. L. (2003). Engineered control of cell morphology *in vivo* reveals distinct roles for yeast and filamentous forms of *Candida albicans* during infection. *Eukaryotic Cell* **2**, 1053–1060.
Schaller, M., Bein, M., Korting, H. C., Baur, S., Hamm, G., Monod, ,M., Beinhauer, S. and Hube, B. (2003). The secreted aspartyl proteinases Sap1 and Sap2 cause tissue damage in

an *in vitro* model of vaginal candidiasis based on reconstituted human vaginal epithelium. *Infect. Immun.* **71**, 3227–3234.
Scholer, H. J. (1960). Experimentalle vaginal candidiasis der ratte. *Pathol. Microbiol.* **23**, 62–68.
Sobel, J. D. and Muller, G. (1983). Comparison of ketoconazole, BAY N7133 and BAY L9139 in the treatment of experimental vaginal candidiasis. *Antimicrob. Agents Chemother.* **24**, 434–436.
Sobel, J. D. and Muller, G. (1984). Comparison of itraconazole and ketoconazole in the treatment of experimental candidal vaginitis. *Antimicrob. Agents Chemother.* **26**, 266–267.
Sobel, J. D., Wiesenfield, H. C., Martens, M., Danna, P., Hooton, T. M., Rompalo, A., Sperling, M., Livengood, C., Horwitz, B., Von Thron, J. *et al.* (2004). Maintenance therapy for recurrent vulvovaginal candidiasis. *N. Engl. J. Med.* **351**, 876–883.
Spellberg, B. J., Ibrahim, A. S., Avanesian, V., Fu, Y., Myers, C., Phan, Q. T., Filler, S. G., Yeaman, M. R. and Edwards, J. E. (2006). Efficacy of the anti-*Candida* rAls3p-N or Als1p-N vaccines against disseminated and mucosal candidiasis. *J. Infect. Dis.* **194**, 256–260.
Steele, C. and Fidel, P. L., Jr. (2002). Chemokine production by human oral and vaginal epithelial cells in response to *Candida albicans*. *Infect. Immun.* **70**, 577–583.
Steele, C., Ozenci, H., Luo, W., Scott, M. and Fidel, P. L. (1999). Growth inhibition of *Candida albicans* by vaginal cells from naive mice. *Med. Mycol.* **37**, 251–259.
Sundstrom, P. (2002). Adhesion in *Candida* spp. *Cell. Microbiol.* **4**, 461–469.
Taschdjian, C. L., Reiss, F. and Kozinn, P. J. (1960). Experimental vaginal candidiasis in mice; its implications for superficial candidiasis in humans. *J. Invest. Dermatol.* **34**, 89–94.
Taylor, B. N., Saavedra, M. and Fidel, P. L., Jr. (2002). Local Th1/Th2 cytokine production during experimental vaginal candidiasis. *Med. Mycol.* **38**, 419–431.
Thienpont, D., Van Cutsen, J. and Borger, S. M. (1980). Ketoconazole in experimental candidosis. *Rev. Infect. Dis.* **2**, 570–577.
Torosantucci, A., Romagnoli, G., Chiani, P., Stringaro, A., Crateri, P., Mariotti, S., Teloni, R., Arancia, G., Cassone, A. and Nisini, R. (2004). *Candida albicans* yeast and germ tube forms interfere differently with human monocyte differentiation into dendritic cells: a novel dimorphism-dependent mechanism to escape the host's immune response. *Infect. Immun.* **72**(2), 833–843.
Trinité, B., Voisine, C., Yagita, H. and Josien, R. (2000). A subset of cytolytic dendritic cells in rat. *J. Immunol.* **165**(8), 4202–4208.
Valentin, A., Bernard, C., Mallie, M., Huerre, M. and Bastide, J. M. (1993). Control of *Candida albicans* vaginitis in mice by short-duration butoconazole treatment in situ. *Mycoses* **36**, 379–384.
Van Cutsen, J., Van Gerven, F. and Janssen, A. J. (1987). Activity of orally, topycally and parenterally administered itraconazole in the treatment of superficial and deep mycoses animal models. *Rev. Infect. Dis.* **9**(Suppl. 1), S 15-S 32.
Ventolini, G., Baggish, M. S. and Walsh, P. M. (2006). Vulvovaginal candidiasis from non-albicans species: retrospective study of recurrence rate after fluconazole therapy. *J. Reprod. Med.* **51**, 475–478.
Weiner, H. L. (1997). Oral tolerance for the treatment of autoimmune diseases. *Annu. Rev. Med.* **8**, 341–351.
Wheeler, R. T. and Fink, G. R. (2006). A drug-sensitive genetic network masks fungi from the immune system. *PloS Pathog.* **2**, e35.
Wisplinghoff, H., Bischoff, T., Tallent, S. M., Seifert, H., Wenzel, R. P. and Edmond, M. B. (2004). Nosocomial bloodstream infections in US hospitals: analysis of 24,179 cases from a prospective nationwide surveillance study. *Clin. Infect. Dis.* **39**(3), 309–317.

Wormley, F. L., Steele, C., Wozniak, K., Fujihashi, K., McGhee, J. R. and Fidel, P. L., Jr. (2001). Resistance of TCR δ chain deficient mice to experimental *Candida* vaginitis. *Infect. Immun.* **69**, 7162–7164.

Zelante, T., De Luca, A., Bonifazi, P., Montagnoli, C., Bozza, S., Moretti, S., Belladonna, M. L., Vacca, C., Conte, C. and Mosci, P. (2007). IL-23 and the Th17 pathway promote inflammation and impair antifungal immune resistance. *Eur. J. Immunol.* **37**, 2695–2706.

15 Mucosal Immunity and Inflammation

Ulrich Steinhoff[1] and Alexander Visekruna[2]
[1] *Max-Planck Institut für Infektionsbiologie, Berlin, Germany;* [2] *Institut für Medizinische Mikrobiologie und Krankenhaushygiene, Philipps-Universität Marburg, Germany*

♦♦

CONTENTS

♦♦♦♦♦♦ I. INTRODUCTION

The intestinal mucosa is the largest lymphoid organ of the whole body. This is easily understood if one considers that at this site continuous antigenic challenge in form of food antigens, antigens of the normal bacterial flora and pathogens occurs (Dahan *et al.*, 2007). The intestinal immune system is therefore confronted with the difficult task to respond to pathogens while remaining relatively unresponsiveness to the commensal microflora and to food antigens. The current view is that despite constant antigenic stimulation, inflammatory processes are controlled in the intestine in order to keep the mucosal barrier intact and to safeguard the complex homeostasis of this organ (Sherman and Kalman, 2004). This complexity became evident by the fact that mutations in genes that affect the innate immune recognition, the adaptive immune system as well as epithelial cell physiology are all associated with gut inflammation (Macdonald and Monteleone, 2005).

The capability of the intestinal immune system to differentiate between dangerous and non-dangerous signals is still not fully understood but seems to rely on multiple non-immune and immune factors (Mowat, 2003). Non-immune factors are related to the luminal epithelium which is the major cell type that produces multiple factors, including mucus, brush border enzymes and antimicrobial

METHODS IN MICROBIOLOGY, VOLUME 37
0580-9517 DOI 10.1016/S0580-9517(10)37015-2

peptides. Immune mechanisms involve both, innate responses mediated by pattern recognition receptors (PRRs), NK cells, macrophages and polymorphonuclear cells (Campbell *et al.*, 1999). Adaptive immunity is mediated by B- and T-lymphocytes which partially exhibit a special and characteristic phenotype in the mucosa (Lambolez et al., 2007). The mucosal immune system is composed of three lymphoid areas: (a) The lamina propria (LP) which lies underneath the basement membrane in the intestinal villi, (b) the intraepithelial compartment above the basement membrane contains the intraepithelial lymphocytes (IELs) and (c) lymphoid follicles which are embedded in the gut wall or organized as Peyer's patches (PPs) (Weigmann *et al.*, 2007). Lymphocytes of the LP, PP and IEL form a complex network that is involved in the maintenance of the intestinal homeostasis, responds to infections and ignores the endogenous flora. Induction of immune responses occurs usually at the inductive sites where antigen is sampled from mucosal surfaces and stimulates cognate naïve B and T cells. These inductive sites for mucosal immunity are constituted by organized mucosa-associated tissue (MALT) and local mucosa-draining lymph nodes (LNs). MALT structures resemble LNs, with variable T-cell zones that intervene between the B cell follicles and contain a variety of antigen presenting cells, including dendritic cells and macrophages (Brandtzaeg et al., 2008). PPs in the small intestine are typical MALT structures that are involved in the induction of antigen (AG)-specific IgA antibody responses as well as cellular immune responses including the development of inflammation (Craig and Cebra, 1971; Kiriya et al., 2007). Interestingly, the MALT lacks afferent lymphatic vessels since sampling of endogenous antigen occurs directly from the mucosal surfaces through a specialized follicle-associated epithelium that contains microfold (M) cells or through direct contact with dendritic cells that open the tight junctions between epithelial cells, send dendrites outside of the epithelium and sample bacteria (Rescigno *et al.*, 2001). There exists an extensive crosstalk both between and within immune cells of the IEL and LPL compartment resulting in the activation or silencing as well as expansion of effector and memory lymphocytes. The composition and function of immune cells within the intestine dramatically influences immunity in an environment that is constantly exposed to a tremendous antigenic burden. Many questions remain till today unsolved, i.e. how intestinal immune responses are regulated by antigens derived from the food, which influence have the complex interactions of the microbiota with the host on the development and function of mucosal as well as systemic immune responses and by which means discriminates the mucosal immune system between commensals and pathogens and how are they eliminated. Approaching many of these questions requires the use of defined experimental systems and a careful analysis of the various immune cells/compartments in the mucosa.

♦♦♦♦♦♦ II. INTRAGASTRIC/ORAL INFECTION WITH BACTERIA

Infection via the oral route is a normal portal of entry for many bacteria, viruses and parasites. Experimental infection via the oral/intragastric route allows the analysis of innate and adaptive immune responses of the mucosal immune system.

Exemplary, we here present the murine infection model of *Listeria monocytogenes* which is a foodborne pathogen that causes listeriosis in humans (Schlech et al., 1983). Mice and guinea pigs can be infected intragastrically or intravenously and virulence is evaluated either by counting the bacterial load in infected tissues or by determining the 50% lethal dose (LD 50) of animals. Since strains of *L. monocytogenes* differ quite substantially in virulence, the EGD strain has been most widely used as reference strain because its genome has been sequenced. Recombinant Listeria expressing ovalbumin or other model antigens allow to monitor elegantly antigen-specific immune responses. The genetic background of the animals is critical for the outcome of the infection (Schlech *et al.*, 1983; Lecuit et al., 2001). *L. monocytogenes* is an organism which requires L-2 biosafety levels and thus guidelines and regulations for the use and handling of pathogenic microorganisms have to be followed. After intragastric inoculation, *L. monocytogenes* crosses the intestinal barrier, replicates in the LP of the small intestine before dissemination to mesenteric lymph nodes and liver. Procedures presented here refer to infection with *L. monocytogenes* strain EGD and recombinant *L. monocytogenes* expressing, e.g., a secreted form of ovalbumin (rLM-ova) in C57BL/6J mice. Since natural Listeria-derived epitopes have not been identified in H-2^b mice, rLM-ova allows visualization of systemic and mucosal $CD8^+$ T-cell responses.

Similarly, oral infections can be performed, e.g., with *Citrobacter rodentium* or *Salmonella typhimurium*, which is one of the few facultative intracellular bacteria that stimulate not only a potent T-cell but also B-cell responses.

A. Intragastric Infection with *L. monocytogenes*

1. Starve animals (giving only water) for approx. 12 h before infection.
   Non-starvation of animals may lead to aspiration of the inoculum in the lung and to a higher variability of the infectivity between animals.
2. Before inoculation, thaw an aliquot of bacteria and keep it on ice. Dilute bacteria appropriately in sterile phosphate-buffered saline (PBS) to achieve 0.2–0.4 ml per mouse.
   The standard dose recommended for *L. monocytogenes* EGD via the intragastric route is 5×10^9 cfu per mouse in a volume of 0.2–0.4 ml.
3. Hold the mouse with the thumb and digit on either side of the base of the neck and fix the tail with the little finger. Try to tilt the head up slightly, thus aligning the oral cavity and pharynx with the oesophagus (Figure 2).
4. Insert the bulbous-ended needle over the tongue into the oesophagus and stomach (Figure 1 and 3).
5. Slowly inject the inoculum.
6. After completing the injections, carefully withdraw the needle and check animals for normal behaviour.
7. Discard the needle and the syringe and disinfect instruments and working area.

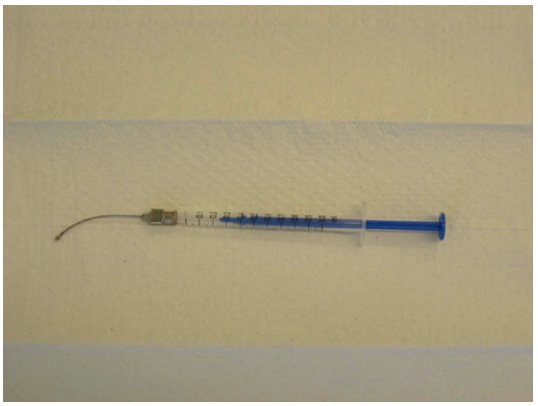

Figure 1. Needle for oral gavage.

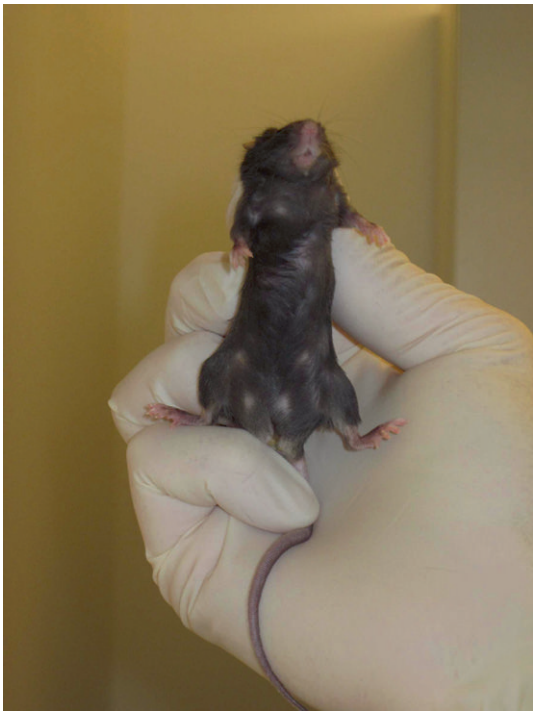

Figure 2. Restraining of mice.

♦♦♦♦♦♦ III. ANIMAL MODELS OF INTESTINAL INFLAMMATION

Animal models of intestinal inflammation have essentially contributed to the current understanding of the pathogenesis of Crohn's disease and ulcerative colitis, the two major forms of inflammatory bowel disease (IBD). Both forms are chronic inflammatory and frequently relapsing disorders of gastrointestinal tract. Recent

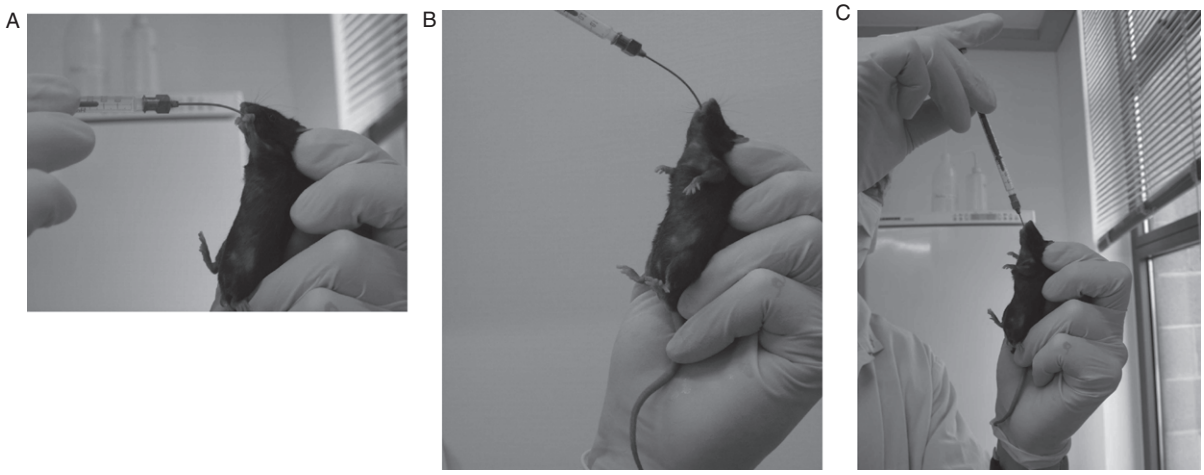

Figure 3. Sequential steps of inserting the gavage needle.

data suggest that the dynamic balance between the composition of commensal gut flora and mucosal immune response has a pivotal role in the initiation and immunopathogenesis of IBD. The complexity of the interactions between commensal bacteria (or their products) and the components of the mucosal immune system is reflected in the heterogeneous characteristics of human IBD. The established murine models of colitis, which seem to be bacteria-driven, share many of the features of human IBD. Notably, animals kept under germ-free conditions do not develop colitis. Thus, the intestinal bacterial flora appears to play a crucial role for understanding the pathogenesis of IBD. A wide variety of mouse models that in some respects resemble mucosal inflammation of the human intestine can be divided into five groups: Chemically induced models [dextran sodium sulphate (DSS) colitis and hapten-based models], immunologically mediated models, infection-induced models, gene-targeted models and spontaneous models. Below is a list of the most commonly applied models of experimental colitis (Table 1).

♦♦♦♦♦♦ IV. CHEMICALLY INDUCED MODELS OF MUCOSAL INFLAMMATION

A. DSS Colitis

Oral administration of DSS induces colitis in mice characterized by ulcerations, infiltration of granulocytes and bloody diarrhoea. DSS is believed to be directly toxic to the epithelial cells of the basal crypts, causing a complete crypt drop-out and disruption of the integrity of the gut epithelial barrier. It has been reported that the adaptive immune system is not required for the induction of acute DSS colitis, as T- and B-cell deficient mice develop severe intestinal inflammation. Thus, the DSS colitis model is particular useful to study the impact of the innate immune system in colitis development. Oral administration of DSS by multiple cycles is able

Table 1. List of murine colitis models

Mouse model	Pathology
Chemically induced	
DSS	Superficial colon, Th1/Th17 (acute),Th1/Th17/Th2 (chronic)
TNBS/DNBS (*hapten-based*)	Transmural, colon, Th1/Th17 (acute, chronic)
Oxazolone	Superficial, colon, Th2 (acute)
Immunologically mediated	
$CD4^{+}CD45RB^{high} \rightarrow RAG^{-/-}$ mice	Transmural, colon/duodenum, Th1/Th17 (acute, chronic) Superficial, colon, Th1/Th17/Th2 (chronic)
Bone marrow → Tgε26 mice	Transmural, small intestine, Th1 (chronic)
Infection induced	
r-Salmonella	Mucosal ulcerations, severe transmural inflammation
Citrobacter rodentium infection	Epithelial hyperplasia, diarrhoea
Gene -targeted	
IL-2 knockout mice	Superficial, colon, Th1/Th17 (acute, chronic)
IL-10 knockout mice	Transmural, colon/small intestine, Th1/Th17 (acute, chronic)
STAT-4 transgenic mice	Transmural, colon/ileum, Th1 (acute, chronic)
Spontaneous	
C3H/HeJ/Bir mice	Superficial/transmural, colon, Th1 (acute, chronic)
SAMP1/Yit mice	Transmural, ileum, Th1 (chronic)

to induce a chronic colitis in several mice strains. Acute phase of DSS colitis is mediated by neutrophils and macrophages, whereas T cells could play an important role during the chronic, regenerative phase of DSS colitis. The following protocols give reproducible results and can be used to induce both acute and chronic DSS colitis in C57BL/6 mice, which show intermediate to high susceptibility to acute DSS colitis.

B. Acute DSS-Induced Colitis

1. Prepare a 2% (w/v) DSS solution for the drinking water. Dissolve 10 g DSS (mol. wt 40 kD) in 500 ml autoclaved drinking water to obtain a 2% solution. Store until use at 4°C.
2. Weigh and mark the mice.
3. Give the DSS receiving mice the DSS solution and control mice the same drinking water without DSS for 7 days. The oral administration of 2% DSS for 7 days induces strong colitis without high mortality rates.
4. Weigh mice daily to monitor inflammation-induced weight loss.
5. Refill the remaining DSS solution at day 3 and 5, respectively, with 2% DSS solution in fresh drinking water.
6. Replace the remaining DSS solution with autoclaved drinking water without DSS on day 7.

C. Chronic DSS-Induced Colitis

1. Requires three cycles of feeding mice with 2% DSS in the drinking water for 7 days.
2. After feeding mice for 7 days with 2% DSS solution, replace the remaining DSS solution on day 8 by autoclaved drinking water without DSS for 2 weeks.
3. Proceed until last step of the acute DSS colitis as described in part 1.
4. From day 22 till day 28, replace normal drinking water with 2% DSS solution.
5. Replace the 2% DSS solution with autoclaved drinking water for next 14 days.
6. Repeat the oral administration of 2% DSS in drinking water from day 43 till day 49.
7. Replace the 2 % DSS solution with autoclaved water on day 50.

♦♦♦♦♦♦ V. HAPTEN-BASED COLITIS (TNBS- AND OXAZOLONE-INDUCED COLITIS)

Trinitrobenzene sulphonic acid (TNBS) and oxazalone are both classic skin – sensitizing agents, able to induce distinct forms of colitis when administered intra-rectally together with ethanol. Ethanol is required to break the function of the epithelial barrier, whereas TNBS and oxazalone have been described to haptenize autologous colonic or microbial proteins, thus rendering them immunogenic to the host immune system. These colitis models are highly strain specific in mice and are frequently used to investigate $CD4^+$ T cell-dependent immune responses. TNBS colitis induces Th1/Th17 cell responses with a transmural inflammation resembling human Crohn's disease, whereas, in contrast, oxazalone elicits a Th2 response mediated by IL-13, resulting in a superficial inflammation that resembles ulcerative colitis. The following procedures can be used to induce TNBS and oxazalone colitis in C57BL/6 mice.

A. TNBS-Induced Colitis

1. Presensitization step is required in order to induce TNBS colitis in C57BL/6 mice: prepare a 1% (w/v) TNBS solution by mixing 4 volume of acetone/olive oil mixture (previously prepared by mixing acetone and olive oil in a 4:1 ratio) with 1 volume of 5% TNBS solution.
2. Select and carefully shave a 2×2 cm area of the skin of the mice. Apply 150 μl of 1% TNBS presensitization solution to the shaved skin. Control mice receive the same solution without TNBS.

3. On day 7 after treating mice with presensitization solution containing TNBS, the mice are anaesthetized by i.p. injection of ketamine/xylazine (80 µl solution per 10 g mouse body weight).
4. Prepare 2.5% TNBS solution by mixing 1 volume of 5% TNBS solution in distilled water with 1 volume of absolute ethanol.
5. Insert the catheter into the colon and slowly administer 150 µl of 2.5% TNBS solution in ethanol into the colon lumen.
6. Remove the catheter slowly from the anus in order to avoid damage of colon wall.
7. Keep the mouse with the head down for 1 min to avoid egressing of TNBS solution from colon.
8. Return the animal to the cage.

B. Oxazolone-Induced Colitis

1. Presensitization step for induction of oxazolone colitis in C57BL/6 mice: to make up a 3% (w/v) oxazolone solution, dissolve 60 mg of oxazolone salt in 2 ml of acetone/olive oil mixture (previously prepared by mixing acetone and olive oil in a 4:1 ratio).
2. Carefully shave a 2×2 cm area of the skin of the mice by using a razor. Apply 150 µl of 3% oxazolone presensitization solution to the shaved skin. Control mice receive the same solution without oxazolone.
3. On day 8 after presensitization, mice are anaesthetized by i.p. injection of ketamine/xylazine (80 µl solution per 10 g mouse body weight).
4. Prepare 1% (w/v) oxazolone by dissolving 20 mg oxazolone salt in 2 ml 50% ethanol
5. Insert the catheter into the colon and slowly administer 150 µl of 1% oxazolone solution into the colon lumen.
6. Remove the catheter carefully from the colon in order to avoid damage of colon wall.
7. Keep the mouse with the head down for 1 min. to avoid oxazolone solution exiting colon.
8. Return the animals to the cage.

♦♦♦♦♦♦ VI. INFECTION-INDUCED MODELS OF MUCOSAL INFLAMMATION

S. typhimurium infection in genetically susceptible mouse strains leads to the spread of bacteria via the gut-associated lymphoid tissue to systemic sites. Lesions and bacteremia in systemic organs resembles typhoidal salmonellosis in

humans. Therefore, the mouse model which relies on a surrogate pathogen as well as host is known as mouse typhoid (Carter and Collins, 1974). Despite this, the murine typhoid model has been extensively used to study immune responses to *S. typhimurium* and bacterial virulence factors which are required for systemic infection.

In genetically resistant, Nramp1$^{+/+}$ mouse strains (e.g. 129SvEv) *S. typhimurium* causes chronic infection of systemic organs, thus providing a good model for persistent systemic infection (Monack et al., 2004). However, in all typhoid mouse models, *S. typhimurium* neither efficiently colonizes the intestine nor causes acute intestinal inflammation. The poor intestinal colonization of the murine intestine has been known for a long time and referred as colonization resistance (Bohnhoff and Miller, 1962). Intestinal colonization with *S. typhimurium*, however, can be achieved by treatment of mice with antibiotics. Therefore we will focus in this chapter on *S. typhimurium*-induced enterocolitis model.

Colonization resistance results from a complex interplay between *S. typhimurium*, the resident microflora, the intestinal mucosa and its associated immune system. Reduction of commensals by antibiotics shifts the balance for the benefit of the incoming pathogen. Streptomycin pre-treated mice provide a mouse model for acute intestinal inflammation in response to oral *S. typhimurium* infection. Oral administration of mice with a single dose of streptomycin (20 mg) results in efficient colonization of *S. typhimurium* in the colon which triggers severe acute inflammation of the colon (colitis) and cecum as early as 8 h post-infection (Barthel et al., 2003; Coburn *et al.*, 2005). Characteristic for the acute inflammation is the massive infiltrations of polymorphonuclear granulocytes in the LP, in the submucosa and in the intestinal lumen. Systemic infection develops slowly with approx. 10^3 cfu in liver and spleen at day 2 after infection. The bacterial load is daily rising by 1.5 logs and terminal systemic disease develops at day 5–6 p.i. (Santos et al., 2001). In this model, it is assumed that the systemic spread of *S. typhimurium* does not influence the acute colitis.

This model thus allows to study the host response and the virulence factors of the pathogen needed for induction of enteric salmonellosis. The infection is performed as follows:

A. Salmonella-Induced Streptomycin Colitis

This model requires specific-pathogen-free (SPF) and genetically susceptible (Nramp1$^{-/-}$) mice (C57Bl/6, Balb/c) which are housed under standard barrier conditions in cages equipped with steel grid floors.

1. Withdraw food and water 4 h before start of treatment.
2. Oral application of streptomycin (20 mg) in sterile water (gavage).
3. Supply animals with water and food *ad libitum*.

4. 20 h after streptomycin treatment, withdraw water and food again for 4 h and infect mice with 10^8 *S. typhimurium* in 200 µl sterile PBS orally. Oral infection is performed by gavage.
5. Return animals to the cage and supply them with water and food *ad libitum*.
6. At desired time points, mice are sacrificed by cervical dislocation and tissue samples from the intestinal tract, mesenteric lymph nodes, spleens and livers were removed for further analysis.

♦♦♦♦♦♦ VII. IMMUNOLOGICALLY MEDIATED MODELS OF INTESTINAL INFLAMMATION

T-cell transfer models are best-characterized models of chronic colitis mediated by disruption of T-cell homeostasis. The most widely used model of T-cell transfer is an adoptive transfer of $CD4^+CD45RB^{high}$ (naïve T cells) into syngeneic recipient mice lacking T and B cells (SCID or $RAG^{-/-}$ mice) (Morrissey *et al*., 1993). The SCID model is highly reproducible and easily manipulated and thus provides a very useful tool for studying mucosal immune regulation. Depending on the strain of the donor and recipient mice, reconstituted animals exhibit varying degrees of transmural inflammation, diarrhoea and weight loss. A protocol for $CD4^+CD45RB^{high}$ transfer colitis is given below.

A. Transfer Colitis

1. C57BL/6 WT mice are used as donor animals, whereas immunodeficient $RAG^{-/-}$ or SCID mice on C57BL/6 background are used as recipient mice.
2. Prepare a single-cell suspension from spleens. The numbers of spleens used depend on the required numbers of purified $CD4^+$ $CD45RB^{high}$ cells. Ten spleens will yield approx. 1×10^7 $CD45RB^{high}$ $CD4^+$ cells.
3. Lyse erythrocytes (distilled water or ammonium chloride buffer).
4. Enrich for $CD4^+$ T cells using magnetic beads. (CD4+ cells are enriched by depleting B cells (anti-B220), $CD8^+$ T cells (anti-CD8) and macrophages (anti-Mac-1). There are several $CD4^+$ T-cell enrichment kits commercially available (e.g. Dynal beads).
5. Stain enriched $CD4^+$ T cells with the antibodies CD4-PE (2 µg/ml) and CD45 RB-FITC (15 µg/ml). Analyze labelled cells on the cell sorter and set appropriate gates using isotype control antibodies. Sort the cell suspension into $CD4^+$ $CD45RB^{high}$ and $CD4^+$ $CD45RB^{low}$ fractions.
6. Check purity of sorted cell populations.
7. Resuspend the cells in 2×10^6/ml in PBS and inject 200 µl (equivalent 4×10^5 cells) intraperitoneally into SCID or RAG mice.
8. When performing transfer of $CD4^+CD45RB^{high}$ cells, ensure that the needle is inserted into the peritoneal cavity. Subcutaneous injection of cells will not result in the induction of colitis.

9. Monitor colitis progression by weighing mice. Recipient mice will start developing disease at 4–5 weeks following T-cell transfer.

♦♦♦♦♦♦ VIII. SAMPLING OF INTESTINAL TISSUES FOR EVALUATION OF THE INFLAMMATION

Development of IBD is characterized by progressive weight loss and loose stools with a high portion of mucus. Diagnosis is based on a histological analysis of the colon. Characteristic for intestinal lesions are infiltrates with mononuclear cells into the mucosa and submucosa, hyperplasia of epithelial cells, development of ulcers and loss of mucin-producing goblet cells.

1. Kill the mouse by cervical dislocation and place the animal with the back on a pad.
2. Open the abdomen by a ventral midline incision and cut the colon below the cecum and above the anus. Transfer the colon into cold PBS and use a blunt-ended needle (gavage needles can also be taken) and wash out the luminal content.
3. Cut a small portion of the ascending, transverse and descending colon and put into a histology cassette. Label each sample and fix the tissue in 4% paraformaldehyde solution for 24 h. Alternatively, tissue samples in PBS can also be shock frozen in liquid nitrogen and stored at –80°C.
4. Paraffin embedded samples or frozen tissues are cut into 5 µm transverse sections, mounted on microscope slides. Immunohistological or HE stainings can be performed in order to evaluate or score the histopathology.

♦♦♦♦♦♦ IX. ISOLATION OF INTESTINAL IMMUNE CELLS

The intestinal mucosal immune system is regionally specialized and is composed of three important lymphoid areas: the LP lying directly underneath the basement membrane and containing LP mononuclear cells (LPMC), IEL which are found within the epithelium in both the small and the large intestine and finally the lymphoid aggregates of the colon and PPs of the small intestine embedded in the gut wall.

This protocol describes a method for isolation of murine colonic LPMC and IEL with high yield, viability and purity. The isolated cells can be subsequently used for further studies such as cell-proliferation assay, analysis of protein and mRNA expression and flow cytometric analysis (Weigmann et al., 2007).

A. Isolation of Mononuclear Cells from the LP

1. Collect the entire colon of mice, cut into 5 cm pieces and wash in ice-cold PBS by flushing intestine with a syringe to remove faecal contents.
2. Remove residual mesenteric fat tissues and lymphoid aggregates.
3. Open colon pieces longitudinally, cut into small pieces and wash in ice-cold PBS.
4. Put pieces of tissues into screw cup tube containing 5 ml HBSS with 5 mM EDTA and 1 mM DTT (prepare the fresh HBSS solution just before use) and incubate colon pieces for 15 min at 37°C in HBSS shaken under slow rotation.
5. Shake tubes vigorously by hand for 20 s to remove epithelial cells and IEL. Pass the content through a 100 μm nylon mesh and transfer the tissue pieces into a new tube.
6. Add 10–20 ml of RPMI 1640 medium supplemented with collagenase D and collagenase VIII (0.4 mg/ml each) under constant stirring at 120 rpm for 1 h at 37°C.
7. Filter the cell suspension through a 120 μm mesh and wash twice with PBS.
8. After centrifugation ($500 \times g$ at 20°C), discard the supernatant and resuspend the pellet in 10 ml of 40% Percoll solution which is diluted in RPMI 1640.
9. Carefully overlay the collected cell suspension on the top of a 5 ml 70% Percoll solution.
10. Centrifuge the 40/70 Percoll gradient cells at $800 \times g$ for 25 min at 20°C without brake.
11. Collect the LPMCs from the interphase between 40 and 70% Percoll solution.
12. Wash the cells with PBS and centrifuge the cell suspension at $500 \times g$ for 10 min.
13. Resuspend the cell pellets in PBS and test the viability and the number of purified cells by trypan blue exclusion.
14. Viable LPMCs can be used for subsequent phenotypic and functional assays.

B. Isolation of IEL

1. Collect the small intestine or colon of mice, cut into 5 cm pieces and wash in ice-cold PBS by flushing intestine with a syringe to remove faecal contents.
2. Remove residual mesenteric fat tissues and lymphoid aggregates.
3. Open colon pieces longitudinally, cut into pieces and wash in ice-cold PBS.
4. Put pieces of tissues into screw cup tube containing 5 ml HBSS with 5 mM EDTA and 1 mM DTT (prepare the fresh HBSS solution just before use)

and incubate intestinal pieces for 15 min at 37°C in HBSS shaken under slow rotation.
5. Shake tubes vigorously by hand for 15 s to remove epithelial cells and IEL. Pass the content through a 100 μm nylon mesh and collect the flow-through.
6. Centrifuge the flow-through (500 × *g* at 20°C), wash the pellet with PBS and resuspend cells in 10 ml of 40% Percoll solution, diluted in RPMI 1640.
7. Carefully overlay cells in the 40% Percoll fraction on the top of a 5 ml of 70 Percoll solution.
8. Centrifuge the 40/70 Percoll gradient at 800 × *g* for 25 min without brake.
9. Following centrifugation, collect the IELs from 40/70 interphase.
10. Wash the cells with PBS and centrifuge the cell suspension at 500 × *g* for 10 min.
11. Resuspend the cell pellets in PBS and test the viability and the number of purified cells by trypan blue exclusion.
12. Viable IELs can be used for subsequent phenotypic and functional assays.

♦♦♦♦♦♦ X. ISOLATION OF MUCOSAL IgA

IgA antibodies are mainly found on the mucosal surfaces of the nose, lung, digestive tract, ears, eyes and vagina and the daily production of secretory IgA is greater than that of any other immunoglobulin class. IgA is mostly exported across mucous membranes and is also found in saliva, tears and blood. While the systemic humoral immune response is dominated by IgG, mucosal immunity is mainly mediated by IgA. Toxins and pathogenic microbes are neutralized by IgA with high affinity and with low-affinity the commensal microflora to contain the dense microflora within the intestinal lumen (Macpherson *et al.*, 2008). Germ-free animals and neonates that have not yet been colonized by commensal microbes are virtually lacking IgA-secreting cells (Benveniste et al., 1971). IgA secretion can be induced by sensitizing animals with the model antigen cholera toxin. In serum, IgA exists primarily as a monomer while polymeric forms such as dimers, trimers and even tetramers are sometimes seen. IgA of external secretions, called secretory IgA consists of a dimer or tetramer. The plasma cell that secretes IgA home to the subepithelial tissue, where IgA binds to a receptor for polymeric immunoglobulin molecules. This poly-Ig receptor is expressed on the surface of most mucosal epithelia and transports the IgA-receptor complex across the epithelial barrier into the lumen of the mucosal tissue (Kraehenbuhl and Neutra, 1992). The poly-Ig receptor is then cleaved enzymatically from the membrane and becomes the secretory component which is bound to and released together with the polymeric IgA into the mucous secretion. The secretory component masks the sites susceptible to protease cleavage, allowing the polymeric molecule to be more resistant against enzymatic cleavage in the protease-rich environment (Crottet and Corthesy, 1998). Intestinal IgA can be easily measured in faecal samples as described by deVos and Dick (DeVos and Dick, 1991).

A. Detection and Isolation of Intestinal IgA

1. Place mice in cages without wood shavings.
2. Collect faecal pellets and weigh them. If processing does not immediately occur, pellets can also be stored at –70°C.
3. Take faecal samples of 0.1 g, put them in a 1.5 ml eppendorf tube and add 1 ml PBS (10 volumes weight/volumes).
4. Incubate mixture at room temperature for 15 min.
5. Vortex sample and incubate for another 15 min and vortex again till all material is dissolved.
6. Centrifuge at 5000 $\times$ *g* for 10 min and remove supernatant.
7. Determine IgA concentration with ELISA by comparing with a known standard probe.

References

Barthel, M., Hapfelmeier, S., Quintanilla-Martinez, L., Kremer, M., Rohde, M., Hogardt, M., Pfeffer, K., Russmann, H. and Hardt., W. D. (2003). Pretreatment of mice with streptomycin provides a Salmonella enterica serovar Typhimurium colitis model that allows analysis of both pathogen and host. *Infect. Immun.* **71**, 2839–2858.

Benveniste, J., Lespinats, G., Adam, C. and Salomon, J. C. (1971). Immunoglobulins in intact, immunized, and contaminated axenic mice: study of serum IgA. *J. Immunol.* **107**, 1647–1655.

Benveniste, J., Lespinats, G. and Salomon, J. (1971). Serum and secretory IgA in axenic and holoxenic mice. *J. Immunol.* **107**, 1656–1662.

Bohnhoff, M., and Miller, C. P. (1962). Enhanced susceptibility to Salmonella infection in streptomycin-treated mice. *J. Infect. Dis.* **111**, 117–127.

Brandtzaeg, P., Kiyono, H., Pabst, R. and Russell, M. W. (2008). Terminology: nomenclature of mucosa-associated lymphoid tissue. *Mucosal Immunol.* **1**, 31–37.

Campbell, N., Yio, X. Y., So, L. P., Li, Y. and Mayer, L. (1999). The intestinal epithelial cell: processing and presentation of antigen to the mucosal immune system. *Immunol. Rev.* **172**, 315–324.

Carter, P. B. and Collins, F. M. (1974). The route of enteric infection in normal mice. *J. Exp. Med.* **139**, 1189–1203.

Coburn, B., Li, Y., Owen, D., Vallance, B. A. and Finlay, B. B. (2005). Salmonella enterica serovar Typhimurium pathogenicity island 2 is necessary for complete virulence in a mouse model of infectious enterocolitis. *Infect. Immun.* **73**, 3219–3227.

Craig, S. W. and Cebra, J. J. (1971). Peyer's patches: an enriched source of precursors for IgA-producing immunocytes in the rabbit. *J. Exp. Med.* **134**, 188–200.

Crottet, P. and Corthesy, B. (1998). Secretory component delays the conversion of secretory IgA into antigen-binding competent F(ab')2: a possible implication for mucosal defense. *J. Immunol.* **161**, 5445–5453.

Dahan, S., Roth-Walter, F., Arnaboldi, P., Agarwal, S. and Mayer, L. (2007). Epithelia: lymphocyte interactions in the gut. *Immunol. Rev.* **215**, 243–253.
DeVos, T. and Dick, T. A. (1991). A rapid method to determine the isotype and specificity of coproantibodies in mice infected with Trichinella or fed cholera toxin. *J. Immunol. Methods* **141**, 285–288.
Kiriya, K., Watanabe, N., Nishio, A., Okazaki, K., Kido, M., Saga, K., Tanaka, J., Akamatsu, T., Ohashi, S., Asada, M. et al. (2007). Essential role of Peyer's patches in the development of Helicobacter-induced gastritis. *Int. Immunol.* **19**, 435–446.
Kraehenbuhl, J. P. and Neutra, M. R. (1992). Transepithelial transport and mucosal defence II: secretion of IgA. *Trends Cell Biol.* **2**, 170–174.
Lambolez, F., Kronenberg, M. and Cheroutre, H. (2007). Thymic differentiation of TCR alpha beta(+) CD8 alpha alpha(+) IELs. *Immunol. Rev.* **215**, 178–188.
Lecuit, M., Vandormael-Pournin, S., Lefort, J., Huerre, M., Gounon, P., Dupuy, C., Babinet, C. and Cossart, P. (2001). A transgenic model for listeriosis: role of internalin in crossing the intestinal barrier. *Science* **292**, 1722–1725.
Macdonald, T. T. and Monteleone, G. (2005). Immunity, inflammation, and allergy in the gut. *Science* **307**, 1920–1925.
Macpherson, A. J., McCoy, K. D., Johansen, F. E. and Brandtzaeg, P. (2008). The immune geography of IgA induction and function. *Mucosal Immunol.* **1**, 11–22.
Monack, D. M., Bouley, D. M. and Falkow, S. (2004). Salmonella typhimurium persists within macrophages in the mesenteric lymph nodes of chronically infected Nramp1+/+ mice and can be reactivated by IFNgamma neutralization. *J. Exp. Med.* **199**, 231–241.
Morrissey, P. J., Charrier, K., Braddy, S., Liggitt, D. and Watson, J. D. (1993). CD4+ T cells that express high levels of CD45RB induce wasting disease when transferred into congenic severe combined immunodeficient mice. Disease development is prevented by cotransfer of purified CD4+ T cells. *J. Exp. Med.* **178**, 237–244.
Mowat, A. M. (2003). Anatomical basis of tolerance and immunity to intestinal antigens. *Nat. Rev. Immunol.* **3**, 331–341.
Rescigno, M., Rotta, G., Valzasina, B. and Ricciardi-Castagnoli, P. (2001). Dendritic cells shuttle microbes across gut epithelial monolayers. *Immunobiology* **204**, 572–581.
Santos, R. L., Zhang, S., Tsolis, R. M., Kingsley, R. A., Adams, L. G. and Baumler, A. J. (2001). Animal models of Salmonella infections: enteritis versus typhoid fever. *Microbes Infect.* **3**, 1335–1344.
Schlech, W. F.III, Lavigne, P. M., Bortolussi, R. A., Allen, A. C., Haldane, E. V., Wort, A. J., Hightower, A. W., Johnson, S. E., King, S. H., Nicholls, E. S. et al. (1983). Epidemic listeriosis – evidence for transmission by food. *N. Engl. J. Med.* **308**, 203–206.
Sherman, M. A. and Kalman, D. (2004). Initiation and resolution of mucosal inflammation. *Immunol. Res.* **29**, 241–252.
Weigmann, B., Tubbe, I., Seidel, D., Nicolaev, A., Becker, C. and Neurath, M. F. (2007). Isolation and subsequent analysis of murine lamina propria mononuclear cells from colonic tissue. *Nat. Protoc.* **2**, 2307–2311.

16 CD8 T-Cell Immunotherapy of Cytomegalovirus Disease in the Murine Model

Niels A W Lemmermann, Jürgen Podlech, Christof K Seckert, Kai A Kropp, Natascha K A Grzimek, Matthias J Reddehase and Rafaela Holtappels
Institute for Virology, University Medical Center of the Johannes Gutenberg-University, Mainz, Germany

♦♦

CONTENTS

♦♦♦♦♦♦ I. INTRODUCTION

Cytomegaloviruses (CMVs) are conditional pathogens that are strictly species specific and are usually well controlled in their respective mammalian hosts by the effector mechanisms of both innate and adaptive immunity [for reviews, see Jonjic *et al*. (2006) and Reddehase (2002)]. Human CMV (hCMV) is mostly acquired perinatally and in early childhood and is transmitted for instance through breast milk and saliva. Whilst the immune response in an immunocompetent host prevents an overt CMV disease and rapidly terminates the productive acute infection, viral genome is maintained in most tissues for the life span of the infected host in a state known as 'viral latency'.

By definition, latency implies that infectious virions are no longer produced so that the host is no longer infectious. According to current views, latent CMV genomes are maintained as episomes, associated with cellular histones in a closed higher order chromatin-like structure in which viral genes are usually silenced.

METHODS IN MICROBIOLOGY, VOLUME 37
0580-9517 DOI 10.1016/S0580-9517(10)37016-4

Stochastic and cytokine-induced episodes of gene desilencing associated with local opening of the viral chromatin, in particular at the regulatory major immediate-early (MIE) gene locus, reactivate viral gene expression. This leads to the presentation of antigenic peptides by MHC class I molecules and to sensing of the reactivation by cognate effector memory CD8 T cells. Thus, viral latency is not a static state but involves a permanent immune surveillance of reactivated viral gene expression. Complete reactivation to the release of infectious progeny virions, an event known as 'virus recurrence', is thought to require gene desilencing at all essential loci, including genes coding for the viral DNA polymerase and the virion structural proteins, as well as an ablation of immune control [for reviews, see Reddehase *et al*. (2008) and Reeves and Sinclair (2008)].

CMV disease with multiple organ manifestations such as interstitial pneumonia, hepatitis, adrenalitis, gastrointestinal disease and bone marrow failure results from primary or recurrent infection of the immunocompromised or immunologically immature host [for a review, see Ho (2008)]. A significant medical problem is the congenital hCMV infection of the embryo or fetus, in particular after primary infection of mothers when protective antibodies are missing. Birth defects include thrombocytopenic purpura, sensorineural hearing loss, eye defects and mental retardation. Additional risk groups for CMV disease are patients with acquired immunodeficiency syndrome or with different forms of hereditary severe combined immunodeficiency. Reactivation of hCMV infection is a frequent complication in recipients of solid organ allografts and of allogeneic haematopoietic stem cell or bone marrow transplantation (HSCT or BMT) who are iatrogenically immunocompromised for prevention of host-versus-graft (HvG) reaction and graft-versus-host (GvH) disease, respectively.

HSCT/BMT combined with donor lymphocyte infusion (DLI) is a promising therapeutic option against haematologic malignancies but bears a risk of hCMV reactivation and consequent CMV disease, of interstitial CMV pneumonia in particular. Reactivation of latent virus followed by recurrence of productive infection can originate from the transplanted cells of a latently infected donor (D^+) and/or from latently infected recipient's own tissues (R^+). Thus, except for a D^-R^- transplantation constellation, in which the only risk is a primary infection after accidental transmission from secretors among visitors or clinic personnel, a reactivation risk exists of either the donor's virus variant (CMV^D in D^+R^-) or the recipient's virus variant (CMV^R in D^-R^+) or of both (CMV^D and CMV^R in D^+R^+) (Emery, 1998).

As CMVs are host species specific, hCMV cannot be studied in animal models. Rhesus CMV is an emerging non-human primate model (Powers and Früh, 2008), but a wider use has obvious ethical and logistic limitations. The mouse model of infection with murine CMV (mCMV) is well established, as it offers all the advantages of mouse genetic engineering technologies and because mCMV pathogenesis and immune control in the mouse resemble those of hCMV in humans in the fundamental principles, despite the undisputable genetic differences between these two virus species. Specifically, the mouse model has proven its predictive value by demonstrating the protective effect of antiviral CD8 T cells in the first experimental trial of an immunotherapy of CMV disease by adoptive cell transfer [Reddehase *et al*. (1985); reviewed in Holtappels *et al*. (2006b)]. These findings provided the conceptual basis for promising clinical trials (Riddell *et al*., 1992; Walter *et al*., 1996; Einsele and Hamprecht, 2003; Peggs *et al*., 2003; Cobbold *et al*., 2005).

Here we focus on the virological methods used to quantitate virus replication in organs of the immunocompromised murine host for documenting the efficacy of CD8 T cell-based immunotherapy as the 'proof of concept' (Holtappels *et al.*, 2008a).

♦♦♦♦♦♦ II. MURINE CMV

A. General Information

mCMV is a member of the herpesvirus family (*Herpesviridae*), subfamily β-herpesviruses (*β-Herpesvirinae*). All herpesvirus family members posses a linear, double-stranded DNA genome. Infection by β-herpesviruses is strictly host species specific. Accordingly, working with mCMV is not associated with any health risk. The US BioSafety Level is 2. The German BioSafety Level is 1 (GenTSV § 5; BVL 78/2009/4) according to a decision of the ZKBS No. A VI-6782-12-96.

The Smith strain of mCMV (Smith, 1954), here referred to as 'wild-type' virus mCMV-WT.Smith, was originally isolated as *Mouse Salivary Gland Virus* (SGV) from salivary gland tissue of naturally infected mice. The virus was distributed by the American Type Culture Collection (http://www.atcc.org/home.cfm) as ATCC number VR-194 and was later re-accessioned as VR-1399.

Experiments in our laboratory refer to mCMV ATCC VR-194 purchased in 1981 and propagated in murine embryonic fibroblasts (MEFs). The virus stocks were passaged in our lab only four times since then. The VR-194 genome was first cloned as library of *Hin*dIII fragments by Ebeling *et al.* (1983) and sequenced by Rawlinson *et al.* (1996) (Acc. no. NC_004065). Recent analyses (Tang *et al.*, 2006) of the coding capacity of the viral DNA confirmed 172 transcribed open reading frames (ORFs). The cloning of the VR-194 genome into an infectious bacterial artificial chromosome (BAC) by Messerle *et al.* (1997) and its modification by Wagner *et al.* (1999) has made the genome accessible for genetic manipulations (Brune *et al.*, 2006; Ruzsics and Koszinowski, 2008). Some work in the literature refers to mCMV Smith strain variant K181, for which the genome was originally cloned as libraries of *Hin*dIII and *Eco*RI fragments by Mercer *et al.* (1983). BAC cloning and sequencing of K181 was performed only recently (Redwood *et al.*, 2005) (Acc. no. AM886412; mCMV strain K181, complete genome). An interesting genotypic analysis revealing variance between these two laboratory strains and 26 isolates from wild mice has been conducted by Smith and colleagues (2006, 2008). The powerful techniques of prokaryotic mutagenesis resulted already in numerous viral mutants and have greatly promoted our knowledge of viral functions.

B. Commentaries

1. Use of Salivary Gland Virus

Salivary glands are an immunoprivileged mucosal site, where mCMV replication is controlled with delayed kinetics despite a vigorous immune response [for a review, see Campbell *et al.* (2008)]. Clearance of salivary gland infection occurs in CD8 T-cell-depleted but not in CD4 T-cell-depleted mice, suggesting a protective role for

CD4 T cells (Jonjic *et al*., 1989, 1990). In immunocompetent mice, virus replication in salivary gland tissue is restricted to glandular epithelial cells, a polar cell type specialized on secretion of saliva components. In these cells, mCMV monocapsid virions accumulate in large amounts in cytoplasmic vacuoles (Jonjic *et al*., 1989) and use the constitutive cellular secretory pathway for their release into the salivary duct, which is the mode of horizontal transmission of the virus from host to host.

Historically, mCMV was isolated from the salivary glands (Smith, 1954) and was usually passaged *in vivo* in salivary glands. Some investigators still use SGV because of increased virulence compared with cell culture-propagated and purified mCMV. The difference in virulence *in vivo* has been discussed in relation to multi-capsid virion formation in cultured MEFs (Chong and Mims, 1981), but rather appeared to result from protection of SGV virions against neutralizing antibodies by binding of non-neutralizing antibodies 'shielding' the virus (Chong *et al*., 1981). The virulence was found to be highest if SGV was harvested 2–3 weeks after infection when non-neutralizing antibodies were already present and neutralizing antibodies not yet present (Chong *et al*., 1981; Selgrade *et al*., 1981). Regarding mCMV morphogenesis, it should be noted that multi-capsid virion formation, that is secondary envelopment of several capsids by one envelope, is not an *in vitro* phenomenon but regularly occurs in immunocompromised mice also *in vivo* in most cell types with the exception of the glandular epithelial cells of the salivary glands (Reddehase *et al*., 1985; Jonjic *et al*., 1989).

The problem of using SGV is, however, that SGV is a relatively crude preparation consisting of diluted and only partially purified homogenate of salivary gland tissue from infected mice. SGV thus represents an undefined mixture of virus, cytokines, TLR ligands, hormones and cellular components. Therefore, some biological differences between SGV and cell culture-propagated, purified virus may be attributed to unknown components other than virus. This excludes controlled experiments. Although one might argue that virus in saliva is the natural route of transmission, one must keep in mind that saliva represents the sequestered contents of the secretory vacuoles and is not at all identical with a homogenate of the whole tissue. The frequently reported control experiment using salivary gland homogenate from uninfected mice is inappropriate, as cytokines derived from inflammatory infiltrates in infected salivary glands are absent in uninfected salivary glands. In fact, SGV, but not cell culture virus, suppresses haematopoiesis in long-term bone marrow cell cultures even after inactivation of viral infectivity (Busch *et al*., 1991) and it causes rapid liver tissue necrosis after intraperitoneal or intravenous inoculation independent of virus replication in the liver. It should be noted that, in our experience, unpurified supernatant from infected cell cultures also shows immediate liver toxicity after intravenous inoculation. A theoretical alternative could be to use virus from saliva or to purify the virus from pooled salivary gland homogenates, but this would involve an unreasonable consumption of mice. *In vivo* passaging in salivary glands followed by a limited period of *in vitro* propagation is a compromise but is not promising in view of the finding that even a single round of SGV growth in cell culture leads to a loss of virulence (Osborn and Walker, 1971). Furthermore, mCMV mutants that show a growth deficiency phenotype in the salivary glands do not yield SGV. In any case, after a first round of replication *in vivo*, progeny virions are likely to be imprinted by the respective

infected tissue cells. The molecular basis for this might be the known incorporation of cellular proteins into the virus particle (Streblow *et al*., 2006). So, hepatocytes produce hepatocyte-imprinted mCMV and endothelial cells produce endothelial cell-imprinted mCMV. Cell-type-specific recombination of fluorescence-tagged reporter virus in hepatocytes and endothelial cells of Alb-cre and Tie2-cre transgenic mice, respectively, may help address this issue (Sacher *et al*., 2008). Differences imprinted by the producer cell type are so far poorly characterized. The source of the inoculum virus, however, may be important for virus dissemination from the portal of entry to distant target sites of infection, but arbitrary non-viral factors need to be excluded. Therefore, the use of purified virus is highly recommended for reliable experiments.

2. Is mCMV a reliable model for hCMV?

The two viruses are related and share a number of mostly essential genes designated in mCMV by capital letter '*M*' to indicate homology to the respective hCMV gene (Rawlinson *et al*., 1996), for instance mCMV *M122* coding for the essential transactivator protein IE3 of mCMV is the homolog of hCMV *UL122* coding for the essential transactivator protein IE2 of hCMV. However, the two viruses also possess a number of 'private genes', designated by lower case letter '*m*' in mCMV. These genes are mostly not essential for virus replication but reflect adaptation to the specific host. So, genes involved in modulating innate and adaptive immunity are usually not homologous between the two viruses. As a consequence, one might think that mCMV is not a good model for hCMV in all the important questions that are related to virus–host interactions. Nevertheless, there appears to be a significant analogy in the fundamental principles of pathogenesis and immune control, indicating a convergent co-evolution of each of the two viruses with its corresponding host. For instance, an immune evasion protein (m152/gp40) inhibiting the presentation of antigenic peptides to CD8 T cells by interfering with MHC class I protein vesicular transport has first been described for mCMV before proteins gpUS2, 3, 6 and 11 of hCMV were found to serve the same purpose, although with differences in the details of the underlying molecular mechanisms [for a review, see Reddehase (2002)].

An issue worth of being considered is the fact that clinical isolates of hCMV differ significantly from cell culture-adapted hCMV laboratory strains and also among each other, both genetically and in fundamental biological properties such as cell-type tropism [for a review, see Sinzger *et al*. (2008)]. So, even if hCMV could be studied in an animal model, one would have difficulty in selecting a particular hCMV strain for the model.

♦♦♦♦♦♦ III. VIRUS PROPAGATION AND PURIFICATION

The cloning of mCMV genomes in *Escherichia coli*-propagated BACs allows the use of the powerful methods of bacterial genetics. In the past decade, an impressive number of BACs carrying recombinant mCMV genomes were constructed and

stored as glycerol stocks. The transfection of purified BAC DNA into permissive cells leads to reconstitution of infectious mCMV.

Procedure: reconstitution of virus from BAC plasmids

1. Inoculate 500 ml of lysogeny broth (LB) medium, containing appropriate antibiotics, with 1 ml of an overnight culture of *E. coli*, containing the mCMV BAC, and incubate for 18–20 h at recommended temperature.
2. Purify BAC DNA on silica columns by anion exchange with the NucleoBond PC 500 Kit (cat. no. 740574; Macherey-Nagel, Düren, Germany) following the manufacturer's instructions for low-copy plasmids and for using the optional filtration step.
3. Dissolve the BAC DNA in an appropriate volume of TE buffer (10 mM Tris, 0.1 mM EDTA, pH 8.0).
   Attention! To avoid BAC DNA shearing, always use cut pipette tips and do not vortex a sample containing intact BAC DNA.
4. Check the DNA integrity by restriction enzyme digest followed by electrophoresis. Only high-quality BAC DNA should be used for transfection in order to maximize transfection efficiency.
5. Prepare MEF in the third passage [for the protocol, see Podlech *et al.* (2002)] in a 6-well plate with a confluence of ~80%.
6. Dilute graded volumes (2.5, 5, 10, 15 µl) of purified BAC DNA with minimal essential medium (MEM) (cat. no. 41090; Invitrogen, Karlsruhe, Germany) to a final volume of 100 µl.
7. Add 10 µl of PolyFect (cat. no. 301105; QIAGEN, Hilden, Germany) to each sample, mix gently by tipping the tube and incubate for 10 min at ~20°C (room temperature).
8. Wash the cells once with PBS and add 1 ml of MEM-FCS medium, containing FCS (10% vol/vol) and antibiotics (penicillin: 100 U ml^{-1}; streptomycin: 0.1 mg ml^{-1}).
9. Add 600 µl of MEM-FCS to each transfection sample and transfer the content to 1 well of the 6-well plate.
10. Incubate for 8–18 h at 37°C.
11. Remove the transfection supernatant, add 3 ml of MEM-FCS and incubate at 37°C for 5–7 days.
12. As soon as most cells show a cytopathic effect (CPE), that is when they become rounded and start to detach, collect the supernatant from each well and centrifuge for 5 min at 800 g to sediment cell debris. Store the supernatant at –70°C.
    Note: All recombinant mCMV genomes based on the BAC plasmid pSM3fr (Wagner *et al.*, 1999) can excise the BAC vector sequence by homologous recombination during viral replication. This is an important feature for avoiding *in vivo* attenuation of the BAC-cloned mCMVs. To eliminate the BAC vector sequence, five rounds of passaging in MEF followed by plaque purification are recommended.

13. To propagate the reconstituted virus, infect confluent MEF grown in 6-well plates with 1 ml (in the case of first propagation passage) or with 1 µl + 999 µl of MEM-FCS (second to fifth propagation passage) of cell-free viral supernatant for 30 min at ~20°C. Add 2 ml of MEM-FCS and incubate at 37°C until 80% of the cells show a CPE. Store the cell-free supernatants of all propagation passages at –70°C.
14. For plaque purification, infect confluent MEF with 1 µl as well as with 1 µl of 1:10 diluted fifth propagation passage supernatant as described. After the incubation, cover the cultures with 2 ml of viscous methylcellulose medium to prevent the formation of secondary plaques.

    Preparation of methylcellulose medium:
    - 8.8 g of methylcellulose (cat. no. 25499.182; VWR, Darmstadt, Germany) suspended in 360 ml of *aqua bidist*.
    - Sterilize the suspension at 121°C.
    - Dissolve the methylcellulose at ~20°C under permanent stirring for ~4 h. Continue stirring at 4°C overnight until the solution gets clear. Storage at 4°C is possible for several months.
    - Before use, add 40 ml of 10× MEM, 20 ml FCS, 5 ml L-glutamine (50 mg ml^{-1}), antibiotics and 8–16 ml $NaHCO_3$ (stock solution: 55 g l^{-1}) until a pH of 7.5 is reached
15. After plaque formation (usually on day 4 p.i.), pick single plaques with a 20 µl pipette and infect MEF to expand a clonal viral population.
16. Verify the deletion of the BAC vector sequence by Southern Blot (Simon *et al.*, 2006) or by quantitative real-time PCR (qPCR).

Procedure: qPCR for verifying the deletion of BAC vector-derived sequence

1. Isolate viral DNA and prepare DNA dilutions as described below.
2. Perform absolute quantitation of mCMV genomes (gene *M55/gB*) and BAC vector sequence (see procedure *Quantitation of viral genomes*). For detection of BAC vector sequences, use BAC-specific primers and probe (Table 1). As an external standard for both reactions, use plasmid pDrive_gB_PTHrP_BAC (Figure 1) in $\log_{10}$ dilutions ranging from 1×10^7 to 1×10^1 plasmids.
3. Determine the ratio between BAC vector sequence and *M55/gB* sequence. A result of $<10^2$ BAC vector sequences in 10^6 viral genomes indicates successful excision of BAC vector sequence.

Table 1. List of primers and probes for established qPCRs and RT-qPCRs

Target sequence	Application	Forward primer	Probe	Reverse primer	Splice junction
GAPDH	T RT-qPCR	5′-TTC ACC ACC ATG GAG AAG GC-3′	5′-TGC ATC CTG CAC CAC CAA CTG CTT AG-3′	5′-GGC ATG GAC TGT GGT CAT GA-3′	Yes
β-actin	T RT-qPCR	5′-GAC GGC CAG GTC ATC ACT ATT G-3′	5′-AAC GAG CGG TTC CGA TGC CC-3′	5′-CAC AGG ATT CCA TAC CCA AGA AGG-3′	Yes
PTHrP	S qPCR	5′-GGT ATC TGC CCT CAT CGT CTG-3′	–	5′-CGT TTC TTC CTC CAC CAT CTG-3′	No
PTHrP	T qPCR	5′-CAA GGG CAA GTC CAT CCA AG-3′	5′-TTG CGC CGC CGT TTC TTC CTC-3′	5′-GGG ACA CCT CCG AGG TAG CT-3′	No
Sry/Tdy	S qPCR	5′-ATG CAT TTA TGG TGT GGT CCC-3′	–	5′-AAG GGC CTT TTT TCG GCT TC-3′	No
Sry/Tdy	T qPCR	5′-AAG CGC CCC ATG AAT GC-3′	5′-AGT TGG CCC AGC AGA ATC CCA GC-3′	5′-CCC AGC TGC TTG CTG ATC TC-3′	No
m123/IE1	T RT-qPCR	5′-TGG CTG ATT GAT AGT TCT GTT TTA TCA-3′	5′-AAC GCT CCT CAC TGC AGC ATG CTT G-3′	5′-CTC ATG GAC CGC ATC GCT-3′	Yes
m128/IE2	T RT-qPCR	5′-GCG TCA GTC TGA AGA ACA AAG G-3′	5′-CGG GTC AGC TAC GCC CCT GCT C-3′	5′-GAT ACG ACC CTA CCT ACG TTA ACG-3′	Yes
M122/IE3	T RT-qPCR	5′-TGA TCC CAC TGA GGA AGA GAA GA-3′	5′-TCT ATG TTC ATC TCG GGT CCT GCA GCA-3′	5′-GAG GCC GCT GCT GTA ACA AT-3′	Yes
M112/E1	T RT-qPCR	5′-TCG AAG AGG AAT GTT CTC CAC G-3′	5′-AGC CCA AGC GCC AGA AGA CCC A-3′	5′-TTG TTG TCC TCC ATC GCT GA-3′	Yes
M55/gB	S qPCR	5′-GAA GAT CCG CAT GTC CTT CAG-3′	–	5′-AAT CCG TCC AAC ATC TTG TCG-3′	No

M55/gB	T qPCR/RT-qPCR	5′-CTA GCT GTT TTA ACG CGC GG-3′	5′-TGC TCG GTG TAG GTC CTC TCC AAG CC-3′	5′-GGT AAG GCG TGG ACT AGC GAT-3′	No
m04	T qPCR	5′-ACG GCA ACG GTG GTA ATC TTT AT-3′	5′-ATC CGA ACG CCA CCA CAG GCA G-3′	5′-TCC GCA AAC GAC ATC TGA CA-3′	No
m06	T qPCR	5′-TAT GGA CGA AAA ATG ACA GCA TCA-3′	5′-CCT GCC GGA CGA CGA CCC G-3′	5′-CAC ACC GCT CAT GTT CTT CAT CT-3′	No
m152	T qPCR	5′-CGT TCG CGA GAC TGA TGT TGT-3′	5′-CCA ACG GAA CCT GAG TGC GCA-3′	5′-GCA ACG GCT ACG TGT CCT GTA-3′	No
m164	T RT-qPCR	5′-CAA CTG ACA GTC GCA GCT CTT C-3′	5′-CCG GTT GAA CTG CGC GCC AC-3′	5′-CGG CGG TAA CCT GCT ATC C-3′	No
M86/MCP	T RT-qPCR	5′-GGT CGT GGG CAG CTG GTT-3′	5′-TCG GCC GTG TCC ACC AGT TTG ATC T-3′	5′-CCT ACA GCA CGG CGG AGA A-3′	No
BAC vector	T/S qPCR	5′-GTT CTG TCA TGA TGC CTG CAA-3′	5′-CAC CGC ACG AAG ATT TCT ATT GTT CCT GA-3′	5′-AAT CCG CTC CAC TTC AAC GT-3′	No

T: TaqMan Probes (qPCR and RT-qPCR), S: SYBR Green (qPCR), BAC: bacterial artificial chromosome, MCP: major capsid protein

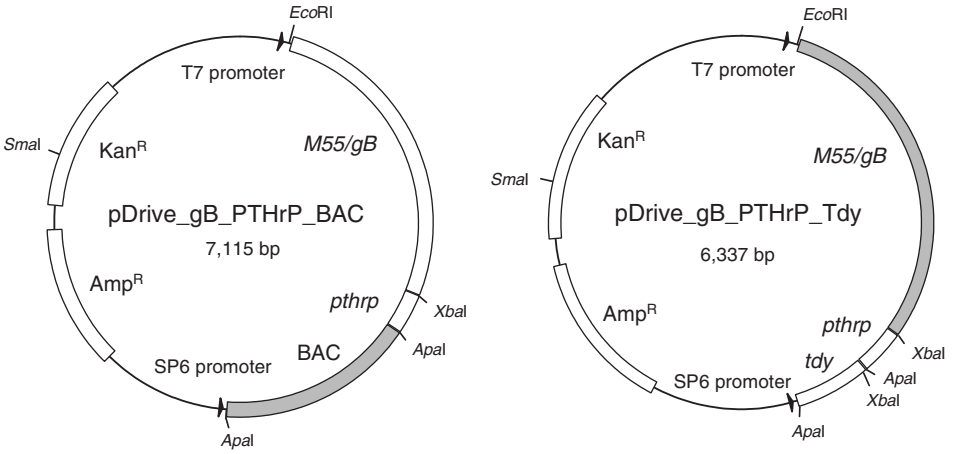

Figure 1. Plasmids for qPCR standardization. Shown are maps revealing restriction enzyme cleavage sites and the positions of resistance genes for selection and target genes for quantitation. Sequences of interest are highlighted by gray shading.

Procedure: large-scale propagation, purification and long-term storage

1. Seed second-passage MEF in 14.5 cm tissue culture dishes. For the protocol of preparing MEF, see Podlech *et al*. (2002). Subsequent steps refer to 40–50 dishes.
2. Infect the cells (per dish) with 0.5–1 $\times$ 10^5 plaque forming units (PFU) of mCMV or with ~60 µl of cell culture supernatant from verified BAC-free mCMV shortly before the cell monolayer is confluent. In detail, remove the culture medium and add the virus (in MEM-FCS) in a total volume of 5 ml. Keep the cultures for 30 min at ~20°C and shake gently from time to time. Add 20 ml of fresh medium.
3. Incubate the dishes under cell culture conditions for 4–5 days, until most cells show a CPE.
4. Collect supernatants and cells in sterile 500 ml centrifugation tubes. Scrape-off adherent cells with a cell scraper (do not use trypsin!).
5. From here on, perform all virus purification steps at 4°C or on ice.
6. Centrifuge for 20 min at 6400 g in order to spin down cell debris and cell nuclei.
7. Collect the supernatants in sterile 250 ml centrifugation tubes.

   Note: If it is the intention to isolate virions with high purity (as in Kurz *et al*., 1997), one should discard the pellets, because cell nuclei contain a high number of non-enveloped, non-infectious nucleocapsids. If it is the intention to get an optimal virus yield, proceed as follows:
8. Resuspend the pellets in 10 ml of MEM-FCS and homogenize the material with a Dounce homogenizer (~20 times). Transfer the homogenate to a 50 ml centrifugation tube and spin down for 20 min at 3600 g. Discard the pellet, collect the supernatant and pool the supernatants of both centrifugations.
9. Centrifuge for 3 h at 26,000 g. Discard the supernatants, except some fluid covering the pellets, and store the tubes on ice overnight.

10. Resuspend the pellets in the residual medium, homogenize again (on ice) and carefully load 2 ml of the homogenate on an 18 ml pre-cooled 15% (wt/vol) sucrose–VSB density cushion in 20 ml polyallomer ultracentrifugation tubes.
    VSB (virus standard buffer): 50 mM Tris (tris-hydroxymethyl-aminomethane), 12 mM KCl and 5 mM Na–EDTA, pH 7.8.
11. Centrifuge for 1 h at 52,800 g (swing-out rotor).
12. Discard the supernatant, cover each pellet with ~0.5 ml of sucrose–VSB and incubate for 4 h on ice.
13. Resuspend the pellets thoroughly with a Pasteur pipette and pool the suspensions in a Dounce homogenizer. Recover residual material from the tubes with a small volume of additional sucrose–VSB. Homogenize the material and store 20–100 µl aliquots at –70°C or in liquid nitrogen.
    Attention! It is essential that the buffer is devoid of Ca^{2+} and Mg^{2+} to preclude aggregation of the virions. Undiluted, purified virus stored in 15% sucrose–VSB solution can be frozen and thawed for up to five times with no loss of infectivity. Do not freeze virus dilutions.

Virus yield

Starting with 50 tissue culture dishes, purification should result in 3–4 ml of virus suspension with an infectivity titre ranging from 5×10^8 to 2×10^9 PFU per ml for mCMV-WT.Smith. Reconstituted BAC-derived recombinants usually reach somewhat lower titres.

Procedure: virus plaque assay in cell culture

General notes: The bioassay for viral infectivity is still the virological gold standard for quantitating functional virus. By definition, 1 PFU is the amount of virus required to cause the formation of a single plaque in a monolayer of permissive cells. It is important to emphasize that PFU is not identical with particle numbers or viral genome numbers (Kurz *et al*., 1997). The virus plaque assay can be performed with purified virions, with supernatant of infected cell cultures and with homogenates of infected cells or organs. There exist two versions of the assay: the standard plaque assay and the more sensitive plaque assay with 'centrifugal enhancement of infectivity, *CEI*' (Hudson *et al*., 1976; Kurz *et al*., 1997).

1. Seed second-passage MEF in 48-well flat-bottomed culture plates for the third passage.
2. Infect the MEF when the cell monolayer is close to confluence. For this, remove most of the cell culture medium in such a way that the cell monolayer remains covered with fluid, and add 100 µl of test suspension in an appropriate dilution.
3. Incubate for ~1 h at 37°C for virus adsorption and penetration. In the case of *CEI*, incubate for ~10 min at 37°C for adsorption and centrifuge the plates for another 30 min with ~760 g at ~20°C for enhanced penetration.

4. Cover the cultures with 0.5 ml of viscous methylcellulose medium to prevent the formation of secondary plaques.
5. Count virus plaques under an inverted microscope after 4 days of cultivation.

Note: Usually, the test suspension is serially diluted in factor-10 steps with 2 or 3 replicate cultures for each dilution. Plaques are counted for the dilution that gives >10 and <60 plaques. In the case of high plaque numbers, plaques may fuse to form doublet, triplet or multiple-leaved structures, which have to be counted accordingly as two, three or more plaques. The virus titre (VT) of the test suspension is calculated according to the formula:

VT [PFU ml^{-1}] = $M \times 10 \times Dilution\ Factor$, where M is the mean value of the plaque numbers counted for the replicate cultures.

Referring to the standard plaque assay, the genome-to-infectivity ratio for mCMV-WT.Smith was reported to be in the region of 500:1 (Kurz *et al.*, 1997). This high ratio is most likely caused by inefficient viral entry rather than by defective viral genomes. This view is supported by the finding that infection of cells under the conditions of *CEI* reduced the genome-to-infectivity ratio to 25:1, indicating a ca. 20-fold enhancement of infectivity. In addition, a ratio of >1 is in part explained also by the formation of multi-capsid virions, a special morphogenetic feature of mCMV characterized by cytoplasmic secondary envelopment of 2–8 capsids thus sharing one envelope (Weiland *et al.*, 1986; Kurz *et al.*, 1997). Specifically, two-thirds of all viral genomes in a purified virion preparation were found to be contained within multicapsid virions (Kurz *et al.*, 1997). Quantitation of viral genomes was previously performed by direct Southern blot hybridization and phosphor-imaging using purified virion DNA as template as well as by PCR followed by Southern blot hybridization. These methods of quantification are nowadays replaced by qPCR. Genome-to-infectivity ratios are routinely used in our lab as a first quality control for the replicative intactness of virus from different preparation batches and in particular of different virus mutants (Table 2). Importantly, within the batch variance observed for mCMV-WT.Smith, BAC-derived mCMV-WT.BAC (MW97.01; Wagner *et al.*, 1999) did not differ.

Procedures: determination of the genome-to-infectivity ratio

Viral DNA isolation and titration

1. Use 15 µl of virus stock solution with a minimal viral titre of 1×10^7 PFU ml^{-1} for DNA isolation. To account for variance during the purification process or subsequent DNA quantitation, prepare triplicate samples.
2. Isolate viral DNA with the kit of your choice according to the respective protocol. We use the High Pure Viral Nucleic Acid Kit (cat. no. 11 858 874 001; Roche, Mannheim, Germany). Viral DNA should be eluted in 100 µl with the appropriate elution buffer.
3. Prepare dilution series of each of the isolated samples, starting with an initial $\log_2$ titration step (25 µl of viral DNA + 25 µl of 10 mM Tris buffer, pH 8.0), followed by 4 $\log_{10}$ dilution steps (5+45 µl Tris) ranging from

0.5×10^{-1} to 0.5×10^{-4}. From the 0.5×10^{-3} dilution step onwards, add 40 ng µl^{-1} of carrier RNA or DNA.

Quantitation of viral genomes

1. Prepare an appropriate volume of qPCR master mix, e.g. the number of reactions planned times a volume of 18 µl of master mix needed per reaction: 10 µl of 2x-QuantiTect SYBR Green PCR Kit (QIAGEN) supplemented with 1.5 µl each of 10 µM forward and reverse primers specific for *M55/gB* (LCgB-forw and LCgB-rev; Simon *et al.*, 2005) (Table 1) and 5 µl of sterile water. The final reaction volume is 20 µl (see step 3).
2. Dilute the standard plasmid pDrive_gB_PTHrP_Tdy (Simon *et al.*, 2005) (Figure 1) in $\log_{10}$ steps from 0.5×10^{7} to 0.5×10^{1} plasmids per microlitre and add 40 ng µl^{-1} of carrier RNA or DNA for plasmid numbers of $<0.5 \times 10^{3}$. Use 2 µl of each titration step for quantitation, ranging from 1×10^{7} to 1×10^{1} plasmids. Perform quantifications for 1×10^{2} and 1×10^{1} plasmids in duplicates and triplicates, respectively. For the preparation of the external plasmid standard, see below.
3. Perform quantification for each of the titrated viral DNA samples. Analyse the 4 $\log_{10}$ titration steps ranging from 0.5×10^{-1} to 0.5×10^{-4} as triplicate measurements. Use 2 µl from each titration step for the quantifications.
4. Estimate the genome-to-infectivity ratio of the virus stock by calculating the median value from the following four quantifications:

Genomes [Mean value of the 0.5×10^{-1} triplicate] :

$$\text{PFU}\left[\frac{\text{Virus titer [PFU ml}^{-1}] \times\ 0.015\ \text{[ml]}}{1\times\ 10^{3}}\right]$$

⇩

Genomes [Mean value of the 0.5×10^{-2}triplicate] :

$$\text{PFU}\left[\frac{\text{Virus titer [PFU ml}^{-1}] \times\ 0.015\ \text{[ml]}}{1 \times 10^{4}}\right]$$

⇩

Genomes [Mean value of the 0.5×10^{-3}triplicate] :

$$\text{PFU}\left[\frac{\text{Virus titer [PFU ml}^{-1}] \times\ 0.015\ \text{[ml]}}{1 \times 10^{5}}\right]$$

⇩

Genomes [Mean value of the 0.5×10^{-4}triplicate] :

$$\text{PFU}\left[\frac{\text{Virus titer [PFU ml}^{-1}] \times\ 0.015\ \text{[ml]}}{1 \times 10^{6}}\right]$$

Table 2. Selected examples of genome-to-infectivity ratios

mCMV variant	Batch #	VT (PFU ml^{-1})	Genome-to-infectivity ratio
WT.Smith	VII	1.4×10^9	397:1
	XIV	7.8×10^8	204:1
	XV	1.1×10^9	397:1
WT.BAC	I	3.5×10^8	249:1
	II	1.3×10^9	212:1
	III	9.3×10^8	434:1
IE1-L176A	II	5.8×10^8	416:1
IE1-A176L	I	2.0×10^8	438:1
m164-I265A	I	8.7×10^7	196:1

PFU: plaque forming unit, VT: virus titre

♦♦♦♦♦♦ IV. QUANTITATION OF VIRAL REPLICATION IN HOST TISSUES

The productive replication cycle of mCMV is cytopathogenic and eventually cytolytic for most permissive cell types. In an immunocompromised and genetically susceptible murine host, for instance in BALB/c mice, mCMV shows a very broad cell-type tropism (Podlech *et al.*, 1998). Specifically, virus replication has been documented *in vivo* for many different cell types, including various types of epithelial cells such as glandular epithelial cells of the salivary glands, pneumocytes, enterocytes, hepatocytes, cortical and medullary cells of the suprarenal glands, glomerular cells in the kidney cortex and ependymal cells lining the brain ventricles. Further permissive cell types include vascular endothelial cells as well as liver sinusoidal endothelial cells (Sacher *et al.*, 2008), heart muscle myocytes, brown fat adipocytes, dendritic cells (Andrews *et al.*, 2001), mature macrophages (Stoddard *et al.*, 1994; Hanson *et al.*, 2001) such as alveolar macrophages in the lungs and Kupffer cells in the liver, connective tissue fibrocytes and bone marrow stromal cells (Mayer *et al.*, 1997). Notably, the *in vivo* cell-type tropism of hCMV is very similar (Plachter *et al.*, 1996). Accordingly, the involvement of multiple organs is a common typical feature of both human and murine CMV disease.

In tissues composed of uniform parenchymal cells permissive for productive mCMV infection, such as in the liver and in the suprarenal glands, viral cytolysis results in three-dimensional plaque-like lesions, literally 'holes' in the tissue. In the histological section, plaques are characterized by a necrotic centre surrounded by a corona of more recently infected cells (Grzimek *et al.*, 1999; Holtappels *et al.*, 2006b) (Figure 5B; Plate 1–B, b). The centre is devoid of nuclei and contains remnants of lysed cells, cytoskeleton components and extracellular matrix components. Plaques expand centrifugally with time of virus replication and cell-to-cell spread (Wirtz *et al.*, 2008; Podlech *et al.*, 2010).

Virus replication in organs can be evaluated (a) in cell cultures of permissive indicator cells infected with organ homogenates, (b) *ex vivo* by quantitation of viral genomes with qPCR and (c) *in situ* by histological methods such as

immunohistochemistry (IHC) for detection of viral proteins and *in situ* hybridization (ISH) for detection of viral nucleic acids in infected tissue cells.

Procedure: VT in organs

1. Dissect organs, transfer them into MEM-FCS and deep-freeze them at –70°C.
2. Thaw them slowly on ice and pass the freeze-thawed, disrupted tissue through a steel mesh. Rinse the mesh with MEM-FCS, so that the organ homogenate reaches a final volume of 2 ml (e.g. for spleen, lungs, salivary glands and suprarenal glands) or of 20 ml in the case of the liver.
3. Prepare dilutions of the homogenate and continue as described above for the *CEI* method of the virus plaque assay.

Note: Organ homogenates may be toxic for the MEF indicator cell monolayer. Therefore, the first suspension to be tested is usually the 1:10 dilution of the homogenate (corresponding to 1:200 and 1:2000 aliquots of various organs and liver, respectively), which defines the detection limit per culture accordingly. The VT is measured under conditions of *CEI* and is usually expressed as PFU per organ.

Attention! In contrast to purified virus stocks, infectivity in organ homogenates is reduced by a factor of ~5 with every freeze-and-thaw cycle.

Procedure: quantitation of viral genomes in host tissues by qPCR

DNA isolation

1. Excise infected organs of interest.
2. Isolate DNA with the kit of your choice according to the respective protocol. We use the DNeasy Blood & Tissue Kit (cat. no. 69504; QIAGEN).
3. Determine the concentration of the isolated DNA samples and adjust them to 50 ng μl^{-1}.

Preparation of an external plasmid standard

General notes: Absolute quantitation requires external standards, preferably plasmids for DNA quantitation. In general, we use plasmid pDrive_gB_PTHrP_Tdy (Figure 1) (Simon *et al.*, 2005) that is derived from the pDrive plasmid (QIAGEN) and encompasses DNA fragments specific for a viral gene (*M55/gB*) and two murine cellular genes (*pthrp* and *tdy/sry*) with a total size of 6337 bp. The cellular single-copy autosomal gene *pthrp* (Mangin *et al.*, 1990) is used for the determination of cellular genomes in the analysed sample. Taking into account that somatic cells are usually diploid with pairs of autosomes, the results of *pthrp* quantitation have to be divided by a factor of 2 to obtain the number of cells per sample. One must consider that cells in cell culture, tumour

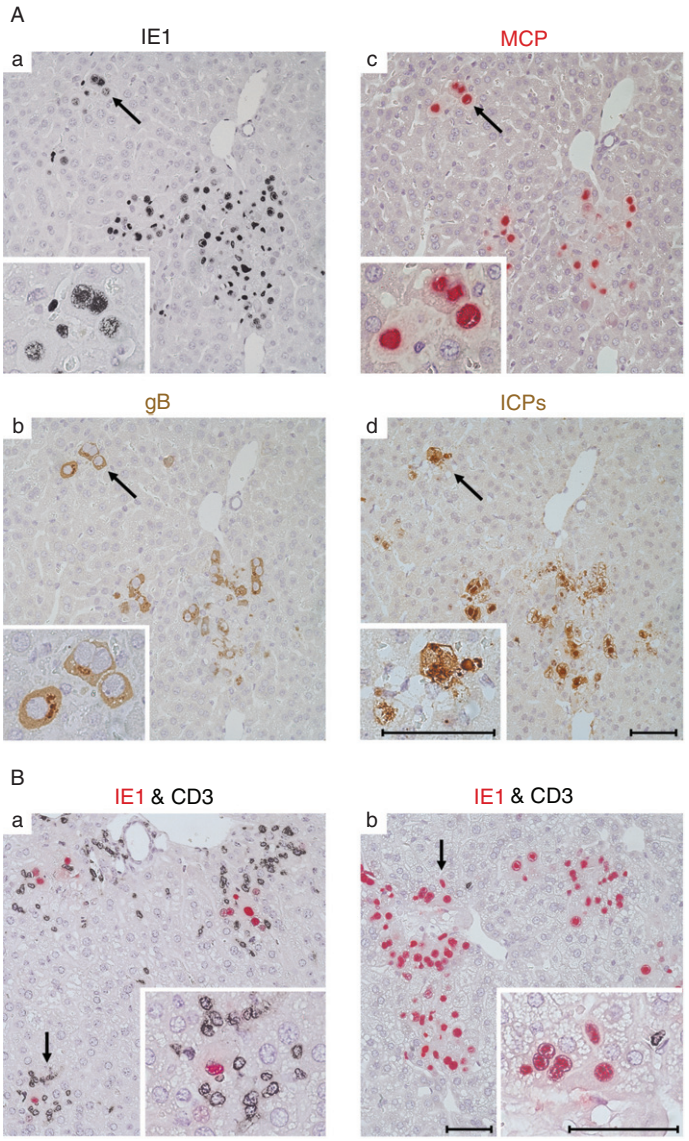
A
IE1
a
MCP
c
gB
b
ICPs
d
B
IE1 & CD3
a
IE1 & CD3
b

cells in particular, may be polyploid. The Y-chromosomal gene *sry* (Koopman *et al.*, 1990) – formerly termed *tdy* (Gubbay *et al.*, 1990) – is present in a single copy in a male cell and can be used as a reporter gene for tracking donor-derived haematopoietic cells in the recipient after sex-mismatched male-into-female BMT (Mayer *et al.*, 1997; Steffens *et al.*, 1998b; Seckert *et al.*, 2008, 2009).

1. Linearize the plasmid by *Sma*I digestion and purify it by gel electrophoresis. Determine the amount of DNA by triplicate OD-measurement and use the mean OD-value for estimating the number of copies per microlitre by using the following formula:

$$\text{Plasmids [copies } \mu\text{l}^{-1}] = \frac{6.022 \times 10^{23} \text{ [copies mol}^{-1}] \times \text{concentration [g } \mu\text{l}^{-1}]}{\text{MW [g mol}^{-1}]}$$

MW: molecular weight of dsDNA = length of plasmid [bp] × 660 [Da bp^{-1}]

2. Adjust the DNA standard to 0.5×10^8 plasmids per microlitre and store the diluted plasmids in 20 µl aliquots at –20°C.
3. For the quantitation of viral and cellular genomes, dilute the standard plasmid pDrive_gB_PTHrP_Tdy in $\log_{10}$ steps from 0.5×10^7 to 0.5×10^1 plasmids per microlitre and add 4 µg of carrier RNA or DNA from the 0.5×10^3 dilution step onwards. Use 2 µl of each titration step as standard for the quantification, ranging from 1×10^6 to 1×10^1 plasmids. Perform measurements for 1×10^2 and 1×10^1 plasmids in duplicates and triplicates, respectively.

Plate 1. Identification of infected cells and CD8 T-cell infiltrates in host tissues by IHC. (A) Demonstration of selected staining options for mCMV-infected cells (see also Table 3). Serial 1 µm liver tissue sections were prepared on day 10 after intraplantar infection of immunocompromised BALB/c mice with 10^5 PFU of mCMV-WT.Smith. Panels a–d show the same tissue site (note the 'landmark' vessels in the upper right corners) with a prominent focus of infection stained for different viral antigens and in different colours. The arrows point to a group of infected cells (primarily hepatocytes) that is resolved to greater detail in the inset images. The bar markers represent 50 µm. (a) Black intranuclear staining of m123/IE1 (ABC technique with peroxidase and DAB-nickel); (b) brown cytoplasmic staining of M55/gB (ABC technique with peroxidase and DAB); (c) red intranuclear staining of M86/MCP (APAAP technique with alkaline phosphatase and Fuchsin); (d) combined brown staining of ICPs in nucleus and cytoplasm as well as at the cell membrane (ABC technique with peroxidase and DAB) using a polyspecific mouse antiserum generated by intraplantar prime-boost-boost infections of BALB/c mice with 10^5 PFU of mCMV-WT.Smith in intervals of 2 weeks and harvested 2 weeks after the last boost. (B) Demonstration of the epitope-specificity of focal T-cell infiltrates. T cells and infected cells present in livers of immunocompromised and infected mice at day 12 after the transfer of 5×10^5 IE1 epitope-specific CTL were visualized by two-colour IHC-staining of CD3ε (black membrane staining; ABC technique with peroxidase and DAB-nickel) and IE1 (red intranuclear staining; APAAP technique with alkaline phosphatase and Fuchsin), respectively. (a) Infection of the transfer recipients with virus mCMV-IE1-A176L expressing the antigenic IE1 peptide (see Table 4); (b) Infection of the transfer recipients with virus mCMV-IE1-L176A lacking the antigenic IE1 peptide due to a point mutation at the C-terminal MHC anchor position. The arrows point to foci that are resolved to greater detail in the inset images. The bar markers represent 50 µm. For the interpretation of the results, see the text of Chapter 15.III.G. (See color plate section).

qPCRs specific for viral and cellular genomes

1. Prepare appropriate volumes of qPCR master mix specific for *M55/gB* and *pthrp*, e.g. respective multiples of 18 µl per sample: 10 µl of 2x-QuantiTect SYBR Green PCR Kit (QIAGEN) supplemented with 1.5 µl each of 10 µM forward and reverse primer for *M55/gB* (LCgB-forw and LCgB-rev; Simon *et al.*, 2005) and *pthrp* (LCpthrp-forw and LCpthrp-rev; Simon *et al.*, 2005), respectively (Table 1), and 5 µl of sterile water to reach a final volume of 20 µl per reaction (see step 2).
2. Perform quantification of tissue sample DNAs in triplicates for *M55/gB* and in one replicate for *pthrp*. Use 2 µl of each DNA test sample or plasmid standard for qPCR reactions.
3. Use the following formula for the normalization of viral genomes to 1×10^6 cells:

$$\text{Viral genomes per } 1\text{x}10^6\text{cells} = \frac{2 \times 10^6}{pthrp \text{ copies}} \times gB \text{ copies}$$

Procedure: detection of infected cells by single-colour IHC

The most sensitive method for the *in situ* detection and quantitation of mCMV-infected cells in paraffin-embedded tissue sections is the staining of the intranuclear viral immediate-early (IE) phase protein IE1 (pp76/89). This protein is expressed abundantly from ca. 2 h after infection onwards and is maintained throughout the virus replication cycle. In the late (L) phase of the cycle, IE1 accumulates in an intranuclear inclusion body, which is the site of nucleocapsid assembly and viral DNA packaging.

Reagents

- Trypsin solution, pH 7.4:
  Dissolve 1.25 g trypsin (cat. no. T 7409; Sigma, Munich, Germany) in 1 l of trypsin buffer:
  - NaCl 8 g (137 mM)
  - KCl 0.2 g (2.7 mM)
  - KH_2PO_4 0.2 g (1.5 mM)
  - Na_2HPO_4 1.15 g (6.5 mM)
  - EDTA 1.25 g (3.4 mM)

  dissolved in 900 ml aqua dist., adjusted to pH 7.4 and filled up to 1 l
- Blocking solution (0.3% H_2O_2 in methanol):
  Add 0.6 ml of a 30% (vol/vol) H_2O_2 solution (in aqua dist.) to 59.4 ml methanol.

- TBS (Tris-buffered saline)
  - Tris 12.1 g (100 mM)
  - NaCl 8.8 g (150 mM)

    dissolved in 900 ml aqua dist., adjusted to pH 7.4, and filled up to 1 l
- Normal rabbit serum (cat. no. R 4505; Sigma)
- Virus-specific antibody:

  Monoclonal antibody (MAb) mouse IgG1, clone CROMA 101, directed against mCMV-IE1 (kindly provided by Prof. S. Jonjic, University of Rijeka, Rijeka, Croatia)
- Polyclonal goat Ab directed against mouse-IgG (Fab), biotin-conjugated and affinity-purified (cat. no. B 0529; Sigma)
  - Mouse IgG1 (cat. no. X 0931; Dako, Hamburg, Germany) serving as an isotype control
- ABC-enzyme kits:
  - Vectastain ABC-peroxidase kit PK-4000 Standard, or (alternatively)
  - Vectastain ABC-alkaline phosphatase kit AK-5000 Standard

    both from Vector Laboratories, Inc. (Burlingame, CA, USA)
- Peroxidase staining substrate:

  10 mg 3,3′-diaminobenzidine tetrahydrochloride (DAB) (cat. no. D 5637; Sigma) and 75 mg ammonium-nickel-sulphate hexahydrate (cat. no. 09885; Fluka, Buchs, CH) dissolved in 50 ml of Tris (50 mM, pH 7.5) and supplemented with 17 µl of 30% (vol/vol) H_2O_2 (in aqua dist.)
- Alkaline-phosphatase staining substrate:

  Fuchsin substrate system (cat. no. K 0625; Dako), consisting of the chromogen Fuchsin, activating reagent, and substrate buffer
- Mayer's haematoxylin (cat. no. MHS-16; Sigma)
- Embedding medium:

  PARAmount (Earth Safe Industries, Belle Mead, NJ, USA)

  Three colour options are used routinely in our lab:
  1. **Black:** Peroxidase combined with DAB-nickel
  2. **Brown:** Peroxidase combined with DAB (with no nickel)
  3. **Red:** Alkaline phosphatase combined with Fuchsin

  Note: Black staining of IE1 with light haematoxylin counterstaining gives the best contrast and the microphotographs can be documented alternatively in colour (Plate 1A, a) or as halftone prints (Figure 5B).

Procedure

1. Prepare 1 µm (for serial sections) or 2 µm sections of paraffin-embedded tissue, deparaffinize and rehydrate according to established histological methods.
2. Partially digest proteins with trypsin solution for 15 min at 37°C.
3. Wash with aqua dist. for 3 min.
4. If it applies (black and brown staining), block endogenous peroxidase with blocking solution for 30 min at ~20°C.
5. Wash with aqua dist. for 3 min.

6. Incubate the slides for 20 min at ~20°C in a 1:10 dilution of normal rabbit serum in TBS. Do not wash after this step, but let the serum run off. Perform all further steps in a humid chamber to avoid drying of the tissue sections.
7. Incubate for ~18 h at 4°C with MAb CROMA 101, diluted 1:500 in TBS. For specificity control, incubate sections accordingly with an isotype-matched Ab.
8. Wash twice with TBS for 3 min.
9. Incubate for 30 min at ~20°C with biotin-conjugated anti-mouse IgG (cat. no. B 0529; Sigma), diluted 1:200 in TBS.
10. Wash twice with TBS for 3 min.
11. Prepare ABC solution from the PK-4000 (alternatively, the AK-5000) kit 30 min before use, according to the product instructions.
12. Incubate the slides for 30 min at ~20°C with the ABC solution.
13. Wash three times for 10 min with TBS.
14. Incubate for 5–10 min at ~20°C with peroxidase or alkaline-phosphatase staining substrate until the coloured precipitate becomes visible.
15. Wash three times for 1 min with aqua dist.
16. Counterstain with haematoxylin solution for 5 s.
17. Let the slides dry. Seal them with PARAmount and a coverslip for storage.

Note: Currently, besides staining of IE1 (m123), reagents (MAbs or custom-made polyclonal anti-peptide sera) and methods are available for staining of the prototypic Early (E)-phase protein E1 (M112-113) (Dobonici *et al.*, 1998), the endoplasmic-reticulum (ER)-resident E-phase glycoprotein gp36.5 (m164) (Holtappels *et al.*, 2006a, Däubner *et al.*, 2010), the virion envelope glycoprotein M55/gB (Böhm *et al.*, 2008b) and the major capsid protein M86/MCP (Wilhelmi *et al.*, 2008) (Table 3). In addition, polyspecific hyperimmune sera directed against an unknown composition of 'infected cell proteins (ICPs)' proved to be specific in the visualization of infectious foci in tissue by combined staining of infected cell nuclei, cytoplasm and plasma membrane. As an example for colour options and different antigens, Plate 1A shows the same tissue site in four serial 1 μm liver tissue sections stained for IE1 (black), MCP (red), gB (brown) and ICPs (brown).

Application example: estimating viral replicative fitness by the determination of viral doubling times in host tissues

For viral mutants generated by reverse genetics, for instance by BAC mutagenesis, and designed to show a selective immunological phenotype, it is important to verify that the introduced mutation does not unintendedly interfere with viral replicative fitness in the absence of an immune response. In addition to the specific mutation of interest, mutagenesis can also lead to spontaneous surplus mutations that do not necessarily affect the intended phenotype but may interfere with virus replication. Therefore, the mutant virus and the corresponding revertant virus

need to be tested for their potential to replicate in host cells. Growth curves in MEF cell cultures were frequently used in the literature to serve this purpose, but MEF are not representative of the many different cell types infected *in vivo* (see above) in the context of tissues where cells are for the most part quiescent. Therefore, in our lab, growth curves are routinely determined for each virus in various organs of immunocompromised mice for calculation of the virus *doubling time* (DT).

An instructive example (Figure 2) compares virus multiplication in the liver, the spleen and the lungs for the BAC-cloned virus mCMV-WT.BAC (MW97.01; Wagner *et al*., 1999), for a virus lacking the expression of the regulatory protein IE1 (Ghazal *et al*., 2005) and for mutant and revertant viruses with a single amino acid replacement Y165C and C165Y in protein IE1, respectively (Wilhelmi *et al*., 2008). The IE1-Y165C mutation is located at the proteasomal cleavage site of the immunodominant IE1 peptide precursor and simultaneously destroys the capacity of IE1 to transactivate cellular genes involved in nucleotide metabolism. The growth analysis revealed that mutant virus mCMV-ΔIE1 is growth-attenuated in all three organs, whereas the mutation Y165C in protein IE1 did not affect virus growth in absence of immune cells (Wilhelmi *et al*., 2008). Notably, recent work by Kropp *et al*. (2009) has exemplarily shown that the DT values differ between different organs but are organ-specific constants independent of the parameter used for their calculation, that is independent of whether virus replication is measured as exponential increase over time in the numbers of PFU, viral genomes or infected tissue cells.

Procedure: calculation of the virus DT

1. Subject mice to haematoablative treatment by total body γ-irradiation with a single dose of 6.5 Gy (BALB/c mice) and 7 Gy (C57BL/6 mice) at 6 and 24 h before infection, respectively, to account for the different radiation sensitivities of these two inbred mouse strains.
2. Infect mice at the left hind footpad (intraplantar infection) with 10^5 PFU (determined by standard plaque assay) of the virus under investigation. For this, dilute the virus stock in physiological saline and inject a volume of not more than 25 µl in order to conform to animal welfare (applies to rules in Germany).
3. Determine the quantitation parameters (PFU, genome numbers, numbers of infected cells per defined tissue section area) for at least three mice per time on days 2, 4, 6, 8 and 10.
4. Plot the logarithmic data (ordinate) versus time (linear scale on the abscissa), as shown in Figure 2, and calculate the log-linear regression line $\log N(t) = at + \log N(0)$, where $N(t)$ is the data determined at time t and a is the slope of the regression line. Use standard statistics software of your choice. We use Mathematica Statistics Linear-Regression software, version 5.1 (Wolfram Research, Inc., Champaign, IL, USA).

Table 3. IHC parameters for the detection of mCMV proteins in host tissues

Viral target	Protein digestion	HIER	Blocking serum	First antibody	Biotin-conjugated second antibody
m123/IE1	Trypsin	Not required	Rabbit serum, diluted 1:10	MAb (murine IgG1) anti-IE1 (clone CROMA 101), diluted 1:500	Polyclonal goat anti-mouse IgG antiserum, diluted 1:200
M112/E1	Trypsin	Required	Rabbit serum, diluted 1:10	MAb (murine IgG1) anti-E1 (clone CROMA 103), diluted 1:500	Polyclonal goat anti-mouse IgG antiserum, diluted 1:200
m164	Proteinase K	Required	Goat serum, diluted 1:10	Polyclonal rabbit anti-m164 antiserum, diluted 1:400	Polyclonal goat anti-rabbit IgG antiserum, diluted 1:500
M55/gB	Trypsin	Required	Goat serum, diluted 1:10	Polyclonal rabbit anti-gB antiserum, diluted 1:500	Polyclonal goat anti-rabbit IgG antiserum, diluted 1:500
M86/MCP	Trypsin	Required	Goat serum, diluted 1:10	Polyclonal rabbit anti-MCP antiserum, diluted 1:1000	Polyclonal goat anti-rabbit IgG antiserum, diluted 1:500
ICPs	Proteinase K	Required	Rabbit serum, diluted 1:10	Polyclonal murine hyperimmune serum, diluted 1:300	Polyclonal goat anti-mouse IgG antiserum, diluted 1:200

IHC: immunohistochemistry, HIER: heat-induced epitope retrieval, MCP: major capsid protein, ICPs: infected cell proteins

5. Calculate DT according to the formula $DT = \log 2\, a^{-1}$. Accordingly, the upper and lower 95% confidence limits of slope a give the 95% confidence interval of DT. Note that one can use any base of the logarithm (ln, $\log_{10}$, $\log_2$), but the base used for calculating DT must be the same as the one used for plotting the data.

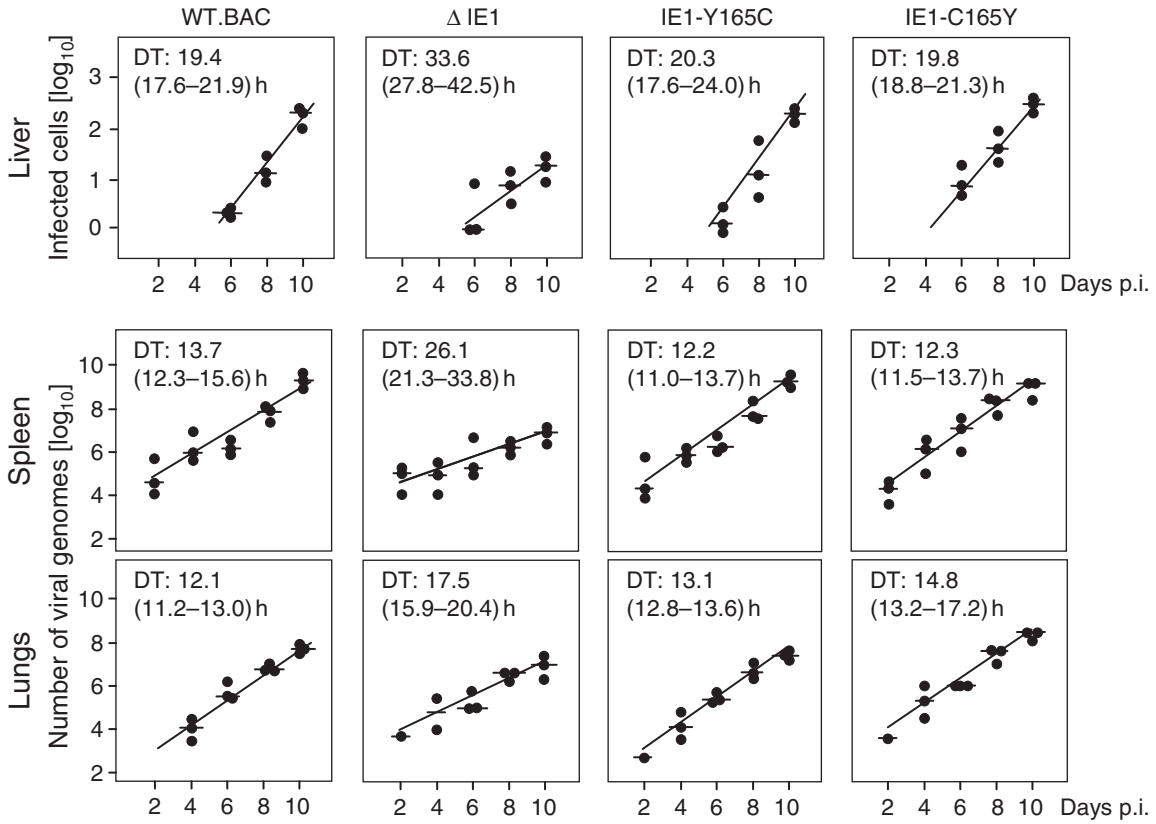

Figure 2. Virus growth curves and DTs in host tissues. BALB/c mice were immunocompromised by 6.5 Gy of γ-irradiation and were infected with 10^5 PFU of mCMV-WT.BAC or the indicated IE1 mutants in the left hind footpad (intraplantar infection). Virus replication in organs was determined at the indicated times after infection. Virus spread in the liver was quantitated by IHC staining of the intranuclear viral protein M86 (MCP) followed by counting of stained cell nuclei in representative 10 mm^2 areas of liver tissue sections. Virus replication in spleen and lungs was measured by quantitation of viral genomes (per 10^6 tissue cells normalized to the cellular gene *pthrp*) with qPCR specific for the viral gene *M55/gB*. Black dots represent data for individual mice. Median values and log-linear regression lines are indicated. DT: doubling time, with the 95% confidence interval given in parentheses (reproduced from Wilhelmi *et al.*, 2008. Copyright © *American Society for Microbiology, Journal of Virology*).

♦♦♦♦♦♦ V. QUANTITATION OF VIRAL GENE EXPRESSION

Quantitation of viral transcripts by reverse transcriptase (RT)-qPCR serves for monitoring the kinetic stage of viral gene expression prior to viral DNA replication and release of infectious virions. This is particularly important in cases in which the productive viral cycle is not completed. Exponential increase in viral transcripts over time can also be employed as a surrogate marker for viral replication and spread in tissues in cases when high amounts of inoculum virion DNA obscure the quantitation of viral DNA replication by qPCR. One must consider the fact that infection with 10^5 PFU is equivalent to application of ~4×10^7 viral DNA molecules, according to the genome-to-infectivity ratios discussed above (Table 2). An example is virus replication in the draining regional lymph node, for instance the popliteal lymph node, shortly after intraplantar infection (Böhm *et al.*, 2008b).

Procedure: preparation of synthetic transcripts as an external standard

General notes: To ensure comparableness between independent RT-qPCR reactions, a reference template is needed for standardization. For absolute quantitation of viral transcripts, this is achieved optimally only with synthetic RNA transcripts as an external standard (Bustin, 2000; Huggett *et al.*, 2005). These molecules can either be derived from *in vitro* transcription or consist of synthetic oligonucleotides. Transcripts of the gene of interest (GOI) are synthesized by *in vitro* transcription. Plasmids carrying the cDNA of the GOI under control of a T7 or SP6 promoter are used as templates for *in vitro* transcription, e.g. with the Megascript Kit (Applied Biosystems, Foster City, CA, USA).

1. Linearize plasmid with a suitable enzyme. The enzyme should cut close to the 3′-end of the GOI and produce blunt ends or 5′-sticky ends to produce *in vitro* transcripts with a defined length.
2. Transcribe GOI cDNA according to the manufacturer's protocol.
3. Determine the concentration of *in vitro* transcripts, for instance with Nanodrop, and calculate the number of transcripts according to the formula

$$\text{Transcripts [copies } \mu\text{l}^{-1}\text{]} = \frac{6.022\times10^{23}\ [\text{copies mol}^{-1}]\times\text{concentration [g }\mu\text{l}^{-1}]}{\text{MW [g mol}^{-1}]}$$

MW: molecular weight of ssRNA = length of the *in vitro* transcript [b] × 340 [Da b^{-1}].

4. Prepare serial dilutions of the transcripts to obtain defined, graded amounts per microlitre (e.g. a series of dilutions containing 10^6–10^1 transcripts μl^{-1}). Because RNA concentration influences the efficiency of the RT, use TE buffer containing 10 ng μl^{-1} of a non-target RNA as carrier RNA

(e.g. *E. coli* rRNA) for preparing the dilutions (Stahlberg *et al*., 2004; Bustin *et al*., 2009). The standards are stored in aliquots at –70°C and can be used several times but should be discarded if the efficiency revealed by the calibration curve drops significantly.

Procedures: purification of RNA derived from cells and tissues

General notes: Work under RNase-free conditions all the time and use a laboratory spatially separated from your PCR laboratory in order to avoid template contamination of your RT-PCR reactions. Workstations with UV irradiation (e.g. Captair Bio; Erlab, Cologne, Germany) can be used to minimize template carryover. QIAGEN reagents were used throughout the protocols to isolate total (viral and cellular) RNA (RNeasy Mini Kit, Qiashredder, and RNase-free DNase Set; refer to the respective manuals for further details).

(A) Preparation of RNA from cell cultures

1. Wash and trypsinize the cells according to standard protocols.
2. Determine cell numbers, spin-down up to 5×10^6 infected fibroblasts in an Eppendorf tube and remove supernatant thoroughly. Note that the exact cell number depends on the cell type. Refer to the QIAGEN RNeasy protocol for further details.
3. Resuspend the cell pellet in RLT buffer to which 2-mercapto-ethanol is added at a concentration of $10\,\mu l\,ml^{-1}$ immediately prior to use. Mix the cell suspension by vortexing.
4. Homogenization of the sample is achieved by using a QIAshredder column and centrifugation for 2 min with 20,000 g. Further processing of the sample is described in the RNeasy manual.
5. To eliminate DNA that can co-purify with the prepared RNA, we use an on-column DNaseI digestion according to the QIAGEN protocol with a 20-min period of incubation.
6. To elute the RNA from the filter, add 50 µl of RNase-free water to the column and incubate for 1 min at ~20°C. The RNA is subsequently eluted into RNase-free 1.5 ml reaction tubes by centrifugation for 1 min with 10,000 g. Store RNA at –70°C.

(B) Preparation of RNA from host organs

General notes: Isolation of RNA from host tissues works essentially as described above for cell cultures, except that additional methods are required for tissue disruption. Sacrifice mice by cervical dislocation or in CO_2 atmosphere and remove organs of interest as fast as possible. Flash-freeze the organs in liquid nitrogen. For easy-to-lyse organs such as liver, lungs, spleen

and salivary glands, use the RNeasy Mini Kit. A broader range of tissues, including also footpad and lymph nodes, can be processed with the RNeasy Lipid Tissue Mini Kit. For disruption of the tissues either the QIAGEN TissueRuptor (for samples containing more than 100 mg of tissue) or a bead mill (Mixer Mill MM300; Retsch, Haan, Germany) with a QIAGEN Tissue Lyser Adaptor Set and steel beads (for samples containing less than 100 mg of tissue) can be used.

Isolation of small samples with the Mixer Mill and the Lipid Tissue Mini Kit

1. Weigh the organs and cut them into pieces of appropriate size. Note that with RNeasy Lipid Tissue Mini Kit up to 100 mg, with the RNeasy Mini Kit a maximum of only 30 mg can be processed.
2. Give steel beads and 1 ml of QIAzol lysis buffer into 2 ml safe-lock tubes. Type and size of beads depend on the specimen and have to be chosen empirically, e.g. two 2 mm bead for a single lymph node and two 4 mm beads for a footpad (see the list below). In order to lyse footpads effectively, use only 300 µl QIAzol and add the remaining 700 µl after disruption of the footpad.
3. Add the tissue specimen (see step 1), close the tubes tightly and homogenize with the mixer mill twice for 3 min with 30 Hz.
4. RNA can then be extracted from the homogenate by adding chloroform followed by centrifugation (for details, see the RNeasy Lipid Tissue Mini Kit manual).
5. Remove DNA by on-column DNaseI digestion for 20 min.
6. To elute the RNA, add 50 µl of RNase-free water and incubate for 1 min followed by a centrifugation step.
7. Store the recovered RNA at –70°C.

Tissue	Frequency (Hz)	Time	Beads	Volume of lysis buffer
Spleen	30	2 × 2 min	2 × 3 mm	600 µl RLT or 1 ml Q
Liver	30	2 × 2 min	2 × 3 mm	600 µl RLT or 1 ml Q
Lungs	30	2 × 2 min	2 × 3 mm	600 µl RLT or 1 ml Q
Salivary gl.	30	2 × 3 min	2 × 3 mm	600 µl RLT or 1 ml Q
Lymph node	30	2 × 3 min	2 × 2 mm	1 ml Q
Footpad	30	2 × 3 min	2 × 4 mm	300 µl Q + 700 µl Q

Q=QIAzol lysis buffer (RNeasy Lipid Tissue Mini Kit)
RLT=RLT lysis buffer (RNeasy Mini Kit)

Isolation of larger samples with the QIAGEN TissueRuptor

1. Add lysis buffer (QIAzol or RLT buffer) to the specimen in a 50 ml Falcon tube. The amount of buffer depends on the weight of the tissue piece (for details, see the kit manual).

2. Keep the tube on ice during the tissue disruption process to prevent heating of the specimen.
3. Take a portion of the sample representing ~30 mg of tissue for further processing. The remaining portion of the homogenate can be stored at –70°C.
4. Further processing is identical with the 'cell-protocol' (see RNeasy manual for details).
5. DNA is removed by on-column DNaseI digestion for 20 min.
6. To elute RNA from the column, add 50 µl of RNase-free water and incubate for 1 min followed by spinning-down.
7. Store the RNA at –70°C.

Procedures: absolute quantitation of viral transcripts

General notes: Absolute quantitation of viral transcripts by RT-qPCR is considered the gold standard for gene expression analysis (Bustin, 2000; Huggett *et al*., 2005). As discussed above, external standards serve to ensure comparableness between RT-qPCRs carried out independently. It is also important to normalize the RT-qPCRs in order to minimize variance (Stahlberg *et al*., 2004; Bustin *et al*., 2009). To maximize reproducibility, we routinely take four actions: (a) Standardization of sample size (i.e., we use the same numbers of cells or amount of tissue for RNA isolation in all the samples of one particular experiment); (b) standardization of the amount of total RNA per reaction to achieve comparable efficiency of reverse transcription; (c) adaptation to the expected amount of target RNA (i.e., we use for instance 10 and 100 ng of total RNA for transcripts of high and low abundance, respectively, and (d) Normalization to a cellular gene. Only genes that are stably expressed under the used experimental conditions, for instance genes whose expression is not regulated by the infection, can be employed as reference genes. This has to be assessed empirically for each experimental setup.

Validation of reference genes

General note: It is often assumed that reference genes used for other methods, such as Northern blotting, are also a good choice for the normalization of RT-qPCR data; yet, this is not always the case (Radonic *et al*., 2004; de Kok *et al*., 2005). So, reference genes need to be validated for the specific experimental purpose. In particular, the quantification cycle (C_q-value), also known as threshold cycle (C_T value), of the reference gene must remain stable under different experimental conditions (Bustin *et al*., 2009), for instance in the comparison between uninfected and infected cells.

1. Prepare RNA, as described above, from cells or tissue pieces in an appropriate number of independent replicates.

2. Make serial dilutions of the isolated RNA in $\log_{10}$ steps, e.g. from 100 to 0.001 ng.
3. Perform RT-qPCR. Ideally, the C_q-values of the replicates of one dilution as well as of the different experimental groups should be identical for each dilution step.
4. Plot C_q-values against RNA amount for each dilution series. The slope of the regression lines should ideally be –3.3 in case of a $\log_{10}$ dilution series, since this corresponds to a PCR reaction efficacy of 100%.

If the reaction efficacy is close to 100% and if the C_q-values are stable for different experimental conditions, the tested gene is suitable as a reference gene for normalization. In our hands, GAPDH as well as β-actin transcripts proved to be reliable as reference (Table 1).

Singleplex RT-qPCR

We use the QIAGEN One-Step RT-PCR Kit to perform the cDNA synthesis and the subsequent PCR reaction in one tube without a need to open the reaction tube for adding any further reagents. PCR runs are performed on an ABIPrism 7500 Real-Time PCR System (Applied Biosystems). Probes are usually labelled with the reporter dye FAM but we also use Cy5, Bodipy TMR, Cy3 and Hex dyes. TAMRA is a frequently used quencher, but Black-hole™ quenchers 1 and 2 (BHQ-1 and BHQ-2) are also used if it is indicated. For a list of primers and probes, see Table 1. We routinely use ROX as a passive reference dye to allow compensation of small pipetting errors and of changes in the reaction volume due to evaporation. Probes and primers are designed with the software *PrimerExpress* 2.0, which is supplied with the ABIPrism 7500 System. Whenever possible, positions of primers or probes are chosen to span a splice junction for minimizing background amplification of contaminating DNA templates.

Reaction mixture

5×PCR buffer	5 µl	
Forward primer 1 (10 µM)	1.5 µl	600 nM
Reverse primer 1 (10 µM)	1.5 µl	600 nM
Probe 1 (10 µM)	0.66 µl	260 nM
Enzyme mixture	1 µl	
ROX (10 µM)	0.33 µl	133 nM
$MgCl_2$ (25 mM)	1.5 µl	1.5 mM
dNTPs (10 mM each)	1 µl	400 µM
Template	xµl	
H_2O	ad 25 µl	

Cycler conditions

PCR program	Time	Temperature	Repeats
cDNA synthesis	30 min	50°C	
Activation of HotStar-Taq polymerase	15 min	95°C	
Denaturation	15 s	94°C	40–50×
Annealing and extension	60 s	60°C	

Multiplex RT-qPCR

The ABIPrism 7500 is a system with five wavelength filters (A–E) and is thus able to detect up to five dyes simultaneously. This allows for a multiplex RT-qPCR in which several probes with distinct labels are monitored in one reaction tube for the same test sample. To establish a multiplex RT-qPCR, suitable labelling dyes for the probes need to be chosen. Optimal are those with the highest difference in emission wavelengths, for instance FAM (Filter A), Bodipy-TMR (Filter C) and Cy5 (Filter E). Filter D is occupied by ROX. Quenchers with auto-fluorescence (e.g. TAMRA) should not be used, as they would occupy filters. We usually use Blackhole™ quenchers (BHQ). The selected probes need to be validated in singleplex, duplex and triplex RT-qPCR assays with corresponding synthetic transcripts as templates. The C_q-values and PCR efficiencies should not differ between the singleplex, duplex and triplex reactions. The standard can consist either of a single synthetic transcript encompassing all test sequences as well as of a mixture of synthetic transcripts, but mixtures have first to be validated.

Reaction mixture (for triplex RT-qPCR)

5×PCR buffer	5 µl	
Forward primer 1 (10 µM)	1 µl	400 nM
Reverse primer 1 (10 µM)	1 µl	400 nM
Forward primer 2 (10 µM)	1 µl	400 nM
Reverse primer 2 (10 µM)	1 µl	400 nM
Forward primer 3 (10 µM)	1 µl	400 nM
Reverse primer 3 (10 µM)	1 µl	400 nM
Probe 1 (10 µM)	0.66 µl	260 nM
Probe 2 (10 µM)	0.66 µl	260 nM
Probe 3 (10 µM)	0.66 µl	260 nM
Enzyme mixture	1 µl	
ROX (10 µM)	0.33 µl	133 nM
$MgCl_2$ (25 mM)	1.5 µl	1.5 mM
dNTPs (10 mM each)	1.67 µl	668 µM
Template	×µl	
H_2O	ad 25 µl	

Cycler conditions

PCR program	Time	Temperature	Repeats
cDNA synthesis	30 min	50°C	
Activation of HotStar-Taq polymerase	15 min	95°C	
Denaturation	15 s	94°C	40–50×
Annealing and extension	60 s	60°C	

♦♦♦♦♦♦ VI. SIMULTANEOUS DETECTION OF TWO VIRUSES IN CO-INFECTED HOST TISSUES

Co-infection of mice with two different viruses, for instance with a gene deletion mutant of mCMV and the corresponding revertant virus, allows a direct comparison of the replicative fitness of the two viruses in the immunocompromised host. In addition, the immune control of the two viruses can be compared in (a) the immunocompetent host, (b) under conditions of immunological reconstitution following BMT and (c) after cytoimmunotherapy by adoptive transfer of immune cells. The main advantage is that the fate of the competing viruses can be compared and made visual by histological imaging in various organs of an individual mouse, so that parameters of individual host variance affect both viruses in like manner. Compared with the infection of two experimental groups of mice with either of the two viruses, co-infection analysis thus reduces the statistical costs for significance. In addition, co-infection helps to identify cooperative effects between virus variants in pathogenesis.

An instructive application was the demonstration of the impact of the mCMV-encoded immunoevasin m152 for the success of immunotherapy with CD8 T cells. In immunocompromised C57BL/6 mice, virus mCMV-Δm152 and the corresponding revertant virus mCMV-Δm152-rev replicated to essentially the same levels. Upon increasing selective force by adoptive transfer of graded numbers of CD8 T cells specific for a D^b-restricted epitope of viral protein M45, the deletion mutant was efficiently controlled, whereas the revertant virus escaped (Holtappels *et al.*, 2004).

Procedure: staining of viral DNA by two-colour ISH

General notes: ISH detects the viral genomic DNA within an intranuclear inclusion body formed in the late (L) phase of the virus replication cycle. Viral DNA is highly accumulated in the intranuclear inclusion body, as this is the site of viral DNA packaging. Cytoplasmic inclusion bodies can be detected by ISH only in infected salivary gland epithelial cells (Podlech *et al.*, 1998), as these cells, unlike other cell types, form vacuoles filled with numerous monocapsid virions for secretion into the salivary duct. As with IHC, there are different colour options for single-colour ISH. Two-colour (black and red) ISH is a method that allows to distinguish between two viruses upon co-infection of mice, for instance with two different mCMV

recombinants. Genomes that carry different sequences can be clearly distinguished by probes directed against these differences and stained in black and red colour, respectively (Plate 2). In such cases, speckled black and red staining of cell nuclei reveals a co-infection at the cellular level. Genomes that differ just by a physical gene deletion, with no replacement by a foreign sequence, are distinguished from the corresponding WT or revertant virus genomes by absence of black staining with a probe directed against the deleted sequence. An optional gene shared between the two viruses (we usually use gene *M55/gB*) is visualized with the respective probe and red staining. Accordingly, the deletion mutant is identified by red staining, whereas WT or revertant virus is characterized by a speckled black and red staining (Holtappels *et al.*, 2004). In such cases, however, co-infection on the cellular level cannot be identified.

Reagents (except those already listed for single-colour IHC)

- Proteinase K buffer:
  - NaCl 0.584 g (10 mM)
  - Tris 6.057 g (50 mM)
  - EDTA 3.722 g (10 mM)

  dissolved in 900 ml aqua dist., adjusted to pH 7.4, and filled up to 1 l
- Proteinase K solution:
  Dissolve proteinase K (cat. no. P 5056; Sigma) in proteinase K buffer. A stock solution of 50 µg in 20 µl is diluted to 1 ml before use.
- Hybridization buffer:
  HybriBuffer ISH (cat. no. R 012-050; Biognostik, Göttingen, Germany)
- Washing solution (SSC, sodium salt citrate); 20-fold conc. stock solution:
  - NaCl 175.32 g (3 M)
  - TSCD 88.23 g (0.3 M)

  (Tri-sodium citrate dihydrate, cat. no. 3580.1; Roth, Karlsruhe, Germany)
  dissolved in 900 ml aqua dist., adjusted to pH 7.0, and filled up to 1 l
- Antibodies:
  - anti-Fluorescein, conjugated with alkaline phosphatase (cat. no. 11 426 338 910; Roche)
  - anti-digoxigenin, conjugated with peroxidase (cat. no. 11 207 733 910; Roche)
- Conjugated nucleotides:
  - Fluorescein-12-dUTP (cat. no. 11 373 242 910; Roche)
  - Digoxigenin-11-dUTP (cat. no. 11 093 088 910; Roche)
- Rubber cement 'Fixogum' (Marabu Company, Tamm, Germany)

Procedure

General notes: Labelled hybridization probes are synthesized by PCR with specific template and primers, using Fluorescein-12-dUTP or Digoxigenin-11-dUTP in the dNTP mix for incorporation into the DNA amplificate. For

optimal staining in ISH, the PCR should be designed so as to result in a probe of >0.5 kbp [for an example and for more PCR details, see Grzimek *et al.* (1999)]. Probes >10 kbp can be derived from labelled plasmids and result in a very strong and specific signal after just a few minutes of development in substrate solution. This is the method of choice for single-colour ISH detecting one type of virus with highest sensitivity (Podlech *et al.*, 1998). Shorter probes are advantageous for the discrimination of virus mutants that differ in single genes or shorter sequences. Oligonucleotide probes give only faint staining even after an extended period of development in substrate solution. If applicable, several oligonucleotides should therefore be used as a probe cocktail. ISH, however, cannot be applied for viruses with a single amino acid point mutation.

Attention! Fluorescein-labelled hybridization probes do not withstand repeated freezing and thawing and should therefore always be frozen in ready-to-use aliquots.

1. Prepare 1 µm (for serial sections) or 2 µm sections of paraffin-embedded tissue, deparaffinize and rehydrate.
2. Digest proteins with proteinase K solution (use ~0.1 ml per slide) for ~18 min at 50°C in a humid chamber.
3. Wash with aqua dist. for 3 min.
4. Block endogenous peroxidase with blocking solution for 30 min at ~20°C.
5. Wash with aqua dist. for 3 min.
6. Dehydrate with graded concentrations of alcohol (50, 70, 90 and 100% isopropanol), 30 s each.
7. Prepare the hybridization solution by adding both labelled probes to the hybridization buffer (0.5–1 µg of each probe per millilitre).
8. Give ca. 5 µl of the hybridization solution onto the dry tissue specimen, cover it with an autoclaved coverslip, seal the edges with rubber cement and let it dry for 1–2 h.
9. Denature at 95°C for 6 min, hybridize at 37°C for ~18 h and remove the sealing.
10. Wash the slides in washing solution, 5 min each in 2x-SSC, 1x-SSC, 0.5x-SSC and 0.1x-SSC.

    Note: From here on, perform all steps in a humid chamber to avoid drying of the tissue sections.
11. Incubate the slides for 30 min at ~20°C with a mixture of the anti-Fluorescein (1:200 in TBS) and anti-Digoxigenin (1:25 in TBS) antibodies.
12. Wash three times with TBS for 5 min.
13. Stain with Fuchsin (cat. no. K 0625; Dako) for 10–50 min, until a red precipitate appears.
14. Wash with TBS for 5 min.
15. Stain with DAB-nickel for 5–10 min, until a black precipitate appears.
16. Wash with TBS for 5 min.
17. Counterstain with haematoxylin solution for 5 s, let the slides dry and seal them with PARAmount and a coverslip for storage.

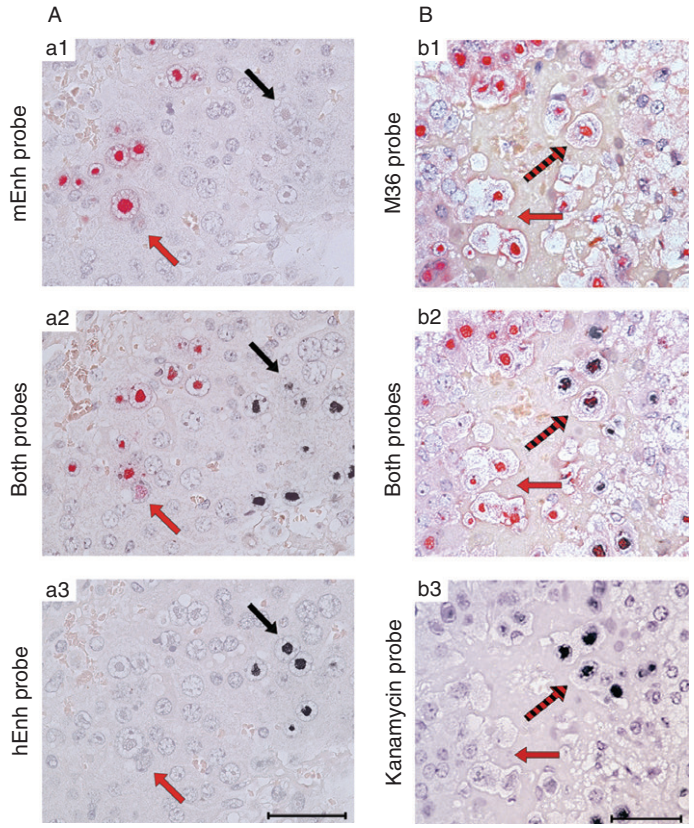

Plate 2. Simultaneous identification of two viruses in co-infected host tissues by two-colour *in situ* DNA hybridization (2C-ISH). (A) Independent replication of an enhancer swap mutant. Immunocompromised BALB/c mice were co-infected with mCMV-WT.Smith and a recombinant virus in which the murine CMV enhancer (mEnh) is replaced with the hCMV enhancer (hEnh). Replication of the two viruses in the co-infected liver was analysed in serial liver tissue sections (a1, a2, a3) by 2C-ISH using DNA probes specific for mEnh (red-stained fluorescein label) and hEnh (black-stained digoxigenin label). The bar marker represents 50 μm. Red and black arrows point to liver cells (primarily hepatocytes) infected with mCMV-WT.Smith and the enhancer swap mutant, respectively. Note the mutually exclusive infection of hepatocytes. For the interpretation of the results, see the text of Chapter 15.III.G. [Modified from Grzimek *et al.* (1999)]. (B) Co-infection of hepatocytes. Immunocompromized BALB/c mice were co-infected with mCMV-WT.BAC and a recombinant virus in which the antiapoptotic gene *M36* is replaced with a kanamycin cassette. Replication of the two viruses in the co-infected liver was analysed in serial liver tissue sections (b1, b2, b3) by 2C-ISH using DNA probes specific for *M36* (red) and the kanamycin sequence (black). The bar marker represents 50 μm. Red and black-and-red-striped arrows point to liver cells (primarily hepatocytes) infected selectively with mCMV-WT.BAC and co-infected with both viruses, respectively. For the interpretation of the results, see the text of Chapter 15.III.G. [Modified from Cicin-Sain *et al.* (2005)]. (See color plate section).

A. Application Example: Independent Replication of An Enhancer Swap Mutant

MIE enhancers of CMVs are key regulators of viral IE transactivator gene expression and are thus regarded as determinants of virus replicative fitness and

pathogenicity in organs of their respective hosts (Stinski and Isomura, 2008). This raised the question of whether CMV enhancers contribute to host species specificity. To test this, the mCMV enhancer was replaced with the hCMV enhancer, and replication of the enhancer swap mutant was compared with that of mCMV-WT. Smith by co-infection of immunocompromised mice. Two-colour ISH with red- and black-stained probes directed against the mCMV and the hCMV enhancer, respectively, revealed distinct foci of infection with either of the two viruses (Plate 2A). This result led to the conclusion that mCMV carrying the hCMV MIE enhancer grows in mouse tissues without a need for trans-complementation of IE gene expression by co-infection of cells with WT virus (Grzimek *et al.*, 1999).

B. Application Example: Trans-Complementation of a Dissemination-Deficient Virus

Deletion of the anti-apoptotic gene *M36* leads to a growth deficiency in macrophages, associated with a dissemination deficiency of the virus from the portal of entry, for instance the footpad tissue after intraplantar infection, to a distant target site such as the liver. This raised the question of whether prevention of apoptosis by trans-complementation of M36 protein upon co-infection with WT virus would enable the deletion mutant to reach the liver. Two-colour ISH with red- and black-stained probes directed against gene *M36* in mCMV-WT.BAC and a kanamycin cassette replacing *M36* in the mutant virus, respectively, revealed frequent co-infection of hepatocytes (Plate 2B). This result led to the conclusion that WT and mutant virus jointly travelled to the liver in co-infected macrophages, in which apoptosis was prevented by M36 protein provided by the WT virus (Cicin-Sain *et al.*, 2005).

♦♦♦♦♦♦ VII. SIMULTANEOUS DETECTION OF TWO PROTEINS IN HOST TISSUES

Detection of two proteins in tissue sections by two-colour IHC allows to relate the expression of two markers in infected host tissues. Ideally, the two proteins should differ in their cellular or subcellular localization. Specifically, antigens should be expressed by different cells or an intranuclear marker should be combined with a cytoplasmic or cell surface marker. The following combinations of markers are technically established for the mCMV model:

1. Viral IE1 (nuclear) and cellular CD3ε (cell membrane) to relate foci of infected cells and T-cell infiltrates within host tissues (Alterio de Goss *et al.*, 1998; Holtappels *et al.*, 1998, 2000; Podlech *et al.*, 2000).
2. Viral IE1 (nuclear) and cellular active caspase-3 (cytoplasm) to relate infection and apoptosis of cells (Cicin-Sain *et al.*, 2008). This showed that deletion of the viral gene *M36* leads to apoptosis of the infected cells rather than to apoptosis of uninfected bystander cells.

3. Viral IE1 (nuclear) and virally encoded GFP (green fluorescent protein) reporter protein (cytoplasmic) to reveal cell-type-specific recombination of floxed reporter virus in infected ($IE1^+$) hepatocytes and endothelial cells of Alb-cre and Tie2-cre transgenic mice, respectively (Sacher *et al.*, 2008).

Procedure: two-colour IHC (2C-IHC)

(for the example of staining for IE1 and CD3ε)

Reagents (except those listed already for single-colour IHC)

- Unmasking solution:

  10 mM Tri-sodium citrate dihydrate, adjusted to pH 6.0
- Dako Biotin Blocking System: Blocking solution (cat. no. X 0590; Dako)
- Antibodies and sera:
  - MAb rat IgG1 directed against the murine CD3ε conserved cytoplasmic epitope ERPPPVPNPDYEPC (clone CD3-12, cat. no. SM1754P; Acris antibodies, Hiddenhausen, Germany)
  - Biotinylated polyclonal goat Ig directed against rat Ig (cat. no. 554014; BD Biosciences)
  - Polyclonal goat antiserum directed against mouse IgG (cat. no. M 5899; Sigma)
  - Alkaline phosphatase anti-alkaline phosphatase (APAAP) soluble complex: mouse MAb, clone AP1B9 (IgG1), conjugated with calf intestine alkaline phosphatase (cat. no. A 7827; Sigma)

Procedure

1. Prepare 1 μm (for serial sections) or 2 μm sections of paraffin-embedded tissue, deparaffinize, rehydrate, wash (aqua dist., 3 min) and partially digest proteins with trypsin solution (see single-colour IHC).
2. Perform *Heat-Induced Epitope Retrieval (HIER)*: boil the slides (in a microwave oven) for 3 min in unmasking solution. Let it cool down to ~20°C (which takes ~45 min) and wash with water.
3. Block endogenous peroxidase and wash with water.

   Note: From here on, perform all steps in a humid chamber to avoid drying of the tissue sections.
4. Block endogenous biotin with the Dako kit, according to the supplier's instructions.
5. Incubate the slides at 4°C for ~18 h with MAb anti-CD3ε, diluted 1:300 in TBS.
6. Wash twice with TBS for 3 min.

7. Incubate at ~20°C for 30 min with biotinylated anti-rat Ab, diluted 1:100 in TBS.
8. Wash twice with TBS for 3 min.
9. Incubate for 30 min at ~20°C with the ABC solution of the ABC-peroxidase kit PK-4000 Standard, freshly prepared 30 min before use, as described by the supplier.
10. Wash three times for 10 min with TBS.
11. Stain for 5–20 min at ~20°C with the peroxidase staining substrate (DAB-nickel), until a black precipitate appears.
12. Wash three times for 10 min with TBS.
13. Incubate the slides for 20 min at ~20°C in a 1:10 dilution of normal rabbit serum in TBS. Do not wash after this step, but let the serum run off.
14. Incubate for ~18 h at 4°C with MAb CROMA 101 (see single-colour IHC).
15. Wash twice with TBS for 3 min.
16. Incubate for 30 min at ~20°C with polyclonal goat antiserum directed against mouse IgG, diluted 1:20 in TBS.
17. Wash twice with TBS for 3 min.
18. Incubate for 30 min at ~20°C with the APAAP complex, diluted 1:50 in TBS.
19. Wash twice with TBS for 3 min.
20. Stain for 10–30 min at ~20°C with the Fuchsin substrate kit, until a red precipitate appears.
21. Wash with TBS for 3 min, counterstain with haematoxylin for 5 s, allow the slides to dry and seal them with PARAmount and a coverslip for storage.

A. Application Example: Epitope-Dependent Infiltration of Infected Liver Tissue by Epitope-Specific CD8 T Cells

Two-colour IHC specific for viral IE1 and cellular CD3ε was used to visualize antiviral protection in the immunocompromised host effected by cytoimmunotherapy with IE1 epitope-specific memory CD8 T cells that were purified by TCR-based cell sorting using MHC-peptide dimers (Pahl-Seibert *et al*., 2005; Böhm *et al*., 2008a) or, alternatively, with cells of an IE1 epitope-specific cytolytic T-lymphocyte (CTL) line (Plate 1B). Typically, infection was confined by focal infiltrates in which few infected hepatocytes were surrounded by infiltrating CD8 T cells (panel **a**). Epitope specificity of the protection was tested by infection with a virus mutant lacking the IE1 epitope due to a point mutation L176A at the C-terminal MHC anchor residue position of the IE1 peptide (Simon *et al*., 2006; Böhm *et al*., 2008a). This indeed abolished the control of virus replication, as it became evident from numerous infected cells localizing around plaque-like tissue lesions (panel **b**). Notably, CD8 T-cell infiltrates were missing after infection with the mutant. This finding showed that formation of focal infiltrates depends on the presentation of the cognate epitope (Böhm *et al*., 2008a).

♦♦♦♦♦♦ VIII. CYTOIMMUNOTHERAPY BY ADOPTIVE CD8 T-CELL TRANSFER

Approaches of experimental cytoimmunotherapy of CMV disease in the murine model were usually performed with mCMV peptide-specific polyclonal cytolytic T-lymphocyte lines (CTLLs) or with *ex vivo* isolated CD8 T lymphocytes derived from the spleen of mCMV-infected mice either as polyclonal and polyspecific populations or after TCR-based cytofluorometric enrichment of defined peptide specificities. The currently known CD8 T-cell epitopes from mCMV are presented either in haplotype *H-2*^{d} or *H-2*^{b}. Therefore, cytoimmunotherapeutic approaches with mCMV-specific CD8 T cells are so far limited to peptides presented by the corresponding MHC class I molecules K^d, D^d and L^d as well as K^b and D^b, respectively. The principles of preemptive and therapeutic CD8 T-cell-based immunotherapy of CMV infection in the murine model have been reviewed recently (Holtappels *et al.*, 2006b, 2008a). We therefore focus here on the methods.

Procedure: generation of CTLLs

1. Sensitize immunocompetent 8- to 10-week-old BALB/c or C57BL/6 mice by subcutaneous infection at one of the hind footpads with 10^5 PFU of cell culture-propagated and purified mCMV.
2. Prepare the spleen cells from the mCMV-infected mice by using standard protocols including red blood cell lysis. Usually, mice at 12 weeks post-infection (p. i.) or later were used as donors of memory CD8 T cells. Generation of CTLLs also works with splenocytes recovered 1 week p.i., which contain recently primed CD8 T cells.
3. Seed 1.5×10^7 spleen cells in 2 ml wells (24-well flat-bottomed culture plates) in 1.5 ml of MEM Alpha + GlutaMAX-I Medium (cat. no. 32561; Invitrogen), supplemented with 7.5% FCS, 100 U ml^{-1} Penicillin, 0.1 mg ml^{-1} Streptomycin, 5×10^{-5} M 2-mercaptoethanol and 10 mM HEPES, with no IL-2 added. For the generation of a stable CTLL, add synthetic peptide in a concentration optimized for every peptide (Table 4). Note that the peptide concentration is critical for the generation of a CTLL, as too low as well as too high doses can be suboptimal.
4. At day 4 after seeding, add recombinant IL-2 in 0.5 ml of fresh medium per well, supplemented as described above. The IL-2 dose required has to be tested for each batch of IL-2. We routinely use a final concentration of 100 U ml^{-1} of recombinant human IL-2 (rhIL-2; 8.2×10^6 U per mg of pure protein; generously supplied by the Sandoz Research Institute, Vienna, Austria).

5. The first restimulation is performed at day 7 by a 1:1 split of the cultures and readdition of 1 ml of stimulation suspension containing supplemented medium, complemented with the appropriate doses of peptide and IL-2, plus 5×10^5 γ-irradiated (30 Gy) normal spleen cells as feeder cells. Further rounds of splitting and restimulation depend on the growth of the particular CTLL, but the time between two restimulations should not exceed 2 weeks.
6. Usually, CTLLs reach epitope-monospecificity after 2–5 rounds of restimulation, but stay polyclonal and retain expression of the CD8 co-receptor molecule (Pahl-Seibert *et al.*, 2005). These parameters, however, need to be tested for each individual CTLL.

Note: All mCMV peptide-specific CTLLs that we have tested so far are efficient in controlling mCMV-WT infection in indicator recipients upon adoptive transfer (Table 4) with the notable exception of CTLLs specific for the D^b-restricted epitope 985-HGIRNASFI-993 derived from protein M45 (Holtappels *et al.*, 2004, 2006a, 2009). Currently (by July 2010) known *H-2*^{d}-restricted mCMV peptides are listed in Table 4, published *H-2*^{b}-restricted peptides are listed in Munks *et al*. (2006).

All CTLLs are routinely tested for their functional avidity in assays of effector cell function (Figure 3). The cytolytic assay (e.g. the ^{51}Cr-release assay) measures lysis of epitope-presenting target cells and reveals the bulk cytolytic activity of the effector cell population. In contrast, the enzyme-linked immunospot (ELISPOT) assay is a single-cell assay that reveals the frequencies of effector cells capable of secreting a cytokine, for instance IFN-γ, upon stimulation with epitope-presenting cells [for the methods, see Podlech *et al*. (2002), and other chapters of this book]. For the calculation of the frequencies and their 95% confidence intervals by intercept-free linear regression analysis, see Pahl-Seibert *et al*. (2005) and Böhm *et al*. (2008b). For the evaluation of functional avidity, effector cell assays are performed with target cells loaded exogenously with the cognate synthetic antigenic peptide at defined concentrations in order to correlate intensity of the effector cell response and epitope presentation density. As shown for the example of a particular CTLL specific for the IE1 epitope (IE1-CTLL), the threshold peptide concentration for triggering cytolytic activity was between 10^{-11} and 10^{-12} M, whereas the threshold for IFN-γ secretion was 10^{-12} M defining the highest functional avidity represented by a low proportion of cells in the effector cell population. As the ELISPOT assay measures cell frequencies, one can determine the avidity distribution for the effector cell population, which, for the specific example, showed a peak frequency (modal value) at 10^{-11} M, and an avidity range from 10^{-12} to 10^{-8} M (Figure 3). For calculating the Gaussian-distributed 'avidity distribution' from the experimentally determined 'cumulative avidity distribution', see Böhm *et al*. (2008b).

Table 4. Antigenic peptides of mCMV in the H-2[d] haplotype

ORF	Protein	Phase	Sequence	Restriction	Antigenicity	Immunotherapy with CTLL	CTLL stimulation concentration	Detection limit(CTL assay)
m04	gp34	E/L	243-YGPSLYRRF(F)-252	D	Subdominant	Positive[a]	10^{-8} M	$10^{-9}/10^{-10}$ M
m18	not defined	E	346-SGPSRGRII-354	D	Subdominant	Positive[b]	10^{-10} M	$10^{-10}/10^{-11}$ M
M45	p150-160	E/L	507-VGPALGRGL-515	D	Subdominant	Positive[c]	10^{-10} M	$10^{-10}/10^{-11}$ M
M83	pp105	E/L	761-YPSKEPFNF-769	L	Subdominant	Positive[d]	10^{-10} M	$10^{-11}/10^{-12}$ M
M84	p65	E	297-AYAGLFTPL-305	K	Subdominant	Positive[d]	10^{-10} M	$10^{-10}/10^{-11}$ M
M105	p111.4	E	207-TYWPVVSDI-215	K	Intermediate	u.i.	10^{-10} M	$10^{-10}/10^{-11}$ M
m123	IE1/pp76/89	IE	168-YPHFMPTNL-176	L	Dominant	Positive[a,e]	10^{-9} M	$10^{-11}/10^{-12}$ M
m145	MHC class I like	E	451-CYYASRTKL-459	K	Intermediate	Positive[f]	10^{-9} M	$10^{-10}/10^{-11}$ M
m164	gp36.5	E	167-AGPPRYSRI-175	D	Dominant	Positive[e]	10^{-9} M	$10^{-9}/10^{-10}$ M

IE: immediate-early, CTLL: cytolytic T-lymphocyte lines, u.i.: under investigation
[a]Holtappels *et al*. (2000).
[b]Holtappels *et al*. (2006b).
[c]Holtappels *et al*. (2006a, 2009).
[d]Holtappels *et al*. (2001).
[e]Holtappels *et al*. (2002).
[f]Holtappels *et al*. (2008b).

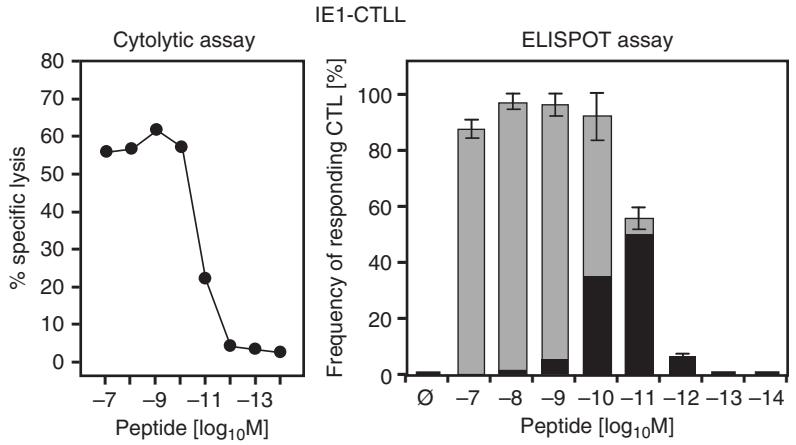

Figure 3. Comparison of functional avidities of a CTLL in two assays of effector cell function. (Left panel), cytolytic (4-h ^{51}Cr-release) assay. (Right panel), IFN-γ-based ELISPOT assay. Target and stimulator cells were P815 mastocytoma cells exogenously loaded with synthetic IE1 peptide (see Table 4) by incubation at the indicated peptide concentrations. Ø: P815 target cells, with no peptide added. Effector cells with cognate TCRs were CTL of an IE1 epitope specific but still polyclonal CTLL (IE1-CTLL). Cytolytic activity was determined at an effector:target cell ratio of 15:1. Dots represent the mean of triplicate measurements. Frequencies of cells responding in the ELISPOT assay by secretion of IFN-γ were determined by seeding graded numbers of effector cells (200, 150, 100 and 50) in triplicates, followed by intercept-free linear regression analysis of spot counts. Gray bars represent the experimentally determined frequencies of responding cells resulting in a cumulative avidity distribution function, with error bars indicating the 95% confidence intervals. Superimposed black bars reveal the corresponding Gaussian avidity distribution of differential frequencies calculated as described previously (Böhm *et al.*, 2008b). Note that the differential frequencies – not the measured frequencies – are the ones that represent cells actually responding at the indicated peptide concentration.

Procedure: immunomagnetic enrichment of CD8 T lymphocytes

General notes: CD8 T cells from the spleens of mice were enriched by positive immunomagnetic cell sorting using the autoMACS system (Miltenyi Biotec Systems, Bergisch Gladbach, Germany) following the protocol recommended by the manufacturer. Usually, a two-column separation was performed to reach a purity of >95%. According to the manufacturer's instructions, separation is efficient for up to 2×10^8 labelled cells and a maximum of 4×10^9 cells in total. *Attention!* Cells and solutions should be kept cold to avoid capping of antibodies.

1. Prepare a single-cell leukocyte suspension, e.g. from spleen and lungs (Podlech *et al.*, 2002).
2. Determine the cell number and resuspend the pelletized cells in 90 µl of MACS buffer (PBS + 0.5% BSA + 2 mM EDTA; pH 7.2) per 1×10^7 total cells.
3. Add 10 µl of CD8a (Ly-2) MicroBeads (cat. no. 130-049-401; Miltenyi Biotec, Bergisch Gladbach, Germany) per 10^7 total cells.

Note: If CD8 T cells are to be isolated from the lungs, use 80 µl of MACS buffer and 20 µl of CD8a beads per 10^7 total cells.

4. Mix thoroughly and incubate for 15 min at 4–8°C. Soft shaking during the incubation period is recommended when high cell numbers are labelled.
5. Wash by adding MACS buffer in the 20-fold labelling volume (e.g. when labelling is performed with 10 µl beads + 90 µl buffer, use 2 ml of MACS buffer for washing).
6. Centrifuge at 300 g for 10 min and remove supernatant completely.
7. Resuspend the pellet (up to 10^8 cells) in 500 µl of MACS buffer.
8. Place the tube containing the magnetically labelled cells into the autoMACS Separator and start the separation program. We routinely use the positive selection program 'Posseld' for the two-column separation.

Ex vivo analysis of epitope-specific CD8 T lymphocytes

For determining the functional activities of epitope-specific CD8 T cells, these cells can be stained and isolated from immunomagnetically enriched *ex vivo* CD8 T-cell populations (see above) by cytofluorometric cell sorting using MHC-peptide dimers as described in detail elsewhere (Pahl-Seibert *et al.*, 2005). Alternatively, other MHC-peptide multimers can be used for the labelling of epitope-specific TCRs.

The frequencies of *ex vivo* CD8 T cells specific for defined antigenic peptides (Table 4) can be determined by using immunomagnetically enriched CD8 T-cell populations as effector cells in the ELISPOT assay and in the cytofluorometric intracellular cytokine assay, as well as by direct cytofluorometric quantitation after staining with MHC-peptide multimers. The recently developed technique of ORF antigenicity screening allows to identify also antigenic ORFs of mCMV for which the corresponding antigenic peptides are not yet known.

Procedure: determination of the specificity repertoire of virus-specific CD8 T lymphocytes by genome-wide mCMV ORF library screening

General note: For monitoring the specificity repertoire of mCMV-primed *ex vivo* CD8 T-cell populations, that is of CD8 T cells engaged in the antiviral response, the recently generated mCMV ORF library, spanning the whole mCMV genome (Munks *et al.*, 2006; Holtappels *et al.*, 2008c), can be employed. It is based on the transfection of cells with mCMV ORF expression plasmids followed by stimulation of effector cell populations with the transfected cells. Activated ORF-specific CD8 T cells are cytofluorometrically identified by intracellular IFN-γ staining. An example for ORF library analysis of the specificity repertoire of spleen-derived CD8 T cells primed at 1 week after intraplantar infection is shown in Figure 4. A list relating ORF library numbers and ORFs is given as a supplemental table in Holtappels *et al.* (2008c).

Loading of DNA-microwell plates

1. Adjust the ORF-plasmid preparations to a concentration of 0.25 μg of DNA per 10 μl.
2. Pipette 20 μl (for transfection in duplicates, see step 7) of each plasmid-DNA into a 96-well round-bottomed microwell plate.

   This is made in advance of the test. The plates can be stored frozen at –20°C.

Day 1: Seeding of APCs

3. Seed transfectable fibroblasts (e.g. SV40-transformed MEF) in 100 μl of culture medium at a density of 12,000 cells per well of a 96-well flat-bottomed microwell plate. Calculate for duplicate transfections.

Day 2: Transfection of APCs

4. The transfection medium consists of a mixture of FuGENE 6 (cat. no. 11 814 443 001; Roche) and OPTI-MEM I + GlutaMAX-I (cat. no. 51985; Invitrogen). The optimal FuGENE:DNA ratio was tested to be 3:1 (vol/wt). As 0.25 μg of DNA proved to be the optimal amount for transfection in 96-well microcultures, 0.75 μl of FuGENE are required per transfection well. Calculate the volume of FuGENE needed for the whole assay. Mix FuGENE with OPTI-MEM + GlutaMAX in a ratio of 1:32 for a final volume of 25 μl per transfection well.
5. Mix the plasmid-DNAs (20 μl per well) in the DNA plates (see step 2) with 50 μl of FuGENE:OPTI-MEM per well and incubate for at least 15 min at ~20°C.
6. Replace the culture medium of the fibroblasts with 40 μl of OPTI-MEM + GlutaMAX-I.
7. Pipette 30–35 μl of the DNA:FuGENE:OPTI-MEM mixture per transfection culture in duplicates.
8. Incubate for at least 3 h at 37°C.
9. Add 100 μl of cell culture medium.

Day 4: Stimulation of the effector cells

10. Prepare the effector cells from organs of interest by using standard protocols, e.g. splenocytes from mCMV-infected mice.
11. Replace the medium of the transfection microcultures with 50 μl of supplemented MEM Alpha + GlutaMAX-I medium (see *Generation of CTLLs*, step 3).
12. Add 1×10^6 effector cells in 100 μl of the medium.
13. For the intracellular cytokine assay, add 50 μl of brefeldin A (BD Golgi-Plug; cat. no. 51-2301KZ; BD Biosciences Pharmingen), diluted 1:250 in the

medium to block secretion of IFN-γ. Note that brefeldin A should be used at a final dilution of 1:1000 in the cultures.
14. Centrifuge for 1 min at 216 g.
15. Incubate for at least 6 h at 37°C.
    Note: For known epitopes, control microcultures of effector cells seeded at a density of 2×10^6 cells per well in a 96-well round-bottomed microwell plate should be stimulated with the respective synthetic peptides (added at the saturating final concentration of 1×10^{-6} M) and incubated in the presence of brefeldin A, accordingly.
16. After incubation, discard 100 µl of the supernatants, combine the effector cells from the duplicate transfection cultures (representing the same ORF) and transfer them into a microculture of round-bottomed 96-well plates.
17. Centrifuge the plates containing the stimulated effector cells for 3 min at 261 g at 4°C.
18. Wash once with 100 µl of FACS buffer.
19. Stain the stimulated effector cells (from both the previous transfection cultures and the peptide control cultures) with PE-Cy5-labelled anti-mouse CD8a (Ly-2) MAb (clone 53-6.7; cat. no. 553034; BD Biosciences Pharmingen) diluted 1:200 in FACS buffer.
20. Wash once with 100 µl of FACS buffer.
21. Fix and permeabilize the cells with 75 µl of BD Cytofix/Cytoperm (cat. no. 51-2090KZ; BD Biosciences Pharmingen).
22. Stain for intracellular IFN-γ with FITC-labelled anti-mouse IFN-γ MAb (clone XMG1.2; cat. no. 554411; BD Biosciences Pharmingen) diluted 1:200 in BD Perm/Wash Buffer-1x (cat. no. 51-2091KZ; BD Biosciences Pharmingen).
23. Wash twice with 100 µl of BD Perm/Wash Buffer-1x.
24. Resuspend the cells in 150 µl of FACS buffer and transfer the probes to microtubes for cytofluorometric analysis. Labelled cells can be stored at this stage at 4°C until the next day.

Day 5: Cytofluorometric analysis

25. Analyse the cells cytofluorometrically by setting electronic gates on lymphocytes and on positive PE-Cy5 fluorescence to restrict the analysis of IFN-γ expression to CD8 T lymphocytes.

Procedure: preemptive CD8 T-cell transfer and infection

1. Subject recipient mice to haematoablative treatment by total body γ-irradiation with a single dose of 6.5 Gy (BALB/c mice) or 7 Gy (C57BL/6 mice), delivered by an appropriate γ-ray source. We use a ^{137}Cs γ-ray source (model OB58 Buchler, now STS Steuerungstechnik & Strahlenschutz

GmbH, Braunschweig, Germany) with a dose rate of ca. 0.6 Gy per minute that is adjusted monthly. This treatment is usually performed at 4 and 22 h prior to the CD8 T-cell transfer for BALB/c and C57BL/6 mice, respectively. Infection is performed ~2 h after the cell transfer.

Note: For therapeutic cytoimmunotherapy [for a review, see Holtappels *et al*. (2008a)] CD8 T cells are transferred on day 6 after local (e.g. intraplantar) infection. At this time, virus has already disseminated to organs and has established organ infection.

2. Warm-up the tail of a recipient mouse gently for ~5 min with an infra-red light bulb (e.g. Philips R95 infraphil, 100 W) to dilate the tail veins.
3. Sterilize the inoculation site with 70% ethanol.
4. Inject 0.5 ml of T-cell suspension (warmed up to body temperature immediately before use) very slowly into one of the two lateral tail veins (i.v.; intravenous cell transfer), while mice are fixed in a special V-shaped device. Use a 2 ml syringe with a 0.45 × 12 mm cannula. To serve as controls, at least 5 mice are left without T-cell transfer.
5. Infect recipient mice at one of the hind footpads (intraplantar infection). In detail, fix the recipient mouse in a V-shaped device, sterilize the footpad surface with 70% ethanol and inject – very slowly – 25 µl of virus suspension in an appropriate dilution of the virus stock (10^5 PFU was mostly used in our experiments) in physiological saline. Use a 1 ml syringe with a 0.4 × 12 mm cannula.

Note 1: Volumes >25 µl as well as inoculation of more than one footpad are not regularly allowed in Germany according to a decision of the Ethics commission at the *Regierungspraesidium Tuebingen*, decision no. AZ 37-9553. In our experience, bilateral intraplantar infection does not give any benefit, as it rather reduces the yield of primed CD8 T cells per popliteal lymph node. Unilateral intraplantar infection proved to result in a well reproducible CD8 T-cell priming in immunocompetent mice and in a low variance of VTs in organs of immunocompromised mice. Therefore, except if the scientific question requires a comparison between ipsilateral and contralateral side (Cicin-Sain *et al*., 2005), unilateral infection is recommended. We do not routinely use the intravenous, intraperitoneal and intranasal routes of infection. Intravenous infection circumvents the local immune control and lymphoid drainage. By reaching the organs directly and within seconds, the tissue infection is higher than for other routes of virus entry.

Note 2: In the murine model of syngeneic BMT [for a review, see Holtappels *et al*. (2006b)], mCMV infection is controlled by CD8 T cells newly generated in the course of lympho-haematopoietic reconstitution. Adoptive transfer of CD8 T cells in addition to endogenous reconstitution after BMT improves the control of acute infection, reduces the load of latent viral DNA and thus also the risk of virus recurrence (Steffens *et al*., 1998a). The method of experimental BMT in the mouse has been described in detail in the second edition of this book (Podlech *et al*., 2002).

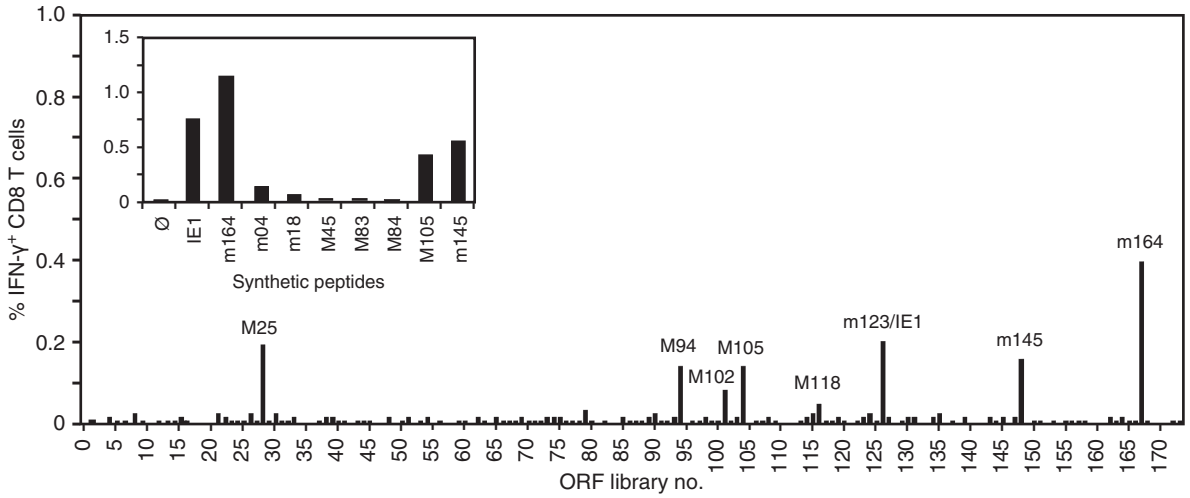

Figure 4. Determination of specificity repertoires by viral genome-wide ORF antigenicity screening. The repertoire of specificities involved in the acute CD8 T-cell response to mCMV in the BALB/c mouse was tested for spleen cells at 1 week after priming by intraplantar infection with mCMV-WT. BAC. The cells were stimulated with SV40-transformed fibroblasts transiently transfected with an ORF library of expression plasmids, and responding CD8 T cells were identified on the basis of IFN-γ production by cytofluorometric intracellular cytokine staining. A list allocating library numbers to ORFs is published elsewhere (Holtappels *et al.*, 2008c, supplemental material, table S1). ORFs eliciting peaks of response are indicated. Note that positive ORFs may represent more than one antigenic peptide. On the other hand, antigen presentation in transfected cells is not necessarily optimal. Thus, to get reference values for the frequencies of effector cells specific for known epitopes, aliquots of the same spleen cell population were stimulated with a saturating concentration (10^{-6} M) of the indicated antigenic synthetic peptides and assayed in parallel to the ORF library (inset figure). Ø: spleen cells, with no viral peptide added.

Monitoring of the Outcome and the Efficiency of Cytoimmunotherapy

Organ infection is monitored between day 11 and 13 after cell transfer, which is the time when immunocompromised mice not receiving therapy (control group) succumb to multiple-organ CMV disease. Virus replication in organs of interest (we usually test spleen, lungs and liver) is evaluated by quantitating infectivity (PFU assay), number of viral genomes (qPCR) and infected cells in tissues (IE1-specific IHC). As an example, Figure 5A shows decreasing infection of organs as a result of increasing numbers of adoptively transferred CTLs and Figure 5B shows immunohistological images illustrating extensive histopathology with plaque-like virus foci (CMV hepatitis) in absence of therapy and the almost complete prevention of liver infection by immunotherapy with 10^6 cells of an epitope (m18)-specific CTLL.

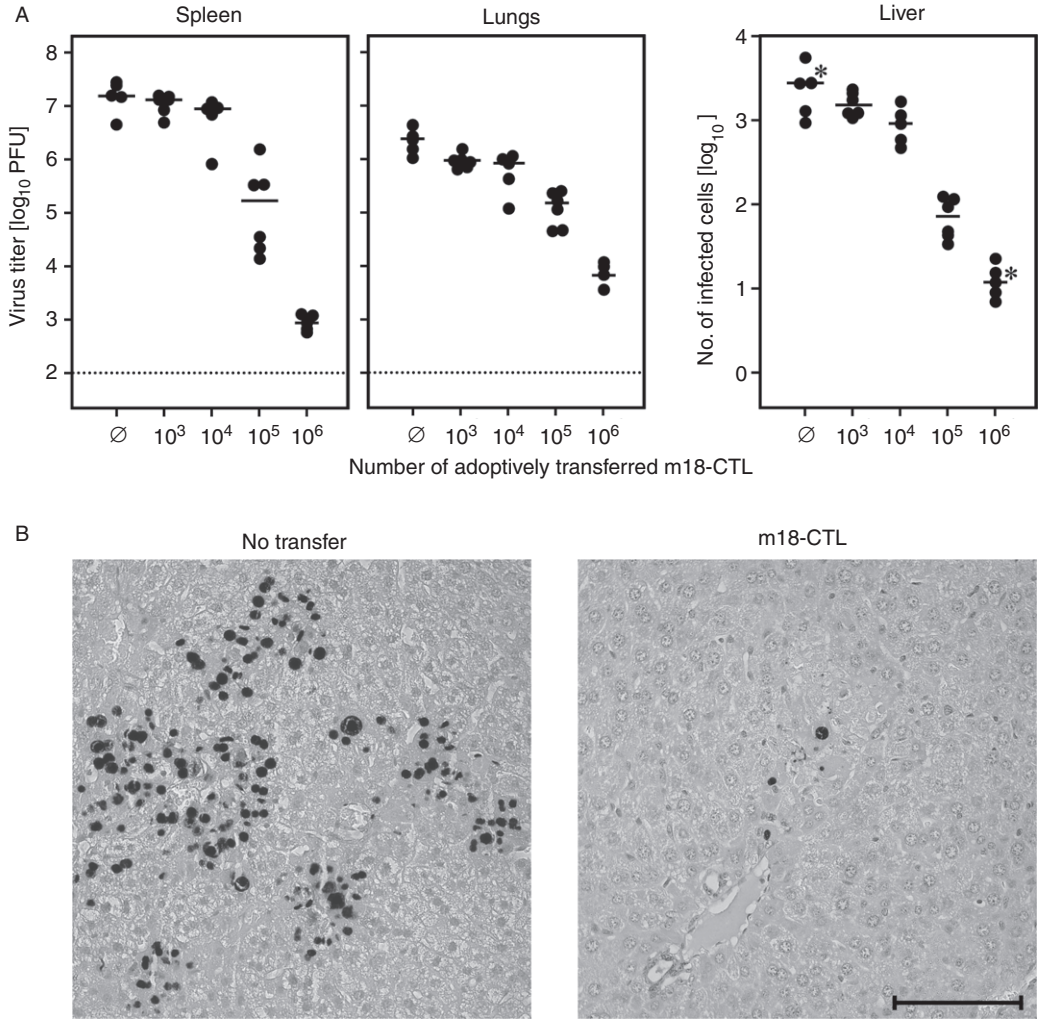

Figure 5. 'Proof of Principle': Control of mCMV infection by adoptive transfer of antiviral CD8 T cells. Graded numbers of cells (m18-CTL) of a CTLL specific for the m18 peptide (see Table 4) were transferred into immunocompromised BALB/c recipients infected with mCMV-WT.Smith. (A) Viral replication was assessed on day 11 after infection and cell transfer by the PFU assay (performed under conditions of *CEI*) in homogenates of spleen and lungs and by counting the number of infected cells (IE1-specific IHC) in representative 10 mm^2 areas of liver tissue sections. Black dots represent data for individual recipients, with the median values marked. Ø: no cell transfer. The dotted line indicates the detection limit of the PFU assay. (B) IHC images (black staining of intranuclear IE1 antigen) of liver tissue sections derived from mice with median infection densities (marked by asterisks in A) for the experimental groups with no cell transfer (left panel; note the plaque-like tissue lesions) and transfer of 10^6 m18-CTL (right panel). The bar marker represents 100 μm.

Contact

Lemmermann@uni-mainz.de	(for all kinds of everything)
Podlech@uni-mainz.de	(for histology & pathology)
Seckert@uni-mainz.de	(for qPCR technologies)
Kai.Kropp@ed.ac.uk	(for qPCR technologies)
Grzimek@uni-mainz.de	(for molecular virology)
Matthias.Reddehase@uni-mainz.de	(for general questions)
R.Holtappels@uni-mainz.de	(for cellular immunology)

Acknowledgements

The authors were supported by the Deutsche Forschungsgemeinschaft, Clinical Research Group KFO 183, individual project TP8 'Establishment of a challenge model for optimizing the immunotherapy of CMV diseases' and collaborative research centre SFB 490, individual projects E2, E3 and E4.

References

Alterio de Goss, M., Holtappels, R., Steffens, H. P., Podlech, J., Angele, P., Dreher, L., Thomas, D. and Reddehase, M. J. (1998). Control of cytomegalovirus in bone marrow transplantation chimeras lacking the prevailing antigen-presenting molecule in recipient tissues rests primarily on recipient-derived CD8 T cells. *J. Virol*. **72**, 7733–7744.

Andrews, D. M., Andoniou, C. D., Granucci, F., Ricciardi-Castagnoli, P. and Degli-Esposti, M. A. (2001). Infection of dendritic cells by murine cytomegalovirus induces functional paralysis. *Nat. Immunol*. **2**, 1077–1084.

Böhm, V., Podlech, J., Thomas, D., Deegen, P., Pahl-Seibert, M. F., Lemmermann, N. A., Grzimek, N. K., Oehrlein-Karpi, S. A., Reddehase, M. J. and Holtappels, R. (2008a). Epitope-specific *in vivo* protection against cytomegalovirus disease by CD8 T cells in the murine model of preemptive immunotherapy. *Med. Microbiol. Immunol*. **197**, 135–144.

Böhm, V., Simon, C. O., Podlech, J., Seckert, C. K., Gendig, D., Deegen, P., Gillert-Marien, D., Lemmermann, N. A., Holtappels, R. and Reddehase, M. J. (2008b). The immune evasion paradox: immunoevasins of murine cytomegalovirus enhance priming of CD8 T cells by preventing negative feedback regulation. *J. Virol*. **82**, 11637–11650.

Brune, W., Wagner, M. and Messerle, M. (2006). Manipulating cytomegalovirus genomes by BAC mutagenesis: strategies and applications. In: *Cytomegaloviruses: Molecular Biology and Immunology* (M. J. Reddehase, ed), pp. 61–89. Caister Academic Press, Norfolk, UK.

Busch, F. W., Mutter, W., Koszinowski, U. H. and Reddehase, M. J. (1991). Rescue of myeloid-lineage-committed preprogenitor cells from cytomegalovirus-infected bone marrow stroma. *J. Virol*. **65**, 981–984.

Bustin, S. A. (2000). Absolute quantification of mRNA using real-time reverse transcription polymerase chain reaction assays. *J. Mol. Genet. Med*. **25**, 169–193.

Bustin, S. A., Benes, V., Garson, J. A., Hellemans, J., Huggett, J., Kubista, M., Mueller, R., Nolan, T., Pfaffl, M. W., Shipley, G. L. *et al.* (2009). The MIQE guidelines: minimum information for publication of quantitative real-time PCR experiments. *Clin. Chem*. **55**, 611–622.

Campbell, A. E., Cavanaugh, V. J. and Slater, J. S. (2008). The salivary glands as a privileged site of cytomegalovirus immune evasion and persistence. *Med. Microbiol. Immunol*. **197**, 205–213.

Chong, K. T., Gould, J. J. and Mims, C. A. (1981). Neutralization of different strains of murine cytomegalovirus (MCMV)-effect of *in vitro* passage. *Arch. Virol*. **69**, 95–104.
Chong, K. T. and Mims, C. A. (1981). Murine cytomegalovirus particle types in relation to sources of virus and pathogenicity. *J. Gen. Virol*. **57**, 415–419.
Cicin-Sain, L., Podlech, J., Messerle, M., Reddehase, M. J. and Koszinowski, U. H. (2005). Frequent coinfection of cells explains functional *in vivo* complementation between cytomegalovirus variants in the multiply infected host. *J. Virol*. **79**, 9492–9502.
Cicin-Sain, L., Ruzsics, Z., Podlech, J., Bubic, I., Menard, C., Jonjic, S., Reddehase, M. J. and Koszinowski, U. H. (2008). Dominant-negative FADD rescues the *in vivo* fitness of a cytomegalovirus lacking an antiapoptotic viral gene. *J. Virol*. **82**, 2056–2064.
Cobbold, M., Khan, N., Pourgheysari, B., Tauro, S., McDonald, C., Osman, H., Assenmacher, M., Billingham, L., Steward, C., Crawley, C. *et al*. (2005). Adoptive transfer of cytomegalovirus-specific CTL to stem cell transplant patients after selection by HLA-peptide tetramers. *J. Exp. Med*. **202**, 379–386.
Däubner, T., Fink, A., Seitz, A., Tenzer, S., Müller, J., Strand, D., Seckert, C. K., Janssen, C., Renzaho, A., Grzimek, *et al*. (2010). A novel transmembrane domain mediating retention of a highly motile herpesvirus glycoprotein in the endoplasmic reticulum. *J. Gen. Virol*. **91**, 1524–1534.
de Kok, J. B., Roelofs, R. W., Giesendorf, B. A., Pennings, J. L., Waas, E. T., Feuth, T., Swinkels, D. W. and Span, P. N. (2005). Normalization of gene expression measurements in tumor tissues: comparison of 13 endogenous control genes. *Lab. Invest*. **85**, 154–159.
Dobonici, M., Podlech, J., Steffens, H.-P., Maiberger, S. and Reddehase, M. J. (1998). Evidence against a key role for transforming growth factor-β1 in cytomegalovirus-induced bone marrow aplasia. *J. Gen. Virol*. **79**, 867–876.
Ebeling, A., Keil, G. M., Knust, E. and Koszinowski, U. H. (1983). Molecular cloning and physical mapping of murine cytomegalovirus DNA. *J. Virol*. **47**, 421–433.
Einsele, H. and Hamprecht, K. (2003). Immunotherapy of cytomegalovirus infection after stem-cell transplantation: a new option? *Lancet* **362**, 1343–1344.
Emery, V. C. (1998). Relative importance of cytomegalovirus load as a risk factor for cytomegalovirus disease in the immunocompromised host. In: *Monographs in Virology 21: CMV-Related Immunopathology* (M. Scholz, H. F. Rabenau, H. W. Doerr, and J. Cinatl, Jr., eds), pp. 288–301. Karger, Basel.
Ghazal, P., Visser, A. E., Gustems, M., García, R., Borst, E. M., Sullivan, K., Messerle, M. and Angulo, A. (2005). Elimination of ie1 significantly attenuates murine cytomegalovirus virulence but does not alter replicative capacity in cell culture. *J. Virol*. **79**, 7182–7194.
Grzimek, N. K., Podlech, J., Steffens, H. P., Holtappels, R., Schmalz, S. and Reddehase, M. J. (1999). *In vivo* replication of recombinant murine cytomegalovirus driven by the paralogous major immediate-early promoter-enhancer of human cytomegalovirus. *J. Virol*. **73**, 5043–5055.
Gubbay, J., Collignon, J., Koopman, P., Capel, B., Economou, A., Münsterberg, A., Vivian, N., Goodfellow, P. and Lovell-Badge, R. (1990). A gene mapping to the sex-determining region of the mouse y chromosome is a member of a novel family of embryonically expressed genes. *Nature* **346**, 245–250.
Hanson, L. K., Slater, J. S., Karabekian, Z., Ciocco-Schmitt, G. and Campbell, A. E. (2001). Products of US22 genes M140 and M141 confer efficient replication of murine cytomegalovirus in macrophages and spleen. *J. Virol*. **75**, 6292–6302.
Ho, M. (2008). The history of cytomegalovirus and its diseases. *Med Microbiol Immunol* **197**, 65–73.
Holtappels, R., Böhm, V., Podlech, J. and Reddehase, M. J. (2008a). CD8 T-cell-based immunotherapy of cytomegalovirus infection: "proof of concept" provided by the murine model. *Med. Microbiol. Immunol*. **197**, 125–134.

Holtappels, R., Gillert-Marien, D., Thomas, D., Podlech, J., Deegen, P., Herter, S., Oehrlein-Karpi, S. A., Strand, D., Wagner, M. and Reddehase, M. J. (2006a). Cytomegalovirus encodes a positive regulator of antigen presentation. *J. Virol*. **80**, 7613–7624.

Holtappels, R., Janda, J., Thomas, D., Schenk, S., Reddehase, M. J. and Geginat, G. (2008b). Adoptive CD8 T cell control of pathogens cannot be improved by combining protective epitope specificities. *J. Infect. Dis*. **197**, 622–629.

Holtappels, R., Munks, M. W., Podlech, J. and Reddehase, M. J. (2006b). CD8 T-cell-based immunotherapy of cytomegalovirus disease in the mouse model of the immunocompromised bone marrow transplantation recipient. In: *Cytomegaloviruses: Molecular Biology and Immunology* (M. J. Reddehase, ed), pp. 383–418. Caister Academic Press, Norfolk, UK.

Holtappels, R., Podlech, J., Geginat, G., Steffens, H. P., Thomas, D. and Reddehase, M. J. (1998). Control of murine cytomegalovirus in the lungs: relative but not absolute immunodominance of the immediate-early 1 nonapeptide during the antiviral cytolytic T-lymphocyte response in pulmonary infiltrates. *J. Virol*. **72**, 7201–7212.

Holtappels, R., Podlech, J., Grzimek, N. K., Thomas, D., Pahl-Seibert, M. F. and Reddehase, M. J. (2001). Experimental preemptive immunotherapy of murine cytomegalovirus disease with CD8 T-cell lines specific for ppM83 and pM84, the two homologs of human cytomegalovirus tegument protein ppUL83 (pp65). *J. Virol*. **75**, 6584–6600.

Holtappels, R., Podlech, J., Pahl-Seibert, M. F., Jülch, M., Thomas, D., Simon, C. O., Wagner, M. and Reddehase, M. J. (2004). Cytomegalovirus misleads its host by priming of CD8 T cells specific for an epitope not presented in infected tissues. *J. Exp. Med*. **199**, 131–136.

Holtappels, R., Simon, C. O., Munks, M. W., Thomas, D., Deegen, P., Kühnapfel, B., Däubner, T., Emde, S. F., Podlech, J., Grzimek, N. K. *et al*. (2008c). Subdominant CD8 T-cell epitopes account for protection against cytomegalovirus independent of immunodomination. *J. Virol*. **82**, 5781–5796.

Holtappels, R., Thomas, D., Podlech, J., Geginat, G., Steffens, H. P. and Reddehase, M. J. (2000). The putative natural killer decoy early gene m04 (gp34) of murine cytomegalovirus encodes an antigenic peptide recognized by protective antiviral CD8 T cells. *J. Virol*. **74**, 1871–1884.

Holtappels, R., Thomas, D., Podlech, J. and Reddehase, M. J. (2002). Two antigenic peptides from genes m123 and m164 of murine cytomegalovirus quantitatively dominate CD8 T-cell memory in the H-2d haplotype. *J. Virol*. **76**, 151–164.

Holtappels, R., Thomas, D. and Reddehase, M. J. (2009). The efficacy of antigen processing is critical for protection against cytomegalovirus disease in the presence of viral immune evasion proteins. *J. Virol*. **83**, 9611–9615.

Hudson, J. B., Misra, V. and Mosmann, T. R. (1976). Cytomegalovirus infectivity: analysis of the phenomenon of centrifugal enhancement of infectivity. *Virology* **72**, 235–243.

Huggett, J., Dheda, K., Bustin, S. and Zumla, A. (2005). Real-time RT-PCR normalisation; strategies and considerations. *Genes Immun*. **6**, 279–284.

Jonjic, S., Bubic, I. and Krmpotic, A. (2006). Innate immunity to cytomegalovirus. In: *Cytomegaloviruses: Molecular Biology and Immunology* (M. J. Reddehase, ed), pp. 285–319. Caister Academic Press, Norfolk, UK.

Jonjic, S., Mutter, W., Weiland, F., Reddehase, M. J. and Koszinowski, U. H. (1989). Site-restricted persistent cytomegalovirus infection after selective long-term depletion of CD4+ T lymphocytes. *J. Exp. Med*. **169**, 1199–1212.

Jonjic, S., Pavic, I., Lucin, P., Rukavina, D. and Koszinowski, U. H. (1990). Efficacious control of cytomegalovirus infection after long-term depletion of CD8+ T lymphocytes. *J. Virol*. **64**, 5457–5464.

Koopman, P., Munsterberg, A., Capel, B., Vivian, N. and Lovell-Badge, R. (1990). Expression of a candidate sex-determining gene during mouse testis differentiation. *Nature* **348**, 450–452.
Kropp, K. A., Simon, C. O., Fink, A., Renzaho, A., Kühnapfel, B., Podlech, J., Reddehase, M. J. and Grzimek, N. K. (2009). Synergism between the components of the bipartite major immediate-early transcriptional enhancer of murine cytomegalovirus does not accelerate viral replication in cell culture and host tissues. *J. Gen. Virol*. **90**, 2395–2401.
Kurz, S. K., Steffens, H. P., Mayer, A., Harris, J. R. and Reddehase, M. J. (1997). Latency versus persistence or intermittent recurrences: evidence for a latent state of murine cytomegalovirus in the lungs. *J. Virol*. **71**, 2980–2987.
Mangin, M., Ikeda, K. and Broadus, A. E. (1990). Structure of the mouse gene encoding parathyroid hormone-related peptide. *Gene* **95**, 195–202.
Mayer, A., Podlech, J., Kurz, S. K., Steffens, H. P., Maiberger, S., Thalmeier, K., Angele, P., Dreher, L. and Reddehase, M. J. (1997). Bone marrow failure by cytomegalovirus is associated with an *in vivo* deficiency in the expression of essential stromal hemopoietin genes. *J. Virol*. **71**, 4589–4598.
Mercer, J. A., Marks, J. R. and Spector, D. H. (1983). Molecular cloning and restriction endonuclease mapping of the murine cytomegalovirus genome (Smith Strain). *Virology* **129**, 94–106.
Messerle, M., Crnkovic, I., Hammerschmidt, W., Ziegler, H. and Koszinowski, U. H. (1997). Cloning and mutagenesis of a herpesvirus genome as an infectious bacterial artificial chromosome. *Proc. Natl. Acad. Sci. U. S.A*. **94**, 14759–14763.
Munks, M. W., Gold, M. C., Zajac, A. L., Doom, C. M., Morello, C. S., Spector, D. H. and Hill, A. B. (2006). Genome-wide analysis reveals a highly diverse CD8 T cell response to murine cytomegalovirus. *J. Immunol*. **176**, 3760–3766.
Osborn, J. E. and Walker, D. L. (1971). Virulence and attenuation of murine cytomegalovirus. *Infect. Immun*. **3**, 228–236.
Pahl-Seibert, M. F., Juelch, M., Podlech, J., Thomas, D., Deegen, P., Reddehase, M. J. and Holtappels, R. (2005). Highly protective *in vivo* function of cytomegalovirus IE1 epitope-specific memory CD8 T cells purified by T-cell receptor-based cell sorting. *J. Virol*. **79**, 5400–5413.
Peggs, K. S., Verfuerth, S., Pizzey, A., Khan, N., Guiver, M., Moss, P. A. and Mackinnon, S. (2003). Adoptive cellular therapy for early cytomegalovirus infection after allogeneic stem-cell transplantation with virus-specific T-cell lines. *Lancet* **362**, 1275–1277.
Plachter, B., Sinzger, C. and Jahn, G. (1996). Cell types involved in replication and distribution of human cytomegalovirus. *Adv. Virus Res*. **46**, 195–261.
Podlech, J., Holtappels, R., Grzimek, N. K. A. and Reddehase, M. J. (2002). Animal models: murine cytomegalovirus. In: *Methods in Microbiology, Immunology of Infection* (S. H. E. Kaufmann and D. Kabelitz, eds), pp. 493–525. Academic Press, London and San Diego, Cal.
Podlech, J., Holtappels, R., Pahl-Seibert, M. F., Steffens, H. P. and Reddehase, M. J. (2000). Murine model of interstitial cytomegalovirus pneumonia in syngeneic bone marrow transplantation: persistence of protective pulmonary CD8-T-cell infiltrates after clearance of acute infection. *J. Virol*. **74**, 7496–7507.
Podlech, J., Holtappels, R., Wirtz, N., Steffens, H. P. and Reddehase, M. J. (1998). Reconstitution of CD8 T cells is essential for the prevention of multiple-organ cytomegalovirus histopathology after bone marrow transplantation. *J. Gen. Virol*. **79**, 2099–2104.
Podlech, J., Pintea, R., Kropp, K. A., Fink, A., Lemmermann, N. A., Erlach, K. C., Isern, E., Angulo, A., Ghazal, P. and Reddehase, M. J. (2010). Enhancerless cytomegalovirus is capable of establishing a low-level maintenance infection in severely immunodeficient host tissues but fails in exponential growth. *J. Virol*. **84**, 6254–6261.

Powers, C. and Früh, K. (2008). Rhesus CMV: an emerging animal model for human CMV. *Med. Microbiol. Immunol*. **197**, 109–115.
Radonic, A., Thulke, S., Mackay, I. M., Landt, O., Siegert, W. and Nitsche, A. (2004). Guideline to reference gene selection for quantitative real-time PCR. *Biochem. Biophys. Res. Commun*. **313**, 856–862.
Rawlinson, W. D., Farrell, H. E. and Barrell, B. G. (1996). Analysis of the complete DNA sequence of murine cytomegalovirus. *J. Virol*. **70**, 8833–8849.
Reddehase, M. J. (2002). Antigens and immunoevasins: opponents in cytomegalovirus immune surveillance. *Nat. Rev. Immunol*. **2**, 831–844.
Reddehase, M. J., Simon, C. O., Seckert, C. K., Lemmermann, N. and Grzimek, N. K. (2008). Murine model of cytomegalovirus latency and reactivation. *Curr. Top. Microbiol. Immunol*. **325**, 315–332.
Reddehase, M. J., Weiland, F., Münch, K., Jonjic, S., Lüske, A. and Koszinowski, U. H. (1985). Interstitial murine cytomegalovirus pneumonia after irradiation: characterization of cells that limit viral replication during established infection of the lungs. *J. Virol*. **55**, 264–273.
Redwood, A. J., Messerle, M., Harvey, N. L., Hardy, C. M., Koszinowski, U. H., Lawson, M. A. and Shellam, G. R. (2005). Use of a murine cytomegalovirus K181-derived bacterial artificial chromosome as a vaccine vector for immunocontraception. *J. Virol*. **79**, 2998–3008.
Reeves, M. and Sinclair, J. (2008). Aspects of cytomegalovirus latency and reactivation. *Curr. Top. Microbiol. Immunol*. **325**, 297–314.
Riddell, S. R., Watanabe, K. S., Goodrich, J. M., Li, C. R., Agha, M. E. and Greenberg, P. D. (1992). Restoration of viral immunity in immunodeficient humans by the adoptive transfer of T cell clones. *Science* **257**, 238–241.
Ruzsics, Z. and Koszinowski, U. H. (2008). Mutagenesis of the cytomegalovirus genome. *Curr. Top. Microbiol. Immunol*. **325**, 41–61.
Sacher, T., Podlech, J., Mohr, C. A., Jordan, S., Ruzsics, Z., Reddehase, M. J. and Koszinowski, U. H. (2008). The major virus-producing cell type during murine cytomegalovirus infection, the hepatocyte, is not the source of virus dissemination in the host. *Cell Host Microbe* **17**, 263–272.
Seckert, C. K., Renzaho, A., Reddehase, M. J. and Grzimek, N. K. (2008). Hematopoietic stem cell transplantation with latently infected donors does not transmit virus to immunocompromised recipients in the murine model of cytomegalovirus infection. *Med. Microbiol. Immunol*. **197**, 251–259.
Seckert, C. K., Renzaho, A., Tervo, H. M., Krause, C., Deegen, P., Kühnapfel, B., Reddehase, M. J. and Grzimek, N. K. (2009). Liver sinusoidal endothelial cells are a site of murine cytomegalovirus latency and reactivation. *J. Virol*. **83**, 8869–8884.
Selgrade, M. K., Nedrud, J. G., Collier, A. M. and Gardner, D. E. (1981). Effects of cell source, mouse strain, and immunosuppressive treatment on production of virulent and attenuated murine cytomegalovirus. *Infect. Immun*. **33**, 840–847.
Simon, C. O., Holtappels, R., Tervo, H.-M., Böhm, V., Däubner, T., Oehrlein-Karpi, S. A., Kühnapfel, B., Renzaho, A., Strand, D., Podlech, J. *et al*. (2006). CD8 T cells control cytomegalovirus latency by epitope-specific sensing of transcriptional reactivation. *J. Virol*. **80**, 10436–10456.
Simon, C. O., Seckert, C. K., Dreis, D., Reddehase, M. J. and Grzimek, N. K. (2005). Role for tumor necrosis factor alpha in murine cytomegalovirus transcriptional reactivation in latently infected lungs. *J. Virol*. **79**, 326–340.
Sinzger, C., Digel, M. and Jahn, G. (2008). Cytomegalovirus cell tropism. *Curr. Top. Microbiol. Immunol*. **325**, 63–83.

Smith, L. M., McWhorter, A. R., Masters, L. L., Shellam, G. R. and Redwood, A. J. (2008). Laboratory strains of murine cytomegalovirus are genetically similar to but phenotypically distinct from wild strains of virus. *J. Virol*. **82**, 6689–6696.

Smith, L. M., Shellam, G. R. and Redwood, A. J. (2006). Genes of murine cytomegalovirus exist as a number of distinct genotypes. *Virology*. **352**, 450–465.

Smith, M. G. (1954). Propagation of salivary gland virus of the mouse in tissue cultures. *Proc. Soc. Exp. Biol. Med*. **86**, 435–440.

Stahlberg, A., Hakansson, J., Xian, X., Semb, H. and Kubista, M. (2004). Properties of the reverse transcription reaction in mRNA quantification. *Clin. Chem*. **50**, 509–515.

Steffens, H. P., Kurz, S., Holtappels, R. and Reddehase, M. J. (1998a). Preemptive CD8 T-cell immunotherapy of acute cytomegalovirus infection prevents lethal disease, limits the burden of latent viral genomes, and reduces the risk of virus recurrence. *J. Virol*. **72**, 1797–1804.

Steffens, H. P., Podlech, J., Kurz, S. K., Angele, P., Dreis, D. and Reddehase, M. J. (1998b). Cytomegalovirus inhibits the engraftment of donor bone marrow cells by downregulation of hemopoietin gene expression in recipient stroma. *J. Virol*. **72**, 5006–5015.

Stinski, M. F. and Isomura, H. (2008). Role of the cytomegalovirus major immediate early enhancer in acute infection and reactivation from latency. *Med. Microbiol. Immunol*. **197**, 223–231.

Stoddard, C. A., Cardin, R. D., Boname, J. M., Manning, W. C., Abenes, G. B. and Mocarski, E. S. (1994). Peripheral blood mononuclear phagocytes mediate dissemination of murine cytomegalovirus. *J. Virol*. **68**, 6243–6253.

Streblow, D., Varnum, S. M., Smith, R. D. and Nelson, J. A. (2006). A proteomics analysis of human cytomegalovirus particles. In: *Cytomegaloviruses: Molecular Biology and Immunology* (M. J. Reddehase, ed), pp. 63–89. Caister Academic Press, Norfolk, UK.

Tang, Q., Murphy, E. A. and Maul, G. G. (2006). Experimental confirmation of global murine cytomegalovirus open reading frames by transcriptional detection and partial characterization of newly described gene products. *J. Virol*. **80**, 6873–6882.

Wagner, M., Jonjic, S., Koszinowski, U. H. and Messerle, M. (1999). Systematic excision of vector sequences from the BAC-cloned herpesvirus genome during virus reconstitution. *J. Virol*. **73**, 7056–7060.

Walter, E. A., Greenberg, P. D., Gilbert, M. J., Finch, R. J., Watanabe, K. S., Thomas, E. D. and Riddell, S. R. (1996). Reconstitution of cellular immunity against cytomegalovirus in recipients of allogeneic bone marrow by transfer of T-cell clones from the donor. *N. Engl. J. Med*. **333**, 1038–1044.

Weiland, F., Keil, G. M., Reddehase, M. J. and Koszinowski, U. H. (1986). Studies on the morphogenesis of murine cytomegalovirus. *Intervirology* **26**, 192–201.

Wilhelmi, V., Simon, C. O., Podlech, J., Böhm, V., Däubner, T., Emde, S., Strand, D., Renzaho, A., Lemmermann, N. A., Seckert, C. K. *et al*. (2008). Transactivation of cellular genes involved in nucleotide metabolism by the regulatory IE1 protein of murine cytomegalovirus is not critical for viral replicative fitness in quiescent cells and host tissues. *J. Virol*. **82**, 9900–9916.

Wirtz, N., Schader, S. I., Holtappels, R., Simon, C. O., Lemmermann, N. A., Reddehase, M. J. and Podlech, J. (2008). Polyclonal cytomegalovirus-specific antibodies not only prevent virus dissemination from the portal of entry but also inhibit focal virus spread within target tissues. *Med. Microbiol. Immunol*. **197**, 151–158.

17 Measuring Immune Responses *In Situ*: Immunofluorescent and Immunoenzymatic Techniques

Antje Müller[1], Torsten Goldmann[2] and Ulrike Seitzer[3]

[1] Department of Rheumatology, University of Lübeck, Lübeck, Germany; [2] Division of Clinical and Experimental Pathology, Department of Pneumology, Research Center Borstel, Borstel, Germany; [3] Division of Veterinary Infection Biology and Immunology, Department of Immunology and Cell Biology, Borstel, Germany

CONTENTS

I. INTRODUCTION

The indirect immunofluorescence technique developed by Coons and Kaplan in 1950 was the first to describe the localization of antigen in tissues using fluorescently labelled antibody. Since then, considerable progress in immunohistochemical procedures has been made, most notably on the application of enzyme-labelled antibodies, signal enhancement and development of new fluorochromes. Enzyme-coupled detection methods were developed primarily because of the limitations of fluorescence techniques, such as naturally occurring autofluorescence, the lack of permanence of the preparations which tend to fade, the difficult correlation to morphological details and the need for expensive equipment. Of a variety of enzymes assayed, the enzymes of choice for direct and indirect procedures became horseradish peroxidase (PO) and calf intestinal alkaline phosphatase (AP) (Nakane and Pierce, 1967). The sensitivity of these immunoenzymatic detection methods was greatly enhanced by the development of the peroxidase anti-peroxidase (PAP) (Sternberger *et al.*, 1970) and the alkaline phosphatase anti-alkaline phosphatase (APAAP) methods (Cordell *et al.*, 1984), which are based on the utilization of non-covalently bound enzyme to enzyme-specific antibodies.

METHODS IN MICROBIOLOGY, VOLUME 37
0580-9517 DOI 10.1016/S0580-9517(10)37017-6

With the advent of monoclonal antibody production techniques developed by Köhler and Milstein in 1975, problems associated with polyclonal antisera could be overcome in immunochemical techniques. Serum-derived antibodies may react with many irrelevant antigens, sometimes making interpretation of results difficult. Monoclonal antibodies help to overcome these difficulties since they recognize only one specific epitope. Due to the homogeneity of monoclonal antibodies, a standardization from laboratory to laboratory has become possible. In addition, hybridoma cell lines provide an unlimited supply of antibodies in contrast to the limited supply of a polyclonal antiserum.

Great effort was also put into making paraffin-embedded material more amenable to immunohistological techniques. Although formalin remains the most popular fixative used, it is not always the best of choice for preserving antigenicity of tissues, due to the intermolecular cross-linking formed between formalin and proteins. Approaches to unmask antigenic sites hidden by cross-linked proteins have been to develop antibodies that can recognize formalin-resistant epitopes, to choose the correct fixative and optimize the duration of fixation and the application of protease digestion. A major advance in antigen retrieval was achieved by Shi *et al*. in 1991 based on microwave heating of tissue sections attached to microscope slides to temperatures up to 100°C (HIER = heat-induced epitope retrieval) in the presence of metal ion solutions. This resulted in the possibility of visualizing antigens that were otherwise undetectable in formalin-fixed, paraffin-embedded tissues and also greatly simplified the method for antigen retrieval. A study undertaken by Cattoretti *et al*. (1993) optimized antigen retrieval techniques for a large number of antibodies to be used on formalin-fixed, paraffin-embedded tissue sections. HIER can be performed in a microwave oven or by steaming devices which are more gentle with regard to mechanic influence onto the specimens. Complementing HIER there are several additional procedures for antigen retrieval by application of enzymes that help to reduce antigen cross-linking (PIER = protein-induced epitope retrieval), such as proteinase K, pepsin and trypsin. The procedures depend on the respective antigen and have to be optimized for each.

The developments from then on were focussed on methods for signal amplification, an important factor when one is confronted with the detection of low antigen levels. Methods which have proven to be of value are the tyramine amplification technique, which can be applied to achieve higher sensitivity and/or to reduce costs for primary antibody (Wasielewski *et al*., 1997), or polymeric conjugate systems (Kammerer *et al*., 2001). Polymeric systems, compared to tyramine, are more easy to control and offer smaller hands on times. To date, polymeric systems, that are available with horseradish PO or AP as a matter of choice, have reached a quality which is clearly superior to APAAP, PAP or biotin-based methods. Rapid progress has also been made in the development of fluorescence techniques with the advancement of confocal laser scanning microscopy (CLSM) and the production of new and more stable fluorochromes (Kumar *et al*., 1999), which may allow the simultaneous description of seven parameters (Tsurui *et al*., 2000). The challenge in this field is to minimize fading of the utilized fluorochromes by the high-energy laser beams (Ono *et al*., 2001).

Key aspects to consider in establishing immunohistoloy methods are however unchanged since the first description of this technology: fixation procedures with

respect to epitope and morphology conservation, specificity of the antibody, antigen retrieval, specificity of the secondary reagents and the properties of the staining reaction. Methods should be chosen and applied which lead to reproducible, reliable and specific results (Burry, 2000). The methods described below are based on the reports found in the literature. They have been developed to yield optimal signal to background ratios and are used routinely in our laboratory with consistently good results. During establishment of staining procedures, operators should be aware that transfer to an automated staining system often requires adjustments to some buffers and reagents.

A. Tissue Arrays

One mentionable breakthrough in immunohistochemistry was the development of tissue arrays (Kononen *et al*., 1998). This technique basically consists of punches taken out of different paraffin blocks, which are arranged in one acceptor block. In this way, up to more than 1000 different specimens can be arranged on a single slide, depending on the sizes of the respective punching needles. The advantages are obvious with regard to high-throughput aspects and inter-specimen comparability with highly reduced costs for consumables. Devices for the building of tissue arrays to date are reliable, with acceptable prices [even home-made devices have been described – (Pires *et al*., 2006)], and the advantages are in good relation to the efforts needed for establishing this technique in the laboratory.

♦♦♦♦♦♦ II. SPECIMEN PREPARATION

For immunoenzymatic techniques, cryostat preparations generally have a superior preservation of antigens than paraffin sections. Morphological details, however, are more readily destroyed in cryostat sections and the great majority of archival material accessible for immunostaining is paraffin embedded. There are alternative fixation protocols to formalin, which deliver excellent preservation of nucleic acids, epitopes and morphology; the most comprehensively studied method is the Hepes-glutamic-acid-buffered-Organic-solvent-Protection-Effect (HOPE) technique (Srinivasan *et al*., 2002; Goldmann *et al*., 2003). This technique has been intensely used for the study of immunorelevant molecules in lung tissues, e.g. Toll-like receptors (TLRs) (Droemann *et al*., 2005, 2007). In the following, the emphasis is on the treatment of cryostat and paraffin sections prior to staining. For other tissue pretreatments and more details on paraffin embedding and sectioning further reading is recommended (Watkins, 1989; Zeller, 1989).

A. Paraffin Sections

For antigen retrieval it may be necessary to try several approaches with respect to the method used or the buffers necessary in preparing paraffin sections for immunoenzymatic staining (Cattoretti *et al*., 1993; Pileri *et al*., 1997; Shi *et al*., 2000).

For no treatment for antigen retrieval, routinely processed paraffin sections are dewaxed by submerging for 10 min in xylene followed by 10 min in acetone and 10 min in a 1:1 mixture of acetone and Tris-buffered saline (TBS). The sections are kept in TBS until staining.

For microwave oven pretreatment, paraffin sections are deparaffinized for 10 min in xylene and rehydrated in a series of ethanols or acetones at 10 min intervals (100, 70, 40, 0%). The slides are transferred to a plastic staining jar filled with 10 mM sodium citrate buffer, pH 6.0. The plastic staining jars are put in the microwave oven and heated for 5 min at 720 W. After 5 min it is essential that the staining jar is refilled with H_2O to prevent drying of the specimens, before heating another 5 min. The frequency of the heating steps depends on the fixation and embedding procedures performed previously and should be optimized. After the microwave treatment the slides are cooled in the staining jar for approximately 20 min at room temperature and washed briefly in TBS before proceeding with immunostaining.

For pressure cooker pretreatment, sections are dewaxed and hydrated as for microwave treatment. Using a normal household pressure cooker (with a 15 psi valve), boil 10 mM citric acid, pH 6.0, before adding the sections. Make up enough buffer to totally submerge the sections (approx. 2 l). Rinse the sections briefly in distilled water and place them into the boiling buffer. Close the lid and heat until top pressure is reached and boil the sections at this pressure. The boiling time must be optimized (approx. 1–10 min). After cooking, immediately cool the pressure cooker under running cold water taking extreme care at this step and absolutely following the instructions of the manufacturer before opening the cooker. The sections are transferred immediately into cold running tap water before proceeding with the immunohistological staining.

B. Frozen Sections

Several steps in the preparation of frozen material are crucial for obtaining samples with well-preserved morphological structure and antigenicity. The following procedure may be followed: Fresh surgical specimens are submerged in flat-bottomed polyethylene tubes (Cat. no. 619-x, Brand Laboratory Equipment Manufacturers, Wertheim, Germany) filled with sterile physiological NaCl, phosphate-buffered saline (PBS) or sterile tissue-freezing medium (Leica Microsystems GmbH, Nussloch, Germany), snap frozen in liquid nitrogen and stored at –70°C. If tissues have not been appropriately snap-frozen, ice crystals will be present in the tissue causing artefactual staining along the fracture lines caused by these crystals. Tissues should always be maintained in a frozen state, since thawing and refreezing will result in extensive damage to the tissue and loss of antigenicity. Cryostat sections of 4–5 μm are air dried for 4–24 h and then fixed for 15–30 min in acetone followed by 15–30 min in chloroform. If the cryostat sections are not meant to be stained the following day, also air dry 4–24 h, fix for 10 min in acetone and store at –70°C. When needed, thaw the sections covered with a paper towel to prevent water condensation on the slides. Fix in acetone and chloroform as mentioned above.

For cytospin specimens, 1 to 5×10^5 cells are applied per slide and centrifuged for 5 min at 220 × g. The cytospins are air dried as above for 4–24 h and stored at –70°C. Before staining, samples are thawed and fixed solely in acetone for 10 min.

For some staining procedures concerning primarily cytokines, the fixing of specimens with paraformaldehyde/saponin may be preferred (Sander *et al.*, 1991). Air dried slides are fixed for 15 min in 4% paraformaldehyde in PBS without NaCl, pH 7.4–7.6, followed by a 15 min treatment in 0.1% saponin/PBS to elute cholesterol from the membranes. Wash thoroughly with PBS before immunostaining.

New and alternative fixation procedures exist in the literature and may be applied if the above procedures do not lead to satisfactory results, such as, for example, the recently described alternative to acetone fixation using pararosaniline (Schrijver *et al.*, 2000).

♦♦♦♦♦♦ III. IMMUNOFLUORESCENCE DETECTION

Fluorescent probes allow the detection of particular components of cells and subcellular structures with a high sensitivity and selectivity. The obtained information can be analysed statistically, quantitatively, temporally and with a high spatial resolution. The use of multicolour probes allows the simultaneous monitoring of different antigens at the same time and can provide information about co-localization of antigens or co-expression of molecules on a single-cell level. The innovative potential of immunofluorescence is reflected by the rising number of applications in fluorescence microscopy, laser scanning microscopy, laser scanning cytometry (Clatch *et al.*, 1998) and flow cytometry (Baumgarth and Roederer, 2000).

A limitation for the combination of fluorochromes is the fact that the emission spectra of the fluorochromes are usually broad and therefore overlap. This drawback can be overcome in part by choosing fluorochromes that have a well-separated emission spectrum and using individual combinations of excitation and emission filters. Fluorescein isothiocyanate (FITC), tetramethyl rhodamine isothiocyanate (TRITC) and rhodamine derivatives are the most common dyes used for commercially available directly conjugated antibodies. New product lines like the ALEXA™ or CY™ dyes are similar in their spectral properties but are improved in brightness and photostability (Panchuk-Voloshina *et al.*, 1999). These dyes can also be conjugated to the antibody of choice using the procedures described by the manufacturer. Counterstaining of DNA is usually performed with UV excitable dyes like DAPI (4′,6-diamidino-2-phenylindole), Hoechst 33258 and Hoechst 33342, with Hoechst 33342 being one of the exceptional dyes that can stain DNA in living cells. On laser-based microscopes that lack an expensive UV light source, these DNA dyes can be replaced by dyes that are excited with a red laser line such as TOTO-3 and TOPRO-3 (Suzuki *et al.*, 1997).

A problem one is confronted with in using fluorochromes in tissue is the presence of autofluorescence. Methods to overcome this problem have been described (Schnell *et al.*, 1999) and additionally excitation and emission in the red spectral region also has the advantage of lowering the background of autofluorescence. Therefore fluorochromes that have red shifted spectral properties, like Cy5, and can be coupled to antibodies are also under current development.

Fluorochrome-labelled antibodies allow a high resolution to be obtained, since subcellular structures can be studied at magnifications beyond the limit of

resolution of the light microscope. Because fluorochromes can be chosen that do not have overlapping emission spectra, double immunofluorescence permits the study of two different antigens in the same specimen even if they have identical subcellular distributions, thus allowing co-localization studies.

Even though conventional fluorescence microscopy is being increasingly substituted by CLSM, it is nonetheless possible to analyse multiple fluorochromes and to use far-red fluorochromes by appropriate selection of filters (Ferri *et al.*, 1997a,b). A possibility to attain CLSM quality in conventional microscopy was described using ultrathin cryosections of skin, which provided convincing comparable images to CLSM (Ishiko *et al.*, 1998).

A. Direct and Indirect Staining

Fluorescence staining can be performed using a primary antibody which is conjugated with a fluorochrome (direct staining) or with an unlabelled primary and a fluorochrome-conjugated secondary antibody directed against the primary immunoglobulin. In both cases, the staining procedure can be performed in the following fashion:

The fixed specimen is incubated for 10 min in TBS/10% bovine serum albumin to block unspecific binding. Wash twice with TBS before applying the directly labelled or unlabelled primary antibody. Incubate for 30 min and wash twice with TBS. When using a directly labelled antibody, proceed with the optional DNA staining and mounting, before viewing under a fluorescence microscope. For the indirect detection procedure, continue with the incubation of the fluorochrome-conjugated secondary antibody for 30 min. For optional DNA staining of nuclei, wash the specimen twice and incubate for 10 min with the bisbenzimide dye Hoechst 33342 (6 μg/ml) or 1 μg/ml DAPI. At this stage it has proven to be useful to fix the stained specimen in 4% paraformaldehyde for 10 min before washing twice in TBS and mounting in 10 μl DABCO (1,4-diazabicyclo [2,2,2] octane) anti-fading solution (Johnson *et al.*, 1982) and viewing under a fluorescence microscope. The specimens can be stored for further viewing at 4°C for several months.

B. Multicolour Immunofluorescence Staining

Two and more fluorochromes can be combined for staining cells and tissue sections, whereby the repertoire used is not restricted to the most commonly used fluorochromes and depends on the microscope and filter sets available. To combine fluorochromes in order to detect multiple antigens several possible strategies present themselves. First, the use of direct staining with a fluorochrome-conjugated primary antibody combined with indirect staining procedures. The advantages of this approach are that it is easy to perform; however, a main drawback is the availability of suitably fluorochrome-conjugated antibodies and the fact that the signal intensity may be too weak. A second approach is to use primary antibodies of different isotypes combined with isotype-specific fluorochrome-conjugated antibodies, bringing the advantage of signal amplification and the choice of up to five different isotypes to be distinguished simultaneously. The inherent restrictions of this method are the availability of primary antibodies of different isotype and of

suitable fluorochrome-conjugated isotype-specific secondary antibodies. A third approach is to use indirect staining with biotin-conjugated antibodies and fluorochrome-conjugated streptavidin.

Critical to any one chosen approach is the staining sequence which is required to combine the chosen primary and secondary antibodies in order to avoid unwanted false-positive results. In addition, it is advised to test the isotype specificity of secondary reagents.

The following staining procedure is an example for the distinction of different cell subsets (T cells, macrophages, dendritic cells and follicular dendritic cells) in cryosections of tonsillar tissue by multicolour immunofluorescence staining (Figure 2A–D). After blocking, sections were incubated with an antibody against the CD4 antigen (BD Biosciences, clone Leu3a, IgG_1) followed by detection with an Alexa-568-conjugated goat-anti-mouse-IgG antibody (Molecular Probes). To detect follicular dendritic cells, the DRC-1 antibody (Dako, IgM) was applied (Naiem *et al*., 1983) followed by incubation with a biotinylated goat-anti-mouse-IgM and streptavidin-Cy5 (Dianova). Lastly, a directly labelled FITC-CD11c (Dako, clone KB90, IgG_1) was applied before fixing the specimens in 4% paraformaldehyde and mounting in DABCO anti-fading medium. The results of the staining procedure were analysed with a confocal microscope (Leica TCS SP, Bensheim, Germany) equipped with a Kr/Ar ion laser. Using this protocol, CD4 is detected on T cells, macrophages and dendritic cells by red fluorescence, DRC-1 reactivity on follicular dendritic cells was shown by blue and CD11c expression by green fluorescence on macrophages and dendritic cells. Only the merged fluorescences allow the clear depiction of red-fluorescing CD4-positive T cells, since macrophages and dendritic cells then appear yellow due to the co-expression of CD11c (Figure 2A–D).

♦♦♦♦♦♦ IV. IMMUNOENZYMATIC DETECTION

The choice of the system to use (AP or PO) depends on several circumstances, such as the species in which the antigen is to be detected and the availability of appropriate primary and secondary antibodies, as well as the presence of non-inhibitable endogenous enzyme activity (e.g. intestinal AP is not inhibited by levamisole). For the APAAP procedure with human tissues, the primary antibody is usually a mouse monoclonal. When using a rabbit antiserum an additional incubation step has to be included to make the antiserum detectable with the system.

In the following procedures, incubation steps are generally followed by washing twice in TBS. Slides are incubated with 100 µl of antibody dilution for 30 min at room temperature in a level humid chamber. Excessive humidity should be avoided since water condensation on the slides will interfere with the staining reaction. Insufficient humidity on the other hand will dry the antibody on the sections, resulting in false-positive staining. Drying is usually most apparent at the edge of sections (rim effect).

A. APAAP Method

This procedure is described according to the method of Cordell *et al*. (1984) and is delineated exemplarily for human tissue and with reagents used routinely in our laboratory. It must be emphasized that the dilutions given may not apply in all cases and should be optimized before routine use.

Incubation for 30 min with the appropriately diluted primary antibody in 10% fetal calf serum (FCS)/TBS is applied to prepared cryosections and cytopreparations directly after the last fixation step and to paraffin sections after washing in TBS. For washing after the first incubation, separate containers are recommended for different antibodies and negative controls.

If the primary antibody is a rabbit antiserum, the following incubation must be performed: 30 min with a monoclonal mouse anti-rabbit immunoglobulin (Cat. no. M 0737, DAKO Diagnostika GmbH, Hamburg, Germany).

The secondary (bridging) antibody [rabbit anti-mouse IgG H+L antiserum (Cat. no. Z 259, DAKO Diagnostika GmbH, Hamburg, Germany)] is diluted 1:20 in TBS, 1:8 inactivated human serum and incubated for 30 min.

The APAAP complex (Cat. no. M 800, Dianova, Hamburg, Germany) is diluted 1:40 in TBS/FCS and also incubated for 30 min.

The incubations with the secondary (bridging) antibody and APAAP complex are repeated once for 15 min each and may be repeated *ad libitum* to increase the detection limit.

For the visualization of the staining, the following developing solution must be prepared freshly each time. Amounts are for one staining jar and the order of addition is essential for results.

Solution A: 35 ml APAAP buffer, 12.5 ml AP buffer, 20 mg levamisole

Solution B: dimethylformamide with 8.3% (w/v) Naphthol-As biphosphate

Solution C: 250 µl $NaNO_3$ solution with 100 µl New fuchsin solution

After 1 min of reaction time 125 µl of solution C is added to 47.5 ml solution A, then 300 µl of solution B is added and the pH is adjusted to 8.8. The solution is filtered before adding the slides and incubating for 20 min on a shaker. Counterstaining is performed in haematoxylin for 90 s, the specimens are washed and left in tap water for 5 min before being mounted with prewarmed (56°C) Kaiser's glycerol gelatine.

B. Indirect Immunoperoxidase Method

The advantage of PO staining is a greater variability and flexibility in the availability and combinations of antibody as well as a less time-consuming procedure. Again, the procedure delineated is exemplarily for human tissue and a mouse or rabbit primary antibody (Figure 1D).

Before proceeding with primary antibody incubations, it may be advisable to block endogenous PO activity in the tissue by preincubating the slides for 20 min in a light-protected staining jar with 1% H_2O_2 in TBS.

The mouse (rabbit) primary antibody is applied in the appropriate dilution in TBS/10% FCS and incubated for 30 min. The first secondary PO-conjugated goat

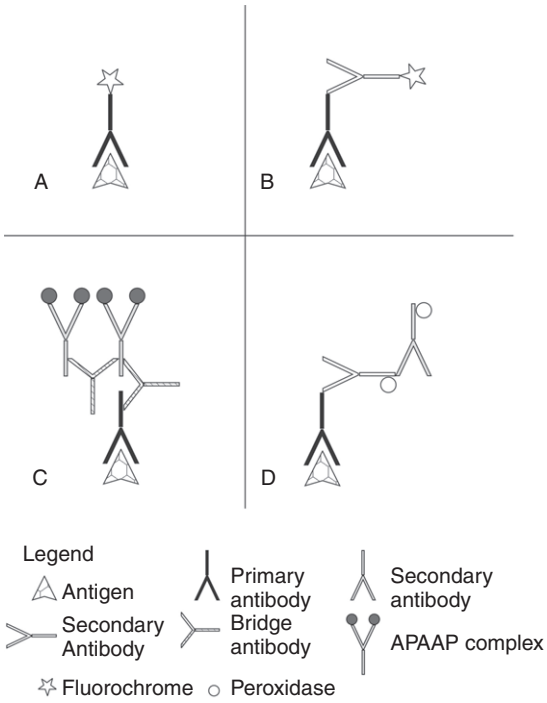

Figure 1. Scheme of the principle of the methods described for immunofluorescence and immunoenzymatic detection of antigens: (A) direct fluorescence, using a fluorochrome-coupled primary antibody; (B) indirect fluorescence with a fluorochrome-coupled secondary antibody; (C) APAAP procedure, performed twice with the bridging antibody and the APAAP complex and (D) indirect immunoperoxidase method using two different PO-conjugated secondary antibodies.

anti-mouse (rabbit) antibody is applied diluted in TBS/10% FCS and inactivated human serum. The second secondary PO-conjugated rabbit anti-goat is also incubated for 30 min. In contrast to the APAAP method, this method is limited to two signal-enhancing steps due to an increase of background staining with further incubation steps.

For development, prepare the developing buffer as described and incubate the slides with 100 µl each. Incubate in the dark in the humid chamber for 3–15 min. The degree of development can be checked microscopically and the incubation stopped at the desired point. Slides are counterstained in haematoxylin and mounted as described for the APAAP procedure.

In analogy to the PO method a combination of two AP-coupled secondary antibodies may also be used applying the detection procedure for AP activity.

1. Immunohistochemistry using a polymer system

After deparaffinization and antigen retrieval by HIER or PIER the endogenous PO is blocked by incubation in 3% H_2O_2 for about 10 min. If a system with AP is used this blocking is omitted. After washing and blocking with blocking solution (included in

the respective system) primary antibody is applied in Tris buffer or commercially available antibody diluent. These diluents make the ready-to-use diluted antibodies stable for weeks, which is of advantage if an automated stainer is used. After washing and application of a postblock reagent (depending on the polymer system used), PO-conjugated polymer is applied for about 20 min at ambient temperature.

After washing colour reaction is performed with substrates for PO, e.g. aminoethylcarbazole (AEC) or diaminobenzidine. Mounting is performed after counterstaining with Mayer's haemalum using Kaiser's glycerol gelatine or another water-compatible mounting medium.

C. Double Staining Procedure

If suitable primary antibodies are available for the antigens of interest (e.g. mouse and rabbit) double immunoenzymatic staining may be performed. Ideally, the rabbit primary antibody is detected using PO-conjugated secondary antibodies while the detection of the mouse monoclonal antibody is subsequently performed using the APAAP procedure. Alternatively, the streptavidin–biotin complex/HRP detection method offered by DAKO may be used for the primary rabbit antibody followed by APAAP detection of the primary mouse antibody. Figure 2A depicts an example of double immunoenzymatic staining in tonsil tissue performed by a different approach. The first antibody used was a mouse monoclonal antibody against the Ki-67 antigen (MIB-1, Dianova) detected with PO-labelled secondary antibodies (PO-goat-anti-mouse, PO-rabbit-anti-goat). The chromogenic substrate was only incubated for 10 min. The subsequent staining procedure for the rabbit-anti-CD3 antiserum (DAKO) was performed using only one secondary AP-conjugated goat-anti-rabbit antibody. The incubation with the chromogenic substrate must then be carefully monitored by microscopic control since the PO reaction tends to continue, causing signal overlap. This is often a drawback in evaluating double-stained specimens; however, digital image analysis may offer the possibility of circumventing this difficulty (Lehr *et al.*, 1999).

D. Detection of Cytokines and Transcription Factors with Immunohistochemistry and/or Immunofluorescence

Cytokines and transcription factors in their functions as regulators and messengers in immune responses are of considerable interest with regard to detection in cells and especially in tissues. However, the investigator will be confronted with problems in obtaining satisfactory results, mainly attributable to the low concentration of cytokines in the tissue specimen, most likely due to the fact that cytokines are usually secreted and that available antibodies often are not well suited for immunohistology, especially in the case of formalin-fixed paraffin-embedded tissues. In choosing an antibody and a protocol for immunostaining one should always be aware of the fact that antibodies directed against cytokines and transcription factors recognize or bind to only a small proportion of the antigen, i.e. one or more epitopes, and that some of these antigens exhibit differing and complex three-dimensional structures. Nonetheless, standard staining procedures can be

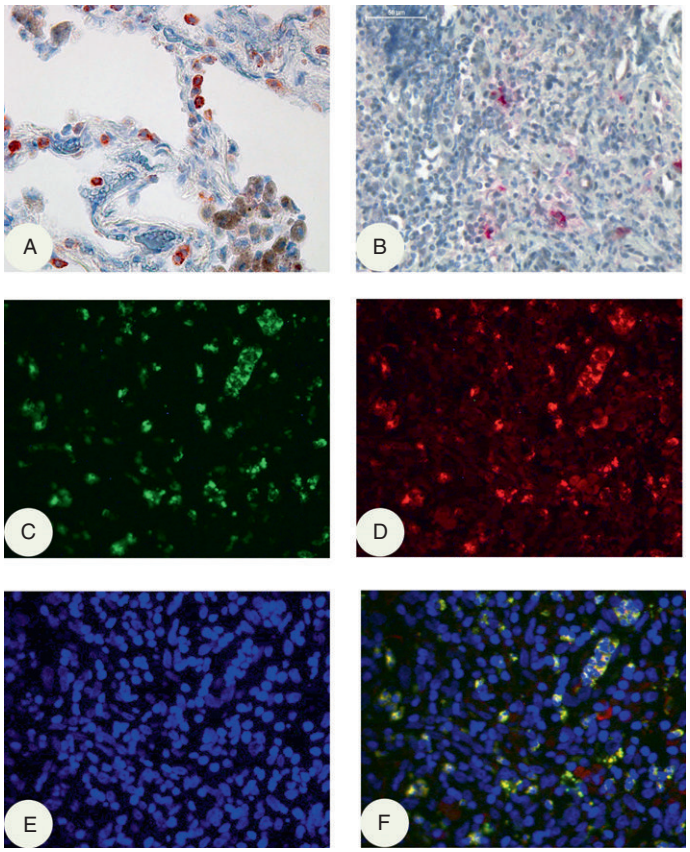

Figure 2. Immunoenzymatic and immunofluorescent detection of antigens in human tissue. (A) Surfactant protein c in alveolar epithelial cells type II in a human lung that was fixed using the HOPE technique. Immunohistochemistry was performed using a Polymer system with horseradish PO and AEC as a substrate (400×). (B) Expression of interleukin-17 in nasal mucosa is detected by a polyclonal anti-IL-17 (R&D Systems, Wiesbaden, Germany) and AP-conjugated secondary reagents. (C–F) Multicolour immunofluorescence staining of nasal mucosa. A deparaffinized section of human nasal mucosa was stained using an indirect immunofluorescence staining procedure. The analysis was performed using conventional immunofluorescence microscopy and corresponding image analysis software (Image J). (C) Detection of proteinase 3/polymorphonuclear neutrophils (green); (D) detection of interleukin-32α (red); (E) detection of nuclei (DAPI stain, blue) and (F) merged image of green, red and blue fluorescence. Cells positive for both proteinase 3 and interleukin-32α appear in yellow due to superposition of the colours green and red. (See color plate section).

modified and lead to good results as shown for instance for interferon-gamma (Scheel-Toellner *et al.*, 1995; van der Loos *et al.*, 2001), tumour necrosis factor alpha (Kretschmer *et al.*, 1990), interleukin-1 beta (Seitzer *et al.*, 1997), interleukin-15 (Maeurer *et al.*, 1999; Capraru *et al.*, 2008), interleukin-17 (Müller and Lamprecht, 2008; Evans *et al.*, 2009) and interleukin-32 (Calabrese *et al.*, 2008).

Because of the lack of visualization of tissue morphology using immunofluorescence staining and detection, the necessity of sufficient control stainings using, for example, appropriate isotypes of the primary antibodies should be emphasized.

Transcription factors are central mediators for initializing or suppressing transcription of DNA and their detection within the cell or even the nuclei is of value in elucidating immune responses in the tissue. Currently, one of the main questions is how to better discriminate between different lineages and different stages during differentiation of T lymphocytes, and in this respect transcription factors play important roles in regulating these mechanisms. Up to now, only a few studies are available demonstrating for instance nuclear staining of either activated or regulatory T cells based upon the forkhead/winged helix (Foxp3) transcription factor in human tissues (Ward *et al.*, 2007). Another transcription factor of relevance for deciphering immune responses is the so-called retinoic acid-related orphan receptor variant 2 (RORγt or RORC2), used as a marker for an interleukin-17-mediated immune response, and to our knowledge thus far only one study showed an immunofluorescence staining of human tissue for RORC2 and Foxp3 (Voo *et al.*, 2009). Another question that is of special importance, especially for tissue reactions, is the development of germinal centres and germinal centre-like formations in lymphoid and non-lymphoid organs/structures. Several transcription factors control these processes and thus analysis of their expression patterns is of relevance. Interferon regulatory factor family 4 (IRF4) and B-cell lymphoma 6 (BCL 6) represent two of these key transcription factors, and it has been shown that for instance the use of different (mono- and polyclonal) antibodies detecting IRF4 indicates a much broader range of mature B cells expressing IRF4 than the use of one antibody alone (Cattoretti *et al.*, 2006).

♦♦♦♦♦♦ V. APPENDIX

A. Antibodies

In general, care should be taken in choosing the correct combination of antibodies for the choice of detection system, i.e. compatibility of antibodies (isotype, species) and prevention of cross reactivity (species from which the antibody originates, species of secondary antibodies, species for which the antigen is to be detected) and choice of serum used to block non-specific reactions. Each first antibody should be titered against a known tissue such as normal lymph node or spleen, before its use in the laboratory. Most antibodies are used in a concentration of 20–40 μg/ml, and most commercially available antibodies are used at titres from 1:20 to 1:200. In our experience, a first evaluation of the correct titre is obtained by using dilution steps of 1:10, 1:30, 1:100, 1:300, 1:1000 and 1:3000. For storage, sterility of antibodies should be maintained, and freezing and thawing should be avoided. Most antibodies are stable for months at 4° C. An important source of information for cluster of differentiation antibodies is the Proceedings (Leukocyte Typing I-VII) of the International Workshop and Conference on White Cell Differentiation Antigens (Oxford University Press). This information is also partly accessible by internet (Protein Reviews On The Web www.sciencegateway.org/resources/prow/).

B. Chemicals and Solutions

Chemicals used for fixation procedures should be of p.a. grade.

Tris-buffered saline: 50 mM Tris (tris(hydroxymethyl)-aminomethane) 150 mM NaCl, pH 7.5.

Phosphate-buffered saline: 150 mM NaCl, 10 mM $NaH_2PO_4 \times H_2O$, pH 7.2.

Haematoxylin stock solution: 1 g haematoxylin, 0.2 g $NaNO_3$, 50 g aluminium potassium sulphate dodecahydrate ($KAl(SO_4)_2 \cdot 12H_2O$), add 1000 ml H_2O. Finally, add 50 g chloral hydrate and 1 g of citric acid.

APAAP-developing buffer: 1.21 g Tris, 5.85 g NaCl, 1000 ml H_2O.

AP buffer: 12.1 g Tris, 5.85 g NaCl, 1000 ml H_2O.

New fuchsin solution: 5 g New fuchsin in 100 ml 2N HCl, store in a dark glass vessel at 4°C.

$NaNO_3$ solution: 6% (w/v) in H_2O.

PO-developing buffer: 6 mg 3,3′-diaminobenzidine tetrahydrochloride is dissolved in 10 ml TBS and is mixed with 100 µl H_2O_2 directly before use.

DABCO anti-fading solution: 2.5% DABCO is dissolved in 90% glycerol overnight. Adjust the pH with 2 N HCl to pH 8.6. Store at room temperature.

C. Controls

Negative controls should include antibody of the same immunoglobulin class at an equivalent concentration (isotype control). The negativity of secondary reagents is confirmed by incubating a sample without the primary antibody (TBS control).

Positive controls should be included where possible to exclude negative results due to incorrect staining procedures and to control specificity of the staining.

Specificity of the primary antibody may be analysed by neutralization experiments to check for blocking of antibody binding resulting in negative staining. This is done prior to the application in immunoenzymatic staining, by preincubating the antibody with recombinant or purified antigen for 30 min at 37°C. It should be kept in mind, however, that the absorption control does not prove the specificity of the antibody for the protein in the tissue (Burry, 2000).

D. Fluorochromes

www.bdbiosciences.com/colors/fluorescence_spectrum_viewer//

Java script generator of spectra of commonly used dyes in microscopy and flow cytometry

https://www.micro-shop.zeiss.com/?s=4648255029efa4&l=en&p=us&f=f
Interactive database of commonly used fluorochromes and corresponding filters

E. Image Analysis Software

http://rsbweb.nih.gov/ij/

List of Suppliers

Antibody resource page: http://www.antibodyresource.com/

Linscott's Directory: http://www.linscottsdirectory.com/search/antibodies

Antibody search at bionity.com: http://www.bionity.com/antibodies/e/

Antibody search at biocompare.com: http://www.biocompare.com/ProductCategories/2045/Antibodies.html

Life Science Information Network: http://www.ihcworld.com/index.htm

Zytomed Systems: http://www.zytomedsystems.de/

BD Biosciences
2350 Qume Drive, San Jose, CA, USA 95131-1807
Tel.: (800) 223-8226
Fax: (408) 954-2347
http://www.bdbiosciences.com/

DAKO Corporation
6392 Via Real, Carpinteria, CA 93013
Tel.: +1 805 566 6655
Fax: +1 805 566 6688
http://www.dako.com

DIANOVA GmbH
Mittelweg 176, 20148 Hamburg
Tel.: +49 (40) 45 06 70
Fax: +49 (40) 45 06 73 90
http://www.dianova.de

Molecular Probes® Fluorescent Dyes & Probes

Invitrogen Ltd (European Headquarters), 3 Fountain Drive, Inchinnan Business Park, Paisley PA4 9RF, UK
Tel.: +44 (0) 141 814 6100
Fax: +44 (0) 141 814 6260
E-mail: euroinfo@invitrogen.com
Technical Services: eurotech@invitrogen.com
http://www.invitrogen.com/site/us/en/home/brands/molecular-probes.html

References

Baumgarth, N. and Roederer, M. (2000). A practical approach to multicolor flow cytometry for immunophenotyping. *J. Immunol. Methods.* **243**, 77–97.

Burry, R. W. (2000). Specificity controls for immunocytochemical methods. *J. Histochem. Cytochem.* **48**, 163–165.

Calabrese, F., Baraldo, S., Bazzan, E., Lunardi, F., Rea, F., Maestrelli, P., Turato, G., Lokar-Oliani, K., Papi, A., Zuin, R. *et al*. (2008). IL-32, a novel proinflammatory cytokine in chronic obstructive pulmonary disease. *Am. J. Resp. Crit. Care Med.* **108**, 894–901.

Capraru, D., Müller, A., Csernok, E., Gross, W. L., Holl-Ulrich, K., Northfield, J., Klenerman, P., Herlyn, K., Holle, J., Gottschlich, S. *et al*. (2008). Expansion of circulating NKG2D+ effector memory T-cells and expression of NKG2D ligand MIC in granulomatous lesions in Wegener's granulomatosis. *Clin. Immunol.* **127**, 144–150.

Cattoretti, G., Pileri, S., Parravicini, C., Becker, M. H.G., Poggi, S., Bifulco, C., Key, G., D'Amato, L., Sabattini, E., Feudale, E. *et al*. (1993). Antigen unmasking on formalin-fixed, paraffin-embedded tissue sections. *J. Path.* **171**, 83–98.

Cattoretti, G., Shaknovich, R., Smith, P. M., Jäck, H. M., Murty, V. V. and Alobeid, B. (2006). Stages of germinal center transit are defined by B cell transcription factor coexpression and relative abundance. *J. Immunol.* **177**, 6390–6399.

Clatch, R. J., Foreman, J. R. and Walloch, J. L. (1998). Simplified immunophenotypic analysis by laser scanning cytometry. *Cytometry* **34**, 3–16.

Coons, A. H. and Kaplan, M. H. (1950). Localization of antigen in tissue cells. II. Improvements in a method for the detection of antigen by means of fluorescent antibody. *J. Exp. Med.* **91**, 1–13.

Cordell, J. L., Falini, B., Erber, W. N., Ghosh, A. K., Abdulaziz, Z., MacDonald, S., Fulford, K. A.F., Stein, H. and Mason, D. Y. (1984). Immunoenzymatic labeling of monoclonal antibodies using immune complexes of alkaline phosphatase and monoclonal anti-alkaline phosphatase (APAAP complexes. *J. Histochem. Cytochem.* **32**, 219–229.

Droemann, D., Albrecht, D., Gerdes, J., Ulmer, A. J., Branscheid, D., Vollmer, E., Dalhoff, K., Zabel, P. and Goldmann, T. (2005). Human lung cancer cells express functionally active Toll-like receptor 9. *Respir. Res.* **6**, 1.

Droemann, D., Rupp, J., Goldmann, T., Uhlig, U., Branscheid, D., Vollmer, E., Kujath, P., Zabel, P. and Dalhoff, K. (2007). Disparate innate immune responses to persistent and acute Chlamydia pneumoniae infection in chronic obstructive pulmonary disease. *Am. J. Respir. Crit. Care Med.* **175**, 791–797.

Evans, H. G., Gullick, N. J., Kelly, S., Pitzalis, C., Lord, G. M., Kirkham, B. W. and Taams, L. S. (2009). *In vivo* activated monocytes from the site of inflammation in humans specifically promote Th17 responses. *Proc. Natl. Acad. Sci.* **106**, 6232–6237.

Ferri, G.-L., Gaudio, R. M., Castello, I. F., Berger, P. and Giro, G. (1997a). Quadruple immunofluorescence: a direct visualization method. *J. Histochem. Cytochem.* **45**, 155–158.

Ferri, G.-L., Isola, J., Berger, P. and Giro, G. (1997b). Direct eye visualization of Cy5 fluorescence for immunocytochemistry and in situ hybridization. *J. Histochem. Cytochem.* **48**, 437–444.

Goldmann, T., Vollmer, E. and Gerdes, J. (2003). What's cooking? detection of important biomarkers in HOPE-fixed, paraffin-embedded tissues eliminates the need for antigen retrieval. *Am. J. Pathol.* **163**, 2638–2640.

Ishiko, A., Shimizu, H., Masunaga, T., Kurihara, Y. and Nishikawa, T. (1998). Detection of antigens by immunofluorescence on ultrathin cryosections of skin. *J. Histochem. Cytochem.* **46**, 1455–1460.

Johnson, G. D., Davidson, R. S., McNamee, K. C., Russel, G., Goodwin, D. and Holborow, E. J. (1982). Fading of immunofluorescence during microscopy: a study of the phenomenon and its remedy. *J. Immunol. Methods* **55**, 231–242.

Kammerer, U., Kapp, M., Gassel, A. M., Richter, T., Tank, C., Dietl, J. and Ruck, P. (2001). A new rapid immunohistochemical staining technique using the EnVision antibody complex. *J. Histochem. Cytochem.* **49**, 623–630.

Köhler, G. and Milstein, C. (1975). Continuous cultures of fused cells secreting antibody of predefined specificity. *Nature* **256**, 495–497.

Kretschmer, C., Jones, D. B., Morrison, K., Schlüter, C., Feist, W., Ulmer, A. J., Arnoldi, J., Matthes, J., Diamantstein, T., Flad, H.-D. *et al*. (1990). Tumor necrosis factor α and lymphotoxin production in Hodgkin's disease. *Am. J. Path.* **137**, 341–351.

Lehr, H.-A., van der Loos, C., Teeling, P. and Gown, A. M. (1999). Complete chromogen separation and analysis in double immunohistochemical stains using photoshop-based image analysis. *J. Histochem. Cytochem.* **47**, 119–125.

van der Loos, C. M., Houtkamp, M. A., de Boer, O. J., Teeling, P., van der Wal, A. C. and Becker, A. E. (2001). Immunohistochemical detection of interferon-gamma: fake or fact? *J. Histochem. Cytochem.* **49**, 699–710.

Müller, A. and Lamprecht, P. (2008). Interleukin-17 in chronic inflammatory and autoimmune diseases: rheumatoid arthritis, Crohn's disease and Wegener's granulomatosis. *Z. Rheumatol.* **67**, 72–74.

Nakane, P. K. and Pierce, Jr. G. B. (1967). Enzyme-labeled antibodies for the light and electron microscopic localization of tissue antigens. *J. Cell Biol.* **33**, 307–318.

Ono, M., Murakami, T., Kudo, A., Isshiki, M., Sawada, H. and Segawa, A. (2001). Quantitative comparison of anti-fading mounting media for confocal laser scanning microscopy. *J. Histochem. Cytochem.* **49**, 305–311.

Panchuk-Voloshina, N., Haugland, R. P., Bishop-Stewart, J., Bhalgat, M. K., Millard, P. J., Mao, F., Leung, W.-Y. and Haugland, R. P. (1999). Alexa dyes, a series of new fluorescent dyes that yield exceptionally bright, photostable conjugates. *J. Histochem. Cytochem.* **47**, 1179–1188.

Pileri, S. A., Roncador, G., Ceccarelli, C., Piccioli, M., Briskomatis, A., Sabattini, E., Ascani, S., Santini, D., Piccaluga, P. P., Leone, O. *et al*. (1997). Antigen retrieval techniques in immunohistochemistry: comparison of different methods. *J. Pathol.* **183**, 116–123.

Kononenk, J., Bubendorf, L., Kallioniemi, A., Barlund, M., Schraml, P., Leighton, S., Torhorst, J., Mihatsch, M. J., Sauter, G. and Kallioniemi, O. P. (1998). Tissue microarrays for highthroughput molecular profiling of tumor specimens. *Nat. Med.* **4**, 844–847.

Kumar, R. K., Chapple, C. C. and Hunter, N. (1999). Improved double immunofluorescence for confocal laser scanning microscopy. *J. Histochem. Cytochem.* **47**, 1213–1217.

Maeurer, M., Seliger, B., Trinder, P., Gerdes, J. and Seitzer, U. (1999). Interleukin-15 in mycobacterial infection of antigen-presenting cells. *Scand. J. Immunol.* **50**, 280–288.

Naiem, M., Gerdes, J., Abdulazizz, Z., Stein, H. and Mason, D. Y. (1983). Production of a monoclonal antibody reactive with human dendritic reticulum cells and its use in the immunohistological analysis of human lymphoid tissue. *J. Clin. Path.* **36**, 167–175.

Pires, A. R., Andreiuolo Fda, M. and de Souza, S. R. (2006). TMA for all: a new method for the construction of tissue microarrays without recipient paraffin block using custom-built needles. *Diagn. Pathol.* **1**, 14.

Sander, B., Andersson, J. and Andersson, U. (1991). Assessment of cytokines by immunofluorescence and the paraformaldehyde-saponin procedure. *Immunol. Rev.* **119**, 65–93.

Scheel-Toellner, D., Richter, E., Toellner, K. M., Reiling, N., Wacker, H. H., Flad, H. D. and Gerdes, J. (1995). CD26 expression in leprosy and other granulomatous diseases correlates with the production of interferon-gamma. *Lab. Invest.* **73**, 685–690.

Schnell, S. A., Staines, W. A. and Wessendorf, M. W. (1999). Reduction of lipofuscin-like autofluorescence in fluorescently labeled tissue. *J. Histochem. Cytochem.* **47**, 719–730.

Schrijver, I. A., Melief, M.-J., van Meurs, M. and Companjen, A. R. (2000). Pararosaniline fixation for detection of co-stimulatory molecules, cytokines, and specific antibody. *J. Histochem. Cytochem.* **48**, 95–103.

Seitzer, U., Scheel-Toellner, D., Toellner, K. M., Reiling, N., Haas, H., Galle, J., Flad, H. D. and Gerdes, J. (1997). Properties of multinucleated giant cells in a new *in vitro* model for human granuloma formation. *J. Pathol.* **182**, 99–105.

Shi, S.-R., Key, M. E. and Karla, K. L. (1991). Antigen retrieval in formalin-fixed, paraffin-embedded tissues: an enhancement method for immunohistochemical staining based on microwave oven heating of tissue sections. *J. Histochem. Cytochem.* **39**, 741–774.

Shi, S.-R., Gu, J., and Taylor, C. R. (eds.) (2000). *Antigen Retrieval Techniques: Immunohistochemistry and Molecular Morphology*. BioTechniques Press, Natick, MA, Eaton Pub.

Sternberger, L. A., Hardy, P. H., Cuculis, J. J. and Meyer, H. G. (1970). The unlabeled antibody-enzyme method of immunohistochemistry Preparation and properties of soluble antigen-antibody complex (horseradish peroxidase-antihorseradish peroxidase) and its use in identification of spirochetes. *J. Histochem. Cytochem*. **18**, 315–333.

Suzuki, T., Fujikura, K., Higashiyama, T. and Takata, K. (1997). DNA staining for fluorescence and laser confocal microscopy. *J. Histochem. Cytochem.* **45**, 49–53.

Srinivasan, M., Sedmak, D. and Jewell, S. (2002). Effect of fixatives and tissue processing on the content and integrity of nucleic acids. *Am. J. Pathol.* **161**, 1961–1971.

Tsurui, H., Nishimura, H., Hattori, S., Hirose, S., Okumura, K. and Shirai, T. (2000). Seven-color fluorescence imaging of tissue samples based on Fourier spectroscopy and singular value decomposition. *J. Histochem. Cytochem.* **48**, 653–662.

Voo, K. S., Wang, Y. H., Santori, F. R., Boggiano, C., Wang, Y. H., Arima, K., Bover, L., Hanabuchi, S., Khalili, J., Marinova, E. *et al*. (2009). Identification of IL-17-producing FOXP3+ regulatory T cells in humans. *Proc. Natl. Acad. Sci.* **106**, 4793–4798.

Ward, S. M., Fox, B. C., Brown, P. J., Worthington, J., Fox, S. B., Chapman, R. W., Fleming, K. A., Banham, A. and Klenerman, P. (2007). Quantification and localisation of FOXP3+ T lymphocytes and relation to hepatic inflammation during chronic HCV infection. *J. Hepatol.* **47**, 316–324.

Wasielewski, Rv.no, Mengel, M., Gignac, S., Wilkens, L., Werner, M. and Georgii, A. (1997). Tyramine amplification technique in routine immunohistochemistry. *J. Histochem. Cytochem.* **45**, 1455–1459.

Watkins, S. (1989). Cryosectioning. In: *Current Protocols in Molecular Biology* (F. M. Ausubel, R. Brent, R. A. Kingston, D. D. Moore, J. G. Seidman, J. A. Smith, and K. Struhl, eds.) pp. 14.2.1–14.2.8. Greene Publishing and Wiley-Interscience, New York.

Zeller, R. (1989). Fixation, embedding, and sectioning of tissues, embryos and single cells. In: *Current Protocols in Molecular Biology* (F. M. Ausubel, R. Brent, R. A. Kingston, D. D. Moore, J. G. Seidman, J. A. Smith, and K. Struhl, eds.) pp. 14.1.1–14.1.8Greene Publishing and Wiley-Interscience, New York.

18 Measuring Human Cytokine Responses

Hans Yssel[1], John Wijdenes[2], René de Waal Malefyt[3], Jean-François Mathieu[4] and Jérôme Pène[1]

[1] Inserm U844, Montpellier, France; [2] Gen-Probe, Besançon, France; [3] Schering-Plough Biopharma, Palo Alto, CA, USA; [4] BD Biosciences, Erembodegem, Belgium

♦♦

CONTENTS

♦♦♦♦♦♦ I. INTRODUCTION

The term *cytokine* has been used to describe a diverse group of low-molecular-weight (generally <20 kD) protein mediators that have a broad spectrum of immunoregulatory effects and which are produced by a variety of cell types. Although many cytokines were originally defined and named after the particular biological functions that they display, the development of recombinant DNA technology has permitted the classification of a plethora of factors and activities into a growing list of well-defined proteins. From a functional point of view, cytokines have several features in common.

- Most, if not all, cytokines have redundant activities, as reflected by their ability to perform similar functions. Among the many examples are interleukin (IL)-2, IL-4, IL-7, IL-10, IL-12, IL-15, IL-21, IL-23, which all have T cell growth-promoting activities, IL-4 and IL-13, which share most of their functional activities, such as induction of B cell proliferation and differentiation, induction of IgG1 and IgE isotype switching, induction of mast cell differentiation and downregulation of secretion of pro-inflammatory cytokines by macrophages, or IL-1, IL-6 and TNF-α, which activate hepatocytes to synthesize acute phase proteins, induce bone marrow epithelium to release neutrophils and act as endogenous pyrogens

METHODS IN MICROBIOLOGY, VOLUME 37
0580-9517 DOI 10.1016/S0580-9517(10)37018-8

on the hypothalamus thereby raising the body temperature, which is believed to help eliminate infections.

- Their effects are pleiotropic, affecting many different target cells, which is reflected by the functional expression of receptors for certain cytokines, such as IL-1, IL-2, IL-4, IL-6 or IL-10 on most cells of the immune system.
- Their secretion is highly regulated, because of the potential for tissue destruction and other adverse effects, and they often are secreted during bursts of immune responses.
- Cytokines interact with specific high-affinity cell surface receptors, which is followed by a cascade of signal transduction events, resulting in mRNA synthesis and, eventually, protein secretion. For a large number of IL receptors, these signal transduction events have been shown to be associated with the phosphorylation of specific tyrosine kinases, members of the Jak-Stat signal transduction system (reviewed in Ihle, 2001). In addition, most cytokines are glycosylated, giving rise to considerable molecular heterogeneity, with the different sugar molecules being important for receptor binding and modulation of receptor-mediated signal transduction.
- Many cytokines are able to induce or inhibit each other's synthesis, including their own, resulting in the creation of regulatory networks. An example of the mutual inducing activity of cytokines, resulting in a positive feedback is the effect of IL-12 and interferon (IFN)-γ on each other's production. Secretion of IL-12 by activated monocytes strongly induces the production of IFN-γ by T cells and natural killer (NK) cells, which in turn enhances the production of IL-12. Moreover, at least in the mouse, IFN-γ induces a functional IL-12R at the cell surface of T cells, rendering them susceptible to the IFN-γ-inducing effect of IL-12. The inhibitory action of cytokines is exemplified by IL-4, IL-10 and IL-13, which all efficiently block the secretion of pro-inflammatory cytokines, such as IL-1, IL-6 and TNF-α, by activated macrophages and furthermore enhance the production of IL-1RA by these cells, thus amplifying a negative feedback mechanism. Another example is IL-10, a cytokine with relatively late production kinetics that is able to inhibit its own synthesis via an autocrine feedback mechanism.
- Mixtures of cytokines often have synergistic effects, as compared to the effect of each of them separately, resulting in an amplification of responses. For example, the pro-inflammatory cytokines IL-1, IL-6 and TNF-α, which are involved in the so-called acute phase response, synergize to mediate inflammation, shock and even death in response to infectious agents.

Cytokines may resemble hormones at first sight, since both are soluble mediators which serve as means of intracellular communication. However, there are important differences between the effects of these two families of mediator molecules. Whereas hormones can be easily detected in the circulation, having endocrine (systemic) effects, most cytokines are released locally. Moreover, hormones are released as a result of internal physiologic variation and therefore are important in maintaining a situation of homeostasis. By contrast, cytokines, are produced in short bursts, following external injury, as well as during developmental and effector phases of immune responses, thereby modulating the function of adjacent

cells or the cells that produce them. Due to a short half-life time in the circulation, cytokines are generally difficult to detect in serum or plasma, although there are a number of exceptions. For example, during acute inflammation or septic shock, IL-1, IL-6 and TNF-α orchestrate a series of events that induce the acute phase response and they can readily be detected in human serum or plasma. The systemic effects of these cytokines, however, may differ significantly from the effects in the local sphere of influence. IL-1, when released by tissue macrophages, is a co-stimulatory factor for T cell activation, whereas high systemic levels of IL-1 result in fewer, leukopenia and, as mentioned above, even shock.

Cytokines can be classified into a number of categories (listed in Table 1), broadly based on their functional properties, i.e. cytokines:

- that are involved in innate immunity,
- that are involved in the regulation of lymphocyte function,
- that are involved in the regulation of haematopoiesis,
- that have anti-inflammatory modes of action,
- that have pro-inflammatory modes of action,
- that have chemoattractant properties.

As is clear from this list, which is not exhaustive, many cytokines feature in more than one category, which is in line with the notion that redundancy serves the purpose of the immune system to mount an effective and rapid response following inflammation or antigenic challenge. The concomitant release of several cytokines will lead to a rapid mobilization of effector cells at the place of injury or insult to produce the desired biological effects. Cytokines with a broad spectrum of action, such as IL-1 and IL-6, are not only involved in innate immune and inflammatory responses, which form the first line of defence of the host against antigenic challenge, but also in adaptive immune responses by exerting co-stimulatory effects on T cells and furthermore induce differentiation and growth of B cells.

Recently, the interest in the role of cytokines in the induction of inflammatory responses has been raised with the description of a T cell population with a particular cytokine production profile, T helper type 17 (Th17) cells, because of their concomitant production of high levels of IL-17 and IL-22, as well as other pro-imflammatory cytokines including TNF-α, TNF-β and IL-26. The activity of the latter cells is distinct from that of the classical Th1 and Th2 cells, characterized by the production of IFN-γ and IL-4, respectively, and although mainly based on the results of experimental animal models, it is currently accepted that activity of the cytokines produced by Th17 cells is strongly associated with excacerbated immune responses that underlie the pathogenesis of various inflammatory diseases such as rheumatoid arthritis, Crohn's disease or multiple sclerosis (reviewed in Korn *et al.*, 2009).

Conversely, in order to prevent exacerbated immune responses, resulting in tissue damage or destruction, many cytokines have downregulatory effects on the production of other cytokines, as well as on their own secretion, in order to dampen the immune response. Examples of such regulatory cytokines are IL-10 and TGF-β, which affect a wide range of target cells. Finally, several cytokines are usually involved in, and required for, the generation of an appropriate immune response and it seems difficult to bestow a more or less prominent role on each of them in view of their interregulatory effects, although there may be a certain

Table 1. Classification of cytokines based on functional properties

Cytokine	Biological action	Produced by
1. Cytokines involved in innate immunity		
IL-1α/β	Mediates host response to infectious agents	Mø, DC, fibroblasts, astrocytes
IL-1RA	Natural antagonist of IL-1, blocks IL-1-mediated signal	Mø
TNF-α	Mediates host response to infectious agents	Mø, T cells
IL-6	Mediates and regulates inflammatory responses Mediates leucocyte chemotaxis and activation	Mø, T cells, fibroblasts, chemokines
2. Cytokines involved in regulation of lymphocyte function		
IL-1	Mediates co-stimulation of T cells Differentiation of Th17 cells	Mø, DC, fibroblasts, astrocytes
IL-2	T cell growth factor, proliferation of B cells	T cells, NK cells
IL-4	T cell proliferation, Differentiation of Th2 cells B cell differentiation, IgG4/IgE switching	Th2 cells, basophils, mast cells
IL-5	Eosinophil growth and differentiation factor	T cells
IL-6	B cell proliferation, enhances Ig secretion in B cells	Mø, T cells
IL-7	Pre-T and pre-B cell proliferation, differentiation LAK and cytotoxic T cells T cells, NK cells	Bone marrow stromal cells
IL-9	Co-stimulator for mast cell-, foetal thymocyte growth	T cells
IL-10-like cytokines: IL-10, IL-19, IL-20, IL-22, IL-24, IL-26		
IL-10	Co-stimulator for T cell, B cell and mastcell growth, downregulation MHC class II/Co-stimulatory molecules on APC	Mø, T cells, keratinocytes
IL-19	Unknown	Mø, B cells
IL-20	Keratinocyte proliferation and differentiation	Keratinocytes, mono
IL-22	Stimulates Mono to make TNF-α	T cells, mast cells
IL-12	Differentiation of Th1 cells, induction of IFN-γ by mono	Mø, B cells
IL-13	B cell differentiation, IgG_4/IgE switching	T cells, B cells, mastcells
IL-15	T cell, mast cell growth factor	Mono
IL-17	Induction of IL-6 and IL-8 production by monocytes induction of CD54 expression by fibroblasts	Th17 cells
IL-18	Induction of IFN-γ production by T/NK cells	Mono
IL-21	Maturation and proliferation of NK cells from BM B cell growth factor, IgG_1/IgG_3 switching	T cells, TFH cells, NK cells
IL-23	Stimulation of IFN-γ production Induction of Th17 cell differentiation/proliferation	DC, Mø
IL-27	B cell growth factor, IgG_1/IgG_3 switching Induction of IL-10 production by Th17 cells	DC, Mø
TNF-β	Stimulates T cell growth	T cells, B cells

Table 1. (*Continued*)

Cytokine	Biological action	Produced by
IFN-γ	Mø/NK cell activation, upregulation MHC class I/II on Mono	Th1 cells, NK cells
3. Cytokines involved in the regulation of haemotopoiesis		
IL-3	Synergistic action in haemotopoiesis	T cells, mast cells
IL-5	Growth/differentiation of eosinophils	T cells, mast cells
IL-6	Growth/differentiation megakaryocytes	Mono, DC, Mø, T cells
G-CSF	Growth/differentiation granulocytic lineage	Mono, DC, Mø, T cells
GM-CSF	Growth/differentiation myelomonocytic lineage	Mono, DC, Mø, T cells
SCF (ckit-L)	Growth/differentiation haemotopoietic precursor cells	Bone marrow stromal cells
Erythropoietin	Growth/diff. erythroid progenitor cells	Kidney cells
4. Cytokines having anti-inflammatory effects		
IL-4	Inhibition of pro-inflammatory cytokines by Mono	
IL-13	Inhibition of pro-inflammatory cytokines by Mono	
IL-10	Inhibition of pro-inflammatory cytokines by Mono, Inhibition MHC class II expression Mono, inhibition of T cell growth, induction of T regulatory cells	
TGF-β	Inhibition of pro-inflammatory cytokines by Mono Induction of T regulatory cells	Chrondrocytes, Mono, DC, Mø, T cells
5. Cytokines having pro-inflammatory effects		
IL-1	Participates in acute phase response	
TNF-α	Participates in acute phase response	
IL-6	Participates in acute phase response	
IL-16	Migratory response in $CD4^+$ T cells/Mono/EO	$CD8^+$ T cells
TGF-β		Induction of Th17 cells with IL-1/IL-6
6. Chemokines (see Zlotnik and Yoshie (2000) for classification of chemokines)		

DC: Dendritic cells, EO: eosinophils, Mono: monocytes, Mø: macrophages, BM: bone marrow.

hierarchy in the action of cytokines, especially with respect to kinetics of production. Therefore, the concomitant inducing and inhibitory effects of many cytokines constitute the basis for the creation of overlapping cytokine networks which are able to tightly regulate an appropriate immune response.

Finally, whereas cytokines play a pivotal role in the generation of immune responses, dysregulation of cytokine production has been shown to result in acute of chronic immunopathology. An example is provided by the above-mentioned activity of IL-17- and/or IL-22-producing cells that, in the absence of regulatory mechanisms, will lead to the induction and perpetuation of various inflammatory diseases. Therefore, the possibility to accurately measure cytokine

production is not only of great importance for scientific purposes, but also for diagnostic purposes and furthermore is useful for the monitoring of clinical therapies.

♦♦♦♦♦♦ II. ASSAYS FOR MEASURING CYTOKINE PRODUCTION

To date, several assays are used to detect and quantify cytokines in serum, body fluids and culture supernatants, as well as their production by cytokine-producing cells. In this chapter we will describe the real-time PCR assay, the enzyme-linked immunosorbent assay (ELISA), ELISPOT assay, the intracellular cytokine staining assay and the BD^{TM} cytometric bead assay. An overview of the advantages and disadvantages of each of these assays, described in this chapter, is shown in Table 2. The detection of cytokines by cell surface staining will be described in Chapter 1 of Volume 32.

Table 2. Advantages and disadvantages of assays for the measurement of cytokines

Bioassay
Very sensitive
Active form of cytokine is detected
Can be performed in the absence of standard: activity expressed in arbitrary biological Units
Requires use of neutralizing anti-cytokine antibodies to demonstrate specificity
Large series of dilutions required to fit results on dose-dependent S-shaped curve
Requires labor-intensive tissue culture for relevant responder cells
Presence of stimulating agent in culture supernatant may act on responder cells
Real time RT-PCR
Quantitation of cytokine transcripts
Expensive, technically demanding and calibration difficult
Suitable for high throughput
Detection of cytokine transcripts only and not (secreted) protein
Intracellular staining
Specific, but not very sensitive for certain cytokines: sensitivity is dependent on antibody and fixation conditions
Requires selection of suitable antibodies that detect chemically fixed cytokines
Use in flowcytometry permits analysis of frequency and phenotype of cytokine-producing cells, as well as kinetics of cytokine production
Simultaneous detection of several cytokines produced by same cell
Results are not affected by the inducing/inhibitory effects of simultaneously produced cytokines
Although theoretically possible, difficult to use under conditions of antigen-specific stimulation
Requires viable cells at the end of the stimulation
Requires exogenous (recombinant) cytokine to confirm specificity
Meaningful interpretation of the results might require kinetics measurements

Table 2. (*Continued*)

ELISA
Specific
Results are easy to fit onto dose-dependent S-shaped curve
Different modes of activation, including antigen-specific stimulation, can be used
Less sensitive than bioassay: sensitivity is dependent on the capture antibody
Non-active form of cytokine is also detected
Laborious and time consuming when multifunctional analysis is performed
Results can be affected by sequestration of cytokines from biological samples by (soluble) cytokine receptors, by inducing/inhibitory effects of simultaneously produced cytokines or by false-positive values with heterophilic antibodies
ELISPOT assay
Specific, and more sensitive than ELISA, because of local release and capture of cytokines
Determination of frequencies of cytokine producing cells although quantification is tedious
Simultaneous (although restricted) detection of cytokine production by the same cell
Possibility to analyse cytokine production by freshly isolated clinical material without prior *in vitro* stimulation
No possibility to combine flowcytometry and cytokine production
Same technical advantages and constraints as ELISA
Cytometric Bead Array (CBA)
Specific
Simultaneous detection and quantification of cytokines by flow cytometry
Assay procedure and data processing more rapid as compared to ELISA
Only very small sample quantities are required for extensive multifunctional analysis
For Bioassay, ELISA, ELISPOT and CBA
Accumulation of secreted cytokines is measured: no constraints regarding kinetics of production

A. Activation Procedure

Since the production of cytokines is tightly regulated, at the transcriptional, as well as the protein level, cell populations need to be appropriately activated for the required amount of time to allow detection of cytokine transcripts and/or production of protein. Activation procedures for each of the cytokine detection assays are nearly identical and will be described first.

1. Protocol

1. Stimulate 10^6–$2.10^6\,ml^{-1}$ peripheral blood mononuclear cells (PBMCs) or 10^6–$4.10^6\,ml^{-1}$ T cells with either of the following agents (see notes 1 and 2):
   - Soluble (for PBMCs) or plate-bound (for purified T cells or T cell lines) anti-CD3 monoclonal (m) antibody (Ab) (SPV-T3b, UCHT-L1, OKT3, B-B11 or equivalent) and soluble anti-CD28 mAb (L293, 9.3, BT-3; $1\,\mu g\,ml^{-1}$). Coat plates with $10\,\mu g\,ml^{-1}$ anti-CD3 mAb diluted in phosphate-buffered saline

(PBS) and incubate for 18 h at 4°C or for 4 h at 37°C, remove mAb solution, wash twice with PBS and once with culture medium and use in experiment (see note 3).
- A combination of mitogenic anti-CD2 mAb (mAb D66 (Rosenthal-Allieri *et al.*, 1995) combined with any sheep red blood cell binding anti-CD2 mAb).
- The combination of 12-O-tetradecanoylphorbol-13-acetate (TPA), also called phorbol-12-myristate-13-acetate (PMA) (1 ng ml^{-1}) and the calcium ionophore A23187 (500 ng ml^{-1}) (Calbiochem: 524400 and 100105, respectively) or Ionomycin (Calbiochem: 524400), respectively.

Use 24-well (final volume 1 ml), 48-well (500 µl) or 96-well (200 µl) plates.

2. When using plate-bound anti-CD3 mAb, spin the culture plates at 100×g for 2 min (see note 3).
3. Incubate the cells at 37°C, 5% CO_2.
4. For *RT-PCR*: harvest the cells after 4–8 h of incubation, spin at 200×g for 10 min at 4°C, carefully remove supernatant and process cells for RNA preparation, as described on page 435.
5. For *ELISPOT*: gently harvest the cells after 6 h of incubation, transfer to ELISPOT plates and incubate for an additional 20 or 40 h at 37°C, 5% CO_2. Analyse filters for presence of cytokines.
6. For *ELISA and Cytometric Bead Array (CBA)* (see note 4): harvest the supernatants after 24–48 h of incubation, spin at 200×g for 10 min to remove residual cells and analyse for cytokine production.
7. For *intracellular staining* (see notes 4 and 5): after 4 h of incubation, add 10 µl of Brefeldin A (A stock solution of 10 mg ml^{-1} Brefeldin A (Epicentre Technologies, Madison, WI: B905MG, or Sigma: B7651) is made in dimethyl sulphoxide (DMSO), diluted 1:10 in PBS, and Brefeldin A is added at a final concentration of 10 µg ml^{-1} to the cell suspension) and incubate the cells for an additional 2 h at 37°C, 5% CO_2. Harvest cells and put on ice, prior to analysis for cytokine production.

2. Notes and recommendations

1. The nature of the cytokine production profile of T cells depends on the mode of activation, and it is therefore recommended to compare different stimulation protocols. Most importantly, these should include activation of the cells with anti-CD3 and anti-CD28 mAbs, which resembles antigen-specific stimulation conditions. Another possibility is the use of superantigens, such as Staphylococcus enterotoxin B (SEB), which bind to certain TCR Vβ gene products. When using PBMC and specific, soluble antigen, use longer incubation periods (up to 4 days) to obtain optimal cytokine production levels. Modes of stimulation involving polyclonal activators, such as the combination of phorbol ester and calcium ionophore or ionomycine, respectively, should be used only as control activations to ensure intrinsic capacity of the cells to produce cytokines or as a positive control in analysis of cytokine production in the intracellular staining assay. It is of note that the combination of phorbolester and ionomycine is almost universially used for the detection of intracellular cytokine production. Although not physiologically comparable to antigen-specific stimulation, this mode of

stimulation indeed results in high frequencies of cytokine-producing cells while maintaining a particular cytokine production profile.

Lipopolysaccharide (LPS, 1 μg ml^{-1}; Sigma ref L-2880) is the stimulation of choice for monocytes. To optimaly induce the production of cytokines by these cells, pre-incubate freshly isolated monocytes with 10 ng ml^{-1} IFN-γ for 18 h and stimulate with LPS at a concentration of 100 ng ml^{-1}.

2. Use Iscove's Modified Dulbecco Medium supplemented with 10% human or foetal calf serum or Yssel's medium (Yssel *et al.*, 1984), supplemented with 1% human serum (detailed procedure for preparation sent upon request).
3. Spinning cells onto anti-CD3 mAb-coated plates will enhance magnitude of stimulation (H. Yssel, unpublished results). This is especially important for short-time kinetics in RT-PCR assays or for the first incubation of cells for the ELISPOT assay prior to transfer to the filters.
4. Since cytokines are secreted with different kinetics, T cells should be stimulated for at least 24 h (48 h is recommended) before harvesting the supernatants for measurement by ELISA or CBA. When not immediately analysed, culture supernatants should be aliquotted and stored at –80°C. Similarly, cytokine standards should be aliquotted and kept frozen. Repetitive freeze/thaw cycles should be avoided, since most cytokines, in particular IFN-γ, will degrade rapidly due to this procedure. For intracellular staining and RT-PCR analysis, 6–8 h of stimulation is optimal for most cytokines.
5. Agents which block intracellular protein transport, such as Brefeldin A and Monensin, have dose- and time-dependent cytotoxic effects and it is not recommended to have either agents included in the cultures for >6 h. Since Monensin has been found to induce the intracellular production of IL-1 and TNF-α in monocytes within 30 min of activation, the use of Brefeldin A, instead of Monensin, is preferred. Brefeldin A is added at a final concentration of 10 μg ml^{-1} to the cell suspension. Brefeldin A is toxic: avoid contact with skin, eyes and mucous membranes.

♦♦♦♦♦♦ III. REAL-TIME QUANTITATIVE PCR 'TAQMAN'

The reverse chain polymerase reaction (RT-PCR) is a powerful technique to analyse gene regulation at the cellular level (Ferre, 1992). However, the advantage of the sensitivity is also a limitation due to the two enzymatic reaction steps. The reverse transcriptase first synthesizes a complementary strand from the RNA with specific, random or oligo dT primers, and this newly synthesized cDNA is subsequently amplified by the Taq polymerase with two specific primers for a sufficient number of times to be analysed. The quantification of a specific cDNA present in the samples is only possible in the exponentiel phase of the enzymatic reaction, where the amount of amplified targets is a linear function of the starting template (Gilland *et al.*, 1990). Real-time quantitative PCR (Higuchi *et al.*, 1992; Higuchi *et al.*, 1993) is a technique that allows for the detection in real time of a PCR product as it accumulates through the successive cycles of a PCR reaction. As a consequence, it is possible to measure product accumulation at the logarithmic amplification phase

of a PCR reaction, independently of the amount of target sequences present at the onset of the reaction. This has the absolute advantage that quantitation of the PCR product is not performed as an endpoint measurement where availability of reaction components or activity of the Taq polymerase become rate limiting. Moreover, this technology allows quantitation with a dynamic range of 7 logs and a sensitivity of less than 10 target sequences per sample. Three different types of chemistry are now applied to detect the accumulation of PCR products: fluorogenic probes, intercalating dyes, such as SYBR Green, and MGB (minor groove binding) probes. All three chemistries are based on the detection of changes in fluorescence levels which are proportional to accumulation of the PCR product.

The first type of chemistry makes use of the 5′ fluorogenic assay (Holland *et al.*, 1991) and measures the amount of PCR product formed as a function of the cleavage of a fluorogenic probe containing a reporter dye and a quencher dye. These probes are called Taqman probes, or FRET (Föster Resonance Energy Transfer) probes. While the probe is intact, the proximity of the quencher dye reduces the fluorescence of the reporter. During the extension phase of PCR, the probe anneals to its target sequence, if present, and is cleaved by the 5′ nuclease activity of Taq DNA polymerase. The resulting separation of the reporter dye from the quencher generates increased fluorescence from the reporter. Since probe cleavage is dependent on polymerization, the increase in fluorescence is proportional to the amount of PCR product formed.

A variant of this chemistry, which has been applied more recently, makes use of modified internal probes that contain a reporter dye at the 5′ end of the sequence, and at the 3′ end a nonfluorescent quencher and a minor groove binder (MGB). There are various names for these probes including MGB probes and Blackhole quenchers. The minor groove binder increases the melting temperature (T_m) and allows for the use of shorter probes. The use of these probes is also dependent on the 5′ nuclease activity of Taq polymerase to generate a signal from the reporter dye that is proportional to the accumulation of the PCR product in the 5′ fluorogenic reaction. The advantage of this approach is the use of shorter probes and the absence of fluorescence from the quencher. The calculations on the increase of fluorescence derived from the reporter dye are more accurate since there is no contribution of fluorescence from the quencher, leading to an increased specificity. This also simplifies the detection of more than one target in a single tube (multiplex reactions), and up to four individual reactions can be monitored simultaneously with four different reporters.

The second type of chemistry is based on the changes in fluorescence of a intercalating dye when it interacts with double-stranded DNA. Again, the accumulation of a PCR product is measured directly by the increase in fluorescence caused by the binding of the SYBR Green dye to double-stranded DNA. This type of reaction is independent of the sequence of the amplified product. It could thus detect amplification of non-specific or contaminant reactions. However, a dissociation or melting curve can be generated as a post-amplification step which determines the T_m of the PCR product and provides information on the amplification and specificity. The advantage of this approach is the elimination of (costly) probes for each different target.

The third type of chemistry is the use of molecular beacons (Tyagi and Kramer, 1996; Tyagi *et al.*, 1998). These are also internal probes that contain the target

sequence in a hairpin loop between with reporter and quencher dyes on short flanking sequences. These probes will hybridize to the target, if present, which will disrupt the hairpin structure and allow for separation of the reporter and quencher dyes, resulting in a fluorescent signal. The fluorescent signal is in this application is recorded during the annealing phase of the PCR reaction. Alternative ways of applying and quantitating gene expression based on these three types of chemistries have also been designed and include incorporation of fluochromes during amplification and addition of quenched probes as hairpin structures at the 5′ or 3′ end of primers (Didenko, 2001). In addition to the wide dynamic range and sensitivity of this type of quantitative PCR, a major advantage of the technology is that post-amplification steps are no longer required, making it very suitable for high throughput analyses. Indeed, 96 and 384 plate formats are currently in use. We will focus in this part on the application of Taqman and SYBR Green assays.

A. Methods

1. Designing specific primers

The design of specific primer and probe pairs is dependent on the chemistry that is used in the application. In general, the melting temperature of the primers in all three chemistry reactions must be between 58°C and 60°C and the maximal difference between the T_m of forward and reverse primer is 2°C. The GC can be variable, but must be between 20 and 80%. More important is that there are no runs of four or more identical bases, in particular no G's, and that the last five bases of the primers contain no more than 2 G/C residues. Primer length can be between 9 and 40 residues with an optimal length of 20. Complementary stretches at the 3′ ends should be avoided to prevent primer–dimer formation, as well as hairpin structures in the primers, which decrease the efficiency of primer annealing. The Taqman probe should have a T_m of 68–70°C, which guarantees annealing of the probe prior to that of primers in the annealing phase of the PCR reaction. Again, runs of four or more identical bases should be avoided, as well as a G residue at the 5′ end. Any G residue adjacent to the reporter dye will quench reporter fluorescence, even after cleavage. Preferably, the strand should be chosen where the number of C residues exceeds the number of G residues. MGB probes should have a T_m of 65–67°C, be as short as possible and contain less than 20 nucleotides.

Since the PCR products do not have to be visualized on gel post amplification, the size of the amplicon can be short, in many cases just encompassing primer and probe sequences. This results in amplicon sizes that are generally less than 150 bp with a variable T_m of around 70°C. All these criteria are difficult to take into account without the use of computation. Primer Express (Perkin Elmer) and other software packages are available to design primer and probes that fit these criteria.

Once primer and probe sequences are designed, an additional check for specificity can be done by blast search against the non-redundant GenBank database (http://www.ncbi.nlm.nih.gov/). Primer design is an empirical process, as even after using the computational design algorithms, the primer and probe combination may not function efficiently. Thus, it may be worthwhile to design and test several primer/probe pairs for a particular target.

Genes encoding cytokines or cytokine receptors, as well as many other genes in the genome, are usually composed of exons, containing coding sequences which are separated by non-coding intron sequences. To prevent amplification of genomic DNA, it is recommended to design one of the primers or the probe over an exon/intron boundary. Primers and probes detecting human cytokine and cytokine receptor expression can be obtained as pre-developed assay reagents (PDAR's) (Perkin Elmer).

2. Primer and probe purification

Due to the high constraints on the efficiency of the PCR reaction, it is worthwhile to purify primers and probe from contaminants. For primer purification a simple desalting step by spin chromatography is usually sufficient. Probes need to be purified by an additional HPLC (high-pressure liquid chromatography) step and preferably a PAGE (poly-acrylamide gel electrophoresis) step to eliminate any fluorochrome residues that are not attached and have to be checked for proper dual labelling. These procedures are usually performed by the manufacturer. Primers and probe concentrations are optimized for use in real-time PCR following design and purification.

3. Protocol

Primers from DNA synthesis facility (20–30 OD) are dissolved in H_2O in 500 µl. Spin Sephadex G25 column (Microspin G-25 Columns: Amersham/Pharmacia 27-5325) for 1 min at $1700 \times g$. Change collecting tube, add 200 µl primer solution and spin Sephadex G25 column for 2 min at $1700 \times g$. Remove tube and read the OD of an aliquot which was diluted 100-fold. Calculate the molarity (M) according to the following formula:

$$\text{Absorbance (260 nm) (OD)} = \frac{\text{sum extinction coefficient contributions of each of the individual bases} \times \text{cuvette pathlength} \times \text{concentration}}{\text{dilution}}$$

The extinction coefficients of the individual bases are

A 15.200/**C** 7.050/**G** 12.010/**T** 8.400

The concentration in M is thus equal to $100 \times \text{OD} / \text{sum extinction coefficient}$ contributions of each of the individual bases when using a pathlength of 1 cm. Dilute primers to 45 µM.

The concentration of primers and probe are important parameters for the efficiency of the PCR reaction. Apart from the design itself, these are the only parameters that are not standardized in a Taqman PCR reaction. Buffer components are optimized for use with a wide variety of primer/probe combinations with respect to Mg^{2+} concentration in the Taqman and SYBR Green Mastermix™ reaction buffers. Primer concentrations for Taqman applications are optimized in a checkerboard configuration at

50, 300 and 900 nM *in duplo*. Prepare in a tube 300 µl mastermix, 5 µl positive control target DNA (stock 10 µg ml^{-1}), 12 µl probe (stock 10 µM, final 200 nM) and 83 µl H_2O. In separate tubes make serial dilutions of forward and reverse primers from the 45 µM stock solution to yield final concentrations of 50, 300 and 900 nM. (Add 6 µl of stock primer to 44 µl H_2O, from this add 16.3–32.6 µl H_2O and from this add 8.3–42.6 µl H_2O.) Assemble 40 µl target/mastermix/probe and 10 µl of each dilution of forward and reverse primers in nine separate tubes, mix and transfer 25 µl to the reaction plate in duplicate wells. Run reactions and select the primer combination that results in the lowest C_T value and the highest ΔRn (see below). Repeat this process with optimized primer concentrations, now varying the probe concentration from 100, 150, 200, 250 to 300 nM. Generally, primer concentrations of 900 nM and probe concentration of 250 nM give optimal results.

4. RNA preparation

There are two preferential ways to purify the RNA, depending mostly on the amount of available material.

5. More than 10^6 cells

Total RNA is isolated and purified using RNAzol [Quantum-Appligene] according to the manufacturer's instructions and quantified by optical density readings. Pelleted cells are lysed with 1 ml of RNAzol and then 0.2 ml of chloroform is added. After centrifugation, the aqueous phase is recovered and precipitated with isopropanol (v/v). The pellet is resuspended in 10 µl of RNAse-free water. It is sometimes necessary to add glycogen or t-RNA as a carrier for better RNA recovery.

6. Less than 10^6 cells

Total RNA is prepared using an affinity column technique (Glassmax from Qiagen, Invitrogen). The Glassmax technique from Invitrogen is used according to the manufacturer's instructions. Briefly, the cells are pelleted and homogenized into 400 µl of the lysis buffer, and then stored at –20°C until use. The homogenate is thawed on ice and pelleted 5 min at 20.000 x *g* with 280 µl of cold ethanol. The pellet is resuspended in 450 µl of the binding buffer and 40 µl of ammonium acetate and applied on a column, spun for 20 s at 20.000 x *g* and washed successively in the same manner with the wash buffer followed by 80% ethanol in water. The RNA is then eluted with 30–50 µl of RNAse-free water, previously heated at 70°C.

7. Reverse transcription

About 1 µg of total RNA (a lower concentration can be used, but for an easier comparison of the different samples, a constant number of cells is recommended) is resuspended in 20 µl of distilled water (H_2O) and 1 µl of oligo-dT at 1 mg ml^{-1} is

added together with 0.1 µl of 40 U ml^{-1} RNAsin (Promega). The samples are heated at 70°C for 10 min and cooled down at room temperature; the samples are briefly spun down in a microfuge after which 15 µl of the enzyme mixture (7 µl of 5X Superscript buffer (Invitrogen), 5 µl of 10 mM dNTP, 1.5 µl of 1 M DTT (Invitrogen), 0.1 µl of 40 U ml^{-1} RNAsin (Promega) and 1.5 µl of Superscript II (Invitrogen)) is added. The samples are then incubated at 42°C for 1 h and heat denatured at 95°C for 3 min, and after rapid cooling on ice, the volume is adjusted to 200 µl with H_2O. The samples are then stored frozen at –20 to –80°C until use for RT-PCR amplification.

8. PCR amplification

Ten to fifty nanogram of cDNA per reaction is used as templates for quantitative PCR and analysis for the expression of human cytokine and cytokine receptor or transcription factor genes by the fluorogenic 5′-nuclease PCR assay using the GeneAmp 5700, ABI Prism 7700 or 7900 Sequence Detection Systems (Perkin-Elmer), Light Cycler (Roche), iCycler iQ (Biorad) or the Stratacycler (Stratagene). PCR reactions are assembled using 2× concentrated buffer solutions Universal PCR Master Mix (Taqman)- or SYBR Green PCR master mix (ABI)-containing enzymes, dNTPs and a inert fluorochrome (ROX) to yield final concentrations of 1× PCR buffer, 200 mM dATP, dCTP, dGTP and 400 mM dUTP, 5.5 mM MgCl2, 1.25 U *AmpliTaq* Gold DNA polymerase, Passive Reference I and 0.5 U Amp-Erase Uracil-*N*-glycocylase (UNG). Forward and reverse primers are added at 900 nM each and FAM labelled probes at 250 nM in Taqman assays, and forward and reverse primers are used at 200 nM in SYBR Green assays.

In a multiplex Taqman assay it is possible to measure additional targets in the same tube (actin, GAPDH, Ubiquitin, 18S rRNA), which can serve as internal controls for amount of input cDNA. For multiplex assays containing 18S rRNA detection reagents, forward primer, reverse primer and VIC labelled probe are all added at primer limiting concentrations of 50 nM in the PCR reaction. The thermal cycling conditions include at step 1 an incubation of 2 min at 50°C to eliminate any PCR-derived DNA contaminants by UNG, at step 2 an incubation of 10 min at 95°C to activate the 'hotstart' Taq Polymerase and at step 3, 40 cycles of amplification alternating between denaturing conditions at 95°C for 15 s and annealing-extension conditions at 55°C for 1 min.

9. Protocol

This protocol is for a multiplex taqman reaction with a final reaction volume of 25 µl. To ensure rigorous mixing and equal loading, 30 µl reactions are prepared, of which 25 µl is transferred to the final 96-well reaction plate. For 100 reactions assemble in a 5-ml polypropylene tube 1500 µl 2× buffer (Mastermix), 60 µl forward primer target (45 µM Stock), 60 µl reverse primer target (45 µM Stock), 75 µl FAM labelled probe target (10 µM Stock), 15 µl forward primer control (10 µM Stock), 15 µl reverse primer control (10 µM Stock) and 15 µl VIC labelled probe

control (10 μM Stock) and 60 μl H_2O. Mix well and distribute 18 μl per well with an electronic multipipettor (Biohit, Eppendorf or Gelman). Add 12 μl of sample DNA solution (containing 12–60 ng cDNA) or standard DNA solutions to the wells, mix well, spin plate 2 min at $770 \times g$ and transfer 25 μl to the final reaction plate using a 12-channel electronic pipettor. Try to avoid as much as possible the formation of airbubbles during transfer. Close the plate with optical caps or adhesive optical cover and run.

To make DNA standard solutions, start with a stocksolution of plasmid or other DNA containing the appropriate target sequence at 10 μg ml^{-1}. In Eppendorf tubes make at least seven tenfold dilutions of the 10 μg ml^{-1} stock in H_2O. From the 10 μg ml^{-1} dilution (third dilution) take 12 μl as the first point of the standard curve, which equals 100 pg in the final reaction. Do not use the first two dilutions as these are too concentrated for the detection system. You can make stocks of these plasmid dilutions.

This protocol can be easily adapted for SYBR Green reactions by replacing the Taqman mastermix by SYBR Green Mastermix and addition of only 13.3 μl target forward primer and 13.3 μl target reverse primer with 274 μl H_2O.

10. Analyses of results and calculations

Following the amplification, the measurements of fluorescence intensity taken at each PCR cycle are collected and normalized by the software. The normalized reporter value Rn is obtained by dividing the emission intensity of the reporter dye (FAM, VIC, SYBR) by the emission intensity of the passive reference (ROX). This step allows for the correction of small changes in volume present in each individual well. If a positive reaction occurs, then the Rn will increase with an increase in cycle number. Rn+ is the Rn value of a reaction that contains all the components, whereas Rn– is the Rn value of an unreacted sample that is obtained from the early cycles in a PCR run (baseline) or from a reaction that did not contain template. The difference in Rn over time in the reaction is given by $\Delta Rn = (Rn+) - (Rn-)$. ΔRn is thus the increase in fluorescent signal, specific for accumulation of the PCR product. Results of a quantitative PCR reaction are expressed as the Threshold cycle or C_T values. The C_T is the first cycle number at which the reporter fluorescence generated by cleavage of the probe passes a fixed threshold above baseline. The C_T value is most accurately obtained from ΔRn values following log transformation. The software allows for easy visualization of Rn, ΔRn and log transformed ΔRn values which is needed to set the baseline and Threshold. The software will then give the C_T values for the PCR reactions. It is important to realize that C_T number is inversely correlated with the amount of target DNA in the sample; i.e. the C_T equals 40 if no target is present.

Using the C_T values, it is possible to perform calculations on absolute and relative quantitation. When a standard curve of target DNA was run, the software calculates the absolute amount of target DNA present in the samples based on the C_T values of standard curve and samples. These values can even be corrected based on the amount of internal control present by multiplication of normalized log transformed C_T values of the internal control reactions. Finally, fold expression over a

calibrator (e.g. a timepoint = 0, or an untreated sample) can be calculated without the need for absolute quantitation by the formula: fold = $2^{1-\Delta\Delta CT}$. The $\Delta\Delta C_T$ is equal to (sample target C_T – sample internal control C_T) – (calibrator sample C_T – calibrator internal control C_T). A full derivation and theory of this latter can be found at http://www2.perkin-elmer.com/ab/about/pcr. These calculations can also be done using C_T values obtained using SYBR Green if the internal control is run on a separate plate. One additional step that is recommended using SYBR Green assays is to analyse the dissociation curve of the PCR products and discount those that do not have the expected T_m.

♦♦♦♦♦♦ IV. INTRACELLULAR CYTOKINE STAINING

The method of staining with cytokine-specific mAbs for the analysis of intracellular cytokines in suspension by immunofluorescence using an UV microscope has originally been described by Anderson *et al.* (1990) Subsequently, it was shown that the presence of intracellular cytokines could be detected using a FACS flow cytometer (Jung *et al.*, 1993; Assenmacher *et al.*, 1994) and recent improvements in the fixation procedure (Openshaw *et al.*, 1995) and the use of Brefeldin as a protein transport inhibitor (Picker *et al.*, 1995) have made the method even more suitable for multiparameter flow cytometry analysis. The advantage of this method over the measurement of cytokines in culture supernatants of activated cells is that it enables to determine the frequency of cytokine-producing cells, as well as kinetics of cytokine production. Moreover, in combination with cell surface staining, the method can be used to identify the phenotype of cytokine-producing cells in a population of non-separated cells, whereas the development of fluorochromes with different emission wavelength and flowcytometers, equipped with dual lasers, has permitted the simultaneous detection of several cytokines, provided the mAbs are directly conjugated with the appropriate fluorescent dyes.

Critical parameters for successful intracellular cytokine staining include the choice of a proper fixation and permeabilization protocol, the inclusion of a protein transport inhibitor, cell type and activation protocol and kinetics of activation (Figure 1).

The principle and sensitivity of the method depends on the availability of mAbs which recognize natural cytokines, in spite of a fixation and permeabilization procedure. Fixation of the cells is required for subsequent treatment with detergent, and ideal fixatives preserve the morphology of the cells and antigenicity of the cytokines with minimal cell loss. Subsequent permeabilization of the cell membranes with the detergent saponin allows fluorochrome-labelled cytokine-specific mAb to penetrate through the cell membrane, cytosol and the membranes of the Golgi apparatus and endoplasmatic reticulum. It should be kept in mind, however, that the method provides a 'snapshot' of cytokine production and the observed frequency of cytokine-producing cells is affected by multiple variables, such as activation conditions and state of cell cycle of the cells.

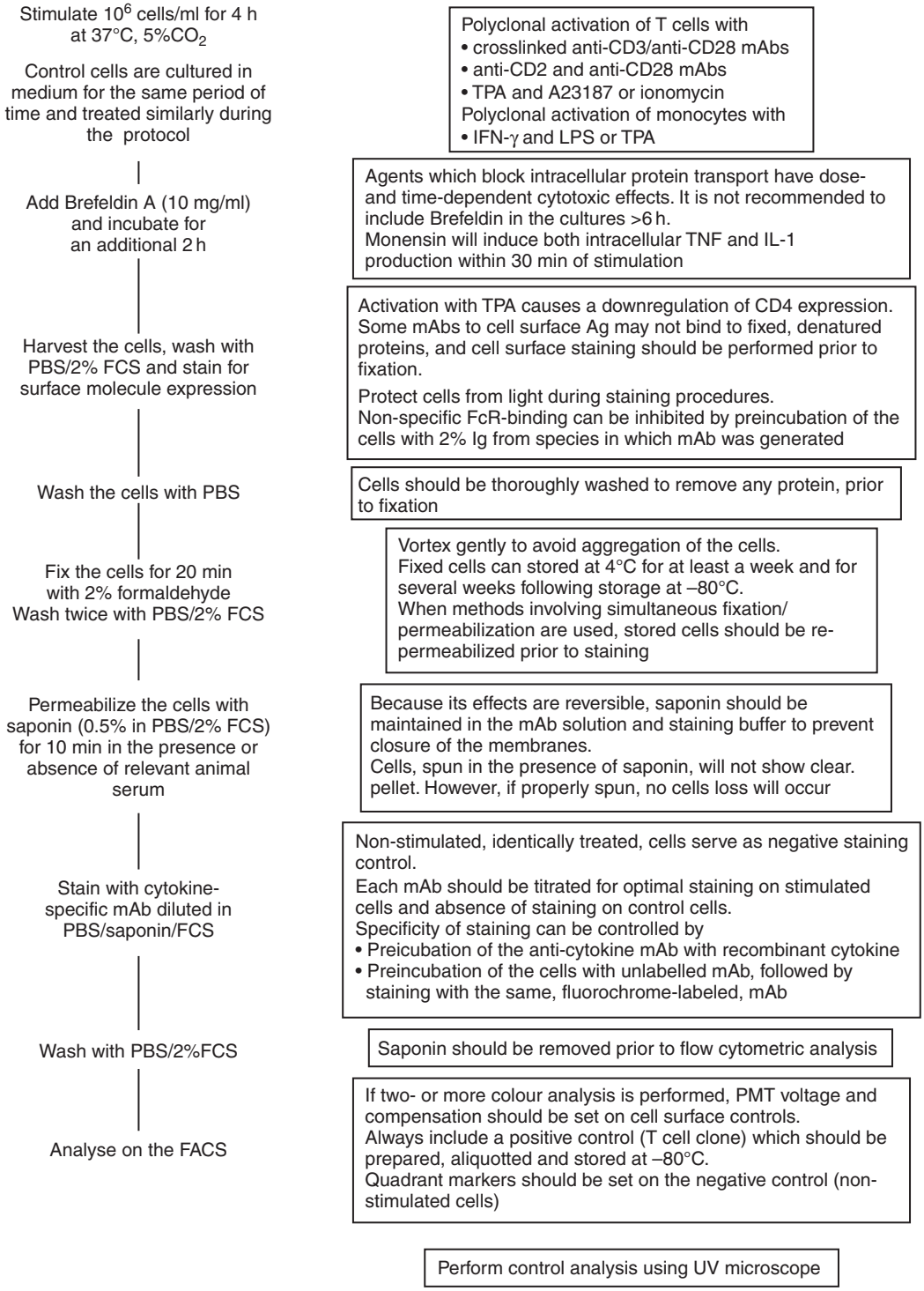

Figure 1. Flowchart for the intracellular staining procedure

A. Reagents and Equipment

- *Washing buffer*. PBS without Ca^{2+} and Mg^{2+}, supplemented with 2% heat-inactivated FCS and 0.1% (w/v) sodium azide (NaN_3) (see note 1). Adjust buffer to pH 7.4 and store at 4°C.
- *Permeabilization buffer*. Washing buffer, supplemented with 0.5% saponin (Sigma; S7900). Make stock solution of 10% saponin in PBS (pH 7.4), dissolve at 37°C, filter solution through a 0.2 μm filter and store at 4°C (see note 1).
- *Formalin* (=37% formaldehyde solution, Sigma F1635). Dissolve 10.8 ml of formalin in 89.2 ml PBS, filter to remove particles and store at 4°C (see note 1).
- *Cytokine-specific mAbs* (preferentially conjugated directly with a fluorochrome (fluorescein isothiocyanate (FITC) phycoerythrin (PE), or Cy5)). A list of mAbs suitable for intracellular staining is shown in Table 3.
- *Second-step fluorochrome-labelled Abs*. Horse–anti-mouse IgG-FITC/PE (Vector; FI 2000/EL 2000). Rabbit–anti-rat IgG-FITC (Vector; FI 4000).
- *For analysis by FACScan flowcytometer*. Vortex; centrifuge with rotor to spin microtitre plates; 96-well V-bottom plates (Falcon, BD Biosciences); FACS tubes (BD Biosciences).

B. Protocol: Staining for Flow Cytometry

The procedure for activating cells is given on page 429 (see notes 2 and 3).

editor: page of activation procedure)

If cell surface staining is performed, start with step 1; for intracellular cytokine staining without cell surface staining, start with step 7 (see note 4).

1. Transfer the stimulated cells to 15-ml centrifuge tube and wash twice with 1 ml of ice-cold washing buffer. Washing with larger volumes will result in cell loss. Spin the cells at $200 \times g$ for 5 min.
2. To block non-specific binding of FcR, add 20 μl of 2% serum (from same animal species as the mAbs used for the immunofluorescence staining) to the cell pellet and incubate cells for 15 min.
3. Wash cells twice with 1 ml of cold washing buffer.
4. Add 20 μl of directly-conjugated anti-cell surface mAb to the cell pellet.
5. Incubate for 15 min on ice.
6. Wash cells twice with 1 ml ice-cold PBS and proceed to step 8.
7. Transfer the stimulated cells to 15-ml centrifuge tube and wash twice with ice-cold PBS.
8. Resuspend the cells at 2×10^6 cells ml^{-1} in cold PBS and add an equal volume of 4% formaldehyde (see note 5). Mix well to prevent aggregates.
9. Incubate for at least 20 min at room temperature.
10. Spin the cells at $200 \times g$ for 5 min and wash once more with 1 ml of cold PBS. At this point the cells can be resuspended in PBS and stored at 4°C in the dark for 1 week or aliquoted and stored at –80°C for at least one month prior to analysis (see note 6).

Table 3. Human cytokine-specific mAbs for intracellular staining

	Coating mAb	Detection mAb	
Cytokine	mAb	Isotype	Source[a]
IL-1β	B-A15	mIgG1	1
IL-2	MQ1-17H12	rIgG2a	2
IL-2	BG-5	mIgG1	1
IL-3	BVD8-3G11	mIgG2a	2/3
IL-3	BVD3-If9	mIgG2a	2/3
IL-4	8D4	mIgG1	3
IL-4	MP4-25D2	rIgG2a	2/3
IL-4	3010.2	mIgG1	3
IL-5	JES-39D10	rIgG2a	2/3
IL-6	MQ2-6A3	rIgG2a	2/3
IL-6	B-E8	mIgG1	1
IL-8	B-K8	mIgG1	1
IL-10	JES8-12G8	rIgG2a	2/3
IL-10	B-N10	mIgG1	1
IL-10	JES3-19F1	mIgG1	2/3
IL-12p40	B-P24	mIgG1	1
IL-12p70	B-T21	mIgG1	1
IL-13	JES10-30F11	rIgG2a	2
IL-13	JES8-5A2	rIgG2a	2/3
IL-13	B-B13	mIgG1	1
IL-15	B-T15	mIgG1	1
G-CSF	BVD13-3A5	rIgG1	2/3
GM-CSF	BVD2-21C11	rIgG2a	2/3
TNF-α	BVD11-37G1	mIgG1	2/3
TNF-α	B-D9	mIgG1	1
TNF-α	MP9-20A4	rIgG1	3
IFN-γ	B27	mIgG1	1
IFN-γ	4S.B3	mIgG1	3
IFN-γ	25723.11	mIgG1	3
IFN-γ	B-B1	mIgG1	1
IL-17	41802	mIgG1	4
IL-22	142928	mIgG1	4

m: mouse mAb, r: rat mAb.
[a]Abs sources are as follows: (1) GenProbe, Besançon, France. (2) Generated at DNAX Research Institute, Palo Alto, CA, USA; relevant hybridomas can be obtained via American Tissue Culture Collection; permission must be obtained from DNAX for acquisition of cell lines from this source. (3) BD Biosciences/PharMingen. (4) R&D Systems.

11. Resuspend the cells in washing buffer and transfer $\pm 10^5$ cells per well of a 96-well V-bottom microtitre plate and spin at $200 \times g$ for 2 min.
12. Remove supernatant by flicking the plate, blot the plate dry on paper tissue and resuspend the cells by gently vortexing.
13. Add 150 µl of permeabilization buffer to the cells and incubate for 10 min at room temperature. A final concentration of 2% serum (as described under step 2) can be added to block non-specific FcR binding of mAbs.
14. Spin the cells at $200 \times g$ for 2 min and remove supernatant.

15. Add 20 µl of cytokine-specific mAb solution to the cell pellet (see note 7).
16. Incubate cells for 20 min at room temperature.
17. When using non-conjugated mAbs, proceed to step 18; for FITC, PE or Cy5-conjugated-conjugated mAbs, proceed to step 22.
18. Add 150 µl of permeabilization buffer, centrifuge the plate at 200 × *g* for 2 min, remove supernatant and resuspend the cells.
19. Repeat washing step.
20. Add 20 µl per well of an appropriate dilution of the second conjugated mAb.
21. Incubate cells for 30 min at room temperature.
22. Add 150 µl of permeabilization buffer, centrifuge the plate at 200 × *g* for 2 min, remove supernatant and resuspend the cells.
23. Repeat washing step.
24. Wash once with washing buffer, resuspend in 200–300 µl PBS and analyse on the FACS flowcytometer as soon as possible.
25. For instrument control and compensation setting, refer to the manufacturer's instructions (see Chapter 1, "Phenotyping and separation of leucocyte populations based on affinity labelling" of Volume 32 and notes 6–9).

C. Notes and Recommendations

1. NaN_3 is known to be toxic, saponin is an irritant and formaldehyde is a suspected carcinogen. Avoid contact with skin, eyes and mucous membranes. Dispose of formaldehyde in container for treatment; do not put formaldehyde-containing waste in sink. Always wear gloves.
2. Since cytokines are produced with different kinetics, optimal time points for the analysis of activated cytokine-producing cells may vary, depending not only on the type of cytokine to be analysed, but also on the mode of stimulation. The peak production of most cytokines, including IL-2, IL-4 and TNF-α, by T cell clones, following stimulation with TPA and A23187, is within the first 6–7 h, whereas others, such as IFN-γ and IL-10, have more long-lasting kinetics. IL-13 is produced early (2 h) following activation, but this cytokine also continues to be produced up to 72 h. Analysis of the cells 4–6 h after activation results in a characteristic staining of the Golgi apparatus/endoplasmatic reticulum, which is bright for cytokines such as IL-2, TNF-α and IFN-γ.
3. The addition of agents which inhibit cellular transport systems, such as Brefeldin A or Monensin, results in an accumulation of newly synthesized protein in the Golgi complex. Although the cellular integrity changes following treatment with intracellular protein transport inhibitors, resulting in a disappearance of Golgi staining and a homogeneously fluorescing cells, their use generally gives a brighter staining pattern and enables the detection of intracellular cytokines that stain only weakly with anti-cytokine mAbs, such as IL-4 and IL-5. However, since these compounds have dose- and time-dependent cytotoxic effects, their use should be limited. Brefeldin A is less toxic than Monensin and should be added to the cultures between 2 and 6 h before harvesting the cells.
4. The staining procedure for flowcytometric analysis is performed in 96-well V-bottom microtitre plates. However, since it is preferable to fix the cells in

15-ml centrifuge tubes, it is recommended to perform staining of cell surface molecules in tubes, followed by fixation and transfer of the cells to microtitre plates. All steps during cell surface staining are carried out at 4°C, in the absence of saponin. Since some mAbs may not bind to fixed, denatured, protein cell-surface staining should be carried out before fixation of the cells. Staining for intracellular cytokines is performed at room temperature in the presence of saponin. All incubation periods during the staining procedures are carried out in the dark.

- Make the Ab dilutions in PBS/2%FCS/NaN_3/0.5% saponin. For each mAb, the optimal titre has to be determined. Generally, final concentrations of mAbs are 1–5 μg per 106 cells. PE-conjugated mAbs are not recommended for analysis on a UV microscope, because of the quick fading of the dye: use Rhodamin-conjugated Abs instead.
- Centrifugation of the Abs at high speed in a microfuge to remove aggregates will improve the quality of the staining.
- If non-conjugated anti-cytokine mAbs are used, obtained from different species, two-colour analysis can be performed. Although cytokine-specific staining signals generally tend to be higher, often increased fluorescence backgrounds are observed, requiring rigid blocking of non-specific mAb binding.

5. Optimal results have been obtained with formaldehyde (Openshaw *et al*., 1995), and although this fixative is less efficient to cross-link and change the tertiary structure of protein as compared to glutaraldehyde, its effect are more gentle and fixation with formaldehyde generally preserves a high degree of antigenicity.
6. *Positive control.* Samples of a resting and activated T clone with a Th0 cytokine production profile can be fixed, aliquotted in PBS, stored at –80°C for several weeks and used in the staining procedure as negative control (to adjust flow-cytometer instrument settings) and positive controls, respectively.
7. *Negative control*. Non-stimulated cells, which have been identically treated during the staining procedure, serve as negative control. Prior to its use in the staining procedure, each anti-cytokine mAb should be titrated at a concentration which gives optimal staining on activated cells and absence of staining on non-stimulated control cells.

   Furthermore, it is recommended to use one of the following controls to confirm specificity of the staining:

   - *Ligand-blocking control.* Pre-incubate mAb with excess of recombinant cytokine in permabilization buffer at 4°C for 30 min. It is recommended to use at least a 50-fold Molar excess of cytokine over mAb. Proceed to step 15 of staining protocol.
   - *Non-conjugated mAb control*. Pre-incubate cells after step 14 of staining protocol with non-conjugated mAb, diluted in permabilization buffer, at 4°C for 30 min, wash cells twice and proceed to step 15 of staining protocol.
   - *Isotype control*. Use an irrelevant mAb of the same isotype as the anti-cytokine mAbs in the staining procedure. Isotype controls can be used to adjust instrument settings, including quadrant markers and compensation of flow-cytometer. In cases where isotype controls give brighter staining than anti-cytokine mAb, rely on non-activated cells as negative control.

8. It should be stressed that when the intracellular staining method, using flow cytometry, is introduced in the laboratory, the results should be confirmed by immunofluorescence using an UV microscope. Intracellular cytokine staining of cells that have been activated less than 6 h in the absence of Brefeldin A will result in distinct staining of the Golgi apparatus and endoplasmatic reticulum, whereas after longer activation periods also cell surface cytokine staining may be detected. Microscopic analysis of cells, activated in the presence of Brefeldin A, shows homogenous staining throughout the cytoplasm, as a result of disintegration of Golgi apparatus and endoplasmatic reticulum.

♦♦♦♦♦♦ V. ELISA

In this section, the antibody sandwich ELISA system is described which is used for the detection of cytokines present in the culture supernatants of *in vitro* activated cells of the immune system or in clinical samples, such as serum, plasma or bronchoalveolar fluid. Although generally not as sensitive as a bioassay, the major advantage of the ELISA is its specificity, enabling the detection of soluble proteins in complex mixtures, which often have overlapping or, by contrast, counter-regulatory activities and which are therefore extremely difficult to detect, based on their biological activities alone. To measure a cytokine in solution, plates are coated with an anti-cytokine mAb which functions as a catcher to bind the cytokine. After removal of unbound cytokine, a second anti-cytokine mAb is added (detection mAb), which is usually biotinylated and which recognizes a different epitope on the cytokine, followed by a washing step and the addition of an enzyme–streptavidin conjugate. The use of such a biotin–streptavidin conjugate in the assay enables amplification of the signal. After removal of unbound conjugate, substrate is added, the hydrolysis oxidation of which by the enzyme–conjugate is proportional to the amount of cytokine present in the solution.

A. Reagents and Equipment

- Cytokine-containing supernatants, cytokine-specific capture mAb; biotin-labelled, cytokine-specific tracer mAbs; PBS; dH20.
- Culture medium to dilute cytokine-containing samples and cytokine standards:

Coating buffer:	Carbonate–bicarbonate buffer pH 7.2 to 7.4.
Washing buffer:	PBS, supplemented with Tween 20 (0.05%).
Tween buffer:	PBS, supplemented with bovine serum albumin (BSA) (0.1%) and Tween 20 (0.02%).
Blocking buffer:	PBS, supplemented with BSA (2%).
Conjugate:	Strepavidine–alkaline phosphatase (AP) conjugate (Southern Biotechnology Associates: 7100-04) or streptavidin–HRP (Prozyme: CJ30H).
ELISA substrate:	Sigma 104 phosphatase substrate (Sigma: 104-0) or ready-to-use 3,3′,5,5′-tretramethylbenzidine (TMB) (Moss: TMBUS).
Substrate buffer:	Diethanol amine: 97 ml in 800 ml dH_20.

0.2 g NaN_3.
0.1 g $MgCl_2.6H_2O$.
Adjust to pH 9.8 with HCl and adjust volume to 1 l with H_2O.

- H_2O_2; PVC U bottom 96-well plates; Immunolon I U bottom 96-well plates; Immunolon II U bottom 96-well plates (Dynatech: 011-010-3450); Microtitre plate reader-spectrophotometer with 405 nm filter or spectro fluorometer (Dynatech: 011-970-1900) with 365 nm excitation filter and 450 nm emission filter.

All reagents should be at room temperature before use in the ELISA. The optimal working concentrations of all Abs should be determined for each ELISA. Usually catcher Ab concentrations range from 1 to 10 $\mu g\,ml^{-1}$. A list of mAbs and polyclonal Abs available for the detection of cytokines by ELISA is shown in Table 4.

Table 4. Human cytokine-specific mAbs for ELISA

Cytokine	Coating mAb	Detection mAb	Source[a] coating/detection
	Designation	Designation	
IL-1α	B–Z3	B-Z5	1/1
IL-1β	B–A15	B-Z8	1/1
IL-2	MQ1-17H12	BG-5	4/1
IL-2	Goat polyclonal Ab	BG-5	1/1
IL-2	5344.111	B333-2	2/2
soluble (s) CD25	BG-3	B-F2	1/1
IL-3	BVD8-3G11	BVD3-IF9	4/4
IL-4	B-R14	B-G28	1/1
IL-4	8D4-8	MP4-25D2	2/2
sIL-4R	S456C9	BB4N1	1/1
sIL-4R	Hil4R-M10.1	HIL4R-M8.2.2	2/2
IL-5	JES-39D10	JES1-5A10	4/4
IL-5	Goat polyclonal Ab	B-Z25	1/1
IL-6	MQ2-39C3	MQ2-13A5	4/4
IL-6	B-E8	B-E4	1/1
sIL-6R	B-N12	B-R6	1/1
SIL-6R	M5	M182	2/2
IL-7	BVD10-40F6	BVD10-11C10	4/4
IL-7	B-N18	B-S16	1/1
IL-8	B-K8	Rabbit polyclonal Ab	1/1
IL-8	G265-5	G265-8	2/2
IL-10	JES3-19F1	JES3-12G8	2/2
IL-10	B-N10	B-T10	1/1
IL-12p40	B-P40	B-P24	1/1
IL-12p40	C8.3	C8.6 (p40/p70)	2/2
IL-12p40	20C2	C8.6 (p40/p70)	2/2
IL-12p70	B-T21	B-P24	1/1
IL-13	JES10-5A2	B69-2	4/4
IL-13	B-B13	B-P6	1/1
IL-15	Goat Polyclonal Ab	B-E29	1/1

(*Continued*)

Table 4. (*Continued*)

Cytokine	Coating mAb	Detection mAb	Source[a] coating/detection
	Designation	Designation	
IL-17	B-C49	B-B51	1/1
IL-17A	41809	Goat Ab	3/3
IL-17A/F	B-C49	B-F60	1/1
IL-17F	B-G46	B-F60	1/1
IL-22	142906	142928	3/3
IL-23	B-Z23	B-F43	1/1
IL-27	B-G44	B-G49	1/1
IL-31	B-S31	B-A51	1/1
IL-33	B-L33	B-S33	1/1
IL-18	Goat polyclonal Ab	Goat polyclonal Ab	1/1
IL-21	J148-1134	I76-539	2/2
G-CSF	BVD13-3A5	BVD11-37G10	4/4
GM-CSF	BVD2-23B6	BVD11-21C11	4/4
TNF-α	MP9-20A4	GMO1–1782	4/4
TNF-α	28401	Goat Ab	3/3
LT-α/TNF-β	359-238-8	359-81-11	2/2
LT-α/TNF-β	5807	Goat Ab	3/3
IFN-γ	A35	B27	1/1
IFN-γ	B-B1	B-G1	1/1
OSM	17001	Goat Ab	3

[a]This list is a selection of (m)Ab for ELISA purposes, but is not exhaustive. (1) Diaclone, Besançon, France; (2) BD Biosciences; (3) R&D Systems; (4) generated at DNAX Research Instititute, Palo Alto, CA, USA; relevant hybridomas can be obtained via American Tissue Culture Collection; permission must be obtained from DNAX for acquisition of cell lines from this source.

B. Protocol

The procedure for activating cells is given on page 429.

1. Coat 96-well assay plate with 100 µl catcher Ab, diluted in carbonate buffer.
2. Seal plate with lid or parafilm and incubate for 2 h at 37°C or overnight at 4°C. Plates can be stored in a sealed pouch with a dessicant bag at 4°C. Before storage, a blocking solution should be added. Avoid storing plates for periods longer than several weeks.
3. Wash wells three times with washing buffer and flick plates dry on absorbent tissue.
4. Add 300 µl of bocking buffer, incubate for 30 min and flick plates dry on absorbent tissue. Do not wash.
5. Dilute the samples and cytokine standard (aliquots stored at –80°C) in Tween buffer, mix well and add 100 µl per well in duplicate at appropriate dilutions.
   - Standard curve: dilute in separate plate in 1:2 dilutions to cover a 1000–20 pg ml^{-1} decreasing range and add 100 µl per well in duplicate.
   - Unknown samples: dilute as needed (see notes) and add 100 µl per well.

6. Incubate plates for overnight at room temperature. When incubation time for the standard or sample is unknown, it is recommended to incubate the plate overnight at 4°C. Alternatively, the biotinylated tracer Ab together with the standard should be incubated overnight at 4°C.
7. Wash three times with washing buffer and flick plates dry on absorbent tissue.
8. Dilute the biotin-conjugated anti-cytokine detection mAb in Tween buffer and add 100 µl per well.
9. Incubate for 1–2 h at room temperature.
10. Wash three times with PBS and flick plates dry on absorbent tissue.
11. Prepare strepavidin–alkaline phosphatase or streptavidin–HRP conjugates in Tween buffer and add 100 µl per well.
12. Incubate for 1 h at room temperature.
13. Wash three times with washing buffer and flick plates dry on absorbent tissue.
14. Prepare the ELISA substrate (Dilute 1 mg ml^{-1} ELISA substrate in 100 ml of substrate buffer. Prewarm at 37°C and add 100 µl per well. TMB substrate is ready to use and should be at room temperature before addition.)
15. Incubate for 30 min at 37°C to let colour develop and read OD at 405–430 nm using a spectrophotometer or spectrofluorometer (Dynatech).
    For TMB, block the reaction with 1N sulphuric acid and read absorbence at 450 nm with a reference filter set at 630 nm.
16. Use the Softmax program (Molecular Devices Corporation) or comparable program to analyse the data.

C. Notes and Recommendations

It is recommended to make several dilutions of cytokine-containing supernatants to be able to measure at the linear part of the standard curve.

It is important to note that the presence or absence of detectable levels of cytokines in clinical samples does not always correlate with their functional activity. Cytokines are often bound to non-specific serum proteins or to soluble cytokine receptors, which will sequester free cytokine from the peripheral circulation and might result in a decrease in detectable cytokine levels, as measured with ELISA. The biological significance of free versus complexed cytokines however is not yet clear. In addition, circulating anti-cytokine Abs, notably in the serum of those who have received cytokine or anti-cytokine therapy, may decrease levels of free cytokine, although they may still be detectable by cytokine-specific mAbs. Conversely, cytokine receptor antagonists may specifically compete with the cytokine for binding to its receptor. For example, despite high levels of IL-1 in certain serum samples, possible receptor occupancy by IL-1RA will prevent IL-1-mediated responses and therefore will prevent a meaningful analysis about its functional activity (Ahrend, 1993). This situation is similar for IL-18 and the IL-18BP (Novick *et al.*, 1999).

The half-life time of many cytokines in serum is very short, generally in the range of minutes, which is one of the reasons that cytokine levels in the peripheral circulation are usually very low in healthy individuals, as measured by ELISA. However, certain cytokines, notably IL-1, IL-6, IL-10 and TNF-α, may be detectable

in the serum following sepsis, trauma or an acute or chronic inflammatory state. It should however be kept in mind that, due to existing cytokine networks, even in above-mentioned pathological situations, the presence in excess of certain cytokines may result in the suppressed production of another and a failure to detect the latter cytokine.

Due to the possible presence of proteases or other (unknown) factors, in clinical samples, as well as culture supernatants, cytokines may be unstable and subject to degradation. Therefore, it is recommended to aliquot and store samples for cytokine measurement at –80°C prior to analysis, especially when prolonged periods of storage are required. Serum may contain certain factors such as heterophilic Abs that have the ability to cross-bridge the capture Ab attached to the solid phase with the biotinylated tracer Ab which may result in false-positive results. The reported incidence of human anti-mouse Abs in the serum of normal individuals is around 3%. Human anti-mouse Abs develop with high incidence in subjects who are in contact with animals or animal products or in patients who have been treated with murine mAbs. Rheumatoid factors (RFs) are polyreactive IgM Abs produced by a subset of B lymphocytes and bind to the Fc portion of the IgG molecule. RF may also interfere in the ELISA assay by bridging the tracer to the capture Ab in the absence of analyte.

Another important issue in immunoassays in general is the calibration of the assay. As the same amount of cytokine will not give the same signal in different assays, it is very important to calibrate the standard to the available international standard in order to be able to compare results.

One last point that should be emphasized is that different monoclonal or polyclonal Ab pairs sometimes give different results which are likely to depend on the different epitopes that are recognized by these Abs. For example, some epitopes might be hidden or denatured by certain cytokine-binding proteins or proteases. Furthermore, the variable level of glycosylation of some cytokines, such as IL-6, may also interfere with the capacity of Abs to fully recognize the natural cytokine. Finally, the capacity of various Abs to detect monomers rather than naturally occurring polymers (TNF-α, IFN-γ, IL-10, IL-12) should also be taken into account when considering the variability between immunoassays.

♦♦♦♦♦♦ VI. ELISPOT ASSAY

The ELISPOT assay is based on immuno-enzyme technology originally developed for the enumeration of Ab-secreting cells (Czerkinsky *et al.*, 1983; Sedwick and Holt, 1983; Czerkinsky *et al.*, 1988). The assay was subsequently adapted to measure cytokine production at the single cell level. The ELISPOT assay is easy to perform and requires, compared to other approaches such as limiting dilution or intra-cellular staining, a minimum *in vitro* cell manipulation, allowing analysis of cells close as the *in vivo* situation. It can be used successfully to measure ongoing cytokine production by freshly isolated mononuclear cells. The technique is designed to determine the frequency of cytokine-producing cells under a given

stimulation, and it enables the follow-up of these frequencies during a treatment and/or different stages of disease.

Cells can either be stimulated directly in wells containing Ab-coated membrane (direct method) or first stimulated for 6 h in 24-well plates, harvested and transferred to ELISPOT plates (indirect method). The choice between the two methods depends on the type of cell to be assayed, the expected frequency of cytokine-producing cells and the mode of stimulation. Stimulation of cells with immobilized anti-CD3 mAb can only be carried out using the indirect stimulation procedure.

The technique includes the following steps: Single cell suspensions are distributed in membrane-bottomed wells previously coated with an anti-cytokine Ab. During cell stimulation, locally produced cytokine molecules will be caught by surrounding capture Ab and accumulate in the close environment of the cell. After cell lysis, trapped cytokine molecules are revealed by a secondary biotinylated detection Ab, which is in turn recognized by streptavidin conjugated to alkaline phosphatase. The enzymatic reaction in the presence of the substrate BCIP/NBT produces a precipitate. Cytokine secreted by individual cells is visualized by sharp blue/purple spots that can be counted on an inverted microscope or a reading system, allowing the numeration of cytokine producing cells under a given stimuli.

The recently developed ELISPOT assays allow to monitor the simultaneous production of two or more cytokines by the same cell population (Figure 2). In this method, Polyvinylidine Fluoride (PVDF) filters in 96-well plates are coated with two different Abs each one specific for one of two cytokines to be analysed. After blocking of non-specific binding sites on the membrane, cells are incubated for the appropriate length of time, in the presence of a stimuli i.e. protein, peptide or tumour cells. After lysing of the cells, cytokine molecules trapped by the catcher Ab are recognized by two differently tagged secondary Abs. For one cytokine, Ab are labelled with biotin; for the other, Abs are conjugated with FITC molecules. These Abs are in turn detected by streptavidin–alkaline phosphatase conjugates, or FITC peroxydase conjugates for the biotinylated and by FITC conjugated Ab, respectively. Finally, addition of BCIP/NBT and AEC, the respective substrates of alkaline phosphatase and peroxidase, will result in blue/purple and red/brownish spots in the presence of their enzyme, allowing the visualization of cytokine molecules produced by the cells. In a recent development, the enzymatic revelation system has been replaced by fluorescent dyes conjugates such as streptavidin–PE and anti-FITC green fluorescent dye. Fluorescent spots are then visualized under a UV light beam on a UV detection system.

A. Reagents and Reagent Preparation

- Capture anti-cytokine mAbs.
- Biotin-conjugated anti-cytokine detection mAbs.

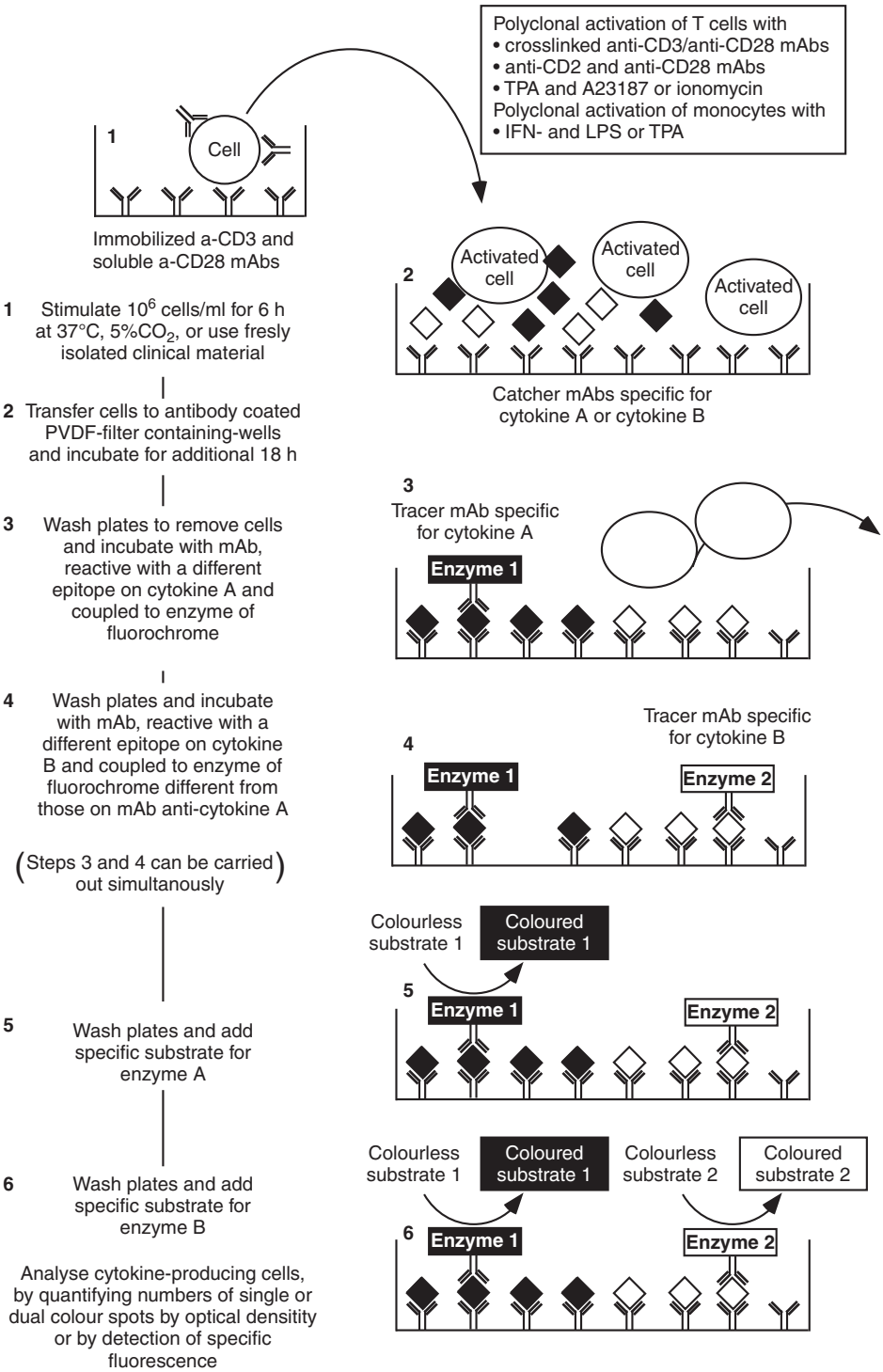

Figure 2. Flowchart for the ELISPOT procedure

- FITC and PE-conjugated anti-cytokine detection mAbs (for dual cytokine ELISPOT).
- Streptavidin alkaline phosphatase conjugate (Prozyme). Dilute 1/1000 in PBS–1% BSA.
- Anti-FITC HRP-conjugated pAb (CTL, Diaclone, MABTECH; for dual ELISPOT). Dilute 1/500 in PBS–1% BSA.
- AEC substrate buffer (for dual ELISPOT). For one plate, mix 1 ml of AEC buffer A with 9 ml of H_2O. Then add 200 µl of AEC buffer B.
- BCIP/NBT substrate buffer.
- PBS, BSA (Sigma: A2153), ethanol (35% in H_2O), Tween 20 (0.05% in PBS).
- 96-well PVDF filter-containing ELISPOT plates (CTL, Millipore MultiScreen; MSIPN4510) are recommended.
- ELISPOT reading system (AELVIS, Zeiss or CTL).

B. Reagent Storage

- If not used within a short period of time, reconstituted detection Ab should be aliquoted and stored at –20°C. Under these conditions, the reagent is stable for at least 1 year.
- Substrate buffers to be stored at 4°C.
- Streptavidin–alkaline phosphatase as well as anti-FITC HRP conjugates should be stored at 4°C.

C. Protocol

The procedure for activating cells is given on page 429 (see notes 2 and 3).

1. Incubate PVDF filter-containing wells of an ELISPOT plate with 100 µl of 35% ethanol for 30 s at room temperature.
2. Empty wells (flick the plate and gently tap it on absorbent paper). Wash three times with 100 µl PBS.
3. Pipette 100 µl of each of the capture mAbs in 10 ml of PBS. Mix and dispense 100 µl into each well, cover the plate and incubate overnight at 4°C.
4. Empty wells and wash plate once with 100 µl of PBS.
5. Dispense 100 µl of complete culture media into wells, cover and incubate for 2 h at room temperature.
6. Empty wells and wash plate once with 100 µl of PBS.
7. Add to a well of an ELISPOT plate between 1.10^5 and 2.5×10^4 of pre-activated cells (indirect method) or cells to be activated with the appropriate stimulator (direct method) in a final volume of 100 µl. Cover the plate with a plastic lid and incubate for 10–15 h at 37°C, 5% CO_2. *During incubation do not disturb the plate.*
8. Empty wells, add 100 µl of PBS–0.05% Tween 20 and incubate for 10 min at 4°C.
9. Empty wells and wash plate three times with 100 µl of PBS–0.05% Tween 20.

10. For one plate, dilute 100 µl of cytokine 1 detection Ab and 100 µl of cytokine 2 detection Ab into 10 ml of PBS containing 1% BSA. Dispense 100 µl into wells, cover the plate and incubate 1 h 30 min at room temperature.
11. Empty wells and wash three times with 100 µl of PBS–0.05% Tween 20.
12. For one plate dilute 20 µl of anti-FITC HRP and 10 µl of streptavidin–alkaline phosphatase conjugates into 10 ml of PBS–1% BSA. Dispense 100 µl of the dilution into wells. Seal the plate and incubate for 1 h at room temperature.
13. Empty wells and wash three times with 100 µl of PBS–0.05% Tween 20.
14. Peel off the plate bottom and wash three times both sides of the membrane under running distilled water. Remove all residual buffer by repeated tapping on absorbent paper.
15. Prepare AEC buffer (see reagents preparation) and add 100 µl of solution to each well.
16. Let colour reaction proceed for 5–15 min at room temperature. When the spots have developed, remove the buffer and dispose of appropriately.
17. Wash both sides of the membrane thoroughly with distilled water and carefully remove residual buffer by tapping the plate on absorbent paper.
18. Dispense 100 µl of ready-to-use BCIP/NBT buffer into wells.
19. Let the colour reaction proceed for about 5–15 min at room temperature. When spots have developed, empty the buffer into an appropriate tray.
20. Wash thoroughly both sides of the membrane with distilled water
21. Dry the membrane by repeatedly tapping the plate on absorbent paper. Store the plate upside down to avoid remaining liquid to flow back onto the membrane. Read spots once the membrane has dried. Note that spots may become more distinct following incubation of the filters at 4°C for 24 h. Store the plate at +4°C away from direct light.

D. Notes and Recommendations

1. AEC and BCIP/NBT buffers are potentially carcinogenic and should be disposed off appropriately. Caution should be taken while handling those reagents. Always wear gloves.
2. While using MSIPN4510 plates, during incubation steps, reagents are leaking through the membrane by capillary action. As this liquid is generally not properly removed during the various washing steps, it will increase the background signal. To avoid this, we recommend that the plate bottom is peeled off at the end of step 9 of the procedure and that the reverse of the membrane is washed with running distilled water, as well as the regular washes with PBS–0.05% Tween 20.
3. Automatization of the ELISPOT technique makes it suitable for use in clinical and hospital settings (Herr *et al.*, 1997). The detection limit of the technique is between one and five cytokine-producing cells for a total of 10^5 cells, which makes it one of the most sensitive techniques for the detection of antigen-specific T cells. However, in contrast to the tetramer-MHC-class II technique, cytokine-producing T cells are only detected following antigen-specific activation of the

Table 5. Human cytokine-specific (m)Abs for ELISpot

Cytokine	Tracer (Phase) mAb	Catcher (m)Ab
IL-1β	B-A15	B-Z8
IL-2	B-G5	Rabbit polyclonal Ab
IL-4	B-R14	B-G28
IL-5	B-Z25	Goat polyclonal Ab
IL-6	B-E8	B-E4
IL-10	B-N10	B-T10
IL-12p70	B-T21	B-P24
IFN-γ	B-B1	B-G1
TNF-α	B-F7	B-C7
IL-17A	B-C49	B-B51
IL-17F	B-G46	B-F60
IL-17A/F	B-C49	B-F60

At present, the most complete, well-characterized set of (m)Abs for use in the ELISPOT assay is available from Diaclone, Besançon, France.

cells. Unless the cells are sorted before the assay, the ELISPOT method does not allow to phenotype the cytokine producing cells, neither to sort cytokine-producing cells. A list of monoclonal and polyclonal Abs available for the detection of cytokines by ELISPOT is shown in Table 5.

♦♦♦♦♦♦ VII. BD™ CYTOMETRIC BEAD ARRAY (CBA)

A. Introduction

Flow cytometry is a powerful analytical tool that enables the characterization of cells and subcellular organelles as well as particles (such as polystyrene beads) on the basis of size and granularity (light scatter characteristics) and a number of different parameters defined by fluorescent probes, including fluorescent antibodies and dyes (Shapiro, 1994, see also Chapter 1, Phenotyping and separation of leucocyte populations based on affinity labelling of Volume 32). Today, flow cytometry is widely applied to the development of multiplex sandwich immunoassays. These particle-based, flow cytometric immunoassays are capable of simultaneously identifying the types and measuring the levels of multiple soluble analytes within small samples of biological fluids. The broad dynamic range of fluorescent detection offered by flow cytometry and the efficient capturing of analytes by suspended particles enables these assays to use fewer sample dilutions and to obtain multiple sample measurements in a short time period. For these reasons, this technology provides an important tool for analysing the networks of biological response modifiers (BRMs) that are coexpressed by cells that mediate immune and inflammatory responses. Biological response modifiers (BRMs), in particular cytokines, chemokines, and their receptors are popular target molecules for study (Chen *et al.*, 1999; Cook *et al.*, 2001; Funato *et al.*, 2002).

The BD™ Cytometric Bead Array (CBA) from BD Biosciences employs a series of suspended beads to simultaneously detect and quantify multiple soluble analytes. Each bead has a unique fluorescence intensity so that they can be mixed and run simultaneously in a single tube to significantly reduce sample requirements and time to results in comparison with traditional ELISA and western blot techniques.

BD CBA solutions are designed for multiplexed analysis providing more data using a single sample. Thus multiplexing is especially useful when only a small amount of sample is available, maximizing the number of proteins that can be analysed. With BD CBA, up to 30 proteins can be analysed with just 25–50 µl of sample. By comparison, other methods such as ELISA and western blot require a similar amount of sample; however, only one protein can be analysed from the same volume.

B. Principle of the Assay

BD CBA employs a series of different single size particles that are stably labelled with one (Kits) or two (Flex Sets) fluorescent dyes the emission wavelength of which is read at ~660 nm and over 680 nm. Each different group of beads is labelled with a discrete level of fluorescent dye so that it can be distinguished by its mean fluorescence intensity (MFI) upon flow cytometric analysis.

For BD CBA Flex Sets, each bead population is given an alphanumeric position designation indicating its position relative to other beads (Figure 3). Beads with different positions can be combined to create a multiplex assay.

In addition, beads within each group are covalently coupled with antibodies that can specifically capture a particular type of molecule present within biological fluids including sera, plasma, tears, tissue culture supernatants or cell lysates. By analogy with the ELISA method (pages 445), the antibody-coupled Capture Beads

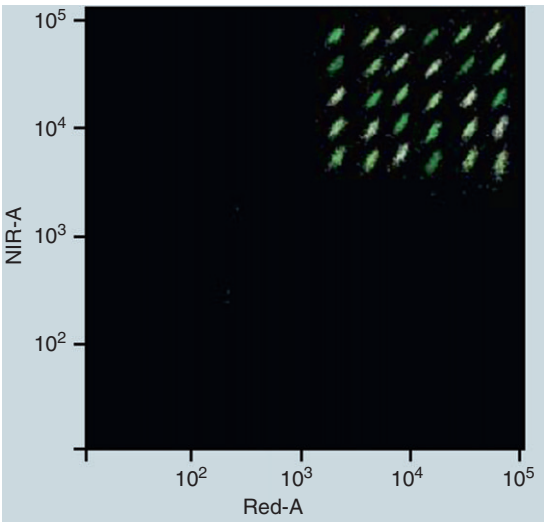

Figure 3. BD CBA 30-plex assay resolved on the BD FACSArray™ bioanalyser (Image from: BD CBA brochure (23-8910-01) p. 5).

Table 6. BD CBA Flex Sets instrument compatibility and associated parameters

Instrument	Reporter parameter	Clustering parameters for BD CBA flex sets	Clustering parameters for BD CBA kits
BD FACSArray™ bioanalyser	Yellow	Red and NIR	Red
BD FACSCanto™ II flow cytometer	PE	APC and APC-Cy7	APC
BD™ LSR II flow cytometer	PE	APC and APC-Cy7	APC
BD FACSAria™ II cell sorter	PE	APC and APC-Cy7	APC
BD FACSCalibur™ flow cytometer	FL2	FL4 and FL3	FL3 or FL4

serve as the solid capture phase for the CBA. The immobilized, high-affinity antibodies function to specifically capture and localize analytes of interest that may be present in biological fluids tested. The captured analyte is then specifically detected by the addition of a fluorescent antibody. PE-coupled (emission at ~585 nm) detection antibodies are most frequently used since the emission wavelength of PE is easily distinguishable from the emission wavelength(s) of the BD CBA capture beads. By including serial dilutions of a standard analyte solution (e.g. a mixture of cytokine protein standards with known concentrations), the BD CBA supports the development of standard curves for each analyte. With multicolour flow cytometric analysis, the levels of analytes captured by the different bead groups are distinguished by looking at the median fluorescence intensity (MFI) of the PE signal, which is in direct proportion to the amount of analyte present.

The data are analysed using FCAP Array™ software to calculate the concentrations of multiple analytes by plotting standard curves and calculating sample concentrations based on these curves. Due to the complexity of the BRM and cell signaling networks that underlie immune function, the capacity of the BD CBA to simultaneously measure multiple analytes in a single small-volume sample is highly advantageous.

BD CBA technology has been optimized for digital flow cytometers but is compatible with virtually all dual-laser flow cytometers capable of detecting and distinguishing fluorescence emissions at 576, 670 and >680 nm (Table 6).

C. BD CBA Flex Sets

1. Introduction

The BD CBA Flex Set system provides an open and configurable menu of bead-based reagents designed to make it easy to create multiplex assays. Available assays include soluble protein assays for detection of human, mouse or rat cytokines, chemokines and growth factors; human immunoglobulins; and cell signaling assays for detection of phosphorylated cell signaling proteins. Using the BD

CBA Flex Set system, up to 30 analytes can be measured simultaneously on a flow cytometer equipped with 488 and 633 nm lasers.

2. BD CBA Soluble Protein Flex Set assays for detection of cytokines

BD CBA Soluble Protein Flex Set assays are available for the detection of cytokines, chemokines, growth factors, and human Ig in serum, plasma or tissue culture supernatant samples.

The antibody pair that comprises each assay is evaluated for dynamic range, sensitivity and parallel titration to native biological samples. The detection antibodies are directly labelled with PE. By avoiding the streptavidin–biotin–PE detection method employed by other assays, direct PE detection reagents minimize the risk of increased background often caused by endogenous biotin in serum and lysate samples.

3. BD CBA Flex Set assay: step by step

BD CBA Flex Sets make it easy to build a multiplex by following three simple steps. First choose the analytes to be measured and the corresponding buffer kit. Then follow the simple formulation instructions in the Master Buffer Kit manual. Assay components are all formulated at 1 μl/test for easy calculations and the unique lyophilized standard pellets facilitate the combination of proteins to make the standards mix. The finished assay can be acquired on a variety of dual-laser flow cytometers and analysed using FCAP Array software.

1. **Choose a human BD CBA Flex Set assay.**
   Each BD CBA Flex Set comes with capture beads, detection reagent and standards. Sufficient reagents are provided to run 100 tests including two standard curves. All assays are available off-the-shelf and ready for mixing.
2. **Choose a 100 or 500 test size BD CBA Flex Set Master Buffer Kit.**
   Each BD CBA Flex Set Master Buffer Kit contains all the assay reagents and instrument setup beads necessary for any size multiplex configured from compatible BD CBA Flex Sets. This means that running a single-plex assay, a 10-plex assay or larger, the buffer reagents are optimized to perform with the customized mixture selected and yield the correct number of assay tests.
3. **Perform the assay following the instructions in the Master Buffer Kit manual.**
4. **Acquire samples on a dual-laser flow cytometer.**
   The BD CBA Flex Set reagents have been validated on a number of BD dual-laser flow cytometry platforms (Table 6). The plate-based BD FACSArray bioanalyser can be used to optimize assay throughput and workflow. Simply prepare samples and standards in a 96-well filter-bottom plate, launch the previously designed FCAP Array template, load the plate and experience truly hands-free sample acquisition.
5. **Analyse data files using FCAP Array multiplex analysis software.**
   Use the intuitive, wizard-driven FCAP Array software to plot standard curves and calculate sample concentrations.

D. Notes and Recommandations

1. Quantitative results or protein levels for the same sample or recombinant protein run in ELISA and BD CBA assays may differ. A spike recovery assay can be performed using an ELISA standard followed by BD CBA analysis to assess possible differences in quantitation. So-called 'Gold Standards' further allow for comparing values obtained using different assay method with those of the National Institute for Biological Standards and Control (NIBSC)/World Health Organization (WHO) International Standards (page 454).
2. When several BD CBA Flex Sets assays are multiplexed, it is possible that the background (MFI of the 0 pg/mL standard point) may increase and the overall assay signals of other standard points may be reduced. This can result in lower dynamic range or loss in sensitivity in some assays. This effect may be greater as more assays are added to the multiplex.
3. For assays that will be acquired on a BD FACSCalibur flow cytometry instrument, it is recommended that additional dilutions of the standard be prepared (i.e. 1:512 and 1:1024) as it is possible that in multiplex experiments containing a large number of assays, the Top Standard, 1:2 and 1:4 standard dilution will not be analysable by the FCAP Array software. In those cases, the Top Standard, 1:2 and 1:4 standard dilutions can be run on the experiment but may need to be excluded from the final analysis in the FCAP Array software (Cat. No. 641488).

E. Material and Reagents

Each BD CBA Flex includes specific Capture Beads, Detection Reagents and Standards. Assay buffers, Flow Cytometer Setup Reagents and Instruction Manual are provided in each BD CBA Flex Set Master Buffer kit. Instruction Manuals, Instrument Setup instructions and Acquisition Templates can be downloaded at **bdbiosciences.com/flexset**

In addition to the reagents provided in the BD CBA Master Buffer Kit and the BD CBA Flex Sets, a dual-laser flow cytometer equipped with a 488 or 532 nm laser, and a 633 or 635 nm laser and capable of distinguishing 576, 660 and >680 nm fluorescence is required for the assay. Refer to Table 6 for examples of compatible instrument platforms. 12×75 mm sample acquisition tubes for a flow cytometer (e.g., BD Falcon™ Cat. No. 352008), and the FCAP Array software (Cat. No. 641488).

1. Required for running experiments on a BD FACSCalibur flow cytometer

- BD CaliBRITE™ 3 beads (Cat. No. 340486)
- BD CaliBRITE APC beads (Cat. No. 340487)
- BD FACSComp™ software

2. Required for plate loader-equipped flow cytometers

- Millipore MultiScreenHTS-BV 1.2 µm clear non-sterile filter plates (Cat. No. MSBVN1210 (10 pack) or MSBVN1250 (50 pack))

- Millipore MultiScreenHTS Vacuum Manifold (Cat. No. MSVMHTS00)
- MTS 2/4 Digital Stirrer, IKA Works, VWR (Cat. No. 82006-096)
- Standard microtitre plate for BD FACSArray Bioanalyzer Setup (BD Falcon Cat. No. 353910)
- Vacuum source
- Vacuum gauge and regulator (if not using recommended manifold)

F. BD CBA Soluble Protein Flex Set assay procedure

1. Overview

Summarized below is the BD CBA Flex Set assay procedure for measuring soluble proteins in human samples (see sections below for details).

1. Perform instrument setup procedure.
2. Dilute samples as appropriate.
3. Reconstitute standards mix and prepare serial dilutions.
4. Prepare (dilute) Capture Beads.
5. Prepare (dilute) PE Detection Reagents.
6. Transfer Capture Beads to tubes or wells.
7. Add standard and sample dilutions to the appropriate tubes or wells.
   Incubate for 1 h at room temperature (protect from light).
8. Add mixed PE Detection Reagent to tubes or wells.
   Incubate for 2 h at room temperature (protect from light).
9. Wash.
10. Analyse.

2. Instrument setup

In order to ensure that the flow cytometer is performing optimally, perform the instrument setup procedure prior to preparing the BD CBA Flex Set assay. Refer to the appropriate flow cytometry instrument setup in the manual included with the Master Buffer Kit for instructions on how to set up your instrument.

3. Preparation of test samples

The standard curve for each BD CBA Soluble Protein Flex Set covers a defined set of concentrations. It may be necessary to dilute test samples to ensure that their mean fluorescence values fall within the limits or range of the generated standard curve. For best results, samples that are known or assumed to contain high levels of a given protein should be diluted as described below.

1. Dilute test sample by the desired dilution factor (i.e. 1:10 or 1:100) using the appropriate volume of Assay Diluent. Serum or plasma samples must be diluted at least 1:4 before transferring the samples to the assay tubes or wells.

2. Mix sample dilutions thoroughly before transferring samples to the appropriate assay tubes containing Capture Beads.
3. In order to facilitate analysis in FCAP Array software, load serially diluted samples in sequential wells from most concentrated to least concentrated (e.g. Sample 1 – 1:4, 1:8, 1:16; Sample 2 – 1:4, 1:8, 1:16; etc.).

4. Preparation of BD CBA Soluble Protein Flex Set standards

For each single bead or multiplex assay, a standard curve will need to be prepared. The protocol below indicates how standards should be mixed and diluted for use in a BD CBA Soluble Flex Set assay.

1. Remove one lyophilized standard vial from each BD CBA Soluble Flex Set.
2. Open each vial of lyophilized standard and pool all lyophilized standard spheres into a single polypropylene tube (Recommended 15-ml Conical Tube, BD Falcon Cat. No. 352097). Label the tube 'Top Standard'.
3. Reconstitute the standards with 4.0 ml of Assay Diluent. Allow the reconstituted standard to equilibrate for at least 15 min before making dilutions. *Mix reconstituted protein by pipette only. Do not vortex or mix vigorously.*
4. Label 12×75 mm tubes (BD Falcon Cat. No. 352008) and arrange them in the following order: 1:2, 1:4, 1:8, 1:16, 1:32, 1:64, 1:128 and 1:256.
5. Pipette 500 µl of Assay Diluent to each of the remaining tubes.
6. Perform a serial dilution by transferring 500 µl from the Top Standard to the 1:2 dilution tube and mix thoroughly. Continue making serial dilutions by transferring 500 µl from the 1:2 tube to the 1:4 tube and so on to the 1:256 tube and mix thoroughly. *Mix by pipette only; do not vortex*. Prepare one tube containing Assay Diluent to serve as the 0 pg/mL negative control (Table 7).
7. It is recommended that the first 10 wells or tubes in the experiment be the standards. Standards should be run in order from least concentrated (0 pg/mL) to most concentrated (Top Standard, see Table 8).

Table 7. Typical BD CBA Human Soluble Protein Flex Set standard concentrations after dilution

BD CBA Human Soluble Protein Flex Set Standard	Top Standard	1:2 Dilution Tube	1:4 Dilution Tube	1:8 Dilution Tube	1:16 Dilution Tube	1:32 Dilution Tube	1:64 Dilution Tube	1:128 Dilution Tube	1:256 Dilution Tube
Protein (pg/ml)	2500	1250	625	312.5	156	80	40	20	10

Note: Refer to the Technical Data Sheet for each individual assay to verify the concentration of the Top Standard.
Table from: Manual for Cat. No. 558264, p. 11.

Table 8. Essential controls

Tube No.		Reagents (All reagent volumes are 50 µl)
1	Negative Control	Capture Beads, Assay Diluent, PE Detection Reagent
2	10 pg/ml Standard	Capture Beads, Standard 1:256 Dilution, PE Detection Reagent
3	20 pg/ml Standard	Capture Beads, Standard 1:128 Dilution, PE Detection Reagent
4	40 pg/ml Standard	Capture Beads, Standard 1:64 Dilution, PE Detection Reagent
5	80 pg/ml Standard	Capture Beads, Standard 1:32 Dilution, PE Detection Reagent
6	156 pg/ml Standard	Capture Beads, Standard 1:16 Dilution, PE Detection Reagent
7	312.5 pg/ml Standard	Capture Beads, Standard 1:8 Dilution, PE Detection Reagent
8	625 pg/ml Standard	Capture Beads, Standard 1:4 Dilution, PE Detection Reagent
9	1250 pg/ml Standard	Capture Beads, Standard 1:2 Dilution, PE Detection Reagent
10	2500 pg/ml Standard	Capture Beads, Standard 'Top Standard', PE Detection Reagent

5. Preparation of BD CBA Soluble Protein Flex Set capture beads

The Capture Beads provided in each BD CBA Soluble Flex Set are at a 50× concentration and must be diluted to their optimal concentration before adding to a given assay tube or assay well.

1. Determine the number of BD CBA Soluble Protein Flex Sets to be used in the experiment (size of the multiplex).
2. Determine the number of tests in the experiment. It is recommended that the user prepare a few additional tests than they will use in the experiment to ensure that there is enough material prepared for the experiment.
3. Vortex each Capture Bead stock vial for at least 15 s to resuspend the beads thoroughly.
4. Determine the total volume of diluted beads needed for the experiment.
   Each tube/well requires 50 µl of the diluted beads. The total volume of diluted beads can be calculated by multiplying the number of tests (determined in step 2) by 50 µl.
   - e.g. 35 tests × 50 µl = 1750 µl total volume of beads
5. Determine the volume needed for each capture bead. Beads are supplied so that 1.0 µl = 1 test. Therefore, the required volume (µl) of beads is equal to the number of tests.
   - e.g. 35 tests require 35 µl of each capture bead included in the assay
6. Determine the volume of Capture Bead Diluent needed to dilute the beads.
   The volume of Capture Bead Diluent can be calculated by subtracting the volume for each bead tested from the total volume of diluted beads needed to perform the assay.
   - e.g. 1750 µl total volume of beads – 35 µl for each bead = volume of Capture Bead Diluent
   - e.g. if testing one analyte: 1750 µl – (35 µl × 1) = 1715 µl Diluent
   - e.g. if testing five analytes: 1750 µl – (35 µl × 5) = 1575 µl Diluent

   Refer to Table 9 for more examples of the calculation.
7. Pipette the Capture Beads and Capture Bead Diluent into a tube labelled Mixed Capture Beads.

Table 9. Capture bead and PE detection reagent diluent calculations

Number of Flex Sets to be used	Volume of each Capture Bead or PE Detection Reagent/ test (µl)	Total Capture Volume/ test (µl)	Volume of Capture Bead or Detection Reagent Diluent/ test (µl)	Total volume of mixed Capture Beads or PE Detection Reagents/ test (µl)
1	1	1	49	50
2	1	2	48	50
3	1	3	47	50
4	1	4	46	50
5	1	5	45	50
6	1	6	44	50
7	1	7	43	50
8	1	8	42	50
9	1	9	41	50
10	1	10	40	50
11	1	11	39	50
12	1	12	38	50
13	1	13	37	50
14	1	14	36	50
15	1	15	35	50
16	1	16	34	50
17	1	17	33	50
18	1	18	32	50
19	1	19	31	50
20	1	20	30	50
21	1	21	29	50
22	1	22	28	50
23	1	23	27	50
24	1	24	26	50
25	1	25	25	50
26	1	26	24	50
27	1	27	23	50
28	1	28	22	50
29	1	29	21	50
30	1	30	20	50

Table from: Manual for Cat. No. 558264, p. 20.

6. Notes and Recommendations

Due to some unspecific binding observed with human serum and plasma samples, a specific Capture Beads procedure has been implemented in order to avoid any interference with the assay. The Capture Bead Diluent for Serum/Plasma is included in the Human Soluble Master Buffer kit (Cat. Nos. 558264 and 558265).

1. Determine the number of BD CBA Human Soluble Protein Flex Sets to be used in the experiment (size of the multiplex).
2. Determine the number of tests in the experiment. It is recommended that the user prepare a few additional tests than they will use in the experiment to

ensure that there is enough material prepared for the experiment. Beads are supplied so that 1.0 µl = 1 test. Therefore, the required volume (µl) of beads is equal to the number of tests.
   - e.g. 35 tests requires 35 µl of each capture bead included in the assay
3. Vortex each Capture Bead stock vial for at least 15 s to resuspend the beads thoroughly.
4. Pipette the appropriate volume (determined in step 2) of each capture bead into a tube labelled Mixed Capture Beads.
5. Add 0.5 ml Wash buffer, centrifuge at 200 × *g* for 5 min.
6. Carefully discard supernatant by aspiration. Avoid aspiration of the bead pellet.
7. Resuspend beads in Capture Bead Diluent for Serum/Plasma to a final volume of 50 µl/test, vortex and incubate for 15 min at room temperature prior to use.
   - e.g. 35 tests × 50 µl = 1750 µl Capture Bead Diluent for Serum/Plasma

7. Preparation of BD CBA Soluble Protein Flex Set PE detection reagents

The PE Detection Reagent provided with each BD CBA Soluble Protein Flex Set is a 50× bulk (1 µl/test). The PE Detection Reagents for all BD CBA Protein Flex Sets used in the assay should be combined, and subsequently diluted to their optimal volume per test (50 µl/test) before adding the PE Detection Reagent Mix to a given tube or assay well.

Note: Protect the PE Detection Reagents from exposure to direct light because they can become photobleached and will lose fluorescent intensity.

1. Determine the number of BD CBA Soluble Protein Flex Sets to be used in the experiment (size of the multiplex).
2. Determine the number of tests to be run in the experiment. It is recommended that the user prepare a few additional tests than they will use in the experiment to ensure that there is enough material prepared for the experiment.
3. Determine the total volume of diluted PE Detection Reagent needed for the experiment. Each tube/well requires 50 µl of the diluted PE Detection Reagent. The total volume of diluted PE can be calculated by multiplying the number of tests (determined above) by 50 µl.
   - e.g. 35 tests × 50 µl = 1750 µl total volume of PE
4. Determine the volume needed for each PE Detection Reagent. The PE Detection Reagent is supplied so that 1.0 µl = 1 test. Therefore, the required volume (µl) of PE Detection Reagent is equal to the number of tests.
   - e.g. 35 tests requires 35 µl of each Detection Reagent included in the assay
5. Determine the volume of Detection Reagent Diluent needed to dilute the PE Detection Reagents. The volume of Detection Reagent Diluent can be calculated by subtracting the volume for each PE Detection Reagent tested from the total volume of diluted PE needed.
   - e.g. 1750 µl total volume PE – 35 µl for each Detection Reagent = volume of Detection Reagent Diluent
   - e.g. if testing one analyte: 1750 µl – (35 µl × 1) = 1715 µl Diluent
   - e.g. if testing five analytes: 1750 µl – (35 µl × 5) = 1575 µl Diluent

Refer to Table 9 for more examples.

6. Pipette the Detection Reagents and Detection Reagent Diluent into a tube labelled Mixed PE Detection Reagents. Store at 4°C, protected from light until ready to use.

G. BD CBA Soluble Protein Flex Set assay procedure

Following the preparation and dilution of the individual assay components, transfer the Standards or samples, mixed Capture Beads and mixed PE Detection Reagents to the appropriate assay wells or tubes for incubation and analysis.

Note: Protect Capture Beads and PE Detection Reagents from direct exposure to light.

1. Overview

	Standards	Samples
Capture Beads Mixture	50 µl	50 µl
Diluted Standards	50 µl	N/A
Samples	N/A	50 µl
Vortex the tubes for 5 s or shake the plates for 5 min and incubate for 1 h at room temperature.		
PE Detection Reagent Mixture	50 µl	50 µl
Mix assay tubes gently or shake the plates for 5 min and incubate for 2 h at room temperature in the dark.		
Apply the plate to the vacuum manifold and aspirate or add 1.0 ml of Wash Buffer to each assay tube, centrifuge at 200 × *g* for 5 min and discard the supernatant.		
Wash Buffer	150 µl for plates or 300 µl for tubes	150 µl for plates or 300 µl for tubes

2. Detailed protocol for plates or tubes

1. Prepare all reagents as described in previous sections before starting the experiment.
2. *For plates:* Pre-wet the plate by adding 100 µl of Wash Buffer to each well. To remove the excess volume, apply to vacuum manifold. Do not exceed 10″ Hg of vacuum pressure. Vacuum aspirate until wells are drained (2–10 s).
3. Vortex the Mixed Capture Beads for at least 5 s. Add 50 µl of the Mixed Capture Beads to each assay well (*plates*) or assay *tube*.
4. Add 50 µl of Standard or sample to the assay wells (*plates*) or each assay *tube*.
5. Mix the plate for 5 min using a digital shaker at 500 rpm (do not exceed 600 rpm) or genly mix the assay tubes and incubate for 1 h at room temperature.

6. Add 50 µl of the Mixed PE Detection Reagent to each assay well (*plates*) or assay *tube*.
7. Mix the plate for 5 min using a digital shaker at 500 rpm or gently mix the assay tubes and incubate at room temperature for 2 h.

8a. For *plates*: Apply the plate to the vacuum manifold and vacuum aspirate (do not exceed 10″ Hg of vacuum pressure) until wells are drained (2–10 s).

8b. Add 150 µl of Wash Buffer to each assay well. Shake microwell plate on a digital shaker at 500 rpm for 5 min to resuspend beads.

9a. For *tubes*: Add 1.0 ml of Wash Buffer to each assay *tube* and centrifuge at 200 × *g* for 5 min.

9b. Carefully aspirate and discard the supernatant from each assay *tube*.

9c. Add 300 µl of Wash Buffer to each assay *tube*. Vortex assay *tubes* briefly to resuspend beads.

10. Analyse the samples on a flow cytometer. Proceed to the appropriate flow cytometry instrument instruction manual (included in the Master Buffer Kit) for acquiring the BD CBA Flex Sets.

    Note: It is best to analyse samples on the day of the experiment. Prolonged storage of samples, once the assay is complete, can lead to increased background and reduced sensitivity.

H. Cytometer setup, data acquisition and analysis

Note: The BD CBA Instrument Setup Templates for different flow cytometers mentioned in this section can all be downloaded at: ***bdbiosciences.com/flexset***

1. For flow cytometers running BD FACSDiva™ software

For optimal performance of a BD CBA assay, it is necessary to properly set up the flow cytometer. The cytometer setup information in this section is to be used for the BD FACSCanto™, BD FACSCanto II, BD™ LSR II, BD FACSAria™ and BD FACSAria II flow cytometers.

2. Preparation of instrument setup beads

Prepare five tubes labelled: *A9, PE-F1, F1, F9* and *A1*. Vortex the stock vials of beads, add 200 µl of Wash Buffer to each tube followed by 25 µl of the corresponding setup beads.

3. Instrument setup

1. Edit the parameters list to display only the following: FSC-A, FSC-W, SSC-A, SSC-W, PE-A, APC-A and APC-Cy7-A.
2. On a global worksheet, create the following plots: FSC-A/SSC-A dot plot, APC/APC-Cy7 dot plot and PE histogram.

3. Set FSC-A and SSC-A to Log and create a statistics view showing the FSC-A and SSC-A means. Set the events to display to 500. Using the A9 setup beads, adjust FSC and SSC so that the singlet beads have a mean of 30,000 for each parameter. Stop acquisition to avoid running out of sample.
4. Adjust the FSC-A and SSC-A thresholds using the mean channel as a guideline. Be sure that the thresholds do not cut into the bead population.
5. In the FSC-A versus SSC-A dot plot, create a region that includes the singlet population of beads. In the Population Hierarchy, rename that region *singlet*.
6. Edit the statistics view to display the PE, APC and APC-Cy7 mean of the singlet beads.
7. Through the singlet gate, run the A9 setup beads and adjust the APC and APC-Cy7 voltages until the mean of each parameter is 160,000 ± 2,000.
8. Through the singlet gate, run the PE-F1 tube and adjust the PE voltage so that the mean is 65 ± 5.
9. Create compensation controls and delete the PE compensation tube. Run beads as follows for compensation controls:
   - Unstained: F1
   - APC Stained: F9
   - APC-Cy7 Stained: A1
10. Calculate compensation.
11. Optional: Verify instrument settings prior to analysing the assay by recording a sample using the remaining mixed capture beads from the Flex Set assay, export as FCS2.0 and go to Tools > Clustering Test in FCAP Array software to see if it can identify the correct number of bead clusters.

4. Verification of Instrument Setup

The BD CBA 30 Plex Bead Mixture (Cat. No. 558522) can be included as an additional sample when performing the instrument setup procedure. This cocktail containing 30 bead populations from the BD CBA Flex Set is useful as a control sample to demonstrate that the instrument has been properly set up for analysis and to guarantee that the instrument and FCAP Array Software can analyse a 30 plex assay correctly.

Recommended Assay Procedure:

1. Vortex the BD CBA 30 Plex Bead Mixture to bring beads into suspension.
2. Transfer 25 µl of the BD CBA 30 Plex Bead Mixture to the appropriate sample well or tube.
3. Add 175 µl of Wash Buffer (from the BD CBA Master Buffer Kit used) to the bead sample. More Wash Buffer (275 µl) may be needed for samples in tubes.
4. Proceed with analysis on a BD flow cytometer that has been set up according to the instrument setup procedure and export the FCS2.0 file for the 30 plex bead mixture.
5. Analyse the 30 plex bead mixture data file using the FCAP Array software clustering tool (see Technical Data Sheet for details). If the FCAP Array software fails to identify 30 bead clusters, repeat steps 4 and 5 after repeating the instrument setup procedure. If the FCAP Array software is unable to identify 30 bead clusters from the repeat sample, instrument service may be required.

Note: Do not store the diluted beads. Prepare a new bead sample for each test.

The same procedure is recommended for verification of instrument setup when using the BD FACSArray bioanalyser.

5. Data acquisition

Set events to record to 300 events per analyte (e.g. 300 × 6 = 1800 events for a 6 plex) and set the singlet gate as the storage gate and stopping gate to ensure that only singlet bead events are recorded. Change events to display to 5000. Record samples and export as FCS2.0 files for analysis in FCAP Array.

The Experiment can be saved as a template for future experiments; however, it is recommended to verify instrument settings (i.e. voltages and compensation) prior to each experiment.

6. Analysis of sample data

The analysis of BD CBA data is optimized when using FCAP Array software. Install the software according to the instructions in the *FCAP Array User's Guide* (available for download at **bdbiosciences.com/fcaparray**).

1. Transfer FCS data files for the experiment to the computer with the FCAP Array software.
2. Place all data files for a given experiment in a single folder.

Follow the instructions in the *FCAP Array Software User's Guide* for creating an experiment and for data analysis.

I. For the BD FACSArray bioanalyser running BD FACSArray software

For experiments requiring higher throughput, BD CBA reagents can optimally be combined with the BD FACSArray bioanalyser. Equipped with a 96-well plate loader, the BD FACSArray offers automated data acquisition. BD FACSArray software is used for instrument setup and sample acquisition. BD FACSArray software is compatible with FCAP Array software to allow for quantitative analysis of BD CBA data. FCAP Array software enables researchers to design and set up their BD CBA experiments and import them to the BD FACSArray bioanalyser in a streamlined workflow. Refer to the *BD FACSArray Bioanalyzer Instrument Setup Manual* for instrument setup and data acquisition. Follow the instructions in the *FCAP Array Software User's Guide* (available for download at **bdbiosciences.com/fcaparray**) for creating an experiment and for data analysis.

J. For the BD FACSCalibur™ flow cytometer

For optimal performance of a BD CBA assay, it is necessary to properly set up the flow cytometer. The cytometer setup information in this section is to be used for the BD FACSCalibur™ flow cytometer. The BD FACSComp™ Software is useful for

setting up the flow cytometer. BD CellQuest™ (or BD CellQuest Pro) Software is required for analysing samples and formatting data for subsequent analysis using FCAP Array software.

1. Instrument setup with BD FACSComp software and BD Calibrite™ beads

1. Perform instrument startup.
2. Perform flow check.
3. Prepare tubes of BD Calibrite™ beads for a four-colour setup.
4. Launch BD FACSComp software.
5. Run BD FACSComp software in Lyse/No Wash mode.
   Note: Time-delay calibration must be performed. For detailed information on using BD FACSComp with BD Calibrite beads to set up the flow cytometer, refer to the BD FACSComp Software User's Guide and the BD Calibrite Beads package insert.
6. Proceed to the next section.

2. Preparation of instrument setup beads

1. Label five 12×75 mm tubes *A, B, C, D* and *E*.
2. Add 25 µl of PE Instrument Setup Bead F1 to tube D.
3. Add 50 µl of PE Positive Control Detector to tube D and vortex tube briefly to mix.
4. Incubate tube D for 15 min at room temperature, protect from light.
5. Add 25 µl of Instrument Setup Bead A9 to tube A.
6. Add 25 µl of Instrument Setup Bead A1 to tube B.
7. Add 25 µl of Instrument Setup Bead F9 to tube C.
8. Add 25 µl of Instrument Setup Bead F1 to tubes A, B, C and D.
9. Add 50 µl of the mixed Capture Beads from the BD CBA Flex Set experiment to tube E.
   Note: The mixed Capture Beads added in step 9 should be beads only and not contain PE detection reagent, standards or sample.

Tube	Setup beads
A	A9 + F1
B	A1 + F1
C	F9 + F1
D	PE-F1 + F1
E	Mixed capture beads

10. Add 300 µl of Wash Buffer to tube D and vortex tube briefly to mix.
11. Add 350 µl of Wash Buffer to tubes A, B, C and E. Vortex each tube briefly to mix.
12. Proceed to the next section.

3. Instrument setup with instrument setup beads

1. Launch BD CellQuest (or BD CellQuest Pro) software and open the BD CBA Flex Set Setup Template.
   Note: The BD CBA Flex Set Setup Template file can be downloaded at ***bdbiosciences.com/flexset***
2. Set the instrument to Acquisition mode.
3. Set SSC and FSC to Log mode.
4. Decrease the SSC PMT voltage by 100 from what BD FACSComp set.
5. Set the Threshold to SSC at 650.
6. In Setup mode, run tube A. Follow the setup instructions on the following pages.

Note: Pause and restart acquisition frequently during the instrument setup procedure to reset detected values after settings adjustments.

Adjust gate R1 so that the singlet bead population is located in gate R1 (Figure 4). Adjust the R2 gate so it gates the brightest bead population (Figure 5). Adjust the FL3 PMT so that the FL3 median of the A9 bead population is around 1500 and then adjust the FL4 PMT so that the FL4 median of the A9 bead population is around 5000.

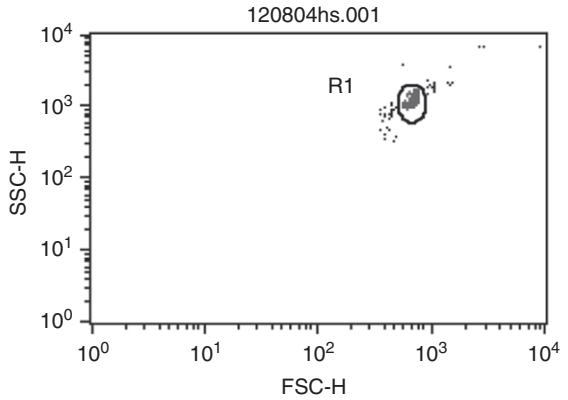

Figure 4. Instrument setup procedure.

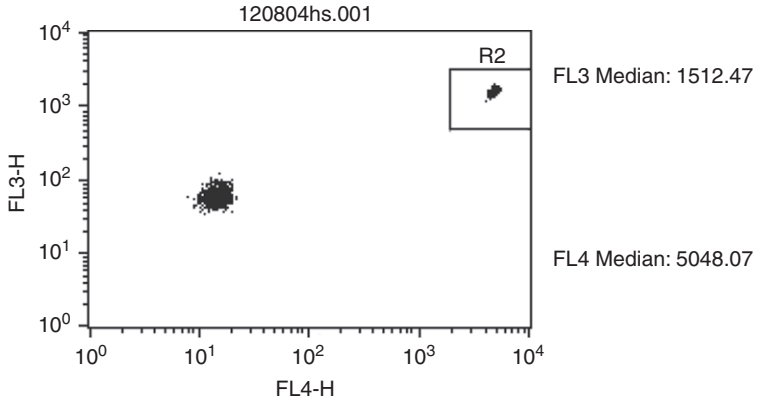

Figure 5. Instrument setup procedure.

Adjust gate R3 so the F1 bead population is inside it (Figure 6). Adjust the FL2 PMT so the FL2 median of the F1 bead population is between 2.5 and 4.0. Proceed to the next page of the setup template.

Run tube B to adjust the compensation settings for FL4 – %FL3.

Adjust gate R4 so the A1 bead population (brightest bead in FL3 channel) is inside it (Figure 7). Ensure that the left edge of gate R4 is touching the *y*-axis boundary of the dot plot. Adjust gate R5 so the F1 bead population is inside it (Figure 7). Using the FL4 – %FL3 control, adjust the median of G4 until it is equal to the median of G5. Proceed to the next page of the setup template.

Run tube C to adjust the compensation settings for FL3 – %FL4.

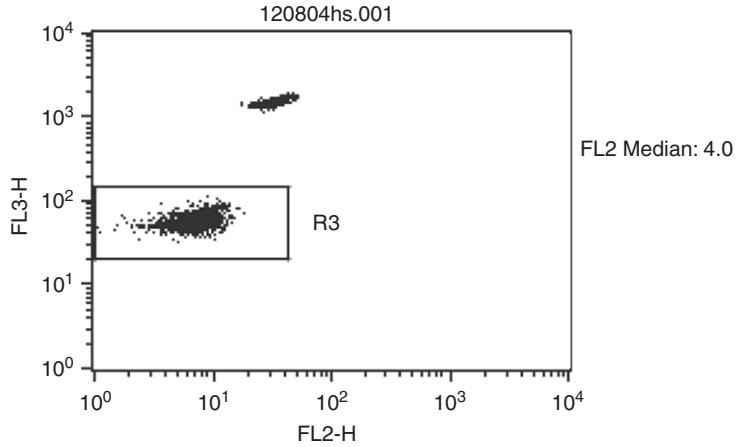

Figure 6. Instrument setup procedure.

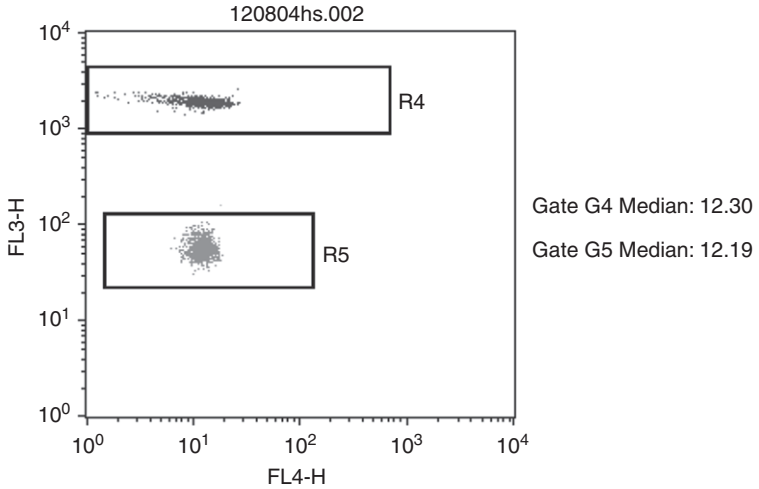

Figure 7. Instrument setup procedure.

Adjust gate R6 so the F1 bead population (dimmest bead in FL4 channel) is inside it (Figure 8). Adjust gate R7 so the F9 bead population is inside it. Using the FL3 – %FL4 control, adjust the median of G7 until it is equal to the median of G6. Proceed to the next page of the setup template.

Run tube D to adjust the compensation settings for FL3 – %FL2.

Adjust gate R8 so the F1 bead population (dimmest bead in FL2 channel) is inside it (Figure 9). Adjust gate R9 so the PE-F1 bead population is inside it. Using the FL3 – %FL2 control, adjust the median of G9 until it is equal to the median of G8. Proceed to the next page of the setup template.

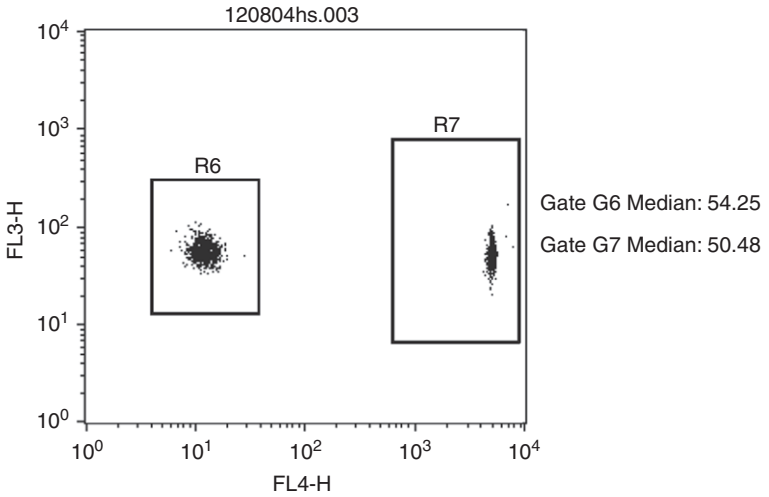

Figure 8. Instrument setup procedure.

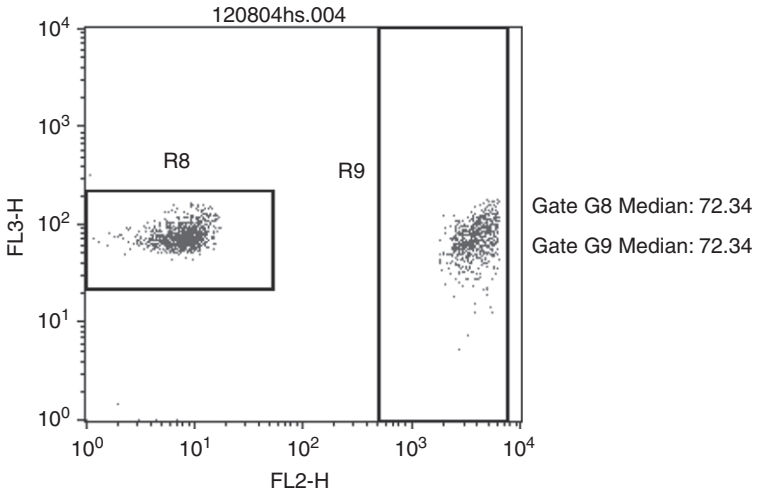

Figure 9. Instrument setup procedure.

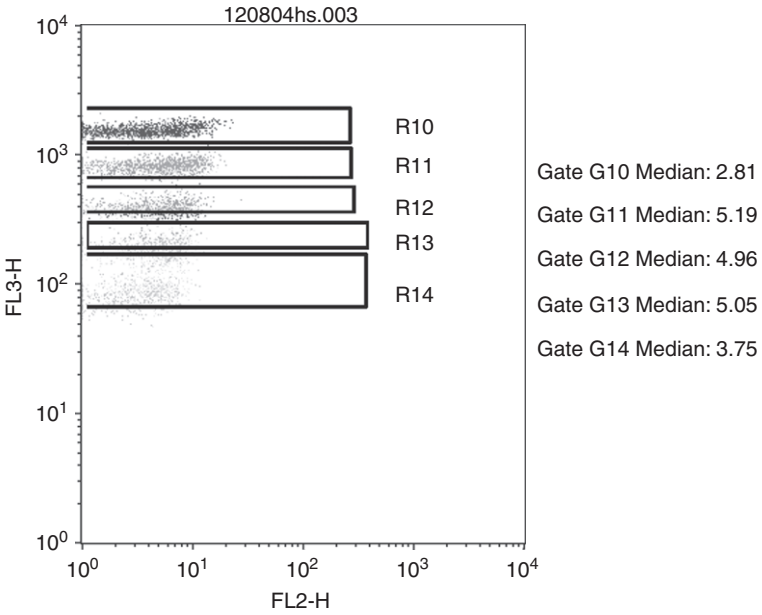

Figure 10. Instrument setup procedure.

Run tube E to adjust the compensation settings for FL2 – %FL3.

Adjust gates R10, R11, R12, R13 and R14 so each bead row falls within only one gate (see Figure 10). Ensure the left edge of each gate is touching the *y*-axis boundary of the dot plot. Using the FL2 – %FL3 control, adjust until the median of any row (G10, G11, G12, G13 or G14) equals 2 – 4.

K. Typical Sample data

Note: It is important not to overcompensate the bead populations in this step. No bead population should have a median below 2.

Note: Not all populations shown in Figure 10 will be displayed in every setup; the populations displayed are dependent on the Flex Set beads used in the experiment.

4. Data acquisition

1. Return to page 1 on the BD CBA Flex Set Setup Template.
2. Set the instrument to Acquisition mode.
3. In the Acquisition and Storage window, do the following:
   a. Set the Acquisition Gate to Accept G1 = R1 events. (This will allow for only the events that fall into R1 to be saved.)
      Note: Be sure that R1 is set correctly to avoid data loss.
   b. Set Collection Criteria for acquisition to stop at 300 × the number BD CBA Flex Set assays being used (e.g. 300 × 6 = 1800 events for a 6 plex). This

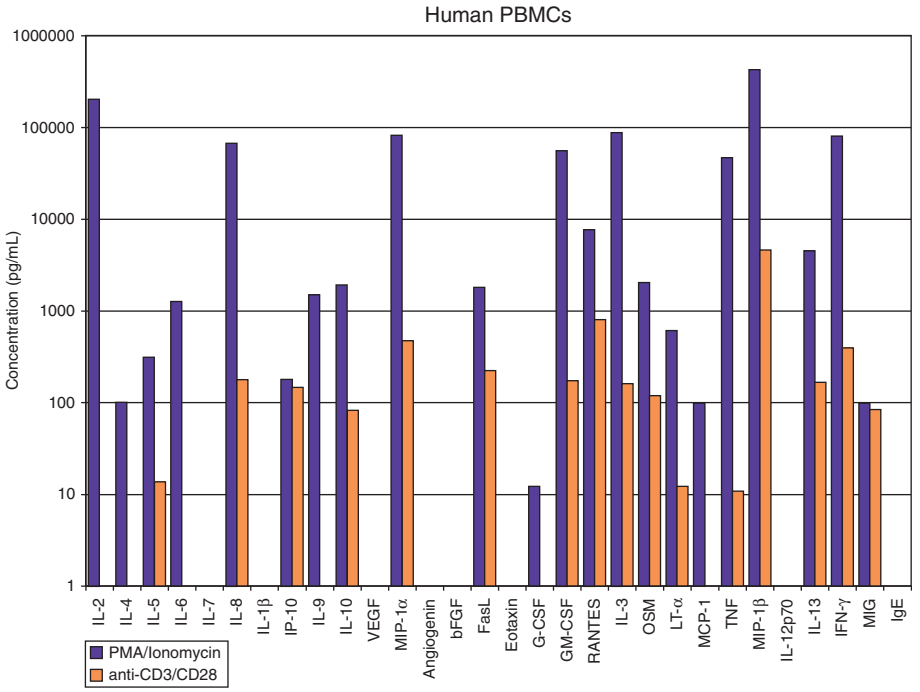

Figure 11. Human peripheral blood mononuclear cells (PBMCs) were stimulated under two different conditions. Supernatants were collected and measured in a BD CBA Flex Set assay (30 plex).

ensures that the sample file contains approximately 300 events of each bead population. Do not acquire more than 300 beads per population.

c. Set Resolution to 1024.
d. Click OK.

4. In setup mode, run tube number 1 and using the FSC versus SSC dot plot, place the R1 region gate around the singlet bead population (see Figure 4).
5. Samples are now ready to be acquired.
6. Begin sample acquisition with the flow rate set to LOW. Using the lowest flow rate can improve resolution of the individual bead populations in the bead plex.

To facilitate analysis of data files using FCAP Array software and to avoid confusion, add a numeric suffix to each file that corresponds to the assay tube number (i.e. Tube No. 1 containing 0 pg/ml could be saved as KT032598.001). The file name must be alphanumeric (i.e. contain at least one letter).

5. Analysis of sample data

The analysis of BD CBA data is optimized when using FCAP Array software. Install the software according to the instructions in the *FCAP Array User's Guide.*

1. Transfer FCS data files for the experiment to the computer with the FCAP Array software.
2. Place all data files for a given experiment in a single folder.

   Follow the instructions for creating an experiment and data analysis in the *FCAP Array Software User's Guide*.

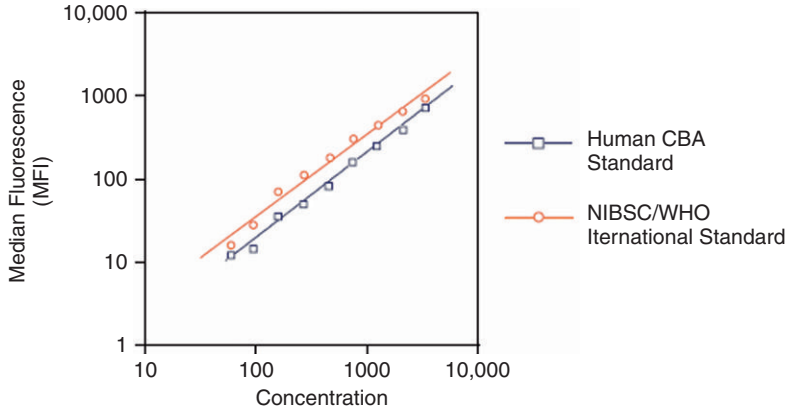

Figure 12. Titration curve comparing the BD CBA Human IFN-γ recombinant standard to the NIBSC/WHO International standard (Image from: BD CBA brochure (23-8910-01) p. 12).

L. Standardization of BD CBA standards to the NIBSC/WHO international standards

Laboratories throughout the world use different assays to measure soluble proteins in biological samples. To support the comparison of values obtained with the BD CBA method, we have evaluated the performance of many of our BD CBA standards with gold standards from the NIBSC. The NIBSC protein standards are recognized by the WHO as international biological standards. They meet established requirements for accuracy, consistency and stability. The NIBSC/WHO standards are assigned potency values in International Units (IU) of biological activity and nominal mass (i.e. not absolute mass values); therefore, they cannot be used to establish absolute concentrations for a cytokine preparation. However, these standards do provide a means to facilitate comparisons of cytokine concentration values determined by experiments conducted within different laboratories or methods.

The source of a recombinant protein (i.e. insect cell, *E. coli*, etc.) and the affinity of antibodies used can affect the measurement and performance of a protein in an immunoassay. The conversion factors provided in Tables 10 and 11 make it possible to compare protein concentrations present in samples measured by different immunoassays that have been standardized to the same NIBSC/WHO standards.

The conversion factor may change based on the batch of either standard. Therefore, the conversion factor is intended to be a guideline indicating whether a BD CBA assay over- or underestimates analyte concentrations relative to the NIBSC/WHO standards. Researchers are advised to incorporate both sets of standards in their assays if they wish to derive data from the NIBSC/WHO standards.

Table 10. NIBSC conversion factor summary for BD CBA Flex Set standards

	NIBSC Standard			Calculated Concentration using BD CBA Flex Set (pg/ml)	Nominal NIBSC Concentration (pg/ml)	BD CBA Flex Set: NIBSC/WHO mass conversion factor
	Code Number	Mass units/ vial	IU Value			
Human b-FGF	90-712	4 μg	1600	1295.87 ± 103.20	2500	1.97
Human G-CSF	88-502	100 ng	10,000	1231.33 ± 87.71	2500	2.06
Human GM-CSF	88-646	1 μg	10,000	1551.45 ± 70.33	2500	1.62
Human IFN-γ	87-586	12.5 ng	250	1287.44 ± 174.12	2500	1.97
Human 1L-1β	86-680	1 μg	100,000	2610.76 ± 129.84	2500	0.97
Human IL-2	86-504	7.6 ng	100	2148.20 ± 193.43	2500	1.17
Human IL-3	91-510	1 μg	1700	1822.31 ± 117.76	2500	1.39
Human IL-4	88-656	100 ng	1000	1535.99 ± 79.24	2500	1.65
Human IL-5	90-586	500 ng	5000	1084.09 ± 254.01	2500	2.38
Human 1L-6	89-548	1 μg	100,000	2041.22 ± 220.02	2500	1.25
Human IL-7	90-530	1 μg	100,000	573.00 ± 94.55	2500	4.44
Human 1L-8	89-520	1 μg	1000	2448.42 ± 153.34	2500	1.04
Human IL-9	91-678	100 ng	1000	601.58 ± 35.24	2500	4.20
Human IL-10	93-722	1 μg	5000	2510.49 ± 144.61	2500	1.01
Human IL-11	92-788	500 ng	5000	13,401.31 ± 1390.37	10,000	0.75
Human IL-12p70	95-544	1 μg	10,000	1307.09 ± 71.6	2500	1.93
Human IL-13	95-622	1 μg	1000	2723.24 ± 660.88	2500	0.93
Human MCP-1	92-794	5 μg	5000 arbitrary units	2280.63 ± 150.6	2500	1.10
Human MlP-lα	92-518	2 μg	200 arbitrary units	1242.93 ± 40.98	2500	2.04
Human OSM	93-564	1 μg	25,000	531.11 ± 34.17	2500	4.75
Human RANTES	92-520	10 μg	100,000 arbitrary units	1589.05 ± 181.79	2500	1.60
Human TNF	88-786	1 μg	46,500	1642.65 ± 99.14	2500	1.54
Human TNFRI	96-528	10 μg	not provided	12,214.45 ± 1165.96	10,000	0.83
Human TNFRII	93-524	10 μg	not provided	707.95 ± 46.45	2500	3.57
Human VEGF	02-286	13 μg	13,000	1250.615 ± 72.77	2500	2.03
Mouse GM-CSF	91-658	1 μg	100,000 arbitrary units	1748.55 ± 132.95	2500	1.46
Mouse IL-1β	93-668	100 ng	100,000 arbitrary units	4531.11 ± 393.89	2500	0.56
Mouse IL-2	93-566	100 ng	10,000 arbitrary	368.74 ± 41.31	2500	6.92
Mouse IL-3	91-662	1 μg	100,000 arbitrary units	1309.44 ± 77.95	2500	1.93
Mouse IL-4	91-656	1 μg	10,000 arbitrary units	439.64 ± 43.03	2500	5.76
Mouse IL-6	93-730	100 ng	10,000 arbitrary units	221.70 ± 49.24	2500	11.40
Mouse TNF	88-532	1 μg	200,000 arbitrary units	1540.95 ± 191.70	2500	1.67

Table from: BD CBA brochure (23-8910-01) p. 13.

Table 11. NIBSC conversion factor summary for BD CBA kit standards

	NIBSC Standard			Calculated Concentration using BD CBA Kit (pg/ml)	Nominal NIBSC Concen-tration (pg/ml)	BD CBA Kit: NIBSC/ WHO mass conversion factor
	Code Number	Mass units/ vial	IU Value			
Human IFN-γ	87-586	12.5 ng	250	4495.12 ± 657.67	5000	1.12
Human 1L-1β	86-680	1 μg	100,000	3463.92 ± 184.87	5000	1.46
Human IL-2	86-504	7.6 ng	100	3118.99 ± 449.33	5000	1.61
Human IL-4	88-656	100 ng	1000	5717.84 ± 632.51	5000	0.88
Human IL-5	90-586	500 ng	5000	3892.01 ± 501.66	5000	1.30
Human 1L-6	89-548	1 μg	100,000	4986.28 ± 633.36	5000	1.01
Human 1L-8	89-520	1 μg	1000	3359.12 ± 319.33	5000	0.74
Human IL-10	93-722	1 μg	5000	4389.72 ± 469.84	5000	1.14
Human IL-12p70	95-544	1 μg	10,000	3764.63 ± 276.73	5000	1.34
Human MCP-1	92-794	5 μg	5000 arbitrary units	2653.49 ± 159.89	5000	0.95
Human RANTES	92-520	10 μg	100,000 arbitrary units	1116.63 ± 90.04	5000	2.26
Human TNF	88-786	1 μg	46,500	3651.85 ± 417.15	5000	1.38
Mouse IL-2	93-566	100 ng	10,000 arbitrary units	627.37 ± 26.29	5000	8.03
Mouse IL-4	91-656	1 μg	10,000 arbitrary units	867.48 ± 59.91	5000	5.81
Mouse IL-6	93-730	100 ng	10,000 arbitrary units	486.43 ± 52.42	5000	10.26
Mouse TNF	88-532	1 μg	200,000 arbitrary units	2328.01 ± 140.83	5000	2.17

Table from: BD CBA brochure (23-8910-01) p. 14.

Acknowledgements

The authors would like to thank Ulf Andersson (Karolinska Hospital, Stockholm, Sweden) and Eric Tartour (Hôpital Européen Georges Pompidou, Paris, France) for sharing information. Schering-Plough Biopharma is supported by Schering-Plough Corporation.

References

Ahrend, W. P. (1993). IL-1 antagonism in inflammatory arthritis. *Lancet* **341**, 155–156.

Andersson, U., Andersson, J., Lindfors, A., Wagner, K., Möller, G. and Heusser, C. H. (1990). Simultaneous production of interleukin 2, interleukin 4 and interferon-γ by activated human blood lymphocytes. *Eur. J. Immunol.* **20**, 1591–1596.

Assenmacher, M., Schmitz, J. and Radbruch, A. (1994). Flow cytometric determination of cytokines in activated murine T helper lymphocytes: expression of interleukin-10 in interferon-γ and in interleukin-4-expressing cells. *Eur. J. Immunol.* **24**, 1097–1101.

Chen, R., Lowe, L., Wilson, J. D., Crowther, E., Tzeggai, K., Bishop, J. E. and Varro, R. (1999). Simultaneous quantification of six human cytokines in a single sample using microparticlebased flow cytometric technology. *Clin. Chem.* **45**, 1693–1694.

Cook, E. B., Stahl, J. L., Lowe, C., Morgan, L. R., Wilson, E. J., Varro, R., Chan, A., Graziano, F. M. and Barney, N. P. (2001). Simultaneous measurement of six cytokines in a single sample of human tears using microparticle-based flow cytometry: allergics vs. non-allergics. *J. Immunol. Methods* **254**, 109–118.

Czerkinsky, C., Andersson, G., Ekre, H. P., Nilsson, L.-A., Klareskog, L. and Ouchterlony, Ö. (1988). Reverse ELISPOT assay for clonal analysis of cytokine production. I. Enumeration of γ-interferon-secreting cells. *J. Immunol. Methods* **110**, 29–36.

Czerkinsky, C., Nilsson, L.-A., Nygren, H., Ouchterlony, Ö and Tarkowski, A. (1983). A solid-phase enzyme-linked immunospot (ELISPOT) assay for enumeration of specific Ab-secreting cells. *J. Immunol. Methods* **65**, 109.

Didenko, V. V. (2001). DNA probes using fluorescence resonance transfer (FRET): designs and Applications. *Biotechniques* **31**, 1106–1121.

Ferre, F. (1992). Quantitative or semi-quantitative PCR: reality versus myth. *PCR Methods Appl.* **2**, 1–9.

Funato, Y., Baumhover, H., Grantham-Wright, D., Wilson, J., Ernst, D. and Sepulveda, H. (2002). Simultaneous measurement of six human cytokines using the Cytometric Bead Array System, a multiparameter immunoassay system for flow cytometry. *Cytometry Res.* **12**, 93–99.

Gilliland, G., Perrin, S., Blanchard, K. and Bunn, H. F. (1990). Analysis of cytokine mRNA and DNA: detection and quantitation by competitive polymerase chain reaction. *Proc. Natl. Acad. Sci. USA* **87**, 2725–2729.

Herr, W., Linn, B., Leister, N., Wandel, E., Meyer zum Buschenfelde, K. H. and Wolfel, T. (1997). The use of computer-assisted video image analysis for the quantification of $CD8^+$ T lymphocytes producing tumor necrosis factor a spots in response to peptide antigens. *J. Immunol. Methods* **203**, 141–152.

Higuchi, R., Dollinger, G., Walsh, P. S. and Griffith, R. (1992). Simultaneous amplification and detection of specific DNA sequences. *Biotechnology* **10**, 413–417.

Higuchi, R., Fockler, C., Dollinger, G. and Watson, R. (1993). Kinetic PCR: real-time monitoring of DNA amplification reactions. *Biotechnology* **11**, 1026–1030.

Holland, P. M., Abramson, R. D., Watson, R. and Gelfand, D. H. (1991). Detection of specific polymerase chain reaction product by utilizing the 5′ to 3′ exonuclease activity of Thermus aquaticus DNA polymerase. *Proc. Natl. Acad. Sci. USA* **88**, 7276–7280.

Ihle, J. N. (2001). The Stat family in cytokine signaling. *Curr. Opin. Cell Biol.* **13**, 211–217.

Jung, T., Schauer, U., Heusser, C., Neumann, C. and Rieger, C. (1993). Detection of intracellular cytokines by flow cytometry. *J. Immunol. Methods* **159**, 197–207.

Korn, T., Bettelli, E., Oukka, M. and Kuchroo, V.K. (2009). IL-17 and Th17 Cells. *Ann Rev Immunol* **27**, 485–517.

Novick, D., Kim, S. H., Fantuzzi, G., Reznikov, L. L., Dinarello, C. A. and Rubinstein, M. (1999). Interleukin-18 binding protein: a novel modulator of the Th1 cytokine response. *Immunity* **10**, 127–136.

Openshaw, P., Murphy, E. E., Hosken, N. A., Maino, V., Davis, K., Murphy, K. and O'Garra, A. (1995). Heterogeneity of intracellular cytokine synthesis at the single-cell level in polarized T helper 1 and T helper 2 populations. *J. Exp. Med.* **182**, 1–11.

Picker, L., Singh, M. K., Zdraveski, Z., Treer, J. R., Waldrop, S. L., Bergstresser, P. R. and Maino, V. C. (1995). Direct demonstration of cytokine synthesis heterogeneity among human memory/effector T cells by flow cytometry. *Blood* **86**, 1408–1419.
Rosenthal-Allieri, M. A., Ticchioni, M., Deckert, M., Breittmayer, J. P., Rochet, N., Rouleaux, M., Senik, A. and Bernard, A. (1995). Monocyte-independent T cell activation by simultaneous binding of three CD2 monoclonal antibodies ($D66^+$ $T11.1^+$ GT2). *Cell. Immunol.* **163**, 88–95.
Sedwick, J. D. and Holt, P. G. (1983). A solid-phase immunoenzymatic technique for the enumeration of specific Ab-secreting cells. *J. Immunol. Methods* **57**, 301–308.
Shapiro, H. (1994). *Practical Flow Cytometry*, (3rd ed.), Wiley-Liss, New York.
Tyagi, S., Bratu, D. and Kramer, F. R. (1998). Multicolor molecular beacons for allele discrimination. *Nat. Biotechnol.* **16**, 49–53.
Tyagi, S. and Kramer, F. R. (1996). Molecular beacons: probes that fluoresce upon hybridization. *Nat. Biotechnol.* **14**, 303–308.
Yssel, H., de Vries, J. E., Koken, M., Van Blitterswijk, W. and Spits, H. (1984). Serum-free medium for the generation and propagation of functional human cytotoxic and helper T cell clones. *J. Immunol. Methods* **72**, 219–227.
Zlotnik, A. and Yoshie, O. (2000). Chemokines: a new classification system and their role in immunity. *Immunity* **12**, 121–127.

Addendum: List of Manufacturers Refered to in This Chapter

AELVIS
Automated Elisa-spot assay videeo analysis systems
http://www.aelvis.net/index.php

American Type Culture Collection
http://www.atcc.org
Hybridomas and antibodies for ELISA, ELISPOT and intracellular staining

Amersham/Pharmacia-General Electric
http://www.apbiotech.com
Columns for primer and probe purification for use in real-time PCR

Applied Biosystems
http://home.appliedbiosystems.com
Reagents for quantitative RT-PCR

BD Biosciences
http://www.bdbiosciences.com
(m)Abs for cellular activation, intracellular staining, BD CBA, flowcytometer equipment

BD Pharmingen PharMingen
http://www.bdbiosciences.com
(m)Abs for cellular activation, ELISA, ELISPOT and intracellular staining

Biosource International
http://www.biosource.com
Reagents for quantitative RT-PCR

Calbiochem-Novabiochem
http://www.calbiochem.com
Reagents for T cell activation

Caltag
http://www.caltag.com
Fluorochrome-conjugated antibodies

Carl Zeiss
http://www.zeiss.de
ELISPOT detection system

Clontech
http://www.clontech.com
Reagents for RT-PCR

CTL-Cellular Technologies LTD
ELISPOT Technology and reagents
http://www.immunospot.com/

DAKO
http://www.dako.com
antibodies for ELISPOT assay

Diaclone Research-Genprobe
http://www.diaclone.com
(m)Abs for cellular activation, ELISA, ELISPOT and intracellular staining

Dynatech Corporation
http://www.dynatech.com/html
Elisa plates and spectrophotometer equipment

Epicentre Technologies
http://www.epicentre.com
Brefeldin A

Eppendorf
http://www.eppendorf.com
PCR machines, multipipetor equipment

Intergen Company
http://www.intergen.com
Reagents for quantitative RT-PCR

Invitrogen (Gibco)
http://www.invitrogen.com
Reagents for RT-PCR

MABTECH
Reagents for ELISPOT assay
http://www.mabtech.com/

Millipore
http://www.millipore.com
ELISPOT plates

Molecular Devices
http://www.moleculardevices.com
Equipment for ELISA, software

Molecular Dynamics
http://www.mdyn.com
Scanning equipment

Molecular Probes
http://www.probes.com
Reagents for RT-PCR

Moss Substrates Inc.
http://www.MossSubstrates.com
Substrates for ELISA

Perkin-Elmer
http://www.perkinelmer.com
PCR machines, reagents for quantitative RT-PCR, software for primer sequence detemination

Promega
http://www.promega.com
Reagents for RT-PCR

Prozyme
http://www.prozyme.com
Enzymes and substrates for ELISA

Quantum-Appligene
http://www.quantum-appligene.com
Products for RNA isolation

Qiagen
http://www.qiagen.com
Reagents for RT-PCR, Reagents for quantitative RT-PCR

R&D Systems
http://www.rndsystems.com
mAbs for cellular activation, ELISA and intracellular staining

Roche
http://www.roche.com
PCR machines, reagents for quantitative RT-PCR

Sigma-Genosys
http://www.genosys.com
Reagents for quantitative RT-PCR

Southern Biotechnology Associates
http://southernbiotech.com
Enzymes and substrates for ELISA

Stratagene
http://www.stratagene.com
PCR machines, Reagents for quantitative RT-PCR, Molecular Beacons

Vector Laboratories
http://www.vectorlabs.com
Fluorochrome-conjugated antibodies

19 Human Dendritic Cell Subsets

Hideki Ueno[1,2], Eynav Klechevsky[1,2], A Karolina Palucka[1,2,3,4] and Jacques Banchereau[1,2,3,4]

[1] Baylor Institute for Immunology Research, Baylor Research Institute, Dallas, TX, USA; [2] INSERM U899, Dallas, TX, USA; [3] Department of Gene and Cell Medicine, Mount Sinai School of Medicine, New York, NY, USA; [4] Department of Medicine, Immunology Institute, Mount Sinai School of Medicine, New York, NY, USA

CONTENTS

I. INTRODUCTION

The immune system is endowed with the ability to recognize a universe of diverse molecules called antigens (Ag), and to generate responses specific to the recognized antigens. An immune response involves both the Ag-nonspecific innate immunity and Ag-specific adaptive immunity. The innate and the adaptive immune systems act in concert to eradicate pathogens through cells, such as macrophages, granulocytes and lymphocytes, and through effector proteins such as antimicrobial peptides, complement, cytokines, cytotoxic granules and antibodies (Batista and Harwood, 2009; Gilliet *et al*., 2008; Kolls *et al*., 2008; Medzhitov and Janeway, 1997; Voskoboinik *et al*., 2006). Dendritic cells (DCs) play a central role to bridge the innate and adaptive immune systems. DCs integrate information obtained from the innate immune system, and deliver the processed information to cells constituting the adaptive immune system, that is, T cells and B cells (Banchereau *et al*., 2000; Banchereau and Steinman, 1998; Shortman and Liu, 2002; Shortman and Naik, 2007; Steinman, 1991) (Figure 1).

DCs reside in peripheral tissues where they are poised to capture antigens. Antigen-loaded DCs migrate from tissues through the afferent lymphatics into the draining lymph nodes. There, they present processed protein and lipid Ags

METHODS IN MICROBIOLOGY, VOLUME 37
0580-9517 DOI 10.1016/S0580-9517(10)37019-X

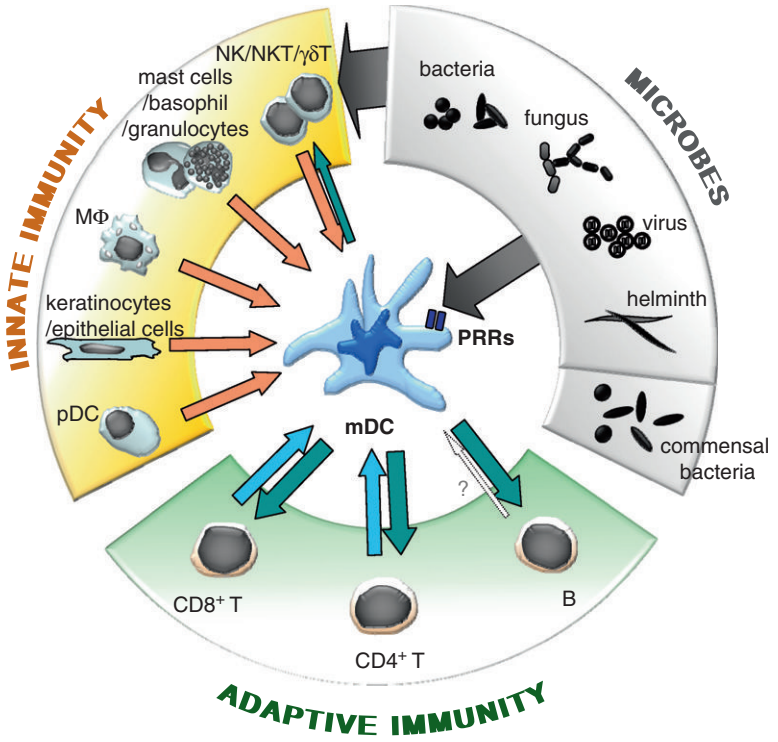

Figure 1. Dendritic cells play a central role in the regulation of immune responses. The innate immune system, which is composed of variable type of cells, recognize microbial invasion through multiple pattern recognition receptors (PRRs) by recognizing microbial pathogen-associated molecular patterns (PAMPs). DCs also act as a component of the innate immune system by directly recognizing PAMPs. Innate immune cells then secrete cytokines and chemokines, which activate DCs and their precursors into mature cells with distinct phenotypes. Activated mDCs migrate to the draining lymph nodes, where they interact with cells of the adaptive immune system, that is, $CD4^+$ and $CD8^+$ T cells and B cells, to induce adaptive immunity. Two major factors, signals from the innate immune system and DC subsets, govern the type of subsequent adaptive immune responses. (See color plate section).

to T cells via both classical (MHC class I and class II) and non-classical (CD1 family) antigen presenting molecules (Banchereau *et al.*, 2000), respectively. Soluble antigens can also reach, through lymphatics and conduits, the draining lymph nodes, and are captured, processed and presented by lymph-node resident DCs (Itano *et al.*, 2003). In the steady state, non-activated (immature) DCs present self-antigens to T cells (Heath and Carbone, 2001; Steinman *et al.*, 2003; Steinman *et al.*, 2000) at periphery, which leads to tolerance. DCs also appear to play a critical role in the regulation of central tolerance in the thymus (Liu *et al.*, 2007). Once activated (mature) in periphery, antigen-loaded DCs are geared towards launching of antigen-specific T cell immunity, which leads to the T cell proliferation and differentiation into helper and effector cells. DCs are also important in launching humoral immunity partly due to their capacity to interact directly with B cells (Jego *et al.*, 2005; Qi *et al.*, 2006). DCs can route antigens into non-degradative recycling compartments, which allow presentation of unprocessed antigens to B cells (Batista

and Harwood, 2009; Bergtold *et al.*, 2005). Thus, not surprisingly, alterations in DC system are involved in the pathogenesis of autoimmune diseases, such as systemic lupus erythematosus (SLE) (Blanco *et al.*, 2001) and in cancer, such as myeloma and breast cancer (Aspord *et al.*, 2007; Cao *et al.*, 2009; Gobert *et al.*, 2009).

Importantly, DCs are composed of multiple subsets with distinct functional properties. The two major subsets are the myeloid DCs (mDCs) and the plasmacytoid DCs (pDCs). Human mDCs are found at least three different sites: (1) peripheral tissue, (2) secondary lymphoid organ and (3) blood. pDCs circulate in the blood and enter lymphoid organs through high endothelial venules (HEV) (Siegal *et al.*, 1999). pDCs are also composed of subsets with different biological properties as described later. We surmise that understanding of the biology of such complex DC system is essential to unravel the pathophysiology of human diseases and design novel vaccines, and thus represents a very important research subject.

Herein, we describe (1) methods to isolate different DC subsets from human skin and blood, (2) *in vitro* culture protocols that allow the generation of distinct DC subsets either from $CD34^+$ hematopoietic progenitor cells (CD34-HPCs) or monocytes and (3) methods to assess the DC functions in the induction of effector $CD4^+$ T cells and $CD8^+$ T cells with different functions.

♦♦♦♦♦♦ II. ISOLATION OF DC SUBSETS

A. Isolation of DC Subsets from Skin

1. Background

There are at least three distinct mDC subsets in the human skin. The epidermis contains only Langerhans cells (LCs), while the dermis contains two DC subsets, $CD1a^+$ DCs and $CD14^+$ DCs (Valladeau and Saeland, 2005). Our recent studies have demonstrated that such skin mDC subsets display distinct phenotype and functional properties (Klechevsky *et al.*, 2009; Klechevsky *et al.*, 2008).

Dermal $CD14^+$ DCs express a large number of surface C-type lectins including DC-SIGN, DEC-205, LOX-1, CLEC-6, Dectin-1 and DCIR, while LCs express the lectins Langerin and DCIR. Dermal $CD14^+$ DCs express multiple Toll-like receptors (TLRs) recognizing bacterial pathogen-associated molecular patterns (PAMPs), such as TLR2, 4, 5, 6, 8 and 10 (Klechevsky *et al.*, 2009; van der Aar *et al.*, 2007). While LCs have been reported to express TLR1, 2, 3, 6 and 10 (Flacher *et al.*, 2006; van der Aar *et al.*, 2007), our own studies using microarray of highly purified LCs failed to show much TLR expression (Klechevsky *et al.*, 2009).

LCs and $CD14^+$ DCs also differ in their cytokine profiles. In response to stimulation via CD40, $CD14^+$ DCs produce a large set of soluble factors including IL-1β, IL-6, IL-8, IL-10, IL-12, GM-CSF, MCP and TGF-β, while LCs produce only a few cytokines, including IL-15 (Klechevsky *et al.*, 2008).

$CD14^+$ DCs derived from CD34-HPCs induce CD40-activated naïve B cells to differentiate into IgM-producing plasma cells through the secretion of IL-6 and IL-12 (Caux *et al.*, 1997). Furthermore, $CD14^+$ DCs induce naïve $CD4^+$ T cells to

differentiate into effectors sharing properties with T follicular helper cells (Tfh) (Klechevsky *et al*., 2008), a $CD4^+$ T cell subset specialized in B cell help (Fazilleau *et al*., 2009; King *et al*., 2008). There, $CD4^+$ T cells primed by $CD14^+$ DCs help naïve B cells to produce large amounts of IgM, and to switch isotypes towards IgG and IgA. This ability to regulate B cell differentiation appears unique to $CD14^+$ DCs, as LCs are unable to do so. Acquisition of Tfh phenotype and function by human $CD4^+$ T cells largely depends on IL-12p70 secreted by DCs (Schmitt *et al*., 2009). IL-12 endows activated $CD4^+$ T cells with the capacity to help the differentiation of antibody-secreting cells (ASCs) via IL-21 (Schmitt *et al*., 2009), a pleotropic cytokine that promotes B cell growth, differentiation, and class-switch recombination (Spolski and Leonard, 2008). Thus, IL-12 secreted by $CD14^+$ DCs appears to contribute to humoral immunity in humans through two different paths: a direct path in DC-B interaction, and an indirect path through DC-T cell interaction and induction of Tfh cells.

In contrast, LCs are remarkably efficient at inducing CTL responses. LCs induce a robust proliferation of naïve allogeneic $CD8^+$ T cells when compared to $CD14^+$ DCs (Klechevsky *et al*., 2008). When pulsed with MHC class I peptides, LCs are far more efficient than $CD14^+$ DCs in the priming of antigen-specific $CD8^+$ T cells. LCs are also efficient in cross-presenting peptides from protein antigens to $CD8^+$ T cells. When compared to those induced by $CD14^+$ dermal DCs, the $CD8^+$ T cells primed by LCs show high avidity and express higher levels of cytotoxic molecules, such as granzymes and perforin. Accordingly, they are remarkably more efficient in killing target cells (Klechevsky *et al*., 2008).

The results summarized above prompted us to hypothesize that the two different arms of adaptive immunity, that is, humoral and cellular arms, are differentially regulated by the two skin mDC subsets. Thus, we surmise that humoral immunity is preferentially regulated by $CD14^+$ dermal DCs, while cellular immunity is preferentially regulated by LCs (Figure 2).

Further characterization of skin DC subsets will be essential to fully understand how immune responses are regulated in human skin, and possibly in many other organs. Notably, while there is no doubt that studies in mice bring fundamental knowledge in basic aspects of DC biology, immune regulation by DC subsets in humans does not appear to be always identical with that in mice. Thus, for better understanding in human immunology, experiments need to be done with human samples.

Here we describe the methodology to isolate DC subsets from human skin tissues. Three mDC subsets, that is, LCs, dermal $CD1a^+$ DCs and dermal $CD14^+$ DCs, can be purified from normal human skin specimens.

2. Technical aspects

1. Cut skin specimens into small pieces (~1–10 mm wide) and incubate them in bacterial protease dispase type 2 (Roche) at a final concentration of 1.2–2.4 U/ml in cRPMI 1640 for 18 h at 4°C.
   Note: To ease the separation process the specimens can be incubated for an additional 2 h at 37°C (optional).

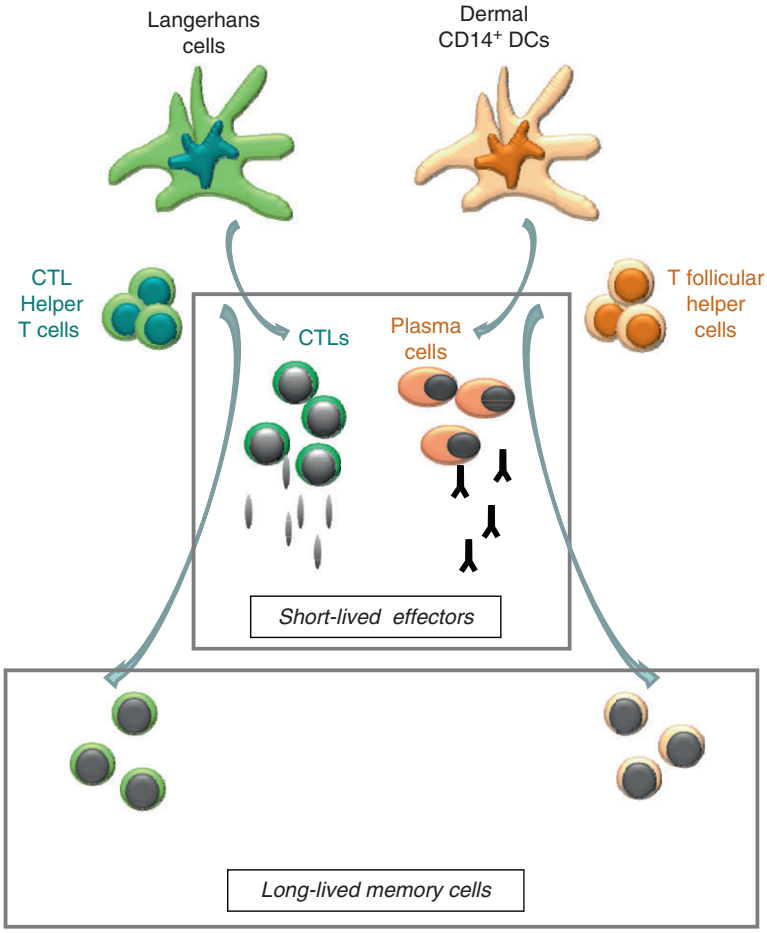

Figure 2. $CD14^+$ dermal DCs preferentially induce humoral immunity, while Langerhans cells induce cellular immunity. LCs are efficient at inducing high avidity-cytotoxic $CD8^+$ T cell responses. In contrast, $CD14^+$ dermal DCs are efficient at inducing the differentiation of naïve B cells into antibody-secreting cells (ASC) and at promoting the development of T follicular helper (Tfh) cells. $CD4^+$ T cells primed by LCs might be efficient at helping the development of CTL responses. Thus, we view that dermal $CD14^+$ DCs are the major DC subset associated with the development of humoral immunity, while epidermal LCs are the major DC subset associated with the development of cellular immunity. (See color plate section).

2. Separate epidermal and dermal sheets with forceps, and place them in separate culture dishes with RPMI 1640 complete medium supplemented with 10% fetal bovine serum (FBS).
   Note: To prevent infection, we recommend supplementing the culture medium with antibiotic antimycotic solution (Gibco).
3. Incubate for 2 days in a humidified incubator at 37°C and 5% CO_2.
4. Collect cells migrating into the medium from epidermal sheets or dermal sheets.
5. Enrich DCs with sodium diatrizoate/Ficoll according to the manufacturer's protocol (Lymphocyte Separation Medium (LSM), Lonza, Switzerland).

6. For the isolation of LCs, stain epidermal cells with anti-CD1a FITC and anti-CD14 APC (BD Biosciences), and sort $CD1a^+CD14^-$ cell population by FACS.
7. For the isolation of dermal DC subsets, stain DCs recovered from dermal sheets with anti-CD1a FITC and anti-CD14 APC, and sort $CD1a^+CD14^-$ cell population (dermal $CD1a^+$ DCs) and $CD1a^-CD14^+$ cell population (dermal $CD14^+$ DCs).
   Note: In our hands, LCs, $CD1a^+$ DCs and $CD14^+$ DCs represent 58, 30 and 12% of the total skin DCs, respectively.

B. Isolation of DC Subsets from Blood

1. Background

Human blood contains mDCs and pDCs, and their subsets. Within blood mDC component, $CD1c^+$ ($BDCA\text{-}1^+$) DCs represent a major population. $BDCA3^+$ mDCs (Dzionek *et al.*, 2000) represent a minute population that uniquely expresses CLEC9A, a C-type lectin with ITAM-like motif (Huysamen *et al.*, 2008).

Blood pDCs can be identified by the expression of high levels of IL-3Rα chain (CD123), as well as some specific markers such as BDCA-2 (Dzionek *et al.*, 2001) within $lin^{neg}HLA\text{-}DR^+$ cells. pDC recognize viral components through TLR7 and TLR9, leading to the secretion of large amounts of Type I IFN (Siegal *et al.*, 1999). Human pDCs are composed of two subsets, distinguished by the expression of CD2 (Matsui *et al.*, 2009). Both subsets secrete IFN-α and express the cytotoxic molecules such as Granzyme B and TRAIL. However, the $CD2^{high}$ pDCs express higher levels of co-stimulatory molecule CD80 upon activation, and are more potent to induce allogeneic T cell proliferation.

In humans, while mDCs are mobilized *in vivo* with by Flt3 ligand, pDCs can be mobilized either Flt3 ligand or G-CSF (Arpinati *et al.*, 2000; Maraskovsky *et al.*, 1996; Pulendran *et al.*, 2000). The differential mobilization of distinct DC subsets or DC precursors by these cytokines offers a strategy to manipulate immune responses in humans (Pulendran *et al.*, 2000; Pulendran *et al.*, 2001).

2. Technical aspect

1. Isolate PBMCs from large blood draw samples (>50 ml) or buffy coats by Ficoll centrifugation.
2. Remove monocytes, T cells, B cells and red blood cells using respective mAbs coupled to microbeads (CD3, CD14, CD19 and glycophorin A; for example, available from Miltenyi Biotec).
   Note: Several companies provide the set of microbeads as a kit, for example, EasySep® Human Pan-DC Pre-Enrichment Kit (Stemcell, BC, Canada).
3. Label DC-enriched PBMCs with CD11c-APC, HLA-DR-PerCP, CD123-PE and a mixture of FITC-mAbs against lineage (Lin) markers: CD3, CD14, CD16, CD19, CD20 and CD56 (lineage cocktail 1, BD Biosciences).
4. Sort mDCs and pDCs by FACS: first gate to $Lin^-HLA\text{-}DR^+$ DC population, and sort $CD11c^+CD123^-$ mDC cells and $CD11c^-CD123^+$ pDC cells.

5. For the isolation of BDCA-3$^+$ mDCs, label DC-enriched PBMCs with Lin FITC, BDCA-3 PE (Miltenyi), CD11c APC, CD123 PE-Cy5 (BD Biosciences) and HLA-DR-Alexa Fluor 700 mAbs (eBioscience), and sort BDCA-3$^+$ cells within the mDC population (Lin$^-$HLA-DR$^+$CD123$^-$CD11c$^+$ cells).
6. Total pDCs as well as pDC subsets can be isolated using antibodies for Lin FITC, HLA-DR PerCP, BDCA-2 PE (Miltenyi) and/or CD2 APC.
   a. For the isolation of total pDCs, label DC-enriched PBMCs with Lin FITC, HLA-DR PerCP, and BDCA-2 PE mAbs, and sort as Lin$^-$HLA-DR$^+$BDCA-2$^+$ cells.
   b. For the isolation of pDC subsets, label DC-enriched PBMCs with the four mAbs described above, and sort CD2$^+$ or CD2$^-$ pDCs found within the Lin$^-$HLA-DR$^+$BDCA-2$^+$ cells.

♦♦♦♦♦♦ III. *IN VITRO* GENERATION OF DC SUBSETS

DCs can be generated *in vitro* from their precursors, CD34-HPCs and monocytes. Different DC precursors cultured in different conditions result in development of DCs with different qualities. Table 1 summarizes a set of parameters in the process of DC generation. *In vitro* generated DCs are amenable to variable purposes, from studies of basic DC biology to clinical applications as vaccines. However, one needs to be aware that each parameter in the DC culture process might largely affect the nature of the subsequent DCs.

Here we describe the methods to isolate the two DC precursors from different sources, and culture conditions to generate DCs *in vitro*. We highly recommend readers to assess how each parameter affects the DC biology in their system, and to select culture conditions that fit their purposes.

Table 1. Parameters in the generation of DCs *in vitro*

Progenitors	Source of cells	Isolation	Culture medium	Serum	Culture cytokines	Culture condition
CD34	G-CSF mobilized blood	CliniMACS®	Yssel's medium	Human AB serum	GM-CSF/ TNF-α/ Flt-3L	Plates
	Fetal liver	CD34$^+$ MACS®	X-VIVO15	Autologous serum		Flasks
	Cord blood	Stemsep®				Bags
Monocytes	Blood	Monocyte Isolation kit II®	RPMI1640	FBS	GM-CSF/ IL-4	Plates
		Elutriation	CellGro® DC Medium	Serum free	GM-CSF/ IFN-α	Flasks
		Adherence			GM-CSF/ IL-15	Bags

A. DC Subsets from CD34-HPCs

1. Background

A method to generate DCs *in vitro* by culturing CD34-HPCs with GM-CSF and TNF-α (CD34-DCs) was introduced in the early nineties (Caux *et al.*, 1992). In the mid-nineties, such CD34-DCs were found to consist of at least two distinct DC subsets, $CD1a^+$ LCs and $CD14^+$ DCs (Caux *et al.*, 1996). This culture system has permitted to determine many differences in phenotypical and functional properties of human mDC subsets (Cao *et al.*, 2007; Caux *et al.*, 1999; Caux *et al.*, 1997; de Saint-Vis *et al.*, 1998; Dieu-Nosjean *et al.*, 2000; Fayette *et al.*, 1997; Fujii *et al.*, 1999; Klechevsky *et al.*, 2008; Rosenzwajg *et al.*, 1996; Strunk *et al.*, 1997; Strunk *et al.*, 1996; Szabolcs *et al.*, 1996; Ueno *et al.*, 2004; Valladeau *et al.*, 2001). Notably, given that IL-4 inhibits the differentiation of LCs from CD34-HPC (Dieu-Nosjean *et al.*, 2001), CD34-DCs developed in the presence of IL-4 likely lack LCs. In contrast, addition of exogenous TGF-β polarized the differentiation of CD34-HPC towards DCs with phenotype typical of LCs, expressing E-cadherin, Langerin and Birbeck granules (Caux *et al.*, 1999). Indeed, epidermal LCs are absent in TGF-β deficient mice (Borkowski *et al.*, 1996), showing that TGF-β is required for the generation of LCs *in vivo*. However, how TGF-β, particularly when used in different doses, affects the biology of *in vitro* generated LCs remains to be established.

There are at least three sources to isolate CD34-HPCs: (1) PBMCs from G-CSF mobilized donors, (2) foetal liver tissues and (3) cord blood samples. We first describe methods for the isolation of CD34-HPCs from these sources, and then methods for the generation and isolation of CD34-DC subsets.

2. Technical aspect

i. Isolation CD34-HPCs from G-CSF mobilized blood apheresis

1. For mobilization of CD34-HPCs to peripheral blood, inject recombinant G-CSF (Neupogen, Amgen) to healthy volunteers 10 μg/kg/day s.c. for 5 days.
   Note: Donor consent and approval of Institutional Review Board (IRB) are required.
2. Isolate CD34-HPCs from blood apheresis samples with CliniMACS® CD34 system (Miltenyi).
   Note: Availability of CliniMACS® might differ according to countries.

ii. Isolation CD34-HPCs from foetal liver tissues

1. Wash fetal liver tissue samples in a 50-ml tube with 25 ml buffer A by gently inverting tube several times.
   Note: Buffer A

500 ml	PBS
20 ml	Fungizone
10 ml	Penicillin/streptomycin

2. Leave tissue at room temperature for 10 min.

3. Repeat step 1 and 2 three times.
4. Place the tissue in a petri dish, and remove fatty or fibrous tissue using forceps.
5. Transfer the tissue into a 50-ml tube, and incubate for 10 min in 20 ml of collagenase D solution.
   Note: Collagenase D solution

20 ml	RPMI1640
200 µL	DNAseI (240 U/ml)
5 ml	collagenase D (5 mg/ml)

6. Disrupt the tissue with a 10-ml pipette and restrain the suspension through a 70-µm filter. Use a syringe plunger to crush the remaining solid tissue and wash with buffer B.

   Note: Buffer B

2.5 g	BSA
5 ml	Penicillin/streptomycin
5 ml	Anticoagulant (ACD or heparin)
500 ml	PBS

   Filter through 0.22 µm, de-gas for at least 45 min and store at 4°C.
7. Spin cells at 1200 rpm for 10 min at room temperature.
8. Resuspend cells with 140 ml with buffer B and then layer 35 ml cell suspension over 15 ml Ficoll. Spin for 25 min at 2000 rpm at room temperature.
9. Collect floating cells over Ficoll, and wash with buffer B in a 50-ml tube.
10. Wash cells again with cold buffer B.
11. Isolate CD34-HPCs using CD34-beads (Miltenyi or Stemsep™, Stemcell, Canada) according to the manufacturers protocol.

iii. Isolation CD34-HPCs from cord blood

1. Dilute cord blood sample with an equal amount of PBS.
2. Layer 35 ml cell suspension over 15 ml Ficoll. Spin for 25 min at 2000 rpm at room temperature.
3. Collect floating cells over Ficoll, and wash three times with PBS supplemented with 1% human AB serum in a 50-ml tube.
4. Isolate CD34-HPCs using CD34-beads according to the manufacturers protocol.

For the generation of DCs, we use three cytokines: GM-CSF, TNF-α and Flt3-L.

Generation and isolation of CD34-DC subsets

1. Resuspend CD34-HPCs at a concentration of 0.5×10^6/ml in Yssel's medium (Gemini Bio-Products, West Sacramento, CA) supplemented with 5% human AB serum, 50 µM 2-β-mercaptoethanol, 1% L-glutamine.
   Note: When CD34-HPCs are obtained from G-CSF mobilized blood, autologous serum obtained after G-CSF mobilization should be used for the optimal growth of cells.
2. Add the three cytokines to the culture: GM-CSF (50 ng/ml; Leukin™, Genzyme), Flt3-L (100 ng/ml; R&D) and TNF-α (10 ng/ml; R&D).

3. Place CD34-HPCs in 12.5 cm^2 flasks, and culture in a humidified incubator at 37°C and 5% CO_2.
4. Refresh half of media at day 5 of culture with supplementation of the cytokines for the full culture volume.
   Note: When cells are proliferating rapidly and the culture medium is getting orange-ish, cell cultures can be split into two (or four) flasks.
5. Harvest cultured cells at day 9 of culture.
6. Label cells with CD1a-FITC and CD14-APC mAbs (BD Biosciences).
7. Sort $CD1a^+CD14^-$ LCs and $CD1a^-CD14^+$ DCs with FACS.
   Note: DC staining and sorting should be performed in the presence of 0.5 mM EDTA in order to avoid cell aggregation.

B. Generation of Different DC Subsets from Monocytes

1. Background

Different cytokines skew the *in vitro* differentiation of monocytes into DCs with different properties. Development of DCs by culturing monocytes with GM-CSF and IL-4 was established in the mid-nineties (Romani *et al.*, 1994), and such IL4-DCs are widely used for the analysis of DC biology and for clinical purposes as DC vaccines. Culture of monocytes in the presence of IFN-α/β or IL-15 yield IFN-DCs, or IL15-DCs, respectively (Banchereau and Palucka, 2005) which display different properties from IL4-DCs. For example, peptide-pulsed IL15-DCs are much more efficient than IL4-DCs for the induction of antigen-specific CTL differentiation *in vitro* (Dubsky *et al.*, 2007). IFN-α-DCs are also efficient for the induction of specific immunity.

Different maturation signals yield DCs with different functional properties. For example, IL-4-DCs activated with a cocktail of IFN-α, polyI:C, IL-1β, TNF, and IFN-γ induce up to 40 times more melanoma-specific CTLs *in vitro* than DCs matured with the 'standard' cocktail of IL-1β/TNF/IL-6/prostaglandin E_2 (PGE_2) (Fujita *et al.*, 2009b; Giermasz *et al.*, 2009; Mailliard *et al.*, 2004).

There are at least three methods for the isolation of monocytes from blood. Here we first describe methods using (1) magnetic beads, (2) elutriation and (3) adherence with sterile culture bags. Elutriation is particularly useful to enrich monocyte fraction from blood apheresis samples. Then, we describe the methods for the generation of monocyte-derived DCs.

2. Technical aspect

i. Isolation of monocytes with magnet beads

Negatively select monocytes using Monocyte Isolation Kit II™ (Miltenyi) according to the manufacturer's protocol.

Note 1: Although monocytes can be positively selected from PBMCs with CD14 magnet beads, we recommend to isolate monocytes by negative selection, as CD14 beads might affect the function of the subsequent DCs (Devitt *et al.*, 1998).

Note 2: Monocyte Isolation Kit II™ (Miltenyi) contains CD16-beads, and thus removes the CD16-expressing monocyte subset. To avoid the loss of the $CD16^+$ population, a mixture of microbeads specific for CD3, CD19, CD56, CD123 and CD235a (Glycophorin A) can be used. However, the negative fraction might contain $CD16^+CD56^-$ NK cells.

ii. Isolation of monocyte-enriched fraction with elutriation

The ELUTRA® cell separation system (CARIDIAN BCT) is used to isolate monocytes from the PBMCs obtained by apheresis. The ELUTRA® is a semi-automatic, closed system centrifuge that uses continuous counter-flow elutriation technology to separate cells into multiple fractions based on size and density. Five fractions are collected, and the Fraction 5 contains an enriched monocyte population (median frequency of $CD14^+$ monocytes: approximately 90%).

iii. Isolation of monocytes with 75 cm^2 culture flasks

1. Resuspend PBMCs with PBS at 1×10^6/ml in PBS supplemented with 0.2% FBS.
2. Place 30 ml PBMC solution into a 75 cm^2 culture flask.
3. Incubate at 37°C for 30 min.
4. Check with a microscope adherent monocytes to the bottom of the flask, and rinse the flask 5–10 times with 10 ml room temperature PBS (per well) using a 10-ml pipette.
5. Change PBS 5–6 times until floating cells become very few.
6. Add culture media to initiate DC generation.

Note: Six well plates can be used as well. There, 3 ml PBMC solution per well should be put.

3. Generation of monocyte-derived DCs

Isolated monocytes can be cultured in plastic culture dishes, flasks and bags. Here we describe outlines of DC generation.

1. When monocytes are isolated either with beads or elutriation, monocytes are resuspended in complete RPMI 1640 media supplemented with 1% l-glutamine, 1% penicillin/streptomycin, 1% sodium pyruvate, 1% non-essential amino acids, 25 mM Hepes pH 7.4 and 10% heat-inactivated FBS at a concentration $\leq 0.3 \times 10^6$ cells/ml.
   Note: DCs can also be generated in serum free media, for example, CellGro DC® (CellGenix, Germany) at 1×10^6 cells/ml.
2. When monocytes are isolated by adherence, add 20 ml media in a 75-ml flask, and 3 ml/well in a 6 well plate.
3. For the generation of IL4-DCs, monocytes are cultured for 6 days with GM-CSF (100 ng/ml; LeukinTM, Genzyme) and IL-4 (50 ng/ml; R&D, or CellGenix). The cytokines are added to the culture every 2 days.

4. For the generation of IL15-DCs, monocytes are cultured for 3 days with GM-CSF (100 ng/ml) and IL-15 (200 ng/ml; R&D).
5. For the generation of IFN-DCs, monocytes are cultured for 3 days with GM-CSF (100 ng/ml) and IFN-α2b (500 IU/ml, Intron-ATM Schering-Plough).
6. Examine the DC morphology with a microscope.
   Note: Make sure that the culture does not contain many lymphocytes. When many lymphocytes are seen in the culture, the generated DCs may show altered phenotype and/or functions, as cytokines secreted by these contaminated cells might affect their biology.

♦♦♦♦♦♦ IV. FUNCTIONAL ASSESSMENT OF DC SUBSETS ON NAÏVE T CELLS

A. Background

As discussed above, DC subsets express different sets of surface molecules as well as secrete different sets of soluble factors. Accordingly, T cells primed by distinct DC subsets display different functional properties. For example, LCs and dermal $CD14^+$ DCs induce $CD4^+$ T cells with different cytokine production profiles. Epidermal LCs induce a potent proliferation of allogeneic naïve $CD4^+$ T cells, which differentiate into cells secreting large amounts of Type 2 cytokines (Klechevsky *et al.*, 2008). A recent report also showed that human LCs promote the development of IL-22-secreting $CD4^+$ T cells, which do not co-express Th1, Th2 or Th17 cytokines (Fujita *et al.*, 2009a). Interestingly, IFN-γ-secreting $CD4^+$ T cells are induced at a similar level by human epidermal LCs and dermal $CD14^+$ DCs. However, the developmental mechanism and the function of Th1 cells induced by the two DC subsets appears be distinct. Consistent with the inability to secrete IL-12, induction of Th1 cells by epidermal LCs was shown to be independent of IL-12 or IL-23 (Furio *et al.*, 2009). As described previously, $CD8^+$ T cells primed by different DC subsets also display distinct cytotoxic abilities.

Thus, analysis of the quality of $CD4^+$ and $CD8^+$ T cells primed by DCs is fundamental to assess the biological functions of DCs. Here we describe methods to purify $CD4^+$ and $CD8^+$ T cells primed by DC subsets. The isolated T cells can be used to assess their qualities through the analysis of molecular expression, cytokine production and gene expression profiling.

B. Technical Aspect

1. Isolation of $CD4^+$ T cells primed by DC subsets

1. Enrich $CD4^+$ T cells from PBMCs by a negative selection using beads coupled with CD8, CD56, CD14, and CD19 mAbs (Miltenyi).
2. Label $CD4^+$ T cell-rich cell populations with mAbs specific for CCR7-PE (R&D), CD45RA-TC (Invitrogen), CD4-APC (BD) and a cocktail of mAbs for CD56, HLA-DR FITC (BD).

Note: The FITC cocktail is important to exclude a contamination of NKT cells and blood DC subsets.

3. Sort naïve $CD4^+$ T cells as FITC cocktail$^-CD4^+CD45RA^+CCR7^+$ cells by FACS.
4. Label naïve $CD4^+$ T cells with 1 μM carboxyfluorescein succinimidyl ester (CFSE, Invitrogen) according to the manufacturer's protocol.
5. Culture CFSE-labelled naïve $CD4^+$ T cells (4×10^5/well) with DCs (5×10^4/well with *in vitro* DCs; 2×10^4/well with skin DCs) in 200 μl of RPMI complete medium supplemented with 10% AB human serum in round-bottomed 96-well plates for 5–7 days.

   Note: DC numbers per well should be adjusted according to the DCs.
6. Stain cells with anti-CD4 APC.
7. Sort $CD4^+$ T cells that underwent cell proliferation ($CD4^+CFSE^-$) by FACS.

For example, cytokine secretion profiles can be determined as follows:

1. Re-stimulate the sorted $CD4^+$ T cells (1×10^5/well) with beads coated with anti-CD3/CD28 (1 μl/well; Dynabeads, Invitrogen) in 200 μl of RPMI complete medium supplemented with 10% AB human serum in round-bottomed 96-well plates for 24 h.
2. Measure cytokine levels in the supernatant with ELISA or multiplex cytokine assays (for example, Luminex, TX).

2. Isolation of $CD8^+$ T cells primed by DC subsets

1. Enrich $CD8^+$ T cells from PBMCs by a negative selection using beads coupled with CD4, CD14 and CD19 mAbs (Miltenyi).
2. Label $CD8^+$ T cell-rich cell populations with mAbs specific for CCR7-PE (R&D), CD45RA-TC (Invitrogen), CD8-APC (BD) and a cocktail of mAbs for CD4 and HLA-DR FITC (BD).
3. Sort naïve $CD8^+$ T cells as FITC cocktail$^-CD8^+CD45RA^+CCR7^+$ cells by FACS.
4. Label naïve $CD8^+$ T cells with 1 μM CFSE.
5. Culture CFSE-labelled naïve $CD8^+$ T cells (4×10^5/well) with DCs (5×10^4/well with in vitro DCs; 2×10^4/well with skin DCs) in 200 μl of RPMI complete medium supplemented with 10% AB human serum and IL-2 (10 U/ml, R&D) in round-bottomed 96-well plates for 5–7 days.

   Note: DC numbers per well should be adjusted according to the DCs.
6. Stain cells with anti-CD8 APC.
7. Sort $CD8^+$ T cells that underwent cell proliferation ($CD8^+CFSE^-$) by FACS.

Acknowledgements

We would like to thank our many post-docs, students, technicians and collaborators who have contributed over more than a decade to many excellent works, which permitted us to write up this chapter. We would particularly like to thank V. Pascual, R. Morita, N. Schmitt, T. Matsui, P. Dubsky and H. Saito, who have contributed to the most recent studies. We thank to Dr. M. Ramsay for continuous

help. This work is supported by NIH grants R01 CA078846, AI067854, R01 AI068842, P50 AR054083, HHSN268200700015C, U19 AI057234, U19 082715, P01 CA85412. **JB holds the W.W. Caruth, Jr. Chair for Transplantation Immunology Research. AKP holds the Ramsay Chair for Cancer Immunology.**

References

Arpinati, M., Green, C. L., Heimfeld, S., Heuser, J. E. and Anasetti, C. (2000). Granulocyte-colony stimulating factor mobilizes T helper 2-inducing dendritic cells. *Blood* **95**, 2484–2490.

Aspord, C., Pedroza-Gonzalez, A., Gallegos, M., Tindle, S., Burton, E. C., Su, D., Marches, F., Banchereau, J. and Palucka, A. K. (2007). Breast cancer instructs dendritic cells to prime interleukin 13-secreting $CD4^+$ T cells that facilitate tumor development. *J. Exp. Med.* **204**, 1037–1047.

Banchereau, J., Briere, F., Caux, C., Davoust, J., Lebecque, S., Liu, Y. J., Pulendran, B. and Palucka, K. (2000). Immunobiology of dendritic cells. *Annu. Rev. Immunol.* **18**, 767–811.

Banchereau, J. and Palucka, A. K. (2005). Dendritic cells as therapeutic vaccines against cancer. *Nat. Rev. Immunol.* **5**, 296–306.

Banchereau, J. and Steinman, R. M. (1998). Dendritic cells and the control of immunity. *Nature* **392**, 245–252.

Batista, F. D. and Harwood, N. E. (2009). The who, how and where of antigen presentation to B cells. *Nat. Rev. Immunol.* **9**, 15–27.

Bergtold, A., Desai, D. D., Gavhane, A. and Clynes, R. (2005). Cell surface recycling of internalized antigen permits dendritic cell priming of B cells. *Immunity* **23**, 503–514.

Blanco, P., Palucka, A. K., Gill, M., Pascual, V. and Banchereau, J. (2001). Induction of dendritic cell differentiation by IFN-alpha in systemic lupus erythematosus. *Science* **294**, 1540–1543.

Borkowski, T. A., Letterio, J. J., Farr, A. G. and Udey, M. C. (1996). A role for endogenous transforming growth factor beta 1 in Langerhans cell biology: the skin of transforming growth factor beta 1 null mice is devoid of epidermal Langerhans cells. *J. Exp. Med.* **184**, 2417–2422.

Cao, W., Bover, L., Cho, M., Wen, X., Hanabuchi, S., Bao, M., Rosen, D. B., Wang, Y. H., Shaw, J. L., Du, Q. *et al*. (2009). Regulation of TLR7/9 responses in plasmacytoid dendritic cells by BST2 and ILT7 receptor interaction. *J. Exp. Med.* **206**, 1603–1614.

Cao, T., Ueno, H., Glaser, C., Fay, J. W., Palucka, A. K. and Banchereau, J. (2007). Both Langerhans cells and interstitial DC cross-present melanoma antigens and efficiently activate antigen-specific CTL. *Eur. J. Immunol.* **37**, 2657–2667.

Caux, C., Dezutter-Dambuyant, C., Schmitt, D. and Banchereau, J. (1992). GM-CSF and TNF-alpha cooperate in the generation of dendritic Langerhans cells. *Nature* **360**, 258–261.

Caux, C., Massacrier, C., Dubois, B., Valladeau, J., Dezutter-Dambuyant, C., Durand, I., Schmitt, D. and Saeland, S. (1999). Respective involvement of TGF-beta and IL-4 in the development of Langerhans cells and non-Langerhans dendritic cells from $CD34^+$ progenitors. *J. Leukoc. Biol.* **66**, 781–791.

Caux, C., Massacrier, C., Vanbervliet, B., Dubois, B., Durand, I., Cella, M., Lanzavecchia, A. and Banchereau, J. (1997). $CD34^+$ hematopoietic progenitors from human cord blood differentiate along two independent dendritic cell pathways in response to granulocyte-macrophage colony-stimulating factor plus tumor necrosis factor alpha: II. Functional analysis. *Blood* **90**, 1458–1470.

Caux, C., Vanbervliet, B., Massacrier, C., Dezutter-Dambuyant, C., de Saint-Vis, B., Jacquet, C., Yoneda, K., Imamura, S., Schmitt, D. and Banchereau, J. (1996). $CD34^+$ hematopoietic progenitors from human cord blood differentiate along two independent dendritic cell pathways in response to $GM\text{-}CSF^+$TNF alpha. *J. Exp. Med.* **184**, 695–706.

de Saint-Vis, B., Fugier-Vivier, I., Massacrier, C., Gaillard, C., Vanbervliet, B., Ait-Yahia, S., Banchereau, J., Liu, Y. J., Lebecque, S. and Caux, C. (1998). The cytokine profile expressed by human dendritic cells is dependent on cell subtype and mode of activation. *J. Immunol.* **160**, 1666–1676.

Devitt, A., Moffatt, O. D., Raykundalia, C., Capra, J. D., Simmons, D. L. and Gregory, C. D. (1998). Human CD14 mediates recognition and phagocytosis of apoptotic cells. *Nature* **392**, 505–509.

Dieu-Nosjean, M. C., Massacrier, C., Homey, B., Vanbervliet, B., Pin, J. J., Vicari, A., Lebecque, S., Dezutter-Dambuyant, C., Schmitt, D., Zlotnik, A. *et al*. (2000). Macrophage inflammatory protein 3alpha is expressed at inflamed epithelial surfaces and is the most potent chemokine known in attracting Langerhans cell precursors. *J. Exp. Med.* **192**, 705–718.

Dieu-Nosjean, M. C., Massacrier, C., Vanbervliet, B., Fridman, W. H., and Caux, C. (2001). IL-10 induces CCR6 expression during Langerhans cell development while IL-4 and IFN-gamma suppress it. *J Immunol.* **167**, 5594–5602.

Dubsky, P., Saito, H., Leogier, M., Dantin, C., Connolly, J. E., Banchereau, J. and Palucka, A. K. (2007). IL-15-induced human DC efficiently prime melanoma-specific naive CD8(+) T cells to differentiate into CTL. *Eur. J. Immunol.* **37**, 1678–1690.

Dzionek, A., Fuchs, A., Schmidt, P., Cremer, S., Zysk, M., Miltenyi, S., Buck, D. W. and Schmitz, J. (2000). BDCA-2, BDCA-3, and BDCA-4: three markers for distinct subsets of dendritic cells in human peripheral blood. *J. Immunol.* **165**, 6037–6046.

Dzionek, A., Sohma, Y., Nagafune, J., Cella, M., Colonna, M., Facchetti, F., Gunther, G., Johnston, I., Lanzavecchia, A., Nagasaka, T. *et al*. (2001). BDCA-2, a novel plasmacytoid dendritic cell-specific type II C-type lectin, mediates antigen capture and is a potent inhibitor of interferon alpha/beta induction. *J. Exp. Med.* **194**, 1823–1834.

Fayette, J., Dubois, B., Vandenabeele, S., Bridon, J. M., Vanbervliet, B., Durand, I., Banchereau, J., Caux, C. and Briere, F. (1997). Human dendritic cells skew isotype switching of CD40-activated naive B cells towards IgA1 and IgA2. *J. Exp. Med.* **185**, 1909–1918.

Fazilleau, N., Mark, L., McHeyzer-Williams, L. J. and McHeyzer-Williams, M. G. (2009). Follicular helper T cells: lineage and location. *Immunity* **30**, 324–335.

Flacher, V., Bouschbacher, M., Verronese, E., Massacrier, C., Sisirak, V., Berthier-Vergnes, O., de Saint-Vis, B., Caux, C., Dezutter-Dambuyant, C., Lebecque, S. *et al*. (2006). Human Langerhans cells express a specific TLR profile and differentially respond to viruses and Gram-positive bacteria. *J. Immunol.* **177**, 7959–7967.

Fujii, S., Fujimoto, K., Shimizu, K., Ezaki, T., Kawano, F., Takatsuki, K., Kawakita, M. and Matsuno, K. (1999). Presentation of tumor antigens by phagocytic dendritic cell clusters generated from human $CD34^+$ hematopoietic progenitor cells: induction of autologous cytotoxic T lymphocytes against leukemic cells in acute myelogenous leukemia patients. *Cancer Res.* **59**, 2150–2158.

Fujita, H., Nograles, K. E., Kikuchi, T., Gonzalez, J., Carucci, J. A. and Krueger, J. G. (2009a). Human Langerhans cells induce distinct IL-22-producing $CD4^+$ T cells lacking IL-17 production. *Proc. Natl. Acad. Sci. U.S.A* **106**, 21795–21800.

Fujita, M., Zhu, X., Ueda, R., Sasaki, K., Kohanbash, G., Kastenhuber, E. R., McDonald, H. A., Gibson, G. A., Watkins, S. C., Muthuswamy, R. *et al*. (2009b). Effective immunotherapy against murine gliomas using type 1 polarizing dendritic cells-significant roles of CXCL10. *Cancer Res.* **69**, 1587–1595.

Furio, L., Billard, H., Valladeau, J., Peguet-Navarro, J. and Berthier-Vergnes, O. (2009). Poly(I:C)-Treated human langerhans cells promote the differentiation of $CD4^+$ T cells producing IFN-gamma and IL-10. *J. Invest. Dermatol.* **129**, 1963–1971.

Giermasz, A. S., Urban, J. A., Nakamura, Y., Watchmaker, P., Cumberland, R. L., Gooding, W. and Kalinski, P. (2009). Type-1 polarized dendritic cells primed for high

IL-12 production show enhanced activity as cancer vaccines. *Cancer Immunol. Immunother.* **58**, 1329–1336.
Gilliet, M., Cao, W. and Liu, Y. J. (2008). Plasmacytoid dendritic cells: sensing nucleic acids in viral infection and autoimmune diseases. *Nat. Rev. Immunol.* **8**, 594–606.
Gobert, M., Treilleux, I., Bendriss-Vermare, N., Bachelot, T., Goddard-Leon, S., Arfi, V., Biota, C., Doffin, A. C., Durand, I., Olive, D. *et al*. (2009). Regulatory T cells recruited through CCL22/CCR4 are selectively activated in lymphoid infiltrates surround ing primary breast tumors and lead to an adverse clinical outcome. *Cancer Res.* **69**, 2000–2009.
Heath, W. R. and Carbone, F. R. (2001). Cross-presentation, dendritic cells, tolerance and immunity. *Annu. Rev. Immunol.* **19**, 47–64.
Huysamen, C., Willment, J. A., Dennehy, K. M. and Brown, G. D. (2008). CLEC9A is a novel activation C-type lectin-like receptor expressed on BDCA3$^+$ dendritic cells and a subset of monocytes. *J. Biol. Chem.* **283**, 16693–16701.
Itano, A. A., McSorley, S. J., Reinhardt, R. L., Ehst, B. D., Ingulli, E., Rudensky, A. Y. and Jenkins, M. K. (2003). Distinct dendritic cell populations sequentially present antigen to CD4 T cells and stimulate different aspects of cell-mediated immunity. *Immunity* **19**, 47–57.
Jego, G., Pascual, V., Palucka, A. K. and Banchereau, J. (2005). Dendritic cells control B cell growth and differentiation. *Curr. Dir. Autoimmun.* **8**, 124–139.
King, C., Tangye, S. G. and Mackay, C. R. (2008). T follicular helper (TFH) cells in normal and dysregulated immune responses. *Annu. Rev. Immunol.* **26**, 741–766.
Klechevsky, E., Liu, M., Morita, R., Banchereau, R., Thompson-Snipes, L., Palucka, A. K., Ueno, H. and Banchereau, J. (2009). Understanding human myeloid dendritic cell subsets for the rational design of novel vaccines. *Hum. Immunol.* **70**, 281–288.
Klechevsky, E., Morita, R., Liu, M., Cao, Y., Coquery, S., Thompson-Snipes, L., Briere, F., Chaussabel, D., Zurawski, G., Palucka, A. K. *et al*. (2008). Functional specializations of human epidermal Langerhans cells and CD14$^+$ dermal dendritic cells. *Immunity* **29**, 497–510.
Kolls, J. K., McCray, P. B.Jr. and Chan, Y. R. (2008). Cytokine-mediated regulation of antimicrobial proteins. *Nat. Rev. Immunol.* **8**, 829–835.
Liu, Y. J., Soumelis, V., Watanabe, N., Ito, T., Wang, Y. H., Malefyt Rde, W., Omori, M., Zhou, B. and Ziegler, S. F. (2007). TSLP: an epithelial cell cytokine that regulates T cell differentiation by conditioning dendritic cell maturation. *Annu. Rev. Immunol.* **25**, 193–219.
Mailliard, R. B., Wankowicz-Kalinska, A., Cai, Q., Wesa, A., Hilkens, C. M., Kapsenberg, M. L., Kirkwood, J. M., Storkus, W. J. and Kalinski, P. (2004). alpha-type-1 polarized dendritic cells: a novel immunization tool with optimized CTL-inducing activity. *Cancer Res.* **64**, 5934–5937.
Maraskovsky, E., Brasel, K., Teepe, M., Roux, E. R., Lyman, S. D., Shortman, K. and McKenna, H. J. (1996). Dramatic increase in the numbers of functionally mature dendritic cells in Flt3 ligand-treated mice: multiple dendritic cell subpopulations identified. *J. Exp. Med.* **184**, 1953–1962.
Matsui, T., Connolly, J. E., Michnevitz, M., Chaussabel, D., Yu, C. I., Glaser, C., Tindle, S., Pypaert, M., Freitas, H., Piqueras, B. *et al*. (2009). CD2 distinguishes two subsets of human plasmacytoid dendritic cells with distinct phenotype and functions. *J. Immunol.* **182**, 6815–6823.
Medzhitov, R. and Janeway, C. A. Jr. (1997). Innate immunity: the virtues of a nonclonal system of recognition. *Cell* **91**, 295–298.
Pulendran, B., Banchereau, J., Burkeholder, S., Kraus, E., Guinet, E., Chalouni, C., Caron, D., Maliszewski, C., Davoust, J., Fay, J. *et al*. (2000). Flt3-ligand and granulocyte colony-stimulating factor mobilize distinct human dendritic cell subsets in vivo. *J. Immunol.* **165**, 566–572.

Pulendran, B., Palucka, K. and Banchereau, J. (2001). Sensing pathogens and tuning immune responses. *Science* **293**, 253–256.
Qi, H., Egen, J. G., Huang, A. Y. and Germain, R. N. (2006). Extrafollicular activation of lymph node B cells by antigen-bearing dendritic cells. *Science* **312**, 1672–1676.
Romani, N., Gruner, S., Brang, D., Kampgen, E., Lenz, A., Trockenbacher, B., Konwalinka, G., Fritsch, P. O., Steinman, R. M. and Schuler, G. (1994). Proliferating dendritic cell progenitors in human blood. *J. Exp. Med.* **180**, 83–93.
Rosenzwajg, M., Canque, B. and Gluckman, J. C. (1996). Human dendritic cell differentiation pathway from $CD34^+$ hematopoietic precursor cells. *Blood* **87**, 535–544.
Schmitt, N., Morita, R., Bourdery, L., Bentebibel, S. E., Zurawski, S. M., Banchereau, J. and Ueno, H. (2009). Human dendritic cells induce the differentiation of interleukin-21-producing T follicular helper-like cells through interleukin-12. *Immunity* **31**, 158–169.
Shortman, K. and Liu, Y.-J. (2002). Mouse and human dendritic cell subtypes. *Nat. Rev. Immunol.* **2**, 151–161.
Shortman, K. and Naik, S. H. (2007). Steady-state and inflammatory dendritic-cell development. *Nat. Rev. Immunol.* **7**, 19–30.
Siegal, F. P., Kadowaki, N., Shodell, M., Fitzgerald-Bocarsly, P. A., Shah, K., Ho, S., Antonenko, S. and Liu, Y. J. (1999). The nature of the principal type 1 interferon-producing cells in human blood. *Science* **284**, 1835–1837.
Spolski, R. and Leonard, W. J. (2008). Interleukin-21: basic biology and implications for cancer and autoimmunity. *Annu. Rev. Immunol.* **26**, 57–79.
Steinman, R. M. (1991). The dendritic cell system and its role in immunogenicity. *Annu. Rev. Immunol.* **9**, 271–296.
Steinman, R. M., Hawiger, D. and Nussenzweig, M. C. (2003). Tolerogenic dendritic cells. *Annu. Rev. Immunol.* **21**, 685–711.
Steinman, R. M., Turley, S., Mellman, I. and Inaba, K. (2000). The induction of tolerance by dendritic cells that have captured apoptotic cells. *J. Exp. Med.* **191**, 411–416.
Strunk, D., Egger, C., Leitner, G., Hanau, D. and Stingl, G. (1997). A skin homing molecule defines the langerhans cell progenitor in human peripheral blood. *J. Exp. Med.* **185**, 1131–1136.
Strunk, D., Rappersberger, K., Egger, C., Strobl, H., Kromer, E., Elbe, A., Maurer, D. and Stingl, G. (1996). Generation of human dendritic cells/Langerhans cells from circulating $CD34^+$ hematopoietic progenitor cells. *Blood* **87**, 1292–1302.
Szabolcs, P., Avigan, D., Gezelter, S., Ciocon, D. H., Moore, M. A., Steinman, R. M. and Young, J. W. (1996). Dendritic cells and macrophages can mature independently from a human bone marrow-derived, post-colony-forming unit intermediate. *Blood* **87**, 4520–4530.
Ueno, H., Tcherepanova, I., Reygrobellet, O., Laughner, E., Ventura, C., Palucka, A. K. and Banchereau, J. (2004). Dendritic cell subsets generated from $CD34^+$ hematopoietic progenitors can be transfected with mRNA and induce antigen-specific cytotoxic T cell responses. *J. Immunol. Methods* **285**, 171–180.
Valladeau, J., Duvert-Frances, V., Pin, J. J., Kleijmeer, M. J., Ait-Yahia, S., Ravel, O., Vincent, C., Vega, F. Jr., Helms, A., Gorman, D. *et al*. (2001). Immature human dendritic cells express asialoglycoprotein receptor isoforms for efficient receptor-mediated endocytosis. *J. Immunol.* **167**, 5767–5774.
Valladeau, J. and Saeland, S. (2005). Cutaneous dendritic cells. *Semin. Immunol.* **17**, 273–283.
van der Aar, A. M., Sylva-Steenland, R. M., Bos, J. D., Kapsenberg, M. L., de Jong, E. C. and Teunissen, M. B. (2007). Loss of TLR2, TLR4, and TLR5 on Langerhans cells abolishes bacterial recognition. *J. Immunol.* **178**, 1986–1990.
Voskoboinik, I., Smyth, M. J. and Trapani, J. A. (2006). Perforin-mediated target-cell death and immune homeostasis. *Nat. Rev. Immunol.* **6**, 940–952.

Index